Using drug treatments to control genome behaviour in normal and Hutchinson-Gilford Progeria Syndrome fibroblasts, with and without hTERT immortalisation

Thesis submitted for the Degree of Doctor

of Philosophy by:

Mehmet Ural Bikkul BSc MSc

College of Health and Life Sciences, Brunel University London, UK

January 2016

Abstract

Hutchinson-Gilford Progeria Syndrome (HGPS) is an exceedingly rare genetic condition with striking features reminiscent of marked premature ageing. HGPS is commonly caused by a ‘classic’ mutation in the A-type lamin gene, *LMNA* (G608G). This leads to the expression of an aberrant truncated lamin A protein, progerin. The nuclear lamina is known to anchor chromosomes, stabilising and regulating the genome. Interphase chromosomes are non-randomly positioned in the nuclei of cells and they occupy specific locations with respect to a radial distribution, gene-poor chromosomes are positioned at the nuclear periphery and gene-rich chromosomes are positioned towards the nuclear interior. The findings indicated that FTI-277, pravastatin, Zoledronic acid, N-acetyl-L-cysteine and all three combination treatments; FG, PZ, FPZ, have a positive effect on anchoring the genome to the nuclear matrix in AG01972 cell line. Furthermore, it was shown that in terms of positiong of chromosomes 18 and X, treatment of AG01972 HGPS cells with FTI + GGTI and FTI-277 + pravastatin + zoledronic acid drug combinations greatly restored the chromosomal organisation as well as the chromosome repositioning. The data in this thesis indicated that HP1α was found affected in T08 cells and upon lovastatin treatment T08 cells exhibited increased HP1α staining which is the good indication of rescue of heterochromatin organization. Whole exome sequencing data obtained from AG08466 atypical HGPS cells revealed that 2457589 position of promoter region is missing on *LMNB2* gene located on chromosome 19.

Intriguinly, the radial positions of chromosomes 10, 13, 18, and X results revealed that first time ever in our lab chromosome X found occupying the nuclear interior in atypical T08 cells. Colocalisation analysis of chromosome and fibrillarin findings

confirmed chromosome positioning results since chromosomes X colocalised with fibrillarin with higher percentages in T08 cells than other cells suggesting the situation appears to be due to elongated telomeres with more chromosome territories being in the nuclear interior associated with nucleoli. M-FISH karyotyping analysis results confirmed unequivocally metaphase chromosome findings that immortalised T08 cell line has aneuoploidy including deletions and translocations. Histone modification marks H3K9me3, H3K27me3, H4K20me3 and HP1α results indicated that proteins were severely affected in T06 cells, suggesting that expression of truncuated progerin protein alters chromatin organization in T06 cells and also the structure of histone marks are severely affected in atypical T08 cells. The structure of nucleolus is affected in both typical and atypical immortalised HGPS cells, suggesting epigenetic regulation to have a crucial role in HGPS. Subsequently, the telomere lengths of immortalised normal and atypical T08 HGPS cell lines were assessed using IQ-FISH. The results indicated that both immortalised cells had chromosomes with relatively longer telomeric repeats in comparison to the control NB1 cells. The small non-peptidic, non-nucleosidic synthetic compounds (BIBR1532) was utilised to target the telomerase/telomere complex of our immortalised cell lines to shorten telomeres in order to test the hypothesis that elongated telomeres had mislocalised chromosomes. Furthermore, the effect of BIBR1532 on telomeres position in cells was assessed. Remarkably, results demonstrated that BIBR1532 is capable of shortening telomere length of immortalised cells to the level of normal NB1 fibroblasts and immortalised cell lines were capable of proliferating after drug treatment. Furher, results revealed that BIBR1532 treatment can restore the position of chromosome X towards the nuclear periphery within the NB1T and T08 nucleus. Furthermore, although BIBR1532 treatment can restore the position of chromosome

18 towards the nuclear periphery in NB1T cells, treatment did not alter the position of chromosome 18 in T08 cells. Finally, the telomere dysfunction-induced foci (TIF) assay was performed to detect DNA damage in NB1T and T08 cells using an antibody against DNA damage marker γ-H2AX and a synthetic PNA probe for telomeres. Surprisingly, results indicated that BIBR1532 treatment of cells did not give rise to high DNA damage response in both NB1T and T08 cells.

Declaration

I hereby declare that the work presented in this thesis has been performed by myself unless stated.

Date: 5/1/2016

Mehmet Ural Bikkul

Acknowledgements

First and foremost, I am highly grateful to my supervisor, Dr. Joanna Bridger, for accepting and giving me the opportunity to be her Ph.D. student. I appreciate for all her supervision, motivation, guidance, friendship and support throughout my Ph.D. Thanks also to Dr.Predrag Slijepcevic, my second supervisor.

I would also like to acknowledge Dr. Ian Kill for his helpful advice and diverse suggestions during this project. It is almost impossible to individually thank everyone who provided assistance during my studies. I want to express my gratitude to the following collaborators who provided me a number of cell lines, without which the studies that presented here would not be complete. Dr. Chris Parris (Brunel University, NB1T), Professor Richard Faragher (Brighton University, TAG06297 and TAG08466).

I would like to thank to the following collaborators: Dr. Rhona Anderson for her guidance on M-FISH analysis work. Dr. Evgeny Makarov for training me for cDNA synthesis and RT-PCR technique. Dr. Joanna Bridger and Dr. Helen Foster for general laboratory support as well as letting me use the FISH scripts developed by Dr. Paul Perry and Prof. Wendy Bickmore. I am sincerely grateful to Dr. Craig Clements for his invaluable suggestions and guidance.

I am very grateful to Dr. Ian Kill, Dr. Predrag Slijepcevic, Dr. Ines Castro, and Dr. Paola Vagnerelli for their generously provided gifts of antibodies. I would like to thank to laboratory technicians: Dr. Matthew Themis, Helen Cox, and Geraldi Hatton for general laboratory support during my studies. Furthermore, I would like to thank and acknowledge: Dr. Parissa, Dr. Yaghoub, Dr. Chetna and Savi for their assistance in general laboratory work.

My acknowledgement also goes for my office colleagues Gemma, Dr. Abdulbasit, Kumar, Dr. Sara, Temi, Dr. Halime, Ezgi, Paudyal, Amir, Amanda.

Last but not least, I am eternally indebted to my parents Saadet and Mengu and my brother Barkin for their devoted support, inspiration and unrelenting love, especially through the challenging times.

Lasty, I would like to dedicate this thesis to my parents and my beloved uncle and auntie. Thank you all!!

Abbreviations

µg	micro gram
µl	micro litre
µm	micro metre
µM	micro molar
^{0}C	degree centigrade
2D	two dimensional
2D-FISH	two dimensional FISH
3D	three dimensional
3D-FISH	three dimensional FISH
4D	four dimensional
53BP1	p53-binding protein 1
APD	accumulated population doublings
ATP	adenosine-5'-triphosphate
BAF	barrier auto-integration factor
BMPs	bone morphogenetic proteins
Bp	base pairs
BSA	bovine serum albumin
CCD	charge coupled device
CcFI	corrected calibrated fluorescence
CDK	cyclin dependent kinase
cDNA	complementary DNA

ChiP	chromatin immunoprecitation
CHO	Chinese hamster ovary
CMT	carboxyl methyltransferase
CMT2B	charcot-marie- tooth disease type 2
CO_2	carbon dioxide
CT	chromosome territories
CT-IC	CT- interchromatin compartment
Da	dalton
DAPI	4', 6-diamidino-2-phenylindole
DCM	dilated cardiomyopathy
DFC	dense fibrillar compartment
DMEM	dulbeco's modified eagle's medium
DMSO	dimethyl sulphoxide
DNA	deoxyribonucleic acid
dNTP	deoxynucleotide triphosphate
DOP-PCR	degenerate oligonucleotide primed-PCR
DSBs	double strand breaks
Ds-DNA	double stranded DNA
EDMD	Emery- Dreifuss muscular dystrophy
EDTA	ethylenediaminetetraaceticacid
ER	endoplasmic reticulum
F-actin	filamentous actin
FBS	foetal bovine serum

FC fibrillar component

FISH fluorescence in situ hybridisation

FITC fluoresceinisothyiocynate

FPLD familial partial lipodystrophy

FRAP fluorescence recovery after photobleaching

FTIs farnesyl transferease inhibitors

G grams

G_0 quiescence

GC granular compartment

GFP green fluorescent protein

GGTI geranylgeranyltransferase inhibitor

G_S senescence

H3 histone 3

H4 histone 4

HA95 heterochromatin associate protein 95

HDAC histone deacetylase

HDF human dermal fibroblast

HGPS Hutchinson Gilford Progeria Syndrome

HMG-Coa 3-hydroxy-3-methylglutarylcoenzyme a

HnRNP heterogenous nuclear ribonucleoprotein

HP1 heterochromatin protein-1

HR head rod

HSTc human stem cells

hTERT human telomerase reverse transcriptase

HU hydroxyurea

ICD interchromosome domain

ICMT isoprenylcysteine CMT

ICN interchromosomal network

IF intermediate filament

IGF1 insulin-like growth factor-1

INM inner nuclear membrane

IQ-FISH interphase quantitative FISH

ITLs interstitial telomere loops

K potassium

KASH klarsicht, anc-1 and syne homology

Kb kilobase(s)

KCl potassium chloride

kDa kilodalton

LADs lamina associated domains

LAP lamina associated polypeptide

LBR lamin B receptor

LBR-TD LBR tudor domain

LCR locus control region

LEM lap2 emerin man1

LGMD1B limble girdle muscular dystrophy 1B

LINC links the nucleoskeleton and cytoskeleton

LIS lithium diodosalicilate

Lt litre

LY-R lymphoma radiation-resistant

LY-S lyphoma radiation sensitive

M Molar

M: A methanol-acetone

MAA methanol acetic acid

MAD Mandibuloacral Dysplasia

MARs matrix-attachment regions

Matr3 matrin 3

MDa million daltons

MDB membrane desalting buffer

MEFs mouse embryo fibroblasts

M-FISH multiplex FISH

Mg miligrams

MgCl magnesium chloride

Min minute(s)

Ml millilitres

mm milimeters

mM Milimolar

mTOR Mammalian target of rapamycin

MW molecular weight

NaCl sodium chloride

na-DNA nucleolus associated DNA

NB1T normal boy 1 transferase

ncRNA noncoding RNA

NCS newborn calf serum

NETs nuclear envelope transmembrane proteins

NLS nuclear localization signal

NM nuclear matrix

NM nuclear membrane

NOR nucleolar organising regions

NPCs nuclear pore complexes

NUP153 nucleoporin 153

ONM outer nuclear membrane

P53 tumour suppressor protein

PARP1 poly (ADP) ribose polymerase 1

PBS phosphate buffer saline

PCNA proliferating cell nuclear antigen

PCR polymerase chain reaction

PEV position-effect variegation

PFA paraformaldehyde

pH $-\log_{10}(a_H+)$

PNA- FISH peptide nucleic acid FISH

PTMs post-translational modifications

Rb retinoblastoma

RBBP4 retinoblastoma binding protein 4

RCE1 RAS converting enzyme 1

RD Restrictive Dermopathy

RNA ribonucleic acid

RNAi RNA interference

RNP ribonucleoprotein

RPC Replication Factor C

RPM rotations per minute

r-RNA ribosomal RNA

RT room temperature

RT-PCR reverse transcriptase PCR

S/MAR scaffold/matrix attachment regions

SAFA scaffold attachment factor

SARs scaffold attachment regions

SDS sodium dodecyl sulphate

SDS-PAGE sodium dodecyl sulphate-PAGE

SEM standard error of mean

siRNA short interfering RNA

SSC saline sodium citrate

SUN sad1 and unc-84

SV-40 simian virus 40

SYNE spectrin repeat- containing nuclear envelope

TIF telomere dysfunction induced foci

TPE	telomere position effect
TRF2	telomeric repeat binding factor 2
TRITC	rhodamine
tRNA	transfer RNA
TSA	trichostatin A
U	enzyme units
UV	ultra violet
VEGF	vascular endothelial growth factor
WB	Western blotting
WCP	whole chromosome probe
WS	werner syndrome
Zmpste24	zinc-metalloprotease related to ste24p
β-actin	beta actin

Contents

Pages

List of Figures

Chapter 1

Chapter 2

Chapter 3

Chapter 6

Pages

List of Tables

Chapter 4

Chapter 5

Chapter 1: Literature review

Introduction

Within the human nuclei the hereditary material DNA is present in a highly compact and organized manner. For the regulation of gene expression and as well as maintenance of the cell, this level of organisation is vital and it is altered in Hutchinson Gilford Progeria Syndrome premature ageing disease *(Puckelwartz, et al.,*2011). In this literature review, nuclear structures and their functions and roles in chromosomal and genome organization in normal cells as well as diseased HGPS cells will be discussed.

1.1 The nucleus and nuclear architecture

The nucleus co-ordinates a wide range of functions, including transcription, replication, repair of DNA and assembly of ribosomes. The nucleus consists of several nuclear compartments; nuclear envelope, the genome, nucleoli, nuclear bodies (Figure 1.1) (Foster and Bridger, 2005). Any misorganization or disruption of this nuclear architecture could lead to diseases including cancer and severe ageing diseases, such as the progeriod syndromes and laminopathies (Bridger *et al.*, 2014; Bourne *et al.*, 2013; Goldman *et al*., 2002).

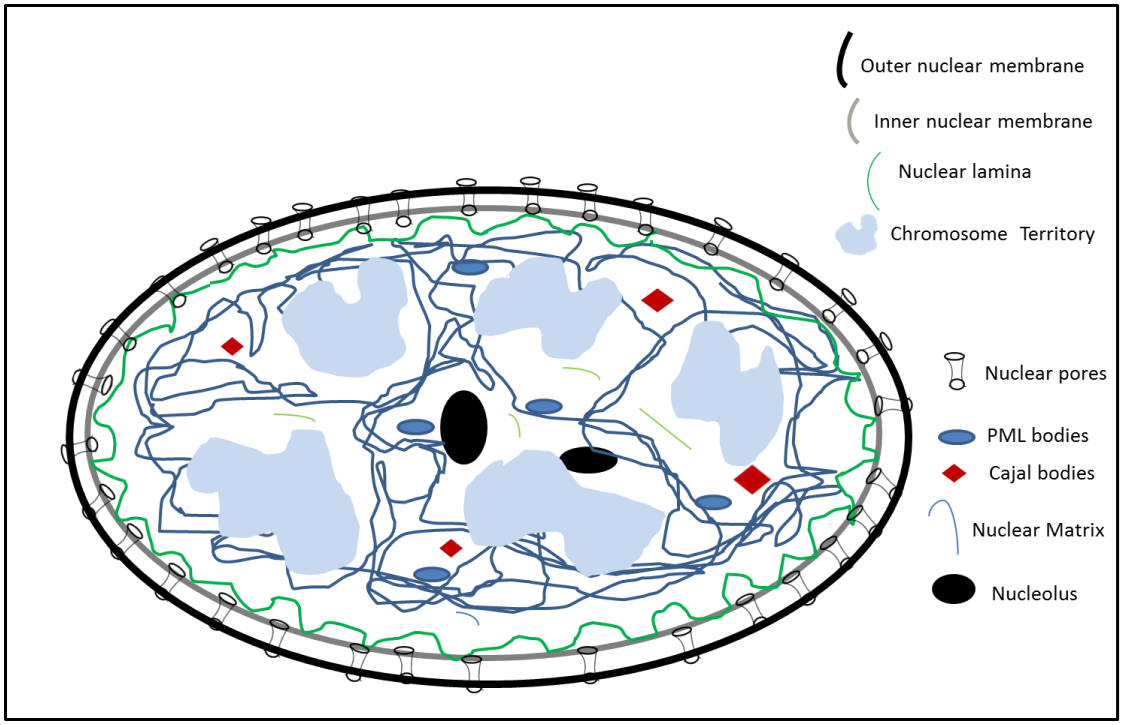

Figure 1.1 This diagram shows components of an interphase nucleus including the nuclear envelope, nuclear bodies, nuclear lamina and the genome.

1.1.1 Nuclear Matrix

Nuclear processes occurring at distinct sites suggest that there may be an underlying structure in the nucleus. Although, nuclei do not contain a structure resembling the cytoskeleton, a filamentous network consisting of protein, DNA and RNA called “the nuclear matrix” may present in the nucleus (Jackson, 2003; Berezney *et al.*, 1995). Mika and Rost’s (2005) study reported that there are over 400 nuclear matrix proteins (NM proteins) and of these, almost 50% are constituents of the inner nuclear membrane and 130 are connected with cell cycle (Mika and Rost, 2005). If nuclei are treated with DNase, detergents, and high salt, this network can be easily visualized compared to the cytoskeleton (Berezney *et al.*, 1995). The nuclear matrix is made up of 10 nm filaments supports DNA replication, repair, and

transcription, maintaining the strict compartmentalization of the nucleus and also providing a scaffold for higher-order chromatin packaging (Berezney *et al.*, 1995). The presence of the nuclear matrix proteins matrin 3(matr3) and scaffold attachment factor A (SAFA) was demonstrated in transcription-associated nuclear environments (Coelho *et al.*, 2015; Malyavantham *et al.*, 2008). It was reported that both matr3 and SAFA bind DNA at sites named scaffold/matrix attachment regions (S/MAR) (Hibino *et al.*, 2000; Göhring and Fackelmayer, 1997). Moreover, SAFA stabilizes specific mRNAs and plays a key role in active transcription through an interaction with RNA polymerase II and actin (Obrdlik *et al.*, 2008; Yugami *et al.*, 2007). Furthermore, DNA halo exctraction together with two-dimensional FISH can be used to reveal the relationship between the genome and nuclear matrix (Elcock and Bridger, 2008). Chromosome territories seem to specifically anchor to the nuclear matrix and a study revealed that chromosomes do not attach to the nuclear matrix similarly, gene-rich chromosome 19 is more tightly associated with the nuclear matrix compared to gene-poor chromosome 18 (Croft *et al.*, 1999). It was demonstrated that following extraction for the nuclear matrix, chromosome territories were maintained intact, however complete extraction of the internal matrix caused disruption of the chromosome territories.

1.1.2 The Nucleolus

The nucleolus is where ribosomal RNAs are synthesized and processed and ribosomal subunits are assembled (Lam and Trinkle-Mulcahy, 2015). In humans the acrocentric chromosomes containing the ribosomal repeat genes are embedded in nucleoli, providing a functional anchorage site for these genes and their chromosomes (Bridger *et al.,* 1998). A nucleolus consists of three sub-

compartments: the fibrillar compartment (FC), dense fibrillar compartment (DFC) and granular compartment (GC) (Bridger *et al.,* 1998). The FC is present throughout the nucleolus and is linked through a network of DFCs. In addition, both FC and DFC are embedded within the GC which consists of granules of 15-20 nm in diameter (Junera *et al.*, 1995). Each of compartments has distinct but associated functions. Ribosome synthesis begins in the DFC with nascent RNA accumulated in this nucleolar domain and in the junctions between DFC and FC (Cmarko *et al.*, 2000). The process of ribosome synthesis continuous in the intracellular regions and in the GC (Fatica and Tollervey, 2002). It is important to note that the function of the nucleolus is not restricted to the biogenesis of ribosomal subunits and there are more than 700 nucleolar proteins which are believed to be involved in various cellular functions (Boisvert *et al.*, 2007). In nucleoli, tRNA genes are clustered where they are transcribed and where tRNA processing begins (Németh *et al.*, 2010; Boisvert *et al.*, 2007).

Mutations in genes coding for nucleolar proteins lead to premature senescence and thus it would be essential to examine whether nucleolar proteins are involved in the HGPS pathology (Rosete *et al.,* 2007). Nucleophosmin also known as B23 is an abundant non-ribosomal nucleolar protein participating in numerous cellular activities, which include ribosome biogenesis, histone assembly, regulation of DNA integrity, cell proliferation, and regulation of tumour suppressors, such as p53, p14arf, and Fbw7γ (Chiarella *et al.*, 2013; Lee *et al.*, 2007). In addition, B23 also plays several roles outside the nucleolus. It shuttles between the nucleus and the cytoplasm and shows molecular chaperone activity (Chiarella *et al.*, 2013). Fibrillarin is highly conserved throughout evolution; for example, human fibrillarin is 67% identical to its yeast homolog named Nop1p (for nucleolar protein 1) (Aris and

Blobel, 1991) and small ribonucleo protein present in the DFC domain of nucleoli that is associated with all Box C/D small nucleolar (sno) RNAs and functions in early processing and modification of pre-rRNA and ribosome assembly. The Human pol I transcription consists of upstream binding factor (UBF), selectively factor 1 (SL1) and pol I with its binding factors (TIF IA and TIF IC) (Grummt, 1998). Transcription by all three classes of RNA polymerase halts or functions decreased as cells go through mitosis. However, in interphase UBF, SL1 and a fraction of Pol I transcription machinery remains associated with mitotic NORs at genes that were active (Sullivan *et al*., 2001). In the case inactive genes, it appears that inactive genes are condensed and are not associated with the Pol I transcription machinery (Prieto and McStay, 2007; Mais *et al.*, 2005). rRNA genes are known to exist in different epigenetic states and changes in the CpG methylation pattern are hallmarks of various diseases and cancer (Oakes *et al.*, 2003). In terms of epigenetic features of rRNA genes, active rRNA genes are defined by demethylation of H3K4me2 and acetylation of histone H4, however repressed rRNA genes are characterised by repressive epigenetic marks such as trimethylation of H3K9, H4K20 and H3K27 and DNA hypermethylation (Grummt and Längst, 2013; Zentner *et al*., 2007). Telomere reverse transcriptase in the nucleolus bound to the nucleolar protein nucleolin until the onset of S-phase of the cell cycle and is vital for addition of telomeric repeats at the ends of newly synthesised chromosomes (Trinkle-Mulcahy and Lamond, 2006). Studies in yeast nucleoli have revealed that Sir complex genes reposition from the telomeres to the nucleoli with age of the organism, suggesting a role of nucleolus in organismal ageing (Guarente, 1997). Chromosomes integrate into the nucleolus via their active Nucleolar organising regions (NORs), inactive NORs and therefore nucleolus is believed to be vital for spatial organisation of the genome within the

nucleus (Zentner *et al.*, 2011; Sullivan *et al.*, 2001). Nemeth and collegues (2010) demonsrated that nucleolous-associated DNA (naDNA) appeared mainly on p-arms of acrocentric chromosomes and pericentromeric regions of chromosomes are enriched in naDNA. Moreover, it was revealed that certain type of satellite repeats, tRNA, 5S RNA genes and members of immunoglobulin gene families constitute the main building blocks of NADs and nine numbers of NADs were shown localising in subtelomeric regions (Németh *et al.*, 2010). Bridger *et al., (*1998) demonstrated colocalization between nucleolar pKi-67 foci and satellite III DNA clusters on human chromosome 1 and Y.

1.2 Nuclear Envelope

The nucleus of a eukaryotic cell is separated from the cytoplasm by a nuclear membrane (NM) which is made up of two membranes, the inner and outer nuclear membranes (Katta *et al.*, 2014). The nuclear envelope contains nuclear pore complexes (NPC) and nuclear lamina and other associated proteins (Grossman *et al.*, 2012). The space between the outer and inner nuclear membranes is called “the nuclear envelope lumen” and is 20-40 nm in width. The outer nuclear membrane is continuous with the endoplasmic reticulum, therefore facing the cytoplasm *(Voeltz, et al.,* 2002). The inner nuclear membrane faces the nucleus and contains a subset of integral membrane proteins (IMPs) (Worman and Dauer, 2014; Trinkle-Mulcahy and Lamond, 2006). Proteomic analysis has identified 67 of these proteins and includes A-type and B-type lamins, lamin B receptor, lamin associated polypeptide 1 and 2, emerin, nesprins, SUN1/2 and also actin (Figure 1.2) (Worman and Schirmer, 2015; Bridger *et al.*, 2007; Broers *et al.*, 2006). NM not only acts as a physical barrier providing structural support for the nucleus but also the NM has numerous other cell-

specific function including regulation of tissue-specific gene expression, nuclear positioning and chromatin organization in cells (Dechat *et al.*, 2008).

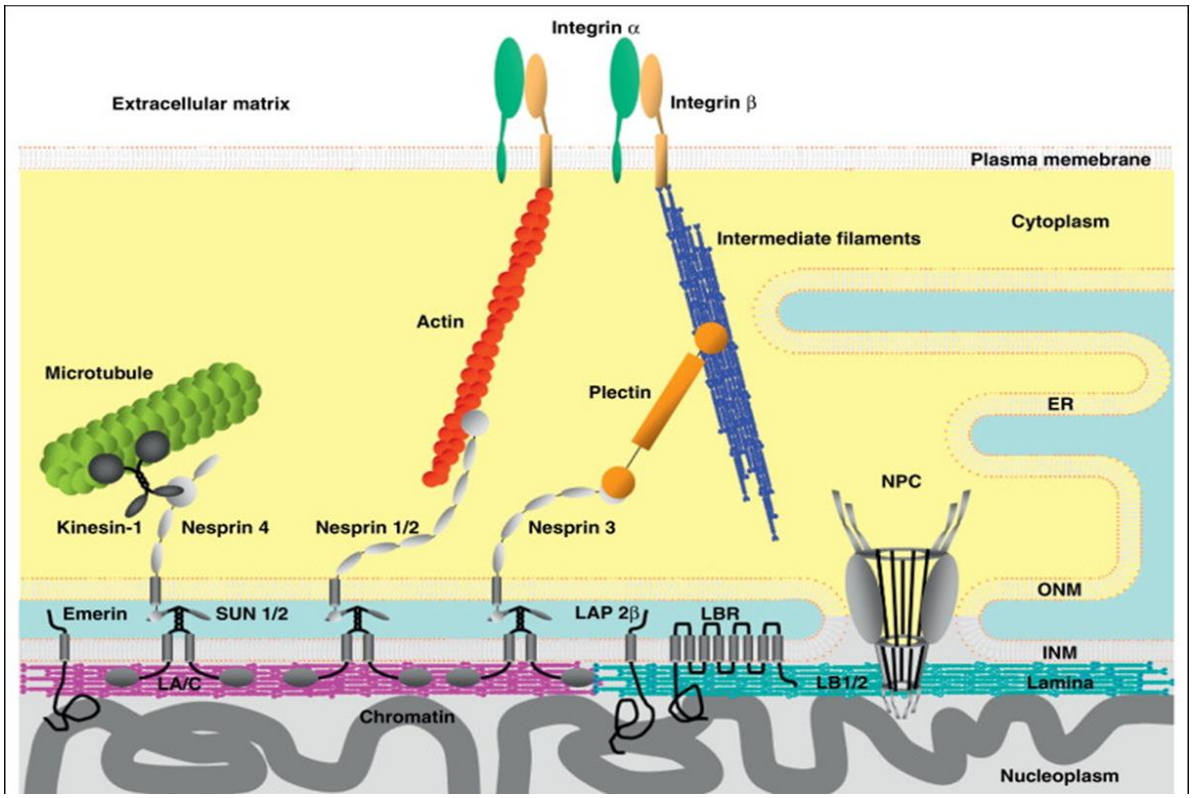

Figure 1.2 Illustration of the various proposed interactions of lamins with inner nuclear memrane proteins, nuclear pores. Lamins bind directly to lamina-associated proteins (LBR, LAP2, emerin, LB1/2, nesprins-1 and -2). All of the lamins and some of the INM proteins interact with chromatin. SUN1 and SUN2 bind to the KASH domain of nesprins in the luminal region between the INM and ONM to form the LINC complex. Nesprins in the ONM bind to cytoskeletal filaments such as actin, microtubules, and intermediate filaments (IFs) directly or indirectly through plectin or kinesin. Actin and IFs are associated with the plasma membrane through integrin complexes (Shimi *et al.,* 2012).

1.2.1 Nuclear pore complexes

Nuclear pore complexes (NPC) are large aqueous channels embedded across numerous perforations in the nuclear envelope with a calculated mass of 40 and 60 million Daltons (MDa) in yeast and vertebrates, respectively being responsible for

bidirectional exchange of proteins, RNAs, and other macromolecules between the nucleus and cytoplasmic compartments (D'Angelo and Hetzer, 2008; Weis, 2007; Tran and Wente, 2006). Furthermore, NPCs remain highly selective and allow the passage of molecules that are larger than 30–40 kDa only when bound to appropriate transport receptors (Tran and Wente, 2006). A typical vertebrate nucleus has approximately 5,000 NPCs scattered over its surface (Wozniak and Lusk, 2003). The overall structure of the NPC can be superficially divided into three basic elements: the nuclear basket, the central region, and the cytoplasmic fibrils (Figure 1.3) (Suntharalingam and Wente, 2003)

Cryoelectron tomography with three dimensional reconstructions has been used to present the highest-resolution structure (approximately 9 nm) of the NPC (Beck *et al.*, 2004). This structure demonstrates that the cytoplasmic filaments adopt a highly "kinked" structure, yielding a length of approximately 35 nm. In spite of their immense size, NPCs are about 30 distinct proteins, collectively named nucleoporins or nups (Tran and Wente, 2006). These nucleoporins are modularly assembled to form subcomplexes within the highly dynamic NPC (Lim and Fahrenkrog, 2006). Zhou's group suggests that as NPC nuclear basket interacts with the nuclear lamina with NUP153 playing an indirect role in maintaining nucleoskeleton and cytoskeleton architecture via the nuclear lamina (Zhou and Panté, 2010). Nup153 has multiple binding sites for both A- and B- type lamins and due to the mutations occurring in the *LMNA* Ig-fold, the interaction is selectively affected given that Nup153 is involved in specific laminopathic diseases (Al-Haboubi *et al.*, 2011).

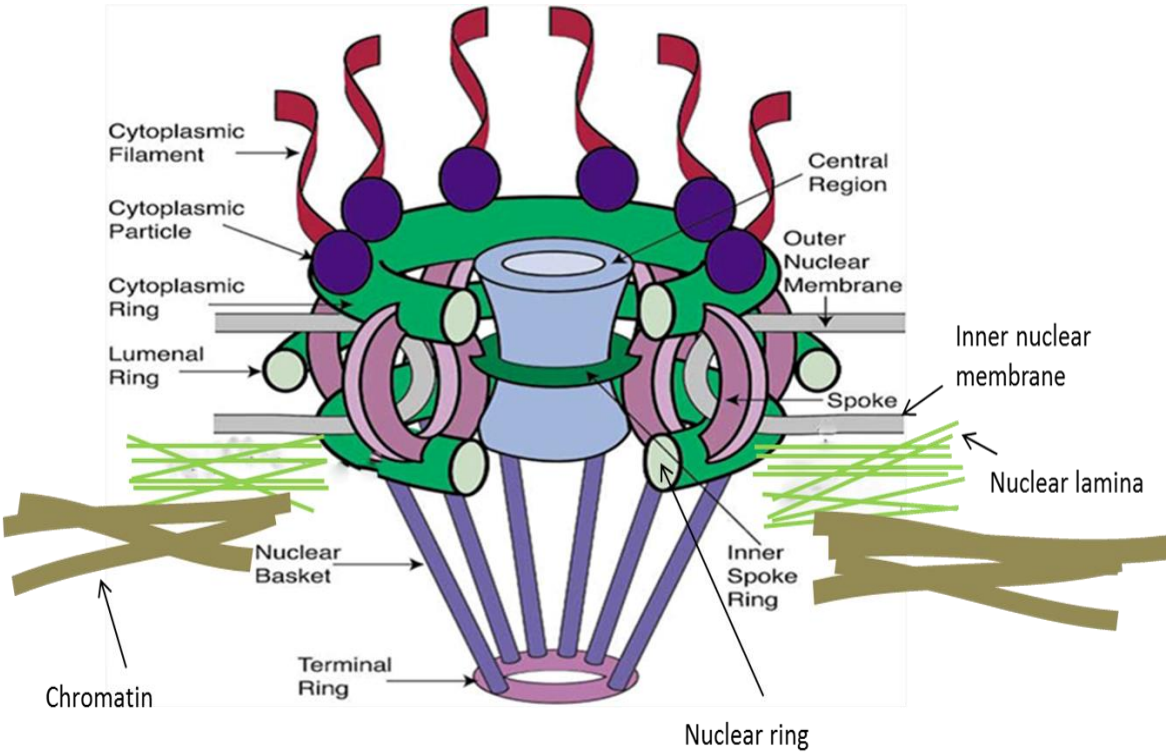

Figure 1.3 Schematic representation of nuclear pore complex. All the structures found in vertebrate NPCs are included, with the cytoplasmic face on top (Suntharalingam and Wente, 2003).

1.3 The nuclear lamina

The nuclear lamina is an intermediate filament meshwork underlying the inner nuclear membrane (INE) and it is a 30-80nm thick network of lamin polymers forming a higher-ordered structure (Worman, 2012; Gerace and Huber, 2012). Lamins seem to be expressed in all metazoans but are absent from unicellular organisms and plant cells (Ciska *et al.*, 2013; Dechat *et al.*, 2010). The A and B type nuclear lamins represent one (type V) of six subtypes of the intermediate filament (IF) superfamily, defined on the basis of the genomic structure and nucleotide sequence and are believed to be the progenitors of all intermediate filaments which constitute the major

components of the nuclear lamina, giving support to the nuclei, tethering specific regions of the genome to the nuclear periphery and regulating gene expression (Dittmer and Misteli, 2011; Wilson and Foisner, 2010; Rodriguez and Eriksson, 2010; Bridger *et al.*, 2007). Nuclear lamins distribute mainly in the nuclear membrane but can also be found in the nucleoplasm (Figure 1.1) (Bercht Pfleghaar *et al.*, 2015; Gesson *et al.*, 2014; Goldman *et al.*, 1992).

1.3.1 Lamin structure

Like other IF proteins, lamins possess a tripartite structure consisting of a central α-helical rod domain of 350 aminoacids containing four coiled-coil domains: 1A, 1B, 2A, and 2B separated by linker regions L1, L12, and L2 , flanked by non-α-helical globular N-terminal(4 KDa) head at one end and a longer carboxy-terminal (20-30 KDa) (Figure 1.4) (Burke and Stewart, 2013; Worman *et al.*, 2009; Bridger *et al.*, 2007; Strelkov *et al.*, 2004; Herrmann and Aebi, 2004). In different lamins, these end domains have different structures and they are known to play important roles in lamin assembly (Moir *et al.*, 2000). 1A, 1B, 2A segments show a distinct pattern of charged amino acid clusters that are important for a given IF protein to assemble into higher order structures (Köster *et al.*, 2015). A nuclear localization signal (NLS) between the central rod and the Ig-fold that is required for the transport of lamins into the nucleus (Burke and Stewart, 2013; Dechat *et al.*, 2008). The Ig domain is common to many proteins and arbitrates various protein-protein and protein-ligand interactions, which involve every surface of the Ig domain (Dittmer and Misteli, 2011; Dhe-Paganon *et al.*, 2002). Lamins have shorter head domains than most cytoplasmic intermediate filament proteins which are about 40 to 100 residues long (Worman, 2012; Dittmer and Misteli, 2011). The basic filament building block is a

lamin–lamin dimer. Lamins dimerize via their α- helical rod domain which contains the characteristic coiled-coil heptad amino acids repeat pattern, thus allowing the lamin monomers to self-interact by parallel interactions to form coiled-coil homodimers (Dittmer and Misteli, 2011; Dechat *et al.*, 2010; Worman *et al.*, 2009).

In vitro, lamins form higher-order polymers and head- to- tail associations between two or more lamin dimers, resulting in a lamin polymer, whereas the head and tail globular domains aid lateral interactions between the dimers to form filaments (Figure 1.5) (Strelkov *et al.*, 2004; Herrmann and Aebi, 2004). These polarized arrays interact in an antiparallel fashion to form filaments and eventually the interaction between lamin non-polar protofilaments leads to the formation of the 10 nm lamin filamentous lattice-work, composed of three or four protofilaments (Gruenbaum and Medalia, 2015; Dittmer and Misteli, 2011; Ben-Harush *et al.*, 2009). Lamin dimers associate by polar “head-to-tail “ interactions in order to form protofilaments. On the other hand, cytoplasmic IF dimers associate by half-staggered, antiparallel side-by-side, which assemble into 10 nm filaments (Dechat *et al.*, 2010; Strelkov *et al.*, 2004). Moreover, vertebrate lamins contain six extra heptads in the central rod domain which may cause assembly differences between cytoplasmic IF and lamins (McKeon *et al*., 1986).

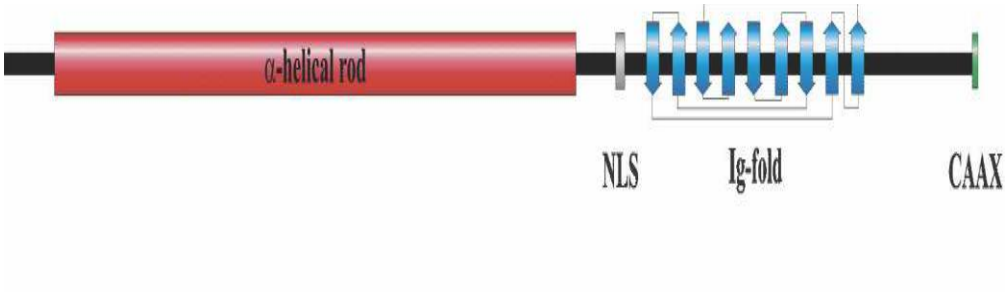

Figure 1.4 A representative image of pre-lamin A polypeptide chain.The central α-helical rod domain (red), the NLS (grey), simplified structure of Ig-fold indicating the nine β- sheets (blue) and the C-terminal −CAAX box (green) are depicted (Dechat *et al.*, 2008).

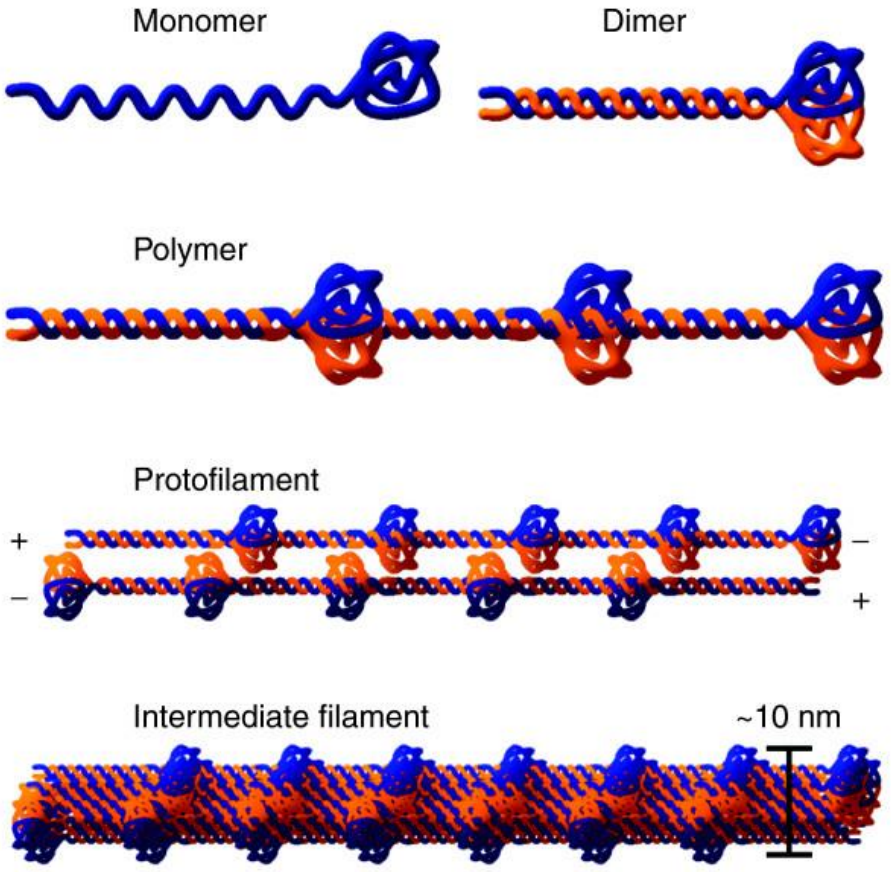

Figure 1.5 A schematic model of lamin assembly. Monomer lamins self assemble head-to-head manner to form a coiled- coil dimer which then join to form by association of dimers in a polar head-to-tail manner. Protofilaments are generated through anti-parallel interaction of two lamin polymers. Eventually, association of three or four protofilaments to form an intermediate filament (Dittmer and Misteli, 2011).

Due to the difficulty in producing 10-nm filament *in vitro*, the study of higher-order lamin structure has been challenging (Chernyatina *et al*.,2015). To date, the *Caenorhabditis elegans* lamin (Ce-lamin) is the only lamin that has been successfully assembled into 10 nm intermediate filament-like filaments based on cryo-electron tomography studies (Dittmer and Misteli, 2011).

1.3.2 Post-translational modifications of lamin proteins

A –CAAX motif, which serves as a substrate for post-translational farnesylation, which is located at the C terminus in all B-type lamins, lamins A and AΔ10 and as these proteins are expressed as prelamins that require sequential posttranslational modifications and cleavage to generate the mature forms of lamin A, lamin B1 and lamin B2 (Rusiñol and Sinensky, 2006). However, lamin C lacks a- CAAX motif and its carboxyl terminus is not further farnsylated or otherwise modified after synthesis (Clarke, 1992). In the first step, the sequential processing of the –CAAX sequence is initiated by the addition of the 15-carbon farnesyl isoprenoid, farnesyl group, to the cysteine residue by farnesyltransferase (Zhang and Casey, 1996; Clarke, 1992). Following the addition of farnesyl, prelamins are then modified by a specific protease. In lamin B, prenyl-CAAX-specific endoprotease (AAX=aliphatic-aliphatic-any amino acid) known as RAS converting enzyme 1 (RCE1) clips off the last three carboxyl-terminal amino acids. However, in A-type lamins residues are removed by a different protease, the Zinc metalloprotease related to Ste24p, Zmpste24 also known as FACE1 (Winter-Vann and Casey, 2005; Boyartchuk *et al*., 1997). In a third step, these prelamins are then the substrate for a second ER-resident enzyme, isoprenylcysteine carboxyl methyl-transferase (ICMT), which methylesterifies the carboxyl-terminal farnesylcysteine (Winter-Vann and Casey, 2005). In this last step, unlike B-type lamins, lamin A undergoes an additional cleavage of 15 amino acids upstream of the farnesylated cysteine by ZMPSTE24, which removes the C-terminal farnesyl group and leaves a tyrosine residue at the carboxyl end of lamin A (Dechat *et al.*, 2010; Corrigan *et al.*, 2005). This final modification step results in the production of mature lamin A lacking the carboxyl-terminal farnesyl- and carboxymethyl-modifications (Figure 1.6) (Dechat *et al.*, 2010). While the maturation

of B-type lamins is terminated at this step resulting in their permanent farnesylation and carboxymethylation (Goldberg *et al.*, 2008). In normal human cells, the post-translational modifications of lamin A has been determined to take approximately three hours (Beck *et al.*, 1990). It is believed that these modifications help the accurate targeting of the final lamin A product to the nuclear envelope as farnesylation and carboxymethylation increase the hydrophobicity of a protein (Candelario *et al.*, 2011) and it is likely that the carboxy terminal peptide cleaved by ZMPSTE24 could remain attached to the membrane or be rapidly degraded (Reddy and Comai, 2012). Although the prelamins can be processed in the cytoplasm, as ZMPSTE24 is located both at the inner nuclear membrane and the endoplasmic reticulum (ER), it is presumed that the location of lamin carboxyl terminal modification processes takes place within the nucleus (Barrowman *et al.*, 2008; De Sandre-Giovannoli and Lévy, 2006; Lutz *et al.*, 1992). The retension of a farnesyl residue attached to B-type lamins may facilitate them to associate more closely with the inner nuclear membrane than lamin A or C (Nigg *et al.*, 1992). Mature lamin A is a soluble protein and so is imported into the nucleus through the nuclear pore complexes (Cau *et al.*, 2014). B-type lamins are not soluble, so localise to the inner nuclear envelope by lateral diffusion through the lipid bilayer (Holmer and Worman, 2001). Lamins are not only modified by farnesylation and carboxymethylation, they are also posttranslationally modified by phosphorylation, sumoylation and possibly by glycosylation (Dechat *et al.*, 2010).

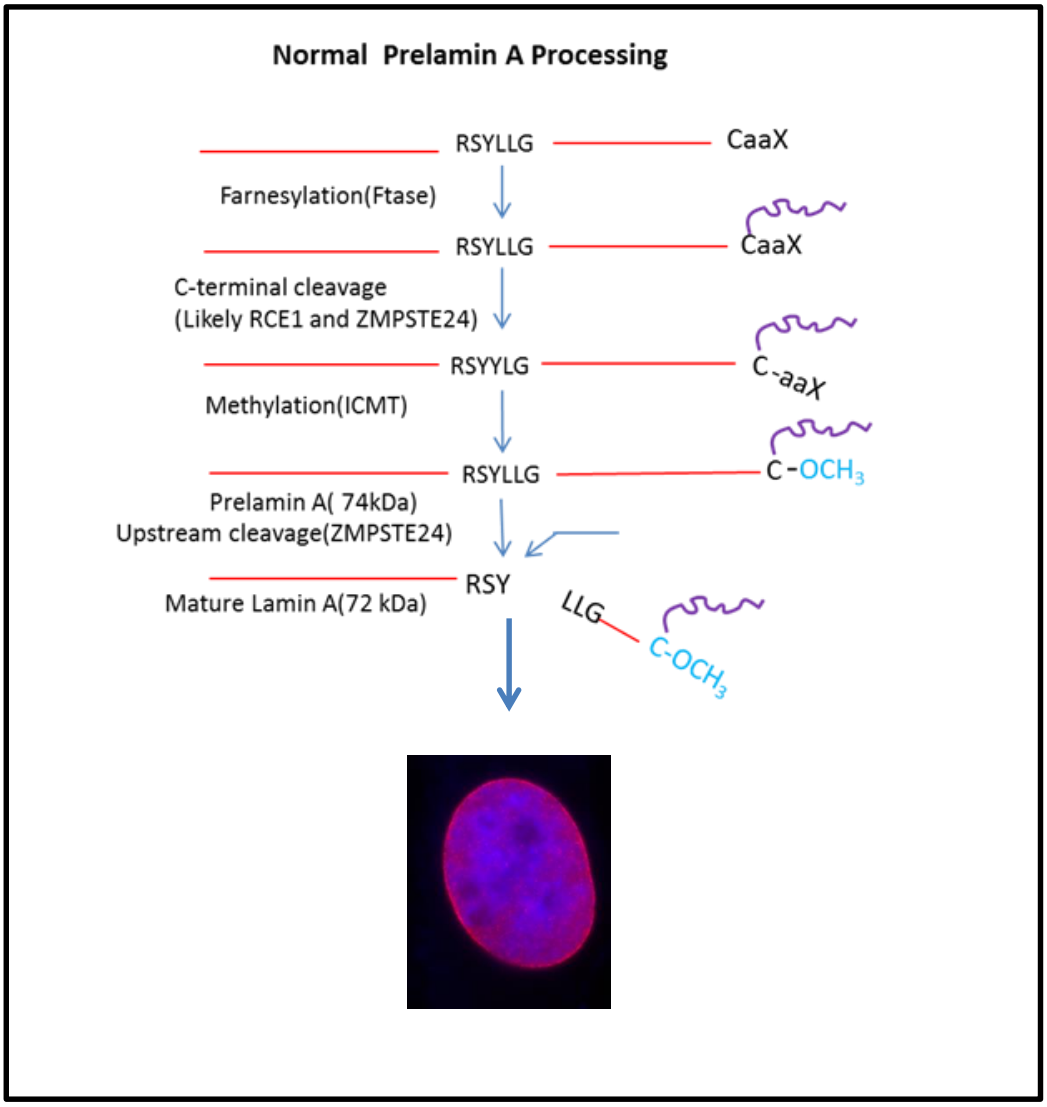

Figure 1.6 Biogenesis of formation of mature Lamin A

Lamin A contains a carboxyl-terminal CAAX box (C is cysteine, A is analiphatic amino acid and X is any amino acid), it is modified by farnesylation. Following farnesylation, the cleavage of the three last amino acids, and methylation of the carboxyl-terminal,an internal proteolytic cleavage takes place removing the last 15 coding amino acids, in order to generate a mature lamin A with 646 amino acids.

1.3.3 The expression of lamin genes

Based on their biochemical and solubility during mitosis, lamins are categorized into A- and B- types (Dechat *et al.*, 2010). In mammals, A-type lamin expression is limited to more differentiated somatic lineages, the lower layer of epidermis. Interestingly, the central nervous system produces little to no lamin A, whereas B-type lamins are constitutively expressed in all cell types both in adults and in embryos (Davidson and Lammerding, 2014; Dreesen *et al.*, 2013a; Jung *et al.*, 2012; Crisp *et al.*, 2005; Goldman *et al*., 2002). Most vertebrates have one A-type lamin and two B-type lamin genes except for *Xenopus*, which has three B-type genes (Tang *et al.*, 2008). The two main isoforms of vertebrate A-type lamins; lamin A and C are encoded by the *LMNA* gene located on chromosome 1q21.2-21.3 and are generated by alternative splicing within exon 10 to produce different isoforms (Worman and Courvalin, 2000; Lin and Worman, 1993). The *LMNA* gene contains 12 exons (Figure 1.7) (Eriksson *et al.*, 2003). Exon 1 codes for the N-terminal head domain and also the initial part of the central rod domain. Exons 7-9 codes for the C-terminal tail domain for lamin A and Lamin C. In exon 7, the nuclear localisation signal (NLS) is located. Exon 10 encompasses a splicing site to produce lamin A and lamin C (Lin and Worman, 1993). The *LMNA* gene encodes four alternatively spliced mRNAs which are translated into the A-type lamin proteins; the predominant isoforms lamin A and lamin C, which differ in the length of their C-terminal tail with lamin A being 74 amino acids longer whereas lamin C has 6 unique C-terminal amino acids (Luo *et al*., 2014). A-type lamins A and C have crucial roles in tissue homeostatis (Eckersley-Maslin *et al.*, 2013; Yang *et al.*, 2013). The less abundant isoform LAΔ10 has 30 amino acid deletion at the C-terminus with exon 10 completely spliced out and so far is found only in a few carcinoma cell lines. Germ

cell specific isoform Lamin C2 is similar to lamin C except that 86 residues at the N-terminus are replaced by six unique residues (Luo *et al*., 2014; Eckersley-Maslin *et al.*, 2013; Yang *et al.*, 2013; Burke and Stewart, 2013; Adam and Goldman, 2012; Vlcek and Foisner, 2007; Foster and Bridger, 2005; Goldman *et al*., 2002; Alsheimer and Benavente, 1996; Furukawa *et al.*, 1994). There are three types of B-type lamins in mammals; lamin B1, B2 and B3 (Gruenbaum and Medalia, 2015). The B-type lamins are encoded separately by *LMNB1* and *LMNB2* genes (Figure 1.8). In humans, *LMNB1* is located on chromosome 5q23.2-q31.3 encodes lamin B1 and *LMNB2* is located on chromosome 19p13.3 encodes lamin B2 (Worman, 2012; Dechat *et al.*, 2008; Lin and Worman, 1997). *LMNB1* contains 11 exons. Exon 1 codes for the N-terminal head domain and the first part of the central rod domain. Exons 2-6 code for the central α- helical rod domain. Exons 7-11 encodes for the C-terminal tail domain of lamin B. In exon 7, the nuclear localisation signal is located. Both lamin B1 and B2 are regulated and expressed in most somatic cells (Reddy and Comai, 2012). On the other hand, Lamin B3 is a small splice variant of lamin B2, encoded by *LMNB2* gene and expression is restricted to spermatogenic cells (Furukawa and Hotta, 1993).

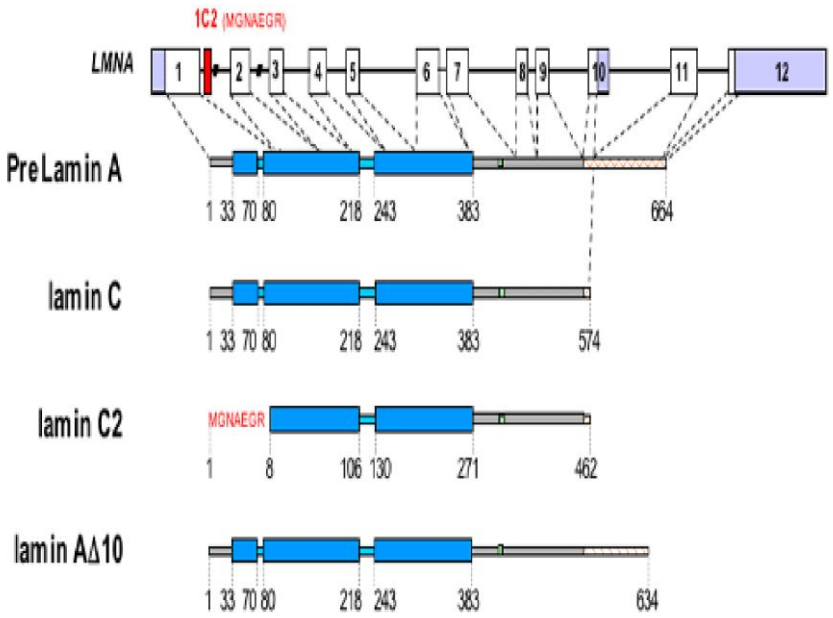

Figure 1.7 A schematic representation of the *LMNA* gene.

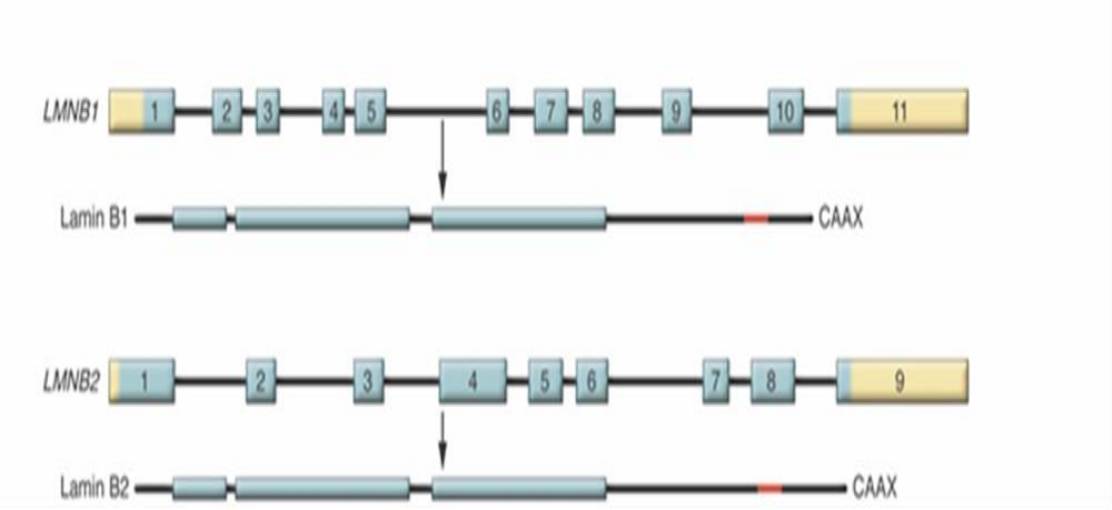

Figure 1.8 The nuclear lamins B1 and B2. *LMNB1* on chromosome 5q23.3–q31.1 encodes lamin B1, and *LMNB2* on chromosome 19p13.3 encodes lamin B2. The nuclear localization signals are located in the C terminal tail domain (indicated in red). Lamin B1 and lamin B2 have carboxyl-terminal CaaX motifs, a signal for protein farnesylation (Worman *et al.*, 2009).

1.3.4 Lamins and Nuclear Functions

More recent data reported roles of lamins both at the NE and in the nuclear interior, based on the identification of novel interaction partners of lamins, including DNA replication, transcription factors, and proteins involved in chromatin organization.

1.3.4.1 Lamins and DNA replication and repair

Metazoan cells comprise ~30,000 replicons, which are spatially and temporally regulated in DNA replication in S-phase (Keller *et al.*, 2002). There are a significant number of studies showing that lamins play an important role in the regulation of this complex process (Dechat *et al.*, 2008; Goldman *et al.,* 2002). The spatial regulation

of replication sites contribute to the replication of specific regions of the genome at precise times of S-phase. For instance, in late S phase in mouse 3T3 cells, it was demonstrated that lamin B1 colocalizes with the replication factor proliferating cell nuclear antigen (PCNA) in replication factories (Moir *et al.,* 1994). In addition, lamin A is associated with sites of early replication in primary fibroblasts (Kennedy *et al.*, 2000a). The lamin binding site for PCNA resides within the highly conserved Ig-fold motif is located in the C terminal of both the lamin A and B (Shumaker *et al.*, 2008). B-type lamins have a significant role in the elongation phase of DNA replication, owing to presence of B-type lamins in intranuclear foci only during S-phase. It is believed that lamins in these foci provide a scaffold needed for assembly of elongation complexes (Moir *et al.*, 1994). The most extensively used kind of extract is that from *Xenopus* oocytes. In this method, extracts contain all the components and DNA is added to them. These extracts contain lamin B3 and smaller amounts of lamins B1 and B2. When compared to control nuclei, assembled DNA replication in *Xenopus* nuclei *in vitro* is hampered by the depletion of lamin B3, which drives the disassembly of the endogenous lamin network (Shumaker *et al.*, 2008; Shumaker *et al.*, 2005; Ellis *et al.*, 1997; Newport *et al.,* 1990). Moreover, in *Xenopus* oocyte extracts, from which lamin B3 had been depleted, addition of the headless nuclear lamin A caused a mislocalization of PCNA and the large subunit of the RFC complex, proteins involved in the elongation phase of replication. Therefore, disruption of nuclear lamin organisation blocks the elongation phase of DNA replication. Furthermore, in the presence of headless lamin A, assembled nuclei were smaller and more fragile compared to control nuclei (Spann *et al.*, 1997). A few studies have demonstrated that nuclear lamins play an essential role in DNA repair as well for example in premature ageing diseases (Gonzalo-Suaraz *et al.,* 2009). It

has been shown in the presence of the HGPS mutant protein, LA50/progerin, DNA repair is defective. For example, the recruitment of the repair factor p53-binding protein (53BP1) to sites of DNA damage is disrupted and the presence of fragmented DNA after irradiation is prolonged in HGPS fibroblasts and in *ZMPSTE24*$^{-/-}$ mouse embryo fibroblasts (MEFs) (Liu *et al.*, 2005). Furthermore, it was shown in *ZMPSTE24*$^{-/-}$ mice that DNA-damaging agents of UV radiation and γ-irradiation caused double strand breaks (DSBs) (Liu *et al.*, 2005). Scaffidi and co-workers have demonstrated that the nuclei of a subpopulation of skin fibroblasts cells obtained from normal old donors, which express an increase in LAΔ50/progerin, showed also a higher percentage of DNA damage than skin fibroblasts from young individuals (Scaffidi and Misteli, 2006).

1.3.4.2 Lamins and Transcription

There are several pieces of experimental evidence that support the view that lamins are involved in transcription (Dittmer and Misteli, 2011). When amino-terminally deleted dominant negative lamins are introduced into nuclei of *Xenopus* embryos, the lamin network is disassembled leading to the synthesis of RNA polymerase II-dependent transcripts being dramatically inhibited. This leads to an impairment of transcription as monitored by a reduction in BrUTP incorporation and also perturbs the localization of the initiation factor TATA-binding protein (Spann *et al.*, 2002; Kumaran *et al.,* 2002). In contrast, the activity of RNA polymerase I or pol III was not found to be inhibited (Spann *et al.*, 2002). Furthermore, silencing of lamin B1 induces a significant inhibition of Pol II transcription in HeLa cells (Shimi *et al.*, 2008). Overexpression of either lamin A or C also leads to a significant reduction in pol II transcription in HeLa cells (Kumaran *et al.*, 2002). Lamins associate with several

transcriptionally active genes. A repressor of collagenase gene, Oct-1 associates with lamin B at the nuclear periphery which appears to be essential for the oxidative stress response in MEFs. When cells become senescent, Oct-1 –gene disassociates from the nuclear periphery leading to a dysregulation of Oct-1 –dependent genes, to a disruption of lamin B1 and to an increase in reactive oxygen species (Malhas *et al.,* 2009; Imai *et al.*, 1997). Lamin A/C associates with numerous transcriptional regulators either directly or indirectly such as; pRB (Zastrow *et al.,* 2004). pRB is involved in the regulation of G1-S transition and silencing E2F/Rb target genes for cell cycle exit (Galderisi *et al.*,2006). Intranuclear lamin A and LAP2α associates with E2F-dependent promoter sequences via binding to Rb, causing hypophosphorylation and therefore reducing E2F-dependent gene expression (Markiewicz *et al.*, 2002). Overexpression of LAP2α caused cell cycle exit and initiation of differentiation, while loss of LAP2α impaired cell cycle arrest (Pekovic *et al.*, 2007). Previous work showed by ChIP and 3D immuno-FISH that LMNA-promoter interaction dynamics upon adipogenic differentiation taking place at the nuclear periphery and in the nuclear interior (e.g., ACTL7A, DNAL4). Furthermore, LMNA-interacting loci with alleles at the nuclear periphery were shown to have alleles in the interior (e.g., DEFA3, SCN10A, TCN1, and ATP5EP2) (Lund *et al.*, 2013).

1.3.5 Intranuclear lamins

Nuclear lamins are not entirely found within the nuclear lamina meshwork lining the inner nuclear membrane, but are also located inside the cell (Moir *et al.,* 1994; Bridger *et al.*, 1993). The structural organization of the nuclear interior is poorly understood. However, with recent advanced techniques it has become increasingly apparent that a fraction of lamins also resides throughout the nuclear interior (Dechat

et al., 2010; Gruenbaum *et al.*, 2005). A few ultrastructural studies suggest presence of lamin filaments or a lamin containing lattice throughout the nuclear interior using indirect immunofluorescence microscopy and analyses of green fluorescent protein (GFP)-tagged lamins in cells (Broers *et al.*, 2005; Bridger *et al.*, 1993). A first genetic proof for the presence of nucleoplasmic lamin was shown in *C. elegans* nuclei, which were partially down regulated for Ce-lamin (Liu *et al.*, 2000). In that study, both peripheral and nucleoplasmic Ce-lamin were down regulated to almost the same extent. Bridger and colleagues (1993) has revealed the presence of lamin foci and filamentous structures within the nucleoplasm of cultured human cells using monoclonal antibodies against the endogenous A-type lamin and these intranuclear lamin A/Cs were most prominent in the G1 phase of the cell cycle and were closely aligned with condensed chromatin (Bridger *et al.*, 1993). Kochin and co-workers (2014) have mapped the phosphorylation sites in lamin A and suggests that phosphorylation at Ser22 and Ser392 in vertebrate lamins A/C, which flank the rod domain from both sides, is involved in solubilizing lamin A in the nucleoplasm (Kochin *et al.*, 2014). Shimi and co-workers have demonstrated that cells transfected with lamin C-GFP had higher intranuclear lamin mobility compared to lamin A-GFP-transfected cells. This finding suggests that lamin C molecules are switched from immobile nuclear complexes into a diffuse nucleoplasmic state. The nucleoplasmic fraction of lamin A but not lamin C had increased mobility in cells with decreased amount of nucleoplasmic lamin B1 (Shimi *et al.*, 2008). Swift and his colleagues (2013) have demonstrated that siRNA was able to knockdown more lamin A compared to lamin C. These findings might indicate that lamin A is less stable and more susceptible to various influences than lamin C (Swift *et al.*, 2013).

In addition to A-type lamins, the presence of a small fraction of B-type lamins was also found to localize in the nuclear interior either in nucleoplasmic foci where its Ig-fold domain interacts (Shumaker *et al.*, 2008; Moir *et al*., 1994). In contrast to nucleoplasmic A-type lamins, there is no soluble fraction of lamin B1 and only small amounts of lamin B2 are present in a soluble fraction of HeLa cells (Moir *et al.*, 2000). Furthermore, in contrast to the mobile nucleoplasmic A-type lamins, B-type lamins residing within the nuclear interior are immobile, similar to those integrated in the nuclear lamina and it is suggested that B-type lamins are associated with more stable structures such as SUN1 (Al-Saaidi and Bross, 2015). Noteworthy, lamin B foci are most prominent during S-phase and do not colocalize with lamin A spots (Stuurman *et al*., 1998). Knock-in mice expressing nonfarnesylated versions of lamin B1 and lamin B2 have shown that mice having nonfarnesylated lamin B2 developed normally and also were free of disease, however mice having nonfarnesylated lamin B1 passed away due to severe neurodevelopmental deficiencies and remarkable nuclear abnormalities in neuronal cells (Jung *et al.*, 2013).

1.3.6 Lamin- interacting proteins

Lamins support a broad range of functions through interactions with a plethora of lamin binding proteins both at the nuclear membrane and/or in the nucleoplasm (Maraldi and Lattanzi, 2005; Schirmer *et al.*, 2003). Proteomic analyses have identified ~80 nuclear envelope transmembrane proteins (NETs) in rat liver and subsequent studies demonstrated that distinct tissues express different set of NETs (Schirmer *et al.*, 2003). It is essential to identify and analyse lamin-binding proteins in order to understand the various cellular functions that are attributed to the nuclear

lamina (Gruenbaum *et al.*, 2005). The nuclear envelope proteins are classified as integral and peripheral proteins. The integral nuclear membrane domains are embedded in both outer nuclear membrane (ONM) and inner nuclear membrane (INM) through transmembrane proteins. The peripheral membrane proteins associate with the lamins forming the nuclear lamina (Schirmer and Gerace, 2005). The vast majority of the transmembrane proteins interact directly or indirectly with lamins and many of them share a common motif of approximately 40 amino acids that folds as two α-helices, known as the LEM domain (Margalit *et al.*, 2005b; Laguri *et al.*, 2001) and this motif was initially detected by Jean-Claude Courvali and its name derives from the INMs; **L**AP2, **E**merin, and **M**an1 (Worman and Courvalin, 2000). The LEM-domain contains a growing family of nuclear proteins including; lamina-associated polypeptides 2 (Berger *et al.*, 1996) and its several isoforms, emerin (Bione *et al.*, 1994), MAN1 (Lin *et al.*, 2000), Lamin B receptor(LBR) (Olins *et al.*, 2010) LEM2, LEM3, several uncharacterized human proteins names; Lem3, Lem4 and Lem5 (Lee and Wilson, 2004). The LEM-domain of all analysed proteins binds a conserved metazoan chromatin associated protein, named Barrier to Autointegration Factor (BAF) (Margalit *et al.*, 2007; Mansharamani and Wilson, 2005). Lamins can also bind chromatin proteins; histone H2A or H2B dimers, kruppel-like protein (MOK2), actin, retinoblastoma (RB) (Gruenbaum *et al.*, 2003). There is a family of large proteins that are proposed to be in NE, mechanically coupling to the nucleoskeleton and cytoskeleton, named 'LINC' (Linker of Nucleoskeleton and Cytoskeleton) complexes (Mejat and Misteli, 2010; Crisp *et al.*, 2005). LINC complexes consist of lamin-binding SUN-domain proteins in the INM that interact in the NE lumen with KASH (Klarsicht, ANC-1, Syne homology) -domain proteins; nesprin 1-α and nesprin-2β (Crisp *et al.*, 2005; Zhang *et al.*, 2005). Lamin-

binding proteins are good candidates for linking heterochromatin to the lamina and are generally characterised by low expression levels, hence the nuclear lamina is considered as an area of transcriptional repression (Guelen *et al.*, 2008; Foster and Bridger, 2005). Furthermore, lamin- binding proteins contribute to nuclear architecture, mechanics also to chromatin organization and signalling (Gruenbaum and Foisner, 2015).

1.3.6.1 BAF

Barrier-to-autointegration factor-1(BAF or BANF1) is a vital component of the lamina and highly conserved double-stranded DNA (dsDNA) binding protein consisting of 89 amino acids and expressed throughout the metazoan kingdom (~9 mM near NE, ~2 mM in nucleoplasm) and furthermore, BAF is essential during embryogenesis (Zhuang *et al.*, 2014; Margalit *et al.*, 2007; Segura-Totten and Wilson, 2004; Holaska *et al.*, 2003; Furukawa *et al.*, 2003; Zheng *et al*., 2000). BAF was initially discovered as a mammalian protein that prevents Moloney murine leukemia virus from integrating into its own genome-autointegration ensuring its integration into host DNA (Lin and Engelman, 2003; Lee and Craigie, 1998). BAF forms helical obligate dimers and each monomer within the dimer possesses two symmetry related DNA binding sites that permit BAF to bind non-specifically to double-stranded DNA by contacting the phosphate backbone of DNA in the minor groove face *in vitro*, allowing it to "bridge" two DNA molecules *in vitro* by creating loops that compact DNA (Skoko *et al.*, 2009; Bradley *et al.*, 2005; Shumaker *et al.*, 2001; Zheng *et al.*, 2000). In viral DNA, DNA bridging by BAF makes it unavailable as a target for integration (Skoko *et al.*, 2009) . Barrier to autointegration factor (BAF) is a fundamental component of the nuclear lamina that binds the LEM domain of the inner nuclear membrane protein

family, lamina associated polypeptide 2β and subsequently shown to bind (LEM) domain of LAP2. BAF also directly binds histones (H3, H4, and certain H1 isoforms) also associates *in vivo* with transcription factors (including Sox2, a master regulator of pluripotency), poly (ADP) ribose polymerase 1 (PARP1) and retinoblastoma binding protein 4 (RBBP4)(Cox *et al.*, 2011; de Oca *et al.*, 2009; Wang *et al.*, 2002). It was demonstrated that when added to cell-free *Xenopus* nuclear assembly reactions, BAF induces higher-order chromatin structure and involved in repression of transcription at specific promoters (Huang *et al.*, 2011; Segura-Totten *et al.*, 2002). BAF plays a substantial role in mitosis to arrange reorganization of the nuclear envelope (Haraguchi *et al.*, 2001). During anaphase, BAF is targeted to chromosomes at “core” regions near the spindle attachment sites of telophase chromosomes (Haraguchi *et al.*, 2001). Lamin A and emerin are recruited to these core regions during reassembly of nuclear envelope (Haraguchi *et al.*, 2001; Dabauvalle *et al.*, 1999). BAF helps bind chromatin to the nuclear envelope (Asencio *et al.*, 2012). In addition, BAF has a critical role in post-mitotic nuclear assembly, cell viability and cell cycle progression (Koch and Holaska, 2014; Furukawa *et al.*, 2003). BAF also influences gene expression at various levels (Shang *et al.*, 2014; Zastrow *et al.*, 2004) For example, by binding it can directly repress gene expression *in vivo* and inhibiting cone-rod homeobox (Crx) and other homeodomain transcription factors *(Puente et al., 2011; Gruenbaum et al., 2005).* BAF seems to have tissue-specific roles, since deletion of BAF in *Caenorhabditis elegans* affect tissue-specific functions, including gonadal cell migration, muscle maintenance and germ-line survival and maturation (Margalit *et al.*, 2007). Due to mutations in BAF that are proposed reduction of protein stability which results in mislocalization of emerin to the cytoplasm cause Nestor-Guillermo progeria syndrome (NGPS) (Puente *et al.*,

2011; Cabanillas *et al.*, 2011). Emerin may also be vital for the DNA damage response as evidence of emerin and BAF association with DNA repair proteins (Cul4a and DDB2) following UV light exposure (de Oca *et al.*, 2009). Van Steensel has revealed that knockdown of BAF significantly increased the contact frequency of several lamina associated domains (LADs) with Lamin B1 (Kind and Van Steensel, 2014). BAF has also been reported to have a role in interphase chromatin organisation and BAF null *Drosphila* displayed aberrant lamina distribution, abnormal nuclear morphology and clumping of chromatin (Margalit *et al.*, 2005a ; Zhuang *et al.*, 2014).

1.3.6.2 Emerin

In 1994, the Emerin gene (*EMD*) was identified by positional cloning of a gene on chromosome Xq28 of X-linked recessive Emery-Dreifuss muscular dystrophy (X-EDMD) (Bione *et al.*, 1994; Emery and Dreifuss, 1966). The emerin gene (*EMD*) consists of six exons and five introns and sequencing demonstrated that it encodes a 254 amino acid type II integral membrane protein with a 220 amino acid hydrophilic N-terminal nucleoplasmic domain, a 23 amino acid C-terminal transmembrane domain and an 11 residue lumenal domain (Koch and Holaska, 2014; Clements *et al.*, 2000; Ellis *et al.*, 1998).

Emerin is a 29 kDa, ubiquitously expressed serine rich protein, principally located at the INM and has been implicated in the regulation of gene expression, cell signaling, and nuclear and genomic architecture in almost every tissue (Huber *et al.*, 2009; Manilal *et al.*, 1996). Newly synthesized emerin in the cytoplasm is inserted into the endoplasmic reticulum (ER) post-translationally and then diffuses through the ER

into the contiguous membranes of the nuclear envelope (Ostlund *et al.*, 2006). Once emerin has reached the inner membrane, emerin is retained and accumulated by binding A-type lamins. Emerin binding to lamins is essential for proper localization to the nuclear envelope, as cells lacking A-type lamins show increased emerin mobility throughout the nuclear envelope and ER (Clements *et al.*, 2000; Manilal *et al.*, 1999; Sullivan *et al.*, 1999; Ostlund *et al.*, 1999). Subpopulations of emerin seem to localize elsewhere, including the NE outer membrane and the plasma membrane (Berk *et al.*, 2013). Emerin has no known secondary structure outside of the LEM-domain and the transmembrane domain. Residues 3–219 mediate the localization of the transmembrane domain of an unrelated protein to the nuclear envelope and deletion of residues 107–175 cause cytosolic aggregation of emerin, which suggest that they are required for emerin's nuclear envelope localization (Tsuchiya *et al.*, 1999). Emerin's functions are masked by collaboration with other nuclear membrane proteins. For example, in *Xenopus* emerin's function overlaps with MAN1 during development of muscle and eye (Reil and Dabauvalle, 2013). Both emerin and LEM-2 are essential for mitotic chromosome segregation, nuclear assembly and embryogenesis in *C. elegans* (Liu et al., 2003), and are required in meiosis for centrosome attachment to the nuclear envelope (Meyerzon *et al.*, 2009). Emerin binds to a number of transcription regulators, including GCL, Btf, Lmo7, catenin, SIKE and regulates the expression of their target genes (Koch and Holaska, 2014). There is accumulating evidence that emerin binds structural components of both the NE proteins; SUN1, SUN2, nesprins and the nucleoskeletal actin (Berk *et al.,* 2013). Furthermore, disruption of telomere anchorage was shown in both carrier and patient X-EDMD (Godwin, 2010).

1.3.6.3 MAN1

MAN1 (also known as LEMD3) is an 82.3 kDa LEM-domain protein located in the inner nuclear membrane encoded by a gene on human chromosome 12q14. MAN1 has two transmembrane domains a nucleoplasmic, N-terminal followed by two hydrophobic segments and a nucleoplasmic, C-terminal tail, MAN1-N and MAN1-C, respectively (Wu *et al.*, 2002; Lin *et al.*, 2000). Indirect evidence suggests that MAN1 interacts with nuclear lamins and emerin, thus playing a role in nuclear organization (Caputo *et al.*, 2006). Protein sequence analysis reveal that MAN1 contains a conserved globular module of approximately 40 amino acids, which has been termed the LEM domain because it is found in LAP2, emerin and MAN1 (Lin *et al.*, 2000; Worman and Courvalin, 2000). In addition to MAN1, the human genome also encodes an uncharacterized homologous protein named LEM2 and three other regions are conserved between human MAN1 and human LEM2 (Mansharamani and Wilson, 2005). MAN1 is part of a protein complex essential for chromatin organization and cell division and which may play a role in sister chromatid separation (Paulin-Levasseur *et al.*, 1996). Furthermore, both MAN1 and emerin can bind to transcription repressors GCL (Holaska *et al.*, 2003). MAN1 is the first lamin-dependent INM protein with a direct role in signal transduction since the binding between the C-terminal domain of MAN1 and receptor-regulated SMAD(R-SMAD) mediate signalling downstream of bone morphogenetic proteins (BMPs) and other members of the TGFβ superfamily (ten Dijke and Hill, 2004).

1.3.6.4 Lamina-associated polypeptide 2(LAP2) family

In 1993, Foisner and his co-workers identified the first member of LAP2 family by means of a monoclonal antibody, which was raised against nuclear envelope fractions of rat liver nuclei and this antibody reacted with a, 55-kDa inner nuclear membrane protein, which was highly enriched in Triton X-100/salt-resistant nuclear lamina fractions and was therefore named Lamina-Associated-Polypeptide (LAP) 2 (Foisner and Gerace, 1993). The LAP2, type II integral membrane proteins are among the best studied lamin-binding proteins and consist of six alternatively spliced LAP2 isoforms, four—LAP2β, -γ, -δ, and -ε— in mice derived from a single gene (Harris *et al.*, 1994). However, only three LAP2 alternatively spliced protein products; LAPα, β, γ have been detected in humans (Harris *et al.*, 1994). LAP2 is polypeptide which is distributed in the inner nuclear membrane and is tightly associated with the nuclear lamina and a large amino-terminal domain of LAP2 which is hydrophilic and exposed to the nucleoplasm (Furukawa *et al.*, 1997). LAP2 specifically binds to B-type lamins and has a direct role in the assembly of the nuclear envelope at the end of mitosis (Furukawa *et al*., 1997). The large nucleoplasmic N-terminus domain of LAP2 includes two non-overlapping nuclear envelope targeting signals and is important for targeting LAP2 to the nuclear envelope. These signals are present in the first half (residues 1-296) and the second half (residues 298-409), respectively (Furukawa *et al*., 1997). The nonmembrane-bound isoform LAP2α is localized throughout the nucleus and has been identified as a specific binding partner of nucleoplasmic A-type lamins (Dechat *et al.*, 2000). Lap2α contains a unique, functionally different C terminus 506 amino acids long and the lamin B-binding

domain in the LAP2β isoform is absent, leading to the prediction that Lap2α have different lamin-binding properties (Dechat *et al.*, 2000).

Lap2α together with lamin A complexes bind directly to pRB and are involved in the pRB activity of E2F/pRB target gene (Wilson and Foisner, 2010). The N-terminal 85 amino acids of LAP2β were found to be sufficient for the interaction with metaphase and anaphase chromosomes. Amino acids 67–137 in LAP2β have been demonstrated to interact with the chromosomal protein BAF (barrier to autointegration factor) by yeast two-hybrid screening (Furukawa, 1999). Furthermore, *in vitro* amino acids 244 to 296 in the nucleoplasmic domain of LAP2β were found to cause nuclear retention of small cytoplasmic proteins and to bind to single- and double strand DNA cellulose (Furukawa *et al*., 1997). Lap2β can bind HA95 which is a chromain protein involved in DNA replication (Dove, 2003; Martins *et al.*, 2003). LAP2β binds a ubiquitous transcriptional regulator that is named as germ cell-less (GCL), which localizes near the INM of the nuclear envelope (Nili *et al.*, 2001).

1.3.6.5 Lamin B receptor (LBR)

LBR, a 58 kDa protein, also known as p58, is an evolutionary conserved and developmentally essential integral membrane protein of the interphase nuclear envelope interacting with chromatin and was initially characterized by virtue of its ability to associate with nuclear lamin B (Olins *et al.*, 2010; Wagner *et al.*, 2004; Worman *et al.*, 1988). Human LBR contains 615 amino acids and harbours two significant domains; a hydrophilic N-terminal domain is 208 amino acids, localized in the nucleoplasm which is interacting with the lamina and the displays consensus phosphorylation sites for CDK1 (Shaklai *et al.*, 2007). The C-terminal contains 407

aa with eight predicted transmembrane segments, localized in the nuclear membrane of nuclear envelope (Worman *et al.*, 1990; Courvalin *et al.*, 1990).The N-terminus of human LBR which is predicted to harbour a Tudor domain (LBR-TD) is capable of binding to heterochromatin protein 1 alpha(HP1α),methyl-CpG-binding protein MeCP2 and B-type lamins (Liokatis *et al.*, 2012; Hirano, 2012). On the other hand, the C-terminus is involved in the conversion of 7-dehydrocholestrol to cholesterol (Silve *et al.*, 1998). LBR kinase phosphorylates serine residues of the RS-rich region of avian LBR (Nikolakaki *et al.*, 1996) . The expression of both Lamin A/C and LBR in neuronal nuclei is temporarily coordinated in the developing retina in mice. First, retinal neurons only express LBR and then LamA/C appears and replaces LBR 10–14 days after the birth of the respective neuronal cell type. Furthermore, absence of both proteins in postmitotic cells in the eye results in inversion of the nuclear architecture with heterochromatin relocalizing from the nuclear envelope to nuclear interior (Solovei *et al.*, 2013). LBR and lamin A/C expression in diverse cell types suggests that peripheral heterochromatin tethers regulate differentiation in a broad range of tissues or perhaps in all cell types (Solovei *et al.*, 2013). Comparison of $Lbr^{-/-}$, $Lmna^{-/-}$, and WT myoblast transcriptomes revealed that a sequential temporal usage of LBR and Lamin A/C tethers during development correlates with their opposite effects on a decrease and increase of the transcription of muscle specific genes (Solovei *et al.*, 2013). Heterozygous mutations in LBR are known to cause human Pelger- Huët anomaly which is characterized by abnormal nuclear shape and chromatin organisation in blood granulocytes (Hoffmann *et al.*, 2002). However, homozygous mutations correlate with developmental delay, skeletal abnormalities and abnormal sterol metabolism (Hoffmann *et al.*, 2007).

1.3.6.6 LINC Complexes

As early as 1982, mechanical links between the plasma membrane and nucleus were suggested and subsequently supported by research in which mechanical force applied to the cell surface caused structural reorganization inside the nucleus (Bissell *et al*., 1982). This connection was discovered when intermediate filament, microtubules and cytoskeletal filaments were revealed to be specifically attached at the nuclear envelope by different types of LINC complexes, which mechanically couple the nucleoskeleton and cytoskeleton (Meinke, 2015; Mejat and Misteli, 2010; Crisp *et al.*, 2005). The fundamental unit of LINC complexes comprise of lamin-binding SUN (Sad1 and UNC-84)-domain containing proteins (encoded by human genes *SUN1, SUN2* and *SUN3)* located in the INM that interact in the NE lumen with KASH (Klarsicht, ANC-1 and SYNE homology)-domain containing nesprins (nuclear envelope spectrin- repeat proteins; encoded by human genes spectrin repeat-containing nuclear envelope 1 (*SYNE1*), *SYNE2*, *nesprin -3* and *nesprin -4*) anchored in the ONM (Figure 1.9)(Mellad *et al*., 2011; Mejat and Misteli, 2010; Padmakumar *et al.*, 2005; Crisp *et al.*, 2005). Mammalian SUN1 and SUN2 proteins were first characterized by bioinformatics analysis as homologues of *C. elegans* UNC-84 and later confirmed in screens for NE components (Malone *et al.*, 1999). The name SUN was based on *S.pombe* Sad1 and *D. Melanogaster* and each have two *SUN* genes: *UNC84* and germ-cell specific *matefin/SUN1* in *C.elegans* and *Klaroid* respectively and *CG6589* in *Drosophila* (Starr, 2009). To date, in mammals several SUN genes have been identified; *SUN1*, *SUN2* and testis-specific genes; *SUN3, SPAG4* and *SPAG4L* (Table 1.1) (Starr, 2009; Starr and Fischer, 2005).

SUN1 and SUN2 are widely expressed, while SUN3 expression is restricted to testes and it is localized in the ER. The expression of SPAG4 protein is restricted to spermatids, pancreas and testes (Shao *et al.*, 1999). Both SUN1 and SUN2 contain three transmembrane domains localized in the INM and with their C-terminal SUN domain crossing the periplasmic space between the INM and ONM. In addition, they also have a coiled-coil domains that mediates to form SUN1 and SUN2 homo- and heterodimers and is involved in binding the KASH domain, whereas their exposed nucleoplasmic N-terminal can interact directly with A-type lamins (Starr, 2009; Tzur *et al.*, 2006; Haque *et al.*, 2006). Nesprins or NUANCE are prototypical ONM components of the LINC complexes, constitute a large family of spectrin repeat (SR) transmemrane proteins. By alternative splicing and transcription initiation of four independent genes, multiple nesprin isoforms are produced (Warren *et al.*, 2005; Zhen *et al.*, 2002). In mammals, the *Nesprin-1 and -2* genes are alternatively spliced in order to produce more than 12 protein isoforms and some isoforms lack the KASH domain and are not membrane localized, however other are localized at the INM (Starr and Fischer, 2005). Sun1 and Sun2 can bind directly to emerin. Indeed, in skin fibroblasts emerin is required to localize the nesprin-2 giant at the ONM (Randles *et al.*, 2010). Spectrin repeat domains in INM-localized isoform nesprin-1α are capable to mediate binding to lamins, emerin and other nesprin-1α molecules (Mislow *et al.*, 2002). Nesprin-1 and 2 are the largest isoforms and can bind actin, whereas nesprin-3 binds plectin that binds cytoplasmic intermediate filament and finally nesprin-4 binds kinesin 1, which is a plus-end-directed microtubule-dependent motor, and is likely to involve in delocalization the Golgi membranes and centrosome away from the nucleus in epithelial cells (Roux *et al.*, 2009).

"LINC" complexes facilitate the regulated, cytoplasmic-motor protein-driven movement of the entire nucleus to different position in the cell and the movement of the entire nuclear envelope-attached chromosomes to new locations (Kracklauer *et al.,* 2013; Starr, 2009; Crisp *et al.*, 2005) and different combinations of SUN- and KASH-domain proteins mediate distinct functions (Luke *et al.*, 2008) such as the stiffness of the cytoskeleton (Stewart-Hutchinson *et al.*, 2008). In *C. elegans,* in order to recruit the proapoptotic protein CED-4 death signalling to the nuclear envelope SUN-domain protein matefin/SUN1 is required (Tzur *et al.,* 2006).

Deletions in the *nesprin-1* or *nesprin-2* genes were shown to destroy endogenous LINC complexes causing failure of nuclei to cluster at neuromuscular junctions and can result in muscular dystrophy in mice (Puckelwartz *et al.*, 2009). Meiotic chromosome clustering and homologous recognition requires both matefin/SUN1 and ZYG-12 for chromosome organization as in matefin/SUN1 mutant strain of *C. elegans* chromosome reorganization is disrupted in early meiosis (Woglar *et al.*, 2013; Penkner *et al.*, 2007). Mammalian SUN1 and SUN2 are associated with telomeres between the leptotene and diplotene stages of meiosis and it was revealed that SUN-1 knockout mice have both impaired homologous pairing and impaired NE-telomere association (Ding *et al.*, 2007). Mammalian SUN proteins do not depend upon A-type lamins in meiosis, whereas in *C. elegans* the nuclear migration and nuclear anchoring functions of LINC complexes require B-type lamins (Lee *et al.*, 2002). However, it is important to note that *S.pombe and S. cerevesia* do not have lamins, whereas SUN- and KASH- dependent pathway exist (Starr, 2009). Horn and colleagues reported that both nesprin-4 and SUN-1 are expressed in mechanosensory hair cells and they play a significant role in the basal positioning of

outer hair cells nuclei and also are essential for the maintenance of cell viability. Moreover, from their experiments, they found that mice deficient in SUN1 displayed loss of nesprin-4 from the NE of hair cells and therefore showed a pattern of hearing loss, similar to *Nesp4* $^{-/-}$ mice (Horn *et al.*, 2013).

Table 1.1 Functions of SUN and KASH proteins (Starr, 2009).

SUN proteins	Characteristics and function(s) at the INM	References
Mammals		
Sun1	Telomere attachment in meiosis and gametogenesis; nuclear-envelope integrity; recruit KASH proteins	(Crisp *et al*., 2006; *Ding et al*., 2007; Haque *et al*., 2006;Padmakumar *et al.,* 2005)
Sun2	Nuclear-envelope integrity; recruit KASH proteins	(Crisp *et al.,* 2006; Hodzic *et al.,* 2004)
Sun3	Testis specific; ER localized; unknown function	(Crisp *et al.*, 2006)
Spag4	Testis specific; not at nuclear envelope; unknown function	(Shao *et al.*, 1999)
C. elegans		
UNC-84	Nuclear positioning; recruit ANC-1 and UNC-83 in somatic cells	(Malone *et al*., 1999; Starr and Han, 2002; Starr *et al.,* 2001)
SUN-1 (matefin)	Centrosome attachment; apoptosis; chromosome pairing in meiosis; recruit ZYG-12 and CED-4	(Malone et al., 2003; Penkner et al., 2007; Tzur *et al.,* 2006)
D. melanogaster		
Klaroid	Recruit Klarsicht in eye disc; nuclear migration in eye disc	(Kracklauer *et al.*, 2007)
CG6589	Unknown	(Kracklauer *et al.*, 2007)
Dictyostelium		
Sun-1	Centrosome attachment; genome stability	(Xiong *et al*., 2008)
S. pombe		
Sad1	Spindle architecture; recruit Kms1	(Chikashige *et al*., 2006; Hagan and Yanmagida, 1995)
S. cerevisiae		

Mps3	SPB duplication; attachment of telomeres to nuclear envelope; recruit Csm4	(Conrad *et al.,* 2008; Jaspersen *et al.,* 2006; Koszul *et al*., 2008)
KASH proteins	Known function(s) at the ONM	References
Mammals		
1) Syne-1 (Nesprin-1)	Anchorage of nuclei to actin filaments	(Apel *et al*., 2000; Zhang *et al.,* 2001; Zhang *et al.,* 2007)
2)Syne-2 (Nesprin-2)	Anchorage of nuclei to actin filaments	(Apel *et al.,* 2000; Zhang *et al*., 2007; Zhen *et al*., 2002)
Nesprin-3	Intermediate-filament interactions with the nucleus	(Ketema *et al.,* 2007; Wilhelmsen *et al*., 2005)
Nesprin-4	Unknown; endocrine specific	(Crisp and Burke, 2008)
C. elegans		
ANC-1	Anchorage of nuclei to actin filaments	(Starr and Han, 2002)
UNC-83	Nuclear migration	(McGee *et al*., 2006; Starr *et al*., 2001)
ZYG-12	Attachment of centrosomes to nuclei	(Malone *et al*., 2003)
D. melanogaster		
Klarsicht	Nuclear migration and centrosome attachment	(Mosley-Bishop *et al.,* 1999; Patterson *et al*., 2004)
MSP-300	Muscle development (?); nuclear anchorage (?)	(Rosenberg-Hasson *et al.,* 1996; Technau and Roth, 2008; Xie and Fischer, 2008; Yu *et al.,* 2006)
S. pombe		
Kms1	Meiotic chromosome movement and pairing via dynein	(Chikashige *et al.,* 2006; Miki *et al*., 2004)
Kms2	Meiotic and mitotic chromosome movement	(Chikashige *et al.,* 2006; King *et al.,* 2008; Miki *et al.,* 2004)
S. cerevisiae		
Csm4	Meiotic actin-driven telomere movements and pairing	(Conrad *et al.*, 2008; Koszul *et al.,* 2008)

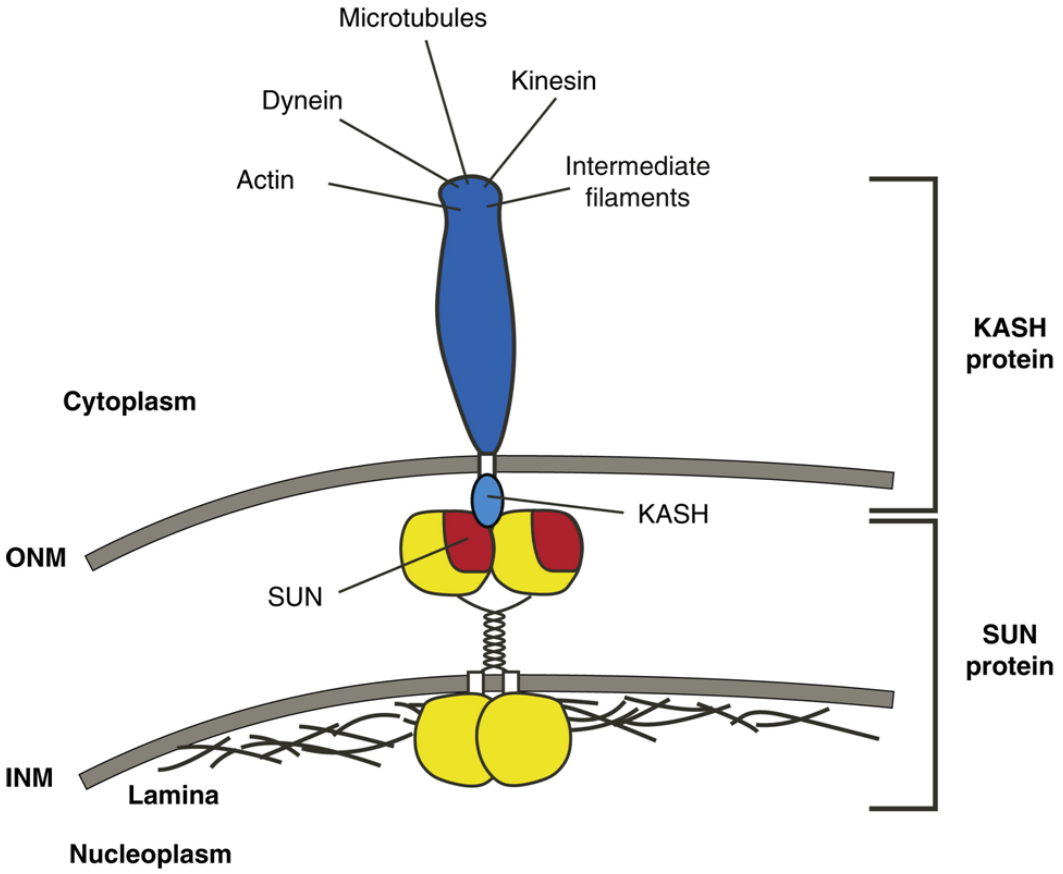

Figure 1.9 SUN proteins represented by yellow and red colours as a dimer span the inner nuclear membrane (INM). KASH proteins represented by blue span the outer nuclear membrane (ONM). The cytoplasmic domains of KASH proteins interact with a variety of cytoskeletal components. The nucleoplasmic domains of SUN proteins interact with lamins or other structural components of the nucleus. SUN proteins interact with the KASH domain in the perinuclear space in order to form the central link of a bridge that spans the nuclear envelope, connecting the cytoskeleton to the nucleoskeleton (Starr, 2011).

1.4 Higher Order Chromatin Organisation

1.4.1 Euchromatin and heterochromarin

It is becoming increasingly evident that the eukaryotic cell nucleus is a highly complex organelle in eukaryotes and accommodates much of the genome and the machinery for its replication, temporal control of gene expression, maintenance and DNA repair (Bourne *et al.*, 2013; Bridger *et al.*, 2007; Branco and Pombo, 2006; Parada and Misteli, 2002). The human cell nucleus is ~10 μm in diameter and contains 22 pairs of autosomes and a pair of sex chromosomes consisting of ~ 2 m of DNA in total (Sun *et al.,* 2000). For more than a century, scientists have been investigating the organization of the nucleus (de Wit and de Laat, 2012). The major chromatin domains are morphologically defined as; euchromatin and heterochromatin (Tamaru, 2010). Heterochromatin appears highly condensed, and brightly stained as the cell makes the transition from metaphase to interphase, whereas, euchromatin is less condensed, gene-rich and decondenses during interphase (Huisinga *et al*., 2006; Hsu, 1962; Heitz, 1928). In the eukaryotic cell nucleus, DNA exists with histone proteins. 147 base pairs (bp) of DNA are wrapped in 1.7 negatively supercoiled turns around the nucleosome core particle consisting of two H3-H4 and two H2A–H2B histone dimers (Woodcock, 2006; Luger *et al.*, 1997). 10–80 bp linker DNA associated with linker histone H1 separates nucleosomes from each other and these portions of genomes are typically gene-poor, however not devoid of genes (Grewal and Elgin, 2002). Heterochromatin and euchromatin have distinct nucleosome modifications (Tamaru, 2010), with heterochromatin characterized by hypoacetylation of histones, H3K9me, association with heterochromatin protein-1(HP1), and DNA cytosine methylation (5mC)(Suzuki and Bird, 2008; Richards and Elgin, 2002; Jenuwein and Allis, 2001; Bannister *et al.*,

2001; Rea *et al.*, 2000; Tschiersch *et al.*, 1994). Whereas euchromatin is typically enriched in acetylated histones H3, H4 and H3K4 methylation (Noma *et al.,* 2001; Grunstein, 1998). Pericentromeric and telomeric sequences are predominantly repetitive DNA sequences, as are satellite sequences and transposable elements, and are the main targets for heterochromatin formation (Schoeftner and Blasco, 2009; Slotkin and Martienssen, 2007). Heterochromatin Protein 1 (HP1) was first identified (James *et al.*, 1989) in a screen with monoclonal antibodies as a protein primarily concentrated in the pericentric heterochromatin and is now known that H3K9me3 marks deposited by the histone methyltransferase, Su(var)3-9, are responsible for recruiting this protein to heterochromatin (Lachner *et al.*, 2001). HP1 is highly conserved from *S.pombe* (Swi6p) to *Homo sapiens (*HP1α, HP1β, and HP1γ) (Eissenberg and Elgin, 2000). In *Drosphila* and mouse, Classical PEV (position-effect variegation), which can encompass genes that are hundreds of kilobases from the heterochromatin/euchromatin boundary occurs when a gene is juxtaposed to heterochromatin and sites buried within repeats could initiate the propagation of a heterochromatic state (Saksouk *et al.*, 2015; Dimitri and Junakovic, 1999). In addition, HP-1 was found at sites of the transposon arrays in polytene chromosomes (Fanti *et al.*, 1998). Although artificially tethered HP1 was shown to silence a transgene without histone methylation and Su (var)3-9 in *Drosophila*, Suv4-20h in human cells it was revealed that repression corresponded to methylation of the targeted region (Li *et al.*, 2003).

1.5 Genome organisation in the interphase nucleus

In mitosis, chromatin becomes tightly packaged and each individual chromosome becomes visible as discrete entities known as chromosome territories (Figure 1.10) (Cremer and Cremer, 2006). The organization of interphase chromosome territories (CT) was first described by Karl Rabl (C and Z, 1885) and Boveri (Boveri, 1909) based on their studies of plants with large genomes and Salamander. In 1974, evidence for the territorial organisation was discovered by Thomas and Christopher Cremer demonstrating the existence of CT in the interphase of nuclei of Chinese Hamster Ovary (CHO) cells by laser UV microbeam irradiation of the chromosomes (Cremer *et al.,* 1974). Cremer et al. demonstrated that UV microbeam induced DNA repair in only a few chromosomes, suggesting that induced chromosomes may not entirely undergo decondensation following mitosis (Cremer *et al.,* 1974). In the following years, the presence of chromosome territories was confirmed using fluorescence in situ hybridisation techniques employing fluorescently labelled chromosome paints and the territorial organisation of chromosomes became accepted scientific dogma (Lichter *et al.*, 1988). Integration of fluoresecenlty tagged nucleotides into chromatin have been used and indicating that chromosomes have their own individual areas (Edelmann *et al.*, 2001; Visser and Aten, 1999; Zink *et al.*, 1998). In 1999, Bickmore and co-workers determined that chromosomes were radially organised in interphase nuclei of fibroblasts and lymphocytes (Croft *et al.*, 1999; Bridger *et al.*, 1999) and moreover, they discovered that there is a strong link between the gene density of a chromosome and its radial location within interphase nuclei (Gilbert *et al.,* 2004; Bridger and Bickmore, 1998). Interestingly, most chromosomes appeared to have mainly conserved positions between the two cell

types but conversely, several chromosomes demonstrated different positioning (Cremer *et al.*, 2003).

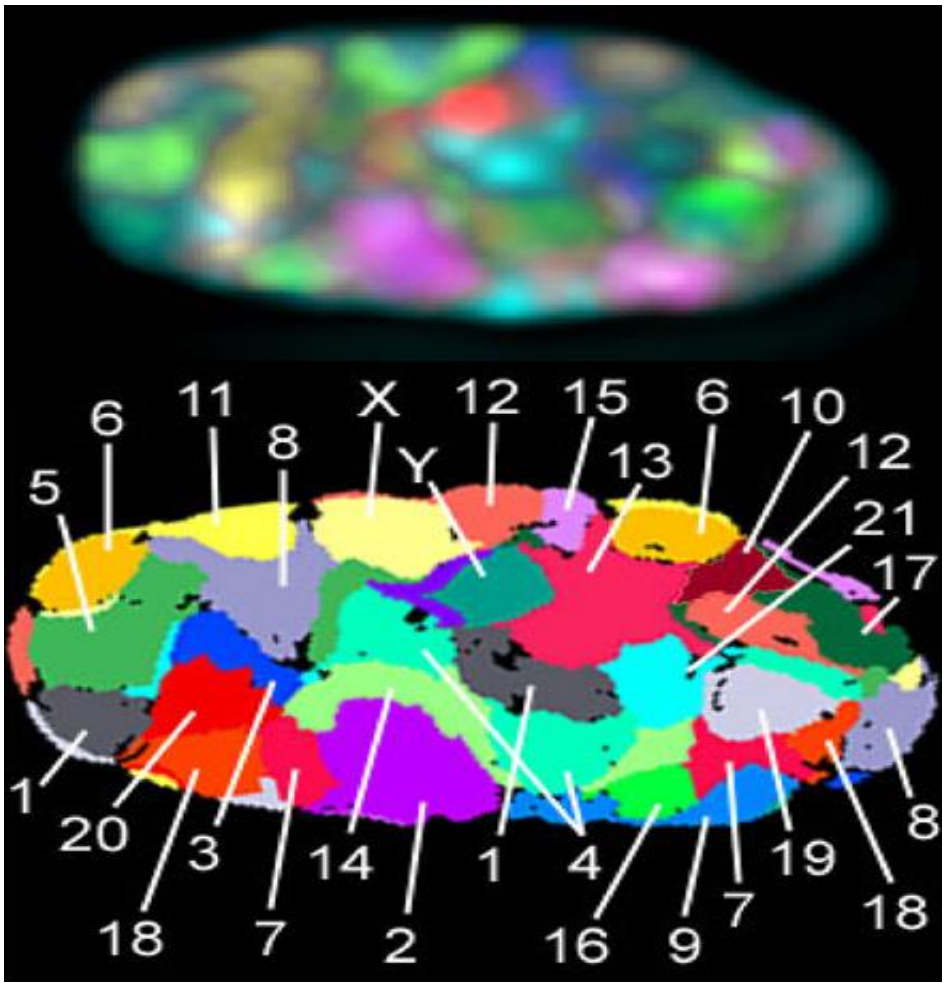

Figure 1.10 Demonstrates false colour representation of the 23 human chromosomes in interphase nuclei occupying specific territories during prometaphase in 3D M-FISH presented fibroblast cells (Bolzer *et al.*, 2005)

.

1.5.1 Interphase chromosome position gene-density theory

According to the gene-density theory, chromosomes are dispersed radially within the nuclear environment according to the density of genes on a chromosome (Figure 1.11) (Croft *et al.*, 1999). Firstly, CT were assessed for the different nuclear positioning of two similarly sized human chromosomes; 18 and 19 in proliferating human dermal fibroblasts and lymphoblasts. Chromosomes HSA18 and HSA19 represent two extremes of the human genome. There are a number of reasons why these two chromosomes make for interesting comparisons: the DNA contents of chromosomes; HSA18 and HSA19 are quite similar, 86 and 72 Mb, respectively (Lander *et al.*, 2001; Morton, 1991), nevertheless their gene densities and replication timing are significantly different: HSA19 is the human chromosome with the highest gene-density carrying a predicted number of 1930 genes (26.8 per Mb). It comprises mostly of early replicating chromatin and has a high number of CpG islands with 43 per Mb compared with an average number of 10.5 per Mb in the human genome and repeats of the Alu family (Craig and Bickmore, 1994; Korenberg and Rykowski, 1988). In addition, replication of most of its DNA starts in the early part of S phase (Dutrillaux *et al.*, 1976). On the contrary, HSA18 has fewer gene assignments (Cross *et al.*, 1997), a low CpG island density and high proportion of late replicating chromatin (Lander *et al.*, 2001). After (2D) and three dimensional (3D) fluorescence in situ hybridisation (FISH), it was revealed that human chromosome 19 was located in a more internal region of the nucleus compared with human chromosome 18 which was located close to the nuclear edge lamina in cells (Croft *et al.*, 1999). Furthermore, Bickmore and colleagues reported that several chromosomes were organised quite differently in senescent and quiescent conditions (Bridger *et al.*, 1999). Under serum-starved conditions, HSA18 territories moved from the nuclear

periphery to a more central position when fibroblasts exit the cell cycle and enter G_0. Under normal culture conditions, this phenomenon was shown to be reversible when fibroblasts re-entered the cell cycle (Bridger *et al.*, 1999). Whereas, chromosomes 4 and X known as larger chromosomes did not alter their position and remained at the nuclear edge in quiescent and senescent cells (Meaburn *et al.*, 2005). In addition to fibroblasts cells, Bickmore and co-workers showed that gene-density theory of chromosome positioning in nuclei applied to chromosome positioning in lymphoblasts and dermal fibroblasts for all chromosomes (Boyle *et al.*, 2001). In CT positioning analysis using 3D-FISH, confocal laser scanning, and 3D-reconstruction of nuclei indicated that HSA19 territories did not reveal any visible contact with the nuclear lamina which is in full agreement with the findings reported by Bickmore and colleagues (Tanabe *et al.*, 2002). On the contrary, HSA18 and HSA19 territories were positioned towards the two-dimensional (2D) the nuclear centre in the rather flat-elliptically shaped nuclei of proliferating amniotic fluid cells (Cremer *et al.*, 2001). After comparative gene mapping, it was revealed that both HSA18 CTs and the chicken homologous CTs of GGA 2 and Z gene-poor chromosomes found at the nuclear periphery, whereas both HSA19 CTs and the chicken homologous the gene-rich microchromosome compartment of GGA 11, 28, and E25C31 found located towards the centre of the cell nucleus (Tanabe *et al.*, 2002; Habermann *et al.*, 2001). Furthermore, investigation of four lymphoblastoid cell lines from three species of Old World monkeys by three-dimensional FISH demonstrated that CT homologous to HSA 18 were located preferentially close to the nuclear edge, however gene-dense human 19 homologous CTs were oriented towards the nuclear centre (Tanabe *et al.*, 2005). The experimental findings of the gene-density-correlated positioning of human 18 and 19 homologous CTs is evolutionarily conserved in vertebrates from

chicken to human over a period of more than 300 million years despite major evolutionary chromosome rearrangements. This remarkable conservation of gene-density-related positioning contributes further support for functionally relevant higher-order chromatin architecture (Tanabe *et al.*, 2005; Tanabe *et al.*, 2002). It is believed that gene-poor chromosomes may be positioned more peripherally than those that are gene rich because they are more transciptionally inactive (Casolari *et al.*, 2004).

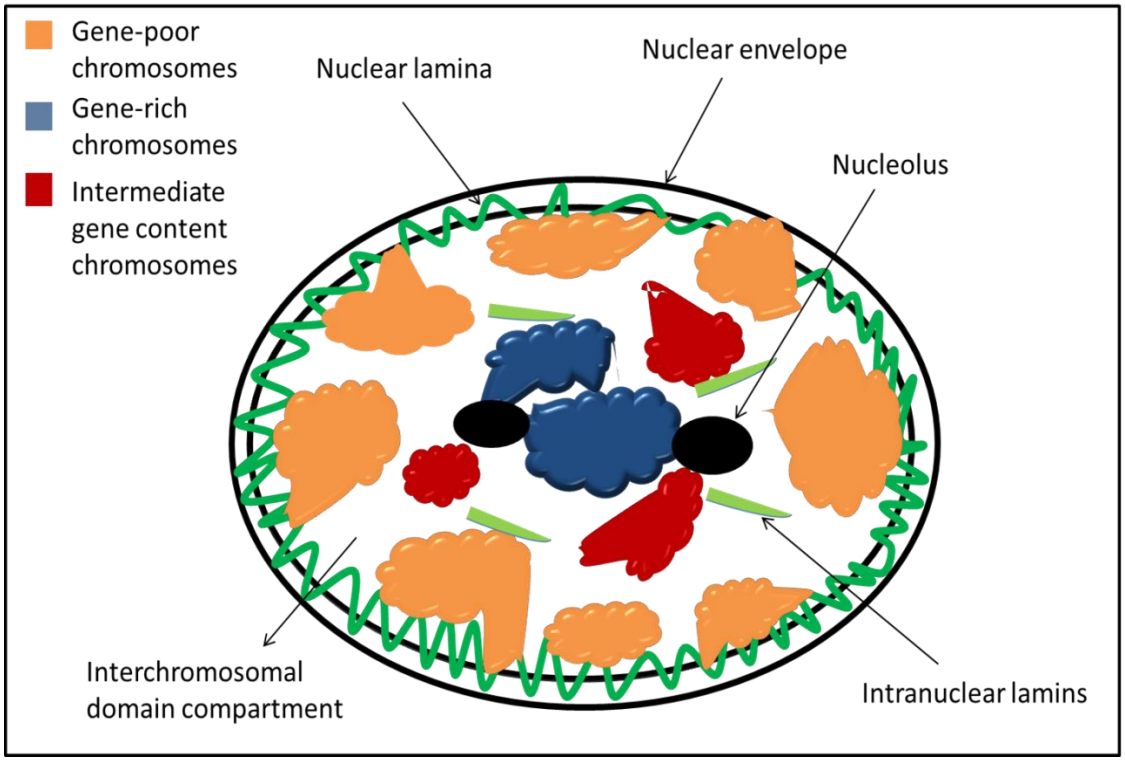

Figure 1.11 Cartoon showing gene density based distribution of chromosome territories in an interphase nucleus.

Nuclear envelope is represented by black double line. Gene-poor chromosomes (orange) are preferentially positioned at the nuclear periphery and in close-contact with the nuclear lamina (Green). Gene-rich chromosomes (blue) are located towards the nuclear interior. The chromosomes with intermediate gene content (red) are preferentially positioned between the gene-rich and gene-poor chromosomes. Interchromosomal domain compartments are where most transcription is believed to occur. Intranuclear lamins (green) can be seen residing throughout the nuclear interior.

1.5.2 The Link between Interphase Chromosome Location and Gene Expression

The nuclear location of a chromosome and/or gene plays a role in regulating specific gene expression (Bickmore, 2013; Malyavanthama *et al.*, 2010; Malyavantham *et al.*, 2008). For example, when resting human lymphocytes are activated by phytohemagglutinin, changes result in the intraorganization of chromosome territories, both in the degree of intermingling between territories and in their volume. More importantly, however, the radial positioning of the chromosome territories is changed. This alteration has been postulated to be a response to an altered transcriptional program (Branco *et al.*, 2008). Furthermore, during *ex vivo* stem cell differentiation into adipocytes, the radial position of important genes involved in adipogenesis altered dramatically, with genes that become switched on moving from the nuclear periphery toward the nuclear interior and back again when switched off. Control genes in this system that were either on or off did not respond to the adipogenic growth factors and did not change location (Szczerbal *et al.*, 2009). In this differentiation system, there was little whole chromosome movement, but genes were looped out from chromosomes into the nuclear interior to associate with the nuclear structure SC35 speckles (Szczerbal and Bridger, 2010). Other studies have gone further, to identify where in the nucleus and to what nuclear structures the genes are targeted. Genes have been found to relocate to structures associated with active transcription and processing of RNA. Indeed, the activation of gene loci can involve a repositioning of genes toward areas of the nucleus where RNA polymerase II molecules aggregate into superstructures called transcription factories (Osborne *et al.*, 2007). Other studies have shown genes becoming associated with other

structures. For example, Dundr et al. inserted an artificial U2 snRNA array into the genome of cells and demonstrated that the array moved toward a stably positioned Cajal body for transcription through long-range chromosomal relocation. This movement was inhibited by an actin inhibitor, implying the involvement of actin in interphase chromosome repositioning (Dundr *et al.*, 2007). Other studies have shown genes increasingly associated with SC35 domains upon upregulation (Szczerbal and Bridger, 2010; Brown *et al.*, 2008). Most excitingly recent 3C (Ferraiuolo *et al.*, 2010) and 4C conformation capture experiments have shown that actively transcribing Hox genes in a cluster are associated with a nuclear compartment for active transcription and that the nontranscribing genes are all located at a region where gene silencing occurs (Noordermeer *et al.*, 2011). When the silenced genes become activated, they then co-compartmentalize with the other active Hox genes. This strict co-compartmentalization of genes explains the strict co-linearity rules associated with the Hox gene clusters where position in the cluster is correlated with the expression zone down the developing embryo. The three-dimensional (3D) structure of the chromosomes within the territories also plays a major role in the control of gene expression. Regions of the chromosomes interact with other regions of the same chromosome, in *cis.* For example, the locus control region (LCR) of the β-globin gene cluster acts as an enhancer of the β-globin genes, although it is more than 50 kb away. However, the LCR is in close physical proximity to an actively transcribed HBB gene, suggesting a direct regulatory interaction (Carter *et al.*, 2002; Tolhuis *et al.*, 2002). This looping in 3D forms an active chromatin hub (ACH) for control of the expression of the β-globin genes (de Laat and Grosveld, 2003) which dynamically associate with the LCR (Gribnau *et al.*, 1998).

1.5.3 Telomere structure and function

Telomeres are highly specialized nucleoprotein structures which are located at the end of linear chromosomes of eukaryotes and some prokaryotes to maintain chromosome stability (Cech, 2004; Blackburn, 2001; Blackburn, 1992). Telomeres are responsible to protect the chromosomes against the loss of genetic material, fusion of fragments of chromosomes and unwanted repair (Blackburn, Greider and Szostak, 2006; Wong and Slijepcevic, 2004). Furthermore, during mitosis and meiosis telomeres play a substantial role in genome segregation. Telomeric DNA is not a linear structure and a T (telomeric)-loop is formed by a number of telomere-associated proteins and a single stranded part of telomeric DNA (Hohensinner, Goronzy and Weyand, 2011; Griffith *et al.*, 1999). In mammalian cells, telomere-associated proteins are; TRF1, TRF2, Rap1, POT1, TIN1 and TIN2 which are known as protective shelterin complex and can directly or indirectly bind telomeric DNA to maintain the T-loop structure by capping the telomeres (Galati *et al.*, 2015; Palm and de Lange, 2008; Liu *et al.*, 2004). Shelterin-associated proteins are known as TNKS1, TNKS2, SMG6, and TEP1 can affect chromosome end integrity and dynamics (Salhab *et al.*, 2008). Formation of the T-loop stops the telomere end from being recognized as a Double Strand Breaks (DSBs) DNA by the DNA repair machinery thus avoiding DNA damage response activation. Genetic and other factors strongly influence telomere length (Allsopp *et al*., 1992; Blackburn, 2000). In normal human somatic cells a small part of telomeric DNA is lost in each successive cell division due to the polymerases enzymes involved in copying DNA can not complete DNA replication, known as the end replication problem (Olovnikov, 1971). When telomeres become critically short, the protective function of telomeres is affected and thus DNA damage response is activated leading inhibition of cell

proliferation referred as cell senescence (O'Sullivan *et al.*, 2002). Different to human somatic cells which have low telomerase activity, human stem cells (HSCs), germ cells and cancer cells are exceptional human cell types that maintain telomere length through expression of telomerase enzyme while continuing to divide (Tian *et al*., 2010; Ingram *et al.*, 2004; Bodnar *et al.*, 1997). In 1985, Carol Greider and Elizabeth Blackburn discovered telomerase, a ribonucleoprotein reverse transcriptase which was firstly isolated from *Tetrahymena thermophilia* extracts (Greider and Blackburn, 1989). Subsequently, human telomerase was isolated from cancer cells indicating that telomerase is required for proliferation of cells towards malignancy (Aubert and Lansdorp, 2008; Hastie *et al.*, 1990). Telomerase is a multi-subunit holoenzyme that consists of three components: the unique catalytic reverse transcriptase unit (hTERT in humans), the RNA template (hTERC in humans) and accessory protein of the nucleolar phosphoprotein dyskerin (Cohen *et al.*, 2007; Cong *et al*., 2002). Dyskerin is essential for stable formation of telomerase complex (Cohen *et al*., 2007). The RNA subunit of telomererase employs a sequence complementary to a 150-250 nucleotides long single-stranded the G-rich telomeric DNA as a substrate to elongate the 3' G-overhang of the telomere in a 5' to 3' direction via reverse transcriptase subunit (hTERT) and not require ATP (Xu, 2011; Autexier and Lue, 2006). Telomeres are physically attached to the nuclear envelope during nuclear reassembly (Crabbe *et al.*, 2012). In previous works, it was shown that in order to reorganize chromatin domains after each cell division telomeres can function as a nuclear envelope tethering point via the shelterin subunit RAP1 to the nuclear envelope protein SUN1, which is part of the LINC complex is required for attachment of telomeres to the nuclear envelope in fission yeast and mice (Crabbe *et al.*, 2012; Kanoh and Ishikawa, 2001).

1.6 Interaction of the genome with other components of the nuclear architecture

The movement of chromatin in nuclei appears to be mostly by constrained diffusion and thus reflects the physical attachment of chromatin to nuclear compartments, such as the nucleolus, nuclear periphery, or a nuclear matrix (Boyle *et al.*, 2001; Andrulis *et al.*, 1998). It is evident that nuclear position has a crucial role for gene regulation and moreover, it has been shown that there is a strong correlation between transcriptionally silent, late replicating chromatin and a nuclear peripheral localization in several model systems (Zhang *et al.*, 2012; Boyle *et al.*, 2001; Andrulis *et al.*, 1998). Chromosomes that contain active nuclear organising regions (NORs), inactive NORs and also other chromosomes integrate into the nucleolus and therefore this nuclear compartment is thought to be crucial for spatial organisation of the genome within the nucleus (Pliss *et al.*, 2015; Sullivan *et al.*, 2001; Bridger *et al.*, 1999). In genome wide screens, two studies have revealed many sites throughout the genome that are anchored at nucleoli including chromosome 17 (van Koningsbruggen *et al.*, 2010) and chromosome 19 (Németh *et al.*, 2010). It was deciphered in G_0 synchronized WI38 fibroblasts that one nucleolus was always associated with more NOR-CT than the other nucleoli leads to a “dominant nucleolus” and several smaller sub-clusters chromosomes that yield their own nucleoli (Pliss *et al*., 2015). These studies demonstrate that the nucleolus is a major player in anchoring and organising chromosome territories in interphase nuclei. Studies on mammalian cell nuclei using fluorescence recovery after photobleaching (FRAP) showed that in time periods of more than 1 hour, chromatin became immobile over distances higher than 0.4 µm (Chubb *et al.*, 2002). Chubb *et al*. demonstrated that nucleoli and the nuclear envelope constrain the motion of

interphase chromosomes that are located at these nuclear structures. In addition they demonstrated that the mobility of chromatin not associated with nucleoli or the nuclear periphery was much less constrained and interaction of nucleolus with chromatin is likely to have a more profound effect on the regulation of chromatin dynamics than interactions with any global structures such as a nuclear matrix (Chubb *et al.*, 2002). Since human chromatin is subject to greater resistance, the diffusion coefficients for human loci is lower than the diffusion coefficients of other organisms such as budding yeast. Whereas, as the size of human nucleus is larger than yeast nucleus, loci are restricted to a much smaller proportion of the total nuclear volume (Chubb *et al.*, 2002)

1.7 Lamins and Genome Organisation

Lamins are heavily implicated in organising the genome. This has been demonstrated by *in vitro* lamins binding directly to chromatin (Taniura *et al.*, 1995). Further, in the early 1990s, studies on *Drosophilia* showed that *in vivo* the distribution of lamin B coincides with peripherally located chromatin. The *Drosophila* lamin Dm0 as well as Vertebrate A- and B- type lamins can bind DNA sequences known as matrix-attachment regions (MARs) or scaffold-attachment regions (SARs) (Lude´rus *et al.*, 1992) . FISH studies revealed that A- and B-type lamins have roles in genome organization (Gruenbaum and Foisner, 2015; Adam and Goldman, 2012). Two gene clusters of chromosome 13; 13A and 13B were shown having significant changes in nuclear localisation moving towards the nuclear interior in *LMNA* E161K mutant fibroblasts suggesting a loss of connection with the nuclear lamina. Furthermore, the region of chromosome 13 having the two gene clusters was

demonstrated being less compact with chromatin in the *LMNA* E161K mutant fibroblasts, however the chromosome 13 volume was shown being smaller (Mewborn *et al.*, 2010). The dense heterochromatin network is thought to reflect the association of transcriptionally inactive genes with the nuclear lamina suggesting that the nuclear membrane and lamina may play an active role in gene repression (Shaklai *et al,* 2007). Lamin-associated domains (LADs) are considered to regulate the interaction of chromatin with the nuclear lamina and LADs are thought to be transcriptionally repressive (Van Steensel and Dekker, 2010; Guelen *et al*., 2008 (Van Steensel and Dekker, 2010). Using DNA adenine methylase (Dam) method, striking alterations in the interactions between chromatin and the nuclear lamina was elucidated in terminal differentiation (Guelen *et al*., 2008). Dam method using lamin B1 in order to map genome-nuclear lamina interactions in progressive stages of the embryonic stems cells and neural differentiation pathway, Lamin-associated domains (LADs) were shown to cover almost 40% of the genome in human cells and moreover, promoters found within LADs generally carried repressive histone marks suggesting that LADs are repressive (Guelen *et al*., 2008). 4,052 genes of the 13,798 tested was demonstrated to have reduced expression and only 215 had enhanced association with the nuclear lamina suggesting that interaction of the genes with the nuclear lamina was shown as not a result of loss of transcriptional activity but a more directed and specific process for certain genes (Peric-Hupkes *et al.*, 2010). Previous work revealed that chromosomes 13 and 18 were found in the nuclear centre in proliferating laminopathy HDFs, different than normal proliferating cells that chromosomes 13 and 18 were found at the nuclear periphery (Mehta *et al*., 2011).

It is noteworthy that localization of chromosome in the nucleus can vary considerably between cell types (Zuleger *et al*., 2011). Sullivan and colleagues (1999) demonstrated that *Lmna* $^{-/-}$ mice cardiomyocytes and MEFs cells show a partial loss of peripheral chromatin integrity associated with blebbing of the NE and lamina and mis-positioning of centromeric heterochromatin (Sullivan *et al.*, 1999). Furthermore, both in *Lmna* $^{-/-}$ MEFs and in cells obtained from patients suffering from some-type of laminopathies, gene-poor chromosomosome 18 is positioned away from the nuclear periphery toward the nuclear interior (Meaburn *et al.*, 2007; Malhas *et al.*, 2007). Silencing of Lamin B1 expression in HeLa cells leads to formation of NE blebs that are lamin A/C rich and lamin B2-deficient (Shimi *et al.*, 2008). Euchromatic chromatin is mainly associated with these NE blebs and consists of gene-rich chromosome regions. This suggests that A-type lamins are preferentially associated with high gene density regions of active chromatin. On the other hand, LB1 seems to be associated with gene-poor regions of chromosomes (Shimi *et al.*, 2008). Lamins have been shown to play a role in the localization of and function of telomeres and centromeres (Solovei *et al.*, 2004). Lamins interact with chromatin associated histone proteins and the expression of mutant lamins leads to global changes in the epigenetic organization of chromatin (Dechat *et al.*, 2008). In cells derived from patients suffering from various laminopathies such as; HGPS. It has been shown that abnormalities in chromatin organization are linked to epigenetic changes, specifically to changes of specific histone methylations known to define heterochromatin (Martin and Zhang, 2005). Due to expression of mutant lamin protein, epigenetic marks; H3K9me3 and H3K27me3 were down-regulated and H4K20me3 was up-regulated (Scaffidi and Misteli, 2005) and moreover, mutant lamin A cause loss of heterochromatin (Capell and Collins, 2006; Shumaker *et al.*,

2006). Analysis of the expression of LEM domain domains in WT retina cells was shown that no individual LEM domain protein could be the universal mediator of the Lam A/C-dependent peripheral heterochromatin tether (Solovei *et al*., 2013).

1.8 Chromosome Movement

It was demonstrated by Simon and colleagues that the mutant lamin A/C tails bound less well than its wild-type to F-actin and even though F-actin is not present in the nucleus by phalloidin staining, the presence of some actin in the nucleus was found in an altered polymeric state (Simon *et al.,* 2010; McDonald *et al.*, 2006). Emerin has been demonstrated to attach the pointed end of actin filaments at the nuclear lamina (Holaska *et al.*, 2004). Puckelwarts and colleagues proposed that mechanosensing defects in LINC complexes lead to aberrant chromosome territories, gene dysregulation and altered lamin-actin interaction (Puckelwartz *et al*., 2011). It is believed that altered lamin-actin interactions cause aberrant chromatin movement (Puckelwartz *et al*., 2011). The energy for the movement of telomeres and chromosomes are generated in the cytoplasm by KASH and SUN proteins (Chikashige *et al.*, 2007). Chikashige and colleagues discovered meiotic-specific proteins bqt1 and bqt2 which are involved in connection of telomeres to Sad1 on the nucleoplasmic face of the INM in yeast (Chikashige *et al.*, 2006). Furthermore, Csm4 is the first KASH protein recognised in budding yeast and it is suggested that cytoplasmic domain of Csm4 is possibly to associate with a component of the actin cytoskleton (Bhalla and Dernburg, 2008; Penkner *et al.*, 2007).

1.9 Laminopathies

In the past decade, our knowledge and interest of the molecular mechanism underlying human ageing has exploded with the discovery that mutations in the genes encoding lamins and associated nuclear envelope proteins cause a diverse range of human diseases (de La Rosa *et al.*, 2013; Vijg and Campisi, 2008). Consequently, research in clinical genetics has changed the way cell biologists view the nuclear lamins and nuclear lamina (Worman *et al.*, 2009). Nuclear functions can easily be perturbed by a wide range of mutations in lamin genes. Many laminopathy syndromes disrupt only one or a few major tissues derived from mesenchymal origin including muscle, adipose tissue and neurons, whereas others affect combinations of tissues (Worman, 2012; Hutchison and Worman, 2004). Remarkably, over 400 discrete disease mutations in the *LMNA* gene have been so far identified, which implicate more than a dozen overlapping or distinct named clinical disorders and these diseases are collectively referred to as “laminopathies” or nuclear envelopathies and are often characterised by the manifestation of disease (Schreiber and Kennedy, 2013; Reddy and Comai, 2012; Dauer and Worman, 2009). These diseases include dilated cardiomyopathy, Emery-dreifuss muscular dystrophy (EDMD)(Puente *et al.*, 2011; Bione *et al*., 1994), limb girdle muscular dystrophy 1B (LGMD1B), familial partial lipodytrophy, Charcot-Marie-Tooth disease type 2 (CMT2B), restrictive dermopathy (RD), Werner’s syndrome, Hutchinson Gilford Progeria Syndrome(Hennekam, 2006) and other atypical progerias (Gotzmann and Foisner, 2006; Somech *et al.*, 2005; Capanni *et al.*, 2005; Navarro *et al.*, 2005).

1.9.1 Hutchinson-Gilford progeria syndrome

The two best-known examples of accelerated ageing syndrome in humans are Hutchinson-Gilford Progeria syndrome (HGPS), 'Progeria of childhood' (Eriksson *et al.*, 2003) and Werner syndrome (WS, 'Progeria of adult') (Sinha *et al*., 2014; Coppedè, 2012, Davis *et al*., 2006). Disruption in lamin expression can lead to a disease condition termed Hutchinson Gilford Progeria Syndrome (HGPS) (OMIM 176670) and which is a rare but the most severe disease of all laminopathies (Tsiligiri *et al.*, 2015). HGPS was first described by general practitioner Jonathan Hutchinson and Hastings Gilford in 1886 and 1904 respectively (Hastings, 1904; Hutchinson, 1886) and is exceedingly rare sporadic disease with an incidence of 1 per 4-8 million live births, dominantly inherited disease characterized by rapid growth deceleration in childhood (Rehman *et al.*, 2015; McClintock *et al.*, 2007). According to data from the progeria research foundation, the total number of known living children with HGPS was 103 worldwide in 2013 and approximately 140 cases have been reported in medical history (Monga *et al*., 2015).

1.9.1.1 Clinical features

Patients with HGPS condition generally appear normal at birth although to some extent small for gestational age and by approximately 1 year of age develop multiple clinical abnormalities with striking features that resemble accelerated ageing with failure to thrive develops, often accompanied by sclerodermatous skin with loss of subcutaneous fat, osteolysis, alopecia, rapid loss of joint mobility and varied skin hyperpigmentation (Chu *et al.*, 2014; Wuyts *et al.*, 2005; Goldman *et al.*, 2004; Brown, 1992). The children also present with prominent scalp veins and clear fontanelles. Almost all patients have a high-pitched voice and a short stature, and are under-weight (Gordon *et al.*, 2007). They have a characteristic facial appearance

with prominent eyes, a beaked nose and facial disproportion due to micrognathia and a large cranium (Hennekam, 2006; Brown, 1992). The children have a normal to above-average intelligence. Strokes are very common, at a median age of 9 years, resulting in seizures and headaches and limb weakness. Other abnormalities observed in HGPS patients are: dental crowding, conductive progressive hearing and bilateral sensorineural loss and a complete absence of spermatogenesis (Monga *et al.*, 2015). Mutation in lamin A appears to affect diverse body sytems including tongue, heart, liver kidney, stomach, bladder, pancreas, spleen, bone, skeletal muscle, heart and large and small arteries (Olive *et al.*, 2010; Mazereeuw-Hautier *et al.*, 2007). The average life expectancy of HGPS patients is around 13.5 years and most frequent cause of demise is heart attack or stroke resulting from progressive arteriosclerotic disease (Kumar, 2011; Goldman *et al.*, 2004).

Typical clinical features of the ageing, such as malignancy is conspicuously absent in patients with progeria which is most probably due to shortened life span of the patients and therefore HGPS is often called “segmental” (Pereira *et al.*, 2008). However, in 1978, King’s group reported the first case of Osteosarcoma diagnosed in a patient with HGPS (King *et al.*, 1978).

1.9.1.2 Genetic basis underlying HGPS

The genetic basics of progeria involving the *LMNA* gene were described by two different groups. One methodology was based on clinical overlaps between patients affected with mandibuloacral dysplasia (MAD), and this disease is one of the disorders caused by mutations in *LMNA* and HGPS. This methodology led to mutational analysis of *LMNA* in two affected children (De Sandre-Giovannoli *et al.*, 2003). The other group performed a different methodology which was a whole-genome scan using microsatellite marker in 12 patients and the aim was looking for regions of homozygosity (Eriksson *et al.*, 2003). In their experiment, Eriksson's group were expecting autosomal recessive inheritance however, surprisingly retrieved two cases with uniparental isodisomy and also one case in the 1q21 region of the chromosome, a 6-megabase paternal interstitial deletion was identified, leading towards candidate gene sequencing in the interval (Eriksson *et al.*, 2003). Both studies identified the most common *de novo* a silent point mutation located in *LMNA* gene exon 11 associated with HGPS. The major mutation associated with HGPS is a heterozygous germline single base-substitution in exon 11 on *LMNA* gene c1824C>T, and at the protein level, p. Gly608Gly, (Figure 1.12)(Cao *et al.*, 2007; Moulson *et al.*, 2007; De Sandre-Giovannoli *et al.*, 2003). Even though, this heterozygous mutation is predicted to be synonymous at the protein level, in reality, there is a formation of an aberrant a cryptic splicing donor site that generates a 150-nucleotide deletion on the mRNA sequence resulting in a truncated pre-lamin A protein called progerin/LAΔ50 (Wang et al., 2012) lacking 50 amino acids near the C-terminus (Scaffidi and Misteli, 2006; Goldman *et al.*, 2004). In HGPS, the deletion of 150 nucleotides due to single base-substitution in exon 11 on *LMNA* gene c1824C>T, does not affect the CaaX motif and protein pre-progerin undergoes normal farnesylation. However, the protein lacks the ZMPSTE24-FACE1 recognition

site for the final cleavage step, therefore leading to retention of farnesyl group on C-terminal cysteine in contrast to the transient farnesylation of prelamin A (Figure 1.13) (Scaffidi and Misteli, 2006; Goldman *et al.*, 2004; Eriksson *et al.*, 2003) . Progerin acts in a dominant negative manner and therefore transfection of wild type A-type lamin is not sufficient to rescue the HGPS cellular phenotype (Scaffidi and Misteli, 2005). The toxic accumulation of farnesylated prelamin A at the nuclear membrane compromises nuclear structure, disrupts the nuclear lamina , leads to herniations and loss of peripheral heterochromatin giving rise to the formation of grossly abnormally shaped nuclei (McCord *et al.*, 2013; Goldman *et al.*, 2004). It is believed that accumulation of farnesylated protein would lead to disruption of lamin–related functions such as gene expression and DNA replication (Pereira *et al.*, 2008). In addition to the mutation in codon 608 of exon 11, other *LMNA* mutations to be associated with HGPS include: a heterozygous base mutation E145K in exon 2, GAG > AAG (Eriksson *et al.*, 2003); a heterozygous base mutation within the same codon, G608S (GGC>AGC)(Eriksson *et al.*, 2003); a *de novo* missense mutation S143F(Kirschner *et al.*, 2005); a heterozygous base mutations R527C (Liang *et al.,* 2009) and R644C (Csoka *et al.*, 2004) on the *LMNA* gene. Homozygous missense base mutation has also been identified, K542N on *LMNA* gene which has an overlap with MAD (Plasilova *et al.*, 2004).

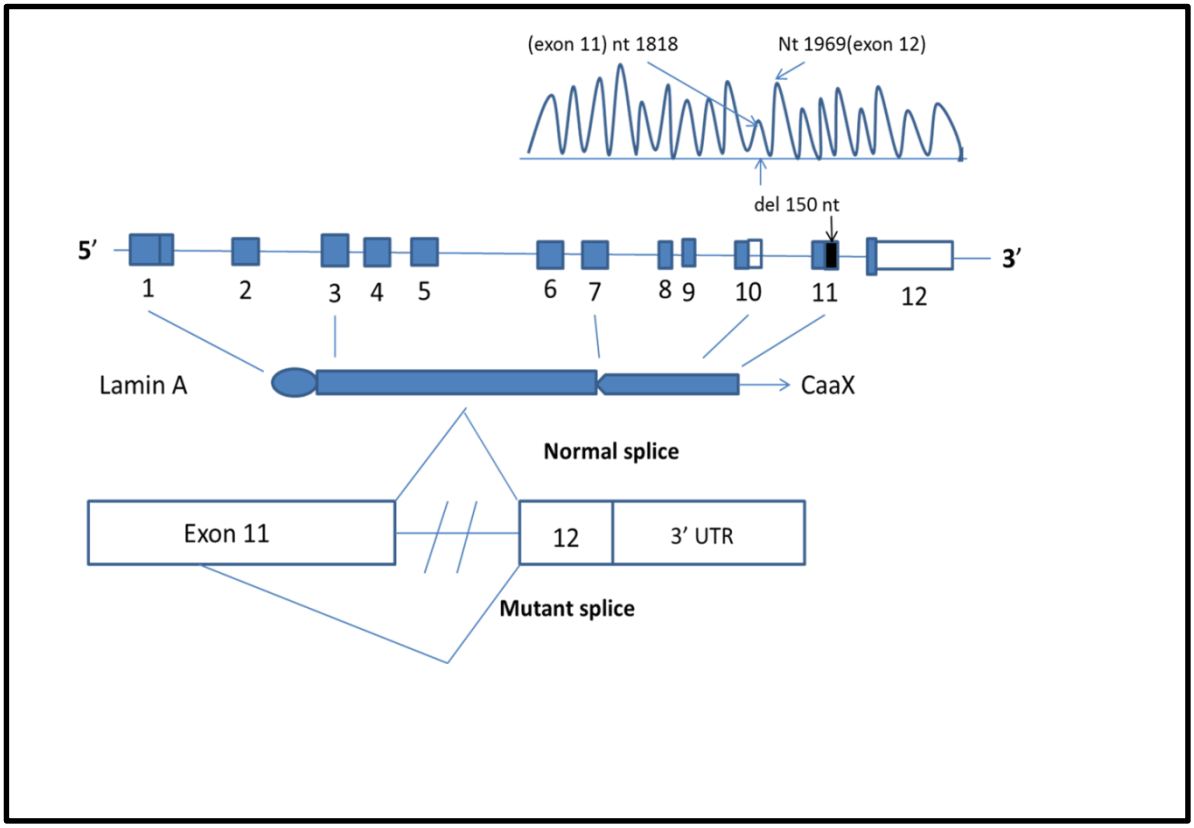

Figure 1.12 Representation of the *LMNA* gene and lamin A protein, correlated by globular domains and rod domain. The deleted LMNA transcript junction sequence is shown. The 150-bp deletion extends from G1819 to exon 11 end (Black box) and is indicated by a black bar in lamin A tail. CAAX, cysteine-aliphatic-aliphatic-any amino acid. Adapted from (Eriksson *et al.*, 2003).

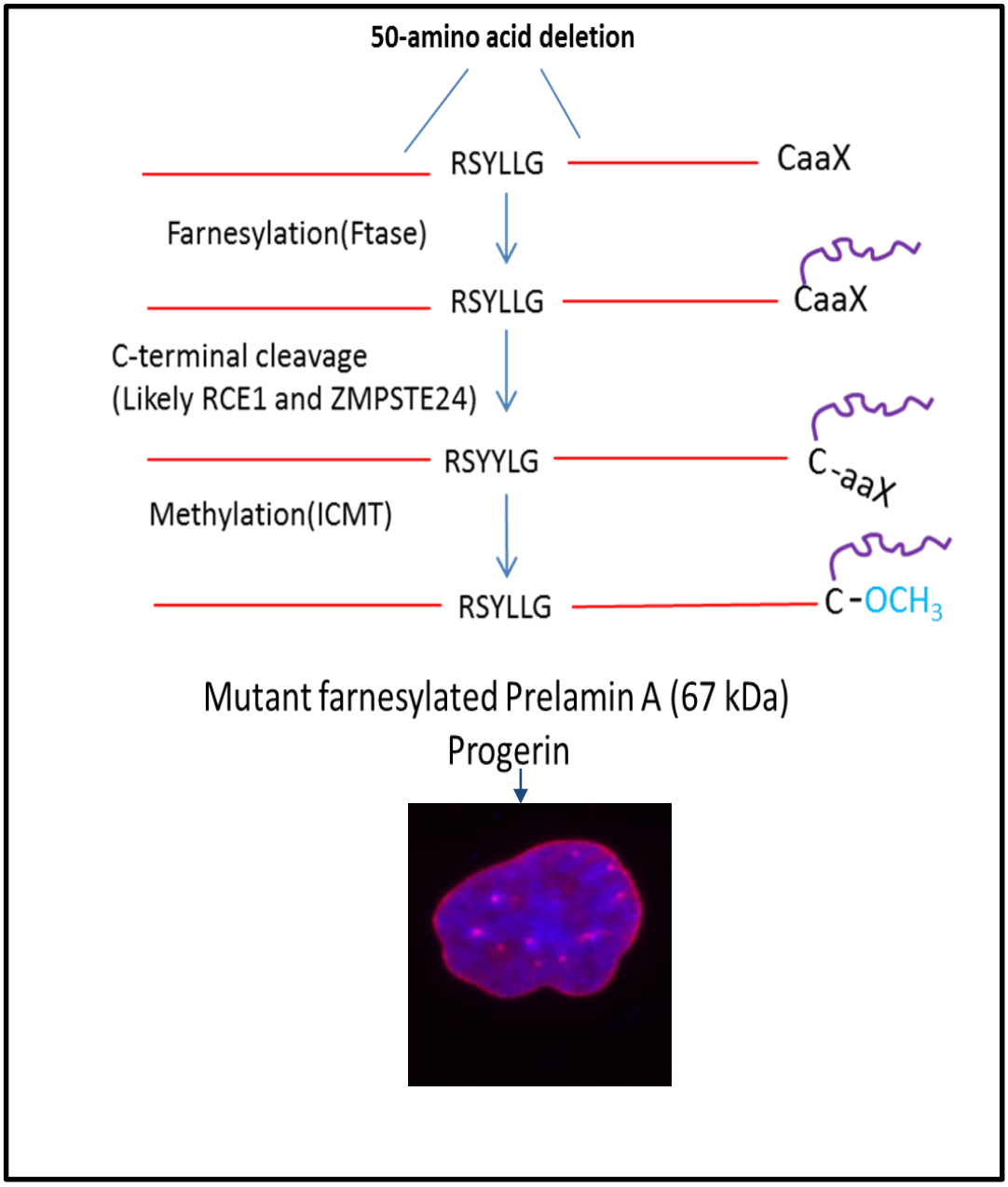

Figure 1.13 The formation of mutant farnesylated prelamin A in HGPS. In HGPS, ZMPSTE24 endoproteinase cannot cleave farnesylated prelamin A, due to lack of 50-amino acid in prelamin A (amino acids 607–656), the site for the second endoproteolytic cleavage (ZMPSTE24). Consequently, no mature lamin A is formed, and a farnesylated mutant prelamin A (progerin) accumulates in cells. A representative image of T06 cells showing nuclear herniations. Lamin A/C is labelled in red.

1.10 Chromosome positioning in Hutchinson-Gilford Progeria Syndrome

The nuclear lamina's association with genome organisation increased interest in chromosome positioning in cases of disruption to the nuclear lamina, such as that seen in HGPS. Nuclear organisation has been shown to be disrupted in cells from HGPS patients.One study compared the nuclear location of three representative chromosomes, in three separate HGPS cell lines and control cells (Mehta *et al.*, 2011). Chromosome 10 had previously been shown to occupy different nuclear locations in proliferating, quiescent and senescent cells (Mehta *et al.*, 2010; Mehta *et al.*, 2007). In normal proliferating cells it was found in an intermediate location, however, in HGPS proliferating fibroblasts it was found at the nuclear periphery. This is in line with the location observed in control quiescent nuclei. Chromosome 18 moves from the nuclear periphery to the nuclear interior during the transition from proliferation to non-proliferation, in normal cells. In HGPS cells, chromosome 18 was found at an interior location during proliferation. This is in line with findings from a previous study, which found chromosome 18 at the nuclear interior in proliferating laminopathy cells, including HGPS cells (Meaburn *et al.*, 2007). Complete reorganisation of the genome was, however, not observed as the X chromosomes were found at the nuclear periphery in both control and HGPS cells. It was concluded that HGPS show nuclear organisation patterns similar to that seen in quiescent normal cell nuclei (Mehta *et al.*, 2011). The association of *LMNA* mutations with altered chromosome territories was shown in *LMNA* mutant fibroblasts as chromosome 13 was displaced to the nuclear interior in *LMNA* E161K mutants cells, whereas chromosome 13 was shown positioning against the nuclear membrane in *LMNA* D596N mutant cells (Puckelwartz *et al*., 2011).

1.11 Senescence and HGPS

Cellular senescence is a state of irreversible cell cycle arrest, commonly reached by replicative (e.g., critically short telomeres) or cell stress (e.g., DNA damage) pathways, and proceeded by signaling of DNA damage response (Campisi, 2005; Blackburn, 2005, 2000). As the process of cellular senescence is defined as a gradual accumulation of non-dividing cells throughout the reproductive life span of culture (Kill *et al.,* 1994), it is a major obstacle to continuous propagation of cell, and therefore is often regarded as a tumour supressing mechanism (Campisi, 2005). How cellular senescence promotes age-related diseases and dysfunction remains one of the important questions in the biology of ageing. The abundance of senescent cells increases in multiple tissues with chronological ageing and in progeroid syndromes (Waaijer *et al*, 2012; Campisi *et al*., 2011; Burton, 2009). Senescent cells produce and secrete a variety of candidate signalling molecules, including ROS (Passos *et al*., 2010), pro-inflammatory interleukins (Kuilman *et al*., 2008), TGFb1 (Debacq-Chainiaux *et al*., 2005) and various IGF-binding proteins (Kim *et al*., 2007; Muck *et al*., 2008) that can all maintain or induce senescence in a cell autonomous or nonautonomous fashion. Senescence-causing inducers include repeated cell division and strong mitogenic signals, telomere shortening, DNA damage and mutations, protein aggregation, and increased ROS (Jeyapalan *et al.*, 2008; Tchkonia *et al.,* .2010; Weyemi *et al*., 2012). These insults activate the p53 and p16INK4a tumor suppressor pathways and potentially other pathways that initiate a senescence response and this feature was termed as ‘ the senescence associated secretory phenotype (SASP)’ (Coppe et al, 2008, 2010b). The SASP is mainly a DDR (Rodier *et al.*, 2009) and the SASP, through the inflammatory, growth-promoting, and remodeling factors that it produces, can potentially explain how

senescent cells alter tissue microenvironments, attract immune cells, and, ironically, induce malignant phenotypes in nearby cells. Proteins that are associated with the SASP, such as TNF-α, IL-6, matrixmetalloproteinases(MMPs), monocyte chemoattractant protein-1 (MCP-1), and IGF binding proteins (IGFBPs), increase in multiple tissues with chronological ageing (Freund *et a*l., 2010). The SASP has been revealed to have potentially both detrimental and beneficial effects, depending upon the biological environment (Freund et al. 2011). Beneficial aspects appear to consist of a reinforcement of the anti-tumour cellular growth arrest (Acosta et al. 2008) and a positive contribution to the clearance of senescent cells by the immune system (Xue et al. 2007). Deleterious effects consist of the promotion of malignant phenotypes of adjacent cells and accelerated tumour growth (Coppe et al. 2010; Gonzalez et al. 2015). Furthermore, many SASP factors are pro-inflammatory, hence the increased accumulation of senescent cells with age (Herbig et al. 2006; Jeyapalan et al. 2007) may contribute to the low-level chronic inflammation that is a hallmark of aged mammalian tissues, and provides one route whereby senescent cells can have detrimental effects in the context of ageing (Brassard et al. 2015; Davis and Kipling 2006; Freund et al. 2011). Cells in a senescent state can remain viable indefinitely in culture. This is true in most cases *in vivo* (Michaloglou *et al*., 2005) as well as *in vitro* with a very few exceptions where some senescent tumour cells of liver carcinomas phagocytose rapidly (Xue *et al*., 2007). Replicative senescence results from the progressive shortening of telomeres as cells divide throughout life (Bodnar et al. 1998). When the telomeres become critically short, they trigger a DNA damage response involving activation of p53, which in turn up-regulates the cell-cycle-inhibitor p21CDKN1 resulting in cell cycle arrest and entry into senescence (Canela et al., 2007 ; Vaziri and Benchimol, 1996).

The increased levels of progerin with age in non-HGPS individuals results in the accumulation of wild-type lamin A at the nuclear periphery (Scaffidi and Misteli 2006). These observations suggest that the mechanisms that lead to aberrant nuclear morphology and chromatin disorganisation in HGPS may also affect aged cells. Remarkably, the cryptic splice donor site that produces progerin is activated in senescent cells (Cao *et al*. 2011a). Telomere attrition results in the alternative splicing of several genes including progerin, thus presenting a complex and synergistic relationship between telomere shortening, progerin and senescence suggesting that progerin accumulation also impacts cell dysfunction and senescence in biological ageing (Cao et al. 2011a). In both human and animal studies, prelamin A accumulation has been shown to occur selectively in the vasculature, and prelamin A–induced VSMC (Vascular Smooth Muscle Cells) calcification and senescence are reiterated in animal models of HGPS and in vascular cells differentiated from induced pluripotent stem cells derived from patients with HGPS (Liu *et al*., 2013). Accumulation of Prelamin A was shown in VSMCs with increasing cell passage number *in vitro* concommitantly with decreased levels of its processing enzyme farnesylated proteins-converting enzyme 1 and increased levels of DNA damage. Furthermore, expression of pre-lamin A in VSMCs was found to increase DNA damage and to promote premature senescence, suggesting a causal link between its accumulation and accelerated VSMC ageing (Ragnauth *et al*., 2010). Examination of the arteries from young children on dialysis who develop hallmarks of premature vascular ageing, including arterial stiffening, VSMC loss revealed that calcifying nodular VSMCs have elevated levels of p16 and increased staining for senescence-associated β-galactosidase compared with monolayer VSMCs, confirming a link between prelamin A accumulation, calcification, and senescence both *in vitro* and *in*

vivo. Furthermore, SASP factors were shown abundantly secreted by prelamin A–expressing VSMCs (Liu *et al*., 2013). The extensive adventitial fibrosis and the frequent atherosclerotic lesions were shown to be present in the arterial histological sections of HGPS patients and intimal lesions were mainly fibrotic and acellular, closely resembling atheromatous lesions in physiological ageing (Olive *et al*. 2010). The autopsy of two HGPS patients of age 11 and 20 revealed an important decrease in VSMCs in the medial layer of the aorta (Stehbens *et al*. 1999). It was demonstrated on senescent vascular smooth muscle cells that baseline apoptosis rates do not change significantly in VSMCs as the fraction of senescent cells within the culture increases suggests that senescent VSMCs may persist *in vivo* long enough to be of physiological significance in the pathogenesis of vascular disease. However, it has been reported that apoptosis is a feature of advanced atherosclerosis and this could promote telomere shortening (and thus senescence) by reducing the number VSMCs capable of replication (Burton *et al*., 2009; Matthews et al., 2006).

1.12 Treatments for Hutchinson-Gilford Progeria Syndrome

1.12.1 Farnesyltransferase inhibitors (FTI)

HGPS is a sporadic autosomal dominant disease and most commonly classical *de novo* a point mutation in exon 11 in *LMNA* gene (c1824C>T) is responsible pGly608Gly on chromosome 1, this leads to a Gly substitution for a Gly the LMNA encodes the nuclear intermediate filament proteins lamin A and C (De Sandre-Giovannoli *et al.*, 2003; Eriksson *et al.*, 2003; Delgado Luengo *et al.*, 2002). Mature lamin A is produced via a pre-lamin A whose C-terminal cysteine residue is initially modified by farnesylation and carboxymethylation followed by enzymatic cleavage of the terminal 15 aminoacids by the ZMPSTE24 endoprotease, releasing the unfarnsylated mature lamin A. However, due to the point mutation that partially activates a cryptic splice site in exon 11 of *LMNA* leads to in-frame deletion of 150 nucleic acids from the lamin A mRNA, since the ZMPSTE24/FACE 1 cleavage site is missing and therefore a permanently farnesylated and carboxymethylayed uncleaved truncated lamin A isoform called progerin is accumulated (Wang *et al.*, 2012; Scaffidi and Misteli, 2006; Eriksson *et al.*, 2003; Goldman *et al*., 2004).

Farnesyl transferase inhibitors (FTI's) have been employed in order to inhibit farnesyltransferase enzyme that transfers the farnesyl group onto Ras and other proteins. FTIs were initially developed as potential anti-cancer agents targeting Ras function (Basso *et al.,* 2006). Although using of FTIs was considered not successful in cancer treatment, a potential success story exists to use FTIs for the treatment of Hutchinson–Gilford Progeria syndrome (HGPS). As a treatment for HGPS, FTI's have been employed to prevent the attachment of a farnesyl group to proteins by irreversibly binding to the CaaX domain and to prevent the accumulation of progerin

at the nuclear envelope and to treat many cellular abnormalities such as nuclear blebbing (Worman *et al*., 2010; Glynn and Glover, 2005). In 2007, the collaboration work of the Progeria Research Foundation with scientists at Children's Hospital, Boston and Schering-Plough Research Institute using an open-label, clinical trial with a single agent named lonafarnib for HGPS patients for 2 years showed the rate of weight gain over baseline for each patient with multiple secondary endpoints plus alterations in cardiovascular function (Gordon *et al.*, 2008). Furthermore, FTI treatment has been used for redistribution of mutant protein from the nuclear envelope and also restores genome localization after mitosis in Hutchinson Gilford Progeria Syndrome (HGPS) cells *in vitro* and in whole organisms (Taimen *et al.*, 2009). Using a FTI alone had only partial effect on lamin A maturation and due to the possibility of FTI drugs may cause an alternative post-translational modification of pre-lamin A which is geranylgeranyltransferase (GGT) that can cause accumulation of progerin, using a FTI together with geranylgeranyltransferase inhibitor (GGTI) concurrently results in accumulation of substantially higher levels of normal pre-lamin A (Mehta *et al.*, 2011; Liu *et al.*, 2010). On the other hand, GGTI-alone showed no effect on Lamin A maturation, indicating farnesyltransferase inhibition induces geranylgeranylation (Liu *et al.*, 2010). Furthermore, pre-lamin A has been shown to accumulate and be over-expressed in MSC derived from HGPS iPS cells (Blondel *et al.*, 2014). The Bridger group reported that FTI alone and together with GGTI cause alteration of the location of chromosome 10 to an intermediate location and also chromosome 18 was repositioned from an internal location to a peripheral one in HGPS cell nuclei. However, chromosome X was not repositioned after FTI alone nor with FTI and GGTI together. By using FTI, the shape of any aberrant, invaginated nuclei was restored to more smoothened ellipsoid shapes (Mehta *et al.*, 2011).

FTI treatment has been shown not only to reposition chromosomes but also to restore the distribution of nuclear motor protein nuclear myosin 1β (NM1β) in nuclei (Mehta *et al.*, 2011). Therefore, by preventing the farnesylation of progerin in HGPS cells chromosomes locate correctly, possibly because of the correct organization of NM1β and there is a good indication that lamin A is involved in regulation of chromosome behaviour through a nuclear motor protein. The Bridger group demonstrated the nuclear distribution of nuclear myosin 1β (NM1β) was aberrant in proliferating HGPS cells and after the treatment with FTI it was distributed and also restored to a similar distribution as in proliferating fibroblasts (Mehta *et al.*, 2011). FTI-277 treatment of HGPS cells has been shown to restore nucleolar antigen localization (Mehta *et al.*, 2009). Adam and coworkers' study on normal cells using FTI treatment demonstrated that after addition of of the drug, within 48-96 hours cells became senescent, larger and adopted a flattened morphology. Furthermore, senescence led cells to a decrease in LB1 expression and accumulation of preLB2 was observed in the nuclei of cells (Adam *et al.*, 2013). FTI treatment has been shown to give rise to the formation of doughnut-shaped nuclei in mice owing to defect in centrosome separation (Verstraeten *et al.*, 2011).

Evidence of improved cardiovascular status, sensorineural hearing, peripheral arterial stiffness and echodense common arteries of children with HGPS has been shown after Lonafarnib (FTI) drug treatment. Although, some children benefitted with respect to rate of gain weight, some did not benefit or have been affected negatively with regards to rate of weight gain (Gordon *et al.*, 2012). Mid-and late-passage HGPS cells treated with FTIs have been shown to cause a substantial reduction in the fraction of abnormally shaped nuclei, whereas, FTI's have been shown not to have any affects on nuclear shape in healthy control cells. FTI's treatment also

contributed improvement of wound healing in healthy control cells (Verstraeten *et al.*, 2008). In both HGPS and healthy control cells, FTI treatment increased the persistence time of cell migration speed. Moreover, it was shown that blocking lamin A/progerin does not have any role on improved wound healing effect (Verstraeten *et al.*, 2008). Over the 2-year period of the trial of Lonafarnib (SCH66336) - a synthetic tricyclic derivative of carboxamide with antineoplastic properties, FTI drug treatment in HGPS patient's revealed improvements in pulse wave velocity, carotid echodensity, headcahes and seizures. Although a statistically significant improvement in the rate of weight gain (36%) was obtained after the drug treatment, the overall poor growth and weight of these patients were not changed (Kieran *et al.*, 2014).

1.12.2 Combination therapy: statins and aminobisphonates

Pravastatin and zoledronic acid (an aminobisphosphonate), which inhibit the HMG-CoA reductase and FPP synthatase enzymes of the mevalonate pathway respectively have been shown to improve longevity in ZMPSTE24 deficient mouse models (Varela *et al.* 2008). A 3 drug combination of lonafarnib, pravastatin and zoledronic acid has been put forward in trial based in the United States at Children's Hospital Boston (Clinical trial ID: NCT00879034). Administration of recombinant IGF-1 protein to the *ZMPSTE24* ($^{-/-}$) mice restores the GH/IGF-1 balance and increases their longevity (Marino *et al*., 2010).

1.12.3 Rapamycin

Rapamycin also known as Sirolimus is a macrolide antibiotic that has been shown to have an impact on a number of biological pathways to extend longevity in mammals. Mammalian target of rapamycin (mTOR) is a main cellular target of rapamycin and a central regulator of cell growth that integrates hormonal signals and therefore regulates diverse cellular processes (Blagosklonny, 2011; Cao *et al.*, 2011b). As mTORC exists in two different complexes as mTORC1 and mTORC2, which control cell growth, rapamycin inhibits mTORC1 and releases the autophagic signalling pathway at low concentrations. However, to inhibit mTORC2, a higher concentration of rapamycin is used (Cao *et al.*, 2011b). Rapamycin has been used for a variety of clinical applications such as a potential anticancer treatment. The characteristic hallmarks of HGPS nuclei are; nuclear blebbing, loss of rim structure of nuclear membrane, punctuate accumulations of progerin in mitotic cytoplasm. Much is being made of rapamycin drug as a new treatment for HGPS and even normal ageing (Mendelsohn and Larrick, 2012). Cao *et al*. study showed that treatment with rapamycin abolished nuclear blebbing and enhanced the degradation of progerin in HGPS cells which lead to decreased formation of insoluble progerin aggregates, therefore increases solubility of lamin A and progerin and also clearance of progerin in normal fibroblasts and more importantly suppressed senescence in non-HGPS mammalian cells (Cao *et al.*, 2011b). In their study, Cenni *et al,* (2011) demonstrated that after Ramapycin drug treatment progerin levels were substantially reduced and LAP2α, BAF proteins were restored and distribution pattern of H3K9ME3 was recovered in HGPS cells (Cenni *et al.*, 2011). Automated image analysis of HGPS cells after rapamycin and RAD001 drugs treatment revealed a reduction of blebbing, invaginations and the area of the nucleus (Driscoll *et al.*, 2012). Ibrahim *et al.,* (2014)

demonstrated that using rapamycin caused reduction of the proliferation of HGPS cells (Ibrahim *et al.*, 2013). Rapamycin drug treatment has been demonstrated to reduce insoluble progerin aggregates within the cell nuclei of HGPS fibroblasts through autophagic degradation and also have a positive outcome on MSC derived from HGPS iPS cells by reducing the number of progerin expressing cells (Blondel *et al*., 2014).

1.12.4 Morpholino oligonucleotides

In 2005, Scaffidi and colleagues designed a modified 25-mer morpholino oligonucleotide (exon11) antisense complementary to the region containing the HGPS mutation in exon 11 in order to block the activated cryptic splice site, leading to reverse the cellular phenotype in HGPS and these studies revealed that the drug enabled correction of aberrant splicing of a LMNA minigene in HeLa cells and also in dermal fibroblast and B-lymphocyte cell lines derived from individuals with HGPS (Scaffidi and Misteli, 2005). Moreover, splicing correction of HGPS cells with exon 11 oligonucleotide corrected the morphological abnormalities of cell nuclei in >90% of cell, the wild-type lamin A protein was restored and lamin B, LAP2 proteins and HP1α was restored in ~90% of treated cells (Scaffidi and Misteli, 2005). Importantly, improvements in nuclear morphology occurred without entering mitosis.

1.13 Brief Summary

Over the past decade, growing evidence has been accumulated that the nuclear lamina and large number of NE-associated and interacting proteins are an emerging class of proteins playing critical roles in genome organization, gene regulation, DNA replication, cell differentiation, apoptosis and many variety of activities. In past years, lamins have received most attention owing to increased number of human diseases asscociated with lamins and lamin-binding proteins to shed light on common mechanism shared by normal ageing and to decipher pathogenic mechanisms. HGPS is a rare and segmental progeroid syndrome, leading to death at an average age of 13 years. In HGPS, it is well known that lamin A does not function as direct component of DNA repair protein complexes in contrast to other progeroid conditions such as Werner syndrome. Therefore, different than in these other syndromes, mutations in *lamin A* gene of HGPS patients give rise to premature stem cells exhaustion in order to produce a highly segmental tissue-specific pattern of premature ageing rather than increased cancer risk (Halaschek-Wiener and Brooks-Wilson, 2007). However, the main question of how farnesylated pre-lamin A named progerin to cause DNA damage, perturb DNA repair and lead to genomic instability remains unanswered. The genome is highly and non-randomly organized within the interphase nucleus and each chromosome occupies a chromosome territory. LINC complex of KASH and SUN proteins form a bridge to transfer forces across the nuclear envelope involved in a variety of cellular processes, including nuclear anchorage, chromosome movements and the notion that mutations in lamin proteins lead to alterations in the nuclear-cytoskeletal link. In previous work, it has been suggested that improper nuclear and chromatin organization lead to accelerated ageing in HGPS patients. To date, there is no effective treatment for a

devastating disease HGPS. Nevertheless, aforementioned promising preclinical findings have recently driven the development of potential therapies which have entered into clinical trials such as FTI's in USA and have been shown to restore the normal nuclear morphology of the cells and to increase average life span of HGPS patients. Moreover, they might be relevant to many other related progeroid syndromes. Clearly, the relationship between progeria and normal physiological ageing still remains to be understood and thus further clinical research will help to solve the puzzle of molecular mechanisms in lamin-linked pathologies and to improve potentially therapeutic understanding of many human diseases from cancer to ageing. This thesis is to investigate aberrant nuclear organisation in progeria cells and how can be restored with drug treatments.

Chapter 2: The effects of drug treatments on chromosome 18 and X territory positions and telomere interactions with the nuclear matrix in primary HGPS

Manuscript in Preparation: C. S. Clements, M. U. Bikkul, I. R. Kill and J. M. Bridger

2.1 Introduction

2.1.1 The nuclear matrix and its composition

In 1966, the nuclear matrix (NM) was defined as a non-chromatin structure of the nucleus readily observed in extracted cells using the electron microscope (Fawcett, 1967). In the early 1960s a fibrogranular ribonucleoprotein (RNP) network was discovered as the principal feature of these non-chromatin nuclear structures (Smetana *et al.*, 1963). Berezney and Coffney coined the term nuclear matrix which was previously described a newly isolated nuclear fraction by treating rat liver nuclei with high salt molarities, non-ionic detergents and DNase I (Berezney and Coffey, 1974). NM constitutes ~1% of the total protein of cells and tissues (Mika and Rost, 2005).

The nuclear matrix is a proteinaceous permanent network of 10-nm core filaments and a dynamic RNA-protein complex which spans the entire mammalian nucleus (Nickerson, 2001). NM is thought to be a network of fibrous proteins that comprised of nuclear lamina inside the cell nucleus and proposed to be a platform for several significant nuclear activities such as DNA repair and replication, transcription and regulating gene expression (Anachova *et al.*, 2005; Bissell *et al.*, 1999; Jackson and Cook, 1985). According to the NM proteome analysis by 2-dimensional gel electrophoresis, over 400 mammalian proteins have been classified as NM proteins and 130 of them have a cell-cycle dependent association with the structure (Mika and Rost, 2005).

In a mammalian nucleus, it is believed that DNA can be organized into approximately 60,000 chromatin loops, each representing an independent regulatory unit (Berezney *et al.*, 1996). DNA is organized in supercoiled loops attached to the NM by non-coding sequences after nuclease treatment known as matrix attachment regions (MARs) or scaffold attachment region (SAR)(Ottaviani *et al.*, 2008). MARs function to bring about the domain organization by the anchorage of the loop bases to the nuclear matrix (Boulikas, 1996). Numerous INM proteins have been shown to be components of the NM including both A-type and B-type lamins in Hela and rat hepatocytes (Barboro *et al.*, 2002; Hozak *et al.*, 1995). One study showed emerin to link to the NM (Squarzoni *et al.*, 1998). Furthermore, other scaffolding proteins such as NuMA, actin and several actin-binding proteins are constitutents of NM (Nickerson, 2001; Zeng *et al.*, 1994). Matrin-3 protein has been found in the nuclear matrix/scaffold “central proteome,” regardless of the method of isolation (Engelke *et al.*, 2014). It is thought that owing to the effects of diverse variations in procedure of the nuclear matrix preparation on protein composition and ultrastructure of the isolated nuclear matrix, it can lead the so-called internal nuclear matrix to be rather unstable and therefore is not preserved under certain conditions of nuclei fractionation (Lebkowski and Laemmli, 1982). The aim of this study is to test whether or not the proposed drugs and combinations of drugs currently used in clinical trials can restore positioning of chromosomes 18 and X in HGPS fibroblasts.

2.1.3 The isolation and visualization of the inner nuclear matrix

In order to isolate and visualise the the inner NM, a variety of methodologies have been developed. A detergent, named Triton X-100 is generally used to extract

plasma and nuclear membranes and this treatment removes the majority of phospholipids and some cellular and nuclear proteins (Aaronson and Blobel, 1974). As nuclear matrix is concealed by chromatin structure, nucleases/DNase 1 is employed to digest nuclei. It is unfortunate that some procedures are not evaluated for preservation of matrix morphology (He *et al.*, 1990). Berezney and colleagues employed isolated nuclei with DNase I and then eluted the partially digested chromatin with 2 M NaCl. The obtained matrix after the treatment retains many important features including the chromatin loop attachment sites, DNA replication complexes as well as most of the heterogenous nuclear RNA or hnRNA (Berezney and Coffey, 1974). On the other hand, Mirkovitch *et al*., treated cells with a strong detergent, lithium diiodosalycilate in order to remove partially digested chromatin. None of these two studies established the morphology of neither the resultant matrix nor its biochemical completeness. Capco *et al*., (1982) and Fey *et al*., (1986) adopted a different procedure to visualise NM structure by skipping the initial isolation of nuclei and extracting with nonionic detergent, chromatin is digested with DNase I to cut chromatin DNA between nucleosomes and removed with low ionic 0.25 M ammonium sulfate. Along with the DNA other soluable proteins are also removed. Thus yielding a more structurally complete nuclear matrix, without contaminating chromatin components (Figure 2.1) *(Fey et al., 1986; Capco et al*., 1982). After high-salt extraction about 70% total nuclear RNA remains and treatment of the core filament preparation with RNase A for 10 min results in their almost complete disappearance of core filaments, leaving an empty nuclear shell and the lamina was unchanged and remains intact by RNase A digestion. Moreover, the intermediate filaments filling the cytoplasmic space could still be seen to associate to the empty nuclear lamina. These findings provide evidence that for the overall

integrity of the filament network, intact RNA is required and RNA is an indispensable component of the inner nuclear membrane (He *et al.,* 1990). Nickerson *et al.* (1997) performed the cross-linking agent named formaldehyde to stabilize the preservation of ultrastucture of NM prior to removal of chromatin (Nickerson *et al.*, 1997). Following extensive formaldehyde cross-linking, 93–99% of 3H-labeled DNA along with its associated histones are removed. Importantly, the visualisation of the nuclear interior by means of these different protocols showed that the internal NM is indeed built upon a highly-branched network of filaments approximately 10 nm in diameter (Wan *et al*., 1999).

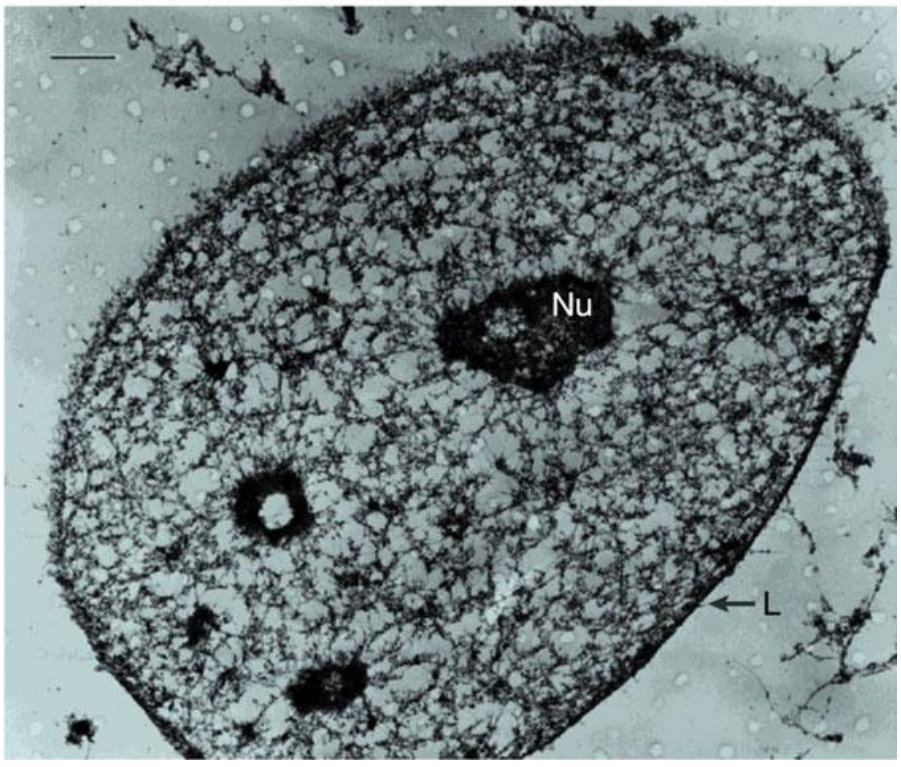

Figure 2.1: The nuclear matrix of a cervical carcinoma cell line was prepared by the crosslink-stabilized nuclear-matrix procedure and visualized by resinless section electron microscopy. The nuclear matrix consists of two parts, the nuclear lamina (L) and a network of intricately structured fibres connected to the lamina and well

distributed through the nuclear volume. The matrices of nucleoli (Nu) remain and are connected to the fibres of the internal nuclear matrix. The structures of three nucleoli can be seen in this section. Figure reproduced from Nickerson *et al.*, 1997.

2.1.4 The role of the NM in genome organization

The nuclear matrix is considered as a structural basis for compartmentalization and after extraction of histones, total nuclear DNA remained bound to nuclear matrix, being organized into topologically closed loops with average size of 50-250 kb in length (Razin *et al.*, 1996). It is believed that these loops are associated to the NM through their MARs or SARs (Heng *et al.*, 2004). In the genome, it is estimated that thousands of MARs regions are present, however relatively few of them have been identified (Bode *et al.*, 2000). It was suggested that the nuclear matrix plays a crucial role in folding of interphase chromosomes (Razin *et al.*, 2014). Moreover, it was also suggested that DNA loops anchored to the nuclear matrix may represent some structural and functional domains of the genome (Georgiev *et al.*, 1981). Remarkably, differentiation (Szczerbal *et al*., 2009) and cellular state have been shown to determine positioning of chromosomes (Mehta *et al*., 2010; Bridger *et al*., 1999). Chromosome arrangement is mediated by the NM and it was demonstrated that extraction of NM leads disruption of these territories (Ma *et al.*, 1999). Studies have demonstrated that there are not any discrepencies between MARs and SARs and recently, instead terms “MAR” or “SAR”, the term “S/MAR” is often referred (Bode *et al.*, 1996). It should be noted that MARs do not have any tissue or species specific properties and in addition, are present inside genes and exons (Fiorini *et al.*, 2006). Although, MARs elements do not share homologous nucleotide sequences, they retain some common properties, including relative enrichment in A/T pairs and

also the ability to be preferentially integrated in super coiled DNA (Bode *et al.*, 2003). Using variety of methods, it has been shown that many proteins adhere to MARs including lamins (Luderus *et al.*, 1994), SATB1 (special ATrich sequence binding 1) and SAFA/hnRNPU (Fackelmayer *et al.*, 1994). Localization of actively transcribing genes was shown at the base of loops or very close to them, whereas silent genes were shown localizing at distal parts of loop. Using a method of DNA loop excision by DNA topoisomerase II of the nuclear matrix (Gromova *et al.*, 1995), permanent sites of DNA attachment to the nuclear matrix were revealed in *Xenopus laevis* and rising size of loops during ontogenesis and alteration in specificity of DNA attachment to the nuclear matrix was also shown (Vassetzky *et al*., 2000). For the regulation of the topology of chromatin regions, it has been proposed that MARs and DNA topoisomerases may function together which lead facilitating transcriptional process (Bode *et al.*, 1992). It has been considered that nuclear matrix function as a platform for assembling and positioning of replication (Wilson and Coverley, 2013; Hozák *et al.*, 1993), transcription factories (Jackson *et al.*, 1998) and splicing speckles (Spector *et al.*, 1991). Researchers indicated that after removal of most of the chromatin essentially all identified nuclear compartments are preserved in isolated nuclear matrix (Mattern *et al.*, 1999; Berezney *et al.*, 1996). In order to transport of RNA to the cytoplasm, replication and transcription factories are positioned at the surface of interchromatin channels which seems that during nuclear matrix isolation, proteins of RNP particles existing inside interchromatin channels aggregate with formation of a network of filaments, which was termed diffuse matrix and it was suggested that indeed, the diffuse nuclear matrix is an artifact structure (Razin and Gromova, 1995; Hozák *et al.*, 1993). It was demonstrated by Gerdes and colleagues that although transcriptionally inactive sequences have loose interaction

with the NM structure, transcriptionally active DNA shows tighter interaction with the NM (Gerdes *et al.*, 1994). Similar results were revealed by Croft *et al.* that gene-dense human chromosome 19 was shown adopting a more internal position than gene-poor human chromosome 18 in the nucleus and to be more extensively interacted with the nuclear matrix (Croft *et al.*, 1999). NM's role for the regulation of DNA repair has been shown as in response to DNA damage, both the level of tumour-suppressor protein named p53 and binding of p53 to the NM increased (Jiang *et al.*, 2001). Furthermore, another tumour-suppressor protein retinoblastoma protein (pRb) is believed to associate with the NM structure (Mancini *et al.*, 1994). It has become apparent that A- and B-type lamins and emerin are MAR-binding proteins and these proteins mediate the NM's role in organizing the genome and therefore, mutations in these proteins can lead to the disruption of chromatin organization and gene expression. Tang et al. have demonstrated that depletion of lamin B1 from human cells lead loss of integrity of the NM, inhibition of RNA synthesis and thus reduced RNA polymerase I and II activity (Tang *et al.*, 2008). Stabilization of the architecture of interphase chromosome is provided by interaction of a set of chromosomal domains with the nuclear lamina (Meister and Taddei, 2013; Guelen *et al.*, 2008) and this stabilization requires long non-coding RNA's associating with nuclear matrix proteins (Hacisuleyman *et al.*, 2014).

2.1.5 Telomeric DNA, nuclear matrix and lamins

Telomeres are essential structures found at the ends of linear eukaryotic chromosomes comprised of multiple repeats of the hexameric conserved G-rich DNA sequences TTAGGG and specific binding proteins (Blackburn, 2001; Zakian, 1995;

Blackburn, 1991). They play a significant role to prevent genomic instability (O'Sullivan and Karlseder, 2010; Slijepcevic *et al.*, 1996). Telomere binding proteins function to form a protective structure which 'caps' chromosome ends and thereby protect from being recognized as double-stranded breaks (de Lange, 2005). *In vivo* and *in vitro*, with each cell division telomeres shorten owing to the 'end replication problem' also sporadic losses due to damage or replication errors (Lansdorp, 2005). Luderus and colleagues have postulated that MARs show affinity to tether to specific areas of mammalian telomeres and suggested that per kb of telomeric sequence, there is at least one MAR is present (Luderus *et al.*, 1996). It has been demonstrated that human telomeres are tethered to the nuclear membrane by their TTAGGG repeats (de Lange, 1992). Most telomeres avoid the nuclear periphery and are dispersed throughout the nuclear interior, suggesting a more specific role for intranuclear lamins in tethering telomeres (Shimi *et al.,* 2008). A repositioning of telomere localization was observed towards the nuclear periphery with the lack of A-type lamins, suggesting an active role of A-type lamins in the positioning of telomeres in the nuclear interior (Gonzales- Syare *et al*., 2009).

In this chapter, a technique known as Halo-FISH is employed to study the association of the genome with the nuclear matrix. Although many variations of this technique exist to examine such genomic associations, majority of methodologies utilizes detergents such as lithium diiodosalicilate (LIS) or high salt solutions in order to extract proteins such as histones, non-soluble proteins and DNA not associated with the nuclear matrix from the nucleus (Elcock and Bridger, 2010; Ma *et al*., 1999; Luderus *et al.*, 1996; de Lange, 1992). Once interphase nuclei are permeabilized and extracted, residual chromatin that is not fixed to an internal structure is released, forming a halo around a residual nucleus. The residual nucleus consists of the NM

and NM-associated DNA; however the halo contains extracted DNA. These structures can be stained with DAPI (4', 6-diamidino-2-phenylindole) to reveal the residual nucleus and the DNA halo. Performing FISH on these preparations, named HALO-FISH using telomere specific probes can delineate specific DNA sequences (Volpi and Bridger, 2008; de Lange, 1992). It is believed that the association of telomeres with the nuclear matrix is disrupted in Hutchinson-Gilford Progeria Syndrome (Elcock and Bridger, 2010). It was demonstrated that an interaction between a telomere-binding protein, TRF-2 and lamin A/C is disrupted in HGPS which give rise to telomere instability (Wood *et al*., 2014). To date, there are no studies looking at the interactions between the genome and the nuclear matrix in HGPS in the context of proposed drug treatments. To address this gap of knowledge, this investigation utilises the DNA halo assay to evaluate the efficacy of these drugs in restoring these interactions.

2.2 Materials and methods

2.2.1 Cell culture

A HGPS cell-line derived from AG01972 (14 years old female primary HGPS) was obtained from Coriell Cell Repositories (New Jersey, USA). The 2DD normal dermal fibroblast cell line was used (Bridger *et al.*, 1993). These cell lines were cultured in T75 tissue culture flasks (Fisher, UK) in Dulbeco's Modified Eagles Medium (DMEM) (Invitrogen, UK), with the following additives: 15% foetal bovine serum (FBS) (Invitrogen), 2% (v/v) streptomycin and penicillin antibiotics (Invitrogen) and 200 mM L-glutamine (Invitrogen) by Dr. Craig clements. The cells were maintained at 37^0C temperature, in a humidified atmosphere containing 5% CO_2. Cells were washed with

3 ml of versene (NaCl 0.8% (w/v), KCl 0.02% (w/v), Na2HPO4 0.0115% (w/v), KH2PO4 0.02% (w/v), 0.2% EDTA (w/v) (Sigma Aldrich)). Followed by 3 ml diluted solution of 0.25 % trypsin (Invitrogen): versene (1:10, v: v) for up to five minutes. As soon as all the cells were detached from the flasks' bottoms, the effect of trypsin solution was neutralized by adding an equal amount of DMEM medium to the dishes. The final suspension was centrifuged at 300-400 g for 5 minutes. The supernatant was removed and the pellet of cells was re-suspended in a known volume of fresh medium.To determine the number of cells in the suspension, a drop of cell suspension was placed onto a haemocytometer (Neubauer, 1/400 mm^2) with a chamber depth of 0.1 mm and then the total number of the cells was calculated for the number of cells in the large squares of the haemocytometer under a 10X lens of a phase contrast light microscope. The total number of the cells was calculated using the following equation:

$$\frac{\text{Number of cells}}{\text{Number of Squares}} \times \text{Volume of cell suspension} \times 10^4$$

The number of cells counted on the haemocytometer, divided by number of Haemocytometer's large squares where the cells have been counted, the result is multiplied by the total volume of the suspension and then by 10^4, the final result equals the total number of the cells in the suspension. The cells were then seeded in T75 new flasks at a density of 5 x 10^5/flask. The volume in each flask was topped up

to 20 ml using fresh media and the cells incubated at 37^0C. To maintain stocks of cells, 1 million cells were frozen down in medium containing 10% dimethyl sulphoxide (DMSO) (v/v) (Sigma). These cells were then transferred to -80^0C freezing box overnight and then placed in liquid nitrogen at –170^0 C until needed. When required, the cells were defrosted rapidly in a water bath at 37^0C and as soon as the cells were thawed, cells were transferred to a tissue culture flask containing medium pre-heated at 37^0C.

2.2.2. Drug treatments

The drugs used were FTI-277, Pravastatin, Zoledronic acid, Rapamycin, Insulin-like Growth Factor 1, N-acetyl-L-cysteine and GGTI-2133 and were all obtained from Sigma Aldrich, UK. Drugs were added to the media and incubated for fixed periods of time by Dr. Craig Clements, Brunel University. The final concentration and duration of drug treatments were: 1) untreated AG01972, 2) AG01972 with FTI-277 (2.5 µM for 48 hours) (Mehta *et al*., 2010), 3) AG01972 with pravastatin (1 µM for 24 hours) (Varela *et al*., 2008), 4) AG01972 with zoledronic acid (1 µM for 24 hours), 5) AG01972 with rapamycin (10 nM for 24 hours) (Cao *et al.*, 2011b), 6) AG01972 with insulin-like growth factor 1 (50.0 ng/mL for 24 hours) (Marino *et al.*, 2010), 7) AG01972 with N-acetyl-L-cysteine (20 µM for one hour) (Richards *et al.*, 2011), 8) AG01972 with FTI-277 and GGTI-2133 (both 2.5 µM for 48 hours) (Mehta *et al.*, 2010; Mehta *et al*., 2009; Kieran *et al.*, 2007), 9) AG01972 with pravastatin and zoledronic acid (both 1 µM for 24 hours) (Varela *et al.*, 2008) and 10) AG01972 with FTI-277 (2.5 µM for 24 hours), pravastatin and zoledronic acid (both 1 µM for 24 hours).

2.2.3 Indirect immunofluorescence

In order to distinguish proliferating cells from non-proliferating cells, 2D- FISH was combined with indirect immunofluorescence staining for antigen Ki-67. PKi-67 is a nucleolar antigen that is only present in cells in proliferative cell cycle (Gerdes *et al*., 1983). The coverslips from the FISH experiments were removed by placing slides in 1X PBS solution for 30 minutes on a shaker until the coverslips detach. The slides were incubated 100 µl of rabbit primary anti pKi-67 (DAKO, A0047) (1:30 dilution in 1% NCS/PBS v/v)- { a kind gift from Dr. Ian Kill, Brunel University, London} and placed in an humidified chamber either for 2-3 hour at room temperature or overnight at 4^{o}C, followed by 27 times washes in 1X PBS. Subsequently, 100 µl fluorochrome-conjugated secondary antibody; the swine anti-rabit (TRITC) antibody (DAKO, R0156) diluted with 1% FBS in 1X PBS was added to the slides. Cells were incubated in the dark for either 30 min at 37^{0}C or 1 hour at room temperature. The cells were washed 27 times in 1X PBS followed by a final wash in double distilled water. A total of 15µl of Vecta-shield anti- fade mounting medium containing 4', 6-diamidino-2-phenylindole (DAPI) (Vector Laboratories) was added to each slide and the coverslip sealed using rubber cement.

2.2.4 Two-dimensional fluorescence in situ hybridisation (2D- FISH)

2.2.4.1 Cell fixation for FISH

Treated and untreated 1972 HGPS cells were fixed by Dr. Craig Clements. As described in section 2.2.1, cells were treated with versene and versene/trypsin and after centrifugation at 300-400g for 5 min, most of the supernatant was removed and

the cells were re-suspended in the remaining media. A hypotonic solution (0,075 M KCl) was added dropwise to the cells at room temperature for 15 min in order to swell the cells and to remove the cytoplasm. Then, the samples were centrifuged at 300g for 5 minutes, most of the supernatant was removed and the cells re-suspended in the residual solution. A fixative mixture of ice-cold methanol: acetic acid (3:1, v/v respectively) was freshly prepared and added drop wise to the sample with constant agitation. The sample was stored at 4^0C for at least 1 hour. The samples were then centrifuged at 300g for five minutes, the supernatant was removed and the fixing procedure was repeated 4-5 more times. The remaining samples in the tubes were stored at -20 °C until required.

2.2.4.2 Slide denaturation

The cells were dropped from a height onto humid or damp SuperFrost™ slides, and then the slides were air dried and observed using the phase contrast to check that most of the cytoplasm had been eliminated. The cells were then aged at 70 °C for 1 hour or for 2 days at room temperature. The aged slides were passed through an ethanol row of 70%, 90% and 100% ethanol for 5 min in each solution and then placed on warm plate to dry. After that the slides were pre-warmed at 70^0C for 5 minutes at oven and transferred into a denaturing solution (70% (v/v) formamide, 2X saline sodium citrate (300mM sodium chloride, 30mM hydrous tri-sodium citrate, pH 7.0) at 70^0C for 2 minutes. The slides were immediately plunged into ice-cold 70% ethanol for 5 min and then again passed through the ethanol row of 90% and 100% ethanol for 5 min in each solution. Afterwards, the slides were air-dried and kept warm until hybridization with the probe.

2.2.4.3 Probe preparation and hybridization

The chromosome templates 18 and X were made in-house by amplifying flow sorted chromosomes by degenerate oligonucleotide primed polymerase chain reaction (DOP-PCR). These chromosome templates were labelled with biotin-16-dUTP(Roche) by DOP-PCR (10 µl of 5x DOP-PCR buffer, 5 µl of dACGTP (2mM), 2 µl of dTTP(2Mm), 10 µl of biotin-16-dUTP, 5 µl of DOP primer(20µM), 1 µl of taq polymerase(1U/ µl), 12 µl of ddH2O, 5 µl of DNA template). The probe mixture was then prepared by ethanol precipitation of the biotin labelled chromosome paint (8 µl per slide) with the addition of human Cot 1 DNA (7 µl per slide) (Roche), herring sperm DNA (3µl per slide), 1/20 the volume of 3 M sodium acetate pH 5 and 2X volume of 38 µl of ice-cold 100% ethanol (per slide). This mixture was incubated at -80^{0}C for at least 30 minutes followed by centrifugation at 1000g for 30 minutes at 4^{0}C. The DNA pellet was then washed with ice cold 70% ethanol and centrifuged again at 1000g for 15 minutes at 4^{0}C. The supernatant was removed and the pellets were allowed to dry at 50^{0}C on a hot block. The probes were then dissolved in 12µl (per slide) of hybridisation mix (50% formamide, 10% dextran sulphate, 10% 20X SSC, 1% Polyoxyethylene sorbitan monoolaurate (Tween 20)) overnight at room temperature. The probes were denatured at 75^{0}C for 5 minutes and then allowed to re-anneal at 37^{0}C for at least 10 minutes or up to 2 hours. 12 µls of the probe was then applied to the slide, covered with pre-warmed 22 x 22 mm coverslip (Fisher) and sealed with rubber cement (Halfords). The slides were allowed to hybridise with the probe in a humid chamber at 37^{0}C for at least 18 hours.

2.2.4.4 Post-hybridisation washes

The rubber cement was removed and the slides were washed three times for 5 minutes each in buffer A (50% v/v formamide, 2X SSC, pH 7.0) preheated at 45^0C and then slides were then washed three times for 5 minutes each in buffer B (0.1X SSC, pH 7.0) preheated at 60^0C but placed in 45^0C water bath and then slides were transferred to 4X SSC at room temperature. The slides were then incubated with a 100µls blocking solution (4% bovine serum albumin; BSA, w/v) for 10 min at room temperature. In order to detect the biotin labelled probes, each slide was incubated in 100µls of 1:200 diluted streptavidin- Cyanine (Cy3) (Amersham Life Science Ltd) at room temperature for 1 hour. The slides were then washed in a 4X SSC solution containing 0.05% Tween 20 in the dark at 42^0C for 15 minutes with three changes of the solution. Afterwards, slides were mounted in in Vectashield.

2.2.4.5 Microscopy and data analysis

All slides were examined using 100X Plan Fluoropar oil immersion lens (Leica) on an Olympus BX41 fluorescence microscope. pKi-67 positive nuclei were selected randomly as per the experiment by following a rectangular scan pattern and grey-scale images of these nuclei with the DAPI signal pseudocoloured in blue were captured and biotin-streptavidin signal pseudocoloured in green. At least 50 images per slide were captured by Smart Capture 3.00 software and converted into TIFF or PICT format. In order to analyse the images, the images were passed through a simple erosion analysis script using IPLab Spectrum software. The script (used with a kind permission of Prof. Wendy Bickmore and Dr. Paul Perry, University of

Edinburgh) was devised to divide each captured nucleus into 5 concentric shells of equal area, the first shell starting at the periphery of the nucleus going to the interior of the nucleus (5th shell) (Figure 2.2). The script measures the pixel signal intensity of DAPI and the chromosome probe in these five shells and puts the data obtained into a table. The background from the FISH signal was removed by subtracting the mean pixel intensity within the segmented nucleus. In erosion analysis, the percentage chromosome signal intensity measurement per shell was divided by the percentage DNA signal intensity measurement of the same shell in order to normalise the data Shell 1 represents the nuclear periphery and shell 5 the nuclear interior. The normalized proportion of probe was calculated in all 5 shells for at least 50 nuclei. Histograms and standard error bars were plotted using these data. Finally, statistical analyses were performed using the two-tailed student t-tests.

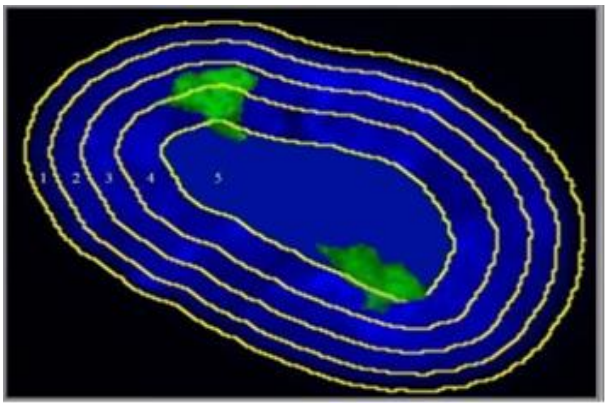

Figure 2.2: Erosion analysis for positioning of chromosome territories. Representative image of erosion analysis script by IP lab software. Shell 5 shows nuclear interior and shell 1 shows nuclear periphery (Croft *et al*., 1999). Chromosomes (green), DAPI (blue).

2.2.5 DNA Halo preparations

DNA Halo was performed by Dr. Craig Clements. Cells were grown for two days on SuperFrost® slides (Fisher, UK) in QuadriPERM^{TM} (Sarstedt, Germany) chambers, at a starting density of 1 x 10^5 and treated as described previously on the day after seeding. The medium was removed and the slides were washed 3 times with 1 X PBS. Slides were then placed in Coplin jars, on ice, containing CSK buffer (10 mM Pipes pH 7.8, 100 mM NaCl, 0.3 M sucrose, 3 mM MgCl2, 0.5% (v/v) Triton-X 100) for 15 minutes. The slides were then washed again three times in 1X PBS. The slides were placed in extraction buffer (2 M NaCl, 10 mM Pipes pH 6.8, 10 mM EDTA, 0.1% (w/v) digitonin, 0.05 mM (v/v) spermine, and 0.125 mM (v/v) spermidine) for 4 minutes. The slides were then rinsed consecutively in 10 **x** PBS, 5 x PBS, 2 x PBS and 1 x PBS, for 1 minute each. The slides were then taken through an ethanol series of 10%, 30%, 70% and 95% (v/v), respectively. The slides were then air dried and stored at 4^0C.

2.2.6 Telomere PNA FISH

In order to detect telomeres on the DNA halo preparations, a telomere PNA FISH/Cy3 kit (Dako) was used following a protocol under the manufacturer's instructions. Unless otherwise stated, the protocol was performed at room temperature. The DNA halo slides were immersed in PBS (pH 7.0) for 15 min with agitation. After that the samples were treated with 4% formaldehyde for 2 minutes and washed in PBS three times for 5 minutes each. To remove unwanted proteins, slides were then immersed and incubated in Coplin jars including preheated 37^0C pre-treatment solution for 10 minutes; a total of 500 µl of pepsin (10 % pepsin; Sigma) was mixed with 50 ml of acidified dH_2O of pH 2 (49.5 ml of deionized water

added to 0.5 ml HCl) and then added to 50 ml PBS and subsequently washed twice with PBS for 5 minutes each. The slides were fixed again with 4% formaldehyde for 2 minutes. The samples were washed two times with PBS for 2 minutes each on the shaking platform. The slides were taken through ethanol series consisting of 70%, 85% and 95% (v/v) ethanol for 5 minutes at each concentration by putting 1 ml on each slide and then air dried at room temperature.

2.2.6.1 Hybridization

20 µl of a Cy3 labelled Oligonucleotide PNA $(CCCTAA)_3$, complementary to telomeres was added to slides. The slides were then placed on a heating block preheated 70-75°C for 2 minutes. Slides were removed from the heating block and incubated in a dark humidified chamber for 2 hours to allow hybridisation.

2.2.6.2 Post-hybridisation washes

The samples were washed twice for 15 minutes in 70% formamide solution in the dark without shaking, followed by washing the slides three times with PBS for 5 minutes each time on the shaker. The halos were then dehydrated in ethanol series (70%, 90%, and 100%) for 5 minutes each by putting 1 ml of ethanol on each slide. Once the slides were air-dried, a total of 15µl of Vecta-shield was added to each slide and the coverslip sealed using rubber cement and the probe was allowed to hybridise on the slide. All slides were examined using 100X oil immersion lens on an Olympus BX41 fluorescence microscope. Fifty images of cell nuclei for each condition were captured at 100X magnification using Smart Capture 3.00 software (Digital Scientific, Cambridge, UK) and were merged as DAPI and CY3. The

proportion of telomeres within the residual nucleus for each treatment were counted and were expressed as a percentage of the total telomeres.

2.2.7 Statistical analysis

Values were expressed as averages ± SEM, and n represents the number of cells analysed. Individual treatments were compared using either two-tailed unpaired t-tests or one-way ANOVAs with Tukey's post-hoc multiple comparison tests where appropriate, and significance was taken as $P \leq 0.05$. The level of significance is indicated as: * $P \leq 0.05$, ** $P \leq 0.01$, *** $P \leq 0.001$ and **** $P \leq 0.0001$.

2.3 Results

2.3.1 Drug treatments alter chromosome territory positions in HGPS fibroblasts

Chromosome 18 positioning

2D-FISH was performed on cells derived from HGPS human dermal fibroblast cell line- AG01972, using whole chromosome paints for chromosome 18. In order to analyse proliferative cells, positive anti Ki-67 staining of cells taken as a marker for proliferation. Figure 2.3 displays representative images for chromosome 18 positioning within HGPS fibroblasts with and without drug treatments. Chromosome 18 territories were predominantly found in the interior of the nucleus (shell 5) in untreated HGPS fibroblasts (Figure 2.4-A) with a value of 1.38 ± signal (%)/ DAPI (%) (n=55). Of the drug treatments studied, two resulted in a significant reduction in the signal (%)/ DAPI (%) ratio for chromosome 18 in shell 5 compared to untreated HGPS fibroblasts. These were FTI-277 + GGTI-2133 (Figure 2.4-F) and FTI-277 +

pravastatin + zoledronic acid (Figure 2.4-B) with signal (%)/ DAPI (%) ratios of 0.58 ± 0.11 ($p<0.001$, n=47) and 0.48 ± 0.11 ($p<0.001$, n=46) respectively. Treatment of HGPS cells with FPZ and N-acetyl resulted in significant increase in the signal (%)/ DAPI (%) ratio for chromosome 18 in shell 2 and shell 4 respectively. FPZ treated cells with signal (%)/ DAPI (%) ratio of 1.51 ± 0.134 ($p < 0.001$, n=48) and N-acetyl treated cells with signal (%)/ DAPI (%) ratio of 1.22 ± 0.12 ($p < 0.01$, n=50).

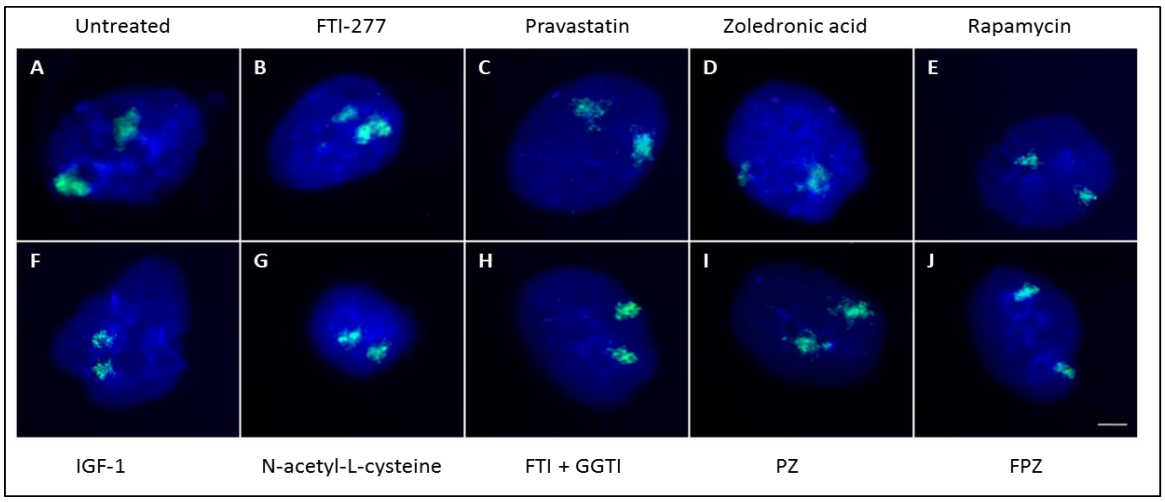

Figure 2.3 Representative images of the position of chromosome 18 within HGPS fibroblast nuclei before and after drug treatments. HGPS fibroblasts derived from laminopathy patient were subjected to 2D-FISH using probes specific to chromosome 18. Whole chromosome painting probes were labelled with biotin and detected using streptavidin conjugated to FITC (green) and the nuclei were counterstained with DAPI (blue). Ki-67 staining is not shown in the images.Magnification: X100 and scale bar = 5 µm.

A

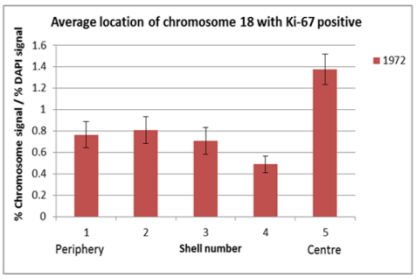
Average location of chromosome 18 with Ki-67 positive
% Chromosome signal / % DAPI signal
1.6
1.4
1.2
1
0.8
0.6
0.4
0.2
0
1
2
3
4
5
Periphery
Shell number
Centre
1972

B

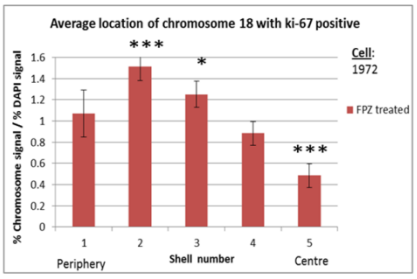
Average location of chromosome 18 with ki-67 positive
% Chromosome signal / % DAPI signal
***
*
***
Cell:
1972
FPZ treated
Periphery
Shell number
Centre

C

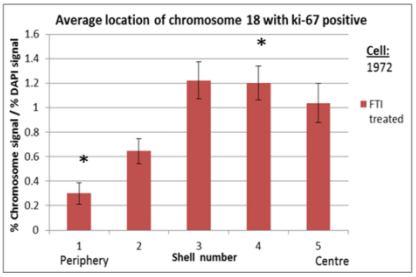
Average location of chromosome 18 with ki-67 positive
% Chromosome signal / % DAPI signal
*
*
Cell:
1972
FTI treated
Periphery
Shell number
Centre

D

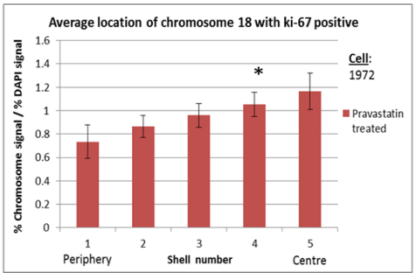
Average location of chromosome 18 with ki-67 positive
% Chromosome signal / % DAPI signal
*
Cell:
1972
Pravastatin treated
Periphery
Shell number
Centre

E

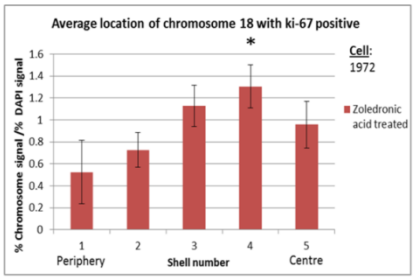
Average location of chromosome 18 with ki-67 positive
% Chromosome signal /% DAPI signal
*
Cell:
1972
Zoledronic acid treated
Periphery
Shell number
Centre

F

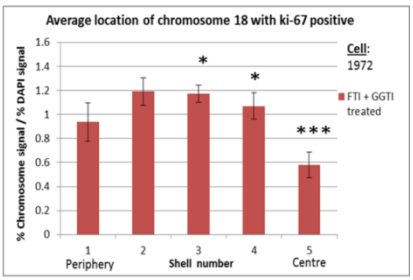
Average location of chromosome 18 with ki-67 positive
% Chromosome signal / % DAPI signal
*
*
***
Cell:
1972
FTI + GGTI treated
Periphery
Shell number
Centre

G

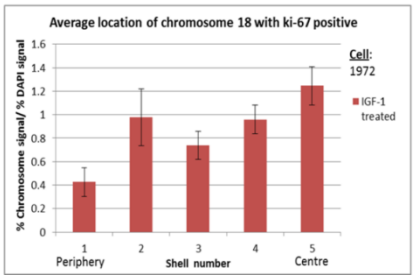
Average location of chromosome 18 with ki-67 positive
% Chromosome signal/ % DAPI signal
Cell:
1972
IGF-1 treated
Periphery
Shell number
Centre

H

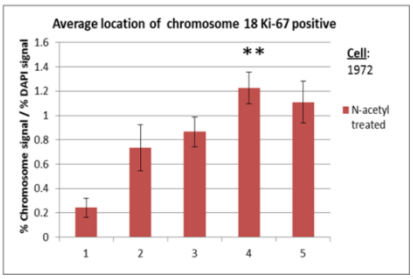
Average location of chromosome 18 Ki-67 positive
% Chromosome signal / % DAPI signal
**
Cell:
1972
N-acetyl treated

I

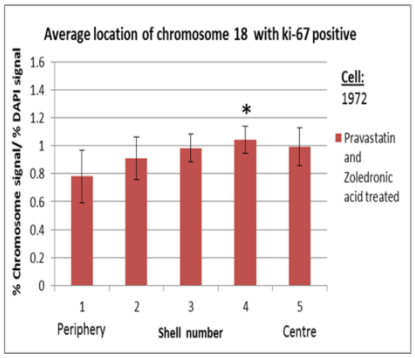
Average location of chromosome 18 with ki-67 positive
% Chromosome signal/ % DAPI signal
*
Cell:
1972
Pravastatin and Zoledronic acid treated
Periphery
Shell number
Centre

J

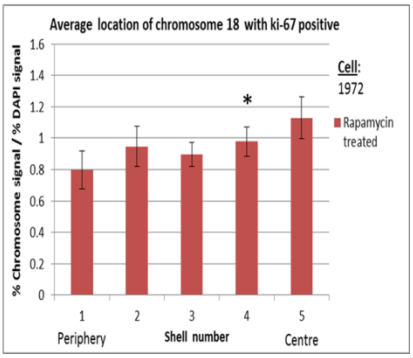
Average location of chromosome 18 with ki-67 positive
% Chromosome signal / % DAPI signal
*
Cell:
1972
Rapamycin treated
Periphery
Shell number
Centre

Figure 2.4 Histograms displaying the position of human chromosome 18 territories with Ki-67 positive in HGPS cells before and after drug treatments. Standard 2D-FISH assay was performed and at least 50 digital images were analysed. Erosion analyses were performed by ascertaining the distribution of the mean proportion of hybridisation signal per chromosome (%), normalised by the percentage of DAPI signal, over five concentric shells of equal area from the nuclear periphery to centre. The x-axis displays the shells from 1–5 (left to right), with 1 being the most peripheral shell and 5 being the most internal shell. The y-axis shows signal (%)/ DAPI (%), from 0 to 1.6 with 0.2 increments.The standard error bars representing the standard error of mean (SEM) were plotted for each shell for each graph (* $P \leq 0.05$, ** $P \leq 0.01$, *** $P \leq 0.001$).

Chromosome X positioning

2D-FISH was performed on cells derived from HGPS human dermal fibroblast cell line- AG01972, using whole chromosome paints for chromosome X. In order to analyse proliferative cells, positive anti Ki-67 staining of cells taken as a marker for proliferation. Figure 2.5 shows representative images for chromosome X positioning within HGPS fibroblasts with and without drug treatments. Chromosome X territories were predominantly found close to the periphery of the nucleus (shell 2) in untreated HGPS fibroblasts (Figure 2.6-A) with a value of 1.31 ± 0.17 signals (%)/ DAPI (%). The signal (%)/ DAPI (%) ratios of the remaining shells are relatively lower. Of the drug treatments studied, none significantly changed the signal (%)/ DAPI (%) ratio for the modal shell 4. However, two of the treatments resulted in a very significant reduction in the signal (%)/ DAPI (%) ratio for chromosome X in shell 5 compared to untreated HGPS fibroblasts. These were FTI-277 (Figure 2.6-D) and FTI-277 + GGTI-2133 (Figure 2.6-C) with signal (%)/ DAPI (%) ratios of 0.29 ± 0.08 ($p<0.01$, $n=50$), and 0.15 ± 0.05 ($p<0.001$, $n=50$) respectively. Four of the treatments resulted

in a significant reduction in the signal (%)/ DAPI (%) ratio for chromosome X in shell 5 compared to untreated HGPS fibroblasts. These were IGF-1 (Figure 2.6-E), Pravastatin (Figure 2.6-F), Zoledronic acid (Figure 2.6-I) and N-acetyl (Figure 2.6-J) with signal (%)/ DAPI (%) ratios of 0.41 ± 0.1 ($P< 0.05$, n=50), 0.37 ± 0.09 ($P<0.05$, n=50), 0.33 ± 0.08 ($P< 0.05$, n=50) and 0.36 ± 0.1 ($P<0.05$, n=50) respectively. Three other drug treatments resulted in a very significant increase the signal (%)/ DAPI (%) ratio for chromosome X in shell 1 compared to untreated HGPS fibroblasts. These were FTI-277 (Figure 2.6-D), FTI-277 + pravastatin + zoledronic acid (Figure 2.6-B), FTI-227 + GGTI (Figure 2.6-C) with signal (%)/ DAPI (%) ratios of 2.04 ± 0.21 ($p<0.001$, n=50), 2.05 ± 0.29 ($p<0.001$, n=49), 1.86 ± 0.22($P< 0.01$, n=50) respectively. Taken together, these data suggest that certain drug combinations (especially those involving FTI-277) can also influence the position of chromosome X towards the nuclear periphery within the HGPS nuclei.

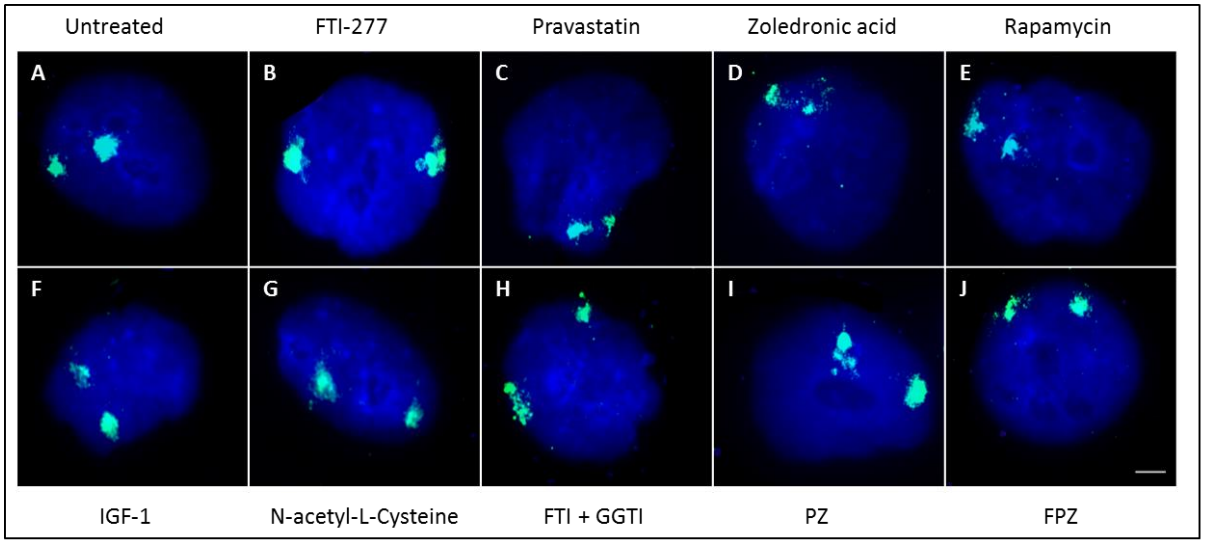

Figure 2.5 Representative images of the position of chromosome X within HGPS fibroblast nuclei before and after drug treatments. HGPS fibroblasts derived from laminopathy patient were subjected to 2D-FISH using probes specific to chromosome X. Whole chromosome painting probes were labelled with biotin and detected using streptavidin conjugated to FITC (green) and the nuclei were counterstained with DAPI (blue). Ki-67 staining is not shown in the images. Magnification = x100.Scale bars = 5 µm

A

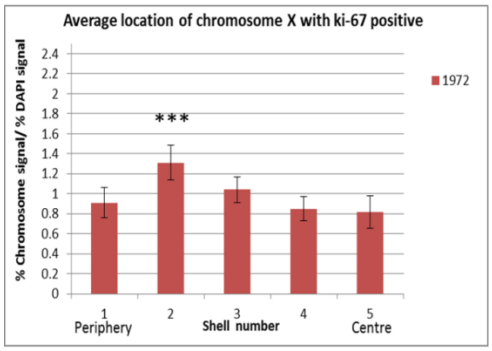
Average location of chromosome X with ki-67 positive
% Chromosome signal/ % DAPI signal
***
1972
1 Periphery
2
3 Shell number
4
5 Centre

B

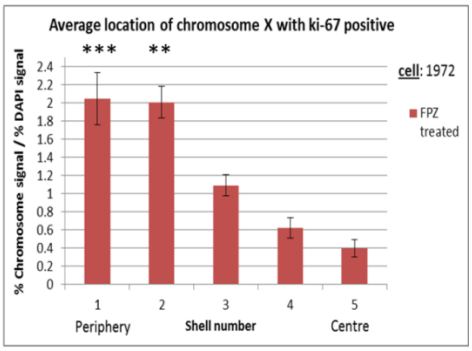
Average location of chromosome X with ki-67 positive
% Chromosome signal / % DAPI signal
*** **
cell: 1972
FPZ treated
1 Periphery
2
3 Shell number
4
5 Centre

C

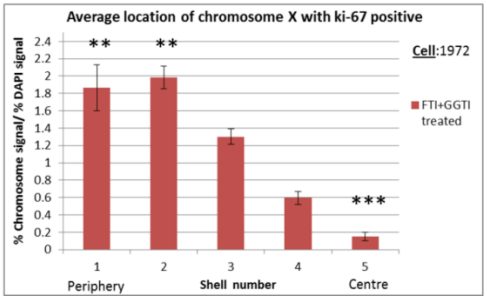
Average location of chromosome X with ki-67 positive
% Chromosome signal/ % DAPI signal
** **
Cell:1972
FTI+GGTI treated
***
1 Periphery
2
3 Shell number
4
5 Centre

D

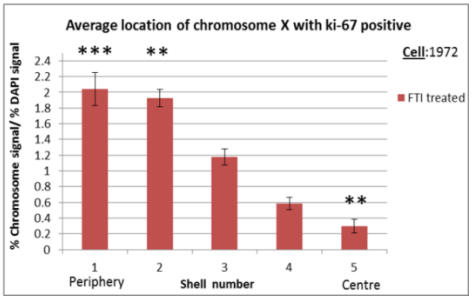
Average location of chromosome X with ki-67 positive
% Chromosome signal/ % DAPI signal
*** **
Cell:1972
FTI treated
**
1 Periphery
2
3 Shell number
4
5 Centre

E

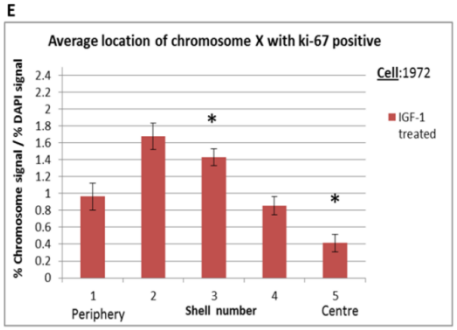
Average location of chromosome X with ki-67 positive
% Chromosome signal / % DAPI signal
Cell:1972
IGF-1 treated
*
*
1 Periphery
2
3 Shell number
4
5 Centre

F

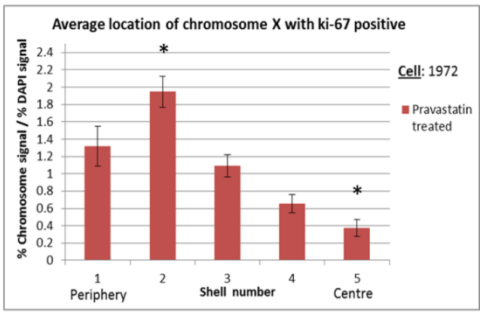
Average location of chromosome X with ki-67 positive
% Chromosome signal / % DAPI signal
*
Cell: 1972
Pravastatin treated
*
1 Periphery
2
3 Shell number
4
5 Centre

G

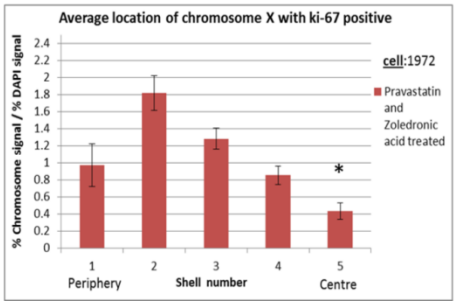
Average location of chromosome X with ki-67 positive
% Chromosome signal / % DAPI signal
cell:1972
Pravastatin and Zoledronic acid treated
*
1 Periphery
2
3 Shell number
4
5 Centre

H

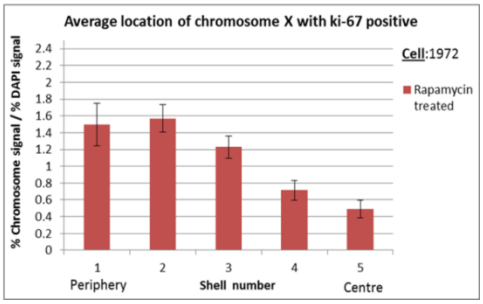
Average location of chromosome X with ki-67 positive
% Chromosome signal / % DAPI signal
Cell:1972
Rapamycin treated
1 Periphery
2
3 Shell number
4
5 Centre

I

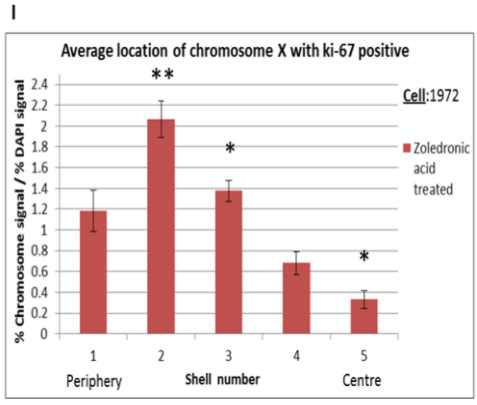
Average location of chromosome X with ki-67 positive
% Chromosome signal / % DAPI signal
**
*
*
Cell:1972
Zoledronic acid treated
1 Periphery
2
3 Shell number
4
5 Centre

J

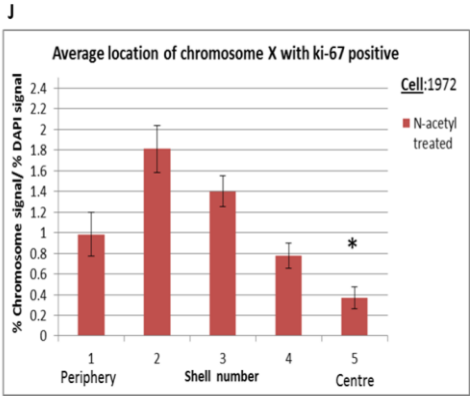
Average location of chromosome X with ki-67 positive
% Chromosome signal/ % DAPI signal
Cell:1972
N-acetyl treated
*
1 Periphery
2
3 Shell number
4
5 Centre

Figure 2.6 Histograms displaying the position of human chromosome X territories with ki-67 positive in HGPS cells before and after drug treatments. Standard 2D-FISH assay was performed and at least 50 digital images were analysed. Erosion analyses were performed by ascertaining the distribution of the mean proportion of hybridisation signal per chromosome (%), normalised by the percentage of DAPI signal, over five concentric shells of equal area from the nuclear periphery to centre. The x-axis displays the shells from 1–5 (left to right), with 1 being the most peripheral shell and 5 being the most internal shell. The y-axis shows signal (%)/ DAPI (%), from 0 to 2.5 with 0.2 increments. The standard error bars representing the standard error of mean (SEM) were plotted for each shell for each graph. Significant differences before and after the drug treatments are denoted by stars (* $P \leq 0.05$, ** $P \leq 0.01$, *** $P \leq 0.001$).

2.3.2 The proportion of telomeres within the residual nuclei of DNA Halo's

Figure 2.7 displays representative images for telomere positioning within HGPS and normal 2DD DNA Halos with and without drug treatments. Table 2.1 summarizes the percentage of interior telomeres in untreated and drug treated 2DD and 1972 HGPS cells. The mean proportion of telomeres with the residual nucleus exhibited by untreated 2DD fibroblasts was 93.9 ± 0.5% (n=31) (Figure 2.8-A). For AG01972 fibroblasts (Figure 2.8-A), the proportion of interior telomeres is 80.0 ± 2.0% (n=22), which is significantly less than the control 2DD. Upon treatment with FTI-277 (Figure 2.8-A), the mean proportion of interior telomeres is increased to 87.9 ± 1.0% (n=37), which is significantly greater than untreated AG01972 fibroblasts (80.0 ± 2.0%, $p<0.0001$, n=22). The mean proportion of interior telomeres in FTI-277 treated AG01972 fibroblasts remained significantly reduced compared to control 2DD fibroblasts (93.9 ± 0.5%, $p<0.001$, n=31). Upon treatment with pravastatin (Figure 2.8-B), the mean proportion of interior telomeres is increased to 93.2 ± 0.4% (n=49),

which is significantly greater than untreated AG01972 fibroblasts. The mean proportion of interior telomeres in pravastatin treated AG01972 fibroblasts was not significantly different compared to control 2DD fibroblasts (93.9 ± 0.5%, n=31). Upon treatment with zoledronic acid (Figure 2.8-C), the mean proportion of interior telomeres is increased to 92.8 ± 1.0% (n=37), which is significantly greater than untreated AG01972 fibroblasts (80.0 ± 2.0%, $p<0.0001$, n=22). The mean proportion of interior telomeres in zoledronic acid treated AG01972 fibroblasts was not significantly different compared to control 2DD fibroblasts (93.9 ± 0.5%, n=31). Upon treatment with rapamycin (Figure 2.8-D), the mean proportion of interior telomeres is to 76.0 ± 1.0% (n=45), which is not significantly different from untreated AG01972 fibroblasts (80.0 ± 2.0%, $p>0.05$, n=22). Upon treatment with N-acetyl-L-cysteine (Figure 2.8-E), the mean proportion of interior telomeres is increased to 92.4 ± 0.7% (n=51), which is significantly greater than untreated AG01972 fibroblasts. Upon combination treatment with FTI-277 and GGTI-2133 (Figure 2.8-F), the mean proportion of interior telomeres is increased to 96.1 ± 0.5% (n=46), which is significantly greater than untreated AG01972 fibroblasts and again similar to control cells. Upon combination treatment with pravastatin and zoledronic acid (Figure 2.8-G), the mean proportion of interior telomeres is increased to 93.6 ± 0.5% (n=48), which is significantly greater than untreated AG01972 fibroblasts (80.0 ± 2.0%, $p<0.0001$, n=22). The mean proportion of interior telomeres in pravastatin and zoledronic acid treated AG01972 fibroblasts was not significantly different compared to control 2DD fibroblasts. Upon combination treatment with FTI-277, pravastatin and zoledronic acid (Figure 2.8-H), the mean proportion of interior telomeres is increased to 92.3 ± 0.8% (n=38), again significantly greater than untreated AG01972 fibroblasts and similar to control cells. Taken together, pravastatin, zoledronic acid, N-Acetyl-L-

cystein and FTI alone and combination of drugs; FTI together with GGTI, FTI together with pravastatin and zoledronic acid, pravastatin together with zoledronic acid are able to to rescue the association of telomeres in DNA halos to the nuclear matrix. However, taken together, these data suggest that rapamycin does not affect any changes.

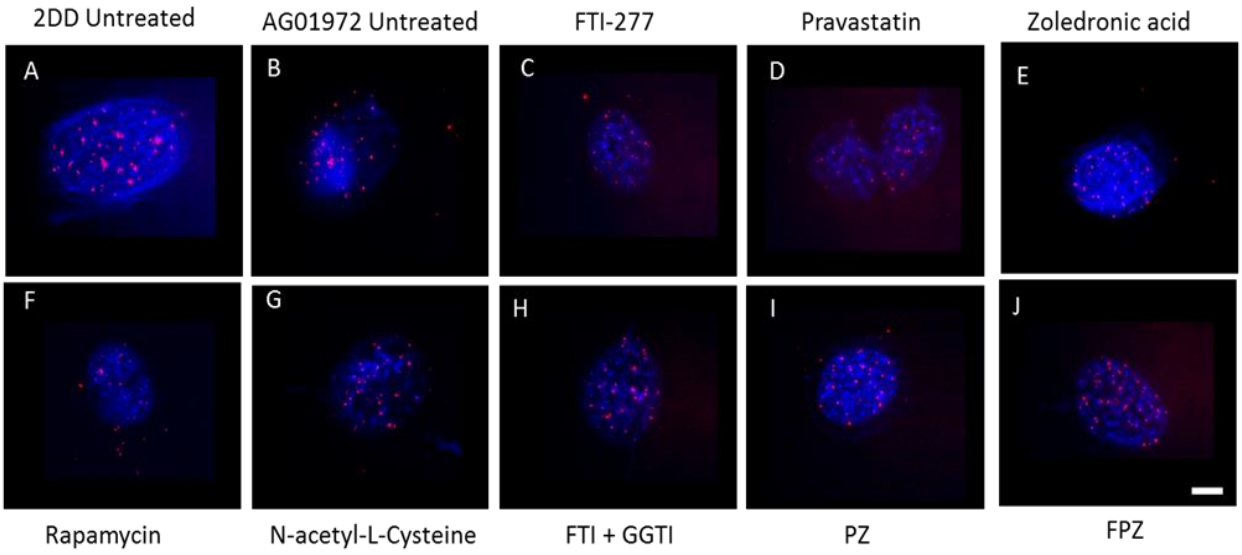

Figure 2.7 Representative images of telomere position of DNA halo preparations of normal and HGPS fibroblasts with and without drug treatment. Images of fixed 2DD and AG01972 DNA halos stained with both DAPI and Cy3 telomeric PNA probes were captured at 100X magnification. Results for the treatments are shown as a) 2DD untreated, b) AGO1972 untreated, c) FTI-277 (2.5 µM for 24 hours), d) pravastatin (1 µM for 24 hours), e) zoledronic acid (1 µM for 24 hours), f) rapamycin (10 nM for 24 hours), g) N-acetyl-L-cysteine (20 µM for one hour), h) FTI-277 and GGTI-2133 (both 2.5 µM for 24 hours), I) pravastatin and zoledronic acid (both 1 µM for 24 hours) and J) FTI-277 (2.5 µM for 24 hours), pravastatin and zoledronic acid (both 1 µM for 24 hours). Magnification = X100.Scale bar = 5 µm.

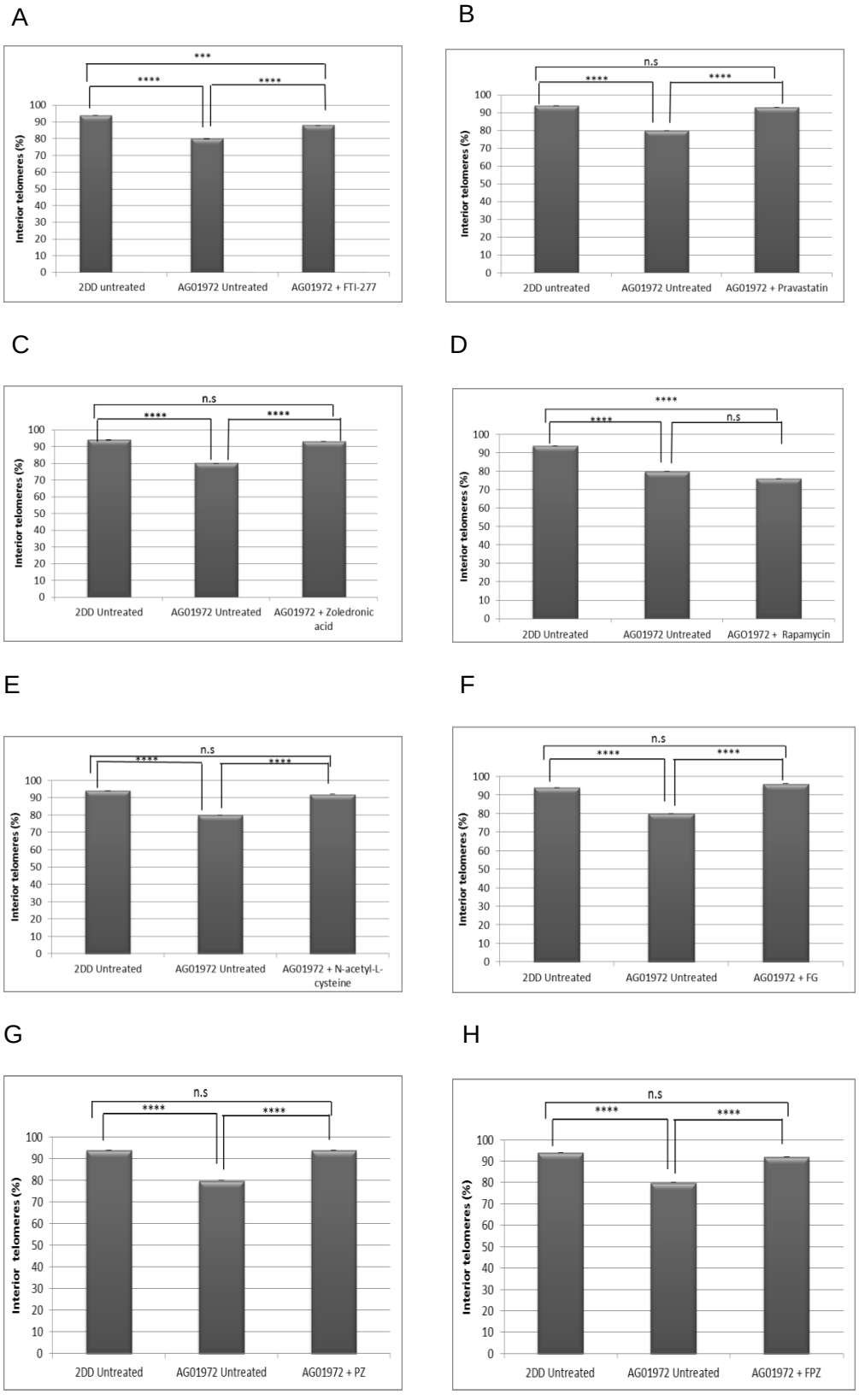

Figure 2.8 Analysis of telomere position of DNA halo preparations of normal and HGPS fibroblasts with and without drug treatment. Results for the treatments are shown as a) 2DD with zoledronic acid (1 µM for 24 hours), b) FTI-277 (2.5 µM for 24 hours), c) pravastatin (1 µM for 24 hours), d) zoledronic acid (1 µM for 24 hours), e)

rapamycin (10 nM for 24 hours), f) N-acetyl-L-cysteine (20 µM for one hour), g) FTI-277 and GGTI-2133 (both 2.5 µM for 24 hours), h) pravastatin and zoledronic acid (both 1 µM for 24 hours) and i) FTI-277 (2.5 µM for 24 hours), pravastatin and zoledronic acid (both 1 µM for 24 hours). The proportion of interior telomeres is expressed as a percentage of the total number of telomeres present. Error bars represent ± SEM. Significant differences are denoted by stars (* P ≤ 0.05, ** P ≤ 0.01, *** P ≤ 0.001, *** P ≤ 0.0001). n.s= not significant.

Table 2.1: The percentage of telomeres associated with nuclear matrix in untreated and treated cells.

	Interior telomeres
2DD untreated	94
AG01972 untreated	80
AG01972 + FTI-277	88
AG01972 + Pravastatin	93
AGO1972 + Zoledronic acid	93
AG01972 + Rapamycin	76
AG01972 + N-acetyl-L-cysteine	92
AG01972 + FG	96
AG01972 + PZ	94
AG01972 + FPZ	92

2.4 Discussion and conclusion

2.4.1 Positioning of chromosomes 18 and X before and after drug treatments in HGPS cells

Gene-rich chromosomes positioned towards the nuclear interior and gene-poor chromosomes towards the nuclear periphery. It has been postulated that nuclear lamina proteins play a role in genome behaviour and stability therefore we wanted to investigate whether whole chromosomes territories of 18 and X would alter their behaviour in HDF cells with mutation in A-type lamin. Chromosome 18 and X are known as gene-poor chromosomes to be positioned at the nuclear periphery

adjacent to the nuclear lamina in control cells. FISH provides a powerful tool to visualize the localization of specific chromosomes within interphase nuclei (Volpi and Bridger, 2008). In order to assess only proliferative cells we used anti-pKi-67 antibody as a proliferation marker. Interestingly, it was shown using 4-HNE as a marker for senescent cells in mouse liver cells that senescent cells induced a bystander effect that spreads DNA damage and eventually induces cell senescence in primary checkpoint-competent cells *in vitro* and possibly *in vivo* (Nelson *et al*., 2012). In previous studies, it has been demonstrated that in the nuclei of proliferating HDFs, interphase chromosome positioning is altered from patients diagnosed with classical HGPS (Mehta *et al*., 2011). In this study, we employed a number of drugs to assess if they could restore chromosome positioning in AG01972 HGPS cells to normal. A positioning of chromosome 18 was shown becoming located more internally in nonproliferating normal human dermal fibroblasts. However, positioning of chromosome X displayed little change at the nuclear periphery both in proliferating and nonproliferating normal HDFs (Meaburn *et al.*, 2007). Meaburn *et al.* (2007) demonstrated that chromosomes 18 located in the nuclear interior in proliferating laminopathy cells (Meaburn *et al*., 2007). Mehta *et al*. (2011) demonstrated that chromosome 18 is located in an interior position in interphase nuclei of senescent HGPS cells and it was revealed that after treatment with FTI-277 alone and together with GGTI-2147, chromosome 18 was repositioned from an internal location to a peripheral one (Mehta *et al*., 2011). We also demonstrated that chromosome 18 occupies an interior location in proliferating untreated HGPS nuclei. Using a combination of drugs; FTI-277 + GGTI-2133 and FTI-277 + pravastatin + zoledronic acid resulted in relocation of chromosome 18 from nuclear interior to nuclear periphery within Ki-67 positive interphase nuclei. Treatment of HGPS cells with a

FTI only showed that chromosome 18 moved towards intermediate location which suggests GGTI is needed to remove geranyl moieties from the lamin. Using other drug treatments; pravastatin, zoledronic acid, rapamycin, insulin-like growth factor 1, N-acetyl-L-cysteine resulted in relocation of chromosome 18 from nuclear interior to an intermediate location in Ki-67 positive interphase nuclei. Since whole chromosome 18s are moved upon treatment, it can be suggested that drugs affect somehow the binding of mutant lamin A or lamin binding proteins with chromosome 18. Taken together, these data suggest that combinations of drugs are able to restore the position of chromosome 18 from an interior position to one that is closer to the nuclear periphery.

Meaburn and colleagues (2007) showed that the X chromosome remains at the periphery in all proliferating laminopathy cells analysed (Meaburn *et al*., 2007). Mehta *et al.* (2011) demonstrated that chromosome X localizes to the nuclear periphery in senescent HGPS cells and it was shown that the X chromosome did not change nuclear position after FTI-277 treatment alone nor with FTI-277 and GGTI-2147 together (Mehta *et al*., 2011). We demonstrated that chromosome X occupies a peripheral location in proliferating untreated HGPS nuclei. Using combinations of drugs; FTI-277 + pravastatin + zoledronic acid and FTI-277 together with GGTI-2133 resulted in relocation of chromosome X more towards periphery within Ki-67 positive interphase nuclei. Furthermore, with FTI alone chromosome X moved more towards periphery as well. Remarkably, chromosome X was not repositioned after rapamycin treatment alone. In line with our results, it was revealed that chromosomes 18 and X are positioned away from the nuclear periphery in proliferating mutant *LMNA* HDF cells (Meaburn *et al.,* 2007). It is noteworthy that in proliferating *LMNA* mutated HDF

cells both chromosome 18 and X mimic their position in non-proliferating control cells (Mehta *et al.,* 2007).

2.4.2 Telomere anchorage by the NM in normal and HGPS fibroblasts before and after drug treatment in the DNA halo assay

Telomeres are shortened with each cell division due to the end replication problem; once telomere length reaches a critical length, the cells enter replicative senescence (Stewart and Weinberg, 2006). It has been demonstrated that such eroded telomeres trigger DNA damage checkpoint responses which in turn leads to this irreversible G1/S cell cycle arrest (d'Adda di Fagagna *et al*., 2003). In light of these facts, we thought it pertinent to examine and compare telomere interactions with the NM in control (2DD) and typical HGPS (AG01972) HDFs by coupling the DNA halo preparation with telomere PNA FISH (Bridger and Lichter, 1999), using combination of drug treatments. We have demonstrated that telomere anchorage with the NM in AG01972 HGPS cell line, which produces a mutant form of lamin A (progerin) is severely perturbed. More than 20% of telomeres were found outside the residual nucleus. De *Vos et al*., (2010) reported that in HDF $^{mut/mut}$ cells, telomere mobility is higher and less confined compared with normal fibroblasts. However, intriguingly in their experiments, it was exhibited that telomere movement appeared more restricted in HGPS cells (De Vos *et al.*, 2010). Remarkably, treatment of HGPS cells with FTI is able to increase telomere mobility (De Vos *et al.*, 2010). It is known that progeria cells have shorter telomeres (Allsopp *et al.*, 1992) and chromosomal aberrations in the setting of telomere dysfunction were shown to be triggered by progerin expression in HGPS cells (Benson *et al.*, 2010). Jegou's group (2009) showed that shorter telomeres have increased telomere mobility in a telomerase negative human

cell line (Jegou *et al.*, 2009) and in line with our findings which has demonstrated that telomere binding to the NM is reduced in HGPS cells. Gonzales-Suarez *et al. (*2009) demonstrated that the accumulation of farnesylated lamin A is concomitant with a migration of telomeres towards the nuclear periphery (Gonzalo-Suaraz, Redwood and Gonzalo, 2009). Raz *et al*. (2008) reported that association of telomeric repeats with lamina intranuclear structure is increased in cells expressing lamin mutants (Raz *et al.*, 2008). It can be suggested that for the correct localization of telomeres within the nucleus, intranuclear lamins play a vital role (De Vos *et al.*, 2010). Whereas, telomere-NM interactions in control cell line (2DD) reveal that approximately 93-94% of telomeres were found within the residual nucleus. The results are also in agreement with earlier study which shows that at least 80% of telomeric DNA is attached to this structure (de Lange, 1992). The findings also confirm previous HALO-FISH experiments using telomere-specific probes (Luderus *et al.*, 1996). Zoledronic acid treated 2DD cells showed that 95-96% of telomeres were found within the residual nucleus which does not change statistically the telomere location. From this study, it is clear that FTI-277, pravastatin, Zoledronic acid, N-acetyl-L-cysteine and all three combination treatments; FG, PZ, FPZ, have a positive effect on anchoring the genome to the nuclear matrix in AG01972 cell line. On the contrary, rapamycin treated AG01972 cells give rise to the reduction of anchorage of telomeres to the nuclear matrix having approximately 76-77% of telomeres which does not show any significant difference compared with untreated AG01972 cells.

In our study we employed a NM extraction followed by telomere PNA FISH to analyse telomere-NM anchorage in HGPS AG01972 cell line harbouring G608G *LMNA* mutation. Our findings indicate that telomere binding to the NM is reduced in

untreated AGO1972 cell line. In contrast, Raz *et al*. (2009) group examined HGPS cell line harbouring R133L and R220Q *LMNA* mutations employing chromatin immunoprecitation (ChiP) and quantitative PCR, whereas De Vos *et al*. (2010) examined HGPS cell line harbouring G608C *LMNA* mutation which produces the same progerin molecule as G608G, employing transfection biology. These two studies' findings revealed that telomere binding to the NM is augmented. Therefore, it can be suggested that using different methodologies and also different mutations in *LMNA* are likely to give rise to have distinct telomere-nuclear matrix anchorage results.

.

Chapter 3: Characterisation of hTERT normal and HGPS fibroblast cell lines

Manuscript in Preparation: M. U. Bikkul, G. Bourne, E. Makarov, R. Faragher, C. Parris, I. R. Kill and J. M. Bridger

3.1 Introduction

A gradually decreasing fraction of proliferating cells give rise to the limited lifespan of human fibroblasts in culture (Kill and Shall, 1990). This technical barrier causes an important obstacle to carry out research on cells. Furthermore, a previous study demonstrated that HGPS fibroblasts had a reduced lifespan in culture by measuring population doublings than a control group of fibroblast cultures (Tollefsbol and Cohen, 1984). HGPS cells are known to become senescent more rapidly compared to normal fibroblast cells (Bridger and Kill, 2004). In our study to overcome this obstacle and have continuous HGPS cells, we employed normal and HGPS human fibroblast cell lines infected with a defective retrovirus encoding human telomerase reverse transcriptase to extend the life span of cell. In other words, cells were immortalised (hTERT) (Wallis *et al.*, 2004). The genes for the human telomerase RNA component-hTR and the catalytic subunit-hTERT were cloned in 1995 and 1997 respectively and sufficient to activate telomerase *in vitro* (Kilian *et al.*, 1997; Weinrich *et al.*, 1997; Feng *et al.*, 1995). Although hTR is present in most adult human cells, hTERT is involved in regulation of telomerase activity (Counter *et al.,* 1998; Kilian *et al.,* 1997; Feng *et al.,* 1995). Normal human somatic cells have limited proliferative lifespan due to lack of telomerase activity leading progressively lose telomeric DNA with each round of cell division and onset of cell sensescence(Harley *et al*., 1990). In order to prevent entry of the normal telomerase-negative cells into senescence, it was shown that introduction of hTERT into cells *in vitro* can lead to an extension of the life-span (Bodnar *et al.*, 1998). Typical progeria cell line, T06 has the classical *de novo* single base substitution, a C>T [Gly608Gly (G608G)] in exon

11 of the *Lamin A* gene (*LMNA*) (De Sandre-Giovannoli *et al.*, 2003). Atypical progeria cell line, T08 has an unknown mutation (Wallis *et al.*, 2004).

The aim of the study within this chapter is to characterise hTERT immortalised normal, typical and atypical HGPS cells. Therefore cell growth, percentage of fraction of proliferating cells, PCNA analysis, nuclear shape, and cell movement of our cells were assessed to compare the differences. Furthermore, lamin A/C, vimentin and progerin proteins were evaluated.

3.2 Materials and methods

3.2.1 Cell Culture

In collaboration with Gemma Bourne, cell culture was performed. hTERT (Human Telomerase Reverse Transcriptase) Human dermal fibroblasts immortalised cell lines: NB1T, TO6 and TO8 have been employed in our experiments. NB1 (normal 8 year old boy) primary cell line was immortalised named NB1T and kindly provided by Dr. Chris Parris, Brunel University, London. AG06297 (typical 8 year old boy) progeria cell line and AG08466(atypical 8 year old female) progeria fibroblast cell line were immortalised, named T06 and T08 respectively and kindly provided by Prof. Richard Faragher, The University of Brighton (Wallis *et al.*, 2004). All cell lines became approximately 80% confluent in three days, therefore these cells were harvested and passaged twice every week. All cell lines have been cultured as described in section 2.2.1.

3.2.2 Serum responsive test and immunostaining

In collaboration with Gemma Bourne, serum responsive test was performed. NB1T, T06 and T08 cell lines were cultured for 1 week. Firstly, these cell lines were cultured in DMEM with the following additives: 0.5 % FBS (Gibco), 2% (v/v) penicillin and streptomycin(P/S) antibiotics (Gibco) and 200 mM L-glutamine (Gibco) in 90 mm of petri dishes for 4 days and the medium was refreshed with 0,5 % medium including FBS and P/S each day and then the amount of serum was increased from 0.5 % to 15% for the rest of the 2 days experiment. All cell lines were stained with Ki-67 during the 1 week experiment as described in the indirect immunofluorescence section 3.2.3.

3.2.3 Indirect Immunofluorescence

3.2.3.1 Fixation

NB1T, T06, T08 cell lines were reseeded into 35 mm petri dishes containing 13 mm circular coverslips and once cell lines reached 80% confluency, the cells were washed three times with 1X phosphate buffered saline (PBS) (NaCl 0.8% (w/v), KCl 0.02% (w/v), Na_2HPO_4 0.0115% (w/v), KH_2PO_4 0.02% (w/v). The cells were then fixed with 3.7 % formaldehyde (w/v) for 7 minutes at room temperature followed by another three washes in 1X PBS. Subsequently, cells were treated with ice-cold methanol-acetone (M:A=1:1, v/v) for 4 minutes at room temperature and then methanol-acetone was removed and the coverslips dried for 7 minutes and subsequently the coverslips were rinsed three times with 1X PBS. The cells were

treated with PBS/ FBS mixture (1:500 dilution) at room temperature for 10 minutes and then transferred to an humidified chamber.

3.2.3.2 Antibody staining

Firstly, the cells were incubated with 10 µl of primary antibody as shown in table 3.1, diluted in 1% (v/v) FBS in 1X PBS, placed in an humidified chamber either for 1 hour at room temperature or overnight at 4^{o}C and washed 27 times in 1X PBS followed by incubation in 10 µl fluorochrome-conjugated secondary antibody as shown in table 3.2, diluted with 1% FBS in 1X PBS. Cells were incubated in the dark for either 30 min at 37^{0}C or 1 hour at room temperature. The cells were washed 27 times in 1X PBS followed with a final wash in double distilled water and coverslips were mounted with mowiol mountant medium containing DAPI counterstain.

Table-3.1: List of primary antibodies used with their appropriate dilution according to manufacturers' instructions.

Primary antibodies	Dilution factors
Goat anti-lamin A (Abcam ab8980-1)	**1:50**
Mouse anti-lamin A/C (NCL-LAM-AC)	**1:100**
Mouse anti-progerin (Enzo Life Sciences , ALX-804-662-R200)	**1:50**
Mouse anti-PCNA (Immunoconcepts-2037)	**1:10**
Rabbit anti-ki67 (DAKO A0047)	**1:30**

Table-3.2: List of secondary antibodies used with their appropriate dilution factor according to manufacturer's instructions.

Secondary antibody	Dilution factor
Goat anti-mouse (FITC)- Sigma- F9006	**1:64**
Goat anti-mouse (TRITC)- Sigma- T-5393	**1:30**
Rabbit anti-goat (FITC)- Sigma- F-7367	**1:50**
Swine anti-rabbit (TRITC)- Dako R0156	**1:25**

3.2.3.3 Image acquisition

All immunostained slides were observed and visualised using 40X or 100X objectives on the Axioplan Zeiss fluorescence microscope. To take images with the 100X objective, 'Immersol 518F' immersion oil was used. In order to capture fluorescence images, 'The Progress' software was used in high resolution of 1290 x 572 VGA and live images in low resolution of 644 x 490 VGA and exposure time was set manually as 80 miliseconds. Images were stored in TIFF format and analysed using 'Image J' software.

3.2.4 Nuclear shape analysis of NB1T, T06 and T08 cell lines

In collaboration with Gemma Bourne, nuclear shape analysis was performed. Randomly selected DAPI stained nuclei (250) for each cell line were captured and analysed by 'Image J' software and converted into TIFF format. The parameters used for the analysis were: Area, perimeter, aspect ratio (major axis/minor axis) and circularity. The raw data obtained from the image analysis software were transferred to a Microsoft Excel worksheet for further analysis. Overlapping nuclei from the results of excel were excluded. Averages and standard deviation were calculated for all parameters. Different attributes of shape such as circularity and aspect ratio were calculated using the formulas below.

$$\text{Circularity} = (4\pi \times \text{Area}) / (\text{perimeter})^2$$

$$\text{Aspect ratio} = \text{Major axis} / \text{minor axis}$$

3.2.5 Cell movement analysis of NB1T, T06 and T08 cell lines

In collaboration with Gemma Bourne and Dr. Ian Kill (Brunel University, London), cell movement analysis was performed. Live fluorescence microscopy was employed to track the movements of individual cells. Petri dishes were placed into the designated mobile incubator to keep the cells alive. CO_2 gas was supplied and temperature was set at 37^{o}C. 180 images were captured automatically in a total of 8

hours for each NB1T, T06 and T08 cell lines with "Axiovision". The parameters of tracking were adjusted to 5 minutes time interval and 0.67 µm distance calibration. In order to analyse the movements of cell lines, 'Image J' software was used. The format of the images was changed to TIFF format and then image section and stack section was chosen to convert the images to video stack. The parameters of drawings were adjusted to dot size; 5 and line width; 3. Subsequently 'add track' section was chosen to commence our cell movement analysis. All the results were transferred to a Microsoft Excel worksheet for further analysis.

3.2.6 Electrophoresis and western blotting

In collaboration with Gemma Bourne and Dr. Ian Kill (Brunel University, London) electrophoresis and western blotting experiments were performed. NB1T, TO6, T08 fibroblast cell lines were cultured for 72 hours. Cell numbers for each cell line were calculated by routine cell culture. One petri dish was used for each cell line and each dish was washed 3 times with 1X PBS and afterwards to lyse the cells 16 µl of 3X SDS sample buffer per 10^6 number of cells was used (100mM Tris-HCL pH6.8 (w/v), 4% SDS (v/v), 0.2% Bromophenol blue (v/v), 20% glycerol, 0.2 % β-mercaptoethanol (v/v) for each cell line. The samples were boiled at 100^{o}C for 3 minutes and stored at -20^{o}C until needed. Before use, cells in 3X sample buffer were defrosted on ice and then boiled for 3 minutes at 100^{o}C and placed on ice. Cells were loaded onto mini-protean 4-20% Tris glycin (Bio-rad) gels at a concentration of 2 x 10^5 per well in 1X SDS-PAGE running buffer (25mM Tris, 192 mM glycine, 0,1 % SDS (W/V) at 100V until the dye front reached the reference line. "Precision Plus Protein™ All Blue Prestained Protein Standards" (Bio-Rad) was used to detect protein size. Proteins were then electrophoretically transferred onto nitrocellulose membrane (Amersham

Hybond –Cextra, Amersham Biosciences) in 1X transfer buffer (50 mM Tris, 380 mM glycine, 20% methanol (v/v)) for 1 hour at 100 V. Membranes were incubated in blocking solution (4%(w/v)) dried milk powder (Marvel) in 1X transfer buffer overnight at 4^{o}C followed by incubation in primary antibodies in 1% FBS/PBS for 1 hour at 4^{o}C, table 3.3. Following two washes for 5 minutes in 1X TBS-Tween 20(50mM Tris pH 7.4, 150 mM NaCl, 0.1 % Tween 20(v/v)) and then membranes were incubated in horseradish peroxidase (HRP) or alkaline phosphatase conjugated secondary antibodies (table 3.4) for 1 hour at room temperature. 1X TBS-Tween 20 washes were then repeated and membranes were then subjected to antibody detection. In order to detect horse radish peroxidase conjugated secondary antibody, chemiluminiscent solution (Solution A: 5 ml Tris pH 8.0, 22 µl courmic acid, 50 µl luminol, Solution B: 5 ml Tris pH 8.0, 3 µl 20% H2O2) were mixed and membranes were incubated in solution for 5 minutes in the dark. In order to detect alkaline phosphatase conjugated secondary antibodies, "Fast red" tablets (Sigma) were dissolved in 10 ml of deionized water then membranes were incubated in the solution until the expected bands appeared on the membrane. Excess reagent was drained and the blot was covered in clear cling film and exposed to UV light by using Bio-rad imaging software.

Table-3.3: List of primary antibodies used with their appropriate dilution factor according to manufacturer's instructions for western blotting.

Primary Antibodies	Dilution factors
Mouse anti-lamin A/C(NCL-LAM-AC)	**1:200**
Goat anti-Vimentin(Sigma V-4630)	**1:200**

Table-3.4: List of secondary antibodies used with their appropriate dilution factor according to manufacturer's instructions for Westernblotting.

Secondary Antibodies	Dilution factors
Rabbit anti-mouse peroxidase Sigma-A9044	**1:160,000**
Rabbit anti-goat Vimentin alkaline Phosphotase Sigma – A8025	**1: 30,000**

3.2.7 Reverse Transcriptase Polymerase Chain Reaction (RT-PCR)

3.2.7.1 RNA purification

RT-PCR was performed in collaboration with Gemma Bourne and Dr. Makarov (Brunel University, London). RNA purification was performed using NucleoSpin® RNA L mammalian total RNA kit (Macherey- Nagel). All cell lines; NB1T, T06 and

T08 were cultured in 90 mm dishes for at least 3 days after seeding, after which the cells were washed with sterile 1X PBS with three changes of the buffer. The cells were lysed and RNases inactivated by incubation in a mixture containing 1.8 ml lysis buffer(buffer RA1) and 18 µl β-mercaptoethanol(β-ME) for no longer than 2 minutes with constant agitation by vortexing. The lysate was applied to a NucleoSpin®Filter L placed in a collection tube and sample was centrifuged for 10 min at 4,500 g. Therefore, the sample was homogenized by removal of residual insoluble material and simultaneous reduction of lysate viscosity. The nucleoSpin® Filter L was discarded and 1.8 ml ethanol (70%) was added to the lysate to isolate RNA from purified samples in a tube and mixed by vortexing 2 x 5 seconds. The lysate-ethanol mixture (maximal 3.8 ml) was loaded onto a Nucleospin® RNA L column and was centrifuged for 3 min at 4,500 g. 2.2 ml Membrane Desalting Buffer (MDB) was added to the Nucleospin®RNA L column and was centrifuged for 3 min at 4,500 g and flow-through was discarded. In a sterile microcentrifuge tube, DNase reaction mixture was prepared (235 µl reaction buffer for rDNase and 25 µl reconstituted rDNase were mixed) per Nucleospin®RNA L column and mixed thoroughly but gently. Isolated RNA from each sample was maintained on ice at all times. DNase reaction mixture (250 µl) was applied directly onto the centre of the silica membrane and was incubated at room temperature for 15 min. The washing consists of three steps: 1) Buffer RA3 (2.6ml) was added to the Nucleospin®RNA L column and was incubated at room temperature for 2 min. Subsequently, the sample was centrifuged 3 min at 4,500 g and then the supernatant was discarded and the column was placed back into the collection tube. 2) Buffer RA3 (2.6ml) was added to the Nucleospin®RNA L column and then, it was centrifuged 3 min at 4,500 g. 3) Buffer RA3 (2.6ml) was added to the Nucleospin®RNA L column and subsequently it was

centrifuged for 5 min at 4,500 g to dry the membrane completely. The column was placed into a fresh collection tube. RNase-free H_2O (500 µl) was pipetted directly onto the centre of the silica membrane and was incubated for 2 min at room temperature and was centrifuged for 3 min at 4,500 g. In order to quantify the RNA, the nano-drop was employed. Firstly, one drop of RNase free H_20 was dropped onto the point and the blank option was selected and afterwards, the point was wiped with tissue and subsequently, samples were dropped onto the point for the quantification sequentially. Purified RNA isolated from each sample was stored at -80^{o}C until further use.

3.2.7.2 cDNA and Reverse Transcriptase Polymerase Chain Reaction(RT-PCR)

First strand cDNA synthesis was performed using Superscript^{TM} II reverse transcriptase kit (Invitrogen). 1 µg of RNA (2, 9 µl RNA + 7,1µl H_20, in total 10 µl RNA) from each NB1T, TO6 and T08 cell lines and purified RNA samples of T06 and T08 cell lines was incubated with 50 ng (2 µl) random oligo primers for 40 sec at 90^{0}C and taken out and kept in room temperature for few minutes. Further, 5X first-strand buffer (250mM Tris-HCL (pH 8.3), 375 mM KCL, 15 mM $MgCl_2$) and 0.1 mM (1,5 µl) DTT , 0.5 µl RNAout and in the last part, 1 µl RT SuperScript^{TM} II reverse transcriptase enzyme was then added to the above mixture and then the constituents were then incubated at 50^{0}C for 1 hour. cDNA synthesised was then stored at -20^{0}C until use.

In order to amplify the gene of interest, cDNA synthesised was subjected to a PCR procedure using enzyme KAPAHIFI DNA polymerase (KAPA biosystems). Two sets of PCR reactions were set: 1-) wild type lamin A and progerin and 2-) internal control actin gene (Table-3.5). For each reaction, PCR reaction mixture containing

cDNA from the above reaction, 36 µl H_20, 5µl of 10 X KAPAHiFi reaction buffer, 1 µl (10 µM) dNTP mix, 2.5 µl (10 µM) final concentration each of gene specific forward and reverse primers and 1U(1µl) of KAPAHiFi DNA polymerase enzyme was prepared. The components were then vortexed and subjected to PCR amplification procedure. In the first set of PCR reactions, the DNA was denatured at 94^0C for 2 minutes followed by 30 cycles at 94^0C for 20 seconds, primer specific annealing temperature at 62^0C for 30 seconds and 72°C for 30 second, the final cycle was followed by 68°C extension for 5 minutes. In the second set of PCR reactions, the DNA was denatured at 94^0C for 2 minutes followed by 30 cycles at 94^0C for 20 seconds, primer specific annealing temperature at 65^0C for 30 seconds and 72°C for 30 second, the final cycle was followed by 68°C extension for 5 minutes. PCR products were then run on 2 % agarose gel and the band size for each product was verified with the expected band size.

Table-3.5: The list of forward and reverse primers for *lamin A* and *ACTN4* genes are displayed in the table below:

Primer name	**Primer sequence 5'→ 3'**
Lamin A (F) Ex10. f1 (annealing at the beginning of Exon 10)	GAAGTGGCCATGCGCAAGCTG
Lamin A (R) Ex12 .r2 (annealing at the Exon 12 in about 50 nucleated downstream of the Lamin A stop codon)	GGTGAGGAGGACGCAGGAAG
ACTN4 (F) Ex7. f1	TGTAAAACGACGGCCAGT
ACTN4 (R) Ex9. r1	CAGGAAACAGCTATGACC

3.2.8 Statistical analysis

Values are expressed as averages ± SEM, and n represents the number of cells analysed. Two-tailed unpaired t-tests used as statistical analysis. The probability-value (p-value) are denoted by stars (* $P \leq 0.05$, ** $P \leq 0.01$, *** $P \leq 0.001$, **** $P \leq 0.0001$).

3.3 Results

3.3.1 Population doubling curve

We compared the growth of 1 normal (NB1T) and 2 HGPS (T06 and T08) immortalised dermal fibroblasts for 50 days. Cells were split twice a week during the experiments and therefore over confluent cell appearance was not observed throughout the experiments. Cell growth was measured at each passage by calculation of population doublings (PD) using the following formula;

$$PD = 3.32 \times (\log H - \log S)$$

Where log H= logarithm of the number of the cells harvested

Log S= logarithm of the number of cells seeded on first day of passage.

Accumulated population doubling (APD) for control and HGPS cells were then plotted (y-axis) against days in culture (x-axis) (figure 3.1).

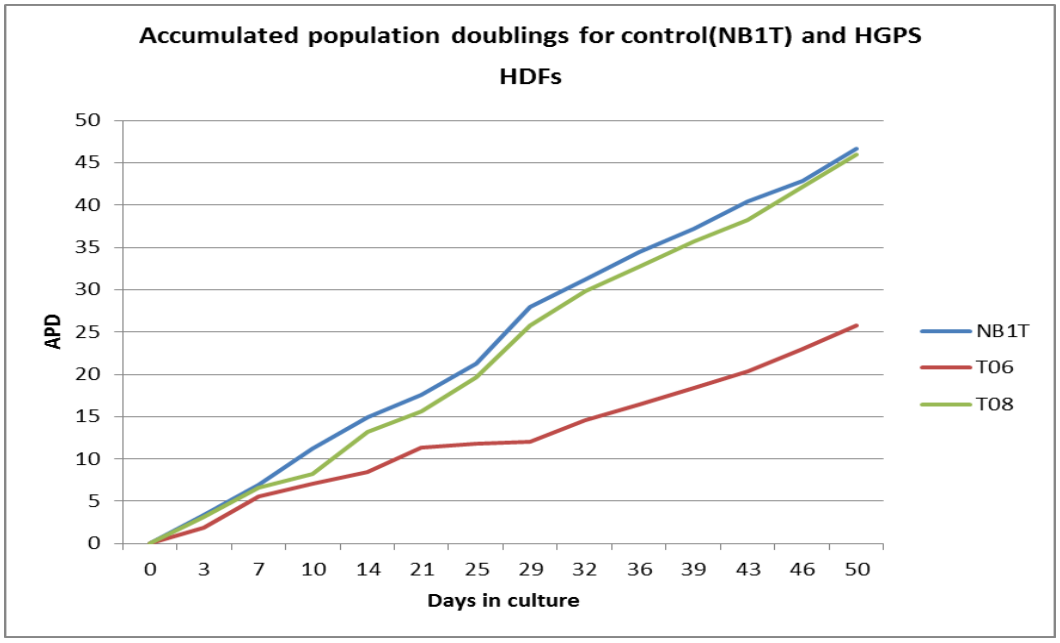

Figure 3.1: Growth rate of control and HGPS fibroblasts in culture. HGPS and control cells were cultured in 15% FBS and passaged twice weekly. The number of cells harvested and the number of cells seeded were recorded at each passage. Cell growth was measured by calculation of accumulated population doublings (APD). In the above graph APD (y-axis) was plotted against days in culture (x-axis).

Shown in Figure 3.1, the data revealed that NB1T and T08 cells have higher growth rate than T06 cell line in 50 days of culture even though all cell lines were immortalised. Control and HGPS fibroblasts were stained with pKi-67 proliferation marker at each passage indicating the fraction of proliferating cells within the culture (Figure 3.2). NB1T and T08 cells have higher proliferation level compared to T06 cell line.

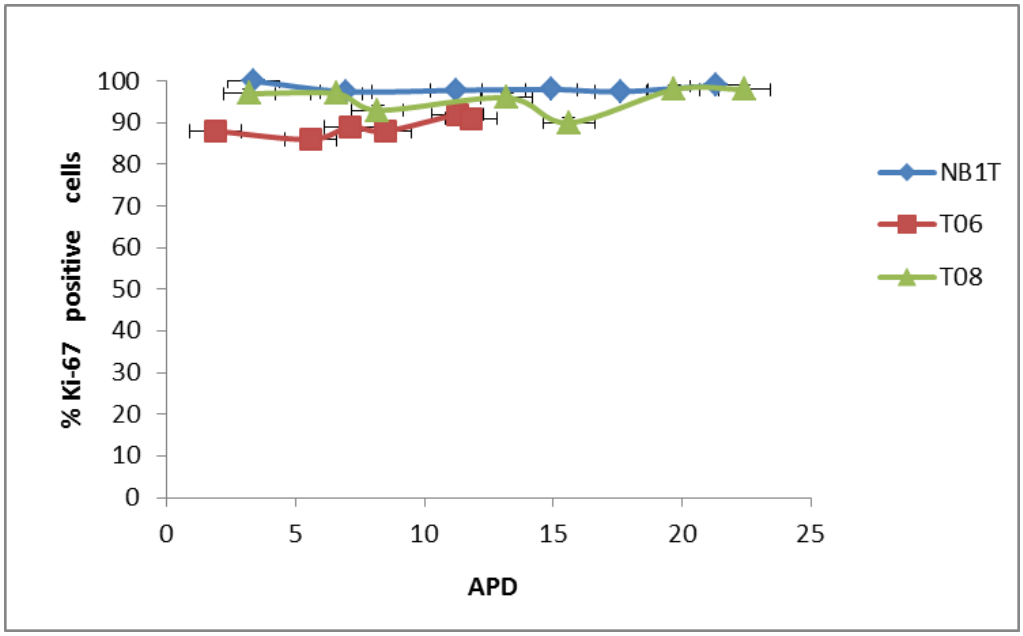

Figure 3.2: The fraction of pKi-67 positive cells against APD. NB1T, T06 and T08 cell lines were fixed with methanol: acetone and stained with pKi-67 antibody at various time points in the culture. The data were obtained from 3 coverslips for each immunostaining of cell line and at least randomly selected 250 nuclei were scored. The fraction of pKi-67 positive cells (y-axis) has been plotted against APD (x-axis) to see the change in fraction of cells showing pKi-67 expression over time in culture. Average number of Ki-67 stained nuclei for each cell line is; NB1T:98.3, T06: 89 and T08: 95.1. One way ANOVA statistical analysis used as statistical analysis. Significance was taken as $P \leq 0.05$ ($p \leq 0.001$).

3.3.2 Nuclear shape analysis

In order to identify if there are any differences in proliferating NB1T, T06 and T08 cell lines in terms of nuclear shape, nuclear shape analysis was carried out for four different parameters. These parameters were: area, perimeter, circularity and aspect ratio. The aspect ratio of nucleus denotes the ratio of the major axis to the minor axis.The cells were fed with fresh DMEM medium containing 15% FBS and grown at 37^0C. To visualize the nuclei, DAPI staining of the nuclear DNA was

performed. Fluorescence images of 250 randomly selected nuclei per cell line were taken with Axioplan Zeiss fluorescence microscope at 100 X magnification (Figure 3.3). The raw data obtained from Image J analysis of the nuclei were transferred to an Excel worksheet where data analysis tools have been utilized to compare the resulting means of each studied parameter(Figure 3.4- A,B,C,D). In terms of area frequency of cells, NB1T, T06 and T08 cell lines have the highest percentage of nuclei with 3000 pixels. In the perimeter parameter analysis of cells, Both NB1T and T08 cells have the highest percentage of nuclei with 250 pixels. On the other hand, T06 cells have the highest percentage of nuclei with 200 pixels. In the circularity parameter analysis of cells, T06 and T08 cell lines have the similar percentage of nuclei with 0.85 pixels. Furthermore, T08 cells are more circular compared to NB1T and T06 cells. In the aspect ratio analysis of cells, all cell lines have the highest aspect ratio with 1.3 in pixels. Figure 3.5 displays average nuclear shape analysis using four different parameters for NB1T, T06 and T08 cell lines. The mean area of the nuclei in NB1T immortalised fibroblasts was 3663.08 ± 57.3 in pixels (n=250). In typical progeria fibroblasts (T06), the mean area was 2703.70 ± 44.05 (n=250) lower than NB1T fibroblast results ($p<0.001$). In atypical progeria fibroblasts (T08), the mean area of the nuclei was 3743.99 ± 47.82(n=250) similar to NB1T fibroblasts results. T08 cells have larger nuclei overall because of higher chromosome number in T08 cells as described in chapter-5. The mean perimeter of the nucleus in NB1T and T08 immortalised fibroblasts was quite similar; 235.33 ± 1.92 (n=250) and 235.92 ± 1.55 (n= 250) respectively in pixels. In terms of T06 immortalised fibroblast the result was 203.16 ± 1.61 (n=250) lower than the two other cell lines ($p<0.001$).The mean circularity of the nucleus in NB1T immortalised fibroblasts was 0.806 ± 0.002 in pixels (n=250). In T06, the mean circularity of the nucleus was

0.805 ± 0.0027 (n=250). Whereas in T08, the result was 0.829 ± 0.0019 (n=250) higher than the two other cell types ($p<0.001$). The mean aspect ratio of the nucleus in NB1T immortalised fibroblasts was 1.32 ± 0.007 in pixels (n=250). In T06 the mean aspect ratio was 1.35 ± 0.009 similar to NB1T fibroblasts results. However, in T08 the result was 1.24 ± 0.008 lower than the two other cell types ($p<0.01$). In figure 3.6-A, B, C of scatter graphs, comparative results of parameters were shown. In figure 3.6-A comparative result of area v aspect ratio illustrates different range of pixels compared to other parameter comparison results. However, NB1T, T06 and T08 cells have very similar aspect ratio v circularity pixels than other results (Figure 3.6-B).

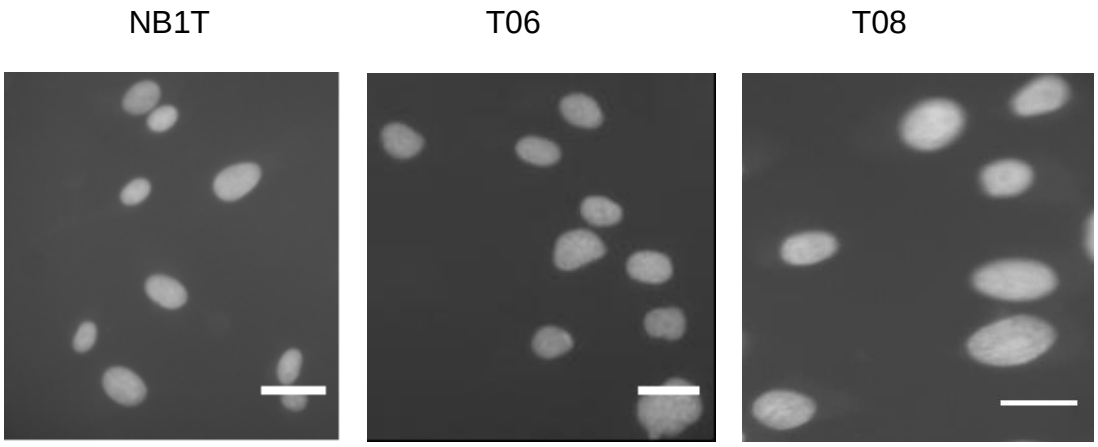

Figure 3.3: Representative gray scale images NB1T, T06 and T08 fibroblasts. Mgnification 40X. Scale bar: 5 µm.

Nuclear shape analysis of NB1T, T06 and T08 cells.

A

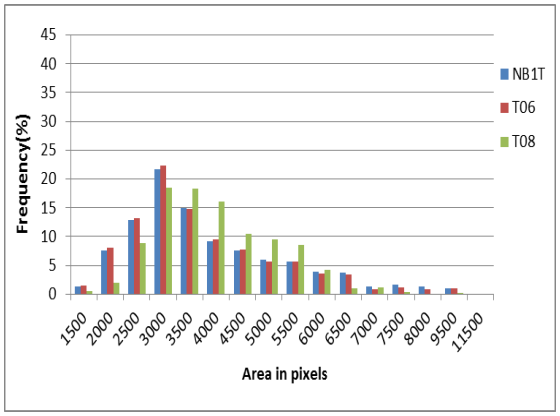

B

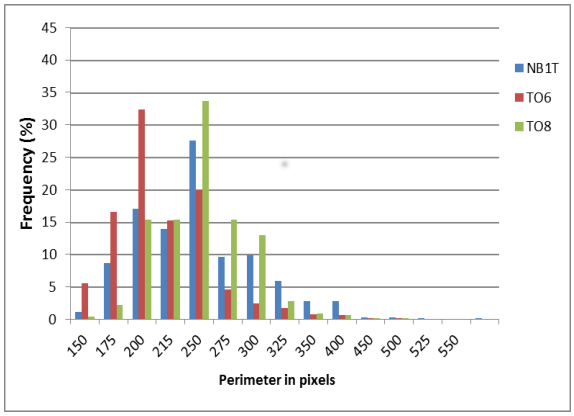

C

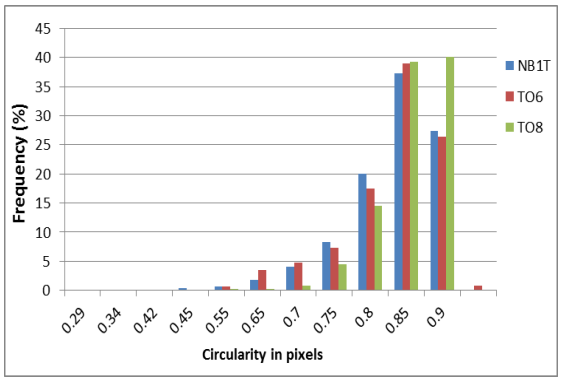

D

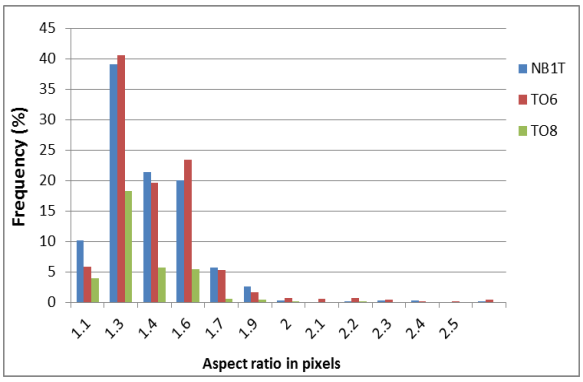

Figure 3.4: Nuclear shape analysis of NB1T, T06 and T08 cells. At least randomly selected 250 DAPI stained nuclei were scored from 3 slides for each cell line. Bin number was chosen for each perimeter frequency results and percentage of frequency was measured. In the graphs, the X- axis illustrates parameter in pixels and Y-axis shows % of frequency. In the charts of A, B, C and D, nuclear shape parameters of area, perimeter, circularity and aspect ratio were shown for NB1, T06 and T08 cells.

Nuclear shape analysis using four different parameters

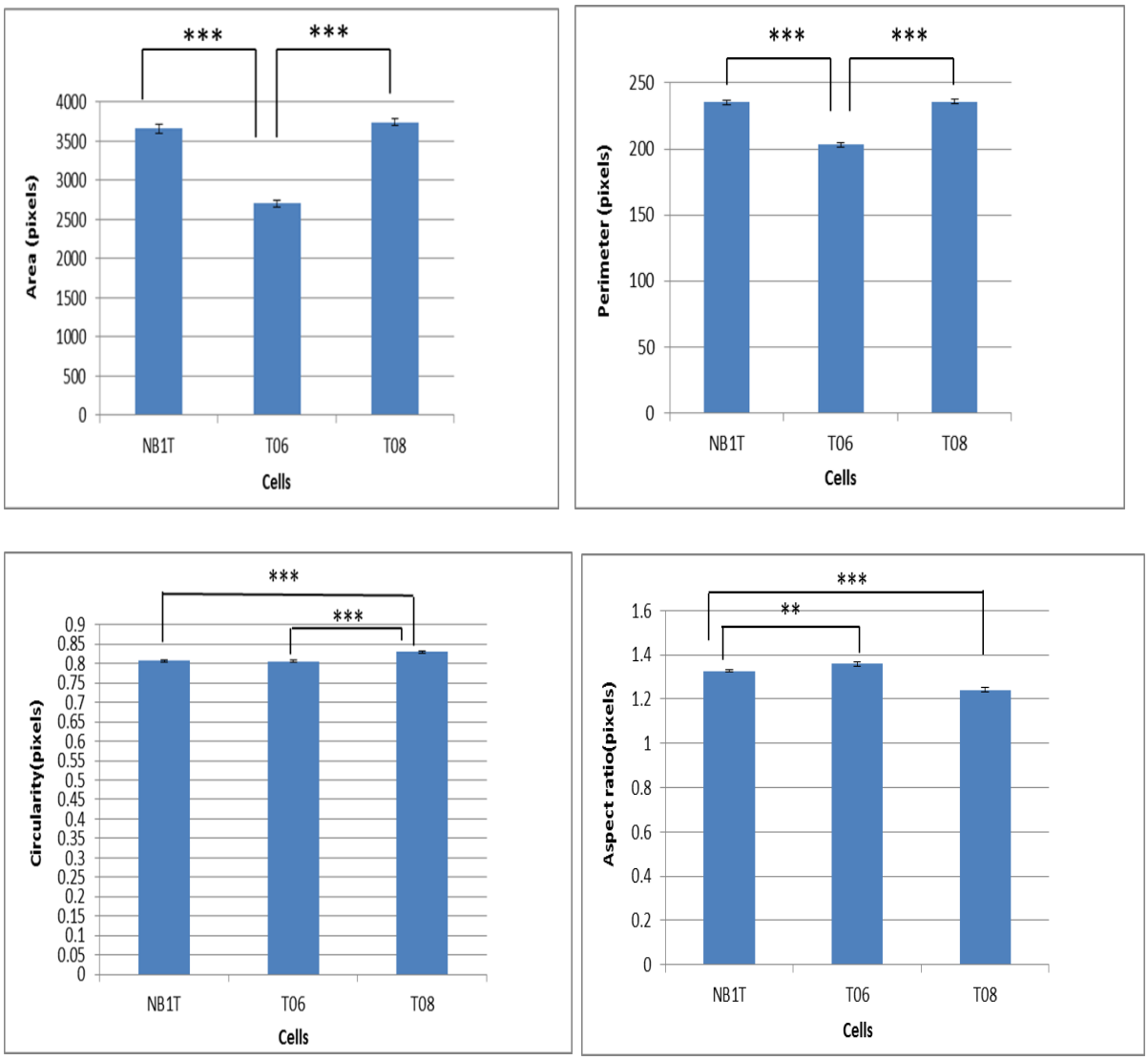

Figure 3.5: Average nuclear shape results using four different parameters for NB1T, T06 and T08 cell lines. At least randomly selected 250 DAPI stained nuclei were scored from 3 slides for each cell line. Standard error bars have been plotted. Significant differences are denoted by star (* $P \leq 0.05$, ** $P \leq 0.01$, *** $P \leq 0.001$).

A

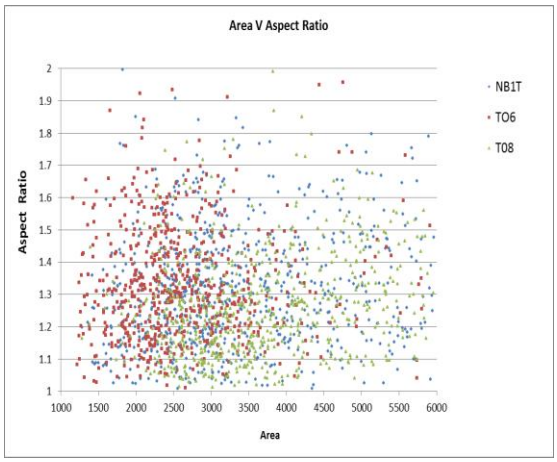

B

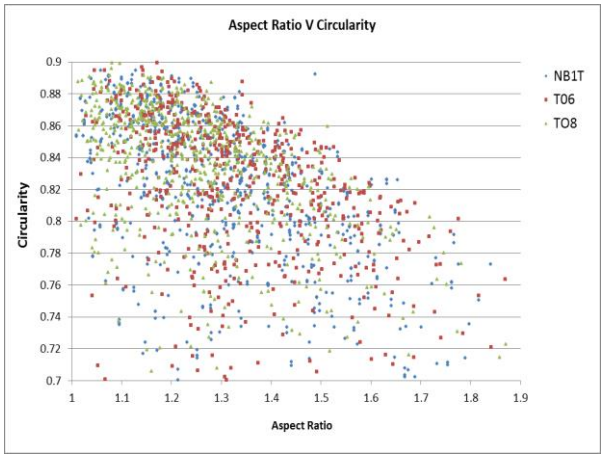

C

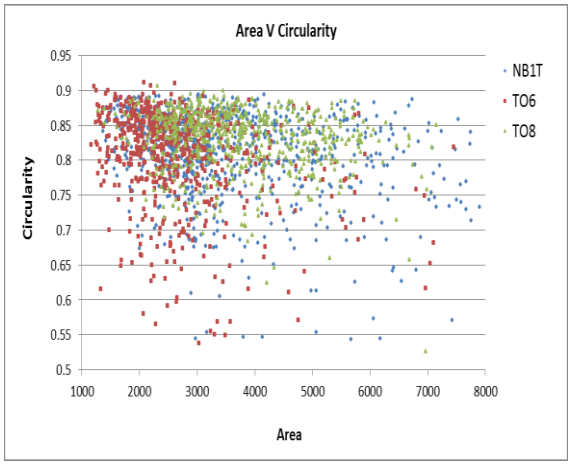

Figure 3.6: In the scatter graphs of A, B and C the parameters were compared with each other by plotting all parameters against the other.

3.3.3 Cell movement analysis

The cell movement analysis was performed by tracking 30 randomly selected cells for each cell line; NB1T, T06 and T08 over an 8 hour duration (Figure 3.7-A, B, C). Cell movement results showed that NB1T cells had the highest average displacement at 109.2 (medial, angular, leftward, and anterior). Another index of directedness of cell movement is meandering. The meandering of cells was obtained as the displacement between the beginning and final points on each the track divided by the total length of the random path. T08 cells have the lowest meandering at 0.19. The average distance of T08 cells are higher than both NB1T and T06 cells (Table 3.6).

A

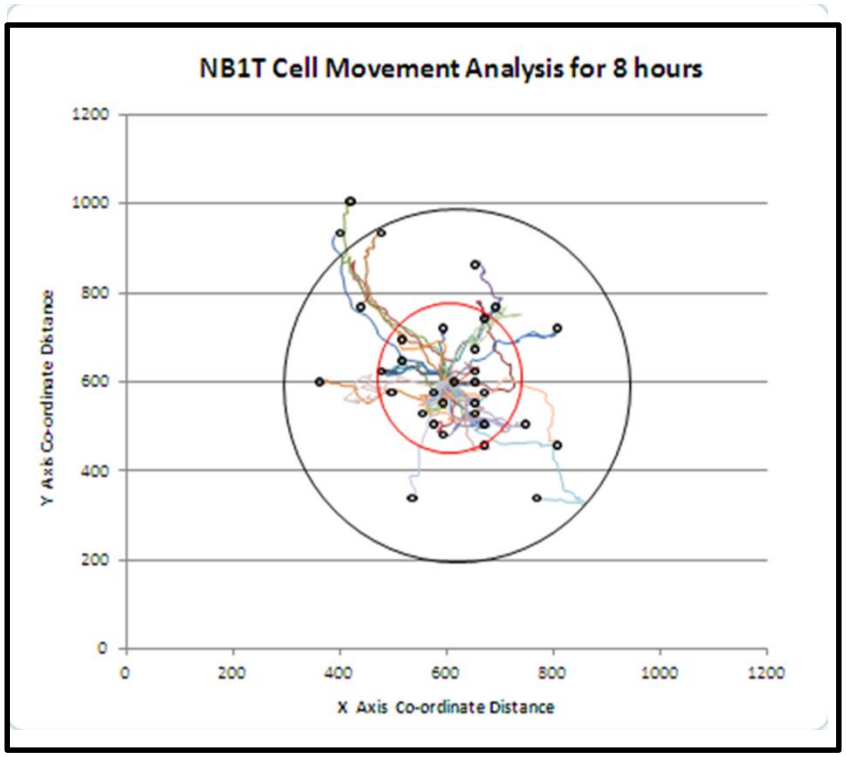

B

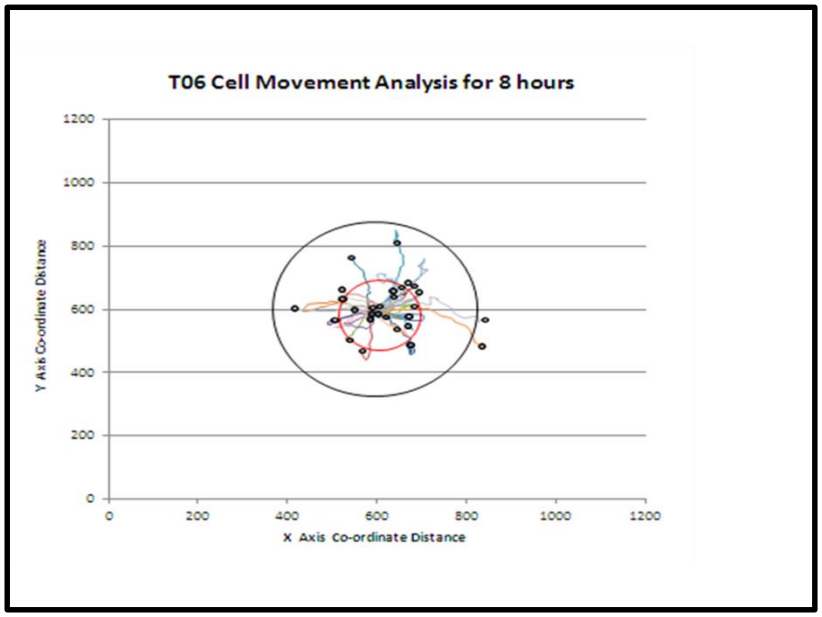

C

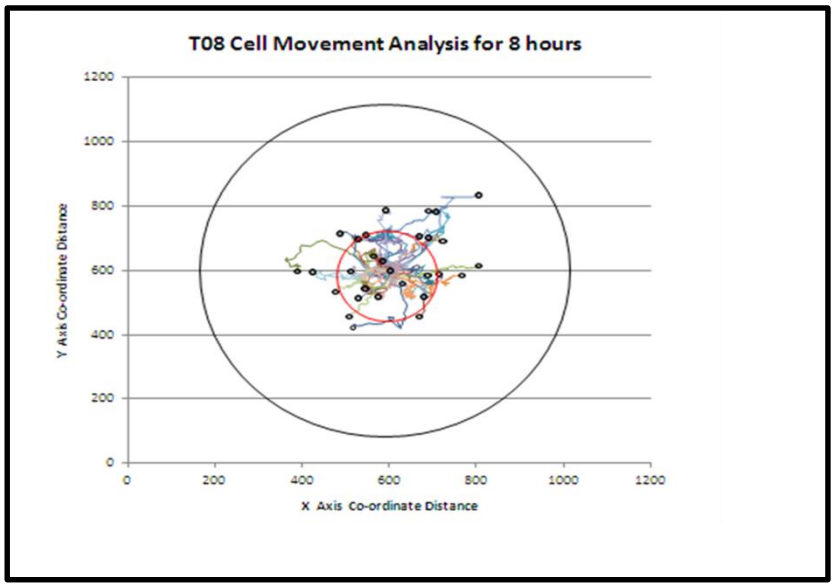

Figure 3.7: In these graphs, three distinct movements for NB1T (A), T06 (B) and T08 (C) fibroblasts for 8 hours can be seen. Each line represents one cell movement. Small black circles show end point for each cell. The outermost large black circle represents average distance moved. The innermost red circle represents average distance moved from the starting position.

Table 3.6: Illustrates average distance, average displacement and ratio meandering of each cell line. Ratio meanderings were obtained by average displacement/ average distance and NB1T cells had the highest ratio meanderings. Distance unit is in µm. The level of significance is indicated as: * P ≤ 0.05, ** P ≤ 0.01, *** P ≤ 0.001 and **** P ≤ 0.0001.

Cell Line	Average Distance	Average Displacement	Ratio (Meanderings)
NB1T	238.2 ± 25.38 (**)	109.2 ± 18.8 (**)	0.31 ± 0.03 (**)
T06	159.6 ± 18.01	66.6 ± 13.4	0.28 ± 0.037 (*)
T08	316.99 ± 23.1(****)	88 ± 11.49 (*)	0.19 ± 0.02

3.3.4 Indirect Immunofluorescence

3.3.4.1 Presence and Distribution of Lamin A,C and Progerin proteins

Antibody staining was performed to identify the presence of specific proteins in the fibroblast cell lines. The nuclei had a smooth surface and a normal ellipsoidal shape in control NB1T cells (Figure 3.8A-b). On the other hand, misshapen nuclei were observed in T06 and T08 cells with herniations and invaginations at the nuclear periphery (Figure 3.8A-e, h). In terms of lamin A staining distribution within nuclei, T06 cells predominantly exhibited higher proportion of cells where rim and speckles (21%) were observed together compared to NB1T(4%) and T08 (6%) cells (Figure 3.9-A). Lamin A staining in NB1T (Figure 3.8A-a) and T08 (Figure 3.8A-g) cells exhibited higher proportion of cells where rim and speckles (96 % and 94 % respectively) was observed relative to T06 (89%) (Figure 3.8 A-D). Lamin A/C staining appeared as thicker nuclear rim in T06 cells than other cells (Figure 3.8B-d), whereas lamin A/C staining appeared as rim and speckles in the nucleoplasm in NB1T and T08 cells (Figure 3.8B-a and Figure 3.8B-g respectively). Using an

antibody specific for progerin, it was revealed that there was no rim staining in of the cells (Figure 3.8-B). Both NB1T and T08 cells exhibited progerin staining in 4% of the cells as small punctuate spots suggesting that progerin is also expressed by cells derived from healthy individuals (Figure 3.9-B). T06 cells exhibited 86% negative staining, 6% a few speckles and 8% small punctuates (Figure 3.9-B).

A

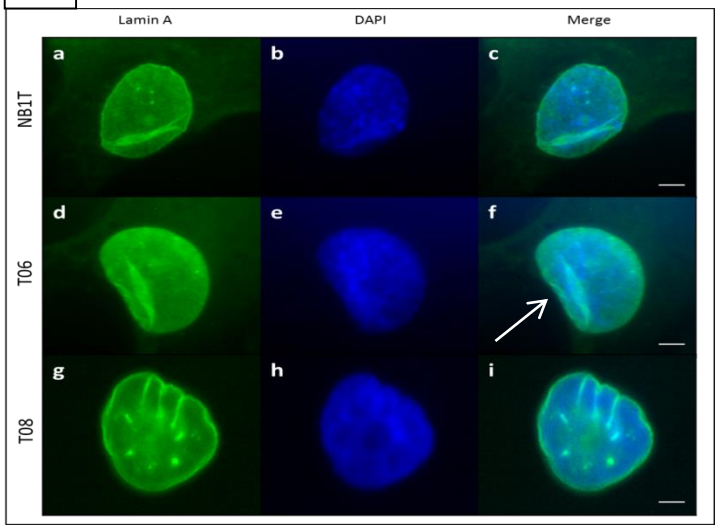

B

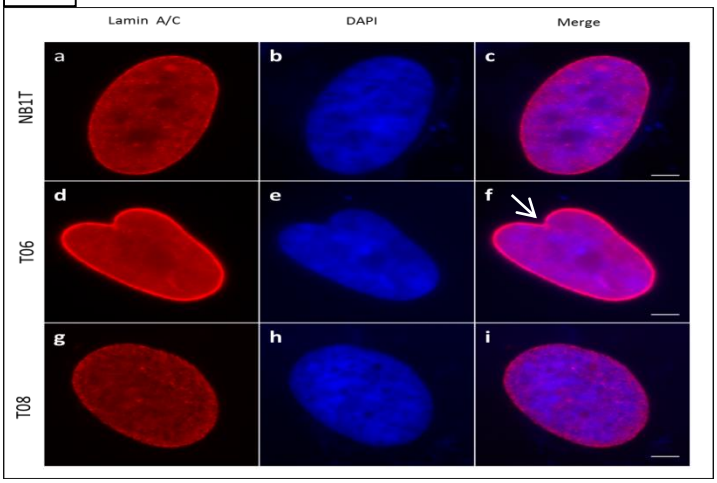

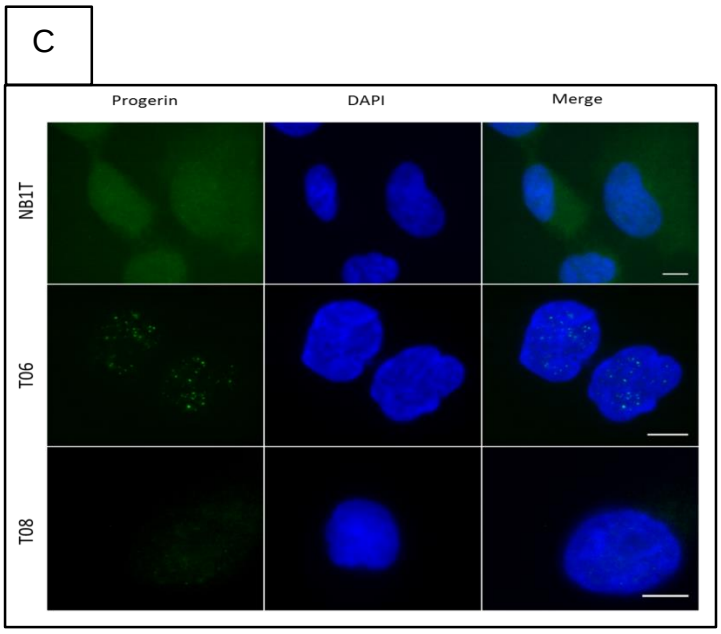

Figure 3.8: Immunodetection of Lamin A (A), Lamin A/C (B) and progerin(C) in NB1T, T06 and T08 cells in green. Nuclei were counterstained with DAPI. White arrows indicate the formation of invagination. Magnification = X100. Scale bars= 5 µm.

A

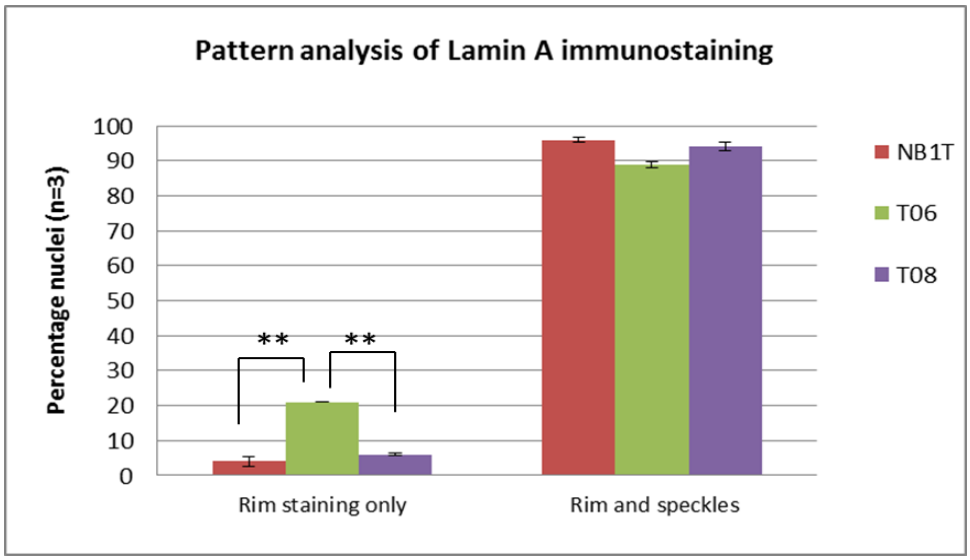

B

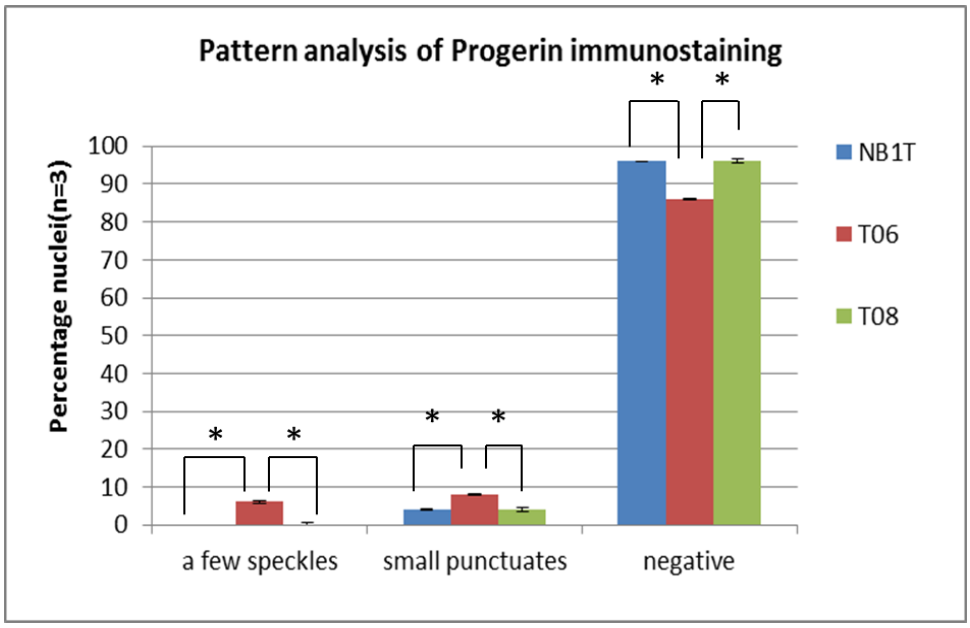

Figure 3.9: Lamin A (A) and progerin (B) staining pattern analysis of NB1T, T06 and T08 cells. N represents number of experiments analysed. Error bars represent standard error of mean (SEM). Significant differences are denoted by star (* $P \leq 0.05$, ** $P \leq 0.01$, *** $P \leq 0.001$).

3.3.4.2 Proliferation of Cells

In order to discriminate between proliferating and nonproliferating nuclei, PCNA and Ki-67 indirect immunostaining was employed to detect Ki-67 antigen. Proliferating nuclear antigen (PCNA), the auxiliary protein of DNA polymerase delta as an indispensable component of the eukaryotic chromosomal DNA replisome appears to have distinctive nuclear distrubutions in S-phase (Maga and Hubscher, 2003; Hutchison and Kill, 1989). Two populations of PCNA exist in nuclei as a soluble form and an insoluble form (Kill *et al.*, 1991) and it is believed that the soluble form is not involved in DNA replication (Kill *et al.*, 1991). A nuclear antigen pKi-67 was firstly discovered by virtue of its reactivity with ki-67 monoclonal antibody (Gerdes *et al.*, 1983) and the antigen is only detected in proliferating cells (Kill *et al.*, 1994). Ki-67 antibodies have been widely employed to evaluate proliferative indices in cancer cells (Luporsi *et al.*, 2012). Although the function of ki-67 is not known yet, there are a number of suggested roles including an involvement with in ribosomal biogenesis and protection of chromosomes from inappropriate contacts with components of mitotic surrondings (Bridger *et al.,* 1998; Hernandez-Verdun and Gautier, 1994). During mitosis pKi-67 is found coating all chromosomes, during G_1 phase it accumulates in nuclear foci and during late G_1, S and G_2 phase it localizes within nucleoli (Bridger *et al.*, 1998). Ki-67 staining results showed different patterns in nuclei. Ki-67 staining was restricted to discrete small foci in pattern I and in another pattern II; Ki-67 was restricted to nucleoli (Figure 3.10). We examined the distribution of PCNA in 250 nuclei in each cell line. Methanol/acetone was used as the fixative of our cells. A bright punctuate pattern was distinct from negatively stained nuclei and therefore represents S phase nuclei. In our experiments, the patterns of PCNA

staining in individual nuclei were classified into three types (Figure 3.11). A regular granular pattern was observerd over the whole of the nucleus (Figure 3.11-a). Punctuated staining but with more significant fluorescence foci over the perinuclear region (Figure 3.11-d) and a few large brightly staining granules (Figure 3.11-g). Three different PCNA patterns were found in NB1T, T06 and T08 cell lines (Figure 3.12). Figure 3.13 displays PCNA positive-negative immunostaining analysis. The patterns of PCNA staining were classified in four types. In type 1, very few foci of PCNA staining were observed; in type 2, a regular granular pattern was observed over the whole of the nucleus; in type 3, the staining was again punctuated but with more significant fluorescence was observed over the perinuclear region; and in type 4, fluorescence was observed in a smaller number of large brightly staining granules (Kill *et al.*, 1991).

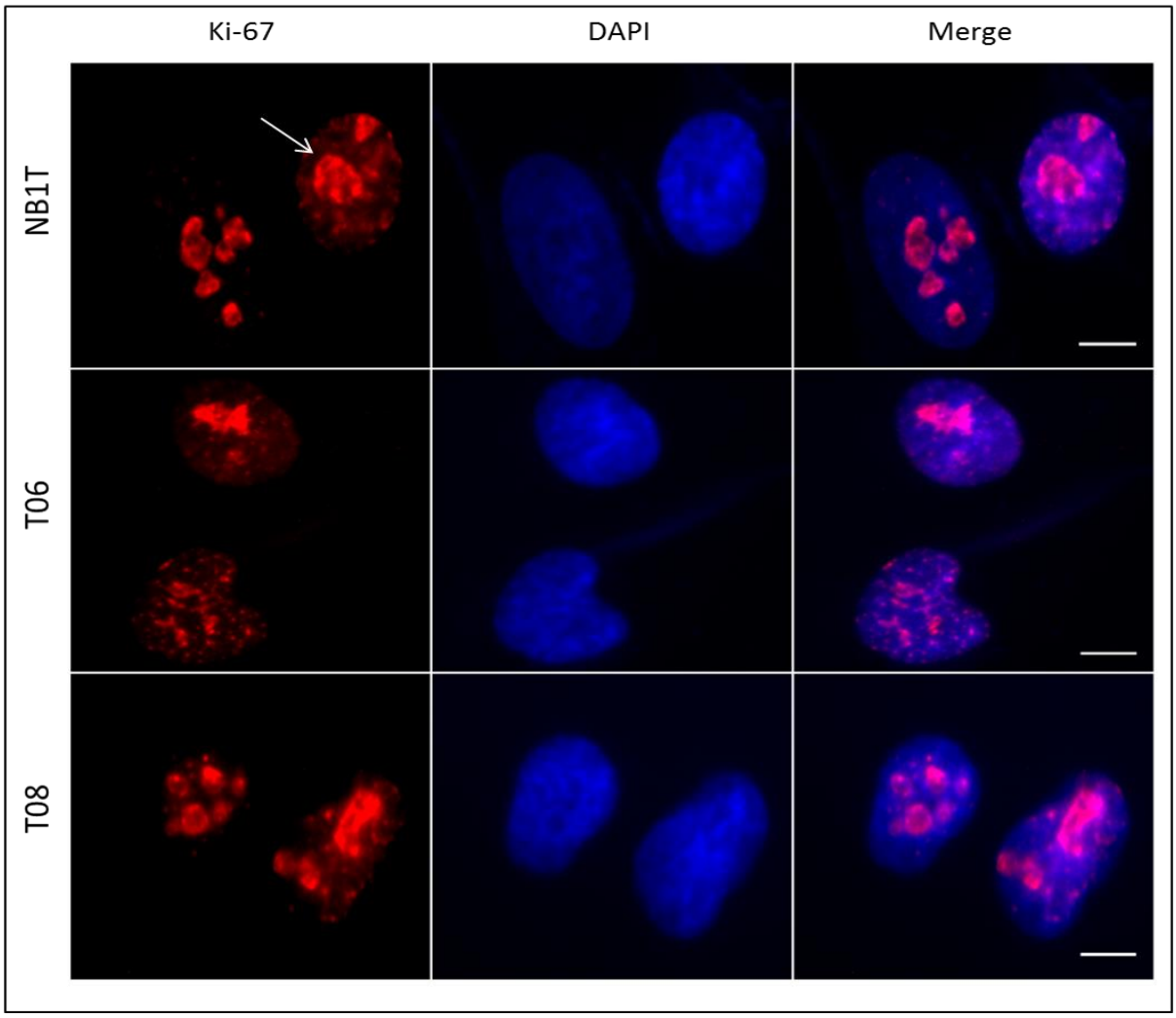

Figure 3.10: Immunodetection of Ki-67 in NB1T, T06 and T08 nuclei in red. White arrow shows restriction of Ki-67 to nucleoli. Magnification = X100. DAPI in blue. Scale bars= 5 μm

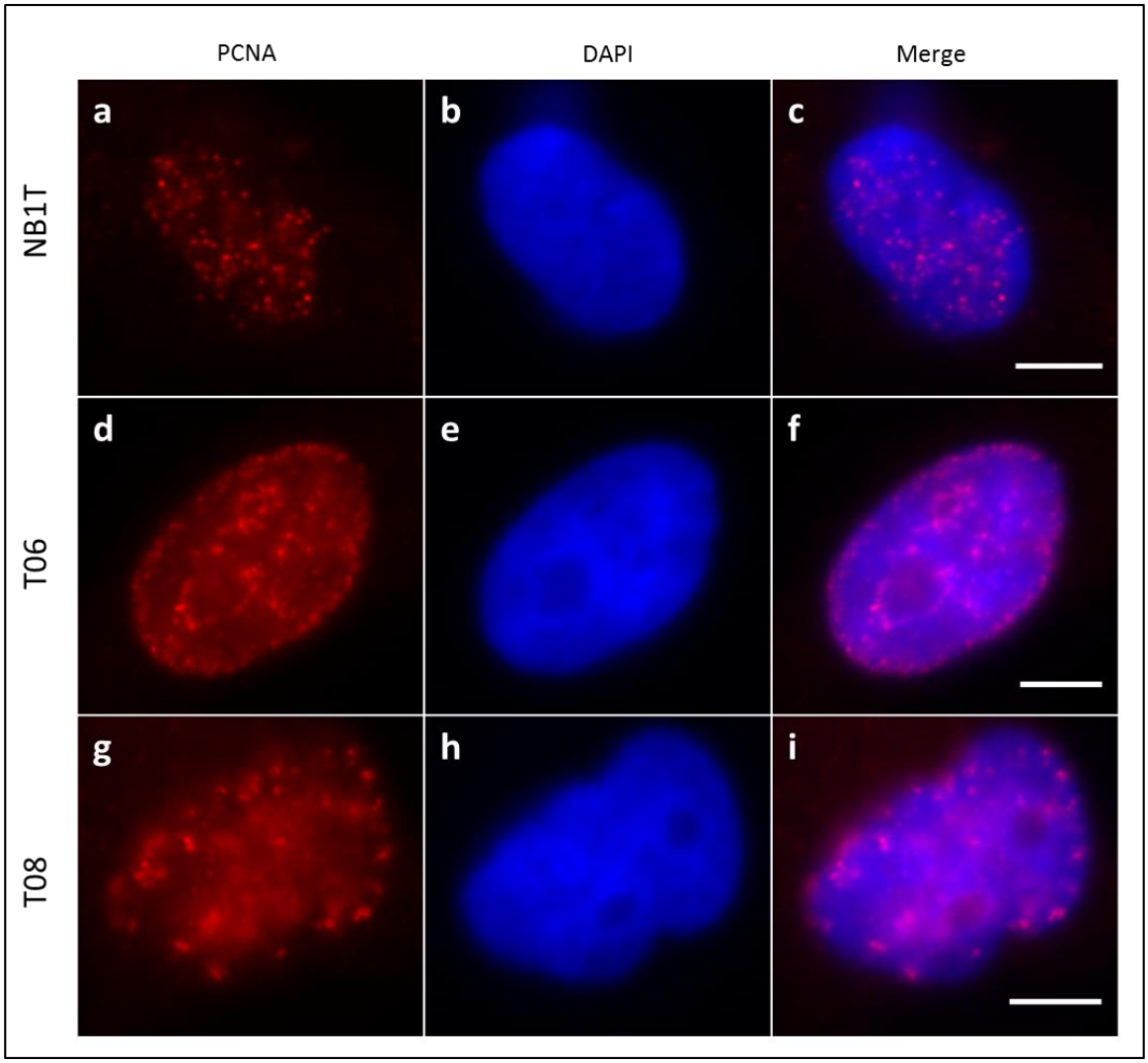

Figure 3.11: Immunodetection of PCNA in NB1T, T06 and T08 nuclei in red. Panels a, d, g illustrate the three different patterns of staining that were observed, described as a regular granular pattern (a), a predominant prenuclear pattern (d) and a few large granules (g). In order to reveal DNA, DAPI was used. Magnification = X100. Scale bars= 10μm.

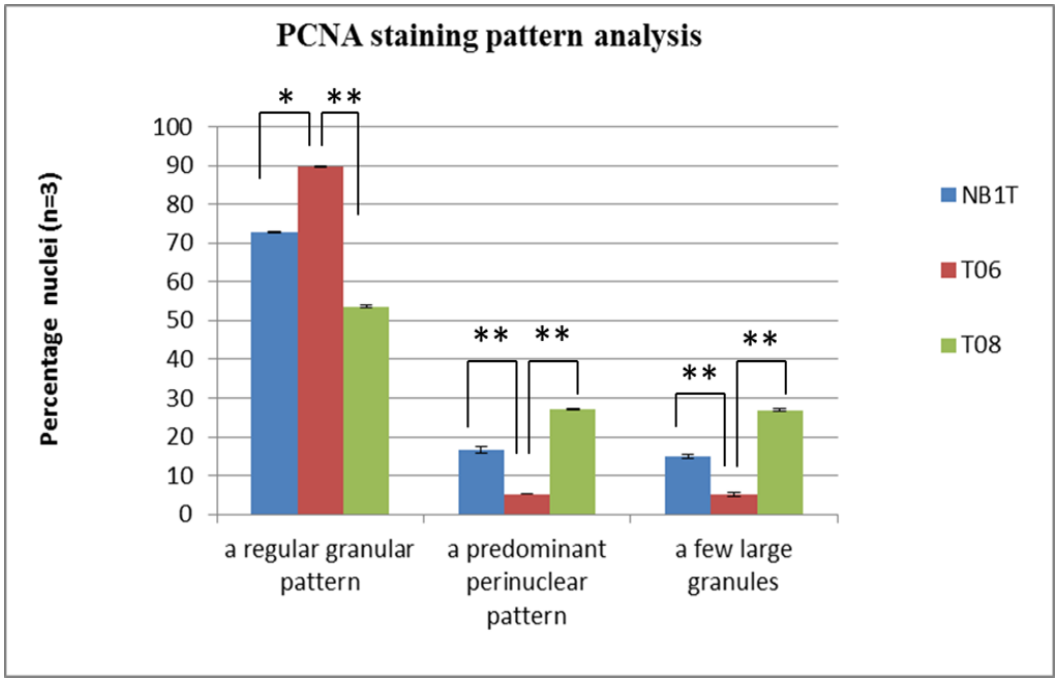

Figure 3.12: PCNA staining pattern analysis shows that there are three types of patterns in NB1T, T06 and T08 cell lines: a regular granular pattern, a predominat perinuclear pattern and a few large granules. N represents number of experiments analysed. Error bars represent standard error of mean (SEM). Significant differences are denoted by star (* P ≤ 0.05, ** P ≤ 0.01, *** P ≤ 0.001).

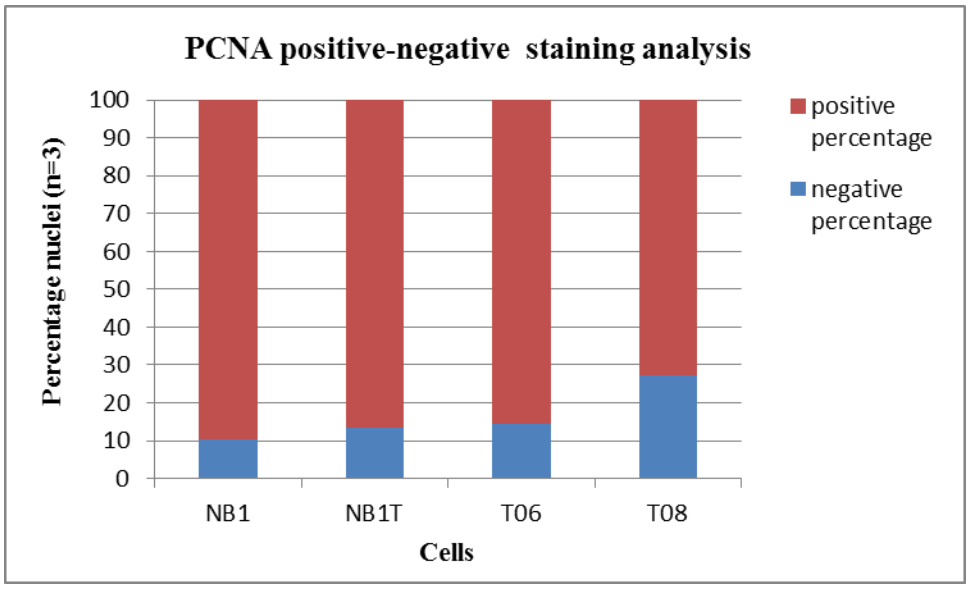

Figure 3.13: PCNA positive-negative staining analysis of NB1T, T06 and T08 cells. N represents number of experiments analysed

3.3.5 Electrophoresis and Westernblotting

The proteins from NB1T, T06, T08 cell lines were separated on 4-20% SDS-PAGE gels and electrophoretically transferred onto a nitrocellulose membrane. Protein expression levels of lamin A, lamin C were then assessed by incubating the membranes with anti- lamin A/C antibody. Lamin A and Lamin C bands appeared on the gel for all cell lines. However, progerin protein was not detected on the gel for T06 cell line (Figure 3.14). Rf (distance the fragment has moved from origin to the reference point) against log MW was plotted for lamin A/C in Figure 3.15 for all cell lines. Vimentin protein was detected by using alkaline phosphatase conjugated secondary antibody (Figure 3.16). Rf (distance the fragment has moved from origin to the reference point) against log MW was plotted for vimentin in Figure 3.17 for all cell lines. The relative density values of lamin A for NB1T, T06 and T08 cells are 1, 0.74 and 1 for NB1T, T06 and T08 cells respectively. The relative density values of Lamin C for NB1T, T06 and T08 cells are 0.46, 1 and 0.41 respectively.

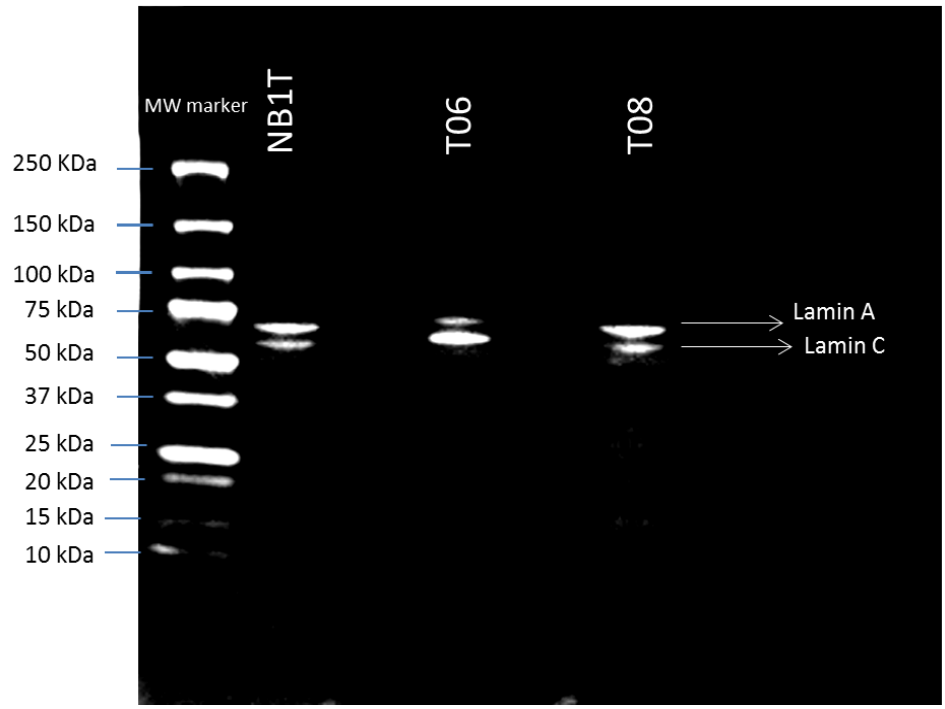

Figure 3.14: Western blotting of NB1T, T06 and T08 cells**.** All samples of cultured cell lines were loaded equally, 2 x 10^5 cells per lane. Molecular weight (MW) of Lamin A: 73 Kilodalton (kDa) and Lamin C: 68 kDa appeared on the gel for NB1T and T08 cells respectively. Molecular weight (MW) of Lamin A: 74 Kilodalton (kDa) and Lamin C: 69 kDa appeared on the gel for T06 cell.

A

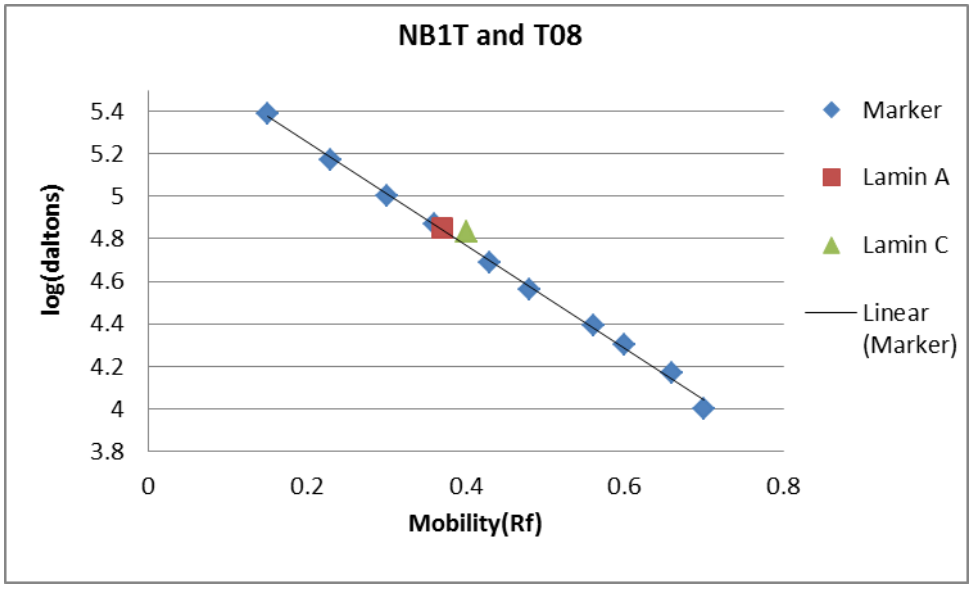

B

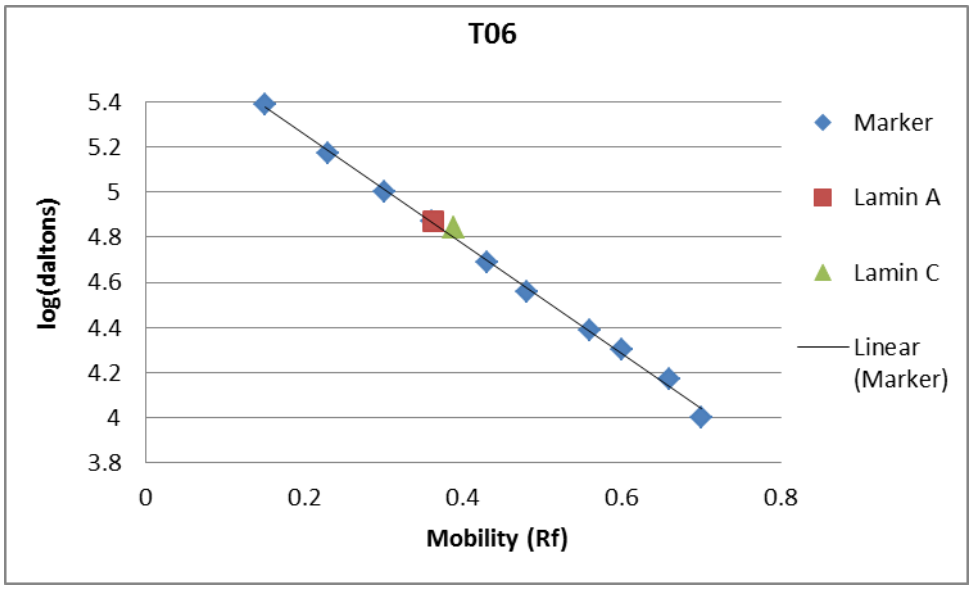

Figure 3.15: Rf(distance the fragment has moved from origin to the reference point) value was plotted on the graph for Lamin A/C for NB1T, T08 cells(A) and T06 cell(B).

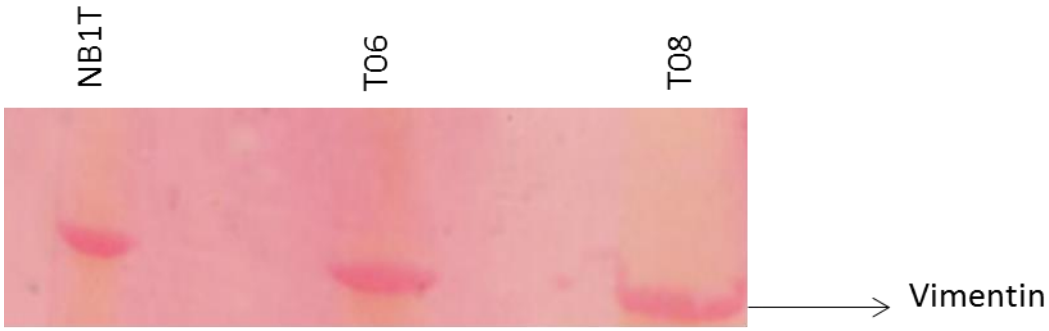

Figure 3.16: All samples of cultured cell lines were loaded equally, 2 x 10^5 cells per lane. Molecular weight (MW) of vimentin: 49 kilodalton (kDa) for NB1T, T06 and T08 cell lines. Vimentin protein was detected using "fast red".

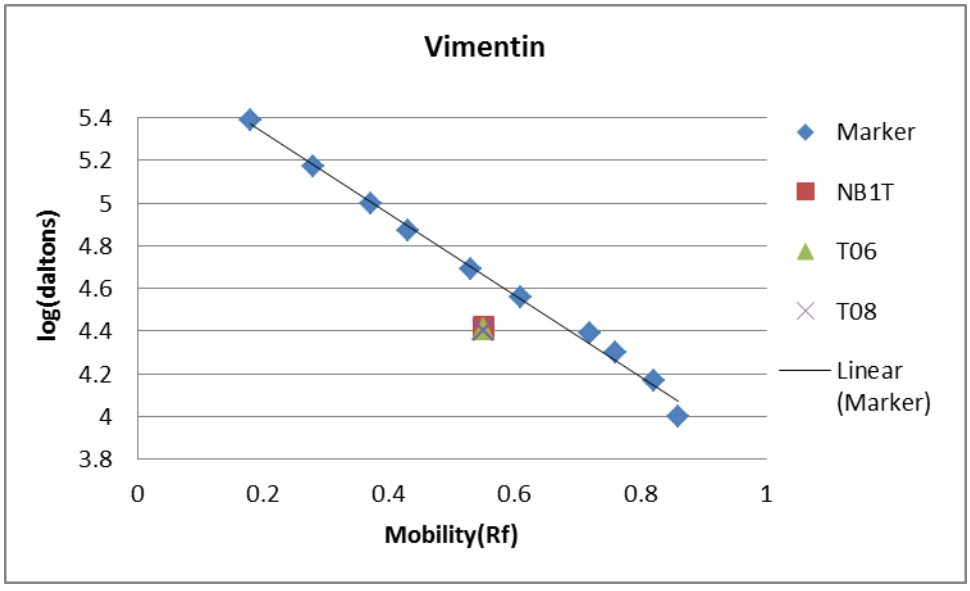

Figure 3.17 Rf (Distance the fragment has moved from origin to the reference point) value was plotted on the graph for Vimentin for NB1T, T06 and T08 cell lines.

3.3.6 RT-PCR of Lamin A and Progerin

An RT-PCR experiment was carried out to see if progerin exists as mRNA in classical progeria T06 cells. Lamin A, progerin and actin primers were used to perform the RT-PCR experiment and then PCR products were then separated on a 2 % agarose gel (Figure 3.18).

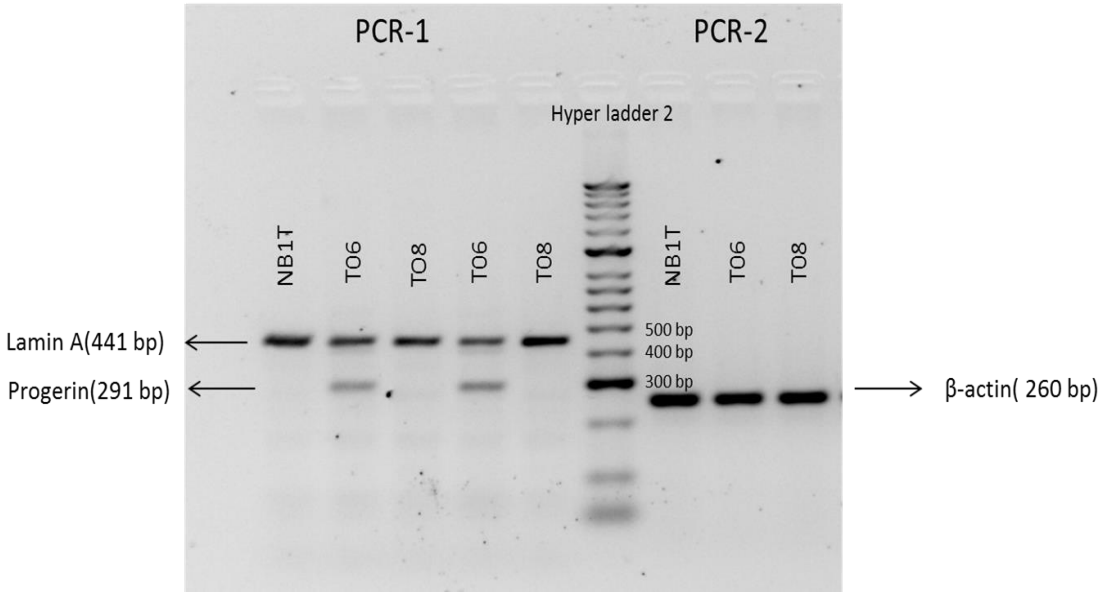

Figure 3.18: Two sets of PCR reactions were performed. PCR-1 reaction for *Lamin A*, and *progerin* detection and PCR-2 was for house-keeping ***β-actin***. Wild type *Lamin A*: 441bp, *Progerin*: 291 bp and house-keeping *ACTN4* gene: 260 bp. Hyperladder™ II 50 bp.

In figure 3.18, NB1T, T06, T08 cell lines were used. The expected band representing *Lamin A gene* appeared on the gel for NB1T cell line. Two bands representing *Lamin A* and *progerin* gene appeared for T06 cell line on the agarose gel. Although one band respresenting *Lamin A* gene appeared on the gel, progerin gene did not appear on the agarose gel for T08 cell line. House-keeping *ACTN4* gene was detected in all lanes.

3.3.7 Serum responsive test and immunostaining

Ki-67 is used as a proliferation marker. Therefore anti-Ki67 immunostaining was performed to see different proliferation level between 15% and 0.5% serum treated in NB1T, T06 and T08 cell lines. Percentage of Ki-67 positive cells against days in culture was plotted in the graph for all cell lines (Figure 3.19).

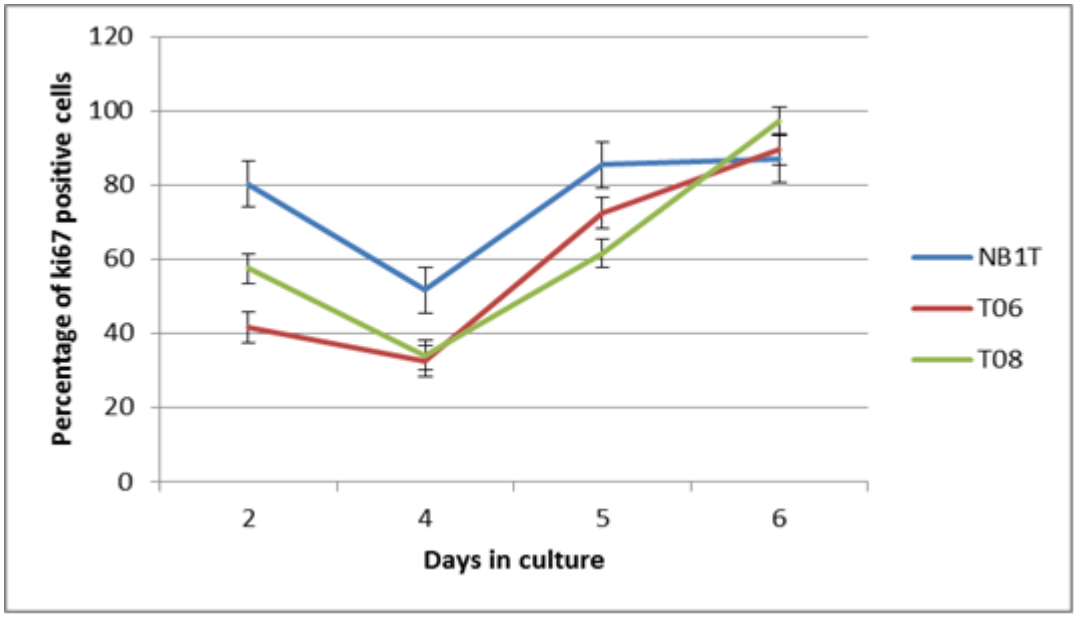

Figure 3.19: Percentage of Ki-67 positive cells for each cell line. First 4 days of the experiment serum were 0.5% and from day 4 to day 6, the percentage of serum was increased from 0.5% to 15%. Standard error bars have been plotted.

The percentage of Ki-67 positive staining reduced dramatically between day 2 and day 4 in all cell lines. Therefore it was a good indication that reduced serum caused low cell proliferation or quiescence for all cell lines. When serum was added at day 4, the percentage of Ki-67 positive staining has risen over 80% after 2 days for all cell lines, because of the increased serum percentage.

3.4 Discussion

In somatic cells, due to lack of telomerase, gradual telomere loss and ultimate senescence is inescapable. The hTERT method enables cells to be immortalised and therefore persistent telomerase expression occurs (Cao *et al.*, 2011a). With regards to the immortalised fibroblast cell line work, Wallis and colleagues showed that forced expression of hTERT, following retroviral infection of HGPS cornea fibroblasts confers telomerase activity and they showed that of the 15 independently isolated clones from the three donors, five failed to immortalise and eventually ceased proliferation and became senescent after an extended lifespan period of only 10-20 population doublings in almost 80 days in culture, in spite of the restoration of telomerase activity (Wallis *et al.*, 2004). The reason for clonal HGPS cells becoming senescent is due to insufficient telomerase activity to maintain telomere length or excessive growth arrests (Wallis *et al.*, 2004).

In our hTERT HGPS skin fibroblast cell growth experiments, increasing numbers of population doublings were observed for immortalised NB1T and T08 cells lines. Despite numbers of population doublings of typical progeria cell (T06) were lower compared to NB1T and T08, T06 cell line has not become senescent over 5 months

of on-going cell culture. Previous studies by Kill & Bridger have shown that in HGPS cell cultures, the fraction of proliferating cells was conserved at relatively high levels compared with normal fibroblast cultures at the same APD level. Whereas a remarkable difference between the growth of normal and HGPS fibroblasts was the rapid decline in proliferating cells observed towards the end of the HGPS culture's life span (Bridger and Kill, 2004). This catastrophe was not observed in the immortalised cells in our hands. Furthermore, it was proposed that in HGPS individuals, mutations in the *lamin A* gene results in deregulation of growth control, hyperproliferation and increased rates of apoptosis and thus there is premature loss of functional 'young' cells and a concomitant premature accumulation of senescent cells (Bridger and Kill, 2004).

One of the hallmarks of HGPS is the abnormal nuclear shape known as blebbing, herniations and invaginations. Formation of nuclear blebbing due to accumulation of progerin on the nuclear membrane has been the main morphological feature to identify HGPS cell lines and has been used to determine the effectiveness of treatments for HGPS. Characterization of nuclear morphological features of HGPS cells may provide insights into mechanisms of HGPS as well as in cellular development (Cao *et al.*, 2011a). From the nuclear shape analysis of area, NB1T and T06 nuclei showed quite similar results. Observations of cells revealed that, both typical and atypical progeria nuclei were more circular than the control cells and from the perimeter results, T06 and T08 nuclei had a smaller perimeter than the control cells. Based on circularity analysis T08 nuclei were rounder than T06 and the control group. HGPS nuclei were characterized by multiple small blebs due to accumulation of truncated lamin A protein on the nuclear membrane, which caused the nuclei to be smaller and rounder.

Cells bind to a surface, extracellular matrix or another cell using cells adhesion molecules such as selectins and cadherins and this process is known as cell adhesion (Gumbiner, 1996). The role of actin polymerization in generating protrusive forces is well established in the lamellipodium, a protruding sheet of membrane at the leading edge of migrating cells (Charras and Brieher, 2016). According to our cell movement analysies, T06 cells had the shortest movement distance than the other cells and there might be variety of reasons for this. However, it is possible that T06 cells have more resilient cell surface adhesion.

To determine the distribution of a range of selected proteins in our cells lines, immunostaining was performed. Performing lamin A/C staining antibody which binds to N-terminal of lamin A/C and progerin proteins, not only enabled us to observe the distribution of lamin a/c and progerin in both classical and unclassical progeria cells and to compare the staining with normal fibroblast cell lines. The results of lamin A/C staining recapitulate that both typical and atypical HGPS cells between passage number 22 and 32 were characterized by a thick lamina and in relation to our study, Goldman and colleagues demonstrated that classical HGPS cells had misshapen or lobulated nuclei with apparent increase in thickness and prominence of the lamina in parallel with nuclear shape changes. However, they stated that control nuclei were never as severely misshapen as those seen in the majority of HGPS cells between passages 13 and 26 (Goldman *et al.*, 2004). These results, along with the data presented in this study, indicate that in our control cell line, lamin A and lamin A/C staining appeared as nuclear rim with a few misshapen nuclei. Our progerin indirect immunostaining analysis showed that none of our cells exhibited rim staining but with T06 cells have the highest proportion of positive staining in speckles. It is noteworthy

that both NB1T and T08 cells showed some foci of progerin adding to evidence that progerin is also expressed in normal cells.

In proliferating cells, the Ki-67 antigen (pKi-67) is detected in all phases of the cell division cycle (Kill, 1996). In our results, Ki-67 staining was restricted to discrete small foci and in another pattern Ki-67 was restricted to nucleoli. Kill (1996) reported that the ki-67 antigen is detected at a large number of discrete foci throughout the nucleoplasm during early G1. During S-phase and G2, Ki-67 antigen is located in the nucleolus and the antigen is present on all chromosomes during mitosis (Kill, 1996). Therefore, based on our numbers the vast majority of our cell lines were proliferating. It is known that active DNA synthesis occurs at sites of PCNA localisation (Zuber *et al.*, 1989). It was revealed that the DNA replication elongation factor PCNA adheres directly to nuclear lamins via their highly conserved Ig-fold motif (Shumaker *et al.*, 2008). In *Xenopus*, the initiation phase of DNA replication was shown not to be affected by the presence of truncated lamins (Mancini *et al.*, 1994; Ozaki *et al.*, 1994). Moreover, the importance of the interaction between lamins and PCNA early in nuclear assembly was demonsrated in *X. laevis* extracts that the reduction of PCNA resulted in the formation of small nuclei with abnormal envelopes that were unable to replicate their DNA (Mattock *et al.*, 2001). Kill *et al*., (1991) demonstrated that following release of hydroxyurea (HU) from HDF cells, four different patterns of PCNA staining that were observed; a few foci, a regular granular pattern, a predominant perinuclear pattern and a few large granules (Kill *et al.*, 1991). The patterns of PCNA in our immortalised cell lines were investigated and found that there are 3 different PCNA patterns exist; a regular granular pattern, a predominant perinuclear pattern and a few large granules. Kill *et al*. (1991) demonstrated using biotin-11-dUTP that PCNA accumulates at the sites of active

DNA synthesis in a pre-initiation complex up to fifteen minutes prior to replication starts (Kill *et al.*, 1991). It has been shown that in G_2 of somatic cell cycle PCNA fluorescence disappears (Celis and Celis, 1985). It is important to note that such DNA replication patterns are dependent upon the method of fixation. In agreement with Kennedy *et al*. (2000) study, we demonstrated that all our immortalised cells have dispersed pattern with sites distributed throughout the nucleus and there was no pattern of a few foci in cells (Kennedy *et al.*, 2000) which suggests that the distribution of PCNA findings are correlated with the period of S-phase rather than G_1/Early S-phase. It was suggested that alterations in the nuclear organisation of DNA replication occur due to immortalisation (Kennedy *et al.*, 2000). In immortalised Lamin A/C-deficient cells, it was shown that the cells enter S phase early with regard to the time spent in G_1 suggesting that Lamin A/C proteins may be essential for function of Rb (Johnson *et al.*, 2004). Progerin accumulates in cultured HGPS cells as an indication of cellular age (Goldman *et al*., 2004). The increased amout of progerin correlates with the progressive alterations in nuclear shape as nuclear herniation and blebbing (Goldman *et al*., 2004). Yang *et al*., (2005) showed using *in vitro* mouse models that progerin was located mainly around the nuclear membrane, whereas following FTI drug treatment the protein was mislocalized to the nucleoplasm.Furthermore, the treatment was shown ameliorating the phenotype by reducing nuclear blebbing (Yang *et al.*, 2005). Our progerin indirect immunostaining analysis showed that none of our cells exhibits rim staining only pattern and furthermore, T06 cells have higher proportion of positive staining than other cells. McClintock et al. and Cao et al. demonstrated the expression of progerin protein in HGPS cells (Cao *et al.*, 2011a; McClintock *et al.*, 2007). Moreover, it was shown that

progerin mRNA was supressed due to the forced elongation of telomeres in human immortalised cells (Cao *et al*., 2011a).

With regards to the western blot results, lamin A and C proteins were expressed in all cell lines. However there was not any expression of progerin protein seen in the T06 cell line. Moreover, the expression of lamin A protein was less in T06 cell line. The reduced expression of lamin A protein is possibly due to reduced lamin A transcription. We assume that the undetected progerin in our T06 HGPS cell lines might be due to proteosomal degradation of the progerin which might be activated by immortalization of cells by hTERT. It was demonstrated that upon sulforaphane (SFN) treatment of HGPS cells, progerin signals were reduced compared with treated control cells. Furthermore, stimulation of proteasome activity and autophagy by employing SFN was revealed in normal and HGPS cells (Gabriel *et al.*, 2014). Because of the widespread use of fibroblasts in tissue culture, vimentin is often taken as a model of intermediate filament behaviour (Eriksson *et al.*, 2009). From the western blot results, we can conclude that vimentin protein is expressed in all normal and progeria cells. Because of undetected progerin protein in progeria cell lines, RT-PCR experiment was carried out and in this study, we have shown that both lamin A and progerin transcripts are present in T06 progeria cells. This is in agreement with findings from an earlier study (Rodriguez *et al.*, 2009), which showed the presence of lamin A and progerin in HGPS cells. With regards to serum responsive results, it was confirmed that in parallel with reduced serum level, the observed Ki-67 positive proliferation marker reduced in all cell lines sharing all the hTERT cells were serum responsive.

3.5 Conclusion

In summary, the hTERT immortalised normal and progeria fibroblasts removed the complication of a limited proliferative life span in culture and greatly facilitate the analysis of HGPS cells. Findings from our results indicate that observed thickening of the nuclear membrane due to accumulation of progerin is concurrent with aberrant nuclear morphology.

Chapter 4: Presence and distribution of lamin and lamin associated proteins in hTERT normal and HGPS fibroblast cell lines

Manuscript in Preparation: M. U. Bikkul, G. Bourne, R. Faragher, C. Parris, I. R. Kill and J. M. Bridger

4.1 Introduction

Other than A- and B- type lamin interactions, there are functionally diverse proteins that are known to interact with the nuclear lamins at the nuclear periphery and internally and these include LAP2 (Lamina-Associated Polypeptides 2)(Laguri *et al.*, 2001), emerin (Cai *et al.*, 2007), LBR (Lamin B receptor)(Olins *et al.*, 2010) and LINC (Linker of Nucleoskeleton and Cytoskeleton) complexes(Mejat and Misteli, 2010) and BAF(Barrier-to Autointegration Factor)(Margalit *et al*., 2007). The nucleoporin 153 (Nup153) is located at the NPC nuclear basket where it interacts with the nuclear lamina playing a vital role in the organization of the NE and in so doing ultimately impacts the architecture of cytoskeletal and mechanical properties of the cell (Zhou and Panté, 2010).

The correct location of lamins and their binding proteins is important for nuclear shape and integrity. In cultured *LMNA*$^{-/-}$ mice fibroblasts, abnormal nuclear shapes was revealed with a reduction of lamin B, LAP2β, NUP153 in nuclear blebs (Sullivan *et al.*, 1999). Depletion of NUP153 caused formation of multiple lobes or membrane invaginations crossing the nuclei, as well as a punctuate distribution of lamin A/C (Zhou *et al*., 2010). Furthermore, depletion of NUP153 was shown to alter the localization of SUN1 and resulted in rearrangement of the cytoskeleton (Zhou *et al*., 2010). Liu and colleagues, 2007 exhibited that SUN1, but not SUN2, was concentrated at NPC in Hela *Lmna* $^{-/-}$ cells (Liu *et al.*, 2007). Even though proteomic analysis had not provided any evidence that SUN1 is an instrinsic part of the NPC. The association of loss of SUN1 and an altered distribution of NPC was correlated in Hela cells leading to aggregation of NPC (Liu *et al*., 2007). Moreover, it was shown that alteration of NPC distribution is specific to SUN1 as depletion of SUN2 did not change the distribution of NPC (Liu *et al.,* 2007).

In cells derived from Familial Partial Lipodystrophy (FPLD), the interaction between NUP153 and lamin A is disrupted owing to Ig-fold mutations, such as the R482W mutation (Al-Haboubi *et al*., 2011). Furthermore, reduction of Nup153 was elicited in cells from a FPLD patient. Tang and colleagues (2008) showed that reduction of the expression of the nuclear lamin B1 using RNAi resulted in specific inhibition of RNA synthesis (*Tang et al.*, 2008). In human *LMNA,* mutations that result in progeria induce an abnormal thickening of the lamina and a loss of peripheral heterochromatin (Shumaker *et al*, 2006). Farnesylated prelamin A is toxic to multiple tissues and is responsible for all of the disease phenotypes associated with HGPS (Gordon *et al.*, 2007). Evidence of progerin toxicity was reported involving *Zmpste24*-deficient (*Zmpste24*$^{-/-}$*)* mice and also half-normal levels of prelamin A (*Zmpste24*$^{-/-}$ *Lmna*$^{+/-}$) and analysis showed that prelamin A levels significantly reduced by 50% which led to fewer misshapen nuclei in *Zmpste24*$^{-/-}$ *Lmna*$^{+/-}$ compared to Zmpste24$^{-/-}$ mice (Fong *et al.*, 2004). Previous study showed using the GFP fusion pre-lamin A mutant R419C protein in HeLa cells that mostly cytoplasmic aggregates being positive after anti-prelamin A immunofluorescence analysis, due to the mutant protein having less CaaX processable substrate whereas, no positive pre-lamin A staining was detected in wild type HeLa cells(Kiel *et al*., 2014). Furthermore, it was observed that the nuclear import of Head Rod (HR)-preLaAWT was as efficient as that of matured HR-LaAWT after lovastatin treatment suggesting that cytoplasmic maturation is not an essential prerequisite for efficient nuclear import of HR-preLaAWT (Kiel *et al*., 2014). Disrupted localization and the reduction of lamin B and LAP2 proteins were demonstrated in HGPS cells (Goldman *et. al*, 2004). Moreover, disruption of pRB-mediated entrance to S-phase was shown and progerin protein was shown interfering with mitosis (Cao *et al*. 2007). During mitosis, progerin was found to be distributed in cytoplasmic aggregates in HGPS cells.

A report revealed that increasing lamin A and lamin C expressions associated with cell and tissue stiffness (Swift *et al.*, 2013). Inhibition of DNA replication by depletion of B-type lamins was shown in Lmnb1 $^{\Delta/\Delta}$ mice (Malhas *et al*., 2007). Silencing of Lamin B1 expression was shown to give rise to a substantial reduction of cell proliferation in U-2-OS cells (Butin-Israeli *et al.*, 2015). In order to knock down the *LMNB1* using lentiviral expression of targeted shRNA in proliferating cells, it was exhibited that lamin B1 protein levels substantially decreased and within two passages cells became senescent (Shah *et al.*, 2013). Malhas *et al*, (2007), found that gene-poor chromose 18 is positioned at the nuclear periphery in three independent wild type and in negative isoprenylcysteine carboxyl methyltransferase mouse cells (ICMT$^{-/-}$). However, it was revealed that chromosome 18 altering its position from periphery to central in both deleted *LMNB* (*LMNB1* $^{-/-}$) and ras converting enzyme 1(*Rce1* $^{-/-}$) cells, suggesting that carboxymethylation is not important for the stability of lamin B1 and in the maintenance of chromosome 18 positioning and thus farnesylated and proteolyzed lamin B1 plays an impfortant role to anchor chromosome 18 to the periphery leading expression of a group of genes on this chromosome (Malhas *et al.*, 2007). LB1 is important to maintain nucler shape and organize the structures of the LA/C and LB2 meshworks and the B-type lamins have a role to position nuclear pore complexes within the lamina (Shimi *et al*., 2008). It was demonstrated in knock-in mice that expression of non-farnesylatable lamin B2 seems to develop in a normal manner, whereas lamin B1 that cannot be farnesylated resulting in severe loss in neuronal development and perinatal death (Jung *et al.*, 2013). Lamin B1-deficient cells were shown having spontaneously rotating nuclei, suggesting loss of nuclear anchoring and thus lamin B1 and B2 are crucial for neuronal migration during brain development (Jung *et al.*, 2013).

In HGPS cells, loss of heterochromatin from the nuclear periphery occurs (Goldman *et al*, 2004). In *C. elegans*, downregulation of Ce-BAF cause defects in chromosome segregation (Zheng et al., 2000). In almost all LAP2 isoforms, the C-terminal regions contain the lamin binding domain (Furukawa *et al*., 1998) and LAP2α is more distantly related amongst all other LAP2 isoforms (Dechat *et al.*, 1998). The disruption of the LAP2β-HA95 was shown to induce protesome-mediated proteolysis of replication factor Cdc6 and thus inhibition of replication (Martins *et al*., 2003). The impact of microinjection of the lamin-binding region of rat LAP2β into early G_1 stage was shown to affect nuclear growth and to inhibit entry of HeLa cells into S-phase (Yang *et al.*, 1997). Introduction of fragments containing the C-terminal chromatin-linked region of LAP2α lead inhibition of assembly of lamins around chromosomes (Vlcek *et al.*, 2002). In LMNA knock-out fibroblasts, the nuclear anchorage of Rb via lamin A/C / LAP2α is destabilized (Johnson *et al*., 2004). In some cells of the lamin A/C knockout mouse, emerin did not localize to the nuclear membrane (Sullivan et al., 1999). Intriguingly, it was shown in $Lmna^{LCO/LCO}$ mice that expression of only lamin C but lack of lamin A and prelamin A caused slight changes in nuclear shape and cells exhibited normal emerin localization (Fong *et al.*, 2006). Elimination of emerin in mice causes nuclei to become fragile (Ozawa *et al.*, 2006) and also to increase autophagic degradation of structurally aberrant regions of the nucleus (Park *et al.*, 2009). It was shown by using electron microscopy that physical damage to skeletal muscle nuclei in EDMD also detachment of membrane from lamina (Squarzoni *et al.*, 1998). Moreover, emerin was shown not localising to the nuclear membrane in some cells in the lamin A/C knockout mouse (Sullivan *et al*., 1999). Solovei and coworkers also revealed LBR and Lamin A/C staining in 39 species of diurnal and nocturnal mammals and found that neither lamin A/C nor LBR were expressed in mammals with inverted rod nuclei. However, either the LBR or Lamin

A/C was shown to be expressed in mammals with a conventional chromatin pattern (Solovei *et al*., 2013). Mice carrying a native (Lbr $^{ic/ic}$) and a transgenic (Lbr $^{GT/GT}$) mutation showed advanced inversion and also absence of Lamin A/C in rod cells (Solovei *et al*., 2013). Also, analysis of the expression of LEM domain proteins in WT retinas showed that both LAP2 and Man1 are present in rod at all phases of differentiation, however Lem2 were found not to be expressed in rods at any stage.In contrast, emerin was found to be expressed in young rod cells but as inversion progressed it became silenced. Interestingly, analysis of adult 6-month-old Emd $^{-/-}$ mice showed that neither nuclear inversion nor persistent LBR expression present in any cell type (Solovei *et al*., 2013).

LINC complexes protein of SUN1 was shown not to depend on the presence of lamins to localize and anchor in human nuclei (Hasan *et al.*, 2006). However, two domains; the N-terminal 299 amino acid and the C-terminal amino acids 500-723 are essential for proper nuclear rim localization of SUN1. Downregulation of lamin A/C and B1 revealed that there was no difference in the localization pattern of SUN1 compared to control cells (Hasan *et al*., 2006). In mammalian somatic cells of *Lmna* $^{-/-}$, it was shown that distribution of SUN2 was not affected having a rim-like pattern encompassing NE (Schmitt *et al.*, 2007). Mattioli and colleagues revealed that overexpression of farnesylated prelamin A in HEK293 human myoblast cells resulted in a remarkable increase of SUN1 and SUN2 staining at the nuclear envelope (Mattioli *et al.*, 2011). In *Lmna* $^{-/-}$ and *Sun1* $^{-/-}$ mice, it was demonstrated that rather than expected severe results than that seen for *Lmna* $^{-/-}$ mice, mice improves in terms of body weight and also pathological phenotype (Chen *et al.*, 2012). Progeria patients' cells nuclei appeared as having defected morphologies and blebs between the INM and ONM which is similar to those observed in other cell lines in which

interactions between SUN and KASH proteins were perturbed (Kandert *et al.*, 2007). In HGPS cells, it was shown that SUN1 formed punctate aggregates with lamin A in metaphase and an uneven distribution of SUN 1 and lamin A during telophases (Chen *et al.*, 2014). In primary spermatocytes from leptotene to diplotenes stages of myosis, telomere-FISH signals overlapped with those of anti- SUN1, indicating colocalization of SUN1 with telomeres and throughout the clustering-dissolution process telomeres were found to attach SUN1. Furthermore, in *SUN1* $^{-/-}$ mice littermates, almost all cells exhibited a zygotene-like SYCP3 staining and the telomeres positioned in the nucleoplasm, showing that SUN1 is essential in order to anchor telomeres at the NE (Ding *et al*., 2007). KASH and SUN proteins were shown to be involved in chromosome movement via meiotic-specific proteins of Bqt1 and Bqt2 to connect telomeres to Sad1 on the nucleoplasmic face of the INM in fission yeast (Chikashige *et al*., 2006). The loss of heterochromatin during the ageing process was first proposed by Villeponteau (1997), causing the derepression of silenced genes and leading to aberrant gene expression patterns (Villeponteau, 1997). Goldman *et al*., (2004) reported loss of peripheral heterochromatin in HGPS fibroblasts (Goldman *et al*., 2004). A reduction in fluorescence instensity and delocalisation for HP1α was shown in HGPS cells (Tsurumi and Li, 2012; Shumaker *et al*., 2006). The accumulation of pre-lamin A in cells affects localization of HP1α and only non-farnesylated intranuclear pre-lamin A gives rise to bright fluorescent nucleoplasmic foci appearance and shown partly overlapping with pre-lamin A aggregates suggesting that farnesylated pre-lamin A might affect the stability of the complex (Lattanzi *et al.*, 2007).

Post-translational modifications (PTMs) are vital biochemical events involved in the regulation of different cellular functions and can occur via the specific effect of a

modification at a single residue or via collective effects over various sites going through the same or distinct modificationsb (Nussinov *et al.*, 2012). Enzymes directly change the chemical structure of the proteins and these enzymes can be proteases, transferases (kinases, acetyltransferases, and methyltransferases) (Lothrop *et al.,* 2013). The common protein modifications contain phosphorylation, acetylation, glycosylation, ubiquitination and methylation (Karve and Cheema, 2011). Moreover, numerous comprehensive studies have shown extensive interactions between different pairs of PTMs such as phosphorylation- acetylation (van Noort *et al.*, 2012) and acetylation- ubiquitylation (Danielsen *et al.*, 2011). Proteolysis is an irreversible PTM process involves the break down of higly-specific hydrolysis of peptide and isopeptide bonds of a protein by a protease which generates new N and C termini. These cleveage events result in entirely altered protein function and they regulate a vast array of biological processes including DNA replication, cell cycle progression, and cell proliferation along with pathological processes such as inflammation, cancer and cardiovascular disease (Rogers and Overall, 2013). Nuclear lamins are regulated by PTMs and farnesylation of nuclear A- and B-type lamins is a type of prenylation involving modification of proteins with lipid intermediates that function in the cholesterol biosynthesis pathway (Snider and Omary, 2014). Farnesyltransferase (FTase) transiently farnesylates lamin A in the maturation process of lamin A and zinc metalloproteinase Ste24 homologue (ZMPSTE24) is involved in the removal of 15 tail domain residues, including farnesylated Cys to complete full maturation of lamin A. However, progerin does not undergo this last step due to missing of the ZMPSTE24 internal cleavage site and as a consequence becomes permanently associated with the inner nuclear membrane (Burke *et al*, 2013). In terms of B-type lamins, they are processed in a similar way to lamin A/C but they do not undergo the

last cleavage step and as a result they permanently retain their farnesyl lipid anchor (Winter-Vann and Casey, 2005).

From literature, it is apparent that nuclear lamin protein network and lamin-associated proteins play an important role to maintain correct nuclear functions and mechanical integrity of cells. Furthermore, perturbions of these proteins cause severe nuclear defects and diseases. The aim of this chapter is to understand the presence and distribution of nuclear envelope proteins within the immortalised HGPS cell lines. To the best of my knowledge, this study is the first study to assess the signal intensity of nuclear lamins and lamin associated proteins in hTERT HGPS cells. To address this gap of knowledge, I have assessed and analysed the distribution and presence of nuclear envelope proteins including nuclear lamins (lamins A/C, B1, and B2), lamin B receptor (LBR), lamin binding proteins; LAP2, emerin, NUP153 and LINC complex proteins; SUN1 and SUN2 in immortalised normal (NB1T) and immortalised HGPS cell lines and compared their localisation to normal fibroblast cell line (NB1) using indirectimmunofluorescence and immunoblotting.

4.1.1 The effects of Lovastatin in HGPS

In the pathology of HGPS, permanently farnesylated lamin A is considered to be the main underlying mechanism and (FTIs) are of great importance to target this mechanism (Snider and Omary, 2014). It was demonstrated in *in vitro* and *in vivo* studies that using FTIs can correct the abnormal structure of the nuclear envelope caused by mutations in *lamin A* (Fong *et al.*, 2006a). The lovastatin drug treatment of HGPS cells caused reduction of the lamin A level. Furthermore lovastatin together

with the histone deacetylase (HDAC) inhibitor TSA drug treatment was shown to abolish the accumulation of progerin in HGPS cells (Columbaro *et al.*, 2005). Swarmy and colleagues, (2002) have shown that Lamin B levels were greatly augmented in colon cancer cells with lovastatin treatment and it was shown that apoptosis was not induced at low dose levels (Swamy *et al.*, 2002).

The data in this chapter show that there is an issue with LB1 and LBR associating with the nuclear envelope in T06 and T08 cell lines respectively. Thus, it was decided to treat T06 and T08 cell lines with lovastatin to see if nuclear structure could be improved. Furthermore, pre-lamin A and HP1α immunofluorescence were assessed in lovastatin treated cells. Finally, we found by performing indirect immunostaining that LINC complex protein of SUN1 was missing at the nuclear membrane of both T06 and T08 cells. However, SUN1 protein was detected at the nuclear membrane of both NB1 and NB1T cells. Furthermore, western blotting results revealed that SUN1 protein is missing in T06 cells, however, a small fraction appeared in T08 cells. In terms of SUN2 protein, both indirect immunostaining and western blotting experiments revealed presence of protein in all cells.

4.2 Materials and Methods

4.2.1 Cell culture

As per chapter 2, section 2.2.1. , NB1 and hTERT human dermal fibroblasts immortalised cell lines: NB1T, TO6 and TO8 have been cultured.

4.2.2 Treatment with Lovastatin

The cells were treated with lovastatin (Sigma- Aldrich) which was dissolved in 100% ethanol at final concentration of 12 µm for 48 hours, (Appendices).

4.2.3 Indirect Immunofluorescence

4.2.3.1 Fixation

As per chapter 3, section 3.2.3.1. In order to carry out costaining experiments, cells were fixed with paraformaldehyde (PFA) 4% (w/v) (Sigma-Aldrich) for 4 minutes at room temperature (RT) followed by 3 washes in 1x PBS and then fixed cells were treated with 1% (v/v) Triton X 100 (Sigma-Aldrich) detergent in PBS for 10 minutes at RT and the washed again 3 times with 1X PBS.

4.2.3.2 Antibody staining

As per chapter 3, section 3.2.3.2

The primary antibodies used were; mouse anti-lamin A/C (diluted 1:100, NCL-LAM-AC), mouse anti-lamin B1 (diluted 1:50, Abcam- ab8982), rabbit anti-lamin B2 (diluted 1:250, Abcam-ab151735), mouse anti- emerin (diluted 1:30, NCL-emerin), mouse anti-LAP2 (diluted 1:100, Abcam- ab66588), rabbit anti- LBR(diluted 1:500, Abcam- ab32535, mouse anti- NUP153(diluted 1:1000, Abcam- ab24700)-{ a kind gift from Dr. Paola Vagnarelli, Brunel Univeristy, London}, rabbit anti -SUN1(diluted 1:100, Abcam-ab124770), rabbit anti-SUN2(diluted 1:50, Abcam-ab124916), goat anti-Pre-lamin A(diluted 1:50, sc-6214), mouse-anti HP1α(diluted 1:500, MAB3584), Rabbit anti-ki67(diluted 1:30, DAKO A0047).

The diluted secondary antibodies were; goat anti-mouse (TRITC) (diluted 1:30, Sigma- T-5393), goat anti-mouse (FITC) (diluted 1:64, Sigma-F9006), Swine anti-rabbit (TRITC) (diluted 1:25, Dako R0156), Rabbit anti-goat (FITC) (diluted 1:50 Sigma- F-7367).

4.2.3.3 Image acquisition

As per chapter 3, section 3.2.3.3. All images were taken at similar exposures within an experiment for each antibody.

4.2.4 Nuclear membrane and nuclei signal intensity analysis

In order to analyse a range of nuclear membrane and nuclei immunostaining results, Image J software was used. In the analysis of the nuclear membrane immunostaining the following steps were applied; the original image was converted to a gray scale image and then converted to binary images by clicking the following sections; process, binary and make binary. In order to make sure that the unit of length is pixels, the following steps were applied; analyse and set scale. Afterwards, the image was adjusted with threshold only covering the whole nucleus by activating the following sections; image, adjust and then threshold. Afterwards, the image was processed and filtered by activating the following sections; process, filters and minimum and 2 pixels were written in the space for radius. The processed image and the original image converted to the binary image were opened concomitantly. In order to obtain only the nuclear edge immunostaining the next step was performed by activating the following sections; process, image calculator, difference and then apply. The final process was performed by activating the following sections; analyse

and then analyse particles. The options for display results, clear results and exclude on edges were all activated and ok button was clicked and number written in the area section was considered as intensity of signal. At least 50 images were used to assess the nuclear membrane signal intesity of all our cell lines. The schematic figure (Figure 4.1) summarizes the application of nuclear membrane signal intensity analysis.

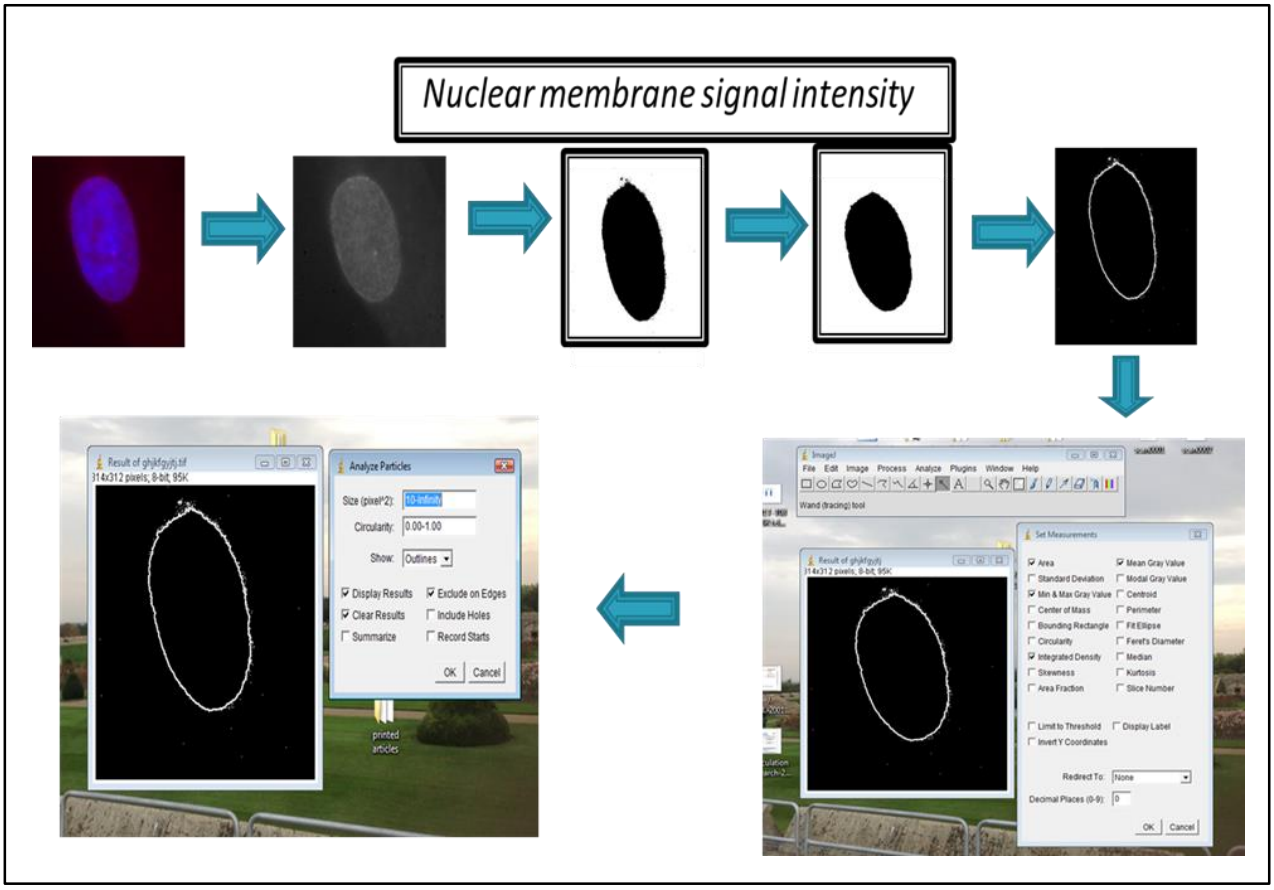

Figure 4.1 The Schematic image showing how to analyze nuclear membrane protein signal intensity by using Image J software.

In the analysis of nuclear only, the following steps were applied; the original image was converted to the gray scale image according to specific colour of secondary antibody and then converted to the mask image by activating the following sections; process, binary, convert to mask. In order to make sure that the unit of length is pixels, the following steps were applied; “analyse and set scale.” Afterwards, the image was adjusted with a threshold covering the whole nucleus by activating the following sections; image, adjust and then threshold. In order to obtain only the nuclei immunostaining, the next step was performed by clicking the following sections; analyse and then analyse particles. 255-infinity in pixels written in the size option was detected. The options for display results, clear results and exclude on edges were all ticked. Finally, ok button was activated and the number written in the area section was considered as intensity of signal. At least 50 images were used to assess the nuclei signal intesity of all our cell lines.

4.2.5 Western blotting

As per chapter 3, section 3.2.6.

The primary antibodies used were; mouse anti-lamin B1 (diluted 1:500, Abcam-ab8982), rabbit anti- LBR (diluted 1:500, Abcam- ab32535), rabbit anti -SUN1 (diluted 1:1000, Abcam-ab124770), rabbit anti-SUN2 (diluted 1:1000, Abcam-ab124916), mouse anti- α-tubulin (diluted 1:4000, Sigma Aldrich-T5168- {a kind gift from Dr. Ines Castro, Brunel University, London}.

The diluted infrared secondary antibodies used for western blotting were; Goat (polyclonal) anti-mouse (diluted 1:15000, LI-COR 926-32210) {a kind gift from Dr. Ines Castro, Brunel University, London}, Donkey (polyclonal) anti-rabbit (diluted

1:15000, LI-COR 926-32213) {a kind gift from Dr. Ines Castro, Brunel University, London}, Goat anti-human (diluted 1:15000, LI-COR 926-32232) {a kind gift from Dr. Ines Castro, Brunel University, London}.

4.2.6 Western blotting protein quantification

In order to analyse and quantify the levels of a range of proteins, Image J software was employed. The relative density values were calculated by dividing the percent value in each row by the percent value of the control protein bands.

4.2.7 Whole exome sequencing

WES was performed at UCL Institute of Child Health as a service using Nextera Rapid Capture Exome Kit (Illumina, FC-140-1001). The sequence data from AG08466 HGPS sample was trimmed down to generate 101 bp and 76 bp, pair-end data sets. Down-sampled subsets of the AG08466 exomes were generated by random selection using the Picard DownsampleSam script and then included in separate BAM files. All sequencing reads were aligned to the human hg19 GENOME using the Burrow-Wheeler Aligner (BWA). The bioinformatics pipeline for data analysis decribed below (Figure 4.2).

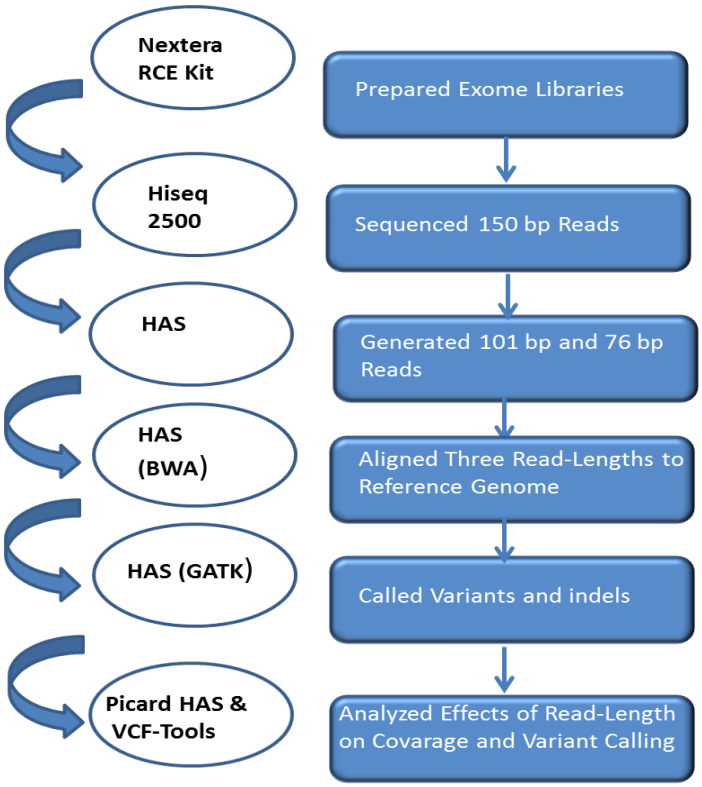

Figure 4.2 Analytical pipeline for WES. Left panel shows program used for each step. Right panel shows analysis steps. Nextera Rapid capture Exome libraries were pooled and sequenced on a Hiseq 2500 System as 2 x 150 bp reads. Reads were trimmed to 101 bp AND 76 BP with Hiseq Analysis software (HAS) and aligned to the reference genome with the Burrows-Wheeler Aligner (BWA). Varient calling and indel realignment were performed with Genome Analysis Tool Kit (GATK). Effect of read length on mean coverage, variant calling, and enrichment performance were analysed with Picard CalculateHsMetrics14 and HAS.

4.2.8 Statistical analysis

Values are expressed as averages ± SEM, and n represents the number of cells analysed. Two-tailed unpaired t-tests used as statistical analysis. Significance was taken as $P \leq 0.05$. The level of significance is indicated as: * $P \leq 0.05$, ** $P \leq 0.01$, *** $P \leq 0.001$ and **** $P \leq 0.0001$.

4.3 Results

4.3.1 Distribution and signal intensity analysis of lamins and lamin binding proteins by indirect immunofluorescence

Lamin and lamin binding proteins are candidates for the mutation in T08 cells. Thus, in this study, I aim to assess and gain insight into the distribution and signal intensity of lamins and lamin binding proteins in human normal fibroblast NB1, immortalised normal fibroblast NB1T and immortalised typical T06 and atypical T08 HGPS cell lines. This was determined by indirect immunofluorescence using a range of antibodies. The cell lines were fixed with methanol: acetone (1:1). In each cell line, for each antibody 50 individual nuclei were scored to analyse signal intensity.

A

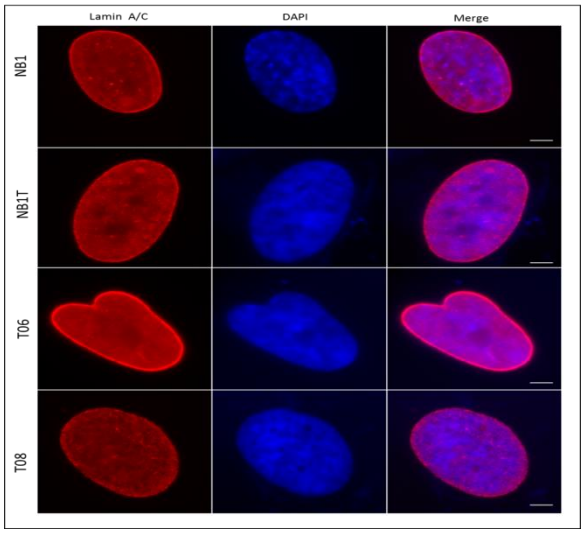
Lamin A/C
DAPI
Merge
NB1
NB1T
TO6
TO8

B

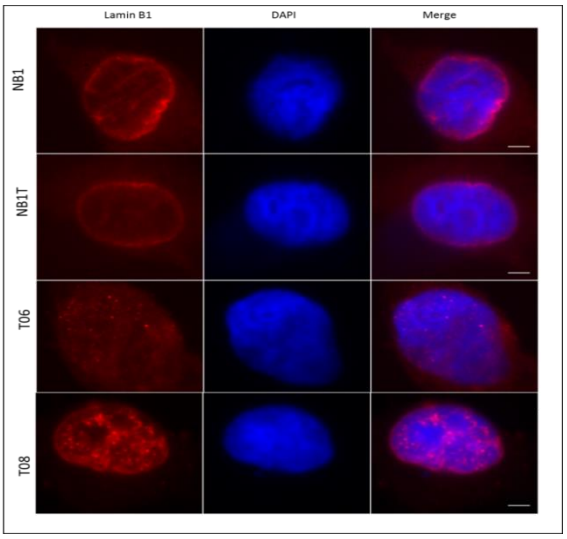
Lamin B1
DAPI
Merge
NB1
NB1T
TO6
TO8

C

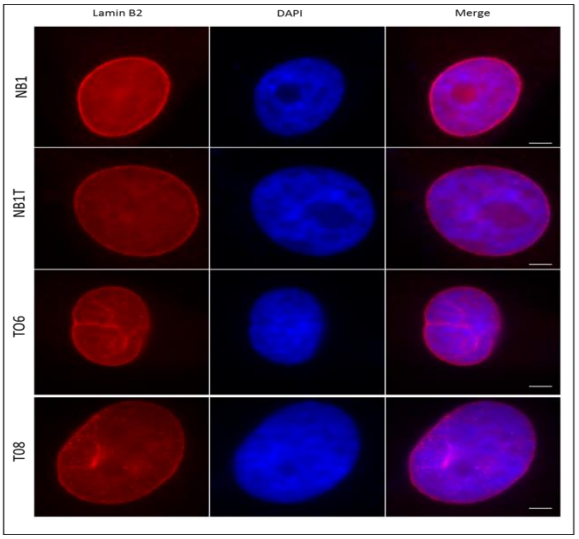
Lamin B2
DAPI
Merge
NB1
NB1T
TO6
TO8

D

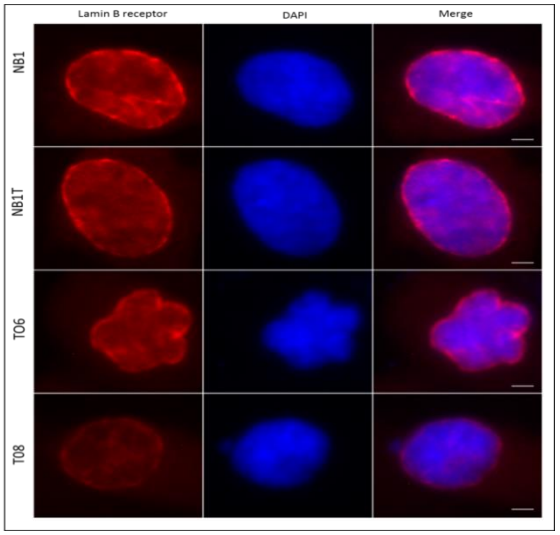
Lamin B receptor
DAPI
Merge
NB1
NB1T
TO6
TO8

E

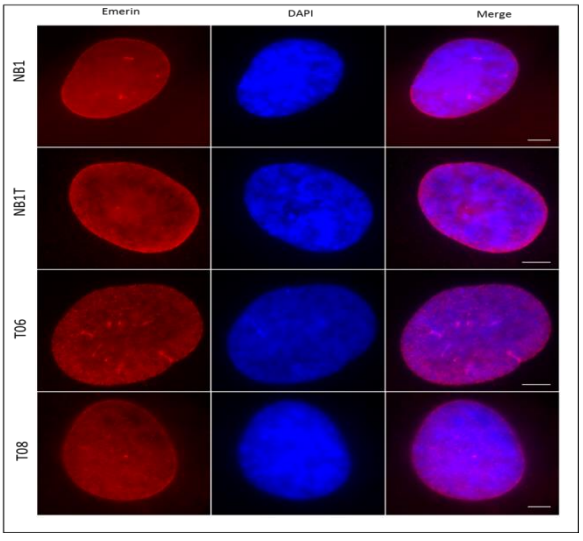
Emerin
DAPI
Merge
NB1
NB1T
TO6
TO8

F

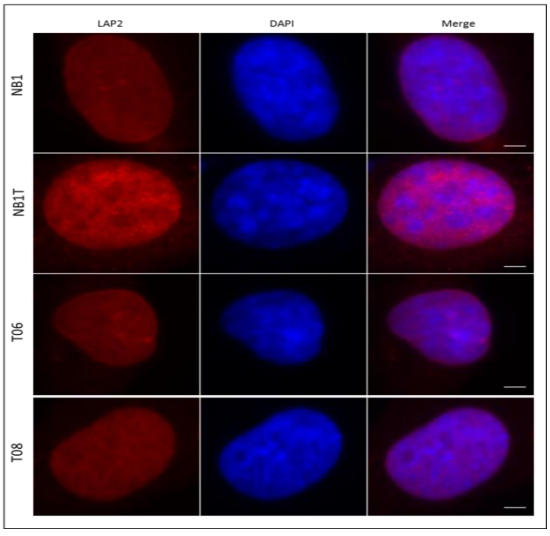
LAP2
DAPI
Merge
NB1
NB1T
TO6
TO8

G

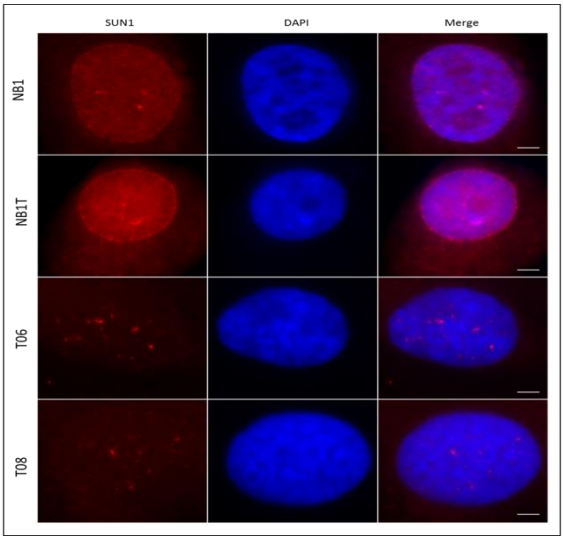

H

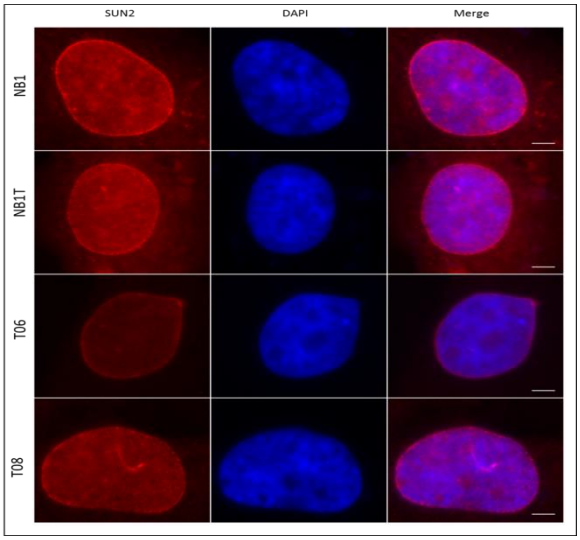

I

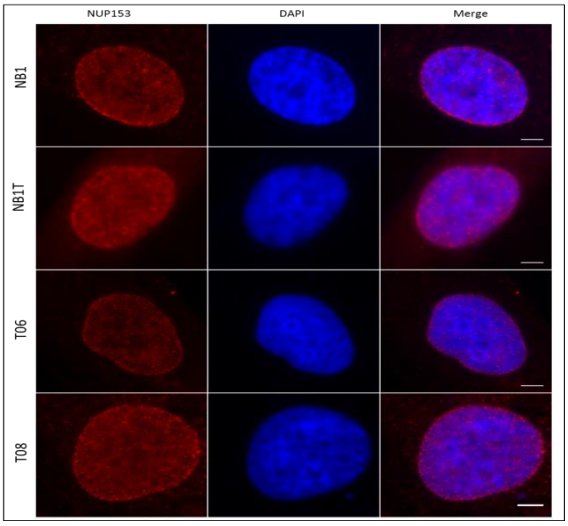

Figure 4.3: Different distributions of nuclear lamins and lamin binding proteins. Representative images of nuclear lamins and lamin binding proteins; Lamin A/C(A)(red), Lamin B1(B)(red), Lamin B2(C)(red), Lamin B receptor(D)(red), Emerin(E)(red), LAP2 (F)(red), SUN1(G)(red), SUN2(H)(red) and NUP153(I)(red) in NB1, NB1T, T06 and T08 cells. The nucleus is counter-stained with DAPI to reveal the DNA (blue). Magnification = X100. Scale bars= 5 μm.

A

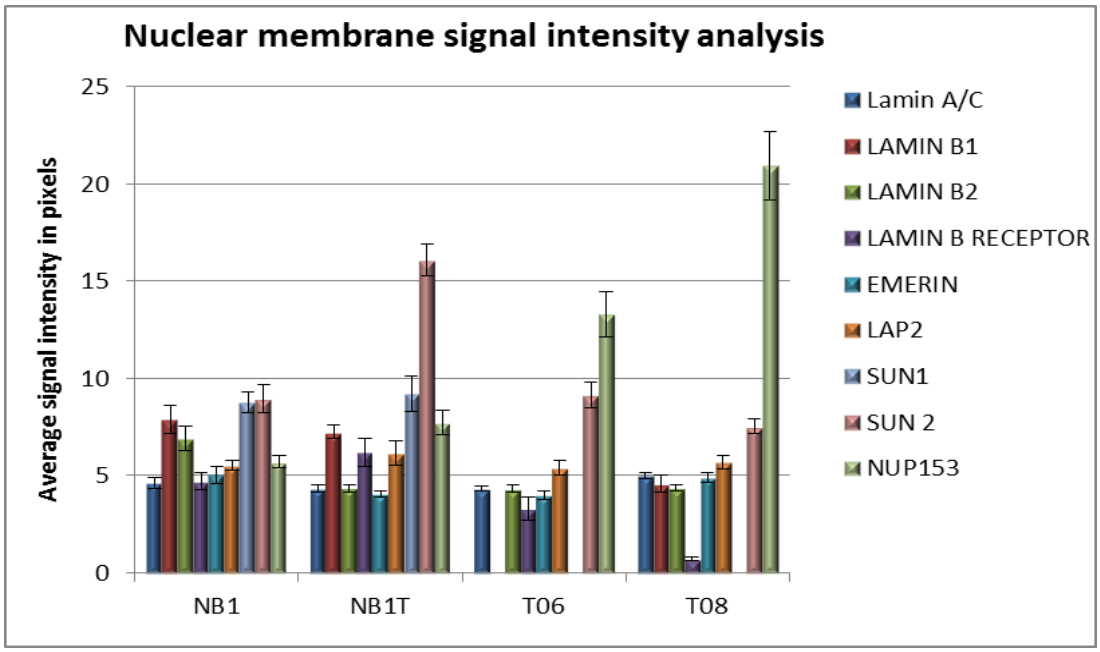

B

	NB1-NB1T	NB1-T06	NB1-T08	NB1T-T06	NB1T-T08	T06-T08
Lamin A/C						
Lamin B1						
Lamin B2						
Lamin B Receptor						
Emerin						
Lap2						
SUN1						
SUN2						
NUP153						

Figure 4.4 Graph displays nuclear membrane signal intensity analysis of lamins and lamin binding proteins; Lamin A/C(A), Lamin B1(B), Lamin B2(C), Lamin B receptor(D), Emerin(E), LAP2 (F), SUN1(G), SUN2(H) and NUP153(I) in NB1, NB1T, T06 and T08 cells.(A) Statistical analysis of nuclear membrane signal intensity analysis using the Student's *t*-test. Green shading indicates no significant difference between the populations, yellow shading depicts a p value < 0.05 and red shading represents p-value <0.01. There is no detected signal intensity at the NE of SUN-1 in T06, T08 cells and no detected signal intensity of Lamin B1 in T06 cells. (B)

A

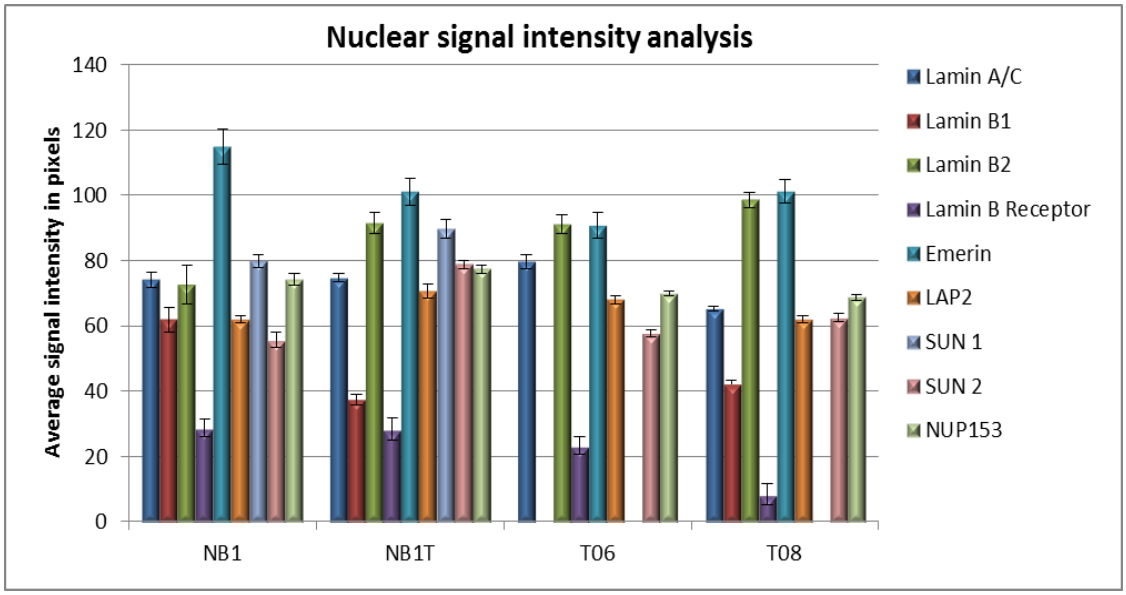

B

	NB1-NB1T	NB1-T06	NB1-T08	NB1T-T06	NB1T-T08	T06-T08
LAMIN A/C						
LAMIN B1						
LAMIN B2						
LAMIN B Receptor						
Emerin						
LAP2						
SUN 1						
SUN 2						
NUP153						

Figure 4.5 Graph displays nuclei signal intensity analysis of lamins and lamin binding proteins; Lamin A/C(A), Lamin B1(B), Lamin B2(C), Lamin B receptor(D), Emerin(E), LAP2 (F), SUN1(G), SUN2(H) and NUP153(I) in NB1, NB1T, T06 and T08 cells.(A) Statistical analysis of nuclear membrane signal intensity analysis using the Student's t-test. Green shading indicates no significant difference between the populations, yellow shading depicts a p value < 0.05 and red shading represents p-value <0.01. There is no detected signal intensity of SUN-1 in T06, T08 cells and no detected signal intensity of Lamin B1 in T06 cells. (B)

Table 4.1: The percentages of nuclear membrane signal intensity of lamins and lamin binding proteins.

	NB1	NB1T	T06	T08
Lamin A/C	4.64 ± 0.28	4.34 ± 0.17	4.32 ± 0.12	5.01 ± 0.14
Lamin B1	7.06 ± 0.71	7.23 ± 0.35	0 ± 0	4.59 ± 0.41
Lamin B2	6.89 ± 0.62	4.35 ± 0.18	4.33 ± 0.18	4.35 ± 0.16
LBR	4.71 ± 0.4	6.18 ± 0.73	3.29 ± 0.6	0.72 ± 0.09
Emerin	5.04 ± 0.43	4.06 ± 0.16	3.99 ± 0.22	4.91 ± 0.26
Lap2	5.5 ± 0.25	6.16 ± 0.64	5.4 ± .04	5.67 ± 0.32
SUN1	8.76 ± 0.52	9.19 ± 0.89	0 ± 0	0 ± 0
SUN2	8.96 ± 0.71	16.08 ± 0.82	9.14 ± 0.65	7.53 ± 0.38
NUP153	5.69 ± 0.3	7.71 ± 0.63	13.27 ± 1.16	20.09 ± 1.76

Table 4.2: The percentages of nuclear signal intensity of lamins and lamin binding proteins.

	NB1	NB1T	T06	T08
Lamin A/C	74.15 ± 2.33	74.72 ± 1.35	79.66 ± 2.26	65.17 ± 0.8
Lamin B1	61.85 ± 3.73	37.41 ± 1.7	0 ± 0	42.1 ± 1.31
Lamin B2	72.58 ± 5.89	91.5 ± 3.35	91.17 ± 2.99	98.25 ± 2.41
LBR	28.67 ± 2.68	28.33 ± 3.29	23.28 ± 2.74	8.46 ± 3.11
Emerin	114.75 ± 5.33	101.08 ± 4.21	90.9 ± 3.94	101.18 ± 3.73
Lap2	61.9 ± 1.05	70.46 ± 2.14	67.9 ± 1.21	62.1 ± 1.11
SUN1	79.8 ± 2.15	89.66 ± 2.79	0 ± 0	0 ± 0
SUN2	55.6 ± 2.25	78.7 ± 1.28	57.72 ± 1.02	62.48 ± 1.13
NUP153	74.21 ± 1.78	77.3 ± 1.21	69.92 ± 0.84	68.79 ± 0.89

The pattern of lamin A/C distribution is a rim staining at the nuclear membrane and a few small foci in the nucleoplasm of NB1, NB1T and T08 cells. In T06 cells lamin A/C shows a thicker rim staining around the nuclear membrane for T06 cells (Figure 4.3-A). In addititon, the numbers of intranuclear spots were observed to be lower in T06 cells relative to other cells. The mean nuclear membrane signal intensity of lamin A/C in NB1 cells is 4.64 ± 0.28 (n=50), which is not significantly different compared to immortalised normal NB1T fibroblasts (4.34 ± 0.17, $p< 0.05$, n=50), immortalised typical T06 fibroblasts (4.32 ± 0.12, $p<0.05$, n=50) and immortalised atypical T08 fibroblasts (5.01 ± 0.14, $p<0.05$, n=50) (Figure 4.4-A). On the other hand, statistical results reveal that the nuclear membrane signal intensity of Lamin A/C in T08 fibroblasts is significantly greater than both NB1T and T06 fibroblasts ($p<0.001$)(Figure 4.4-A,B). The pattern of lamin B1 staining in both NB1 and NB1T

cells appeared as rim staining. However, in T06 and T08 cells, the loss of lamin B1 at the nuclear edge is apparent (Figure 4.3-B). Specifically, there is a complete loss of rim staining of lamin B1in T06 fibroblasts which give rise no detection of signal at the nuclear envelope compared with controls (Figure 4.4-B). Further, nuclei of T06 cells do display a few speckles of LB1 in the nucleoplasm (Figure 4.5-A). In T08 fibroblasts, Lamin B1 staining shows an aberrant rim distribution in addition to many spots throughout the nucleoplasm. The mean nuclear membrane signal intensity of Lamin B1 in NB1 cells is 7.86 ± 0.71 (n=50), which is not significantly different compared to NB1T fibroblasts (7.23 ± 0.35, $p>0.05$, n=50), whereas it is significantly greater than T06 fibroblasts (0, $p<0.001$, n=50) and T08 fibroblasts (4.59 ± 0.41, $p<0.001$, n=50) (Figure 4.4-A, B). The lamin B2 displays a normal distribution in the nuclei of NB1 and NB1T cells, with some internal speckles; whereas T06 and T08 cells show a partial loss of lamin B2 staining in the nuclear interior. Furthermore, T06 and T08 cells exhibit significantly higher number of speckles in the nucleoplasm (Figure 4.3-C). The mean nuclear membrane signal intensity of Lamin B2 in NB1 fibroblasts is 6.89 ± 0.62 (n=50), which is significantly greater than NB1T (4.35 ± 0.18, $p<0.001$, n=50), T06 (4.33 ± 0.18, $p<0.001$, n=50) and T08 (4.35 ± 0.16, $p<0.001$ n=50) fibroblasts (Figure 4.4-A, B). The distribution of LBR is at the nuclear rim staining in all cell lines. However, T08 cells display a partial loss and a faint rim staining compared to other cell lines (Figure 4.3-D). The mean nuclear membrane signal intensity of LBR in NB1 fibroblasts is 4.71 ± 0.4 (n=50), which is not significantly different than NB1T fibroblasts (6.18 ± 0.73, $p>0.05$, n=50). However, it is significanty different from T06 fibroblasts (3.29 ± 0.6, $p< 0.05$, n=50) and significantly greater than T08 fibroblasts (0.72 ± 0.09, $p < 0.001$, n=50) (Figure 4.4-A, B). Emerin is normally distributed at the nuclear rim in all cells and can be seen in internal foci as well (Figure 4.3-E). The mean nuclear membrane signal intensity of

emerin in NB1 fibroblasts is 5.04 ± 0.43 (n=50), which is not significantly different than NB1T fibroblasts (4.06 ± 0.16, p > 0.05, n=50), T06 fibroblasts (3.99 ± 0.22, p>0.05, n=50) and T08 fibroblasts (4.91 ± 0.26, p >0.05, n=50) (Figure 4.4-A, B). The distribution of LAP2 is also at the nuclear rim and a homogenous nucleoplasmic distribution of many small spots in all the cell lines.However, NB1T cells seem to display more spots than other cell lines (Figure 4.3-F). The mean nuclear membrane signal intensity of LAP2 in NB1 fibroblasts is 5.5 ± 0.25, n=50, which is not significantly different compared to NB1T fibroblasts (6.16 ± 0.64, p >0.05, n=50), T06 fibroblasts (5.4 ± 0.4, p> 0.05, n=50) and T08 fibroblasts (5.67 ± 0.32, p >0.05, n=50) (Figure 4.4-A, B). SUN1 is normally distributed at the nuclear rim in both NB1 and NB1T cells and can be seen as a few speckles as well. However, T06 and T08 cells show aberrant distribution of SUN1 with it being found in the nucleoplasm with many speckles and no nuclear rim staining (Figure 4.3-G). The mean nuclear membrane signal intensity of SUN1 in NB1 fibroblasts is 8.76 ± 0.52, n=50, which is not significantly different than NB1T fibroblasts (9.19 ± 0.89, p > 0.05, n=50). However, significantly greater than both T06 fibroblasts (0 ± 0, p < 0.01, n=50) and T08 fibroblasts (0 ± 0, p < 0.01, n=50) (Figure 4.4-A, B). SUN2 is distributed at the nuclear rim and as a few speckles in the nucleoplasma in all cells. In addition to that, T08 cells display less nuclear membrane staining compared to other cell lines (Figure 4.3-H). The mean nuclear membrane signal intensity of SUN2 in NB1 fibroblasts is 8.96 ± 0.71, n=50, which was significantly different compared to NB1T fibroblasts (16.08 ± 0.82, p < 0.05, n=50), whereas not significantly different than T06 fibroblasts (9.14 ± 0.65, p>0.05, n=50) and T08 fibroblasts (7.53 ± 0.38, p> 0.05, n=50) (Figure 4.4-A, B). The distribution of NUP153 exhibits a rim staining around the nuclei in all cell lines. Intriguingly, T08 cells display intense nuclear envelope staining compared to other cell lines (Figure 4.3-I). The mean nuclear envelope

signal intensity of NUP153 in NB1 fibroblasts was 5.69 ± 0.3, n=50, which is significantly smaller than NB1T fibroblasts (7.71 ± 0.63, p< 0.01, n=50), T06 fibroblasts (13.27 ± 1.16, p< 0.01, n=50) and T08 fibroblasts (20.9 ± 1.76, p< 0.01, n=50) (Figure 4.4-A, B). Table-4.1 displays the percentages of nuclear membrane signal intensity of proteins in each of cell lines.

The mean nuclear signal intensity of Lamin A/C in NB1 cells is 74.15 ± 2.33, n=50, which is not significantly different than NB1T fibroblasts (74.72 ± 1.35, p>0.05, n=50) and T06 fibroblasts (79.66 ± 2.26, p> 0.05, n=50) whereas significantly greater than T08 fibroblasts (65.17 ± 0.8, p < 0.01, n=50) (Figure 4.5-A, B). The mean nuclear signal intensity of Lamin B1 in NB1 cells is 61.85 ± 3.78, n=50, which is significantly greater than NB1T fibroblasts (37.41 ± 1.7, p<0.01, n=50), T06 fibroblasts (0 ± 0, p<0.01, n=50) and T08 fibroblasts (42.1 ± 1.31, p<0.01, n=50) (Figure 4.5-A, B). The mean nuclei signal intensity of Lamin B2 in NB1 fibroblasts is 72.58 ± 5.89, n=50, which is significantly smaller than NB1T fibroblasts 91.5 ± 3.35, p<0.01, n=50), T06 fibroblasts (91.17 ± 2.99, p<0.01, n=50) and T08 fibroblasts (98.5 ± 2.41, p< 0.01, n=50) (Figure 4.5-A, B).The mean nuclear signal intensity of lamin B receptor in NB1 fibroblasts is 28.67 ± 2.68, n=50 , which is not significantly different than NB1T fibroblasts (28.33 ± 3.29, p> 0.05, n=50) and T06 fibroblasts (23.28 ± 2.74, p>0.05, n=50). However, significantly greater than T08 fibroblasts (8.46 ± 3.11, p<0.01, n=50) (Figure 4.5-A, B). The mean nuclear signal intensity of emerin in NB1 fibroblasts is 114.75 ± 5.33, n=50, which is significantly different than NB1T fibroblasts (101.08 ± 4.21, p<0.05, n=50) and T08 fibroblasts (101.18 ± 3.73, p<0.05, n=50) and significantly greater than T06 fibroblasts (90.9 ± 3.94, p<0.01, n=50) (Figure 4.5-A, B). The mean nuclear signal intensity of LAP2 in NB1 fibroblasts is 61.9 ± 1.05, n=50, which is significantly smaller than NB1T (70.46 ± 2.14, P<0.01,

n=50) and T06 fibroblasts (67.9 ± 1.21, p<0.01, n=50) and not significantly different than T08 fibroblasts (62.1 ± 1.11, p>0.05, n=50) (Figure 4.5-A, B). The mean nuclei signal intensity of SUN1 in NB1 fibroblasts is 79.8 ± 2.15, p<0.01, n=50), which is significantly greater than T06 (0 ± 0, p<0.01, n=50) and T08 (0 ± 0, p<0.01, n=50) fibroblasts. However, significantly smaller than NB1T fibroblasts (89.66 ± 2.79, P<0.05, n=50) (Figure 4.5-A, B). The mean nuclei signal intensity of SUN2 in NB1 fibroblasts is 55.6 ± 2.25, n=50, which is significantly greater than NB1T (78.7 ± 1.28, P<0.01, n=50) and T08 fibroblasts (62.48 ± 1.13, p<0.01, n=50) and not significantly different than T06 fibroblasts (57.72 ± 1.02, p<0.05, n=50) (Figure 4.5-A, B). The mean nuclei signal intensity of NUP153 in NB1 fibroblasts is 74.21 ± 1.78, n=50, which is not significantly different than NB1T fibroblasts (77.3 ± 1.21, p>0.05, n=50) whereas, significantly different than T06 (69.92 ± 0.84, p<0.05, n=50) and significantly greater than T08 fibroblasts (68.79 ± 0.89, p<0.01, n=50) (Figure 4.5-A, B). Table-4.2 displays the percentages of nuclear signal intensity of proteins in each of cell lines.

A

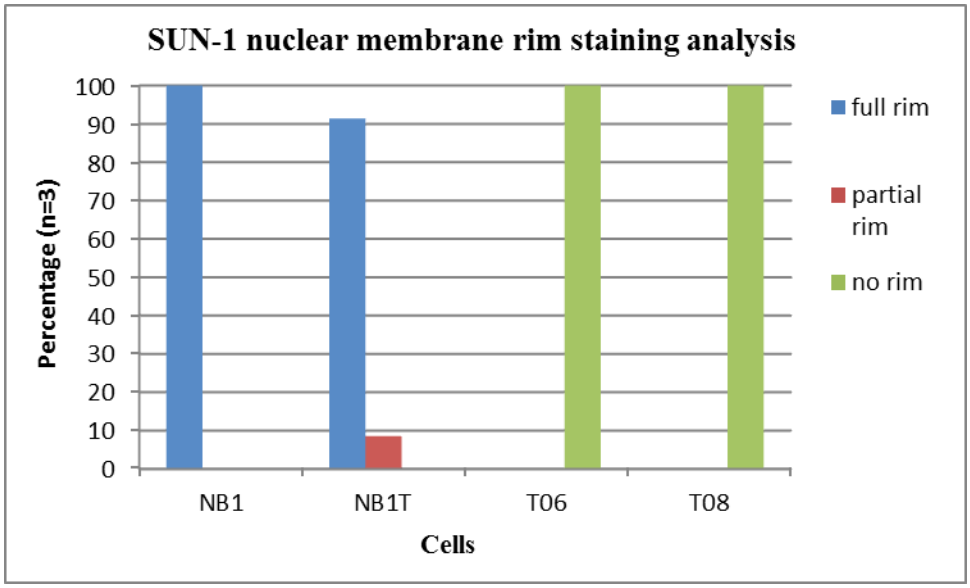

B

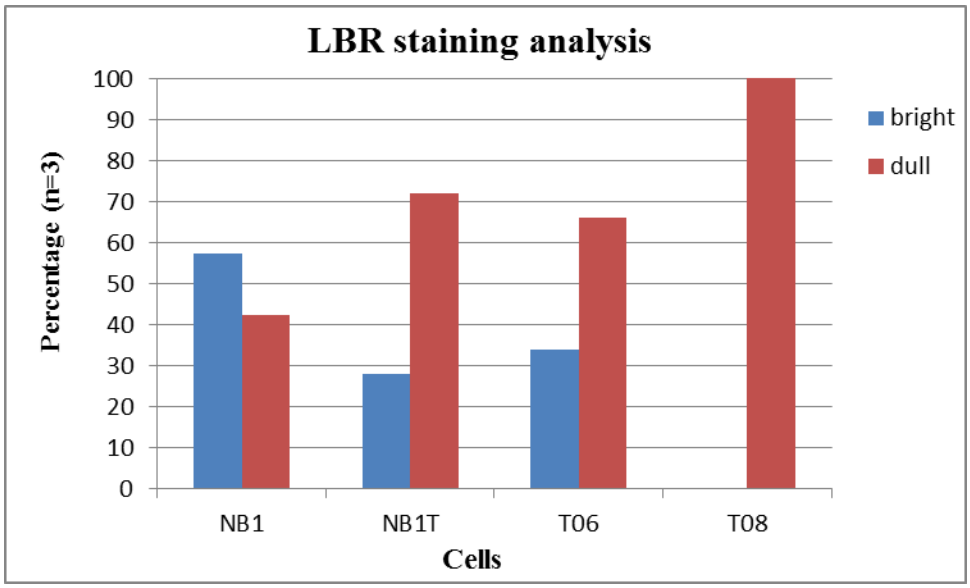

Figure 4.6 SUN1 (A) and LBR (B) immunostaining pattern analysis of NB1, NB1T, T06 and T08 cells. N represents number of experiments analysed. These percentages were calculated by counting at least 200 cells for each cell line. The cells were fixed with metahanol: aceton, 1:1.

Figure 4.6-A and B displays the percentages of SUN1 and LBR staining pattern analysis for NB1, NB1T, T06 and T08 cells. Full rim SUN1 staining was found in high percentages in NB1 (100%) and NB1T (91.4%) cells. However, no rim SUN1 staining was found in high percentages in T06 (100%) and T08 (100%) cells. LBR staining of cells demonstrate that NB1 cells (57.5) have higher percentage of bright staining than other cells whereas dull LBR staining was found in higher percentage in T08 cells (100%).

A

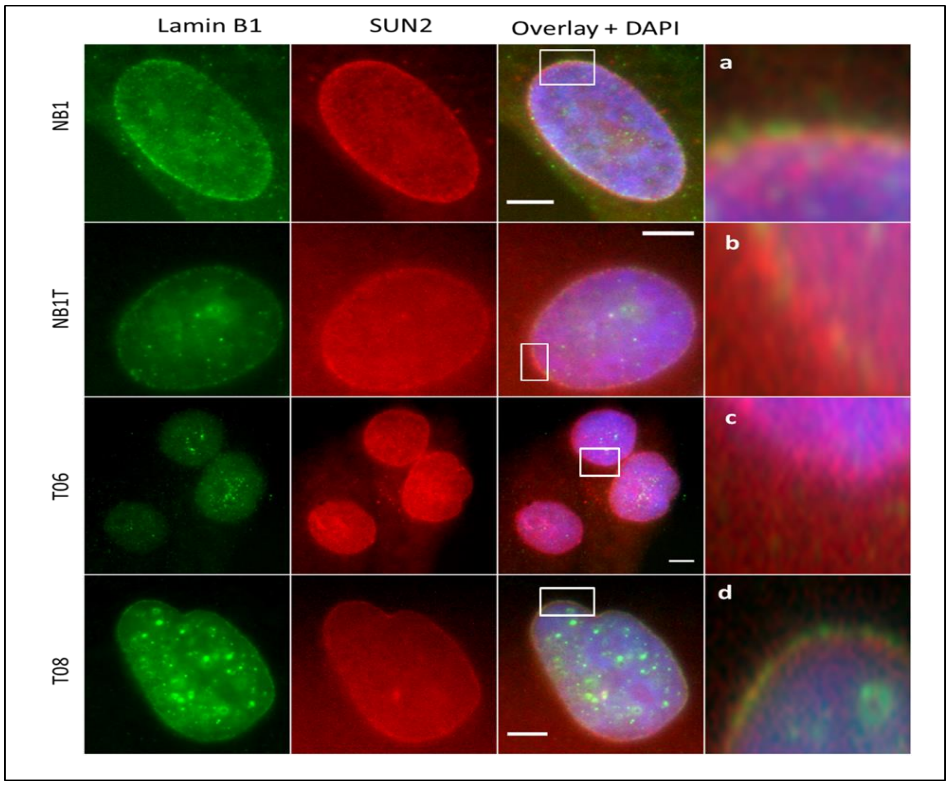
Lamin B1
SUN2
Overlay + DAPI
NB1
NB1T
T06
T08
a
b
c
d

B

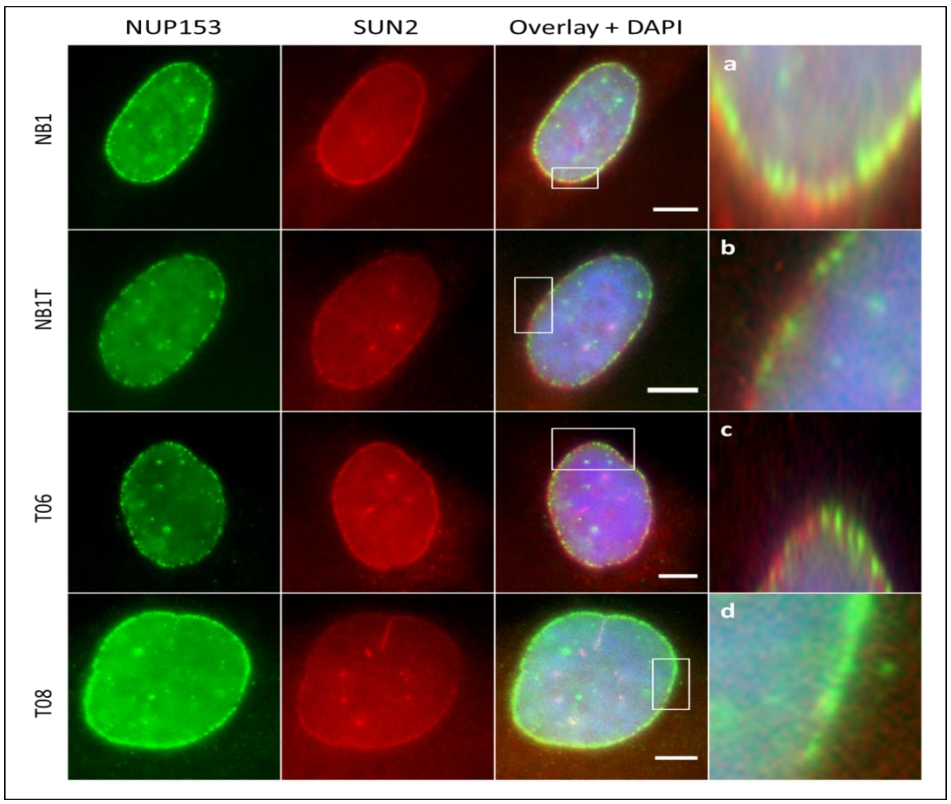
NUP153
SUN2
Overlay + DAPI
NB1
NB1T
T06
T08
a
b
c
d

Figure 4.7 NB1, NB1T, T06 and T08 cells were immunostained by using antibodies directed against Lamin B1 and SUN2 (A) and NUP153 and SUN (B). Enlargements (x 5) of the overlay areas indicated by white boxes are shown as a, b, c, and d. The nucleus is counter-stained with DAPI to reveal the DNA. Magnification = X100. Scale bars= 5 μm.

Co-staining analysis of LB1 and SUN2 showed that LB1 colocalizes with SUN2 at the NE in NB1, NB1Tand T08 cells. However, it was confirmed that LB1 staining is disrupted in T06 cells (Figure 4.7-A). Co-staining analysis of NUP153 and SUN2 exhibited that NUP153 colocalizes with SUN2 at the NE in all cell lines. Furthermore, it was confirmed that NUP153 is overexpressed in T08 cells (Figure 4.7-B).

4.3.2 Western blotting

In order to determine if the aberrations seen in immunofluorescence were due to truncated proteins, western blotting was performed for Lamin B1, LBR, SUN1 and SUN2 proteins. Data were obtained by performing triplicate independent western blots. The size and amount of the proteins were examined, with the aim of confirming that if these proteins are normally expressed in cells. Using NB1T, T06 and T08, whole cell lysates were sampled. The western blots results can be seen in Figure 4.8. Where lamin B1 was detected, a single band was present for NB1T and T08 cells at a molecular weight of 68 kDa. In agreement with the immunofluorescence staining, no Lamin B1 band was detected in T06 cells. The relative density values of Lamin B1 for NB1T, T06 and T08 cells are; 0.938,0 and 1 respectively. SUN1 was detected in NB1T and T08 cells at a molecular weight of 100 kDa with a very faint band for SUN1 was detectable in T08 extracts. In line with immunofluorescence staining results, no SUN1 band was detected for T06 cells. The relative density values of SUN1 for NB1T, T06 and T08 cells are 1, 0 and 0.078 respectively. NB1T,

T06 and T08 cell lines stained SUN2 with the expected single band with molecular weight of 80 kDa. The relative density values of SUN2 for NB1T, T06 and T08 cells are 0.87, 0.93, and 1 respectively. LBR band was detected in all cell lines. In agreement with the immunostaining results, a smaller fraction LBR was detected in T08 cells with the relative density values of 0.372. The relative density values representing the signal intensity values for NB1T and T06 cell lines were 0.674 and 1.048 respectively. α-tubulin was used to normalize the levels of protein detected by confirming that protein loading is the same across the gel. The representative image showing the loading control protein α-tubulin with molecular weight of 58 kDa was detected along with Lamin B1. α-tubulin detected in cells with the relative density values representing the signal intensity for NB1T, T06 and T08 cell are 0.97, 0.95, and 1 respectively.

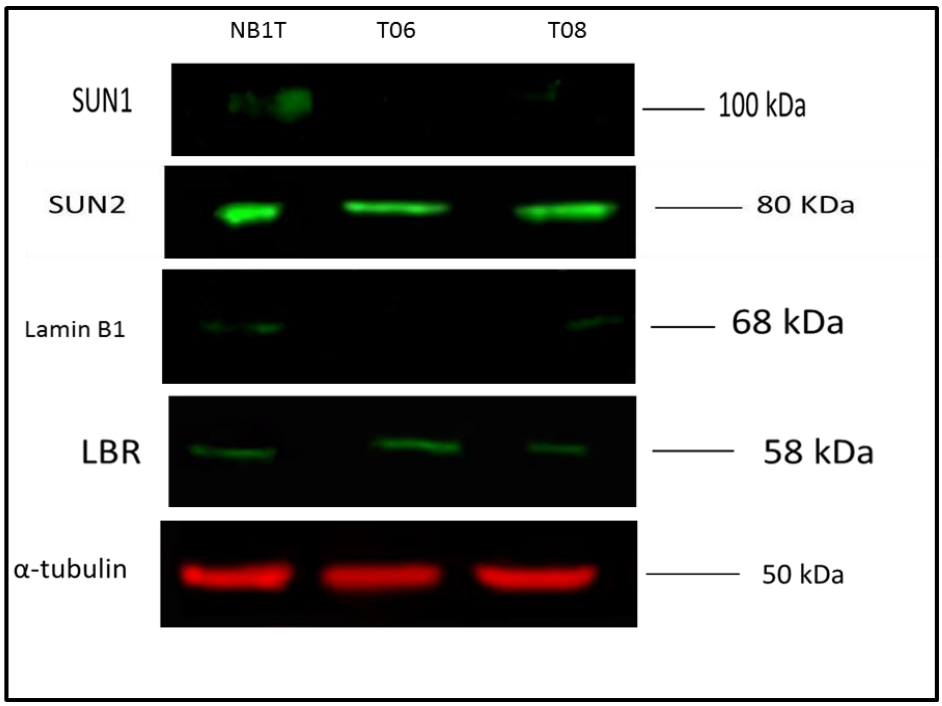

Figure 4.8 Samples of cultured immortalised NB1T control and immortalised typical (T06) and atypical (T08) cell lines in SDS sample buffer were resolved on 10% SDS-PAGE gels, and anti-Lamin B1, anti-SUN1 and anti-SUN2 and LBR antibodies were

used to identify Lamin B1, SUN1, SUN2 and LBR. All samples were loaded equally, 2 x 10^5 cells per lane. α-tubulin was used to normalize the level of proteins.

4.3.3 Whole exome sequencing

Atypical AG08466 cells were previously described as been derived from a HGPS patient having progeria on the Coriell website. Furthermore, it was decribed as mother, father and sister of the patient are not affected. Nonetheless, according to Nicolas Levy's group AGO84466 cells do not harbour a *LMNA* the G608 mutation at exon 11 (Personal communication, Dr. N. Levy), suggesting that the genetic cause of HGPS occurred in either another gene or other genes. Therefore, we do not think, it is a classical mutation and we hypothesise that mutations might be found in genes that encode related nuclear envelope proteins. Previous report noted that AG08466 cells were elucidated as having a greater growth potential and a reduced number of fractions of morphologically abnormal nuclei such as; blebs, herniations (Bridger and Kill, 2004). As decribed in Godwin L. S., study (2010), investigation on exome sequencing of the candidate genes; *ZMPSTE2, LAP2* and *EMD* revealed that these genes are unlikely to harbour the mutation in AG08466 cells either. It has been reported that about 85 % of all mutations related with Mendelian diseases occur in exome boundaries (Wang *et al.*, 2013). In order to determine if the aberrant distribution of proteins were associated with a mutation, whole-exome sequencing (WES) was performed by UCL genomics, London to identify varients associated with HGPS. WES is unbiased and comprehensive technique, which has been employed in the clinical setting to detect pathogenic variation, to enrich characterisation of genomic architecture and for a variety of diseases to discover the underlying genetic origin of disease on a research basis (Picoraro and Chung, 2015). Based on my

findings from immunostaining and western blotting on T08 cells (immortalised AG08466 cell), there are 3 candidate genes which might harbour the mutation and resulted in the clinical phenotype shown by HGPS patients. These genes are; *LMB1, LBR* and *UNC84A*. From the nextera rapid capture exome data provided by UCL genomics for AG08466 HGPS cells, we revealed that 2457589 position of promoter region is missing on *LMNB2* gene located on chromosome 19.

4.3.3 Lovastain treatment and restoration of Pre-lamin A and HP1α in AG08466 cells

Statins or the HMG-CoA reductase inhibitors have been used in order to decrease the cholesterol levels in the serum and to inhibit mevalonate biosynthesis pathways by hampering the enzyme named 3-hydroxy-3-methylglutarylcoenzyme A(HMG-CoA) reductase (Tsiligiri *et al.*, 2015). Lovastatin is a statin that interferes on this pathway. NB1T, T06 and T08 cells were treated with lovastatin, at concentration of 12 µm for 48 hours. It was demonstrated by Corcos and Le Jossic-Corcos, 2013 and Ahmed M.M.H, 2013 that in terms of proliferation of the cells, this concentration is the best concentration of drug to use (Corcos and Le Jossic-corcos, 2013). Lovastatin treatment was shown to increase expression of *lamin B1* and *LBR* genes in cancer cells (Hassan Ahmed, 2013). The cells were treated with different lovastatin concentrations (0 µM, 12 µM) for 48 hours. The distributions of post treatment of Pre-lamin A, LBR and HP1α, Lamin B1 in NB1T, T06 and T08 cells were assessed in triplicate. In the control NB1T cells, pre-lamin A is processed rapidly and thus there was no positive staining for pre-lamin A. However, the untreated T08 cells displayed prelamin A as a weak rim staining in addition to internal speckles suggesting that in HGPS fibroblasts, pre-lamin A is accumulating at foci within the nucleoplasm but also additionally at the nuclear rim (Figure 4.9-A).

However, following lovastatin treatment both NB1T and T08 cells displayed a strong nuclear rim of pre-lamin A at the NE with in addition internal foci (Figure 4.9-A). In order to confirm that using 12 µm concentration of drug is not harmful and whether it caused growth arrest, cells were stained with Ki-67. The proportion of cells exhibiting Ki-67 positive staining upon drug treatment in NB1T and T08 were 70.6% and 73% respectively, which indicates that the chosen concentraton of drug did affect proliferation (Figure 4.9-B). Taken together the data generated by these analyses reveal that lovastatin inhibits the farnesylation of lamin A in NB1T and T08 cells allowing increased pre-lamin A staining at the nuclear envelope, with internal foci. Interestingly, it was found that lovastatin treatment caused complete absence of LBR nuclear membrane staining in both NB1T and T08 cells and cytoplasmic aggregation (Figure 4.10-A). HP1α was dramatically reduced in T08 cells compared to normal NB1T cells and but following lovastatin treatment, the staining of HP1α strikingly was increased in T08 cells. However, following drug treatment no change was seen in NB1T cells (Figure 4.10-B). Lamin B1 immunostaining of NB1T cells following drug treatment was significantly decreased at NE staining and accumulation of internal foci. Furthermore, we found that drug treatment of T06 cells did not cause any alterations of lamin B1 staining(Figure 4.10-C).

A

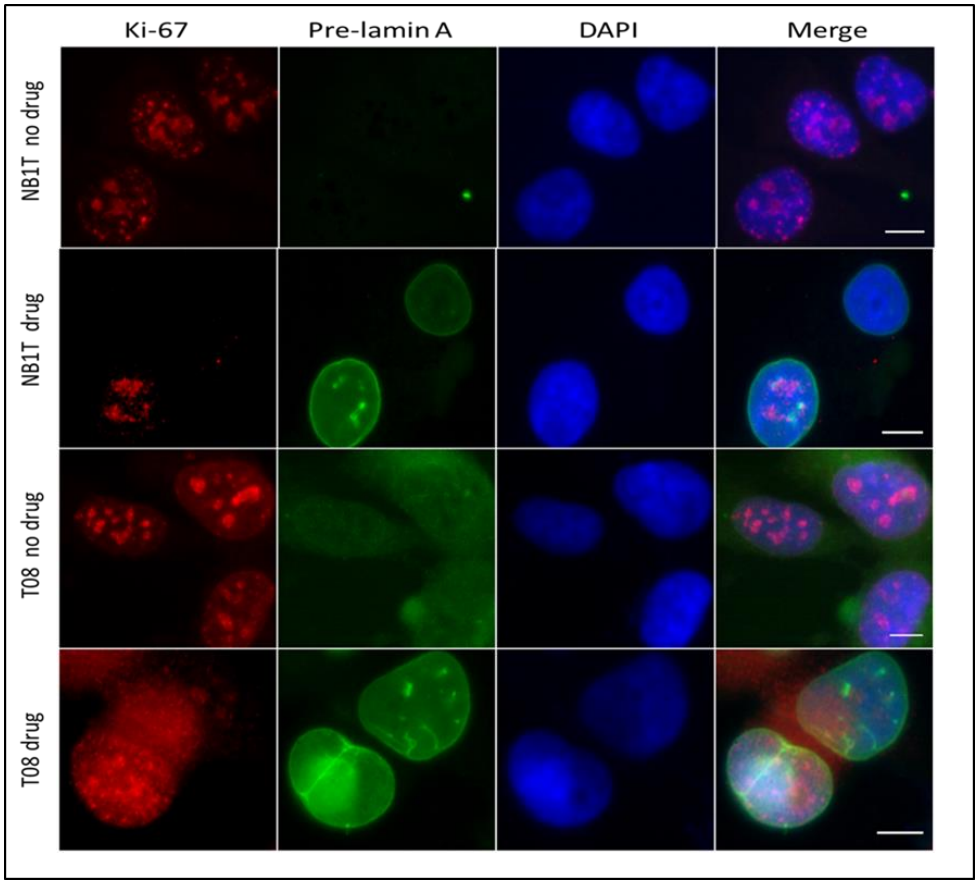
Ki-67
Pre-lamin A
DAPI
Merge
NB1T no drug
NB1T drug
T08 no drug
T08 drug

B

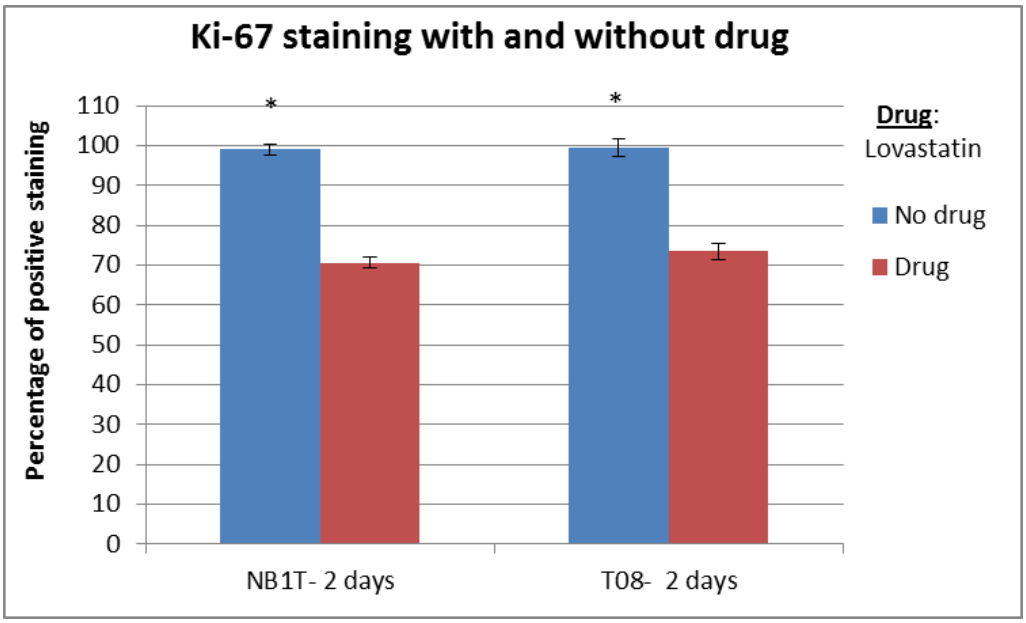
Ki-67 staining with and without drug
Percentage of positive staining
110
100
90
80
70
60
50
40
30
20
10
0
*
*
NB1T- 2 days
T08- 2 days
Drug:
Lovastatin
No drug
Drug

Figure 4.9 The presence and distribution of Pre-lamin A in NB1T, T06 and T08 cell lines before and after treatment with Lovastatin at 12 µm for 48 hours were determined by indirect immunofluorescence. NB1T and T08 cells were immunostained with Pre-lamin A along with Ki-67 (A). A graph shows percentage of Ki-67 positive staining before and after the drug treatment (B). The nucleus is counter-stained with DAPI to reveal the DNA. Error bars represent standard error of mean (SEM). The level of significance is indicated as: * $P \leq 0.05$. Magnification = X100. Scale bars= 10 µm.

A

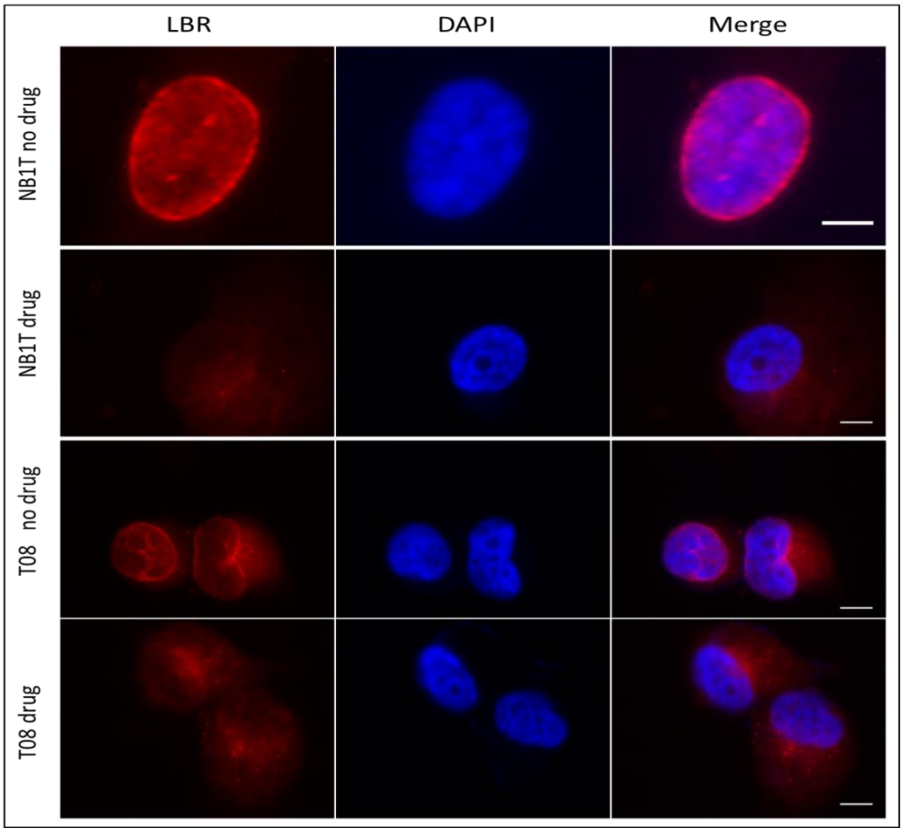
LBR
DAPI
Merge
NB1T no drug
NB1T drug
T08 no drug
T08 drug

B

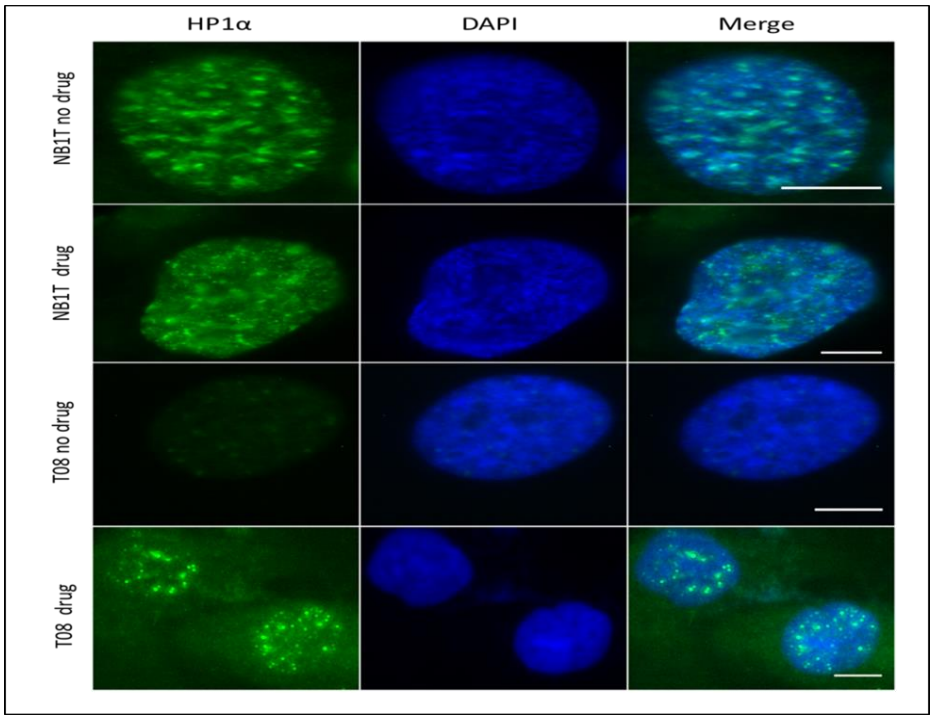
HP1α
DAPI
Merge
NB1T no drug
NB1T drug
T08 no drug
T08 drug

C

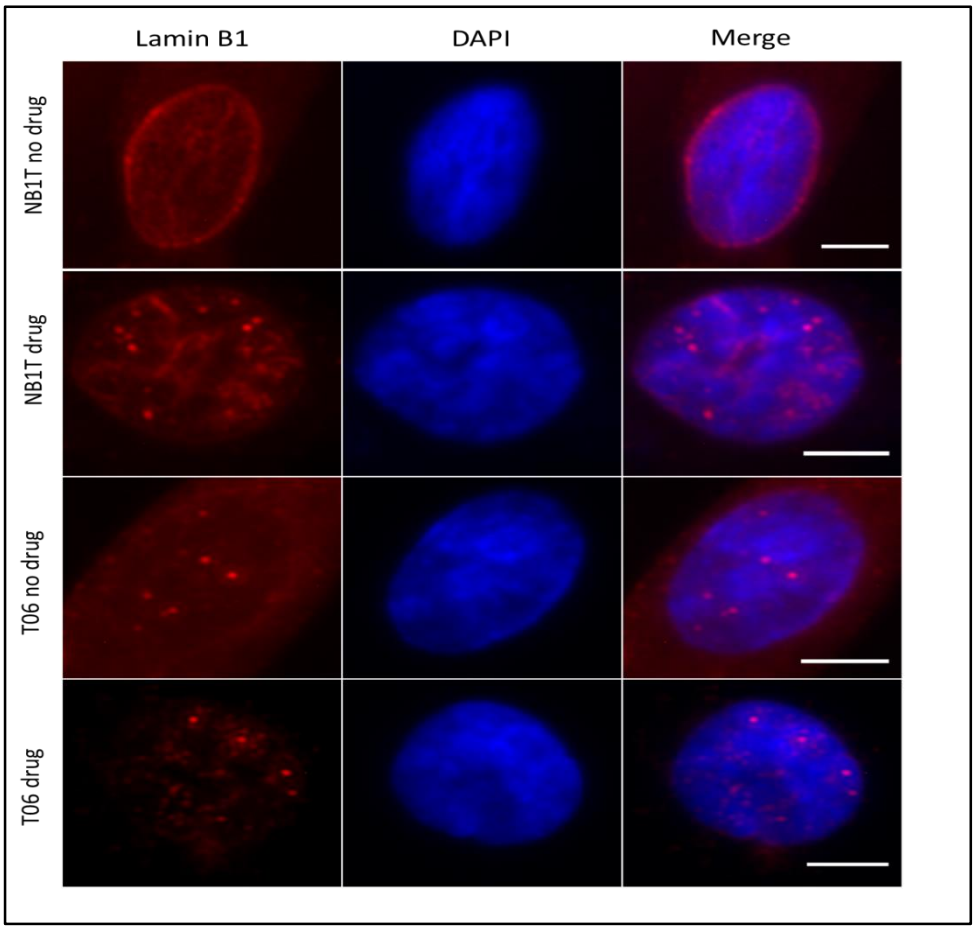

Figure 4.10 The presence and distribution LBR, HP1α and LB1 proteins in NB1T, T06 and T08 cell lines before and after treatment with Lovastatin at 12 μm for 48 hours were determined by indirect immunofluorescence. NB1T and T08 cells were immunostained with LBR (A). NB1T and T08 cells were immunostained with HP1α (B). NB1T and T06 cells were immunostained with LB1 (C). The nucleus is counter-stained with DAPI to reveal the DNA. Magnification = X100. Scale bars= 10 μm.

4.4 Discussion

The architecture of cell nuclei is often changed in HGPS cells. Alterations in nuclear structures could severely affect gene expression and normal function of the cells. The aim of this chapter was to assess and compare the distribution and presence of lamin and lamin associated proteins in hTERT immortalised HGPS fibroblasts with immortalised control NB1T fiboblasts. I found that some of the lamin binding proteins, nuclear pore protein (NUP153) and chromatin binding protein of heterochromatin protein 1 α(HP1α) and also 'LINC' (Linker of Nucleoskeleton and Cytoskeleton) complexes are altered in the immortalised typical (T06) and atypical (T08) HGPS cells. Western blotting results confirmed my findings obtained from immunostaining nuclear membrane and nuclei signal intensity analysis of Lamin B1, SUN1, SUN2 and LBR proteins.

Mutations occurred in human *LMNA* gene cause abnormal thickening of the nuclear lamina (Goldman *et al*., 2004). My nuclear membrane signal intensity analysis of Lamin A/C data presented here demonstrates that T08 atypical progeria cells have the highest signal intensity. However, the nucleoplasm signal intensity analysis revealed that T08 cells have the lowest signal intensity. It was observed from the microscopic images that both T06 and T08 progeria cells have an apparent thicker lamin A/C staining around the nuclei. Lamins are known to assemble into a dense network in the nuclear lamina. However, Lamins A and C are also can be found in the nuclear interior (Adam and Goldman, 2012). In the nucleoplasm of NB1 and NB1T cells, more spots of lamin A/C were detected than in T06 and T08 progeria cells. In my all analysed cells, all cells apart from T06 exhibited Lamin B1 a rim staining around the nucleus. Furthermore, low nuclear membrane signal intensity was detected with many spots found throughout the nucleoplasm in T08 cells.

Scaffidi and Mistelli, (2005) showed the reduction of LB1 in HGPS cells. The nucleoplasmic B-type lamins could form a polymer network structure that provides a scaffold to interact with A-type lamins and also other unknown factors. Even though B-type lamins are known to play a prominent role in nuclear structure and stability and mainly in cells devoid of A-type lamins, in cells expression of both types of lamin levels of A-type lamins correlate more strongly with nuclear stiffness compared to B type lamins(Swift *et al*., 2013) .The mutant Lamin B1 expression in mice was shown to die at birth (Harborth *et al.*, 2001) and in terms of cell proliferation B-type lamins are required rather than A-type lamins. A dramatic decrease of LB1 expression was shown at passage number 42 of HeLa cells when the cells stopped proliferating indicating that the loss of Lamin B1 is a senescence marker in normal diploid cells (Bercht Pfleghaar *et al.*, 2015). Lamin B1 is required for the regulation of gene expression and splicing (Camps *et al.,* 2015). Mouse embryonic fibroblasts missing Lamin B1 grown in *in vitro* condition showed nuclear aberrations, premature senescence and disrupted proliferation (Dreesen *et al.*, 2013b). I showed that the nuclear membranes of typical progeria T06 cells are devoid of Lamin B1 staining. Furthermore, LB1 staining of T08 cells appeared to be disrupted as many spots in the nucleoplasm were detected. Co-staining findings revealed that both LB1 and SUN2 disperse as punctuates around the nuclear membrane in NB1T cells. Furthermore, fewer numbers of foci of SUN2 staining were observed in T06 cells which show loss of LB1 nuclear membrane staining. My immunoblotting findings confirmed the loss of LB1 protein in T06 cells. It was shown that blebs enriched in LA/C, with little or no staining with LB2 antibody (Shimi *et al*., 2008). My observations revealed that herniations on the nuclear membrane, there is little or loss of rim staining with lamin B2. These results suggest strong interaction between LA/C, LB1 and LB2 and lack of or partial loss of LB1 in cells dramatically altered nuclear

membrane staining of LA/C and LB2. While, whole WES data for AG08466 cell reveals that *LMNB2* gene is one of the list of the predicted deleterious varients, I showed that expression of LMNB2 protein is almost the same in analysed cells. It was revealed by amplification of 12 exons plus > 50 nt at each intron-exon boundary of LMNB2 genes that four heterozygous genomic sequence variants of *LMNB2* exist in five APL subjects and these varients were described as exon 1 c82G → A, intron 1- 6G → T, exon 5 c.643G → A (p. R215Q; in two patients), exon 8 c 1218G → A (p.A407T) (Hegele *et al*., 2006). Immunostaining results of lamin binding protein of LBR revealed that staining is severely affected in T08 cells as having great loss of nuclear membrane staining which is in aggrement with my western blotting results exhibiting small fraction of LBR band. The similarity of the distribution between lamin A and emerin and quite different distribution between A-type lamin and emerin were shown in distinct cell types in the heart (Manilal *et al*., 1999). My findings of emerin immunostaining revealed normally distribution of nuclear rim staining of the emerin protein in all cells. A reduced expression of LAP2α was shown in human dilated cardiomyopathy (DCM) (Taylor *et al*., 2005). It was suggested that the lack of LAP2α may play a role for cellular senescence (Pekovic *et al*., 2007). As my control and progeria cells are immortalised leading them be highly proliferative, I demonstrated that the distribution of LAP2α was similar in all cells. Furthermore, NB1T cells exhibited more spots in nucleoplasm relative to other cells with some indication of aggregation inside the nucleus. It was revealed in HGPS cells that physical interaction between progerin and the LAP2 is decrased. However, it is important to note that total LAP2α levels were shown to remain stable in protein samples. Furthermore, loss of close physical proximity between LAP2α and the telomeres were shown in HGPS cells (Chojnowski *et al.*, 2015). In the early phases

of nuclear reassembly, partial overlap of telomeric TTAGGG repeat binding factor 2 (TRF2) structures with LAP2α on chromatin consistent with a targeting of LAP2α to telomeric regions was shown. In addition, by performing fluorescence recovery after photobleaching (FRAP) analysis in cells expressing GFP-LAP2α it was revealed that photobleached regions in the nucleoplasm turned over rapidly to almost their prebleach intensity within 8 seconds in interphase whereas, bleached areas recovered to only about 10% of their prebleach intensity in telophase proposing that LAP2α was stably associated with these core structures (Dechat *et al.*, 2004).

The LINC complex proteins are known to connect the nucleoplasm with the cytoskeleton and have roles in nuclear anchorage and cell polarity (Crisp *et al*., 2006). SUN1 is normally located around the nuclear membrane, positioned by mechanisms but may depend on interaction with intermediate filament protein lamin A (Haque *et al.*, 2006). The signal intensity findings revealed bright staining of SUN1 as a rim around the nuclear membrane in both NB1, NB1T cells. However the signal intensity analysis revealed that SUN1 protein is missing on the nuclear membrane of both T06 and T08 cells. Furthermore, accumulation of SUN1 seen as speckles in nucleoplasm was observed in both T06 and T08 cells lines. In agreement with immunostaining results, the western blotting findings confirm missing SUN1 expression in T06 cells. Moreover, a small fraction of SUN1 band was detected for T08 cell line. Mislocation and over-accumulation of SUN1 in the Golgi having pathogenic and cytotoxic effects causing nuclear herniations were shown in LAΔ50 mice cells. Intriguingly, previous study exhibited the elevated expression of SUN1 in HGPS *(LMNA* c.1824C>T) human fibroblasts compared to control cells by immunostaining and western blotting analysis and cells stained brightest for SUN1 were shown having larger nuclei and more severe nuclear morphological aberrations

and knockdown of SUN1 ameliorated cellular aberrancies and longevity defects (Chen *et al.,* 2012). In contrast to Chen *et al.,* (2012) findings, I did not observe any nuclear defects in both NB1 and NB1T cells showing elevated expression of SUN1. Taken together, the findings demonstrate that both LB1 and SUN1 are perturbed in typical T06 cells which could suggest that B-type lamins may be required to retain SUN1 at the nuclear membrane. Aqueous channels that span the NE are occupied by nuclear pore complexes (NPCs) (Tran and Wente, 2006). Using an antibody against NUP153, my results revealed that NUP153 is distributed uniformally as foci around the nuclear membrane in NB1, NB1T and T06 cells whereas NUP153 localises as clusters in T08 cells. Co-staining findings revealed that NUP153 and SUN2 overlap more in T08 cells than other cells.

I demonstrated that there is a loss of LB1 expression in typical HGPS T06 cells by performing immunostaining and westernblotting and lovastatin treatment did not cause significant changes in LB1 distribution in T06 cells. In contrast, this was not the case for NB1T cells as it was observed that drug treatment leads to a loss of LB1 staining on the nuclear membrane of control NB1T cells. In conjunction with, NB1T cells exhibited significantly higher proportion of speckles in the nucleoplasm after drug treatment. In contrast to my findings, it was shown that upon treatment with pravastatin- zoledronate, nucleoplasmic aggregates of lamin B1 disappeared in HGPS cells (Varela et al., 2008). In line with these findings, Adam *et al.*, 2013 revealed a decrease in the amount of LB1 in normal human foreskin fibroblasts even treated with a low concentration (0.5 μm) of farnesyltramsferase inhibitor (FTI) lonafarnib and LB1 was not detected in HGPS cells before or after drug treatment (Adam, *et al*., 2013). Furthermore, it was shown that normal and HGPS patient dermal fibroblasts became senescent within 4 days after drug addition (Adam, et al.,

2013). Farnesylated pre-lamin A is known to be intrinsically toxic protein if left uncleaved and embedded in the nuclear rim causing misshapen nuclei and severe disease phenotypes such as in HGPS (Davies *et al.*, 2011). Statins are amongst the approved drug to block synthetic metabolic pathway of farnesyl pyrophosphate and geranylgeranyl pyrophosphate. Thus in this study I evaluated the effects of lovastatin on immortalised normal (NB1T) and HGPS atypical (T08) fibroblasts. I elucidated that control NB1T cells do not show any pre-lamin A staining since it is processed rapidly. However atypical HGPS T08 cells exhibit a weak nuclear rim staining and internal speckles. It was revealed that lovastatin drug treatment gives rise to a strong accumulation of pre-lamin A around the nuclear membrane in both in NB1T and T08 cells. Furthermore, I showed that staining of pre-lamin A in the nucleoplasm increased significantly in lovastatin treated NB1T and T08 cells. These data suggest that because pre-lamin A is farnesylated and rapidly converted to mature lamin A, the pre-lamin A antibody does not detect prelamin A in untreated cells. However, in the presence of lovastatin, pre-lamin A processing is blocked, and easily detectable in both NB1T and T08 cells. It is noteworthy that expression of permanently farnesylated pre-lamin A variant prelamin A ′L647R′ caused a substantial defect in proliferation, which is similar to that of cells expressing progerin or elevated levels of pre-lamin A, compared to control cells. In addition, it was demonstrated that HGPS cells and cells expressing high levels of wild-type pre-lamin A show a high frequency of nuclear membrane morphology aberrations, including nuclear membrane lobulation and blebbing (Candelario *et al.*, 2011).

It has been suggested by several studies that pre-lamin A's hydrophobic lipid anchor is substantial for targeting of the protein to the inner nuclear membrane (Sinensky *et al.*, 1994). In agreement with my findings, Sinensky *et al*, (1994) showed that Hela

cells treated with lovastatin resulted in accumulation of pre-lamin A, different than untreated cells which gives little or no signal (Sinensky, Fantle and Dalton, 1994). It was exhibited using combination of pravastatin and zoledronate drugs that pre-lamin A was accumulated in the nuclear matrix in both normal and HGPS-treated cells (Varela *et al*., 2008). It was revealed by silencing the expression of *LMNA* with specific siRNAs to cause accumulation of pre-lamin A, leading increased intracellular ROS levels, altered mitochondrial potential and gene expression (Sieprath *et al.*, 2015).

I found that LBR is affected in atypical HGPS cells compared to NB1T cells. Intriguingly, my immunofluuorcence analysis indicated that drug treatment gave rise to a complete absence of nuclear membrane LBR staining in both NB1T and T08 cells. Furthermore, upon drug treatment it was observed that LBR was found in cytoplasmic aggregates both in NB1T and T08 cells. To maintain an extensive range of cellular processes such as gene silencing, genomic integrity and cell division, the correct regulation and spatial organization of heterochromatin is essential (Dambacher *et al.*, 2013). It has previously been described that downregulation and loss of heterochromatin are pathological hallmarks of HGPS cells (Shumaker *et al*., 2006) and in agreement with this I found that HP1α is affected in our immunostained HGPS atypical T08 cells. Interestingly, upon lovastatin treatment T08 cells exhibited increased HP1α staining which is the good indication of rescue of heterochromatin organization. Columbaro and colleagues, (2005) exhibited by performing lovastatin plus trichostain A (TSA) treatment on HGPS cells that heterochromatin organization was restored (Columbaro *et al*., 2005).

The WES data for AG08466 (T08 parental line) cells obtained from UCL Institute of Child Health. The candidate genes of *SUN1*, *LBR* and *LMNB1* were analysed in the

raw list of predicted deleterious varients and there were no matches. By searching other possible candidate genes such as *LMNB2*, we found that chromosome 19: 2457589, *LMNB2* gene has a variant in its promoter and transcription is regulated by BRCA1. The *BRCA1* tumour-suppressor gene was defined by its mutation in inherited breast and ovarian cancer (King *et al.*, 2003; Miki *et al.*, 1994). Furthermore, missing of BRCA1 was shown resulted in dispersal of focal staining of H3meK9 and also loss of asynchronous X-chromosome replication, suggests that BRCA1 might be involved in the regulation of the structure and function of heterochromatin (Lachner and Jenuwein, 2002). Importantly, loss of tumour suppressor proteins; BRCA1 and 53BP1 has been evidenced to cause accumulation of DNA damage and genomic instability and also augmented cancer incidence (Morales *et al.*, 2003; Scully and Livingston, 2000). Bridger *et al*., (2004) showed that AG08466 cells exhibits increased rate of apoptosis in cultures. In Lmna $^{\Delta 8\text{-}11/\Delta 8\text{-}11}$ fibroblasts, genomic instability- telomere shortening was shown to increase leading to reduction of BRCA1, indicating deregulated transcription (Das *et al.*, 2013). Human HCC1937 cell line deficient with *BRCA1* was exhibited to repress the expression of satellite DNA transcripts almost 20-fold (Zhu *et al.*, 2011). In 2006, after sequencing of the *LMB2* gene, Hagele and his colleagues revealed novel four heterozygous genomic sequence variants of *LMNB2* in patients with Acquired Partial Lipodystropyhy (APL)(Hegele *et al.*, 2006).

4.5 Conclusion

Mutations occurring in nuclear envelope proteins are responsible for an intriguing variety of inherited diseases in humans. Lamin and lamin binding proteins are connected with each other and function in a harmony as having essential diverse roles such as in transcription, genome organization and DNA replication. In addition, LINC complex proteins of SUN1 and SUN2 are involved in nuclear-cytoskeletion intereactions. So far there are known or unknown mutations identified in human cells causing a group of diseases called laminopathies leading disruption of protein structure, nucleus integrity and genome organisation and result in patients with decrased longevity such as in HGPS. Even though there are several proposed models showing the interaction between lamins and SUN proteins, it still remains as an unresolved mystery whether mutations in lamin and lamin binding proteins can lead to alterations in the nuclear-cytoskeletal link and also in the distribution of NPCs. Thus, it is essential to investigate more regarding the structure and function of individual nucleoskeletal entity. The recent work have shown presence and disrubution of a number of proteins from normal and diseases cells that will undoubtedly have far-reaching consequences for our comprehension of pathogenesis of the rapid ageing phenotype of HGPS. The findings from this study suggest that *Lamin B2* is likely to be the site of the disease-causing mutation in AG08466 cells. Although, lovastatin is shown to be a promising treatment for the restoration of LB1 and LBR proteins of cancer cells, our findings from the treatment of LB1 and LBR affected progeria cells with lovastatin bring a vital question of how reliable using lovastatin is for the treatment of children afflicted with progeria? Lovastatin treatment leaves HGPS cell with nonfarnesylated pre-lamin A, which give rise to another issue as the nonfarnesylated proteins could have their own toxicities

over the long term causing defective DNA repair and genome instability, although it is conceived that non-farnesylated progerin is less toxic relative to farnesylayed progerin. Finally, further research on the farnesylation of lamins is required in order to determine the functional role of these modifications into treatment of HGPS such as by assessing the suitability of IF PTMs as potential therapeutic targets.

Chapter 5: Aberrant genome behaviour in immortalised control and progeria fibroblasts

Manuscript in Preparation: M. U. Bikkul, G. Bourne, R. Anderson, R. Faragher, C. Parris, I. R. Kill and J. M. Bridger

5.1 Introduction

Mutations in the *LMNA* gene is known to cause a dramatic loss of peripheral chromatin leading to alterations in histone methylation and mispositoning of chromosomes (Mehta *et al.,* 2011; Goldman *et al*., 2004; Shumaker *et al*., 2006, Meaburn *et al*., 2007). Furthermore, it is known that the nuclear lamina has an important role in regulation of genes at the nuclear periphery. It has been demonstrated that artificially binding of chromosomes to the NE repressed of transcription of several genes (Finlan *et al.*, 2008; Kumaran and Spector, 2008). In HeLa cells, down-regulation of LB1 results in lamin B2 deficient microdomains defined by the lack of heterochromatin (Shimi *et al*., 2008). Methylation of H3K9, H3K27 and H4K20 all lead to transcriptional repression and heterochromatin formation (Kotake *et al.*, 2007; Sims *et al*., 2003). Furthermore, trimethylation of these marks are found in pericentromeres, subtelomeres and telomeres of non-coding regions of the genome. Suv39h1 and Suv 39h2 enzymes are involved in catalysing methylation of H3K9me3 (constitutive heterochromatin) found in heterochromatin associated with pericentric regions. However, as mammalian cells have multiple enzymes catalysing H3K9me3, the process of methylation is not mostly affected in other sites of the genome (Tachibana *et al.*, 2002; Peters *et al.*, 2001). The histone-binding protein heterochromatin-associated protein 1 (HP1) is required for epigenetic silencing through constitutive HC formation and maintenance which is conserved from Schizosaccharomyces pombe (Swi6) to mammals, in which three HP1 isoforms exist: HP1-α, β and γ (Maison and Almouzni, 2004; Zhang and Reinberg, 2001). Methylation of H3K9me3 through Suv39h1/2 enzymes leads tethering of HP1 proteins and thereafter recruitment of the Suv4- 20h1/2 enzymes

responsible for deposition of H4K20me3 histone marks in pericentric heterochromatin of mammalian cells (Schotta *et al.*, 2008). It was demonstrated that the lack of *Suv4-20h/1h2* $^{-/-}$ in mice resulted in complete loss of tri-methylated H4K20 which gave rise to defective double-strand DNA break repair and also aberrations of chromosomes in cells of the immune system (Schotta *et al.*, 2008). H3K9me3 is involved in tethering human beta globulin gene to the nuclear membrane (Bian *et al.*, 2013). Furthermore, binding sites named YY1 (Ying-Yang1) has been shown to facilitate ectopic formation of LAD dependent on H3K27me3 and H3K9me2/3(Harr *et al.*, 2015). In cells devoid of Suv4-20h, reduction of peripheral heterochromatin was revealed, indicating that either Suv4-20h2 or H4K20me3 or both play a part help in attachment of heterochromatin to the nuclear lamina (Hahn *et al.*, 2013). The polycomb repressive complex 2 (PRC2) is evolutionarily conserved from *Drosophila* to mammals which consists of the EZH1/2 catalytic subunit, SUZ12, EED, and RBBP7/4 involved in catalysation of trimethylation of H3K27 (Margueron and Reinberg, 2011). The barrier between constitutive and facultative chromatin is more tolerant and epigenetic markers have an important role to maintain the repressive state of chromatin (Boros *et al.*, 2014). H1 and HP1 were shown having influence on expression of Hox gene via their tethering to the repressive form of H3K27me3 (facultative heterochomatin) (Jedrusik-Bode, 2013). In HGPS, it is thought that deformed lamin A protein-progerin plays a role for chromosome relocation. Lamins have been elucidated as having a prominent role in the positioning and function of telomeres and centromeres in the nucleus (Solovei *et al*., 2004; Gonzales-Suarez *et al*. 2009). In mammalian cells, centromeres cluster closely associated to the NE or the nucleolus. Moreover, the number of centromeric foci differs from 6 to 25 compared with 46 centromeres present in the cells (Alcobia *et al*., 2000). Centromeres cluster within large sites of heterochromatin called chromocenters.

rDNA genes present on chromosomes; 13, 14, 15, 21, 22 could cause tendency of passive clustering close the nucleosome. In the initial stages of mouse embryogenesis, it was depicted that clustering of centromeres close to the nucleolous includes all chromosomes and is essential for chromocenter and heterochromatin formation. Telomeres are not clustered in cycling cells and depending on a cell stage, telomeres show different positioning. Telomeres are positioned internally in interphase cells, whereas in postmitotic nuclear assembly, they are found at the NE (Crabbe *et al*., 2012; Amrichová *et al*., 2003). Heterochromatin is important to maintain telomere function and nuclear localisation (Uhlířová *et al*., 2010; Michishita *et al*., 2008). In MEFs, a reduction in both lamin A and histone methylation was shown to influence localisation of telomeres (Uhlířová *et al*., 2010).

The aim of the study is to determine if there are any genomic aberrations in the progeria cell lines and to do this I investigated alterations in the epigenetic histone marks, histone H3 trimethylated on lysine 9 (H3K9me3), histone H3 trimethylated on lysine 27 (H3K27me3) and histone H4 trimethylated on lysine 20 (H4K20me3) in NB1 normal and immortalised NB1T and HGPS T06, T08 cells. I performed 2D-FISH to compare the positions of chromosome territories, centromeres and telomeres in immortalised typical T06 and atypical T08 HGPS fibroblasts to that in control immortalised NB1T fibroblasts in order to determine whether hTERT treatment or mutation in LMNA gene (T06) and unknown mutation (T08) could cause alteration in chromosome positioning and genomic instability in immortalised cells; NB1T, T06, T08. Furthermore, as increased number of chromosomes was observed in T08 cells in this chapter, we employed M-FISH to analyse 23 pair of chromosomes in T08 cells.

The distribution of major nucleolar proteins, including nucleophosmin, fibrillarin and RNA Pol I was assessed in immortalised T06 and T08 HGPS fibroblasts and their distribution compared to those in control NB1 and immortalised NB1T fibroblasts. Colocalisation experiments of fibrillarin-chromosome, Ki-67-centromere were performed to determine the proportion of colocalisation in immortalised T06 and T08 HGPS fibroblasts and compare their distribution to those in control NB1 and immortalised NB1T fibroblasts. Furthermore, Mander's overlap coefficient was calculated to determine the colocalisation of HP1α- centromere utilising Image J software in cells.

5.2 Materials and Methods

5.2.1 Cell culture

As per chapter 2, section 2.2.1., NB1 and hTERT human dermal fibroblasts immortalised cell lines: NB1T, TO6 and TO8 have been cultured.

5.2.2 Indirect immunostaining

5.2.2.1 Fixation

As per chapter 3 section 3.2.3.1 and costaining was performed as per chapter 4 section 4.2.3.1.

5.2.2.2 Antibody staining

As per chapter 3, section 3.2.3.2

The primary antibodies used were; rabbit anti pKi-67 (DAKO, A0047) (1:30 dilution in 1% NCS/PBS v/v), CREST human anti-serum (diluted 1:1000, protein reference unit, Royal Hallamshire Hospital, Sheffield), mouse anti-HP1α (diluted 1:500, Sigma Aldrich- mab3584), mouse anti-H3me3k9 (1:100 dilution, Abcam-ab6001), rabbit anti-H3ME3K27 (1:100 dilution, SAB4800015-50UG), rabbit anti-H4ME3K20 (1:100 dilution, Abcam-ab9053), mouse anti- nucleophosmin (1:2000 dilution, ab86712),

mouse anti- RNA POL I POL1 (1:100 dilution, Abnova- H00084172-M10), goat anti-Fibrillarin (1:100 dilution, Santa Cruz, sc-11336), rabbit anti- Ki67 (1:200 dilution, Abcam, ab15580).

The secondary antibodies were; goat anti-mouse (TRITC) (diluted 1:30, Sigma- T-5393), goat anti-mouse (FITC) (diluted 1:64, Sigma-F9006), Swine anti-rabbit (TRITC) (diluted 1:25, Dako R0156), Rabbit anti-goat (FITC) (diluted 1:50 Sigma- F-7367), goat anti-human (FITC) (1:100 dilution, Jackson human research, 800-367-5296).

5.2.2.3 Image acquisition

As per chapter 3, section 3.2.3.3

5.2.3 Two-dimensional fluorescence in situ hybridisation (2D-FISH) and immunofluorescence

2D-FISH was performed as described in chapter 2, section 2.2.3 using whole chromosome paints; 10, 13, 18 and X and analysed for NB1T, T06 and T08 cells. Chromosomes signal positions were identified in at least 49 nuclei from NB1T, T06 and T08 cells. To combine immunofluorescence with FISH in cells fixed with methanol-acetic acid, after detection of the hybridisation signals, slides were incubated for 1 h at room temprerature, with a 1:200 dilution of rabbit poyclonal anti-pKi67 antibody (ab15580 abcam) and with a goat polyclonal fibrillarin antibody(1:100 dilution, Santa Cruz- sc-11336). After PBS washes, these slides were incubated with secondary antibodies as described in section 5.2.2.2 for 1 hour at room temperature. Slides were rinsed again in PBS and counter stained by mounting in DAPI in Vecta-shield-mounting medium.

5.2.4 2D-FISH chromosomes, centromeres and 2D-FISH telomeres positioning analysis

Telomere PNA FISH was performed for NB1, NB1T, T06 and T08 cells as described in chapter 2, section 2.2.6. As per chapter 2, section 2.2.4.5, telomere and centromere signal positions were identified in at least 45 nuclei from NB1, NB1T, T06 and T08 cells. Chromosome signal positions were identified in at least 40 nuclei from NB1, NB1T, T06 and T08 cells.

5.2.5 Metaphase chromosome fixation and detection of genomic instability

NB1T, TO6 and T08 cell lines were fixed for metaphase chromosome preparation. The medium was changed the night before and 1% colcemid solution was added to each dish for one hour prior to fixation. Fixation was performed using methanol: acetic acid solution. "Metafercell Software" was used for the detection of metaphases by using 10 X or 63X (immersion oil) objectives for each cell line. Furthermore, chromosome counting and enhancement of brightness of images for each cell line were performed by using Image J software.

5.2.6 Multiplex fluorescence in situ hybridization (M-FISH) assay

M-FISH assay was performed collaboration with Dr. Rhona Anderson's group, Brunel University, London. 24-colour karyotyping (M-FISH) was used to paint the T08 cell line using a modified method of the Metasystems^{TM} protocol as described previously (Foster *et al*., 2013). Digital images were captured using a charged-coupled device (CCD) camera (Photometrics Sensys CCD) coupled to and driven by ISIS (MetasystemsTM). Structural chromosomal abnormalities were identified as colour-junctions down the length of individual chromosomes and/or by the presence of chromosome fragments. The M-FISH paint composition was used to identify the

chromosomes involved in the abnormality and the abnormalities were described according to International System of Cytogenetic Nomenclature (Shaffer *et al,* 2013)

5.2.7 Statistical analysis

Values are expressed as averages ± SEM, and n represents the number of cells analysed. Two-tailed unpaired t-tests used as statistical analysis. One-way ANOVA statistical test with Excel software programme was employed to statistically compare the position of chromosomes; 10, 13, 18 and X within NB1T, T06 and T08 nuclei. The probability-value (p-value) are denoted by stars (* $P \leq 0.05$, ** $P \leq 0.01$, *** $P \leq 0.001$). $P< 0.05$ was considered significant and $p> 0.05$ was considered no significant difference in position.

5.3 Results

5.3.1 Distribution of histone modification proteins

The distribution of histone modification and nucleolar proteins in human normal fibroblast NB1, immortalised normal fibroblast NB1T and immortalised typical T06 and atypical T08 HGPS cell lines was determined by indirect immunofluorescence using a range of antibodies. The cell lines were fixed with methanol: acetone (1:1). Histone modification distribution was assessed. Figure 5.1 represents epigenetic histone marks; H3K9ME3, H3K27ME3, H4K20ME3 and Hp1α for NB1, NB1T, T06, and T08 cells.

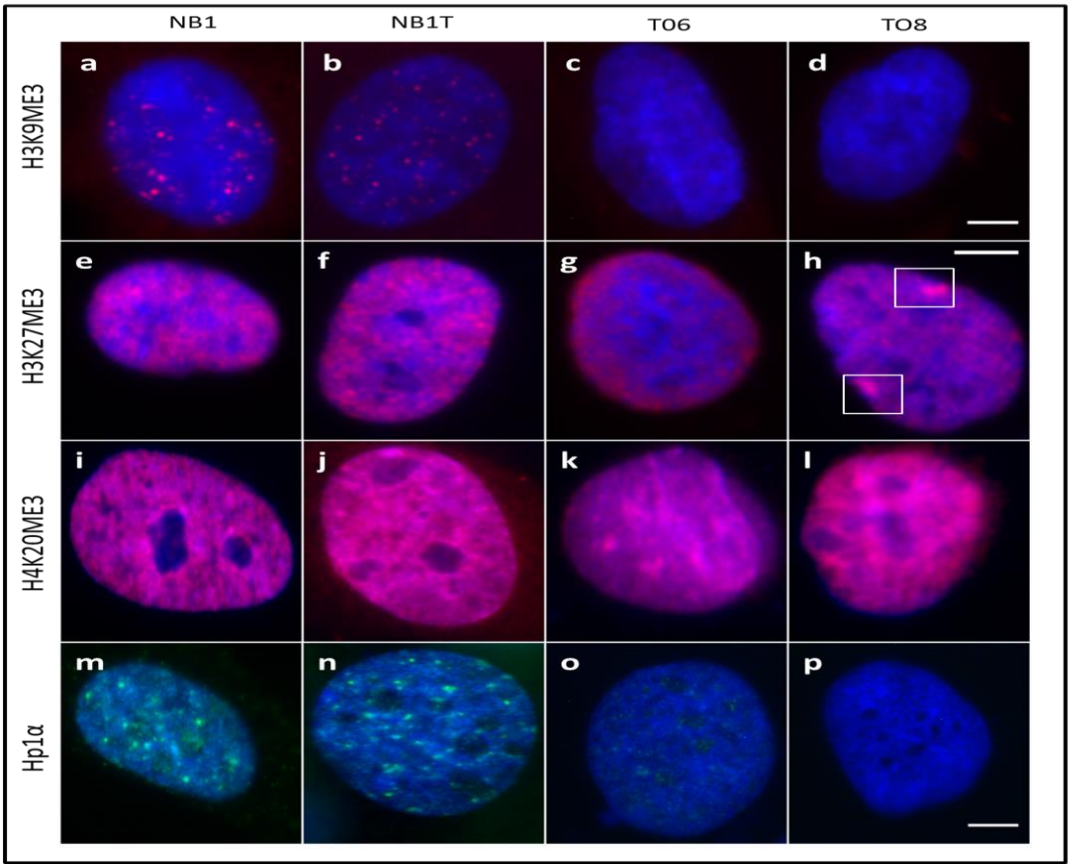

Figure 5.1: NB1, NB1T, T06 and T08 cells were immunostained by using antibodies directed against epigenetic histone marks; H3K9ME3, H3K27ME3, H4K20ME3 and Hp1α. The H3K9ME3 staining pattern consisted of small foci dispersed throughout the nucleoplasm in control cells. (a, b) In hTERT HGPS cells, nuclei exhibited an overall loss of H3K9ME3 staining compared with control cells. (c, d) H3K27ME3 decreases in both T06 and T08 cells (g-h) and the Xi appeared as a uniformly stained compact domain in T08 cells. (h) Xi staining is shown in the white boxes. (h) NB1 and NB1T cells displayed punctuate H3K27ME3 staining throughout the nucleus. (e-f) Nuclei of control cells showed foci of H4K20ME3 throughout the nucleoplasm. (i-j) In HGPS T06 and T08 cells, the H4K20ME3 staining pattern consisted of much larger bright staining structures. (k, i) Hp1α antibody stained large and small foci throughout the the nucleoplasm in controls. (m,n) T06 cells displayed reduction of Hp1α staining. (o) T08 cells great reduction of Hp1α staining. (p) The nucleus is counter-stained with DAPI to reveal the DNA. Magnification = X100. Scale bars= 5 μm.

Nuclei in control NB1 and NB1T cells display H3K9ME3 foci dispersed throughtout the nucleoplasm (Figure 5.1-a, b). Both T06 and T08 cells show reduction of H3K9ME3 staining in the number of nucleoplasmic nuclei (Figure 5.1-c, d).

H3K27ME3 is involved in silencing of the Xi. In control NB1 and NB1T cells, punctuate H3K27ME3 staining was present throughout the nucleoplasm (Figure 5.1-e,f). T06 cells displayed a reduction in overall staining relative to control cells (Figure 5.1-g). Multiple Xi was stained with H3K27ME3 in the nuclei of T08 cells (Figure 5.1-h). The presence of epigenetic mark of H4K20ME3 indicates pericentric heterochromatin. In both H4K20ME3 stained T06 and T08 cells, there is an increase in the number and size of brightly stained nuclear foci relative to control cells (Figure 5.1-I, j and k, l. In terms of heterochromatin protein 1 α (Hp1α), both NB1 and NB1Tcells showed many bright foci throughout the nucleoplasm (Figure 5.1-m, n). However, the overall Hp1α appeared significantly altered in T06 and T08 cells (see chapter 4). Hp1α staining was significantly reduced in T06 cells (Figure 5.1-o) and there is a loss of Hp1α staining in T08 cells (Figure 5.1-p).

5.3.2 Distribution of nucleolar proteins

Mehta *et al.* (2010) demonstrated atypical distribution of nucleophosmin and different distribution of fibrillarin in non-proliferating HGPS cells. In order to assess distribution of nucleolar proteins; nucleophosmin, fibrillarin and RNA pol I, the cell lines were fixed with methanol: acetone (1:1) and an indirect immunofluorescence assay was performed. Nucleolar proteins distribution was assessed by counting at least 200 nuclei. Figure 5.2 represents nucleolar proteins for NB1, NB1T, T06, and T08 cells.

A

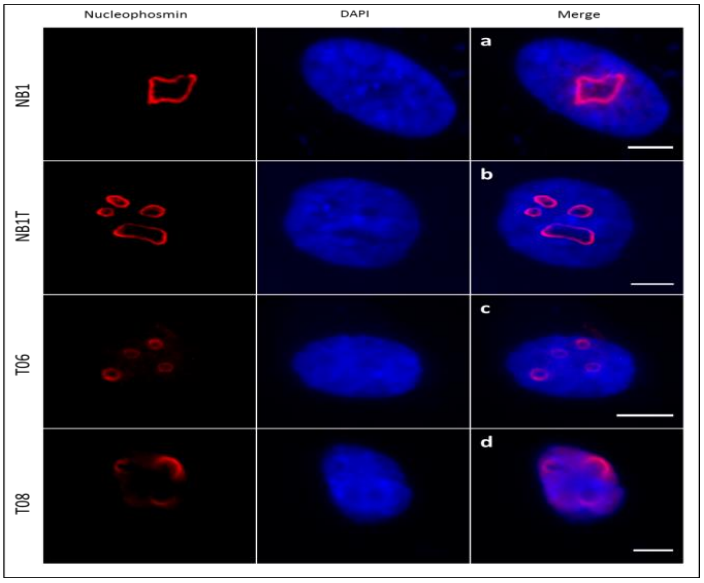
Nucleophosmin
DAPI
Merge
NB1
NB1T
T06
T08
a
b
c
d

B

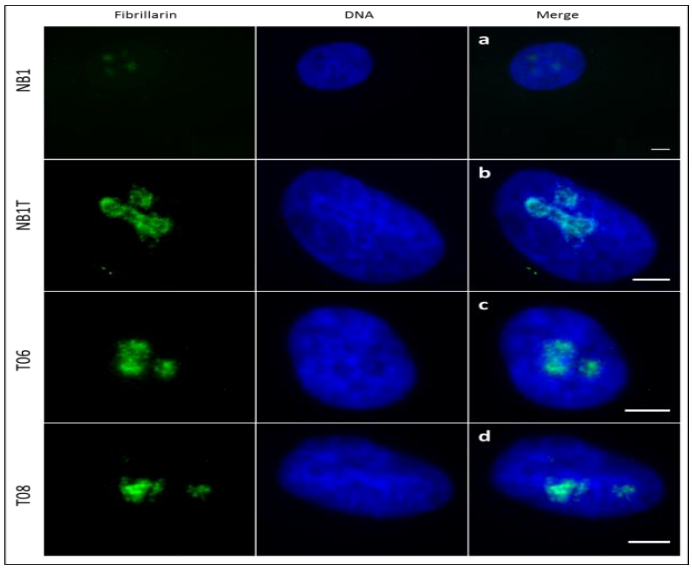
Fibrillarin
DNA
Merge
NB1
NB1T
T06
T08
a
b
c
d

C

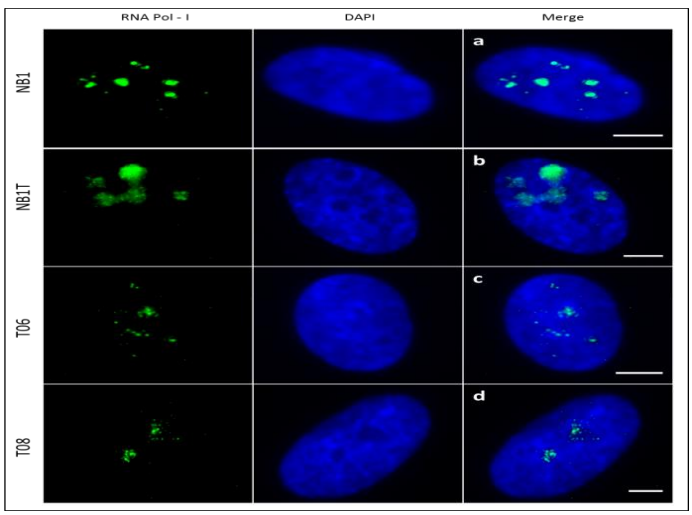
RNA Pol - I
DAPI
Merge
NB1
NB1T
T06
T08
a
b
c
d

Figure 5.2: NB1, NB1T, T06 and T08 cells were immunostained by using antibodies directed against nucleolar proteoins; Nucleophosmin (A), Fibrillarin (B) and RNA Pol I (C). The nucleus is counter-stained with DAPI to reveal the DNA. Magnification = X100. Scale bars= 5 µm

A

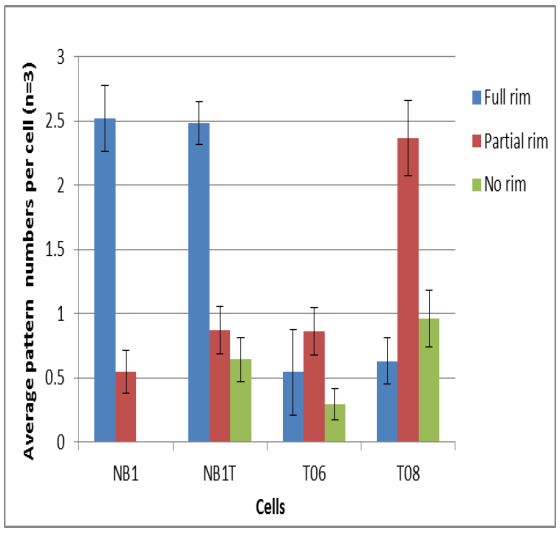

B

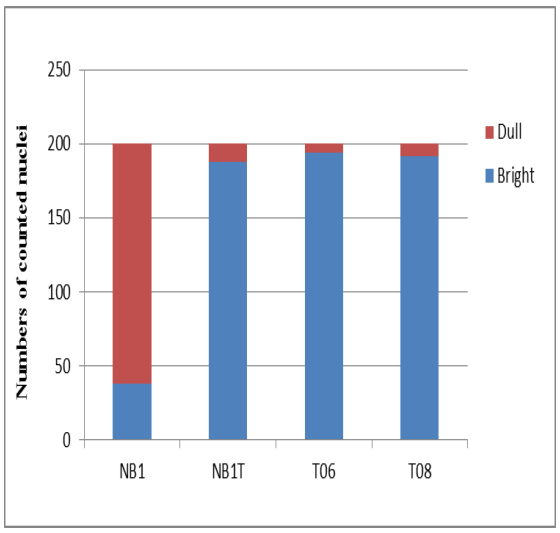

C

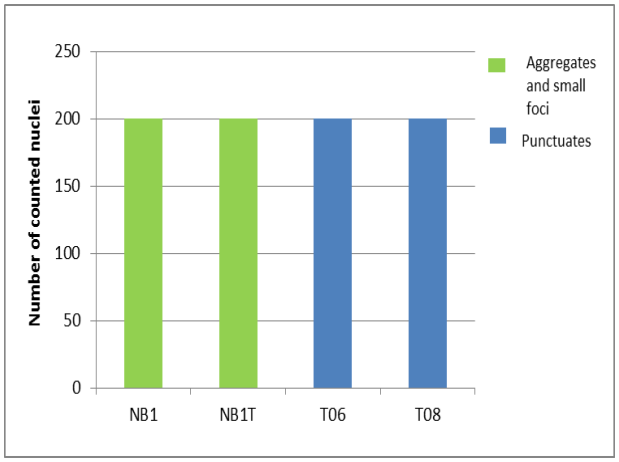

Figure 5.3: Nucleophosmin (A), fibrillarin (B) and RNA POL1 (C) stainings pattern analysis of NB1, NB1T, T06 and T08 cells. N represents number of experiments analysed. Error bars represent standard error of mean (SEM).

Figure 5.3 displays the staining pattern findings of nucleophosmin (A), fibrillarin (B) and RNA POL1 (C) proteins for NB1, NB1T, T06 and T08 cells. Nucleophosmin indirect immunostaining results reveal that cells can be categorized into 3 patterns: 1- full rim, 2- partial rim and 3- no rim. It is evident from the images as well as analysis of counts (Figure 5.3-A) that both NB1 and NB1T cells (Figure 5.2.A-a,b) show typical distribution of full rim, at the nucleolar periphery in the granular centre (GC) domain pattern per cell higher than T06 and T08 cells (Figure 5.2.A-c,d). However, T08 cells show higher number of partial rim pattern per cells around the nucleolar periphery than other cells (Figure 5.2.A-d). NB1 cells did not display any negative nucleophosmin rim pattern per cell (Figure 5.3-A). A subset of T06 and T08 cells also illustrates a typical distrubution of nucleophosmin similar to NB1 and NB1T cells (Figure 5.2-A and Figure 5-3-A).

It is evident from the slides (Figure 5.2-B) that there was no difference in fibrillarin localisation in control cells as compared to HGPS cells. Fibrillarin protein was located in the nucleolar DFC domain as punctuate foci at all times and furthermore, no cytoplasmic staining was detected. Intriguingly, analysis of counts of fibrillarin stained nuclei reveals that the number of dull fibrillarin staining in NB1 cells is greater compared to other cells, suggesting a distinct signal intensity of the protein in immortalised cells (Figure 5.3-B). Distribution of RNA POL 1 was compared between control and HGPS cells by performing indirect immunofluorescence. In both T06 and T08 cells, RNA POL 1 is distributed in the DFC of the nucleolous as small foci at all times (Figure 5.2.C- c, d and Figure 5.3-C). However, it was found as aggregates and small foci distributed in the DFC of the nucleolous in both NB1 and NB1T cells. (Figure 5.2.A-a, b and Figure 5.3-C).

5.3.3 Metaphase chromosome number analysis

"Metafercell Software" was employed for the detection of chromosome number. The chromosome spreads were of a good quality in NB1T and T06 cells compared with T08 cell line. Therefore, the number of metaphase chromosome spread detected by metafercell software was low for T08 cells. Representative images of metaphase chromosomes for NB1T, T06 and T08 cells (Figure 5.4-A, B, C). The number of metaphase cells for NB1T, T06 and T08 cells were 84, 136, and 54 respectively. The bin for chromosome numbers against frequency (%) for each cell line was plotted on a graph (Figure 5.5). NB1T and T06 cells have 46 chromosomes in 30.5 % and 28.5 % of cells respectively. However, TO8 cells have the highest number of chromosomes with an average of 78 (6.9%) and numbers of chromosomes are scattered from 11-20 to 81-90.

A

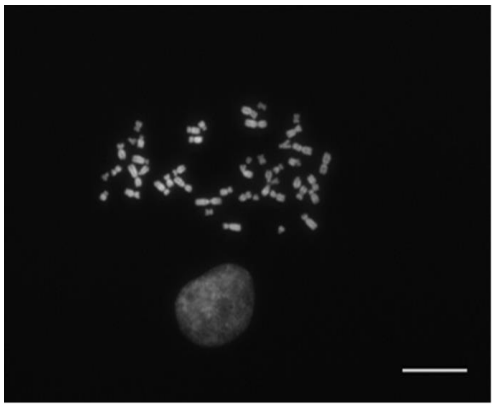

B

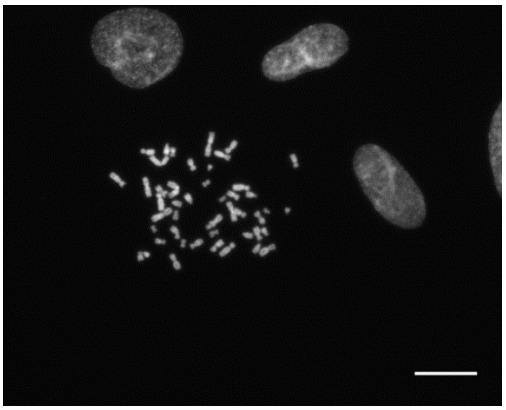

C

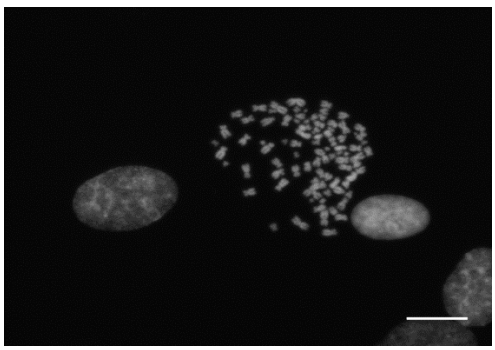

Figure 5.4: A representative image of metaphase chromosome spread of NB1T (A), T06 (B) and T08 (C) cells. Scale bar: 5 µm.

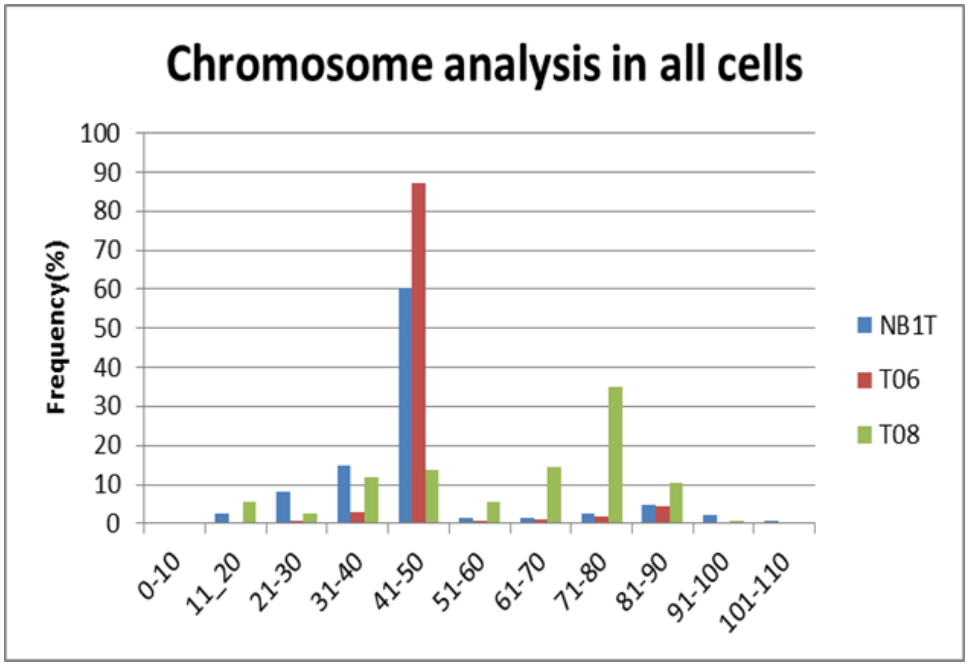

Figure 5.5: Number of chromosomes against frequency (%) was plotted on the graphs for each cell line. Bin for chromosome numbers was chosen and percentage of frequency was measured

5.3.4 M-FISH analysis of T08 cells

T08 cells were assayed by M-FISH, captured and analysed as standard. 17 number of T08 cells were fully karyotyped and notated according to ISCN (An International System for Human Cytogenetic Nomenclature) 2009 (Appendices, M-FISH, Table 1). The karyotypes as near-tetraploid (92, XXXX) as noted in the Tables in appendices. All cells were abnormal containing multiple structural (Appendices, M-FISH, Table 2 and 3) and numerical (Table 4) aberrations. Refer to appendices for more karyotyping data for T08 cells. Figure 5.6 displays karyotypic analysis showing

number of chromosome loss for T08 cells. Figure 5.7 demonstrates M-FISH karyotype of a T08 cell indicating aneuploidy.

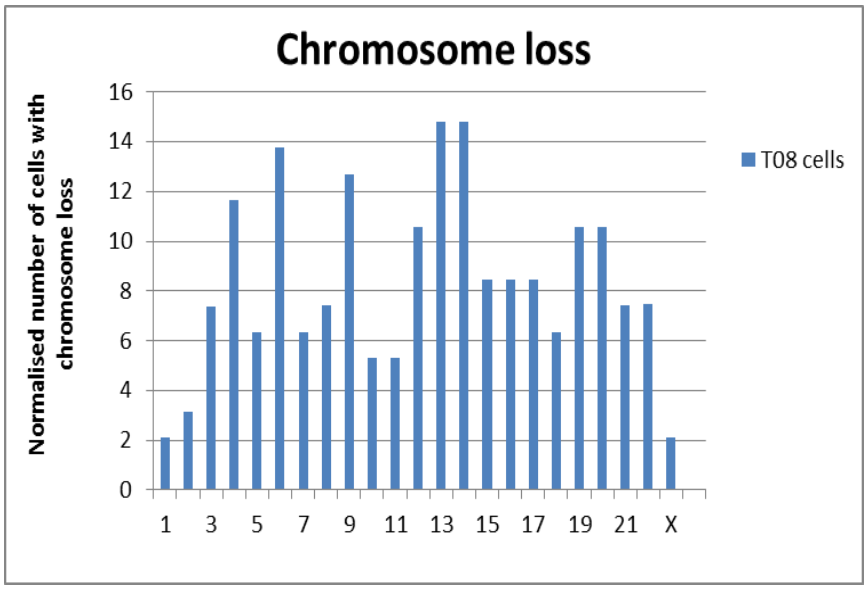

Figure 5.6: Number of chromosome loss for T08 cells. X-axis shows analysed 23 pair of chromosomes including chromosome X. Y-axis displays number of cells with chromosome loss normalised to 18 cells.

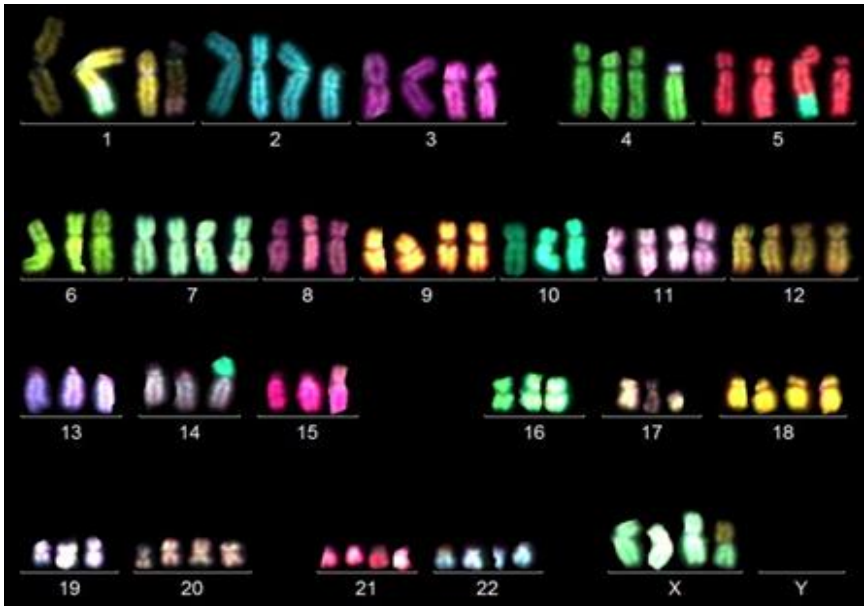

Figure 5.7: Representative M-FISH karyotype of T08 cell line. Cell 21 showing 83,XXX,t(X;1),ins(1;14),der(1)t(14;1;17),del(2p),del(3p),der(4)t(4;19),der(5)t(5;10), del(5p),-6,der(7)t(7;21),-13,-14,der(14)t(10;14),-15,der(15)t(8;15),-16,del(17q)

5.3.4 2D- Telomeres and Centromeres positioning

2D positioning of telomeres and centromeres were determined by employing IPLab Spectrum software as described in chapter 2. Representative example of the hybridization with telomeric PNA in NB1, NB1T, T06 and T08 cells is shown in Figure 5.8-A. Telomeres were predominantly found in the interior of the nucleus (shell 5) in all analysed 4 different fibroblasts with signal (%)/DAPI (%) ratios of 1.17 ± 0.06(n=45) , 1.24 ± 0.04(n=47), 1.25 ± 0.05 (n=47), 1.36 ± 0.04 (n=51) for NB1, NB1T, T06 and T08 cells respectively (Figure 5.8-B). The signal (%)/DAPI (%) ratio for telomeres in shell 4 in T08 cells is significantly different compared with T06 cells ($p<0.01$). The signal (%)/DAPI (%) ratio for telomeres in shell 5 in T08 cells is significantly different relative to other cells ($p<0.05$).

A

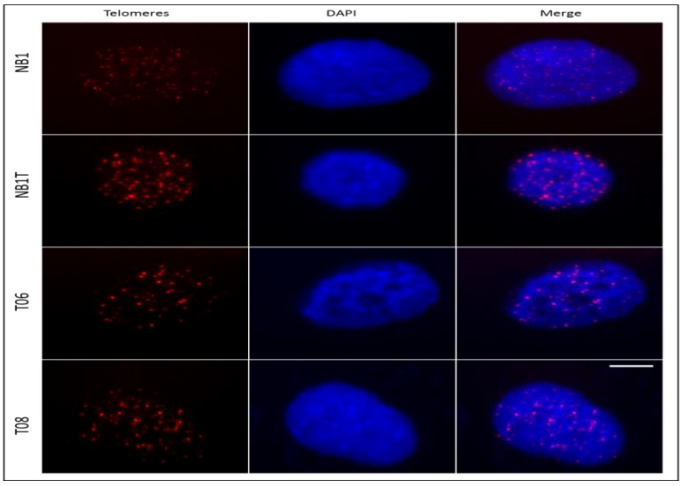

B

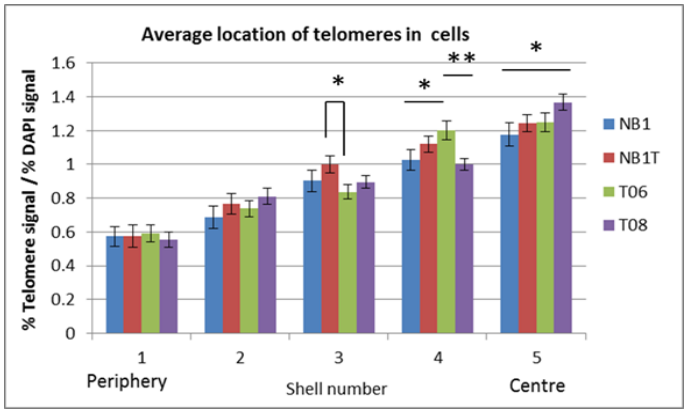

Figure 5.8: Representative digital images of NB1, NB1T, T06 and T08 cells in interphase after hybridization with cy3 conjugated telomeric PNA oligonucleotides (A). Histograms display the position of telomeres in NB1, NB1, T06 and T08 cells. Erosion analyses were performed by ascertaining the distribution of the mean proportion of hybridisation telomeres signal (%), normalised by the percentage of DAPI signal, over five concentric shells of equal area from the nuclear periphery to centre. The x-axis displays the shells from 1–5 (left to right), with 1 being the most peripheral shell and 5 being the most internal shell. The y-axis shows signal (%)/ DAPI (%), from 0 to 1.6 with 0.2 increments. The standard error bars representing the standard error of mean (SEM) were plotted for each shell for each graph. Significant differences are denoted by stars (* P ≤ 0.05, ** P ≤ 0.01) (B). In order to reveal DNA, DAPI was used. Magnification = 100x. Scale bar = 5 µm.

A

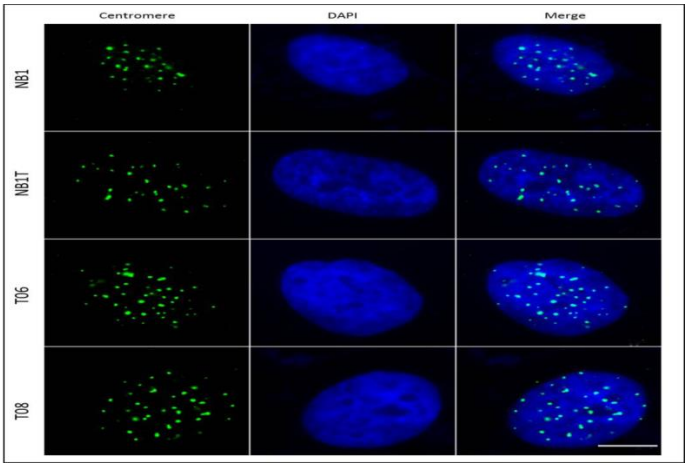

B

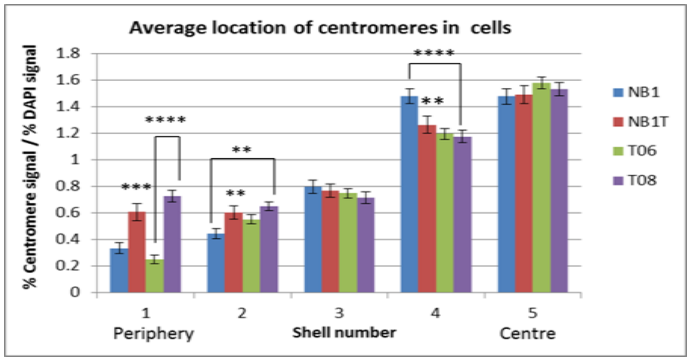

Figure 5.9: Representative images of M:A fixed NB1, NB1T, T06 and T08 cells immunostained with antibody directed against centromere (green). (A). Histograms display the position of centromeres in NB1, NB1, T06 and T08 cells. Erosion analyses were performed by ascertaining the distribution of the mean proportion of

centromeres signal (%), normalised by the percentage of DAPI signal, over five concentric shells of equal area from the nuclear periphery to centre. The x-axis displays the shells from 1–5 (left to right), with 1 being the most peripheral shell and 5 being the most internal shell. The y-axis shows signal (%)/ DAPI (%), from 0 to 1.6 with 0.2 increments. The standard error bars representing the standard error of mean (SEM) were plotted for each shell for each graph. Significant differences are denoted by stars (* P ≤ 0.05, ** P ≤ 0.01, *** P ≤ 0.001, **** P ≤ 0.0001) (B). In order to reveal DNA, DAPI was used. Magnification = 100x. Scale bar = 5 µm.

Figure 5.9-A demonstrates representative images of centromeres immunostaining in four different proliferating cells. Centromeres were predominantly found in the interior of the nucleus (shell 5) in analysed NB1T, T06 and T08 fibroblasts with signal (%)/DAPI (%) ratios of 1.49 ± 0.06 (n=49), 1.57 ± 0.04 (n=47) and 1.53 ± 0.05 (n=50) for NB1T, T06 and T08 cells respectively (Figure 5.9-B). Furthermore, centromeres were predominantly found in the interior of the nucleus positioning in shell 4 and 5 in analysed NB1 cells with signal (%)/DAPI (%) ratios of 1.479 ± 0.055 (n=48) and 1.478 ± 0.058 (n=48) respectively. The signal (%)/DAPI (%) ratio for centromeres in shell 1 in NB1T and T08 cells is significantly different compared with NB1, $P<0.001$ and T06 cells, $P<0.0001$. The signal (%)/DAPI (%) ratio for centromeres in shell 4 in NB1 cells is significantly different relative to other cells NB1T, $P<0.01$ and T08, $P< 0.0001$.

5.3.5 2D-FISH chromosome positioning analysis

Interphase chromosome positioning for chromosomes; 10, 13, 18 and X was assessed in NB1T, T06 and T08 cell lines. Images taken for each cell type, with each chromosome paint were subjected to an erosion analysis script that divided the nucleus into five concentric shells of equal area as in chapter 2. Figure 5.10 displays the representative images of chromosome territory delineation and position of chromosomes in the three analysed cell types in proliferating nuclei respectively. Furthermore, 2D-FISH interphase chromosome positioning for chromosomes; 10,

13, 18 and X was shown in control fibroblast cells (Mehta *et al.,* 2011) (Table 5.2). One-way ANOVA statistical analysis was performed, if the P value is lower than P=0.05, the result was deemed significant (Table 5.1).

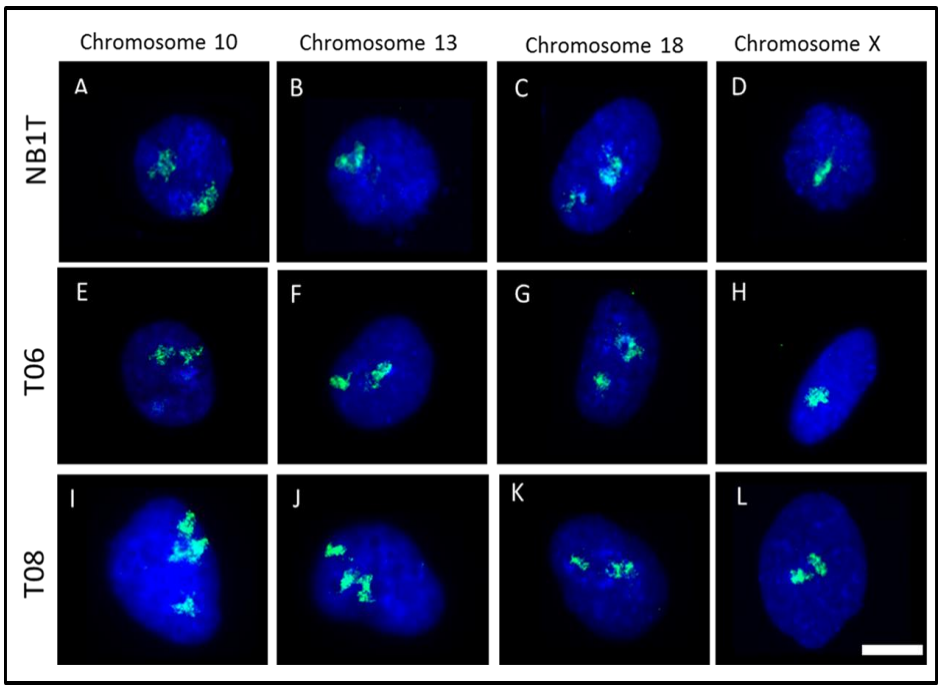

Figure 5.10: Representative 2D images displaying examples of peripherally, intermediately and internally positioned chromosome territories in proliferating NB1T, T06 and T08 cell lines. Whole chromosome painting probes were labelled with biotin and detected using streptavidin conjugated to FITC (green) and the nuclei were counterstained with DAPI (blue). Scale bar, 5 μm.

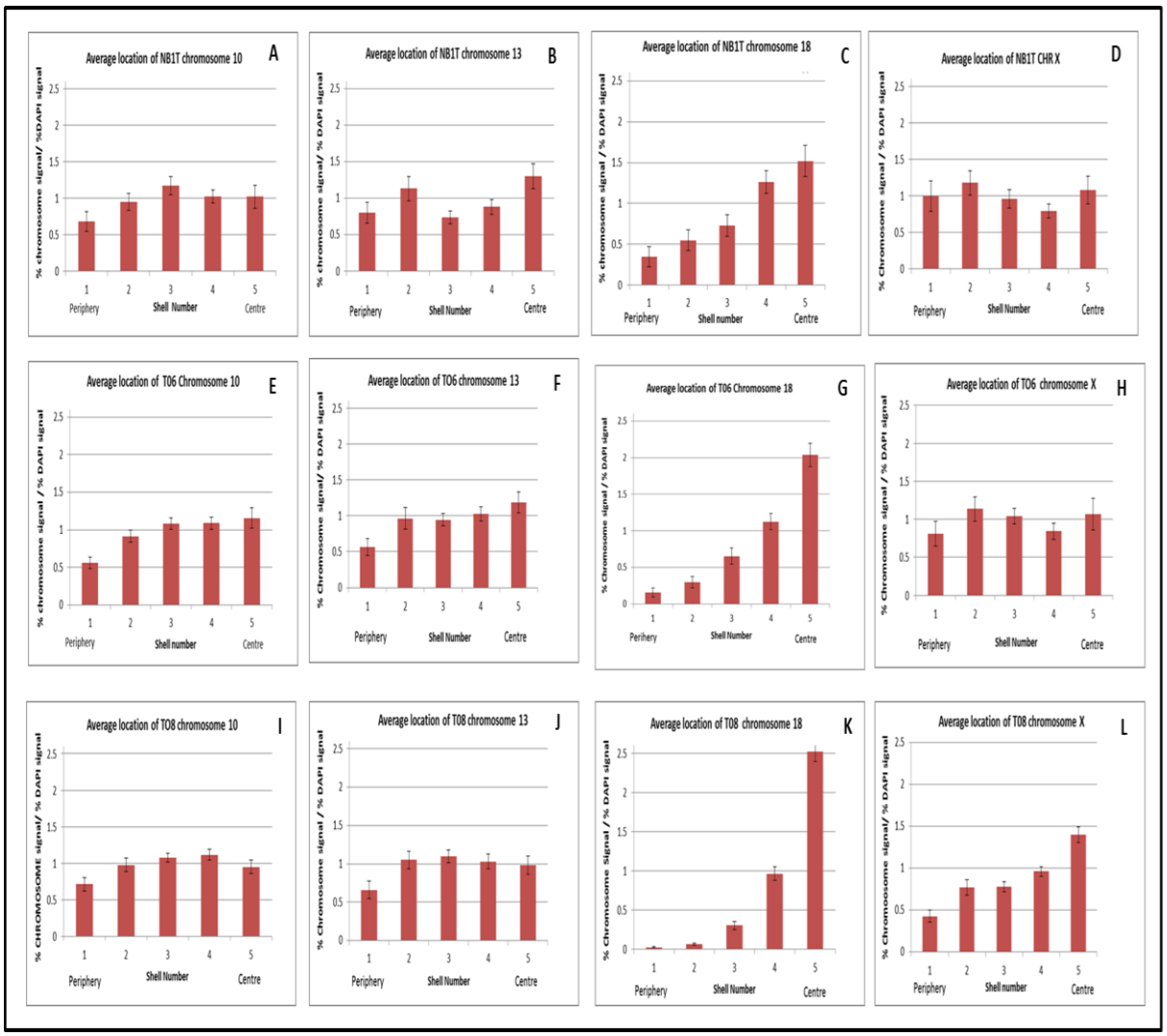

Figure 5.11: The histograms in panel A-L display the distrubition of the chromosome signal in 50-55 nuclei for each chromosome for as analysed by simple erosion analysis for NB1, T06 and T08 cells. The x-axis displays the shells from 1-5 (left to right) with 1 being the most peripheral shell and 5 being the most internal shell. The y-axis shows % chromosome signal/DAPI signal, from 0 to 2.5 with 0.5 increments. Bars represent the mean normalised proportion (%) of chromosome signal for each human chromosome. Error bars represent standard error of mean (SEM).

Table 5.1: One way ANOVA statistical analysis of Chromosomes; 10, 13, 18 and X in NB1T, TO6 and T08 cells. S: Significant; NS: not significant.

Statistical analysis of all chromosome positions		by erosion analysis		
Chr.	Shell	All culture cells		
	1	NS		
	2	NS		
10	3	NS		
	4	NS		
	5	NS		
	1	NS		
	2	NS		
13	3	S P=0.0157		
	4	NS		
	5	NS		
	1	SP= 0.007171		
	2	SP= 0.000161		
18	3	SP= 0.00646		
	4	NS		
	5	SP= 0.000166		
	1	SP= 0.00297		
	2	SP= 0.000157		
X	3	SP= 0.007936		
	4	NS		
	5	SP= 0.019216		

Statistical results revealed that there was significant difference in the interphase position of chromosomes; 13, 18 and X between all cells (Table 5.1). Whereas there is no significant difference in the interphase position of chromosome 10 between all cells. Table 5.2 summarises the positioning of all chromosomes in each cell line.

Table 5.2: The nuclear location of four chromosomes in each cell line.

Chromosomes	10	13	18	X
Control cells (Mehta *et al*, 2011)	Intermediate	Peripheral	Peripheral	Peripheral
NBIT	Intermediate	Bimodal	Interior	Bimodal
T06	Intermediate	Intermediate	Interior	Bimodal
T08	Intermediate	Intermediate	Interior	Interior

The interphase position of chromosome 10 is in an intermediate nuclear location in all proliferating cells (Figure 5.10 panels A, E and I and Figure 5.11-A, E and I). The data demonstrated in Figure 5.10 panels F, J and Figure 5.11- F, J reveal that the interphase position of chromosome 13 is in an intermediate nuclear location in proliferating T06 and T08 cells. However, chromosome 13 showed bimodal positioning in NB1T cells (Figure 5.10 panel B and Figure 5.11-B). In all analysed cells, chromosome 18 was found in the nuclear interior (Figure 5.10 panels C, G, and K and Figure 5.11-C, K and G). Moreover, as Figure 5.10-D, H and Figure 5.11-D, H display, chromosome X demonstrated bimodal positioning in both NB1T and T06 cells. Most interestingly, when the nuclear position of chromosome X was determined in proliferating T08 cells, chromosome X was found in an interior nuclear position (Figure 5.10 panel L and Figure 5.11-L). Noteworthy that it is first time ever we found chromosome X located in an interior nuclear position in all studied normal and disease human fibroblasts.

5.3.7 Assessment of colocalisation of chromosomes with nucleoli

Chromosomes were found moving interior. Thus, the colocalisation of chromosomes; 10, 13, 18 and X with fibrillarin nucleolar antigen was assessed in hTERT NB1T, T06 and T08 cell lines by indirect immunostaining. Combined FISH and immunofluorescence in MAA fixed nuclei were hybridised with whole human chromosome paints (red) and with antibody against fibrillarin nucleolar antigen (green). Chromosome-fibrillarin colocalisation was identified in at least 40 nuclei from NB1T, T06 and T08 cells. This was to test if extra-long telomeres caused chromosomes to attach to nucleoli and consequently chromosomes to be located in the nuclear interior. Figure 5.12 displays representative images of colocalisation of chromosomes with fibrillarin in the three analysed cell types in proliferating nuclei.

A

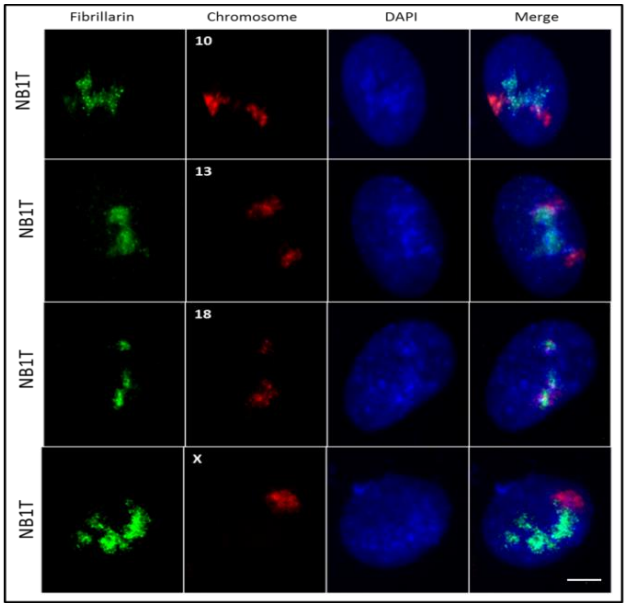
Fibrillarin
Chromosome
DAPI
Merge
NB1T
NB1T
NB1T
NB1T
10
13
18
X

B

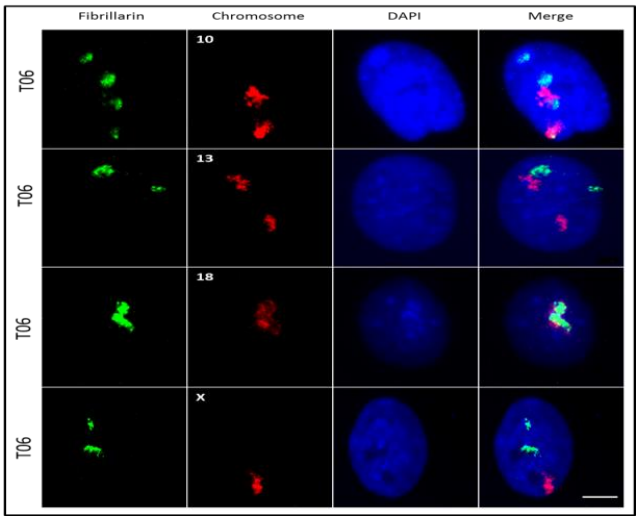
Fibrillarin
Chromosome
DAPI
Merge
T06
T06
T06
T06
10
13
18
X

C

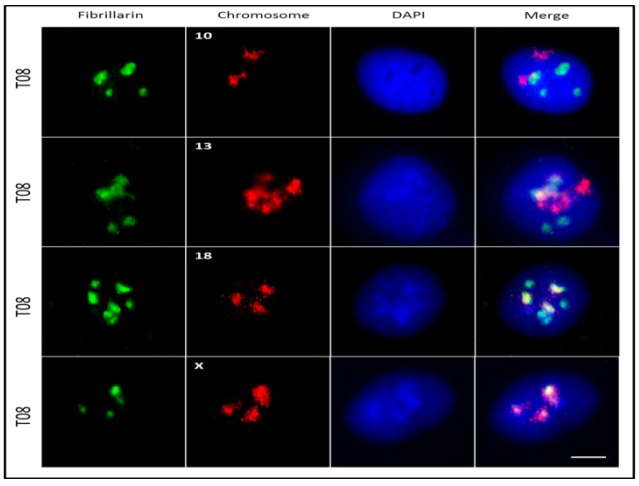
Fibrillarin
Chromosome
DAPI
Merge
T08
T08
T08
T08
10
13
18
X

Figure 5.12: Representative 2D-FISH images displaying examples of peripherally, intermediately and internally positioned chromosome territories within NB1T (A), T06 (B) and T08(C) cell lines immunostained with fibrillarin antibody. Whole chromosome painting probes were labelled with biotin and detected using streptavidin conjugated to cy3 (red), fibrillarin conjugated to FITC(green) and the nuclei were counterstained with DAPI (blue). Scale bar= 5 µm.

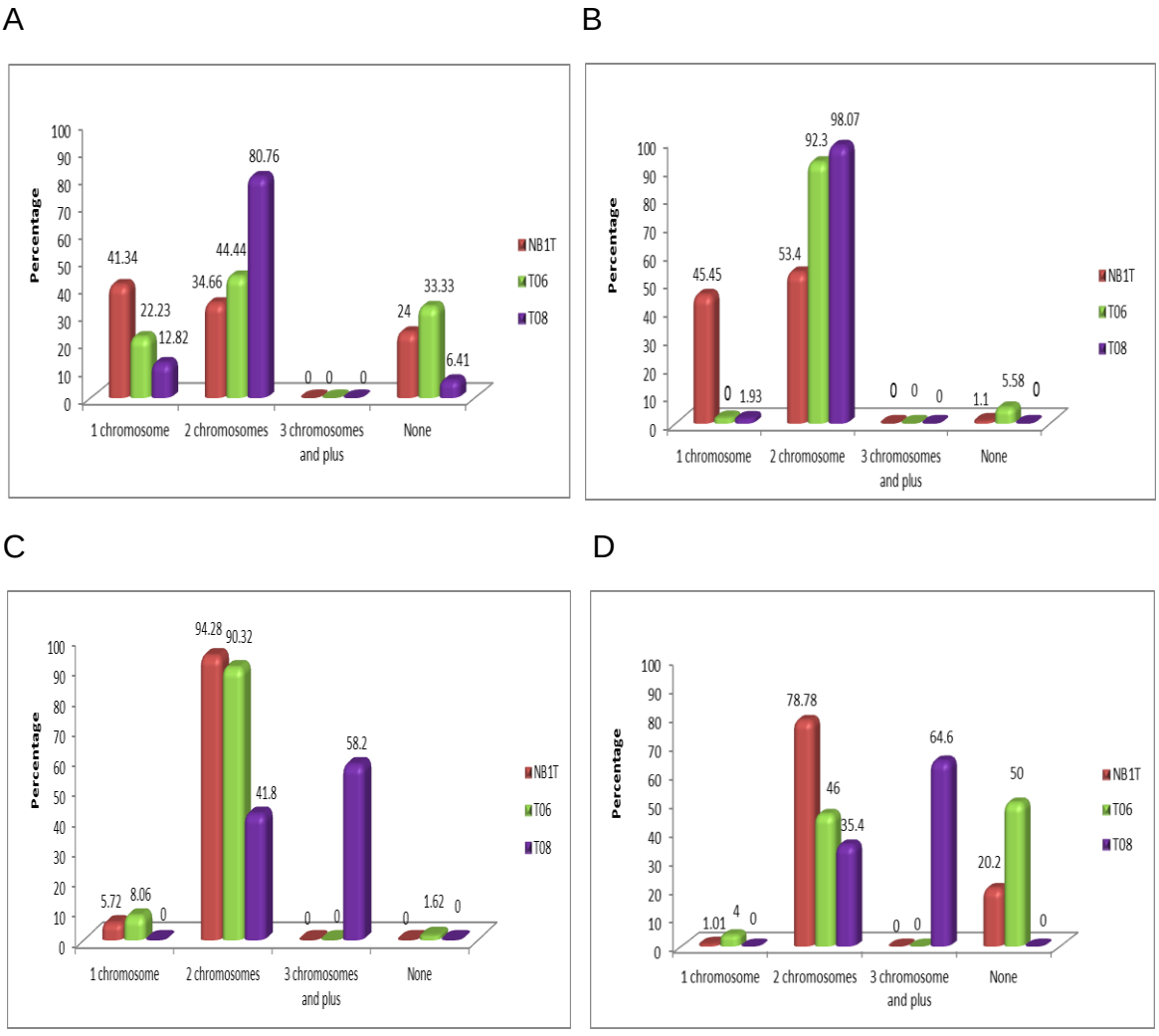

Figure 5.13: Colocalisation of chromosomes; 10, 13, and 18 and X with fibrillarin nucleolar antigen was plotted in histograms. A, B, C, D represent chromosome 10, 13, 18 and X respectively. The x-axis and y-axis display the number of colocalized chromosomes and the percentage of colocalized chromosomes with fibrillarin respectively in each cell line.

In terms of chromosome 10, NB1T cells have the greatest percentage of colocalisation of 1 chromosome with fibrillarin (41.34 %). T08 cells show the highest percentage of colocalisation of 2 chromosomes with fibrillarin (80.76 %) and also have the lowest percentage of none colocalisation (6.41 %). Furthermore, there is no observed colocalisation of 3 chromosome 10s with fibrillarin in all 3 cell lines (Figure 5.13-A). In terms of chromosome 13, NB1T cells show the highest percentage of colocalisation of 1 chromosome with fibrillarin (45.45 %). On the other hand, T06 and T08 cells show the greatest percentage of colocalisation of 2 chromosomes with fibrillarin (92.3 % and 98.07 % respectively). Moreover, T08 cells have the greatest percentage of none colocalisation (5.58 %). There is no observed colocalisation of 3 chromosomes with fibrillarin in all 3 cell lines (Figure 5.13-B). In terms of chromosome 18, NB1T cells have the highest percentage of colocalisation of 1 chromosome with fibrillarin (8.06 %). T06 and T08 cells show the greatest percentage of colocalisation of 2 chromosomes with fibrillarin (94.28 % and 90.32 % respectively). T08 cells have the greatest colocalisation of 3 chromosomes with fibrillarin (58.2 %). Furthermore, T08 cells show the highest percentage of none colocalisation (1.62 %) (Figure 5.13-C). In terms of chromosome X, T06 cells have the greatest percentage of colocalisation of 1 chromosome with fibrillarin (4 %). NB1T cells exhibit the greatest percentage of colocalisation of 2 chromosomes with fibrillarin (78.78 %). T08 cells show the highest percentage of colocalisation of 3 chromosomes with fibrillarin (64.6 %). Furthermore, T06 cells have the greatest percentage of none colocalisation (50 %) (Figure 5.13-D).

5.3.8 Assessment of colocalisation of centromeres with Ki-67

The colocalisation of centromeres with a nucleolar marker p-Ki-67 was assessed in NB1 and hTERT NB1T, T06 and T08 cell lines by indirect immunostaining. The mean percentage of centromere-ki-67 colocalisation per cell was identified in at least 45 nuclei in each cell line. Figure 5.14 displays representative images of colocalisation analysis in four different proliferating cells. A histogram illustrates colocalisation of centromere and Ki-67 in cells in Figure 5.15. Costaining analysis revealed that NB1T and T08 cells have almost the same proportion of costaining with percentage of 44.3 ± 0.75 (n=46) and 45.9 ± 0.86 (n=45) respectively. Furthermore, NB1 and T06 cells show almost the same proportion of costaining with 33.3 ± 0.51 (n=51) and 34.3 ± 0.49 (n=49) respectively.

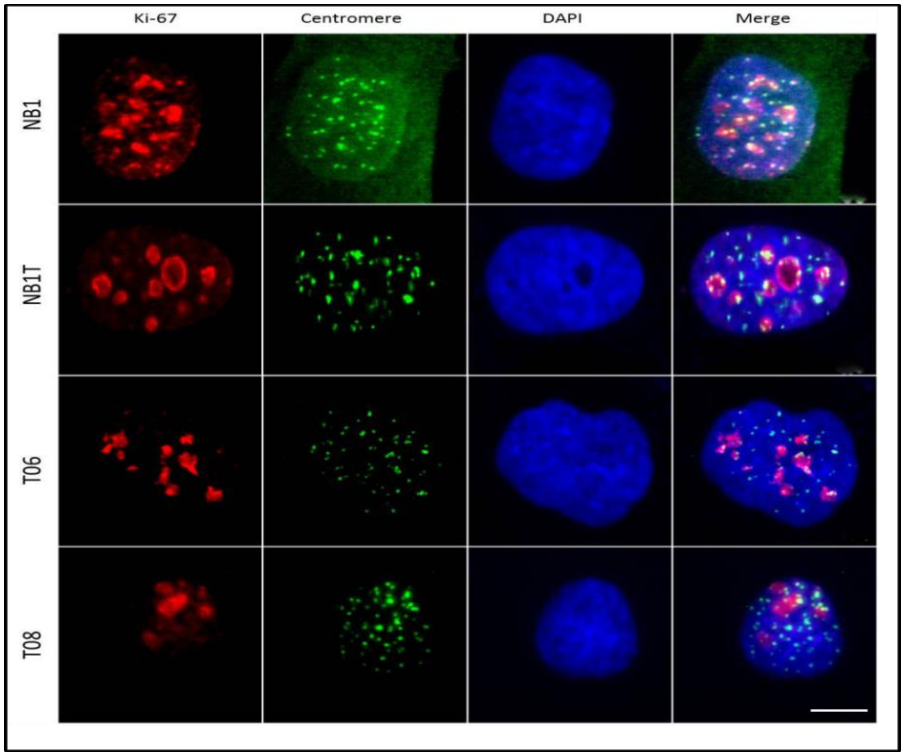

Figure 5.14: M:A fixed NB1, NB1T, T06 and T08 cells were costained with antibodies directed against ki-67 (red) and and centromere (green). The nucleus is counter-stained with DAPI to reveal the DNA. Magnification = X100. Scale bar= 5 µm.

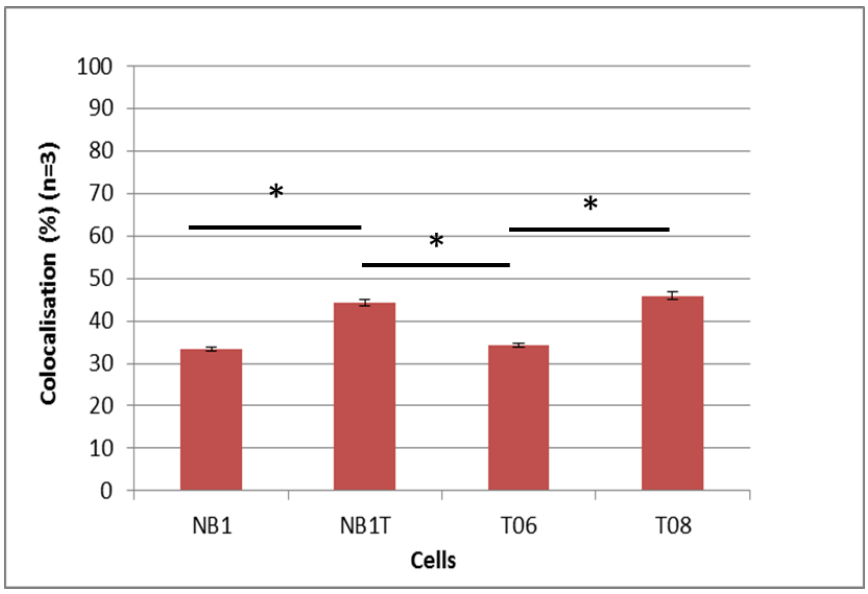

Figure 5.15: A graph to demonstrate the mean percentage of centromere-ki-67 colocalisation per nucleus in at least analysed 45 nuclei for NB1, NB1T, T06 and T08 cells. N represents number of experiments analysed. Error bars represent standard error of mean (SEM). Significant differences are denoted by stars (* P ≤ 0.05, ** P ≤ 0.01).

5.3.9 Assessment of colocalisation of HP1α with centromeres

The colocalisation of centromeres with HP1α was assessed in NB1 and hTERT NB1T, T06 and T08 cell lines by indirect immunostaining. The mean Mander's overlap coefficient of HP1α – centromere colocalisation per cell was identified at least 48 nuclei in each cell line by performing Image J software. Figure 5.16 displays representative images of colocalisation analysis in four different fibroblasts. A histogram illustrates colocalisation of centromere and HP1α in cells in Figure 5.17. Costaining analysis revealed that NB1 cells have Mander's overlap coefficient with 0.83 ± 0.01 (n=50), which is significantly greater than T06 (0.54 ± 0.03, n=45, P ≤ 0.001) and T08 (0.6 ± 0.02, n=48, P ≤ 0.001) cells. Furthermore, costaining analysis revealed that NB1T cells have Mander's overlap coefficient with 0.78 ± 0.03 (n=46), which is significantly greater than both T06 and T08 cells (Figure 5.17).

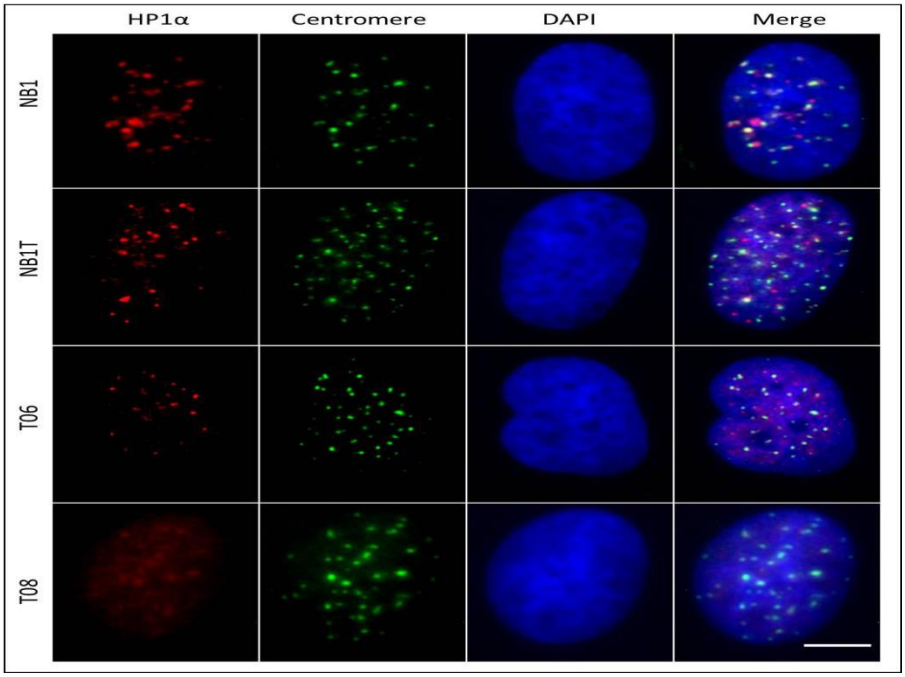

Figure 5.16: M:A fixed NB1, NB1T, T06 and T08 cells were costained with antibodies directed against HP1α (red) and and centromere (green). The nucleus is counter-stained with DAPI to reveal the DNA. Magnification = X100. Scale bar= 5 µm.

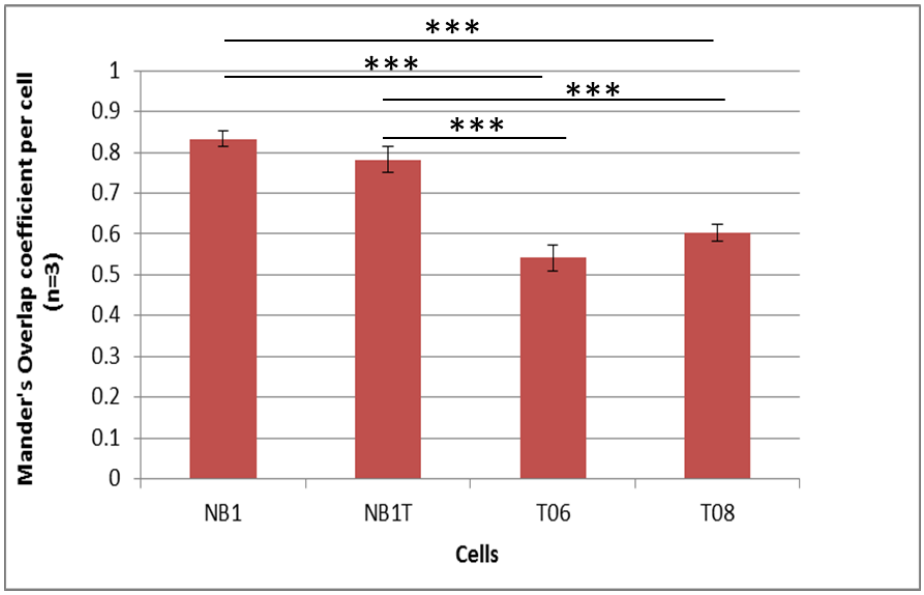

Figure 5.17: A graph to demonstrate the mean Mander's overlap coefficient of centromere - HP1α colocalisation per nucleus in at least analysed 48 nuclei for NB1, NB1T, T06 and T08 cells. The Y-axis ranges between 1 and zero with 1 being high-colocalization, zero being low. N represents number of experiments analysed. Error bars represent standard error of mean (SEM). Significant differences are denoted by stars (* $P \leq 0.05$, ** $P \leq 0.01$, *** $P \leq 0.001$).

5.4 Discussion

Nuclear lamin proteins have been proposed to take part in genome behaviour and stability and therefore we wanted to examine whether in cells with mutations in A-type lamin (T06) and the unknown mutation (T08), chromosomes would change their behaviour. We determined the radial positions of four representative chromosomes in interphase nuclei of immortalised normal (NB1T) and typical (TO6) and atypical (TO8) HGPS proliferating cells. These chromosomes were; 10, 13, 18 and X. It is worthwhile to point out that, all analysed cell lines were proliferating cells due to hTERT expression. Chromosome 10 positioning results demonstrate that chromosome 10 is found occupying the nuclear intermediate in proliferating immortalised control, typical and atypical HGPS nuclei. Mehta et al. (2011) showed that chromosome 10 occupies an intermediate location in normal primary proliferating control nuclei. On the other hand, chromosome 10 was exhibited positioning towards the nuclear periphery in proliferating HGPS nuclei (Mehta *et al.*, 2011). I obtained two different positioning results for chromosome 13 in three different lines. Chromosome 13 positioning findings reveal bimodal distribution in proliferating control nuclei. However chromosome 13 was found occupying an intermediate location in both typical and atypical nuclei. Chromosome 18 was found to be located in the nuclear interior in all proliferating control, typical and atypical HGPS nuclei. Chromosome 13 and 18 results are in agreement with Meaburn *et al.* (2007) results. Meaburn *et al*., (2007) chromosome positioning analysis for chromosomes 13 and 18 in proliferating laminopathy cells and an X-EDMD fibroblast revealed that both chromosome 13 and 18 were found away from the nuclear periphery, located in the nuclear interior. Furthermore, it was revealed that in R482L or r527H $^{-/-}$ mutated cells, chromosome 13 was found in an intermediate location

(Meaburn *et al*., 2007). Mehta *et al*. (2011) demonstrated that the positioning of chromosomes; 13 and 18 in proliferating laminopathy cells is similar to that non-proliferating control cells, given that smaller chromosomes are found in the nuclear interior in the latter (Mehta *et al.*, 2011). More interestingly, chromosome X positioning results revealed bimodal positioning in control and typical nuclei, whereas in atypical nuclei chromosome showed chromosome X occupying the nuclear interior. It is important to note that this is the first time that chromosome X has been seen in the nuclear interior in our laboratory. In contrast, in previous work of Meaburn *et al*., (2007) it was demonstrated that in both proliferating and nonproliferating of mutant HDF cell lines chromosome X was always found at the nuclear periphery. I hoped to determine if chromosomes have association with nucleolus in hTERT cells. Colocalisation analysis of chromosome and fibrillarin findings confirmed chromosome positioning results since chromosomes 18 colocalised with fibrillarin with different chromosome numbers and proportions in all cells and there is no observed none colocalisation of chromosomes with fibrillarin almost in any cells. Further, chromosome X and fibrillarin colocalisation analysis confirmed my chromosome X positioning analysis in T08 cells since findings reveal that chromosomes X colocalised with fibrillarin with different chromosome numbers with higher percentages than other cells and there is no observed none colocalisation of chromosomes with fibrillarin in T08 cells. Colocalization of human acrocentric chromosomes; HSA 13, 14, 15, 21, and 22 with mouse nucleolar fibrillarin was shown with higher percentages compared with chromosome X with fibrillarin in mouse hybrid cells, indicating human acrocentric chromosomes have affinity with mouse nucleoli (Sullivan *et al*., 2001). Taken together, from these findings it can be hypothesised that hTERT made chromosomes become more interior. Telomeres have an affinity for nucleoli and the extra elongated telomeres

may unusually pull chromosomes to the nucleolus, whilst they also have affinity and binding with the nuclear periphery. Furthermore, lamin A/C binding proteins being may be affected by the formation of progerin protein and which might alter the correct positioning of the chromosomes, creating less anchorage points at the nuclear periphery as in the case of chromosome X in T08 cells. It has been shown that repositioning of genes from the periphery to a more interior position can correlate with inappropriate activation of that gene. The formation of chromatin loops for expression from repressed chromatin territories has been suggested as a mechanism of genome regulation, for example, for Hox gene activation (Chambeyron and Bickmore, 2004).

The karyotype of our each progeria cells; T06 and T08 were defined as having 46 numbers of chromosomes prior to hTERT immortalisation application (Coriell Institute). Because of the limited life span of normal and progeria cells, all cells were immortalised by ectopic expression of hTERT. In previous studies by Mukherjee & Costello have shown that both earlier and later passage cells from the HGPS patients consistently exhibited the highest aneuploidy levels in each of the seven chromosomes studied (Mukherjee and Costello, 1998). Furthermore, it was revealed in the stably hTERT transfected sheep fibroblast that although all highly expressing lines showed a virtually normal karyotype, following about 220 population doublings, lower hTERT expressing clones of 1-1 and 2-13, started to display a high frequency of abnormal karyotype corresponding to 20% or more cells (Cui *et al.*, 2002). In order to answer the question of whether or not our cell lines have any genomic instability after hTERT application, metaphase chromosome fixation was carried out. From the results, it is obvious that T08 cell line genomic instability. Several studies showed that the ectopic expression of hTERT can extend the life span without

altering the characteristic phenotypic properties of the cells (Ouellette *et al.*, 2000; Jiang *et al.*, 1999). Our data in M-FISH karyotyping analysis confirms unequivocally our metaphase chromosome findings that immortalised T08 cell line has aneuoploidy including deletions and translocations. In previous work, it was demonstrated that untransformed typical HGPS cell line (AG11498) has a normal 46, XY karyotype although it was noted that the frequency of chromosome loss does appear high (Anderson and Bridger, unpublished data).

In this chapter, I demonstrated that there are significant alterations in the epigenetic control of both consitututive and facultative heterochromatin in hTERT T06 and T08 cells. I observed significant reducution in H3K9me3 and HP1α marks in both T06 and T08 cells compared with NB1 and NB1T cells. In line with Shumaker *et al.*, 2007 findings, I revealed the loss of H3K27me3 mark in T06 cells. Interestingly, although loss of the H3K27me3 histone epigenetic mark was observed in T08 cells, H3K27me3 in T08 cells showed association with the Xi. Furthermore, in agreement with Dechat et al., 2008 study, my findings from the presence of H4K20me3 in both T06 and T08 cells revealed that there is a significant increase compared with NB1 and NB1T cells. My overall data of epigenetic modifications of histones suggest that expression of truncuated progerin protein alters chromatin organization in HGPS T06 cells and also the structure of histone marks are severely affected in atypical HGPS T08 cells. It has been proposed that cooperative mechanism exists in between H3K27and H3K9 methylation marks give rise to contribution to both the stable repression of developmentally regulated genes and the maintenance of constitutive heterochromatin (Boros *et al*., 2014).

In the present study, a possible relationship between the disease pathology and abnormal nucleolar domain structure was elucidated by assessing distinctions in the

distribution of 3 major nuclolar proteins including nucleophosmin, fibrillarin and RNA pol I proteins between NB1 and immortalised control NB1T and typical and atypical HGPS cells in order to discover whether an abnormal lamina have impact on other nuclear structures. Both NB1 and NB1T cells displayed higher typical distribution of NPM full rim, at the nucleolar periphery in the granular centre (GC) domain pattern relative to both T06 and T08 cells showing aberrant nuclear structure. In interphase, NPM is mainly located in the dense fibrillar components and granular components of nucleoli (Amin *et al.*, 2008). It was demonstrated that reduction of NPM gives rise to distortion and fragmentation of nucleolar structures by RNAi in HeLa cells leading to striking alterations in nuclear morphology with multiple micronuclei formation, due to the distortion of cytoskeletal structure through actin and tubulin fibres resulting from the defects in centrosomal microtubule nucleation (Amin *et al.*, 2008).

This study revealed that fibrillarin was distributed as the punctutate foci in the DFC domain in all cells. Further, the signal intensities of fibrillarin immunostaining in NB1 cells appeared to be lower compared with other cells suggesting that fibrillarin epitopes may be masked in NB1 fibroblasts. Interestingly, it was demonstrated that staining patterns for fibrillarin in HGPS fibroblasts appeared abnormal with reduced intensity and lack of any punctate structure (Mehta *et al.*, 2009). In previous study, NPM reduction was shown not significantly affecting the expression of fibrillarin compared with mock-treated cells suggesting that despite the fact that NPM and fibrillarin interact with each other throughout the cell cycle, among them only NPM would play a vital role to maintain the structural integrity by keeping nucleolar proteins compact at the nucleoli (Amin *et al.*, 2008). Most importantly, the localization pattern and expression of the lamin A/C was shown to be intact in NPM-reduced cells and also in the mock-treated cells suggesting that nuclear aberrations are likely

not depending on the post-mitotic nuclear assembly. Since NPM has binding capacity with the nucleic acid, it has been suggested that NPM being involved in chromosomal organisation (Brady *et al.*, 2004). Thus, defected distribution of NPM may cause aberrations in chromosome positioning in diseased cells such as in HGPS. RNA pol I analysis revealed different findings between control and progeria cells as RNA pol I was found as aggregates and small foci distributed in the DFC of the nucleolous in both NB1 and NB1T cells, whereas RNA pol I was only found as punctuates in both TO6 and T08 cells.

In line with Crabbe *et al*., (2012) findings, it is evident from my results that telomeres are positioning internally in all cells. Moreover, centromeres were found internally in all cells. However, location of centromeres in T08 cells was found moving towards periphery relative to other cells. In interphase nucleus, location of centromeres was shown near the nuclear periphery (Solovei *et al*., 2004). Shimi *et al*., (2008) revealed in cells that all lamin-B2 deficient, there is a lack of centromeres at the nuclear edge suggesting B-type lamins are involved in to tethering centromeres to the nuclear lamina. The findings of our colocalisation analysis of Ki-67 and centromeres indicate that the average proportion of colocalisation number is lower than the total number of centromeres for each cell type. It is known that Ki-67 antigen is detected in all phases of the cell division cycle suggests depending on the phase of cell cycle, chromosomes elicit different binding affinity to Ki-67 via their centromeres. We examined the relationship between HP1α and kinetochores using CREST autoimmune serum and results show that these two proteins are more closely associated in both NB1 and NB1T cells than T06 and T08 cells.

5.5 Conclusion

The underlying mechanism of genomic instability of hTERT progeria fibroblasts remain unknown at the moment and further research is required to enlight it. This chapter demonstrates that the structure of nucleolus is affected in both typical and atypical immortalised HGPS cells. Further, it can be hypothesized that epigenetic regulation to have a crucial role in HGPS.

Chapter 6: Telomere erosion corrects chromosome 18 positioning in control immortalised fibroblasts but not in immortalised progeria fibroblasts

Manuscript in Preparation: M. U. Bikkul, Predrag Slijepcevic, R. Faragher, C. Parris, I. R. Kill and J. M. Bridger

6.1 Introduction

In previous chapter, we revealed that elongated telomeres cause mispositioning of chromosomes 13, 18 and X in immortalised T08 cells and thus It is hypothesised that this is due to elongated telomeres in these cells. Murata *et al*., (2007) study evaluated positioning of chromosomes 10, 19 and X in normal thyroid tissue and in adenomatous goiters, papillary carcinomas, and undifferentiated carcinomas. According to their findings, chromosomes 10 and 18 were found locating toward the nuclear periphery and chromosome 19 was found in nuclear interior in both normal and goiter tissue. Nevertheless, in the papillary carcinoma tissue chromosome 19 was found positioning centrally in fewer cells. Furthermore, assessment of positioning of chromosomes 10, 18 and 19 revealed mispositioning of chromosomes (Murata *et al.*, 2007). Repositioning of chromosome 18 was shown moving toward the nuclear interior in cell differentiation of nonneoplastic cervical squamous epithelium (Wiech *et al.*, 2009). A subsequent paper also noted a reduction of the roundness of chromosome 8 territories, and chromosome 8 was mispositioned in pancreatic cancer cells that have elongated telomeres (Timme *et al.*, 2011).

Overexpression of mutant lamin-A in HGPS cells causes accelerated rates of loss of telomeres and shortened replicative lifespans (Wood *et al.*, 2014; Huang *et al.*, 2008). In previous work, it has been shown that telomere length is shorter in HGPS cells as opposed to age-matched control cells due to lamin A malfunction and disruption of normal telomere biology (Allsopp *et al*., 1992). Decker and colleagues exhibited by employing Q-FISH that due to mutant lamin A, telomere length is substantially shorter in HGPS cells compared to normal cells (Decker *et al.*, 2009). Chromosome 18 and chromosome 19, which are gene-poor and gene-rich

respectively in HGPS cells have been shown having similar telomere length (Decker *et al*., 2009).

Ectopic expression of telomerase *in vitro* can extend the proliferative lifespan of a cell without causing any genomic instability (Oulette *et al*., 2000), however ectopic expression of telomerase in mice *in vivo* was elucidated to cause increased incidence of cancer (Tomás-Loba *et al.*, 2008). Gonzalez-Suarez *et al*., (2009) elucidated a direct association between telomeres and lamina employing chromatin immunoprecipitation (ChIP) assay in mice. The elevated level of γH2AX was shown in Lmna $^{-/-}$ MEFs, demonstrating increased basal DNA damage (Gonzales-Suarez *et al.*, 2009).

In mice, at the round spermatid stage telomeres were observed assembling around the nucleolous in the center of the nucleus and in the subsequent the elongating stage, telomeres dispersed all over the nuclei (Tanemura *et al.*, 2005). Formations of t-loops in a TRF2-dependent fashion at interstitial telomere repeat sequences are termed intersititial telomere loops (ITLs) (Wood *et al*., 2014; Simonet *et al.*, 2011). It was proposed that ITL formation involves the interaction of repressed, telomeric DNA with normal chromatin (Wood *et al*., 2014). Shortening of telomeres induced genetic changes and ultimately leading to cell senescence. Alterations in the expression of genes are found neighbouring to telomeres, named Telomere Position Effect (TPE) (Ottaviani *et al.,* 2008). The telomere position effect (TPE) phenomenon was first defined in *Drosophila* as chromatin modifications such as DNA methylation and histone methylation plays an essential role in the silencing of genes that are in close proximity to the telomeres (Baur *et al.*, 2001; Levis *et al.,* 1985). A member of the repressive machinery, HP1 is found accumulating at telomeres and is not seen at

affected genes whereas, it was observed that TRF2 is accumulated at promoters of these affected genes and a lack of TRF2 association is detected in cells with shortened telomeres which suggests that TRF2 is essential to enable long-range telomere looping (Wood *et al.*, 2014; Robin *et al.*, 2014). The expression of ISG15 (interferon-stimulated gene) was shown to increase when telomeres become short and interestingly, genes located between ISG15 and telomeres did not elicit any telomere-length regulation (Lou *et al.*, 2009). Robin *et al*., (2014) exhibited by performing 3D image analysis that shortening of telomeres lead to a dramatic change of chromatin organization at distal chromosome region. SubTel 12p and ISG15 probes were observed being adjacent in cells with long telomere length. However probes were observed being separated in cells with short telomeres (Robin *et al*., 2014).

The small non-peptidic, non-nucleosidic synthetic compounds (BIBR1532) were shown as a cancer treatment by inhibiting the catalytic component hTERT leading to progressive telomere shortening and a proliferation arrest in cancer cells (Bashash *et al.*, 2013; Ruden and Puri, 2013; El-Daly *et al.*, 2005) (Figure-6.1). BIBR1532 was employed to target the telomerase/telomere complex of our immortalised cell lines to shorten telomeres in order to test the hypothesis that elongated telomeres had mislocalised chromosomes. Furthermore, the effect of BIBR1532 on telomere position was assessed in the cells. This study, the first to report on telomere length in ectopically expressed hTERT in normal and HGPS T08 cells demonstrating that BIBR1532 drug treatment has shorthen the telomeres of both control and HGPS hTERT cell lines.

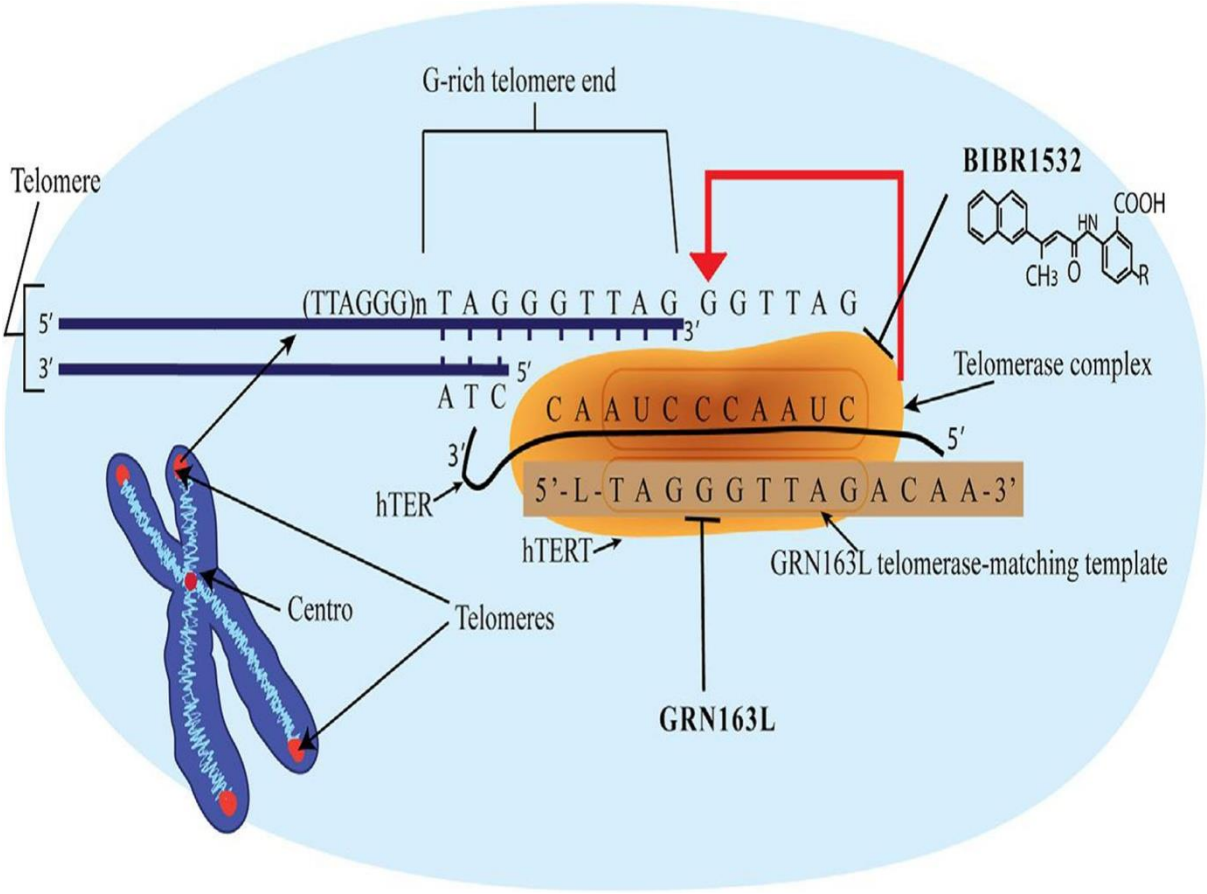

Figure 6.1: Telomeres consists of 1000–2000 oligonucleotides of non-coding tandem repeats of G-rich nucleotide sequences, (TTAGGG) n, forming a 30 - overhang on the 3' end of chromosomes. The RNA template of telomerase (hTER) is composed of a total of 451 nucleotides of which nucleotides 46 through 56 (50 - CUAACCCUAAC-30) serve as a template to add new telomeric repeats. GRN163L functions by inhibiting telomerase by acting as a direct telomerase RNA template antagonist binding with high specificity and affinity at the active site of hTER, leading to a complete inhibition of the enzyme, consist of a 13-mer oligonucleotide.BIBR1532(2-[E)-3-naphtalen-2-yl-but-2-enylylamino]-benzoic acid) is a non-nucleotidic mixed type hTERT active site telomerase inhibitor, which impairs the elongation of DNA substrate upon template copying by reducing the number of TTAGGG repeat (Ruden and Puri, 2013).

6.2 Materials and Methods

6.2.1 Cell Culture and BIBR1532 treatment

As per chapter 2, section 2.2.1. , NB1 and hTERT (Human Telomerase Reverse Transcriptase) fibroblasts: NB1T and TO8 have been cultured. Mouse lymphoma LY-R (radio-resistant) and LY-S (radio-sensitive) cells were used as a reference to measure telomere length using Q-FISH (IQ-FISH) technique-{a kind gift from Dr. Parissa Ka and Dr. Chetana Sharma, Brunel University, London}. Cell culture was carried out with the exception of colcemid treatment. A stock solution of BIBR1532 (Tocris biosciences) at a concentration of 10 mM was prepared by dissolving the compound in 0.1% sterile dimethylsulfoxide (DMSO) and divided into aliquots and stored at -20^{0}C until use. Furthermore, relevant amounts of BIBR1532 stock solution to attain concentrations of 10, 50 and 100 µM were prepared. The culture medium contained 10 µM of BIBR1532 was replenished at every 3 days. NB1T and T08 cells were treated with 10 µM of BIBR1532 for 8 weeks and 6 weeks respectively. Control cells were treated with corresponding solvent concentrations.

6.2.2 Assessment of cell logarithmic growth

In order to investigate effects of BIBR1532 on cell viability, NB1T and T08 cells were seeded at 2 x 10^5 cells/mL and incubated in the presence of 0 µM, 10 µM, 50 µM and 100 µM of BIBR1532. In addition, control cells were treated with a corresponding concentration of DMSO as an alternative negative control. Cultures were maintained for 6 days in 24-well plates as triplactes, re-feeded with medium + drug in day 3 serially and every 24 hours, cell viability was assessed by cell growth analysis.

6.2.3 Interphase Quantitative Fluorescence in situ hybridization (IQ-FISH)

6.2.3.1 Cell Fixation

As per chapter 2, section 2.2.6 NB1, BIBR1532 treated and untreated NB1T and T08 cells were fixed every 2 weeks prior to IQ-FISH experiment.

6.2.3.2 Pre Hybridization washes

Prepared with fixed cell on slides were aged overnight at 55 °C. The rest of the pre hybridisation washes was carried out as per chapter 2, section 2.2.6.

6.2.3.3 Hybridization with the telomeric probe

As per chapter 2, section 2.2.6.1 hybridization was performed. In order to detect telomeres in mouse cell lines L5178Y (LY-R) and L5178Y-S (LY-S), a FITC labelled a telomere PNA FISH/FITC kit (Dako) was used following a protocol under the manufacturer's instructions- {a kind gift from Dr. Predrag Slijepcevic, Brunel University} . A TRITC labelled a telomere PNA FISH/TRITC kit (dako) was used for NB1, NB1T and T08 cells- {a kind gift from Dr. Predrag Slijepcevic, Brunel University, London}.

6.2.3.4 Post-hybridization washes

As per chapter 2, section 2.2.6.2 post-hybridization washes were performed.

6.2.3.5 Image capture for telomere length analysis

At least 30 interphase cells have to be analysed for each cell line and each measurement was repeated 3 times. A 63X objective on an Axioplan 2 Zeiss fluorescent microscope equipped with a CCD camera and the Smart capture 2 image acquisition software (Digital Scientific, Cambridge, UK) was employed to capture images of interphase cells. We used a single exposure time of 0.5 sec and analysed telomere fluorescence intensity in a single microscopy session for LY-R/LY-S cells and human control and immortalised fibroblast samples respectively to reduce the chances of microscope lamp variability. IP Lab software was used to measure telomere signal intensity which is proportional to telomere length. The IP lab software produces a combined image of the detected telomeres and the cell nucleus boundaries which are superimposed onto the telomere image. It is crucial to use appropriate controls for the experiment to maintain the accuracy of IQ-FISH experiment due to intensity of the fluorescence microscope lamp intensity is not constant. Therefore, two mouse cell lines, LY-R and LY-S, with long and short telomeres respectively were used as calibration standards in order to ensure the accuracy of fluorescence intensity measurement (McIlwraith and West, 2001). We captured images of LY-R and LY-S cells together with the human cells in each experiment. The detailed description of the procedure for IQ-FISH is in a PhD thesis (Ojani, 2012).

6.2.4 Telomere dysfunction-induced foci (TIF) Assay

γ-H2AX assay is used to detect DNA double strand breaks in interphase cells employing a monoclonal antibody against the γ-H2AX protein. In this study, I combined γ-H2AX antibody detection with hybridization with synthetic telomeric PNA and this assay is named “TIF” assay. Firstly, as described previously in section 6.2.2, IQ-FISH was performed. Subsequently, cells were washed 15 minutes two times with PBS in a coplin jar. 100 µl of γ-H2AX antibody (dilution of 1:500 with 1% PBS/ FCS, Upstate) solution was added to slides for one hour in damp and room tempereature then after which slides were washed with PBS for 5 minutes, three times on a shaker. 100 µl of goat anti-mouse (FITC) (diluted 1:64 with 1% PBS/FCS, Sigma-F9006) secondary antibody was added for one hour in dark, damp conditions and then rinsed with PBS for five minutes, three times in a dark Coplin jar and on an orbital shaker. Finally, the slides were analysed for the presence of TIF signals.

6.2.5 Two-dimensional fluorescence in situ hybridisation (2D- FISH)

As per chapter 2, section 2.2.3 2D-FISH was performed for untreated NB1, NB1T and T08 fibroblasts. Every 2 weeks, 2D-FISH was performed to assess positioning of chromosomes; 18 and X for BIBR1532 treated NB1T and T08 cell lines. Chromosomes 18 and X signal positions were identified in at least 49 nuclei from NB1 and untreated and treated NB1T and T08 cells.

6.2.6 Telomere distribution using 2D telomere FISH

Every 2 weeks, telomere signal positions were identified in at least 45 nuclei from NB1 and untreated and treated NB1T and T08 cells as described in chapter 2, section 2.2.4.5.

6.2.7 Indirect immunofluorescence

As per chapter 3, section 3.2.3, anti-Ki-67 immunostaining was performed every 2 weeks for BIBR1532 treated and untreated NB1T and T08 cells. In addition, Ki-67 immunostaining was assessed for NB1 fibroblasts.

6.2.8 Statistical analysis

Values are expressed as averages ± SEM, and n represents the number of cells analysed. Two-tailed unpaired t-tests used as statistical analysis. Significance was taken as $P \leq 0.05$. The level of significance is indicated as: * $P \leq 0.05$, ** $P \leq 0.01$, *** $P \leq 0.001$ and **** $P \leq 0.0001$.

6.3 Results

6.3.1 Cell viability analysis of BIBR1532 treated cells

It is important to note that as we only aim to shorthen the telomere length without causing growth arrest of our cells lines by pharmological telomerase inhibition, previously we evaluated cytotoxic effect of the drug at different concentrations by assessing cell viability. Telomerase inhibitor treated NB1T and T08 cells were maintained for a minimum of 6 days, and serially, every 24 h the number of total mean viable cells was evaluated. As dead cells disattached from the surface of the tissue culture dish, the remaining cells were considered as viable cells.

A

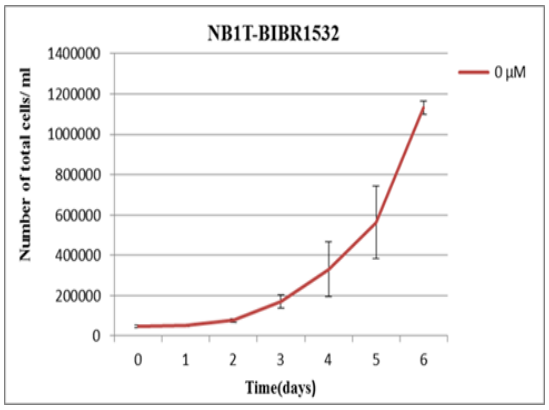
NB1T-BIBR1532
Number of total cells/ ml
1400000
1200000
1000000
800000
600000
400000
200000
0
0 µM
0 1 2 3 4 5 6
Time(days)

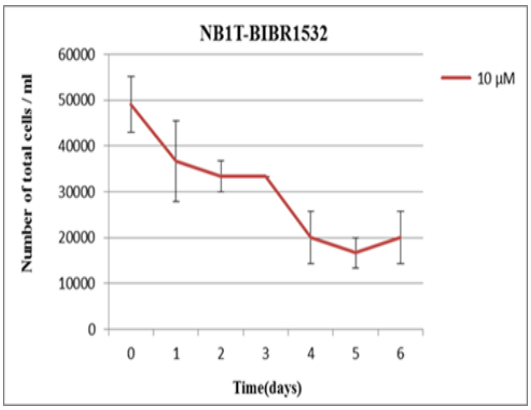
NB1T-BIBR1532
Number of total cells / ml
60000
50000
40000
30000
20000
10000
0
10 µM
0 1 2 3 4 5 6
Time(days)

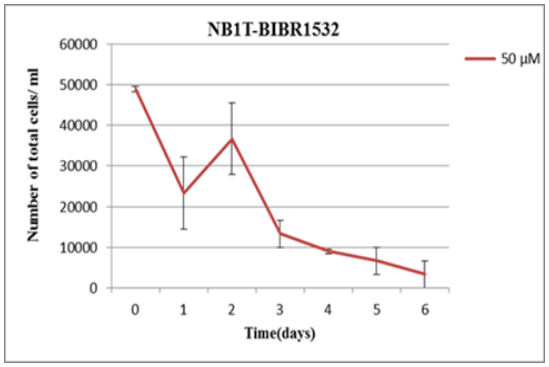
NB1T-BIBR1532
Number of total cells/ ml
60000
50000
40000
30000
20000
10000
0
50 µM
0 1 2 3 4 5 6
Time(days)

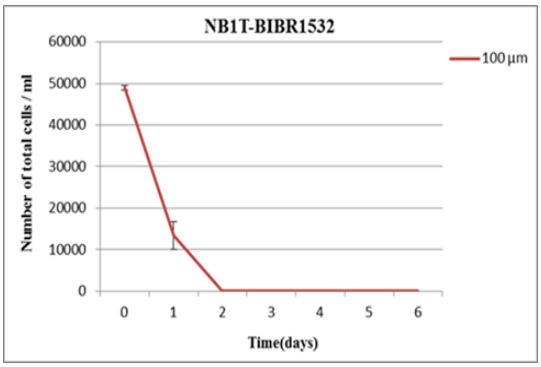
NB1T-BIBR1532
Number of total cells / ml
60000
50000
40000
30000
20000
10000
0
100 µm
0 1 2 3 4 5 6
Time(days)

B

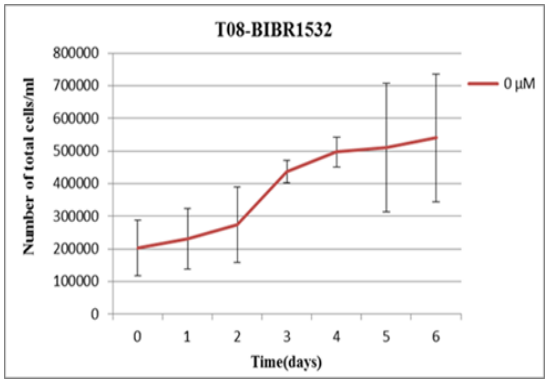
T08-BIBR1532
Number of total cells/ml
800000
700000
600000
500000
400000
300000
200000
100000
0
0 µM
0 1 2 3 4 5 6
Time(days)

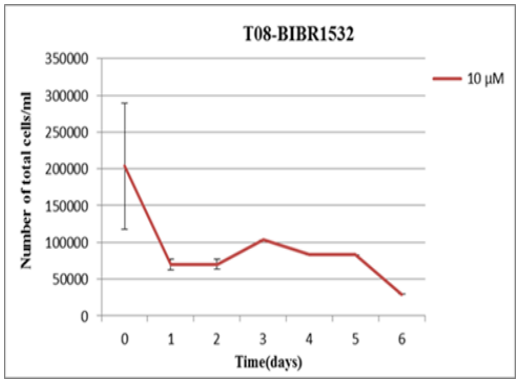
T08-BIBR1532
Number of total cells/ml
350000
300000
250000
200000
150000
100000
50000
0
10 µM
0 1 2 3 4 5 6
Time(days)

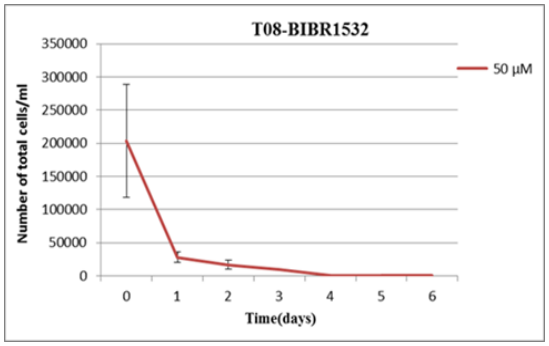
T08-BIBR1532
Number of total cells/ml
350000
300000
250000
200000
150000
100000
50000
0
50 µM
0 1 2 3 4 5 6
Time(days)

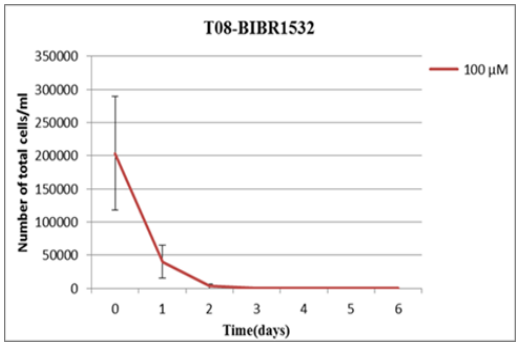
T08-BIBR1532
Number of total cells/ml
350000
300000
250000
200000
150000
100000
50000
0
100 µM
0 1 2 3 4 5 6
Time(days)

Figure 6.2: BIBR1532 gives rise to a direct inhibitory effect on viability of cells. Cells were treated with the desired concentrations of BIBR1532, cultures were maintained a minimum of 6 days and every 24 h the number of total mean viable cells was assessed. The viability index of treated cells lessened in a dose-dependent manner, indicative of a direct short-term cytotoxic effect of BIBR1532 on NB1T (A) and T08 (B) cells.

As shown in Figure 6.2, cell viability of treated cells decreased significantly in a dose-dependent manner, indicative of a direct short-term cytotoxic effect of BIBR1532 on NB1T and T08 cells. Negative control NB1T and T08 cells only treated with DMSO showed increasing total number of cell within 6 days. However, using high concentrations of BIBR1532 (50 and 100 µM), we found substantial decreases in the viability index of treated cells within 2 days. Cell logarithmic growth assessment during continuous treatment of cells for 6 days using concentration of 10 µM demonstrated that both NB1T and T08 cells survived the drug. Given that we decided to perform BIBR1532 drug treatment of our NB1T and T08 cells using concentration of 10 µM.

6.3.2 Interphase quantitative fluorescence in situ hybridisation (IQ-FISH) analysis of cells

Interphase Q-FISH (IQ-FISH) method was employed to assess average telomere lengths in the cell lines using digital microscopy. The advantages of using IQ-FISH to assess telomere length are; the problem of auto-fluorescence specific to flow-FISH is eliminated by using of microscopy, no need to require metaphase cells and IQ-FISH allow assessing telomere length in tissues. Initially, telomere PNA FISH experiment was performed for two lymphoblastoid in origin mouse cell lines L5178Y (LY-R) and

L5178Y-S (LY-S) used as calibration standards. It was shown previously by Q-FISH that the parental L5178Y (LY-R) cell line has telomere length of 49 kb and the LY-S cell line, derived from the LY-R cell line has telomere length of 7 kb (McIlwraith *et al*., 2001). The average telomere length measured with Southern blot analysis in DBA mice from which LY-R cells had been isolated were shown to have terminal restriction fragments (TRFs) ranging from 20 to 150 kb (Zijmans *et al*., 1997). In Figure 6.3, typical interphase LY-R and LY-S cells after hybridization with telomeric PNA oligonucleotides are shown. It is evident from the figures below that the strength of fluorescence in LY-R cells is higher than LY-S cells. The strength of fluorescence signals between normal (NB1) and immortalised cell lines (NB1T and T08) can be seen in Figure 6.4.

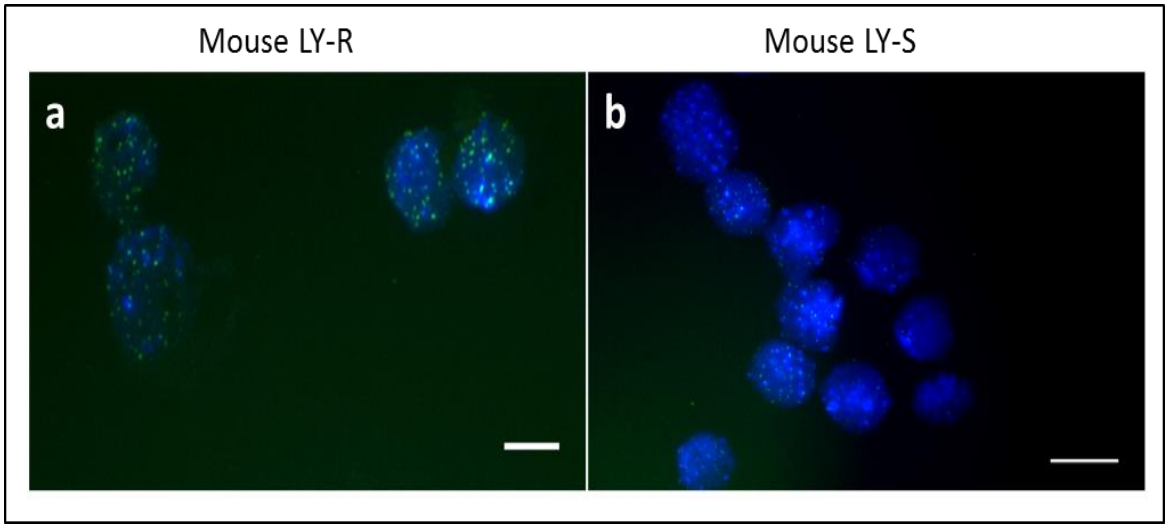

Figure 6.3: Digital images of interphase cells derived from mouse cell lines LY-R (a) and LY-S (b) after hybridization with FITC telomeric PNA oligonucleotides. Magnification= x63. Scale bars= 5 µm.

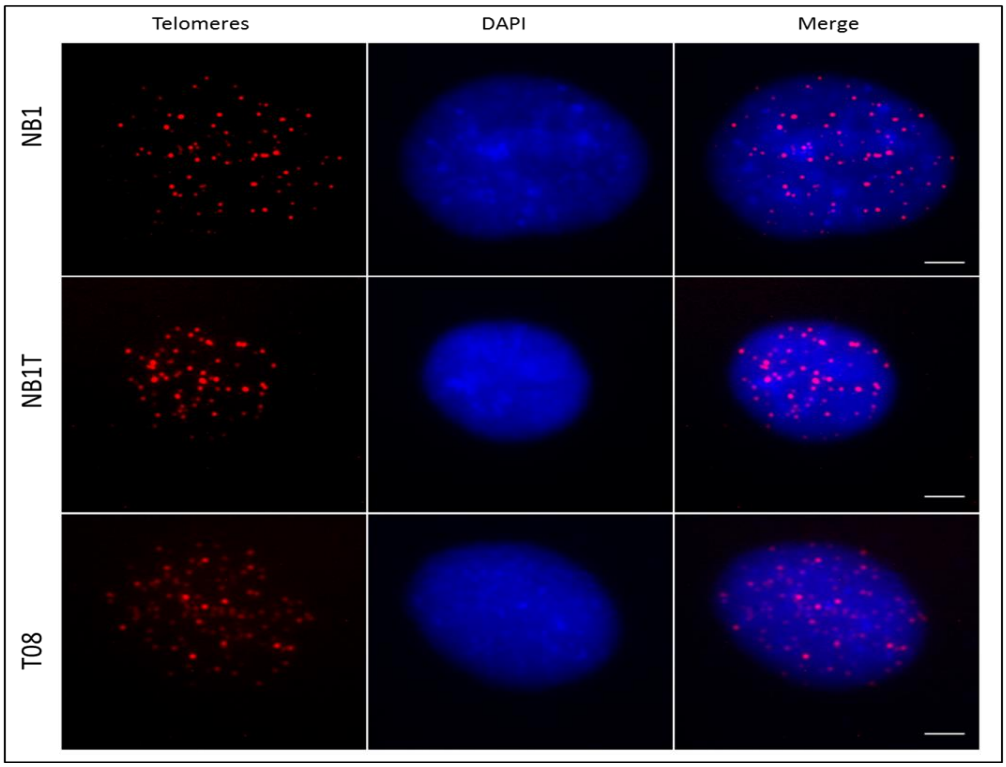

Figure 6.4: Representative images of telomere PNA FISH experiment of control (NB1), Immortalised normal (NB1T) and atypical HGPS (T08) fibroblasts. Fixed cells were stained with both DAPI and Cy3 telomeric PNA probes and captured at 100X magnification. Scale bars= 5 µm

In order to assess the telomere length of these two mouse cell lines as calibration standards, Dr. Slijepcevic's group has before described a modified Q-FISH method (Wong and Slijepcevic 2004). In Q-FISH method, the calibration process is essential to ensure reproducibility of findings. In Q-FISH experiments, as microscope fluorescence bulb intensity changes over time, the length of exposure time is required in order to capture images of telomeric signals which will be subject to fluorescence intensity measurement performing appropriate software programmes. I measured fluorescence intensity of LY-R and LY-S telomeres on five different dates and statistically analysed the results. Previously, it has been demonstrated that this

method works well using different cell lines (Wong and Slijepcevic 2004) and also in IQ-FISH protocol developed by Maryam Ojani (Ojani, 2012). As described in Dr. Slijepcevic's group, IPLab software package was used to measure fluorescence intensity of telomeres in interphase cells (Ojani, 2012). By using IPLab software package, densitometry analysis was performed providing "mean" values representing an average telomere fluorescence intensity value for each assessed cell. It was shown performing IPLab software that scoring of 25 nuclei for each cell line, the average telomere length in LY-R cells is 6.9 times longer than in LY-S cells (Wong and Slijepcevic 2004). My aim is to analyse telomere fluorescence using IPLab software in mouse L5178Y (LY-R) and L5178Y-S (LY-S) cell lines used as calibration standards and in human normal (NB1) as control and immortalised human normal (NB1T) and atypical HGPS (T08) fibroblasts. As described in Ojani (2012), the term named "unmodified fluorescence" was used referring that no internal control was used in order to correct for variations related with fluorescence microscopy (Ojani, 2012). The telomere fluorescence intensity measurement of LY-R and LY-S cell lines performing the IPLab software are shown in Figure 6.5.

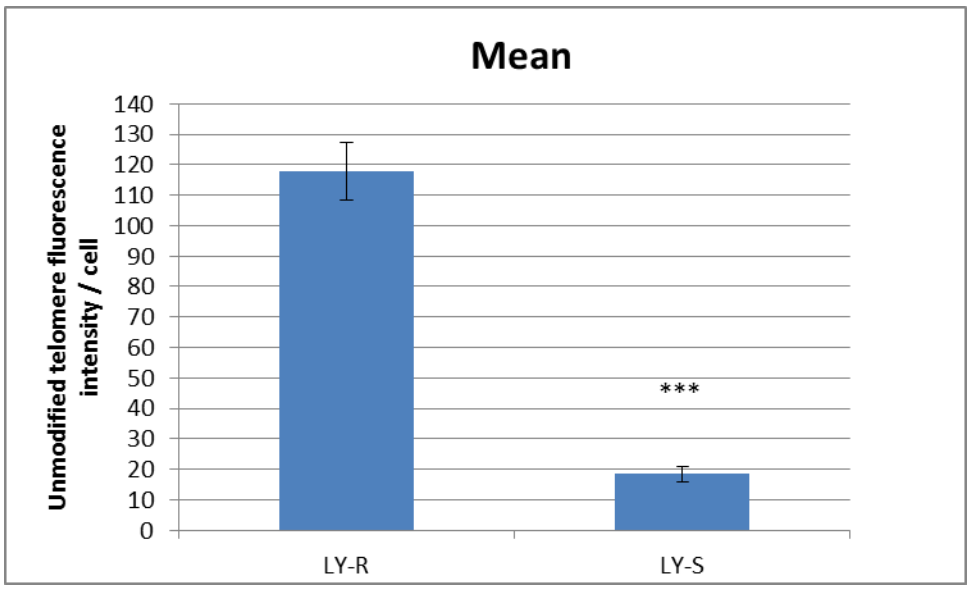

Figure 6.5: Mean Unmodified Telomere Fluorescence Intensity measurements at 0.5 seconds exposure time in LY-R and LY-S per cell**.** ***= P<0.001, Error bars represent SEM.

The telomere fluorescence analysis showed that the average telomere fluorescence, expressed as the mean unmodified fluorescence in IPLab is 6.4 times greater in LY-R than in LY-S cells (Figure 6.5). Previous studies showed that the ratios of telomere fluorescence analysis between LY-R and LY-S are as 6.6 (McIlrath *et al*. 2001) and 7 (Ojani, 2012). Following the calibration method using LY-R and LY-S, I decided to use NB1 fibroblasts as a control cell. As described in previous chapters, both NB1T and T08 cells have the robust telomerase activity. As described in Ojani (2012), in order to obtain arbitrary unit as "CCFL" representing Corrected Calibrated FLuorescence, the values of telomere fluorescence in NB1 cells generated during the 5 different measurement sessions (Ojani,2012).

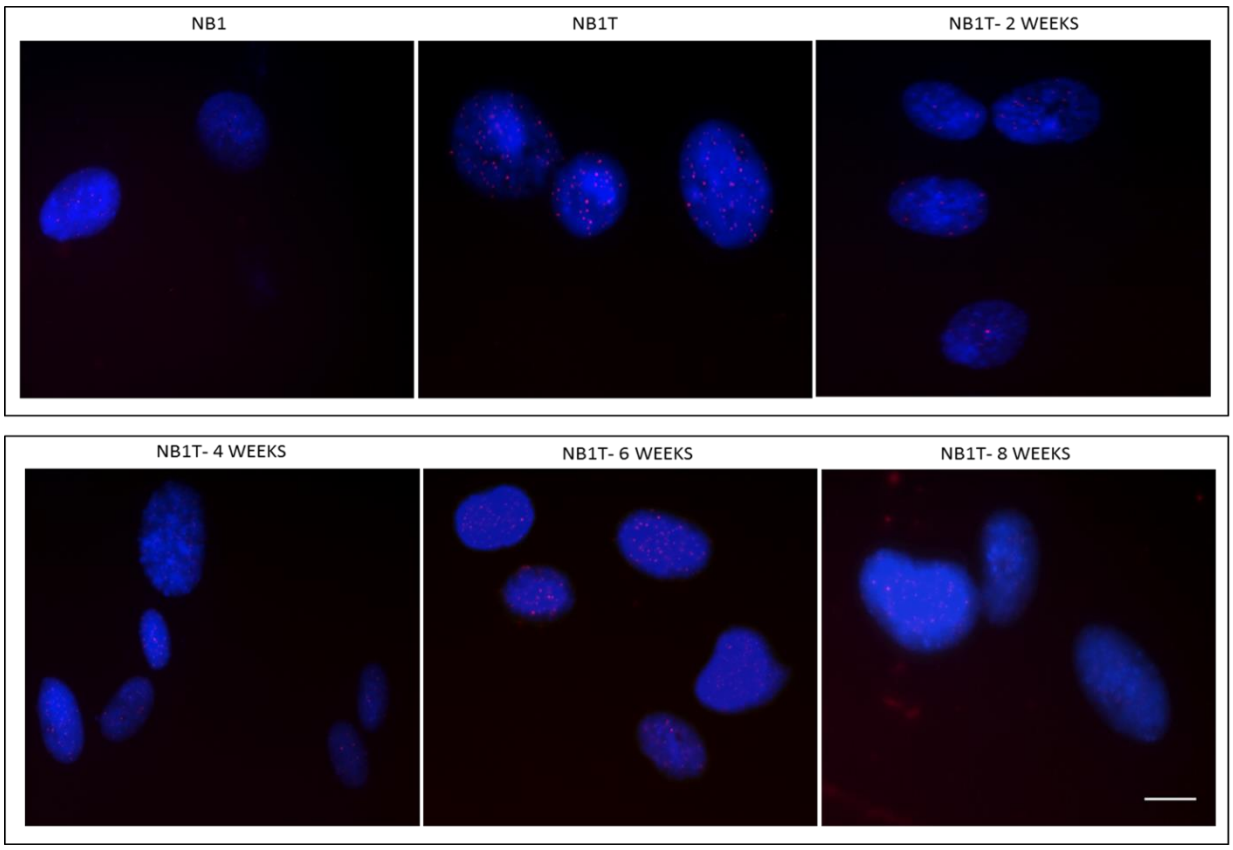

Figure 6.6: Representative digital images of NB1, NB1T and 2, 4, 6 and 8 weeks BIBR1532 drug treated NB1T fibroblast cells in interphase after hybridization with telomeric PNA oligonucleotides. Magnification = x63. Scale bar= 5 µm.

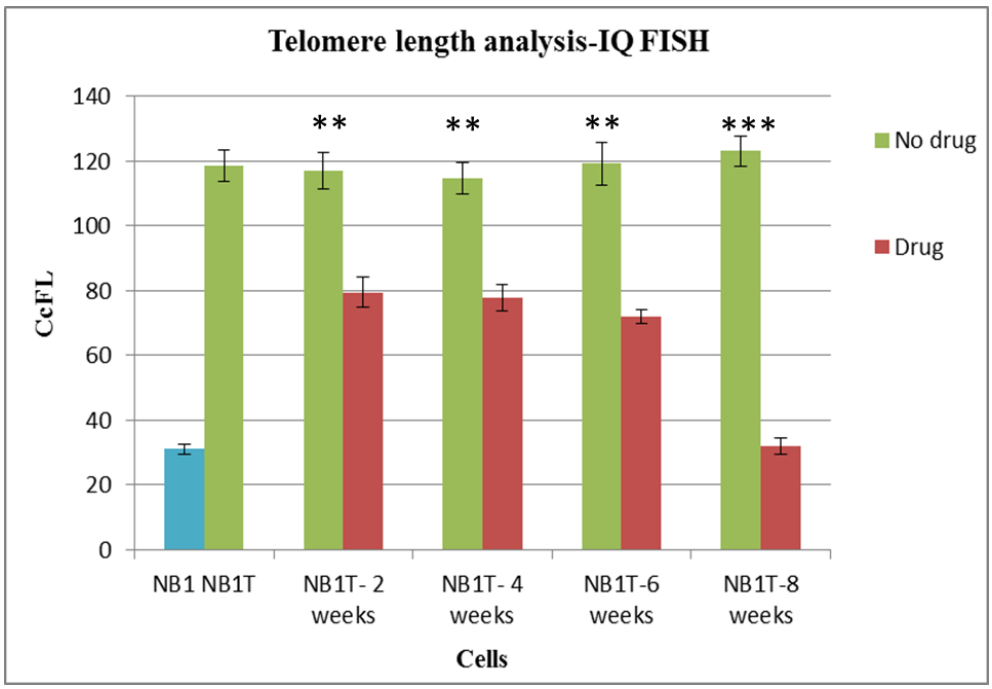

Figure 6.7: Corrected calibrated fluorescence (CcFl) before and after treatment with BIBR1532 NB1T cell line relative to the control NB1 cell line. Every 2 weeks treated and untreated NB1T cells were measured for telomere fluorescence intensity by performing IQ-FISH. Drug treated NB1T cells after 8 weeks showed approximately 4x shorter telomeres compared to the NB1T untreated cells. The telomere fluorescence signal intensity of drug treated NB1T cells for 8 weeks was similar to the control NB1 cell line. **=P<0.01, ***=P<0.001. Error bars represent SEM.

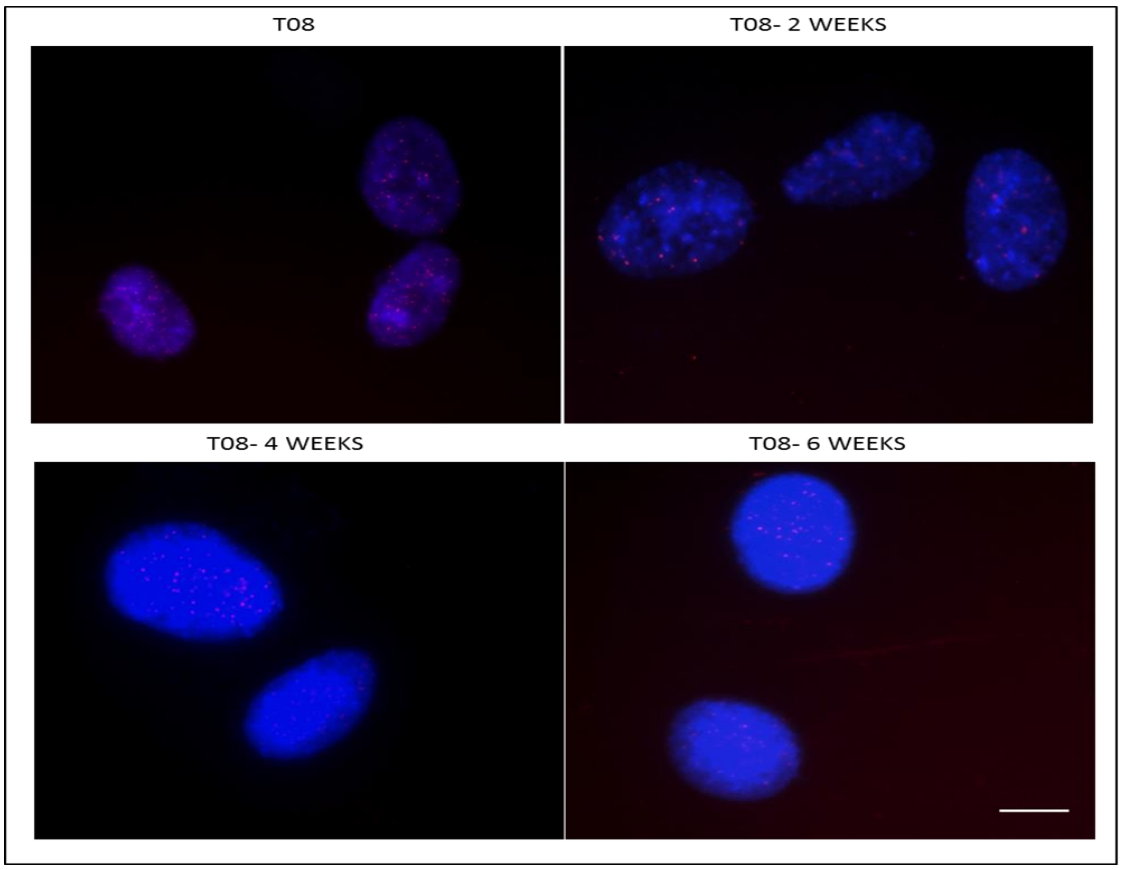

Figure 6.8: Representative digital images T08 and 2, 4, 6 weeks BIBR1532 drug treated T08 fibroblasts in interphase after hybridization with telomeric PNA oligonucleotides. In order to reveal DNA, DAPI was used. Magnification = x63. Scale bar = 5 µm.

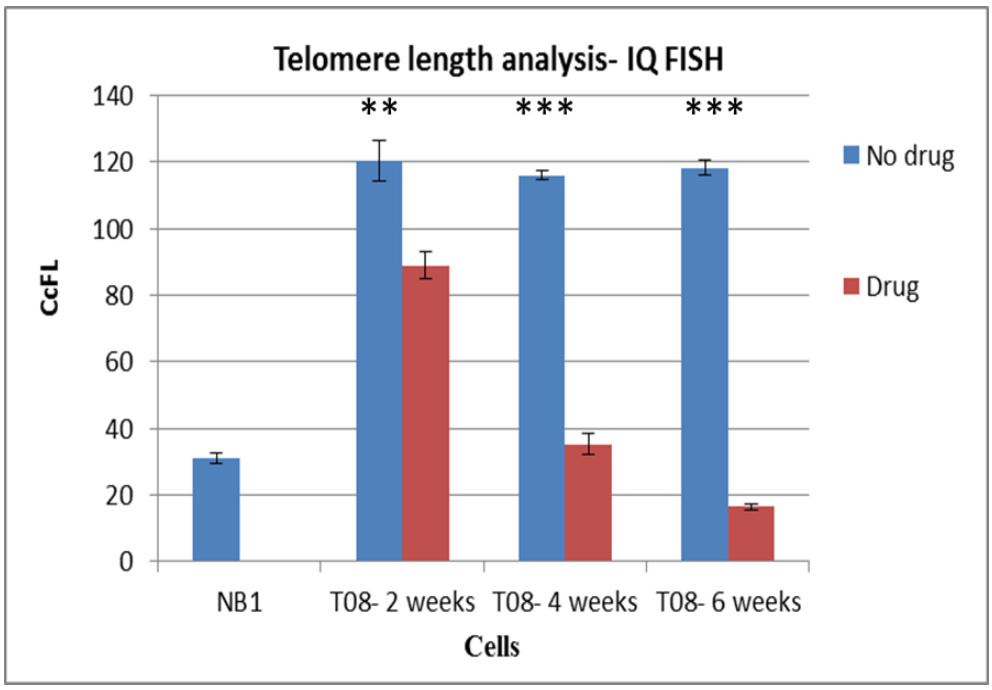

Figure 6.9: Corrected calibrated fluorescence (CcFl) before and after treatment with BIBR1532 T08 cell line relative to the control NB1 cell line. Every 2 weeks treated and untreated T08 cells were measured for telomere fluorescence intensity by performing IQ-FISH. Drug treated T08 cells after 8 weeks showed approximately 6 x shorter telomeres compared to the T08 untreated cells. The telomere fluorescence signal intensity of drug treated T08 cells for 6 weeks was shorter to the control NB1 cell line. ***=P<0.001, ***=P<0.01. Error bars represent SEM.

A representative example of the hybridizations with telomeric PNA in NB1, NB1T and drug treated NB1T cells are shown in Figure 6.6. It is evident from the images that the strength of fluorescence in NB1T cells is higher than NB1 and drug treated NB1T cells. Our IQ-FISH results reveal that treatment of NB1T cells with BIBR1532 gave rise to gradually shortening of telomeres. CcFL at 8 weeks drug treated NB1T cells show 4x shorter telomeres as compared to NB1T cells (P<0.001) and almost the same telomere length with internal control NB1 cells (Figure 6.7). A representative example of the hybridization with telomeric PNA in T08 and drug treated T08 cells

are shown in Figure 6.8. It is evident from the image that the strength of fluorescence in T08 cells is higher than drug treated T08 cells. Our IQ-FISH results reveal that treatment of T08 cells with BIBR1532 give rise to shortening of telomeres. CcFL at 6 weeks drug treated T08 cells show almost 6x shorter telomeres compared to T08 cells ($P<0.001$) and even shorter telomere length with internal control NB1 cells (Figure 6.9). CcFL at 4 weeks drug treated T08 cells show almost 6x shorter telomeres compared to T08 cells ($P<0.001$) and shows similar telomere length with internal control NB1 cells (Figure 6.9).

6.3.3 Telomere dysfunction-induced foci (TIF) Assay analysis in normal and immortalised NB1T and T08 cell lines

When telomeres become critically short in telomerase negative cells, they lose their protective function and are subsequently detected by the DNA damage response proteins as sites of DNA damage which results in replicative cell senescence. In addition to measurement of telomere length, DNA damage response in the same cells lines was investigated using a DNA damage marker, a phosphorylated form of histone H2AX, which enables the direct analysis of DNA damage at telomeres in interphase cells to determine whether shortening of telomeres causes any DNA damage by a technique called TIF (Telomere dysfunction Induced Foci) (Min *et al.*, 2012). A representative example of a TIF observed in NB1 and drug treated NB1T, T08 cell lines are shown in (Figure 6.10). Detection of at least one telomeric signal co-localized with a γ-H2AX signal was considered as a TIF positive cell.

A

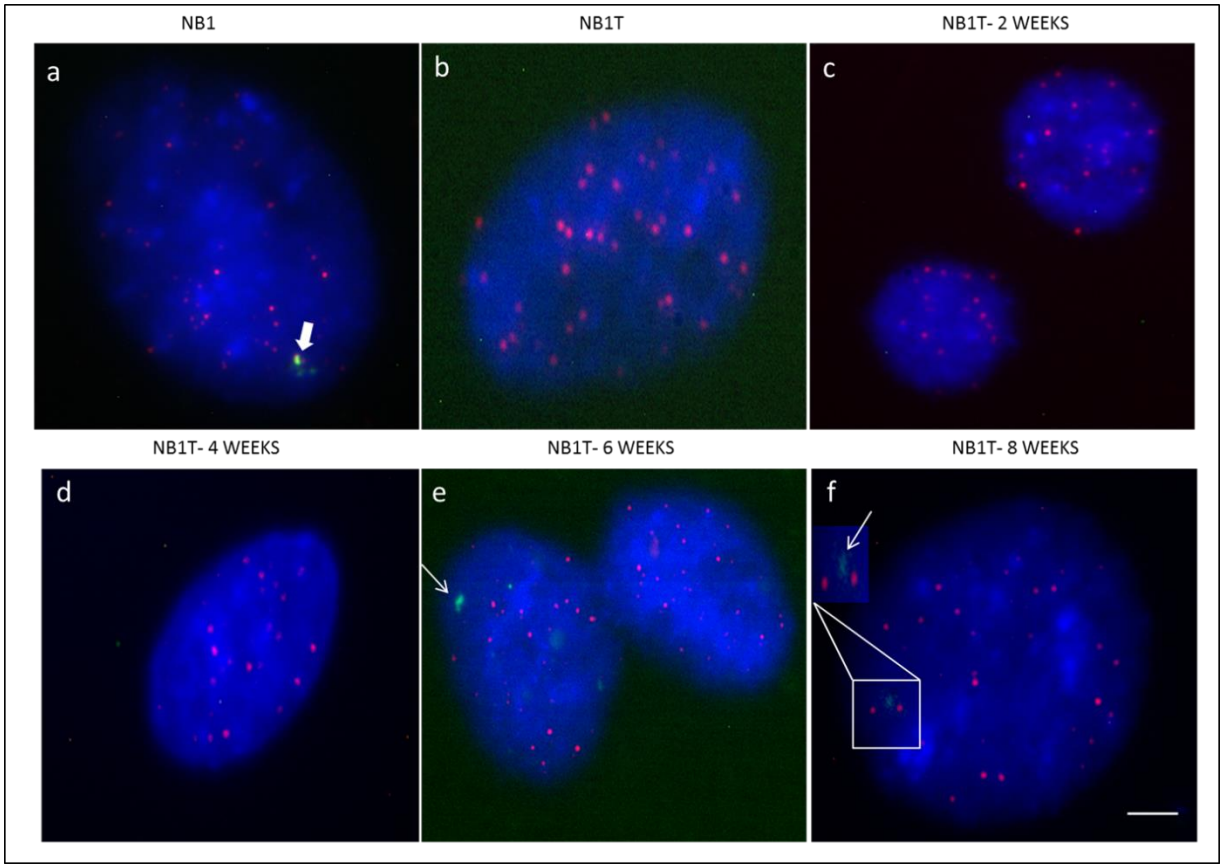
NB1
NB1T
NB1T- 2 WEEKS
a
b
c
NB1T- 4 WEEKS
NB1T- 6 WEEKS
NB1T- 8 WEEKS
d
e
f

B

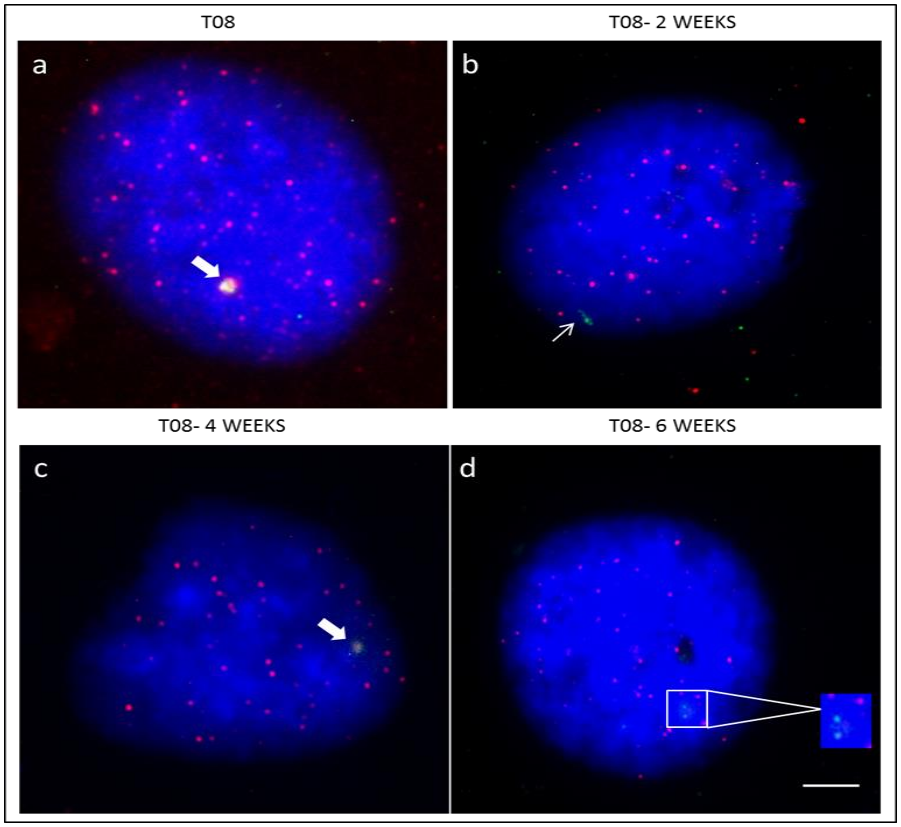
T08
T08- 2 WEEKS
a
b
T08- 4 WEEKS
T08- 6 WEEKS
c
d

Figure 6.10: Representative images of γ-H2AX foci (A) and TIF assay (B) of BIBR1532 treated NB1, NB1T and T08 cells. Red and Green fluorescence in the merged images represents telomeres and H2AX respectively. Thin white arrow in the images indicates H2AX foci and the yellow dots (indicated by thick arrow) represent the co-localization of γ-H2AX and TTAGGG repeats in nuclei. Innermost pictures show enlargements (x 5) of the white boxes. In order to reveal DNA, DAPI was used. Magnification = x100. Scale bar=5 μm

The frequency of γ-H2AX foci/cell represents the total DNA damage in the genome are presented in Figure 6.11-A, B. The frequency of γ-H2AX foci/cell in NB1, NB1T and T08 cells are; 1.44, 0.04 and 2.89 respectively. Upon treatment with BIBR1532 for 8-weeks, the frequency of γ-H2AX foci/cell in NB1T cells is increased to 0.57 which is significantly greater than the frequency of γ-H2AX foci/cell in untreated NB1T cells ($p<0.001$). However, treatment with BIBR1532 for 2-weeks the frequency of γ-H2AX foci/cell in NB1T cells was not significantly different compared to untreated NB1T cells ($p>0.05$). Upon treatment with BIBR1532 for 2-weeks, the frequency of γ-H2AX foci/cell in T08 cells is reduced to 0.12, which is signifantly greater than untreated T08 cells ($p<0.001$). Furthermore, treatment with BIBR1532 for 6-weeks the frequency of γ-H2AX foci/cell in T08 cells was not significantly different compared to untreated T08 cells ($P>0.05$) (Figure 6.11-A). TIF analysis allows us to estimate the proportion of DNA damage occurring at terminal telomeric sequences. In NB1 and T08 cells, TIF frequencies were 0.3 and 0.42 respectively, whereas NB1T cells did not show any TIF/cell. The number of TIF/cell observed in 8-weeks BIBR1532 drug treated NB1T was increased to 0.41, which is significantly greater than untreated NB1T cells ($p<0.01$). The number of TIF/cell observed in 2-weeks BIBR1532 drug treated T08 was reduced to to 0.04, which is significant compared to untreated T08 cells ($p<0.05$)(Figure 6.11- B). It is noteworthy that

although drug treatment was shown causing significant differences in DNA damages for both NB1T and T08 cells, the average number of TIF/cell was less than 1 for both cells.

A

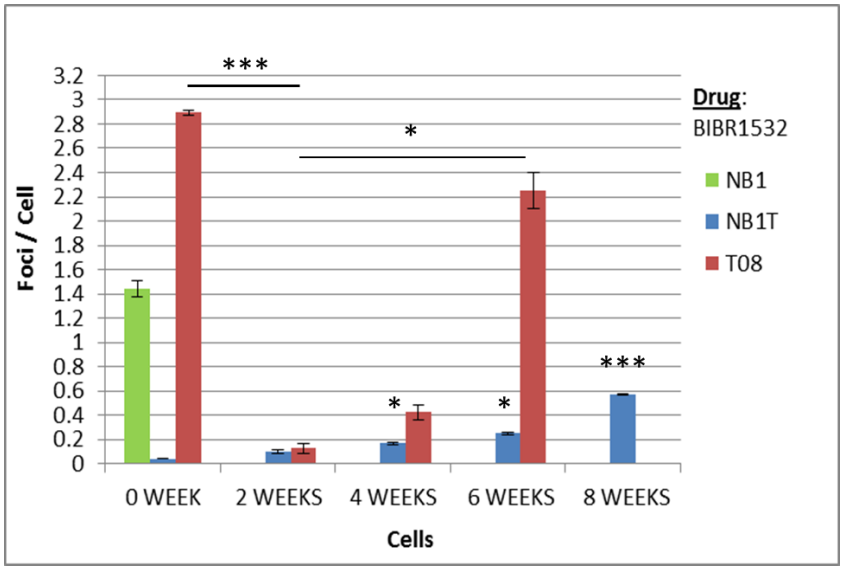

B

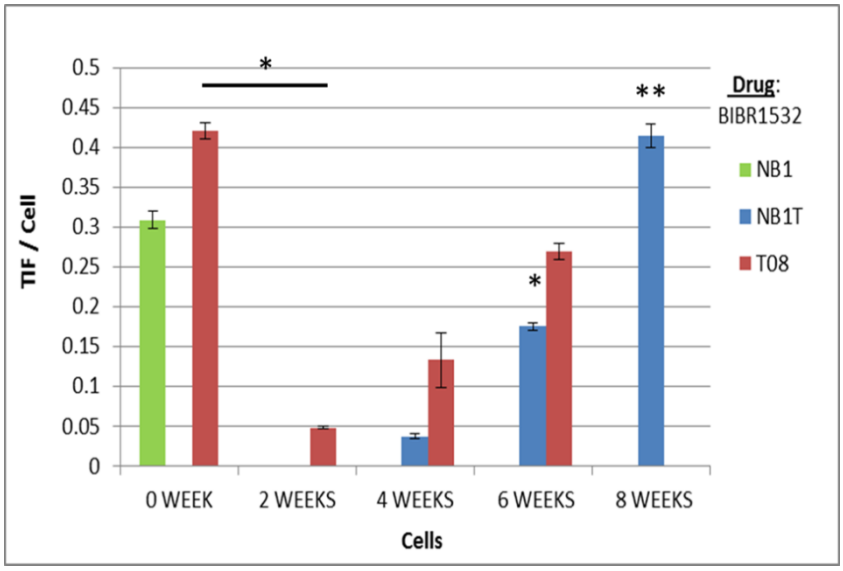

Figure 6.11: The frequency of γ-H2AX foci/cell in NB1, NB1T and T08 cells before and after BIBR1532 treatment. (A) Average number of TIF per cell before and after BIBR1532 treatment. (B) * =P<0.05, ** =P<0.01, *** =P<0.001, Error bars represent SEM.

6.3.4 Ki-67 staining of BIBR1532 treated cells

Ki-67 indirect immunostaining was performed every 2-weeks of drug treated NB1T and T08 cells in order to assess if BIBR1532 drug treatment causes cells to become senescent and leave the proliferaton cell cycle. Representative images of positive and negative Ki-67 staining of BIBR1532 treated NB1T and T08 cells plus NB1 cells in Figure 6.12. Results of our analysis are presented in Figure 6.13-A, B. Proliferation marker of Ki-67 indirect immunostaining findings reveal that percentage of ki-67 staining for 8-weeks treated NB1T and 6-weeks treated T08 cell lines were 74.3 and 48.9 respectively.

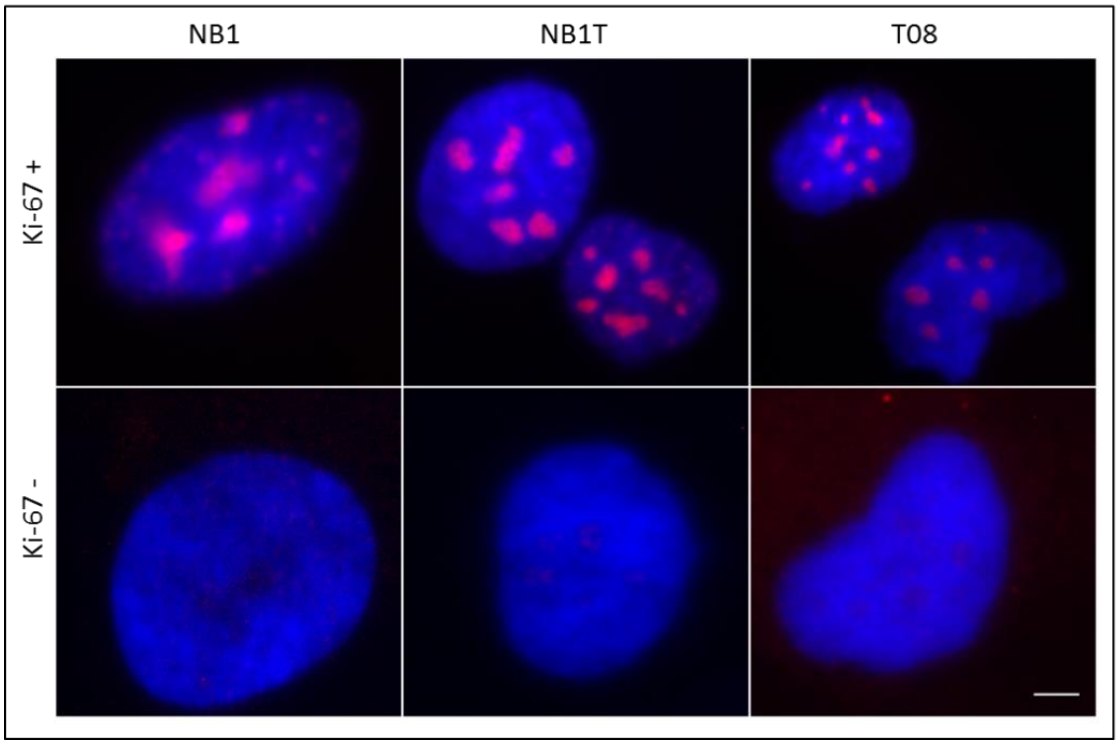

Figure 6.12: Immunodetection of Ki-67 in NB1, untreated NB1T, T08 and BIBR1532 treated NB1T and T08 cells. In order to reveal DNA, DAPI was used. Magnification = X100. Scale bar = 5 µm.

A

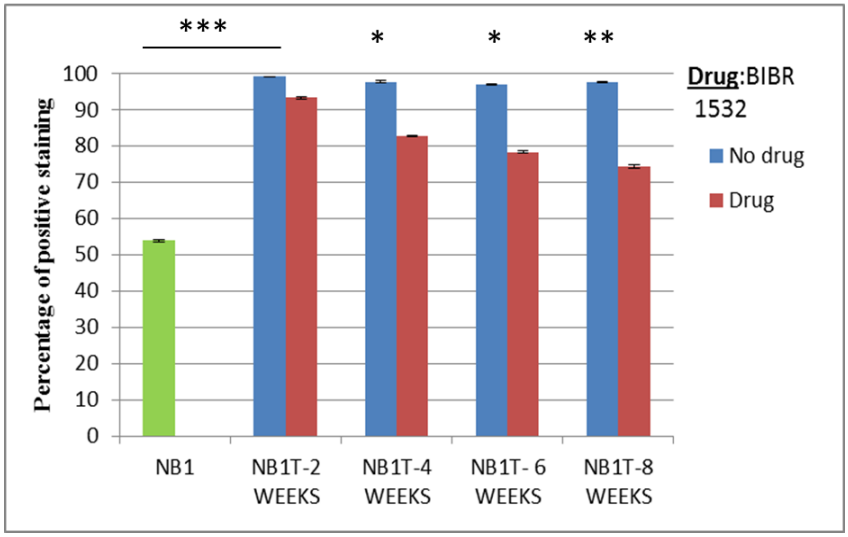

B

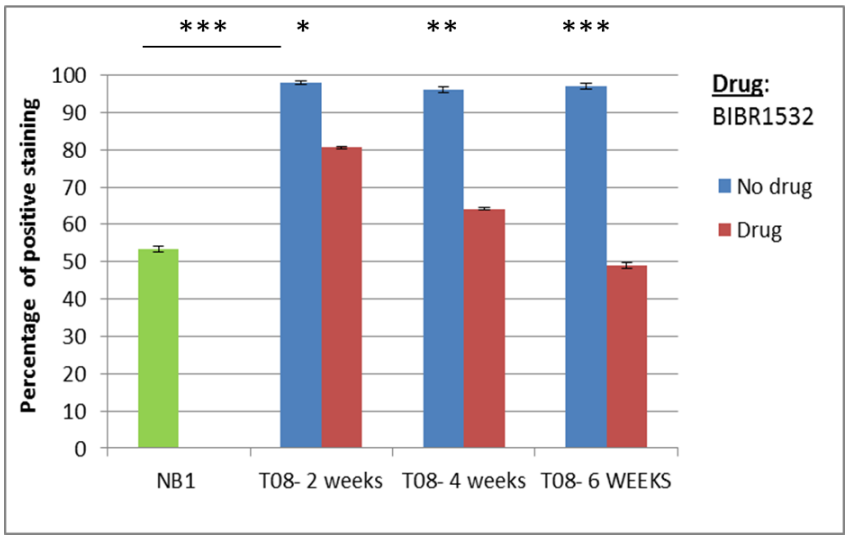

Figure 6.13: NB1, untreated and BIBR1532 treated NB1T (A) and T08 (B) cell lines were fixed with methanol: acetone and stained with pKi-67 antibody every 2-weeks in the culture. The data were obtained from 3 coverslips for each immunostaining of cell line and at least randomly selected 250 nuclei were scored. * =P<0.05, ** =P<0.01, *** =P<0.001, error bars represent SEM.

6.3.5 Telomere positioning of BIBR1532 treated cells

To assess the correlation of reduction of telomere length of BIBR1532 treated cells is positive with telomere positioning, IPLab Spectrum software was used as described in chapter 2. Telomeres were predominantly found in the interior of the nucleus (shell 5) in NB1 and NB1T cells with signal (%)/DAPI (%) ratios of 1.17 ± 0.06(n=45) and 1.24 ± 0.04(n=47) respectively. Upon treatment of NB1Tcells for 8-weeks with BIBR1532, the signal (%)/DAPI (%) ratio for telomeres in shell 1 is increased to 0.89 ± 0.08(n=48), which is significantly greater than NB1 and 2, 4 and 6 weeks BIBR1532 treated NB1T cells ($p<0.001$) (Figure 6.14-A). Telomeres were predominantly found in the interior of the nucleus (shell 5) in T08 cells with signal (%)/DAPI (%) ratio of 1.36 ± 0.04(n=51). Upon treatment of T08 cells for 6-weeks with BIBR1532, the signal (%)/DAPI (%) ratio for telomeres is significantly decreased to 1.02 ± 0.05(n=46, $p<0.001$) in shell 5 (Figure 6.14-B).

A

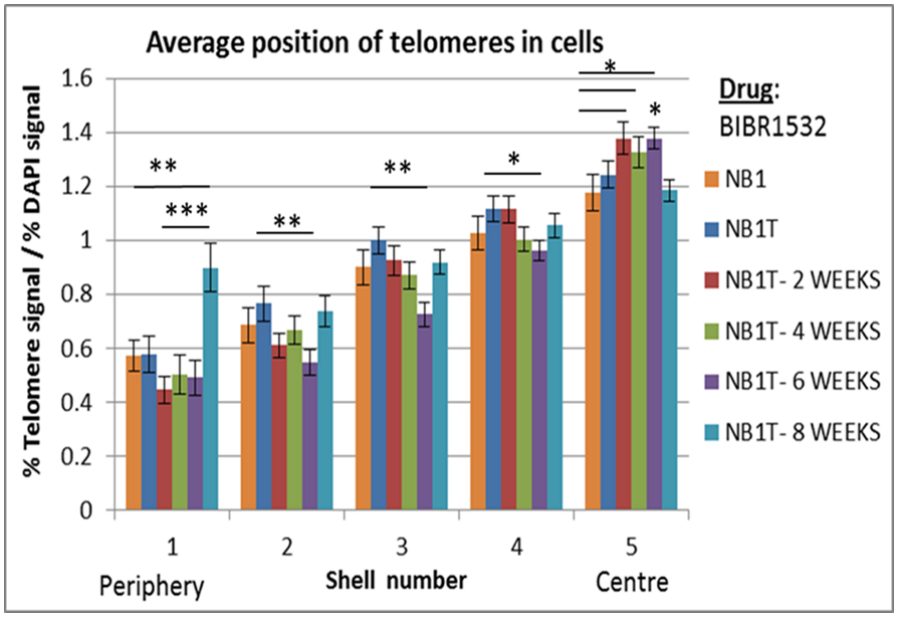

B

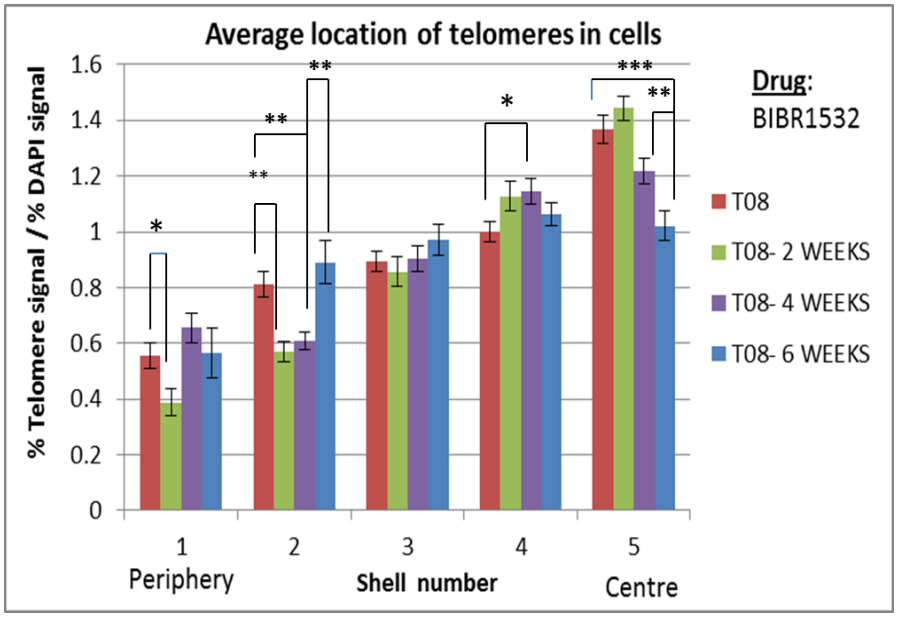

Figure 6.14: Histograms displaying the position of telomeres in NB1, NB1T and T08 before and after drug treatments (A, B). Erosion analyses were performed by ascertaining the distribution of the mean proportion of hybridisation signal of telomeres (%), normalised by the percentage of DAPI signal, over five concentric shells of equal area from the nuclear periphery to centre. The x-axis displays the

shells from 1–5 (left to right), with 1 being the most peripheral shell and 5 being the most internal shell. The y-axis shows signal (%)/ DAPI (%), from 0 to 1.6 with 0.2 increments. The standard error bars representing the standard error of mean (SEM) were plotted for each shell for each graph. Significant differences before and after the drug treatments are denoted by stars (* P ≤ 0.05, ** P ≤ 0.01, *** P ≤ 0.001).

6.3.6 BIB1532 treatment alters chromosome territory positions in NB1T and T08 cells

Chromosome 18 and X positioning in drug treated NB1T cells

2D-FISH was performed on cells derived from human dermal fibroblast cell line; NB1 and immortalised NB1T and T08 cells, using whole chromosome paints for chromosome 18 and X. Only Ki-67 positive cells were analysed when we assessed the chromosome positioning of drug treated cells. Figure 6.15 displays representative images for chromosome 18 and X positioning within fibroblasts with and without BIBR1532 treatments. Chromosome 18 territories were found occupying towards the nuclear periphery in nuclei (shell 2) and (shell 3) in proliferating control NB1 cells with a values of 1.55 ± 0.15 and 1.52 ± 0.08 signal (%) / DAPI (%) (n=51) respectively, which are signicantly greater than the intermediate nucleus (shell 2) and (shell 3) in proliferating control immortalised NB1T cells with a values of 0.29 ± 0.06 and 0.44 ± 0.07 signal (%) / DAPI (%) respectively (n=53, p<0.001)(Figure 6.16-A). Chromosome 18 territories were predominantly found in the interior of the nucleus (shell 5) in untreated NB1T fibroblasts with a value of 1.94 ± 0.15 signals (%)/ DAPI (%) (n=53) which is significantly greater than NB1 cells (0.43 ± 0.08, n=51, p<0.0001) (Figure 6.16-A). Treatment of NB1T cells with BIBR1532 for 6 and 8 weeks resulted in a significant reduction in the signal (%)/ DAPI (%) ratio of chromosome 18 in shell 5 with values of 1.13 ± 0.11, n=49, (p<0.001) and 0.72 ± 0.1, n=50, (p<0.0001) respectively compared to untreated NB1T cells in shell 5 with

a value of 1.94 ± 0.15, n=53 signal (%) / DAPI (%). Furthermore, treatment of NB1T cells with BIBR1532 for 8 weeks resulted in a significant increase in the signal (%)/ DAPI (%) ratio of chromosome 18 in both shell 2 and shell 3 with values of 0.95 ± 0.14, n=50 and 1.23 ± 0. 1, n=50 respectively compared to untreated NB1T cells in both shell 2 and shell 3 with values of 0.29 ± 0.06, n=53 ($p< 0.0001$) and 0.44 ± 0.07 , n=53 ($p<0.0001$) respectively in the signal (%) / DAPI (%) in Figure 6.16-A. Chromosome X territories were found occupying the nuclear periphery of the nucleus (shell 2) in proliferating control NB1 and in immortalised NB1T cells with values of 1.63 ± 0.19(n=50) and 1.52 ± 0.13(n=52) signal (%) / DAPI (%) (n=51) respectively (Figure 6.16-B). Treatment of NB1T cells with BIBR1532 for 8 weeks resulted in significant increase in the signal (%)/ DAPI (%) ratio of chromosome X in shell 1 with a value of 1.34 ± 0.27, (n=52) compared to untreated NB1 cells in shell 1 with a value of 0.71 ± 0.18, n=50 ($p<0.05$) signal (%) / DAPI (%), in Figure 6.16-B. Treatment of NB1T cells with BIBR1532 for 8 weeks resulted in significant decrease in the signal (%)/ DAPI (%) ratio of chromosome X in shell 5 with a value of 0.35 ± 0.08(n=52) compared to untreated NB1T cells in shell 5 with a value of 0.92 ± 0.011, n=50 ($p<0.05$) signal (%) / DAPI (%) in Figure 6.16-B.

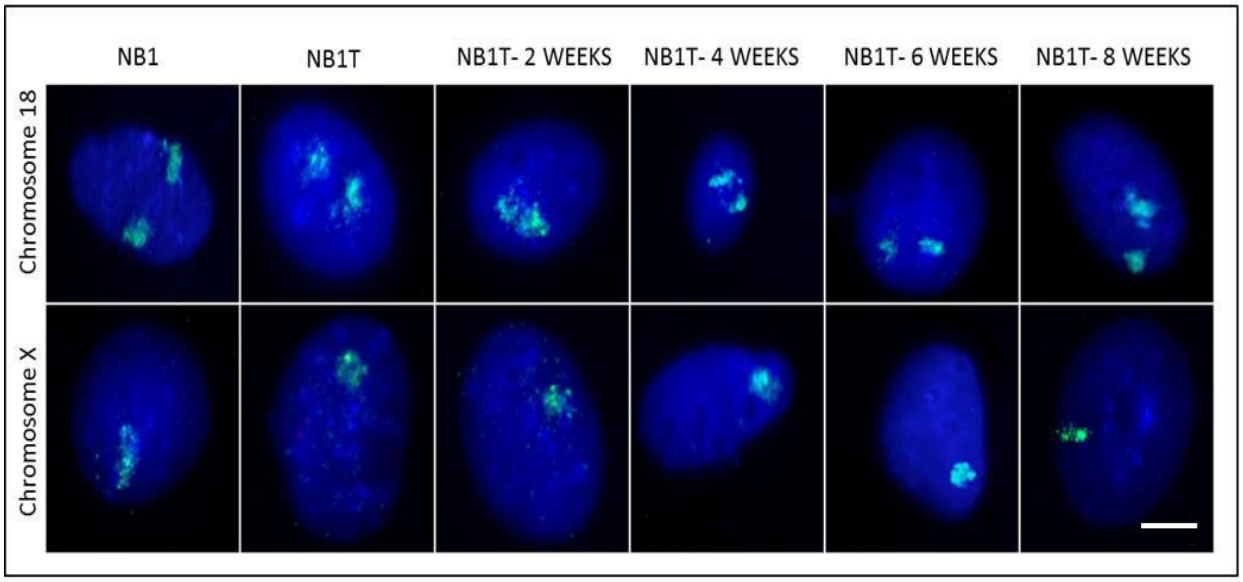

Figure 6.15: Representative images of the position of chromosome 18 and X within NB1 and NB1T fibroblasts nuclei before and after drug treatment. Fibroblasts were subjected to 2D-FISH using probes specific to chromosome 18 and X. Whole chromosome painting probes were labelled with biotin and detected using streptavidin conjugated to FITC (green) and the nuclei were counterstained with DAPI (blue). Ki-67 staining is not shown in the images. Magnification: X100 and scale bar = 5 µm.

A

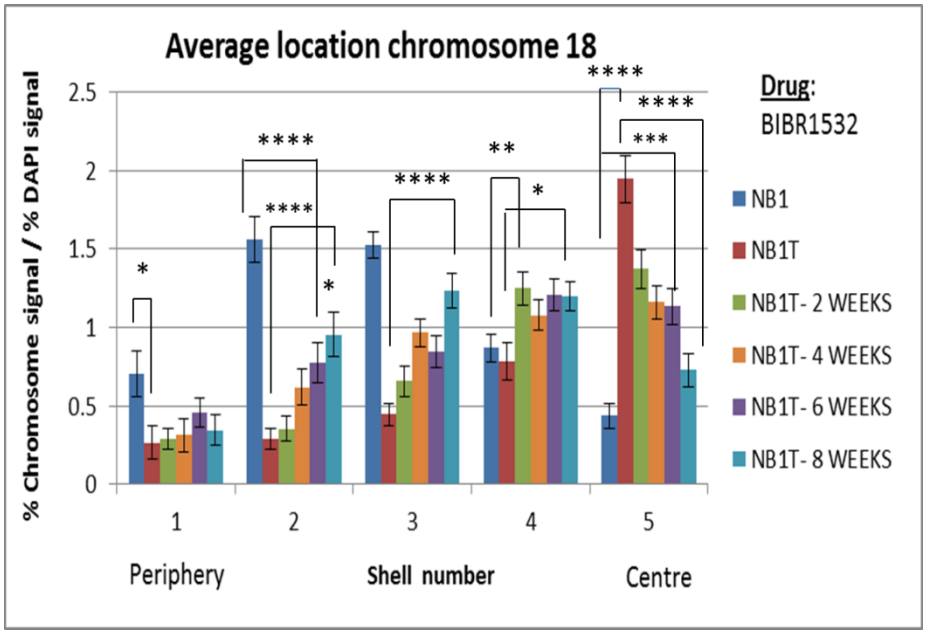

B

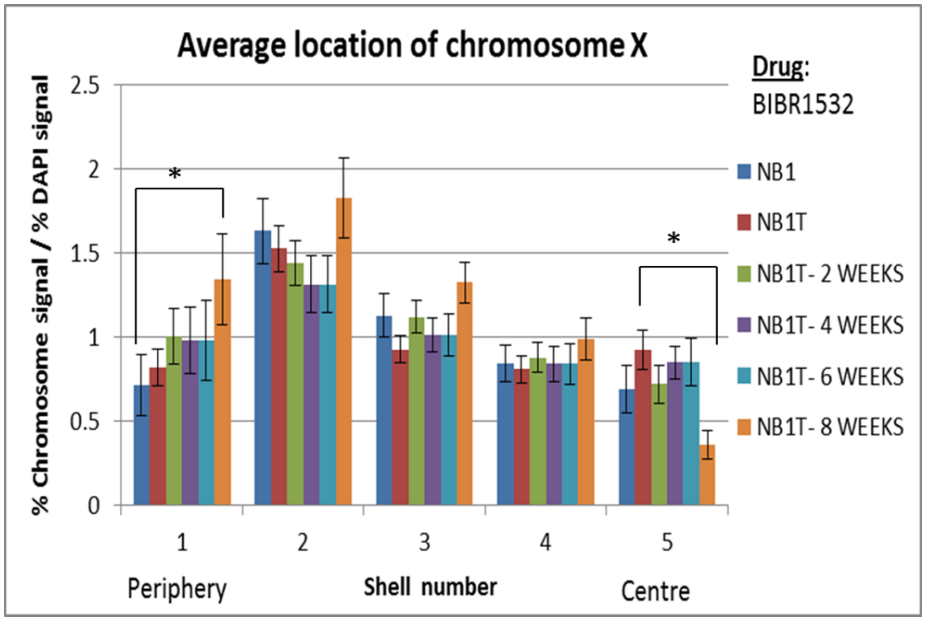

Figure 6.16: Histograms displaying the position of human chromosome 18 (A) and X (B) territories with Ki-67 positive in NB1 and NB1T cells before and after drug treatments. Standard erosion analyses were performed by ascertaining the distribution of the mean proportion of hybridisation signal per chromosome (%), normalised by the percentage of DAPI signal, over five concentric shells of equal area from the nuclear periphery to centre. The x-axis displays the shells from 1–5 (left to right), with 1 being the most peripheral shell and 5 being the most internal shell. The y-axis shows signal (%)/ DAPI (%), from 0 to 2.5 with 2.5 increments.The standard error bars representing the standard error of mean (SEM) were plotted for each shell for each graph(* P ≤ 0.05, ** P ≤ 0.01, *** P ≤ 0.001, **** p ≤ 0.0001).

Chromosome 18 and X positioning in drug treated T08 cells

Figure 6.17 displays representative images for chromosome 18 and X positioning within T08 fibroblasts with and without BIBR1532 treatments. Chromosome 18 territories were predominantly found occupying the nuclear interior of the nucleus (shell 5) in proliferating immortalised T08 cells with a value of 1.59 ± 0.14 signal (%) / DAPI (%), (n=49). Upon treatment with BIBR1532 for 2, 4, 6 weeks, chromosome 18 territories were not significantly different from the untreated T08 cells ($p>0.05$) (Figure 6.18-A). Chromosome X territories were predominantly found occupying the nuclear interior of the nucleus (shell 5) in proliferating immortalised T08 cells with a value of 1.4 ± 0.08 signal (%) / DAPI (%), (n=54) (Figure 6.18-B). Treatment of T08 cells with BIBR1532 for 6 weeks resulted in significant increase in the signal (%)/ DAPI (%) ratio of chromosome X in shell 1 and shell 2 with values of 1.34 ± 0.26 and 1.45 ± 0.17 signal (%) / DAPI (%) respectively, (n=49) compared to the signal (%)/ DAPI (%) ratio of chromosome X in shell 1 and shell 2 with values of 0.4 ± 0.07($p< 0.001$) and 0.7 ± 0.09($p<0.01$) respectively, (n=49) in untreated T08 cells. Furthermore, treatment of T08 cells with BIBR1532 for 6 weeks resulted in significant decrease in the signal (%)/ DAPI (%) ratio of chromosome X in shell 5 with a value of 0.69 ± 0.11 ($p<0.001$) than untreated T08 cells with a value of 1.4 ± 0.08 signal (%) / DAPI (%), ($p<0.001$,n=54) (Figure 6.18-B). Taken together, these data suggest that BIBR1532 treatment can restore the position of chromosome X towards the nuclear periphery within the NB1T and T08 nucleus. Furthermore, although BIBR1532 treatment can restore the position of chromosome 18 towards the nuclear periphery in NB1T cells, treatment did not alter the position of chromosome 18 in T08 cells.

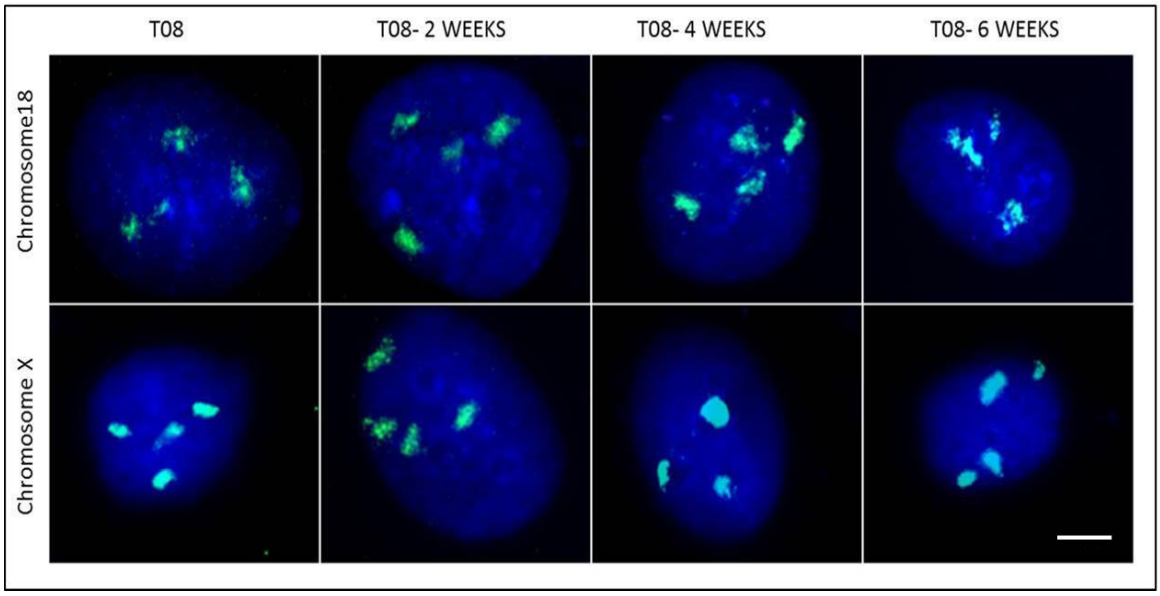

Figure 6.17: Representative images of the position of chromosome 18 and X within T08 fibroblasts nuclei before and after drug treatment. Fibroblasts were subjected to 2D-FISH using probes specific to chromosome 18 and X. Whole chromosome painting probes were labelled with biotin and detected using streptavidin conjugated to FITC (green) and the nuclei were counterstained with DAPI (blue). Ki-67 staining is not shown in the images. Magnification: X100 and scale bar = 5 µm.

A

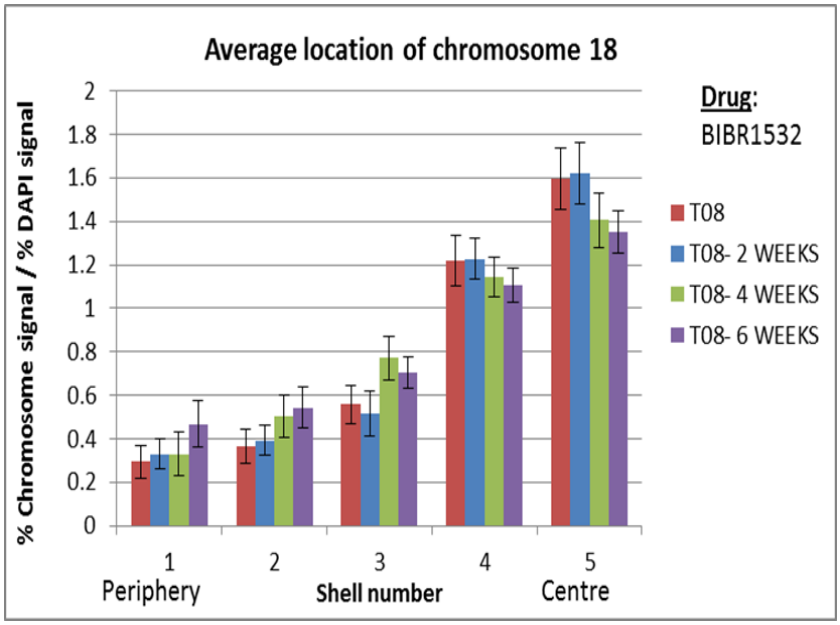

B

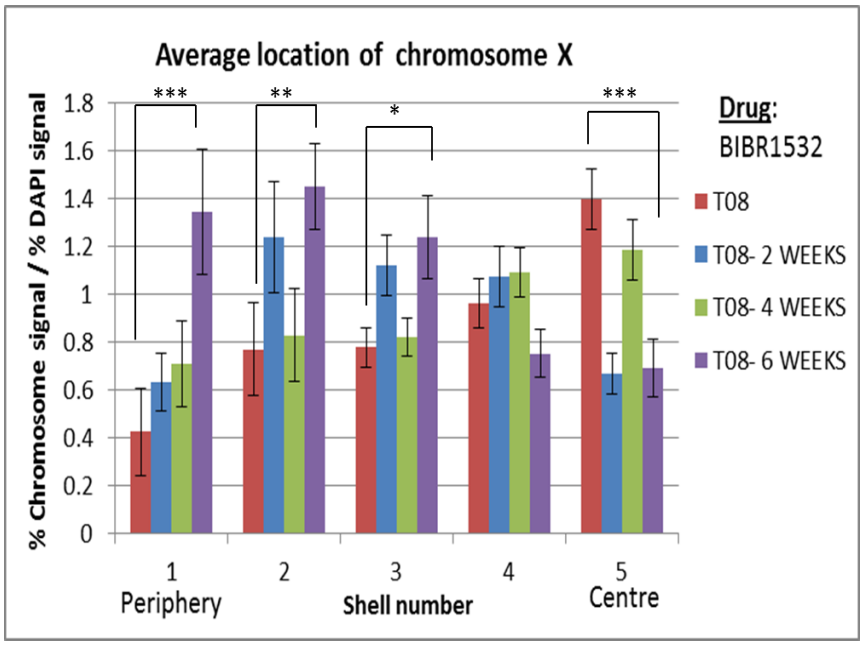

Figure 6.18: Histograms displaying the position of human chromosome 18 (A) and X (B) territories with Ki-67 positive in T08 cells before and after drug treatments. Standard erosion analyses were performed by ascertaining the distribution of the mean proportion of hybridisation signal per chromosome (%), normalised by the percentage of DAPI signal, over five concentric shells of equal area from the nuclear periphery to centre. The x-axis displays the shells from 1–5 (left to right), with 1

being the most peripheral shell and 5 being the most internal shell. The y-axis shows signal (%)/ DAPI (%), from 0 to 2 with 0.2 increments.The standard error bars representing the standard error of mean (SEM) were plotted for each shell for each graph (* P ≤ 0.05, ** P ≤ 0.01, *** P ≤ 0.00).

6.4 Discussion

Results presented in this chapter indicate that telomerase-mediated immortalised dermal fibroblasts (NB1T and TO8) have longer telomeres relative to appropriate control cell line (NB1) in Figure 6.13 and it was shown in chapter 5 that T08 immortalised cells have different chromosome positioning compared to NB1T control cells. Given that the purpose of this study was to target the telomerase/telomere complex by employing the novel synthetic nom-peptidic small molecule BIBR1532 in order to progressively shorten telomere length and in addition to that concomitantly 2D-FISH was employed to determine the impact of the treatment in positioning of chromosomes and telomeres. BIBR1532 has been employed as anti-cancer thereapeutics since it was shown that treatment of cancer cells with this drug leads to progressive telomere shortening and consecutively growth senescence after a lag period (Bashash *et al*., 2013; El-Daly *et al*., 2005). Cell logarithmic growth of the cells was assessed every 24 h, incubated in the presence of different concentrations of BIBR1532. I showed a direct short-term cytotoxic effect of BIBR1532 on cells as the viability index of treated cells lessened in a dose-dependent manner in Figure 6.2. In line with Bashash *et al*. (2013) findings, I demonstrated that culture of cells maintained for 6 days in the presence of BIBR1532 is resistant to drug at a concentration of 10 µM. Furthermore, Parsch *et al*., (2008) showed that long-term treatment of the telomerase positive chondrosarcoma cell line with BIBR1532 at a concentration of 10 µM caused reduction of growth beginning at passage 8 (Parsch

et al., 2008). However, Ruden and Puri, (2013) have showed that BIBR1532 treatment of germ cell tumours did not entirely inhibit tumour cell proliferation. IQ-FISH method demonstrated that in contrast to untreated NB1T and T08 cells, treatment of NB1T and T08 cells with 10 μM BIBR1532 for 8 and 6 weeks respectively gave rise to significant decrease of telomere length (Figure 6.13). El-Daly *et al*., (2005) exhibited by performing Q-FISH method based on telomere length measurement of metaphase chromosomes that BIBR1532 treatment leads to telomere shortening. In late passage of cancer cells, induction of senescence associated β-galactosidase was revealed (Damm *et al.*, 2001). The small synthetic molecule telomererase inhibitor BIBR1532 is capable of shortening telomere length of immortalised cells to the level of normal NB1 fibroblasts and immortalised cell lines were capable of proliferating after drug treatment. Nevertheless, a fraction of cells became senescent due to BIBR1532 drug treatment. It was suggested in previous work that a related feature of BIBR1532-treated cancer cells may be up-regulation of $p21^{Waf1}$, a cyclin-dependent kinase inhibitor whose induction induces growth arrest associated with senescence (Chang *et al*., 2000).

Telomere uncapping is completed through inactivation of the duplex TTAGGG repeat binding factor TRF2, which is important for telomere protection and loss of TRF2 function can give rise to increased activity of the DNA-damage response pathway and cell cycle arrest (Wood *et al*., 2014 ; Takai *et al*., 2003). If uncapped telomeres resemble damaged DNA, they might become associated with DNA damage response (DDR) factors such as H2AX and 53PB1 (Paull *et al.*, 2000; Schultz *et al.*, 2000). TIFs (Telomere Dysfunction-induced foci) are defined as foci of DNA damage response factors that coincide with telomeric PNA signals. In IR-induced cells, most of the TIF-positive cells were shown containing more than four 53BP1 foci at

telomeres (mean 12.6). Whereas, the fraction of TIF-positive cells were shown to be negligible in control cultures (Takai *et al*., 2003). The frequencies of total DNA damage positive foci in control (NB1) and drug treated immortalised cells (NB1T and T08) were examined by the γ-H2AX assay. The treatment of NB1T cells with BIBR1532 for 8-weeks significantly increased the frequency of γ-H2AX foci/cell. Furthermore, treatment of T08 cells with BIBR1532 for 6-weeks shows that the frequency of γ-H2AX foci/cell was not significantly different than in untreated T08 cells. My examination of DNA damage kinetics suggested that damage at telomeres, in forms of TIFs, significantly higher in 8-weeks BIBR1532 drug treated NB1T cells, whereas, the number of TIF/cell in T08 cells after 8-weeks of drug treatment was not significanlty changed. It is important to note that the frequency of γ-H2AX foci/cell and TIFs in both NB1T and T08 cells after 8-weeks and 6-weeks of BIBR1532 drug treatment respectively were not significantly different relative to NB1 cells (Figure 6.11). In line with my findings, in wild-type fibroblasts expressing progerin, damage of telomeres and proliferative inhibition was reversed by hTERT telomerase activation (Kudlow *et al., 2008*). In HGPS, it was presented that the levels of DDR is increased and damage at telomeres are elevated (Benson *et al.,* 2010). Furthermore, accumulation of TIFs in progerin-expressing cells was shown inducing senescence (Benson *et a*l., 2010). In normal fibroblasts, ectopic expression of progerin was shown to give rise to elevated damage signalling at telomeres (Benson et al., 2010). The increase of γ-H2AX coupled with telomeres in senescencing mesenchymal cells led accumulation of telomeres with intranuclear lamin structures (Raz *et al*., 2008). Taken together, BIBR1532 treatment of cells did not give rise to high DNA damage response in our experiment.

The radial positions of two representative chromosomes in interphase nuclei of control (NB1) and untreated and BIBR1532 treated immortalised NB1T and T08 proliferating cells was determined by 2D - FISH. These chromosomes were; 18 and X. It is worthwhile to note that only positive Ki-67 staining cells were used for the analysis of chromosome positioning. Meaning that senescent cells where the chromosome positioning would be altered were not included. It may be that cells on their way to be Ki67 negative and senescent might be included but the numbers would be small and should not influence the overall picture of chromosome location. Chromosome 18 territories were predominantly found occupying nuclear periphery and nuclear interior of the nucleus in proliferating NB1 and NB1T cells respectively. Treatment of NB1T cells for 6 and 8-weeks induced a repositioning of chromosome 18 moving towards the periphery of the nucleus. Chromosome X territories were found more towards the nuclear periphery of nuclei in both proliferating control NB1 and NB1T cells. However, after treatment of NB1T cell with 8-weeks there was a significant shift more towards the nuclear periphery (Figure 6.16). Chromosome 18 territories were predominantly found occupying the nuclear interior of the nucleus in proliferating T08 cells. Intriguingly, treatment of T08 cells did not cause significant alteration of chromosome 18 territories. Chromosome X territories were predominantly found occupying the nuclear interior of the nucleus in proliferating T08 cells. However, treatment of T08 cells with BIBR1532 for 6 weeks resulted in chromosome X moving towards periphery of the nucleus (Figure 6.18).

Subsequently, the influence of drug treatment in telomere positioning in NB1T and T08 cells was determined by employing 2D approach. Telomeres were predominantly found in the interior of the nucleus in NB1, NB1T and T08 cells. Treatment of NB1T and T08 cells with BIBR1532 for 8-weeks and 6-weeks

respectively resulted in telomeres moving towards periphery of the nucleus (Figure 6.14). In *Lmna* $^{-/-}$ mice, due to deficient lamin A telomeres positioning is altered towards the nuclear periphery (Gonzalo-Suaraz, Redwood and Gonzalo, 2009).

6.5 Conclusion

A promising synthetic non-peptidic small molecule BIBR1532 was employed to target telomerase of hTERT NB1T and T08 cells. This study provides evidence by performing drug treatment that shortening of the telomeres was achieved with minimal cytotoxicity and without causing high DDR and more importantly, without inducing high replicative senescence. Furthermore, shortening of telomeres led to restoration of chromosome territories for both cells. Overall, results presented here reveal that BIBR1532 drug treatment gave rise to telomeres to disperse throughout the nuclei in control and diseased cells. There are several proteins involved for the attachment of telomeres to the nuclear membrane and the nucleolus. Future work is required to investigate the mechanism of how shortening of telomere length can induce different chromosome and telomere positioning in hTERT immortalised cells.

Chapter 7: General discussion

This thesis addresses the elucidication of nuclear organisation and interphase chromosome positioning in normal and immortalised typical and atypical HGPS and control fibroblasts before and after treatment with specific drugs. While extensive studies looking at the effects of drug treatments on nuclear shape in HGPS have been performed, studies looking specifically at the distribution of chromosome territories within nuclei following this variety of drug treatments have not been previously studied. To address these issues, 2D- FISH was performed on cells derived from HGPS primary human dermal fibroblast cell line- AG01972, using whole chromosome paints for chromosome 18 and X. (Chapter 2). Furthermore, it was hypothesised that the association of telomeres with the nuclear matrix is disrupted in Hutchinson-Gilford Progeria Syndrome and to address this issue, DNA halo preparations were performed on cells derived from human dermal fibroblat cell line- 2DD (Bridger, 2003) and on HGPS AG01972 fibroblast cell line. The data from this study shows that HGPS fibrobasts treated with pravastatin, zoledronic acid, rapamycin, insulin-like growth factor 1, N-acetyl-L-cysteine resulted in relocation of chromosome 18 from nuclear interior to an intermediate location in Ki-67 positive interphase nuclei. Furthermore, it was shown that FTI-277 (and combinations) leads to more peripheral position of chromosome 18 in the interphase nuclei (Figure 2.4). The data from this study shows that HGPS fibroblasts treated with with FTI alone, chromosome X moved more towards the nuclear periphery within Ki-67 positive interphase nuclei. Furthermore, using combinations of drugs; FTI-277 + pravastatin + zoledronic acid and FTI-277 together with GGTI-2133 resulted in relocation of chromosome X even more towards periphery. Intriguingly, chromosome X was not repositioned after rapamycin treatment alone. Additionally, we revealed that that there is a strong link between the nuclear matrix and disease pathology as after visualisation of telomere-Nuclear matrix tethering in *LMNA* mutated HGPS, telomere anchorage is perturbed. Treatment of AG01972 cell line with FTI-277, pravastatin,

zoledronic acid, N-acetyl-L-cysteine and all three combination treatments; FG, PZ, FPZ was shown having a positive effect on anchoring the genome to the nuclear matrix (Table 2.1) (Chapter 2), suggesting that toxic progerin disturbs the NM and the genome binding to it.

HGPS cells become senescent more rapidly than normal fibroblast cells (Bridger and Kill, 2004). Therefore, in order to overcome this obstacle, we used normal and HGPS human fibroblast cell lines infected with a defective retrovirus encoding human telomerase reverse transcriptase to extend the life span of the cells (Wallis et al., 2004). hTERT normal and diseased T06 and T08 cells were characterised in terms of cell growth, percentage of fraction of proliferating cells, nuclear shape, and cell movement and furthermore lamin A/C, vimentin and progerin proteins were assessed (Chapter 3). In hTERT skin fibroblast cell growth experiment, increasing number of population doublings were observed for immortalised NB1T and T08 cells lines. We demonstrated that although numbers of population doublings of typical progeria cell (T06) were lower compared to NB1T and T08, T06 cell line has not become senescent over 5 months of on-going cell culture.

In proliferating cells, the Ki-67 antigen (pKi-67) is detected in all phases of the cell division cycle (Kill, 1996). Based on our results from proliferation marking of cells, it can be revealed that the vast majority of the immortalised cells were proliferating. It has been suggested that active DNA synthesis occurs at the sites of PCNA localisation (Zuber *et al*., 1989). We showed by PCNA indirect immunostaining that all our immortalised cells have dispersed pattern with sites distributed throughout the nucleus and there was no pattern of a few foci in cells. Even though, alterations in the nuclear organisation of DNA replication occur due to immortalisation (Kennedy *et al.*, 2000). HGPS cells are known having the abnormal nuclear shape as blebbing also herniations and invaginations (Cao *et al.*, 2011a). Furthermore, HGPS nuclei are characterized by

multiple small blebs due to accumulation of truncated lamin A protein on the nuclear membrane, which caused the nuclei to be smaller and rounder (Bridger and Kill, 2004). From the nuclear shape analysis of circularity, we revealed that T08 nuclei were rounder than T06 and the control group (NB1T). It was shown that HGPS cells having common 1824 C → T LA mutation had misshapen or lobulated nuclei, furthermore there was also an apparent increase in thickness and prominence of the lamina parallel with nuclear shape changes (Goldman *et al.*, 2004). Our data presented in this study indicate that in our control cell line, lamin A and lamin A/C staining appeared as nuclear rim and there were few misshapen nuclei as well. Using an antibody specific for progerin, we revealed vast majority of NB1T and T08 cells exhibited no progerin staining however T06 cells was found exhibiting a higher proportion of positive staining with a few speckles and small foci. Our western blotting findings revealed that lamin A and C proteins were expressed in all cell lines. Previously, it was shown that progerin mRNA was supressed due to the forced elongation of telomeres in human immortalised cells (Cao *et al*., 2001) (Chapter 3). We confirmed by RT-PCR that both lamin A and progerin transcripts are present in T06 progeria cells. Furthermore, serum responsive results revealed low serum treatment of cells gives rise to reduced Ki-67 positive proliferation marker (Chapter 3).

Nuclear lamin protein network and lamin-associated proteins have a crucial role maintaining correct nuclear functions and genome organisation. The presence and distribution of nuclear envelope proteins within the immortalised HGPS cell lines were explored (Chapter 4). It was shown that there is an issue with LB1 and LBR associating with the nuclear envelope in T06 and T08 cell lines respectively. Furthermore, it was found that LINC complex protein of SUN1 is absent at the nuclear membrane of both T06 and T08 cells and HP1α is affected in HGPS atypical T08 cells.

A drug named Lovastatin is known to prevent the prenylation, as a post-translational modification process of proteins; through the melovonate pathway similar to pravastatin, zoledronic acid and biphosphonates (Chapter 4). Given that the effects of drug to restore the disrupted localization of a number of proteins in HGPS fibroblasts was assessed. It is found that drug treatment led to a loss of LBR on nuclear membrane in both NB1T and T08 cells. Further, treatment of T06 cells exhibited no alteration of LB1 immunostaining. Before and after the treatment, Lamin B1 was found as foci in the nucleoplasm in T06 cells. However, the expression and distribution of HP1α was increased and improved after the drug treatment in T08 cells. Lovastatin treatment revealed an accumulation of prelamin A at the nuclear rim in both immortalised normal (NB1T) and atypical HGPS (T08) fibroblasts. If 2 days lovastatin drug treatment were arresting proliferation of cells was investigated by performing Ki-67 immunostaining and it was revealed that almost 70% of cells were proliferating (Chapter 4). It was demonstrated using low levels of lovastatin in SV40-transformed human skin fibroblasts for 3 days that lovastatin treatment did not have noticeable effect on lamin B1 farnesylation and did not cause donut-shaped nuclei, whereas high levels of lovastatin gave rise to inhibition of lamin B1 farnesylation (Verstraeten *et al.,* 2011). Although indirect immunostaining findings revealed that Lamin B2 protein is almost the same in all analysed cells, WHS data obtained in collaboration with UCL demonstrated that *LMNB2* gene is one of the genes with predicted deleterious varients in AG08466 (parental cells for T08s) cells. Furthermore, it was revealed that AG08466 cells are devoid of promoter on *LMNB2* gene and transcription is regulated by BRCA1. In S phase in MCF7 cells, it was shown that Rad51 localizing in the same nuclear foci with BRCA1, indicating that BRCA1 is involved in DSBR and and in response to DNA damage (Scully *et al.*, 1997). It was demonstrated that level of *c-Myc* expression was elevated in atypical AG08466 HGPS cells (Nakamura *et al.,* 1988).

C-Myc protein is a multifunctional protein that plays a role in apoptosis and cell progression, suggesting that due to *LMNB2* gene has a variant in its promoter in AG08466 cells level of *c-Myc* expression was elevated. Bridger *et al*., (2004) showed that AG08466 cells exhibits increased rate of apoptosis in cultures.

In chapter 5, alteration of epigenetic histone marks, nucleolar proteins were investigated. Furthermore, the position of chromosomes 10, 13, 18 and X and also centromeres, telomeres in cells were determined. We revealed that NB1T cells behave strangely with respect to chromosome position as well as T08 cells. Remarkably, 2D-FISH chromosome positioning analysis of T08 cells demonstrated that first time in our laboratory chromosome X is located in the nuclear interior. Given that we decided to perform colocalisation analysis of fibrillarin and chromosomes in order to investigate whether chromosome X had a having higher colocalisation with nucleoli. Chromosome X was found colocalising with fibrillarin nucleolar protein in higher proportion in T08 cells. In proliferating HGPS cells it was observed that gene-poor chromosomes 13 and 18 alter their location from nuclear periphery to the nuclear interior (Meaburn *et al.,* 2007). Furthermore, a large part of chromosome 19 was shown to associate with the central regions of the nucleus, being associated the nucleolus (Croft *et al*., 1999). I showed that the structure of histone marks are severely affected in atypical HGPS T08 cells (Chapter 5). Deletion of individual H1 subtypes in mice ESCs resulted in increased repressive H3K27me3 mark at specific Hox genes however the global level of this protein was reduced suggesting that distinct posttranslational modification and/or transcription factors tethering to H1 and thus modulating the effects of H1 on gene silencing (Fan *et al.*, 2005). Enrichment of H3K9me3 and H3K27me3 modifications was shown at 4q subtelomeric *D4Z4* repeats and at telomeres (Arnoult *et al.*, , 2012; Zeng *et al.*, 2009). Moreover, enrichment of tri-methylation of H3K9 and H3K27 was revealed at the *FXN*locus of Friedreich ataxia-derived cells (De Biase *et al.*, 2009). Assessment of

histone posttranslational modifications using a quantitative mass spectrometry performed on mononucleosomes bound by the chromo domain (CD)-containing heterochromatin protein 1 (HP1) revealed associated enrichment of H3K9me3 and H3K27me3 (LeRoy *et al.*, 2012) (Chapter 5).

Centromeres and telomeres positioning of my results revealed that they are both positioned internally in all cells. The centromeres were demonstrated to compact in neoplastic breast tissue, conferring the repositioning of the centromere to a more internal location (Wiesc *et al*., 2005). In support of our genomic instability findings obtained from metaphase chromosome analyses in T08 cells, our M-FISH results with collaboration with Dr. Anderson (Brunel University, London) revealed that T08 fibroblast cell line has aneuoploidy. M-FISH karyotyping of hTERT T06 fibroblast was shown having a karyotype of 46,XY[25]/47,XY,+7[16]/48,XY,+7,+11[3]/46,XY,t(15p;16?q)[1]/ 47,XY,+7,t(15p;16?q)[1]. (Square brackets denote number of cells abnormality was observed in)(Anderson and Bridger, Brunel University, London) (Chapter 5), indicating that T08 cells have different behaviour than T06 cells as showing aneuploidy. Assessment of nucleolar proteins revealed that both nucleophosmin and RNA pol I exhibited distinct patterns in hTERT T06 and T08 cells than NB1 and hTERT NB1T cells. Moreover, fibrillarin pattern analysis revealed that NB1 cells have dull staining than other cells (Chapter 5). Colocalisation analysis of HP1α- centromere exhibited that Mander's overlap coefficient number representing colocalisation is less in HGPS fibroblasts than control cells.

As we are all ageing, to understand the mechanism of ageing and what factors that are involved in the longevity of a person's life has become an active area of research. It is well known that external factors contribute to these changes. However, internal factors should also be considered for in depth exploration of complex process of ageing and it can be found out by examining an indivual cell to reveal the relation with ageing at the

subcellular level, for examples alteration occurred in telomere length (Kirkwood, 2015; Kirkwood and Austad, 2000) (Chapter 6). In human cells and all other vertebrates studied, TTAGGG was identified as the telomere repeat (O'Sullivan and Karlseder, 2010). It is known that both the length of telomeres and the sequence vary between species (Moyzis *et al.*, 1988). In chapter 6, it was aimed to shorten telomeres by utilising the novel synthetic non-peptidic small molecule named BIBR1532 to see if location of chromosomes 18 and X can be restored in NB1T and T08 cells. Ki-67 proliferation marker results exhibited that although a fraction of both NB1T and T08 cells were observed to become senescent, cells were proliferating after drug treatment. Previous work showed a time-dependent reduction of telomere lenth in cancer cells with 10 µM BIBR1532 for 15 passages by quantitative PCR (Parsch *et al.*, 2008). Surprisingly, drug treatment was observed not causing DNA damage response in our experiments. Determination of positioning of telomeres after drug treatment showed that telomeres moving towards periphery of the nucleus in both NB1T and T08 cells.

In treatment of several cancer lines it was demonstrated that BIBR1532 can repress telomerase activity and cause tumour cell growth arrest without triggering acute cytotoxicity (Parsch *et al*., 2008). Remarkably, data revealed telomeres lengths for NB1T and T08 cells got shorten gradually every 2- weeks after the drug treatment and also BIBR1532 treatment helped for the restoration of position of chromosome 18 and X in NB1T cells and chromosome X in T08 cells, indicating that telomeres are totally responsible for misposition of chromosomes. Furthermore, chromosomes 18 and X need different situations to be tethered at the periphery as BIBR1532 was not able to restore the position of chromosome 18 in T08 cells, indicating that one or more proteins are missing in T08 cells.

References

Aaronson, R.P. and Blobel, G. (1974) 'On the attachment of the nuclear pore complex', *The Journal of cell biology,* 62(3), pp. 746-754.

Acosta, J.C., O'Loghlen, A., Banito, A., Guijarro, M.V., Augert, A., Raguz, S., Fumagalli, M., Da Costa, M., Brown, C., Popov, N., Takatsu, Y., Melamed, J., d'Adda di Fagagna, F., Bernard, D., Hernando, E., Gil, J. (2008) Chemokine signaling via the CXCR2 receptor reinforces senescence. *Cell* 133(6), pp. 1006–1018

Adam, S.A., Butin-Israeli V - Cleland, Megan,M., Cleland MM, Shimi T - Goldman, Robert,D. and Goldman, R.D. (2013) 'Disruption of lamin B1 and lamin B2 processing and localization by farnesyltransferase inhibitors', *Nucleus (Austin, Tex.),* 4(2), pp. 1-9.

Adam, S.A. and Goldman, R.D. (2012) 'Insights into the differences between the A- and B-type nuclear lamins', *Advances in Biological Regulation,* 52(1), pp. 108-113.

Alcobia, I., Dilao, R. and Parreira, L. (2000) 'Spatial associations of centromeres in the nuclei of hematopoietic cells: evidence for cell-type-specific organizational patterns', *Blood,* 95(5), pp. 1608-1615.

Al-Haboubi, T., Shumaker, D.K., Köser, J., Wehnert, M. and Fahrenkrog, B. (2011) 'Distinct association of the nuclear pore protein Nup153 with A-and B-type lamins', *Nucleus,* 2(5), pp. 500-509.

Allsopp, R.C., Vaziri, H., Patterson, C., Goldstein, S., Younglai, E.V., Futcher, A.B., Greider, C.W. and Harley, C.B. (1992) 'Telomere length predicts replicative capacity of human fibroblasts', *Proceedings of the National Academy of Sciences of the United States of America,* 89(21), pp. 10114-10118.

Al-Saaidi, R. and Bross, P. (2015) 'Do lamin A and lamin C have unique roles?', *Chromosoma,* 124(1), pp. 1-12.

Alsheimer, M. and Benavente, R. (1996) 'Change of Karyoskeleton during Mammalian Spermatogenesis: Expression Pattern of Nuclear Lamin C2 and Its Regulation', *Experimental cell research,* 228(2), pp. 181-188.

Amin, M., Matsunaga, S., Uchiyama, S. and Fukui, K. (2008) 'Depletion of nucleophosmin leads to distortion of nucleolar and nuclear structures in HeLa cells', *Biochem.J,* 415, pp. 345-351.

Anachkova, B., Djeliova, V. and Russev, G. (2005) 'Nuclear matrix support of DNA replication', *Journal of cellular biochemistry,* 96(5), pp. 951-961.

Andrulis, E.D., Neiman, A.M., Zappulla, D.C. and Sternglanz, R. (1998) 'Perinuclear localization of chromatin facilitates transcriptional silencing', *Nature,* 394(6693), pp. 592-595.

Aris, J.P. and Blobel, G. (1991) 'cDNA cloning and sequencing of human fibrillarin, a conserved nucleolar protein recognized by autoimmune antisera', *Proceedings of*

the National Academy of Sciences of the United States of America, 88(3), pp. 931-935.

Arnoult, N., Van Beneden, A. and Decottignies, A. (2012) 'Telomere length regulates TERRA levels through increased trimethylation of telomeric H3K9 and HP1α', *Nature structural & molecular biology,* 19(9), pp. 948-956.

Asencio, C., Davidson, I.F., Santarella-Mellwig, R., Ly-Hartig, T.B.N., Mall, M., Wallenfang, M.R., Mattaj, I.W. and Gorjánácz, M. (2012) 'Coordination of kinase and phosphatase activities by Lem4 enables nuclear envelope reassembly during mitosis', *Cell,* 150(1), pp. 122-135.

Aubert, G. and Lansdorp, P.M. (2008) 'Telomeres and aging', *Physiological Reviews,* 88(2), pp. 557-579.

Autexier, C. and Lue, N.F. (2006) 'The structure and function of telomerase reverse transcriptase', *Annu.Rev.Biochem.,* 75, pp. 493-517.

Bannister, A.J., Zegerman, P., Partridge, J.F., Miska, E.A., Thomas, J.O., Allshire, R.C. and Kouzarides, T. (2001) 'Selective recognition of methylated lysine 9 on histone H3 by the HP1 chromo domain', *Nature,* 410(6824), pp. 120-124.

Barboro, P., D'Arrigo, C., Diaspro, A., Mormino, M., Alberti, I., Parodi, S., Patrone, E. and Balbi, C. (2002) 'Unraveling the organization of the internal nuclear matrix: RNA-dependent anchoring of NuMA to a lamin scaffold', *Experimental cell research,* 279(2), pp. 202-218.

Barrowman, J., Hamblet, C., George, C.M. and Michaelis, S. (2008) 'Analysis of prelamin A biogenesis reveals the nucleus to be a CaaX processing compartment', *Mol Biol Cell,* 19(12), pp. 5398-5408.

Bashash, D., FAU, G.S., Mirzaee, R.F., Alimoghaddam, K.F. and Ghavamzadeh, A. (2013) 'Telomerase inhibition by non-nucleosidic compound BIBR1532 causes rapid cell death in pre-B acute lymphoblastic leukemia cells', *Leukemia & lymphoma,* 54(3), pp. 561-568.

Basso, A.D., Kirschmeier, P. and Bishop, W.R. (2006) 'Lipid posttranslational modifications. Farnesyl transferase inhibitors', *Journal of lipid research,* 47(1), pp. 15-31.

Baur, J.A., Zou, Y., Shay, J.W. and Wright, W.E. (2001) 'Telomere position effect in human cells', *Science (New York, N.Y.),* 292(5524), pp. 2075-2077.

Beck, L.A., Hosick, T.J. and Sinensky, M. (1990) 'Isoprenylation is required for the processing of the lamin A precursor', *J Cell Biol.,* 110(5), pp. 1489-1499.

Beck, M., Förster, F., Ecke, M., Plitzko, J.M., Melchior, F., Gerisch, G., Baumeister, W. and Medalia, O. (2004) 'Nuclear pore complex structure and dynamics revealed by cryoelectron tomography', *Science,* 306(5700), pp. 1387-1390.

Ben-Harush, K., Wiesel, N., Frenkiel-Krispin, D., Moeller, D., Soreq, E., Aebi, U., Herrmann, H., Gruenbaum, Y. and Medalia, O. (2009) 'The Supramolecular

Organization of the C. elegans Nuclear Lamin Filament', *Journal of Molecular Biology,* 386(5), pp. 1392-1402.

Benson, E.K., Lee, S.W. and Aaronson, S.A. (2010) 'Role of progerin-induced telomere dysfunction in HGPS premature cellular senescence', *Journal of cell science,* 123, pp. 2605-2612.

Bercht Pfleghaar, K., Taimen, P., Butin-Israeli, V., Shimi, T., Langer-Freitag, S., Markaki, Y., Goldman, A.E., Wehnert, M. and Goldman, R.D. (2015) ' Gene-rich chromosomal regions are preferentially localized in the lamin B deficient nuclear blebs of atypical progeria cells.' 6(1), pp. 66-76.

Berezney, R. and Coffey, D. (1974) 'Identification of a nuclear protein matrix', *Biochem Biophys Res Commun,* 60, pp. 1410-1419.

Berezney, R., Mortillaro, M.J., Ma, H., Wei, X. and Samarabandu, J. (1996) 'The nuclear matrix: a structural milieu for genomic function', *International review of cytology,* 162, pp. 1-65.

Berezney, R., Mortillaro, M.J., Ma, H., Wei, X. and Samarabandu, J. (1995) 'The nuclear matrix: a structural milieu for genomic function', *International review of cytology,* 162A, pp. 1-65.

Berger, R., Theodor, L., Shoham, J., Gokkel, E., Brok-Simoni, F., Avraham, K.B., Copeland, N.G., Jenkins, N.A., Rechavi, G. and Simon, A.J. (1996) 'The characterization and localization of the mouse thymopoietin/lamina-associated polypeptide 2 gene and its alternatively spliced product', *Genome Res,* 6(5), pp. 361-370.

Berk, J.M., Tifft, K.E. and and Wilson, K.L. (2013) 'The nuclear envelope LEM-domain protein emerin', *Nucleus,* 4(4), pp. 298-314.

Bhalla, N. and Dernburg, A.F. (2008) 'Prelude to a division', *Annual Review of Cell and Developmental Biology,* 24, pp. 397-424.

Bian, Q., Khanna, N., Alvikas, J. and Belmont, A.S. (2013) 'beta-Globin cis-elements determine differential nuclear targeting through epigenetic modifications', *The Journal of cell biology,* 203(5), pp. 767-783.

Bickmore, W.A. (2013) 'The spatial organization of the human genome', *Annual review of genomics and human genetics,* 14, pp. 67-84.

Bione, S., Maestrini, E., Rivella, S., Mancini, M., Regis, S., Romeo, G. and Toniolo, D. (1994) 'Identification of a novel X-linked gene responsible for Emery-Dreifuss muscular dystrophy', *Nat Genet.,* 8(4), pp. 323-327.

Bissell, M.J., Weaver, V.M., Lelièvre, S.A., Wang, F., Petersen, O.W. and Schmeichel, K.L. (1999) 'Tissue structure, nuclear organization, and gene expression in normal and malignant breast', *Cancer research,* 59(7 Supplement), pp. 1757s-1764s.

Bissell, M.J., Hall, H.G. and Parry, G. (1982) 'How does the extracellular matrix direct gene expression?', *Journal of theoretical biology,* 99(1), pp. 31-68.

Blackburn, E.H., (2005). Telomeres and telomerase: their mechanisms of action and the effects of altering their functions. *FEBS Lett*. 579 (4), pp.859–862.

Blackburn, E.H., (2000). Telomere states and cell fates. *Nature* 408 (6808), pp. 53–56.

Blackburn, E.H (2001) 'Switching and signaling at the telomere', *Cell,* 106(6), pp. 661-673.

Blackburn, E.H (1992) 'Telomerases', *Annual Review of Biochemistry,* 61(1), pp. 113-129.

Blackburn, E.H., Greider, C.W. and Szostak, J.W. (2006) 'Telomeres and telomerase: the path from maize, Tetrahymena and yeast to human cancer and aging', *Nature medicine,* 12(10), pp. 1133-1138.

Blackburn, E.H (1991) 'Structure and function of telomeres', *Nature,* 350(6319), pp. 569-573.

Blagosklonny, M.V. (2011) 'Progeria, rapamycin and normal aging: recent breakthrough', *Aging,* 3(7), pp. 685-691.

Blondel, S., Jaskowiak, A.L., Egesipe, A.L., Le Corf, A., Navarro, C., Cordette, V., Martinat, C., Laabi, Y., Djabali, K., de Sandre-Giovannoli, A., Levy, N., Peschanski, M. and Nissan, X. (2014) 'Induced pluripotent stem cells reveal functional differences between drugs currently investigated in patients with hutchinson-gilford progeria syndrome', *Stem cells translational medicine,* 3(4), pp. 510-519.

Bode, J., Goetze, S., Heng, H., Krawetz, S. and Benham, C. (2003) 'From DNA structure to gene expression: mediators of nuclear compartmentalization and dynamics', *Chromosome Research,* 11(5), pp. 435-445.

Bode, J., Schlake, T., Rios-Ramirez, M., Mielke, C., Stengert, M., Kay, V. and Klehr-Wirth, D. (1996) 'Scaffold/matrix-attached regions: structural properties creating transcriptionally active loci', *International review of cytology,* 162, pp. 389-454.

Bode, J., Benham, C., Knopp, A. and Mielke, C. (2000) 'Transcriptional augmentation: modulation of gene expression by scaffold/matrix-attached regions (S/MAR elements)', *Critical reviews in eukaryotic gene expression,* 10(1), pp. 73-90.

Bode, J., Kohwi, Y., Dickinson, L., Joh, T., Klehr, D., Mielke, C. and Kohwi-Shigematsu, T. (1992) 'Biological significance of unwinding capability of nuclear matrix-associating DNAs', *Science (New York, N.Y.),* 255(5041), pp. 195-197.

Bodnar, A., Lichtsteiner, S., Kim, N. and Trager, J. (1997) 'Reconstitution of human telomerase with the template RNA component hTR and the catalytic protein subunit hTRT', *Nat Genet,* 17, pp. 498-502.

Bodnar, A.G., Ouellette, M., Frolkis, M., Holt, S.E., Chiu, C.P., Morin, G.B., Harley, C.B., Shay, J.W., Lichtsteiner, S. and Wright, W.E. (1998) 'Extension of life-span by introduction of telomerase into normal human cells', *Science (New York, N.Y.),* 279(5349), pp. 349-352.

Boisvert, F.M., van Koningsbruggen, S., Navascues, J. and Lamond, A.I. (2007) 'The multifunctional nucleolus', *Nature reviews.Molecular cell biology,* 8(7), pp. 574-585.

Bolzer, A., Kreth, G., Solovei, I., Koehler, D., Saracoglu, K., Fauth, C., Muller, S., Eils, R., Cremer, C., Speicher, M.R. and Cremer, T. (2005) 'Three-dimensional maps of all chromosomes in human male fibroblast nuclei and prometaphase rosettes', *PLoS biology,* 3(5), pp. 826-842.

Boros, J., Arnoult, N., Stroobant, V., Collet, J.F. and Decottignies, A. (2014) 'Polycomb repressive complex 2 and H3K27me3 cooperate with H3K9 methylation to maintain heterochromatin protein 1alpha at chromatin', *Molecular and cellular biology,* 34(19), pp. 3662-3674.

Boulikas, T. (1996) 'Chromatin domains and prediction of MAR sequences', *International review of cytology,* 162, pp. 279-388.

Bourne, G., Moir, C., Bikkul, U., Ahmed, M.H., Kill, I.R., Eskiw, C.H., Tosi, S. and Bridger, J.M. (2013) 'Interphase chromosome behavior in normal and diseased cells', in *Human Interphase Chromosomes.* Springer, pp. 9-33.

Boveri, T. (1909) 'Die Blastomerenkerne von Ascaris megalocephala und die Theorie der Chromosomenindividualitat', *Archiv fiir Zellforschung,* 3, pp. 181-268.

Boyartchuk, V.L., Ashby, M.N. and Rine, J. (1997) 'Modulation of Ras and a-factor function by carboxyl-terminal proteolysis', *Science,* 275(5307), pp. 1796-1800.

Boyle, S., Gilchrist, S., Bridger, J.M., Mahy, N.L., Ellis, J.A. and Bickmore, W.A. (2001) 'The spatial organization of human chromosomes within the nuclei of normal and emerin-mutant cells', *Human molecular genetics,* 10(3), pp. 211-219.

Brady,S.N.; Yu,Y.; Maggi,L.B.,Jr; Weber,J.D. (2004) 'ARF impedes NPM/B23 shuttling in an Mdm2-sensitive tumor suppressor pathway' Mol.Cell.Biol., 2004, 24(21), pp. 9327-9338.

Bradley, C.M., Ronning, D.R., Ghirlando, R., Craigie, R. and Dyda, F. (2005) 'Structural basis for DNA bridging by barrier-to-autointegration factor', *Nature structural & molecular biology,* 12(10), pp. 935-936.

Branco, M.R., Branco, T., Ramirez, F. and Pombo, A. (2008) 'Changes in chromosome organization during PHA-activation of resting human lymphocytes measured by cryo-FISH', *Chromosome research,* 16(3), pp. 413-426.

Branco, M.R. and Pombo, A. (2006) 'Intermingling of chromosome territories in interphase suggests role in translocations and transcription-dependent associations', *PLoS biology,* 4(5), pp. e138.

Brassard, J.A., Fekete, N., Garnier, A., Hoesli, C.A. (2015) 'Hutchinson-Gilford progeria syndrome as a model for vascular aging.' *Biogerontology.* 7(1), pp. 129-45

Bridger, J.M. and Lichter, P. (1999) 'Analysis of mammalian interphase chromosomes by FISH and immunofluorescence', *Chromosome structural analysis.Oxford University, Oxford,* pp. 103-123.

Bridger, J.M., Arican-Gotkas, H.D., Foster, H.A., Godwin, L.S., Harvey, A., Kill, I.R., Knight, M., Mehta, I.S. and Ahmed, M.H. (2014) 'The non-random repositioning of whole chromosomes and individual gene loci in interphase nuclei and its relevance in disease, infection, aging, and cancer', in *Cancer Biology and the Nuclear Envelope.* Springer, pp. 263-279.

Bridger, J.M., Boyle, S., Kill, I.R. and Bickmore, W.A. (1999) 'Re-modelling of nuclear architecture in quiescent and senescent human fibroblasts', *Current biology,* 10(3), pp. 149-152.

Bridger, J.M., Foeger, N., Kill, I.R. and Herrmann, H. (2007) 'The nuclear lamina. Both a structural framework and a platform for genome organization', *The FEBS journal,* 274(6), pp. 1354-1361.

Bridger, J.M., Kill, I.R., O'Farrell, M. and Hutchison, C.J. (1993) 'Internal lamin structures within G1 nuclei of human dermal fibroblasts', *Journal of cell science,* 104, pp. 297-306.

Bridger, J.M. and Kill, I.R. (2004) 'Aging of Hutchinson–Gilford progeria syndrome fibroblasts is characterised by hyperproliferation and increased apoptosis', *Experimental gerontology,* 39(5), pp. 717-724.

Bridger, J.M., Kill. I, R. and Lichter, P. (1998) 'Association of pKi-67 with satellite DNA of the human genome in early G1 cells', *Chromosome research : an international journal on the molecular, supramolecular and evolutionary aspects of chromosome biology JID - 9313452,* 6, pp. 13-24.

Bridger, J.M. and Bickmore, W.A. (1998) 'Putting the genome on the map', *Trends in Genetics,* 14(10), pp. 403-409.

Broers, J.L.V., Ramaekers, F.C.S., Bonne, G., Ben Yaou, R. and Hutchison, C.J. (2006) 'Nuclear Lamins: Laminopathies and Their Role in Premature Ageing', *Physiol Rev,* 86(3), pp. 967-1008.

Broers, J.L., Kuijpers, H.J., Ostlund, C., Worman, H.J., Endert, J. and Ramaekers, F.C. (2005) 'Both lamin A and lamin C mutations cause lamina instability as well as loss of internal nuclear lamin organization', *Exp Cell Res,* 304(2), pp. 582-592.

Brown, J.M., Green, J., das Neves, R.P., Wallace, H.A., Smith, A.J., Hughes, J., Gray, N., Taylor, S., Wood, W.G., Higgs, D.R., Iborra, F.J. and Buckle, V.J. (2008) 'Association between active genes occurs at nuclear speckles and is modulated by chromatin environment', *The Journal of cell biology,* 182(6), pp. 1083-1097.

Brown, W.T. (1992) 'Progeria: a human-disease model of accelerated aging', *The American journal of clinical nutrition,* 55, pp. 1222-1224.

Burke, B. and Stewart, C.L. (2013) 'The nuclear lamins: flexibility in function', *Nature reviews,* 14, pp. 13-24.

Burton DG. (2009) Cellular senescence, ageing and disease. *Age (Dordr),* 31(1), pp. 1–9

Burton, D.G., GileS, P.J, Sheerin, A.N., Smith, S.K., Lawton, J.J., Ostler, E.L., Rhys-Williams, W., Kipling, D., Faragher, R.G.A (2009) Microarray analysis of senescent vascular smooth muscle cells: A link to atherosclerosis and vascular calcification, *Experimental Gerontology,* 44, pp. 659–665.

Butin-Israeli, V., Adam, S.A., Jain, N., Otte, G.L., Neems, D., Wiesmuller, L., Berger, S.L. and Goldman, R.D. (2015) 'Role of lamin b1 in chromatin instability', *Molecular and cellular biology,* 35(5), pp. 884-898.

C, R. and Z, U. (1885) 'Morphologisches', *Jahrbnch,* 10, pp. 14-330.

Cabanillas, R., Cadiñanos, J., Villameytide, J.A., Pérez, M., Longo, J., Richard, J.M., Álvarez, R., Durán, N.S., Illán, R. and González, D.J. (2011) 'Néstor–Guillermo progeria syndrome: A novel premature aging condition with early onset and chronic development caused by BANF1 mutations', *American Journal of Medical Genetics Part A,* 155(11), pp. 2617-2625.

Cai, M., Huang, Y., Suh, J.Y., Louis, J.M., Ghirlando, R., Craigie, R. and Clore, G.M. (2007) 'Solution NMR structure of the barrier-to-autointegration factor-Emerin complex', *The Journal of biological chemistry,* 282(19), pp. 14525-14535.

Campisi J, Andersen JK, Kapahi P, Melov S. (2011) Cellular senescence: a link between cancer and age-related degenerative disease? *Semin Cancer Biol*. 21(6), pp.354–359

Campisi, J., (2005). Senescent cells, tumor suppression, and organismal aging: good citizens, bad neighbors. *Cell* 120 (4), pp. 513–522.

Camps, J., Erdos, M.R. and Ried, T. (2015) 'The role of lamin B1 for the maintenance of nuclear structure and function', *Nucleus,* 6(1), pp. 8-14.

Candelario, J., Borrego, S., Reddy, S. and Comai, L. (2011) 'Accumulation of distinct prelamin A variants in human diploid fibroblasts differentially affects cell homeostasis', *Experimental cell research,* 317(3), pp. 319-329.

Canela, A., Vera, E., Klatt, P., Blasco, M.A. (2007) ' High-throughput telomere length quantification by FISH and its application to human population studies.' *Proc. Natl. Acad. Sci. U.S.A.,* 104, pp. 5300–5305.

Cao, K., Blair, C.D., Faddah, D.A., Kieckhaefer, J.E., Olive, M., Erdos, M.R., Nabel, E.G. and Collins, F.S. (2011a) 'Progerin and telomere dysfunction collaborate to trigger cellular senescence in normal human fibroblasts', *The Journal of clinical investigation,* 121(7), pp. 2833-2844.

Cao, K., Capell, B.C., Erdos, M.R., Djabali, K. and Collins, F.S. (2007) 'A lamin A protein isoform overexpressed in Hutchinson-Gilford progeria syndrome interferes with mitosis in progeria and normal cells', *Proceedings of the National Academy of Sciences of the United States of America,* 104(12), pp. 4949-4954.

Cao, K., Graziotto, J.J., Blair, C.D., Mazzulli, J.R., Erdos, M.R. and Collins, F.S. (2011b) 'Rapamycin reverses cellular phenotypes and enhances mutant protein clearance in Hutchinson-Gilford progeria syndrome cells', *Science translational medicine,* 3(89), pp. 1-11.

Capanni, C., Mattioli, E., Columbaro, M., Lucarelli, E., Parnaik, V.K., Novelli, G., Wehnert, M., Cenni, V., Maraldi, N.M., Squarzoni, S. and Lattanzi, G. (2005) 'Altered pre-lamin A processing is a common mechanism leading to lipodystrophy', *Human molecular genetics,* 14(11), pp. 1489-1502.

Capco, D.G., Wan, K.M. and Penman, S. (1982) 'The nuclear matrix: three-dimensional architecture and protein composition', *Cell,* 29(3), pp. 847-858.

Capell, B.C. and Collins, F.S. (2006) 'Human laminopathies nuclei gone genetically awry', *Nature,* 12, pp. 940-952.

Caputo, S., Couprie, J., Duband-Goulet, I., Kondé, E., Lin, F., Braud, S., Gondry, M., Gilquin, B., Worman, H.J. and Zinn-Justin, S. (2006) 'The carboxyl-terminal nucleoplasmic region of MAN1 exhibits a DNA binding winged helix domain', *J Biol Chem.,* 281(26), pp. 18208-18215.

Carter, D., Chakalova, L., Osborne, C.S., Dai, Y. and Fraser, P. (2002) 'Long-range chromatin regulatory interactions in vivo', *Nature genetics,* 32(4), pp. 623-626.

Casolari, J.M., Brown, C.R., Komili, S., West, J., Hieronymus, H. and Silver, P.A. (2004) 'Genome-wide localization of the nuclear transport machinery couples transcriptional status and nuclear organization', *Cell,* 117(4), pp. 427-439.

Cau, P., Navarro, C., Harhouri, K., Roll, P., Sigaudy, S., Kaspi, E., Perrin, S., De Sandre-Giovannoli, A. and Lévy, N. (2014) 'Nuclear matrix, nuclear envelope and premature aging syndromes in a translational research perspective', *Seminars in cell & developmental biology,* 29, pp. 125-147.

Cech, T.R. (2004) 'Beginning to understand the end of the chromosome', *Cell,* 116(2), pp. 273-279.

Celis, J.E. and Celis, A. (1985) 'Cell cycle-dependent variations in the distribution of the nuclear protein cyclin proliferating cell nuclear antigen in cultured cells: subdivision of S phase', *Proceedings of the National Academy of Sciences of the United States of America,* 82(10), pp. 3262-3266.

Cenni, V., Capanni, C.M., Ortolani, M., D'Apice, M.R., Novelli, G., Fini, M., Marmiroli, S., Scarano. E, Maraldi, N.M., Squarzoni, S., Prencipe, S. and Lattanzi, G. (2011) 'Autophagic degradation of farnesylated prelamin A as a therapeutic approach to lamin-linked progeria', *European journal of histochemistry,* 55(4), pp. 201-205.

Chambeyron, S. and Bickmore, W.A. (2004) 'Chromatin decondensation and nuclear reorganization of the HoxB locus upon induction of transcription', *Genes & development,* 18(10), pp. 1119-1130.

Chang,B.D., Watanabe, K., Broude, E.V., Fang,J., Poole,J.C., Kalinichenko, T.V., and Roninson, I and B. (2000) 'Effects of P21$^{WAF1/CIP1/Sdil}$ on cellular gene expression: implications for carcinogenesis, senescence, and age-related diseases'. *Proc. Natl Acad. Sci. USA*, 97, pp. 4291-4296.

Charras, G. and Brieher, W.M. (2016) ' Regulation and integrated functions of actin cytoskeleton'. Molecular Biology of the cell, 27, 881.

Chen, C.Y., Chi, Y.H., Mutalif, R.A., Starost, M.F., Myers, T.G., Anderson, S.A., Stewart, C.L. and Jeang, K.T. (2012) 'Accumulation of the inner nuclear envelope protein Sun1 is pathogenic in progeric and dystrophic laminopathies', *Cell,* 149(3), pp. 565-577.

Chen, Z.J., Wang, W.P., Chen, Y.C., Wang, J.Y., Lin, W.H., Tai, L.A., Liou, G.G., Yang, C.S. and Chi, Y.H. (2014) 'Dysregulated interactions between lamin A and SUN1 induce abnormalities in the nuclear envelope and endoplasmic reticulum in progeric laminopathies', *Journal of cell science,* 127(Pt 8), pp. 1792-1804.

Chernyatina, A.A., Guzenko, D. and Strelkov, S.V. (2015) 'Intermediate filament structure: the bottom-up approach', *Current opinion in cell biology,* 32(0), pp. 65-72.

Chiarella, S., De Cola, A., Scaglione, G.L., Carletti, E., Graziano, V., Barcaroli, D., Lo Sterzo, C., Di Matteo, A., Di Ilio, C., Falini, B., Arcovito, A., De Laurenzi, V. and Federici, L. (2013) 'Nucleophosmin mutations alter its nucleolar localization by impairing G-quadruplex binding at ribosomal DNA', *Nucleic acids research,* 41(5), pp. 3228-3239.

Chikashige, Y., Haraguchi, T. and Hiraoka, Y. (2007) 'Another way to move chromosomes', *Chromosoma,* 116, pp. 497-505.

Chojnowski, A., Ong, P.F., Wong, E.S., Lim, J.S., Mutalif, R.A., Navasankari, R., Dutta, B., Yang, H., Liow, Y.Y. and Sze, S.K. (2015) 'Progerin reduces LAP2α-telomere association in Hutchinson-Gilford progeria', *eLife,* , pp. e07759.

Chu, Y., Xu, Z., Xu, Z. and Ma, L. (2014) 'Hutchinson–Gilford Progeria Syndrome Caused by an LMNA Mutation: A Case Report', *Pediatric dermatology,* .

Chubb, J.R., Boyle, S., Perry, P. and Bickmore, W.A. (2002) 'Chromatin motion is constrained by association with nuclear compartments in human cells', *Current biology,* 12, pp. 439-445.

Ciska, M. and Moreno Díaz de la Espina, Susana (2013) 'NMCP/LINC proteins: putative lamin analogs in plants?', *Plant signaling & behavior,* 8(12), pp. e26669.

Clarke, S. (1992) 'Protein isoprenylation and methylation at carboxyl-terminal cysteine residues', *Annu Rev Biochem,* 61, pp. 355-386.

Clements, L., Manilal, S., Love, D.R. and Morris, G.E. (2000) 'Direct Interaction between Emerin and Lamin A', *Biochemical and biophysical research communications,* 267(3), pp. 709-714.

Cmarko, D., Verschure, P.J., Rothblum, L.I., Hernandez-Verdun, D., Amalric, F., van Driel, R. and Fakan, S. (2000) 'Ultrastructural analysis of nucleolar transcription in cells microinjected with 5-bromo-UTP', *Histochemistry and cell biology,* 113(3), pp. 181-187.

Coelho, M.B., Attig, J., Bellora, N., Konig, J., Hallegger, M., Kayikci, M., Eyras, E., Ule, J. and Smith, C.W. (2015) 'Nuclear matrix protein Matrin3 regulates alternative splicing and forms overlapping regulatory networks with PTB', *The EMBO journal,* 34(5), pp. 653-668.

Cohen, S.B., Graham, M.E., Lovrecz, G.O., Bache, N., Robinson, P.J. and Reddel, R.R. (2007) 'Protein composition of catalytically active human telomerase from immortal cells', *Science (New York, N.Y.),* 315(5820), pp. 1850-1853.

Collado, M., Blasco, M.A., Serrano, M., (2007) 'Cellular senescence in cancer and aging.' *Cell.*, 130(2), pp. 223–233

Columbaro, M., Capanni, C., Mattioli, E., Novelli, G., Parnaik, V.K., Squarzoni, S., Maraldi, N.M. and Lattanzi, G. (2005) 'Rescue of heterochromatin organization in Hutchinson-Gilford progeria by drug treatment', *Cellular and molecular life sciences,* 62, pp. 2669-2678.

Cong, Y.S., Wright, W.E. and Shay, J.W. (2002) 'Human telomerase and its regulation', *Microbiology and molecular biology reviews : MMBR,* 66(3), pp. 407-25, table of contents.

Coppe, J.P. Patil, C.K., Rodier, F., Sun, Y., Munoz, D.P., Goldstein, J., Nelson, P.S., Desprez, P.Y., Campisi, J. (2008) Senescence-associated secretory phenotypes reveal cell-nonautonomous functions of oncogenic RAS and the p53 tumor suppressor. *PLoS Biol* , 6, pp. 2853–2868

Coppe, J.P., Patil, C.K., Rodier, F., Krtolica, A., Beausejour, C.M., Parrinello, S., Hodgson, J.G., Chin, K., Desprez, P.Y., Campisi, J. (2010) 'A human-like senescence-associated secretory phenotype is conserved in mouse cells dependent on physiological oxygen.' *PLoS One* 5(2), pp. 9188

Coppedè, F. (2012) 'Premature aging syndrome in *Neurodegenerative Diseases.'* Springer, pp. 317-331.

Corcos, L. and Le Jossic-corcos, C. (2013) 'Statins: Perspectives in cancer therapeutics', *Digestive and Liver Disease,* 45(10), pp. 795-802.

Corrigan, D.P., Kuszczak, D., Rusinol, A.E., Thewke, D.P., Hrycyna, C.A., Michaelis, S. and and Sinensky, M.S. (2005) 'Prelamin A endoproteolytic processing in vitro by recombinant Zmpste24', *Biochem,* 387, pp. 129-138.

Counter, C.M., Meyerson, M., Eaton, E.N., Ellisen, L.W., Caddle, S.D., Haber, D.A. and Weinberg, R.A. (1998) 'Telomerase activity is restored in human cells by

ectopic expression of hTERT (hEST2), the catalytic subunit of telomerase', *Oncogene,* 16(9), pp. 1217-1222.

Courvalin, J.C., Lassoued, K., Worman, H.J. and Blobel, G. (1990) 'Identification and Characterization of Autoantibodies Against the Nuclear Envelope Lamin B Receptor from Patients with Primary Biliary Cirrhosis', *J Exp Med,* 172(3), pp. 961-967.

Cox, J.L., Mallanna, S.K., Ormsbee, B.D., Desler, M., Wiebe, M.S. and Rizzino, A. (2011) 'Banf1 is required to maintain the self-renewal of both mouse and human embryonic stem cells', *Journal of cell science,* 124(Pt 15), pp. 2654-2665.

Crabbe, L., Cesare, A.J., Kasuboski, J.M., Fitzpatrick, J.A. and Karlseder, J. (2012) 'Human telomeres are tethered to the nuclear envelope during postmitotic nuclear assembly', *Cell reports,* 2(6), pp. 1521-1529.

Craig, J.M. and Bickmore, W.A. (1994) 'The distribution of CpG islands in mammalian chromosomes', *Nature genetics,* 7(3), pp. 376-382.

Cremer, M., von Hase, J., Volm, T., Brero, A., Kreth, G., Walter, J., Fischer, C., Solovei, I., Cremer, C. and Cremer, T. (2001) 'Non-random radial higher-order chromatin arrangements in nuclei of diploid human cells', *Chromosome research,* 9(7), pp. 541-567.

Cremer, C., Zorn, C. and Cremer, T. (1974) 'An ultraviolet laser microbeam for 257 nm', *Microscopica acta,* 75(4), pp. 331-337.

Cremer, M., Kupper, K., Wagler, B., Wizelman, L., von Hase, J., Weiland, Y., Kreja, L., Diebold, J., Speicher, M.R. and Cremer, T. (2003) 'Inheritance of gene density-related higher order chromatin arrangements in normal and tumor cell nuclei', *The Journal of cell biology,* 162(5), pp. 809-820.

Cremer, T. and Cremer, C. (2006) 'Rise, fall and resurrection of chromosome territories: a historical perspective. Part II. Fall and resurrection of chromosome territories during the 1950s to 1980s. Part III. Chromosome territories and the functional nuclear architecture: experiments and models from the 1990s to the present', *European journal of histochemistry,* 50(4), pp. 223-272.

Crisp, M., Liu, Q., Roux, K., Rattner, J.B., Shanahan, C., Burke, B., Stahl, P.D. and Hodzic, D. (2005) 'Coupling of the nucleus and cytoplasm: role of the LINC complex', *The Journal of cell biology,* 172(1), pp. 41-53.

Croft, J.A., Bridger, J.M., Boyle, S., Perry, P., Teague, P. and Bickmore, W.A. (1999) 'Differences in the localization and morphology of chromosomes in the human nucleus', *The Journal of cell biology ,* 145(6), pp. 1119-1131.

Cross, S.H., Lee, M., Clark, V.H., Craig, J.M., Bird, A.P. and Bickmore, W.A. (1997) 'The chromosomal distribution of CpG islands in the mouse: evidence for genome scrambling in the rodent lineage', *Genomics,* 40(3), pp. 454-461.

Csoka, A.B., Cao, H., Sammak, P.J., Constantinescu, D., Schatten, G.P. and Hegele, R.A. (2004) 'Novel lamin A/C gene (LMNA) mutations in atypical progeroid syndromes', *Journal of medical genetics,* 41(4), pp. 304-308.

Cui, W., Aslam, S., Fletcher, J., Wylie, D., Clinton, M. and Clark, A.J. (2002) 'Stabilization of telomere length and karyotypic stability are directly correlated with the level of hTERT gene expression in primary fibroblasts', *The Journal of biological chemistry,* 277(41), pp. 38531-38539.

D'Adda di Fagagna F, Reaper PM, Clay-Farrace L, Fiegler H, Carr P, Von Zglinicki T, Saretzki G, Carter NP and Jackson SP (2003) A DNA damage checkpoint response in telomere-initiated senescence. Nature, 426 (6963), 194-198.

D'Angelo, M.A. and Hetzer, M.W. (2008) 'Structure, dynamics and function of nuclear pore complexes', *Trends in cell biology,* 18(10), pp. 456-466.

Dabauvalle, M., Müller, E., Ewald, A., Kress, W., Krohne, G. and Müller, C.R. (1999) 'Distribution of emerin during the cell cycle', *European journal of cell biology,* 78(10), pp. 749-756.

Dambacher, S., Hahn, M. and Schotta, G. (2013) 'The compact view on heterochromatin', *Cell cycle (Georgetown, Tex.) ,* 12(18), pp. 2925-2926.

Damm, K., Hemmann, U., Garin-Chesa, P., Hauel, N., Kauffmann, I., Priepke, H., Niestroj, C., Daiber, C., Enenkel, B., Guilliard, B., Lauritsch, I., Muller, E., Pascolo, E., Sauter, G., Pantic, M., Martens, U.M., Wenz, C., Lingner, J., Kraut, N., Rettig, W.J. and Schnapp, A. (2001) 'A highly selective telomerase inhibitor limiting human cancer cell proliferation', *The EMBO journal ,* 20(24), pp. 6958-6968.

Danielsen, J.M., Sylvestersen, K.B., Bekker-Jensen, S., Szklarczyk, D., Poulsen, J.W., Horn, H., Jensen, L.J., Mailand, N. and Nielsen, M.L. (2011) 'Mass spectrometric analysis of lysine ubiquitylation reveals promiscuity at site level', *Molecular & cellular proteomics : MCP,* 10(3), pp. M110.003590.

Das, A., Grotsky, D.A., Neumann, M.A., Kreienkamp, R., Gonzalez-Suarez, I., Redwood, A.B., Kennedy, B.K., Stewart, C.L. and Gonzalo, S. (2013) 'Lamin A Δexon9 mutation leads to telomere and chromatin defects but not genomic instability', *Nucleus,* 4(5), pp. 410-419.

Dauer, W.T. and Worman, H.J. (2009) 'The nuclear envelope as a signaling node in development and disease', *Developmental cell,* 17(5), pp. 626-638.

Davidson, P.M. and Lammerding, J. (2014) 'Broken nuclei – lamins, nuclear mechanics, and disease', *Trends in cell biology,* 24(4), pp. 247-256.

Davies, B.S., Coffinier, C., Yang, S.H., Barnes, R.H., Jung, H., Young, S.G. and Fong, L.G. (2011) 'Investigating the purpose of prelamin A processing', *Nucleus,* 2(1).

Davis, T., Faragher, R.G.A, Jones, C,J., Kipling, D., (2006) 'Investigation of the Signaling Pathways Involved in the Proliferative Life Span Barriers in Werner Syndrome Fibroblasts', *Annals of the New York*, 1019, 274-277.

De Biase, I., Chutake, Y.K., Rindler, P.M. and Bidichandani, S.I. (2009) 'Epigenetic silencing in Friedreich ataxia is associated with depletion of CTCF (CCCTC-binding factor) and antisense transcription', *PLoS One,* 4(11), pp. e7914.

de La Rosa, J., Freije, J.M., Cabanillas, R., Osorio, F.G., Fraga, M.F., Fernández-García, M.S., Rad, R., Fanjul, V., Ugalde, A.P. and Liang, Q. (2013) 'Prelamin A causes progeria through cell-extrinsic mechanisms and prevents cancer invasion', *Nature communications,* 4.

de Laat, W. and Grosveld, F. (2003) 'Spatial organization of gene expression: the active chromatin hub', *Chromosome Research,* 11(5), pp. 447-459.

de Lange, T. (2005) 'Shelterin: the protein complex that shapes and safeguards human telomeres', *Genes & development,* 19(18), pp. 2100-2110.

de Lange, T. (1992) 'Human telomeres are attached to the nuclear matrix', *The EMBO journal,* 11(2), pp. 717-724.

de Oca, R.M., Shoemaker, C.J., Gucek, M., Cole, R.N. and Wilson, K.L. (2009) 'Barrier-to-autointegration factor proteome reveals chromatin-regulatory partners', *PLoS One,* 4(9), pp. e7050.

De Sandre-Giovannoli, A. and Lévy, N. (2006) 'Altered splicing in prelamin A-associated premature aging phenotypes', in *Alternative Splicing and Disease.* Springer, pp. 199-232.

De Sandre-Giovannoli, A., Bernard, R., Cau, P., Navarro, C., Amiel, J., Boccaccio, I., Lyonnet, S., Stewart, C.L., Munnich, A., Le Merrer, M. and Levy, N. (2003) 'Lamin a truncation in Hutchinson-Gilford progeria', *Science (New York, N.Y.) JID - 0404511,* 300, pp. 2055-2056.

De Vos, W.H., Houben, F., Hoebe, R.A., Hennekam, R., van Engelen, B., Manders, E.M., Ramaekers, F.C., Broers, J.L. and Van Oostveldt, P. (2010) 'Increased plasticity of the nuclear envelope and hypermobility of telomeres due to the loss of A–type lamins', *Biochimica et Biophysica Acta (BBA)-General Subjects,* 1800(4), pp. 448-458.

de Wit, E. and de Laat, W. (2012) 'A decade of 3C technologies: insights into nuclear organization', *Genes & development,* 26(1), pp. 11-24.

Debacq-Chainiaux, F., Borlon, C., Pascal, T., Royer, V., Eliaers, F., Ninane, N., Carrard, G., Friguet, B., de Longueville, F., Boffe, S., Remacle, J., Toussaint, O. (2005) 'Repeated exposure of human skin fibroblasts to UVB at subcytotoxic level triggers premature senescence through the TGF-beta1 signaling pathway'. *J. Cell Sc*i. 118(Pt 4), pp. 743–758.

Dechat, T., Gesson, K. and Foisner, R. (2010) 'Lamina-Independent Lamins in the Nuclear Interior Serve Important Functions', *Cold Spring Harbor Symposia on Quantitative Biology,* 75, pp. 533-543.

Dechat, T., Korbei, B., Vaughan, O.A., Vlcek, S., Hutchison, C.J. and and Foisner, R. (2000) 'Lamina-associated polypeptide 2a binds intranuclear Atype lamins', *J. Cell Sci.,* 113, pp. 3473-3484.

Dechat, T., Pfleghaar, K., Sengupta, K., Shimi, T., Shumaker, D.K. and Solimando, L. & Goldman, R.D. (2008) '"Nuclear lamins: major factors in the structural organization and function of the nucleus and chromatin', 22(7), pp. 832-853.

Dechat, T., Adam, S.A., Taimen, P., Shimi, T. and Goldman, R.D. (2010) 'Nuclear lamins', *Cold Spring Harbor perspectives in biology ,* 2, pp. 1-22.

Dechat, T., Gajewski, A., Korbei, B., Gerlich, D., Daigle, N., Haraguchi, T., Furukawa, K., Ellenberg, J. and Foisner, R. (2004) 'LAP2alpha and BAF transiently localize to telomeres and specific regions on chromatin during nuclear assembly', *Journal of cell science,* 117(Pt 25), pp. 6117-6128.

Dechat, T., Gotzmann, J., Stockinger, A., Harris, C.A., Talle, M.A., Siekierka, J.J. and Foisner, R. (1998) 'Detergent-salt resistance of LAP2alpha in interphase nuclei and phosphorylation-dependent association with chromosomes early in nuclear assembly implies functions in nuclear structure dynamics', *The EMBO journal,* 17(16), pp. 4887-4902.

Decker, M.L., Chavez, E., Vulto, I. and Lansdorp, P.M. (2009) 'Telomere length in Hutchinson-Gilford Progeria Syndrome', *Mechanisms of ageing and development,* 130(6), pp. 377-383.

Delgado Luengo, W., Rojas Martínez, A., Ortíz López, R., Martínez Basalo, C., Rojas-Atencio, A., Quintero, M., Borjas, L., Morales-Machín, A., González Ferrer, S. and Pineda Bernal, L. (2002) 'Del (1)(q23) in a patient with Hutchinson-Gilford progeria', *American Journal of Medical Genetics,* 113(3), pp. 298-301.

Dhe-Paganon, S., Werner, E.D. and Chi, Y.I. & Shoelson, S.E. (2002) 'Structure of the globular tail of nuclear lamin', *J Biol Chem,* 277(20), pp. 17381-17384.

Dimitri, P. and Junakovic, N. (1999) 'Revising the selfish DNA hypothesis: new evidence on accumulation of transposable elements in heterochromatin', *Trends in Genetics,* 15(4), pp. 123-124.

Ding, X., Xu, R., Yu, J., Xu, T., Zhuang, Y. and Han, M. (2007) 'SUN1 is required for telomere attachment to nuclear envelope and gametogenesis in mice', *Developmental cell,* 12(6), pp. 863-872.

Dittmer, T.A. and Misteli, T. (2011) 'The lamin protein family', *Genome biology JID - 100960660,* 12(222), pp. 1-14.

Dove, A.W. (2003) 'An interaction that gets things started', *J Cell Biol,* 162(2), pp. 162.

Dreesen, O., Ong, P.F., Chojnowski, A. and Colman, A. (2013a) 'The contrasting roles of lamin B1 in cellular aging and human disease.' *Nucleus,* 4(4), pp. 283-290.

Dreesen, O., Chojnowski, A., Ong, P.F., Zhao, T.Y., Common, J.E., Lunny, D., Lane, E.B., Lee, S.J., Vardy, L.A., Stewart, C.L. and Colman, A. (2013b) 'Lamin B1 fluctuations have differential effects on cellular proliferation and senescence', *The Journal of cell biology,* 200(5), pp. 605-617.

Driscoll, M.K., Albanese, J.L., Xiong, Z.M., Mailman, M., Losert, W. and Cao, K. (2012) 'Automated image analysis of nuclear shape: what can we learn from a prematurely aged cell?', *Aging ,* 4(2), pp. 119-132.

Dundr, M., Ospina, J.K., Sung, M.H., John, S., Upender, M., Ried, T., L, H.G. and Matera, A.G. (2007) 'Actin-dependent intranuclear repositioning of an active gene locus in vivo', *The Journal of cell biology JID - 0375356,* 179(6), pp. 1095-1103.

Dutrillaux, B., Couturier, J., Richer, C. and Viegas-Péquignot, E. (1976) 'Sequence of DNA replication in 277 R-and Q-bands of human chromosomes using a BrdU treatment', *Chromosoma,* 58(1), pp. 51-61.

Eckersley-Maslin, M.A., Bergmann, J.H., Lazar, Z. and Specto, D.L. (2013) 'Lamin A/C is expressed in pluripotent mouse embryonic stem cells.', 4(1), pp. 53-60.

Edelmann, P., Bornfleth, H., Zink, D., Cremer, T. and Cremer, C. (2001) 'Morphology and dynamics of chromosome territories in living cells', *Biochimica et Biophysica Acta (BBA)-Reviews on Cancer,* 1551(1), pp. M29-M39.

Eissenberg, J.C. and Elgin, S.C. (2000) 'The HP1 protein family: getting a grip on chromatin', *Current opinion in genetics & development,* 10(2), pp. 204-210.

Elcock, L.S. and Bridger, J.M. (2010) 'Exploring the relationship between interphase gene positioning, transcriptional regulation and the nuclear matrix', *Biochemical Society transactions ,* 38(1), pp. 263-267.

Elcock, L.S. and Bridger, J.M. (2008) 'Exploring the effects of a dysfunctional nuclear matrix', *Biochemical Society transactions JID - 7506897,* 36, pp. 1378-1383.

El-Daly, H., Kull, M., Zimmermann, S., Pantic, M., Waller, C.F. and Martens, U.M. (2005) 'Selective cytotoxicity and telomere damage in leukemia cells using the telomerase inhibitor BIBR1532', *Blood,* 105(4), pp. 1742-1749.

Ellis, J.A., Craxton, M., Yates, J.R. and Kendrick-Jones, J. (1998) 'Aberrant intracellular targeting and cell cycle-dependent phosphorylation of emerin contribute to the EmeryDreifuss muscular dystrophy phenotype', *J Cell Sci,* 111(6), pp. 781-792.

Ellis, D.J., Jenkins, H., Whitfield, W.G. and Hutchison, C.J. (1997) 'GST-lamin fusion proteins act as dominant negative mutants in Xenopus egg extract and reveal the function of the lamina in DNA replication', *Journal of cell science,* 110 (Pt 20)(Pt 20), pp. 2507-2518.

Emery, A.E. and Dreifuss, F.E. (1966) 'Unusual type of benign x-linked muscular dystrophy', *J Neurol Neurosurg Psychiatry,* 29, pp. 338-342.

Engelke, R., Riede, J., Hegermann, J., Wuerch, A., Eimer, S., Dengjel, J. and Mittler, G. (2014) 'The quantitative nuclear matrix proteome as a biochemical snapshot of nuclear organization', *Journal of proteome research,* 13(9), pp. 3940-3956.

Eriksson, J.E., Dechat, T., Grin, B., Helfand, B., Mendez, M., Pallari, H.M. and Goldman, R.D. (2009) 'Introducing intermediate filaments: from discovery to disease', *The Journal of clinical investigation,* 119(7), pp. 1763-1771.

Eriksson, M., Brown, W.T., Gordon, L.B., Glynn, M.W., Singer, J., Scott, L., Erdos, M.R., Robbins, C.M., Moses, T.Y., Berglund, P., Dutra, A., Pak, E., Durkin, S., Csoka, A.B., Boehnke, M., Glover, T.W. and Collins, F.S. (2003) 'Recurrent de novo point mutations in lamin A cause Hutchinson-Gilford progeria syndrome', *Nature,* 423(6937), pp. 293-298.

Fackelmayer, F.O., Dahm, K., Renz, A., Ramsperger, U. and Richter, A. (1994) 'Nucleic-acid-binding properties of hnRNP-U/SAF-A, a nuclear-matrix protein which binds DNA and RNA in vivo and in vitro', *European Journal of Biochemistry,* 221(2), pp. 749-757.

Fan, Y., Nikitina, T., Zhao, J., Fleury, T.J., Bhattacharyya, R., Bouhassira, E.E., Stein, A., Woodcock, C.L. and Skoultchi, A.I. (2005) 'Histone H1 depletion in mammals alters global chromatin structure but causes specific changes in gene regulation', *Cell,* 123(7), pp. 1199-1212.

Fanti, L., Dorer, D.R., Berloco, M., Henikoff, S. and Pimpinelli, S. (1998) 'Heterochromatin protein 1 binds transgene arrays', *Chromosoma,* 107(5), pp. 286-292.

Fatica, A. and Tollervey, D. (2002) 'Making ribosomes', *Current opinion in cell biology,* 14(3), pp. 313-318.

Fawcett, D.W. (1967) *An atlas of fine structure: The cell; Its organelles and inclusions.* Saunders.

Feng, J., Funk, W.D., Wang, S.S., Weinrich, S.L., Avilion, A.A., Chiu, C.P., Adams, R.R., Chang, E., Allsopp, R.C. and Yu, J. (1995) 'The RNA component of human telomerase', *Science (New York, N.Y.),* 269(5228), pp. 1236-1241.

Ferraiuolo, M.A., Rousseau, M., Miyamoto, C., Shenker, S., Wang, X.Q., Nadler, M., Blanchette, M. and Dostie, J. (2010) 'The three-dimensional architecture of Hox cluster silencing', *Nucleic acids research,* 38(21), pp. 7472-7484.

Fey, E.G., Krochmalnic, G. and Penman, S. (1986) 'The nonchromatin substructures of the nucleus: the ribonucleoprotein (RNP)-containing and RNP-depleted matrices analyzed by sequential fractionation and resinless section electron microscopy', *The Journal of cell biology,* 102(5), pp. 1654-1665.

Finlan, L.E., Sproul, D., Thomson, I., Boyle, S., Kerr, E., Perry, P., Ylstra, B., Chubb, J.R. and Bickmore, W.A. (2008) 'Recruitment to the nuclear periphery can alter expression of genes in human cells', *PLoS Genet,* 4(3), pp. e1000039.

Fiorini, A., Gouveia, F.d.S. and Fernandez, M. (2006) 'Scaffold/matrix attachment regions and intrinsic DNA curvature', *Biochemistry (Moscow),* 71(5), pp. 481-488.

Foisner, R. and Gerace, L. (1993) 'Integral membrane proteins of the nuclear envelope interact with lamins and chromosomes, and binding is modulated by mitotic phosphorylation', *Cell,* 73(7), pp. 1267-1269.

Fong, L.G., Frost, D., Meta, M., Qiao, X., Yang, S.H., Coffinier, C. and Young, S.G. (2006a) 'A protein farnesyltransferase inhibitor ameliorates disease in a mouse model of progeria', *Science (New York, N.Y.),* 311(5767), pp. 1621-1623.

Fong, L.G., Ng, J.K., Lammerding, J., Vickers, T.A., Meta, M., Cote, N., Gavino, B., Qiao, X., Chang, S.Y., Young, S.R., Yang, S.H., Stewart, C.L., Lee, R.T., Bennett, C.F., Bergo, M.O. and Young, S.G. (2006) 'Prelamin A and lamin A appear to be dispensable in the nuclear lamina', *The Journal of clinical investigation,* 116(3), pp. 743-752.

Fong, L.G., Ng, J.K., Meta, M., Cote, N., Yang, S.H., Stewart, C.L., Sullivan, T., Burghardt, A., Majumdar, S., Reue, K., Bergo, M.O. and Young, S.G. (2004) 'Heterozygosity for Lmna deficiency eliminates the progeria-like phenotypes in Zmpste24-deficient mice', *Proceedings of the National Academy of Sciences of the United States of America,* 101(52), pp. 18111-18116.

Foster, H.A. and Bridger, J.M. (2005) 'The genome and the nucleus: a marriage made by evolution. Genome organisation and nuclear architecture', *Chromosoma,* 114(4), pp. 212-229.

Freund, A., Orjalo, A.V., Desprez, P.Y., Campisi, J. (2010) 'inflammatory networks during cellular senescence: causes and consequences.' *Trends Mol Med*. 16(5), pp. 238–246.

Freund, A., Patil, C.K., Campisi, J., (2011) 'p38MAPK is a novel DNA damage response-independent regulator of the senescenceassociated secretory phenotype.' *EMBO J*, 30(8), pp. 1536–1548.

Furukawa, K. (1999) 'LAP2 binding protein 1 (L2BP1/BAF) is a candidate mediator of LAP2-chromatin interaction' *, J. Cell Sci.,* 112, pp. 2485-2492.

Furukawa, K. and Inagaki, H. & Hotta, Y. (1994) 'Identification and Cloning of an mRNA Coding for a Germ Cell-Specific A-Type Lamin in Mice', *Experimental cell research,* 22(2), pp. 426-430.

Furukawa, K. and Hotta, Y. (1993) 'cDNA cloning of a germ cell specific lamin B3 from mouse spermatocytes and analysis of its function by ectopic expression in somatic cells.', *EMBO,* 12(1), pp. 97-106.

Furukawa, K., Sugiyama, S., Osouda, S., Goto, H., Inagaki, M., Horigome, T., Omata, S., McConnell, M., Fisher, P.A. and Nishida, Y. (2003) 'Barrier-to-

autointegration factor plays crucial roles in cell cycle progression and nuclear organization in Drosophila', *Journal of cell science,* 116(Pt 18), pp. 3811-3823.

Furukawa, K., Glass, C. and Kondo, T. (1997) 'Characterization of the Chromatin Binding Activity of Lamina-Associated Polypeptide (LAP) 2', *Biochemical and biophysical research communications,* 238(1), pp. 240-246.

Gabriel, D., Roedl, D., Gordon, L.B. and Djabali, K. (2014) 'Sulforaphane enhances progerin clearance in Hutchinson–Gilford progeria fibroblasts', .

Galati, A., Micheli, E., Alicata, C., Ingegnere, T., Cicconi, A., Pusch, M.C., Giraud-Panis, M.J., Gilson, E. and Cacchione, S. (2015) 'TRF1 and TRF2 binding to telomeres is modulated by nucleosomal organization', *Nucleic acids research,* 43(12), pp. 5824-5837.

Galderisi, U., Cipollaro, M. and Giordano, A. (2006) 'The retinoblastoma gene is involved in multiple aspects of stem cell biology', *Oncogene,* 25(38), pp. 5250-5256.

Georgiev, G., Bakayev, V., Nedospasov, S., Razin, S. and Mantieva, V. (1981) 'Studies on structure and function of chromatin', *Molecular and cellular biochemistry,* 40(1), pp. 29-48.

Gerace, L. and Huber, M.D. (2012) 'Nuclear lamina at the crossroads of the cytoplasm and nucleus', *Journal of structural biology,* 177(1), pp. 24-31.

Gerdes, J., Schwab, U., Lemke, H. and Stein, H. (1983) 'Production of a mouse monoclonal antibody reactive with a human nuclear antigen associated with cell proliferation', *International journal of cancer,* 31(1), pp. 13-20.

Gerdes, M.G., Carter, K.C., Moen, P.T.,Jr and Lawrence, J.B. (1994) 'Dynamic changes in the higher-level chromatin organization of specific sequences revealed by in situ hybridization to nuclear halos', *The Journal of cell biology,* 126(2), pp. 289-304.

Gesson, K., Vidak, S. and Foisner, R. (2014) 'Lamina-associated polypeptide (LAP) 2α and nucleoplasmic lamins in adult stem cell regulation and disease', *Seminars in cell & developmental biology.* Elsevier, 116-124.

Gilbert, N., Gilchrist, S. and Bickmore, W.A. (2004) 'Chromatin organization in the mammalian nucleus', *International review of cytology,* 242, pp. 283-336.

Glynn, M.W. and Glover, T.W. (2005) 'Incomplete processing of mutant lamin A in Hutchinson-Gilford progeria leads to nuclear abnormalities, which are reversed by farnesyltransferase inhibition', *Human molecular genetics,* 14(20), pp. 2959-2969.

Godwin, L.S. (2010) 'The role of lamin A and emerin in mediating genome organisation' .

Göhring, F. and Fackelmayer, F.O. (1997) 'The scaffold/matrix attachment region binding protein hnRNP-U (SAF-A) is directly bound to chromosomal DNA in vivo: a chemical cross-linking study', *Biochemistry,* 36(27), pp. 8276-8283.

Goldberg, M.W., Huttenlauch, I., Hutchison, C.J. and Stick, R. (2008) 'Filaments made from A- and B-type lamins differ in structure and organization', *J Cell Sci.,* 121(2), pp. 215-225.

Goldman, A.E., Moir, R.D., Montag-Lowy, M., Stewart, M. and Goldman, R.D. (1992) 'Pathway of incorporation of microinjected lamin A into the nuclear envelope', *The Journal of cell biology,* 119(4), pp. 725-735.

Goldman, R.D., Gruenbaum, Y. and Moir, R.D. (2002) 'Nuclear lamins: building blocks of nuclear structure and function', *Novartis Foundation symposium JID - 9807767,* 16, pp. 533-547.

Goldman, R.D., Shumaker, D.K., Erdos, M.R., Eriksson, M., Goldman, A.E., Gordon, L.B., Gruenbaum, Y., Khuon, S., Mendez, M., Varga, R. and Collins, F.S. (2004) 'Accumulation of mutant lamin A causes progressive changes in nuclear architecture in Hutchinson-Gilford progeria syndrome', *Proceedings of the National Academy of Sciences of the United States of America,* 101(24), pp. 8963-8968.

Gonzalez. L.C., Ghadaouia, S., Martinez, A., Rodier, F. (2015)' Premature aging/senescence in cancer cells facing therapy: good or bad?' *Biogerontology*. pp/. 9593-9599.

Gonzalo-Suaraz, I., Redwood, A.B. and Gonzalo, S. (2009) 'Loss of A-type lamins and genomic instability', *Cell cycle,* 8, pp. 3860-3865.

Gordon, L.B., Harling-Berg, C.J. and Rothman, F.G. (2008) 'Highlights of the 2007 Progeria Research Foundation scientific workshop: progress in translational science', *J Gerontol A Biol Sci Med Sci,* 63(8), pp. 777-787.

Gordon, L.B., Kleinman, M.E., Miller, D.T., Neuberg, D.S., Giobbie-Hurder, A., Gerhard-Herman, M., Smoot, L.B., Gordon, C.M., Cleveland, R., Snyder, B.D., Fligor, B., Bishop, W.R., Statkevich, P., Regen, A., Sonis, A., Riley, S., Ploski, C., Correia, A., Quinn, N., Ullrich, N.J., Nazarian, A., Liang, M.G., Huh, S.Y., Schwartzman, A. and Kieran, M.W. (2012) 'Clinical trial of a farnesyltransferase inhibitor in children with Hutchinson-Gilford progeria syndrome', *Proceedings of the National Academy of Sciences of the United States of America ,* 109(41), pp. 16666-16671.

Gordon, L.B., McCarten, K.M., Giobbie-Hurder, A., Machan, J.T., Campbell, S.E., Berns, S.D. and Kieran, M.W. (2007) 'Disease progression in Hutchinson-Gilford progeria syndrome: impact on growth and development', *Pediatrics,* 120(4), pp. 824-833.

Gotzmann, J. and Foisner, R. (2006) 'A-type lamin complexes and regenerative potential: a step towards understanding laminopathic diseases?', *Histochemistry and cell biology,* 125(1-2), pp. 33-41.

Greider, C.W. and Blackburn, E.H. (1989) 'A telomeric sequence in the RNA of Tetrahymena telomerase required for telomere repeat synthesis', *Nature,* 337(6205), pp. 331-337.

Grewal, S.I. and Elgin, S.C. (2002) 'Heterochromatin: new possibilities for the inheritance of structure', *Current opinion in genetics & development,* 12(2), pp. 178-187.

Gribnau, J., de Boer, E., Trimborn, T., Wijgerde, M., Milot, E., Grosveld, F. and Fraser, P. (1998) 'Chromatin interaction mechanism of transcriptional control in vivo', *The EMBO journal,* 17(20), pp. 6020-6027.

Griffith, J.D., Comeau, L., Rosenfield, S., Stansel, R.M., Bianchi, A., Moss, H. and De Lange, T. (1999) 'Mammalian telomeres end in a large duplex loop', *Cell,* 97(4), pp. 503-514.

Gromova, I.I., Thomsen, B. and Razin, S.V. (1995) 'Different topoisomerase II antitumor drugs direct similar specific long-range fragmentation of an amplified c-MYC gene locus in living cells and in high-salt-extracted nuclei', *Proceedings of the National Academy of Sciences of the United States of America,* 92(1), pp. 102-106.

Grossman, E., Medalia, O. and Zwerger, M. (2012) 'Functional architecture of the nuclear pore complex', *Annual review of biophysics,* 41, pp. 557-584.

Gruenbaum, Y. and Foisner, R. (2015) 'Lamins: Nuclear Intermediate Filament Proteins with Fundamental Functions in Nuclear Mechanics and Genome Regulation', *Annu Rev Biochem,* 13(14), pp. 1-34.

Gruenbaum, Y., Margalit, A., Goldman, R.D., Shumaker, D.K. and Wilson, K.L. (2005) 'The nuclear lamina comes of age', *Nature reviews.Molecular cell biology ,* 6(1), pp. 21-31.

Gruenbaum, Y., Goldman, R.D., Meyuhas, R., Mills, E., Margalit, A., Fridkin, A., Dayani, Y., Prokocimer, M. and Enosh, A. (2003) 'The Nuclear Lamina and Its Functions in the Nucleus', *International review of cytology,* 226(0), pp. 1-62.

Gruenbaum, Y. and Medalia, O. (2015) 'Lamins: the structure and protein complexes', *Current opinion in cell biology,* 32(0), pp. 7-12.

Grummt, I. (1998) 'Regulation of mammalian ribosomal gene transcription by RNA polymerase I', *Progress in nucleic acid research and molecular biology,* 62, pp. 109-154.

Grummt, I. and Längst, G. (2013) 'Epigenetic control of RNA polymerase I transcription in mammalian cells', *Biochimica et Biophysica Acta (BBA)-Gene Regulatory Mechanisms,* 1829(3), pp. 393-404.

Grunstein, M. (1998) 'Yeast heterochromatin: regulation of its assembly and inheritance by histones', *Cell,* 93(3), pp. 325-328.

Guarente, L. (1997) 'Link between aging and the nucleolus', *Genes & development,* 11(19), pp. 2449-2455.

Guelen, L., Pagie, L., Brasset, E., Meuleman, W., Faza, M.B., Talhout, W., Eussen, B.H., de Klein, A., Wessels, L., de Laat, W. and van Steensel, B. (2008) 'Domain organization of human chromosomes revealed by mapping of nuclear lamina interactions', *Nature,* 453(7197), pp. 948-951.

Gumbiner, B.M. (1996) 'Cell Adhesion: The Molecular Basis of Tissue Architecture and Morphogenesis', *Cell,* 84(3), pp. 345-357.

Habermann, F.A., Cremer, M., Walter, J., Kreth, G., von Hase, J., Bauer, K., Wienberg, J., Cremer, C., Cremer, T. and Solovei, I. (2001) 'Arrangements of macro- and microchromosomes in chicken cells', *Chromosome research : an international journal on the molecular, supramolecular and evolutionary aspects of chromosome biology,* 9(7), pp. 569-584.

Hacisuleyman, E., Goff, L.A., Trapnell, C., Williams, A., Henao-Mejia, J., Sun, L., McClanahan, P., Hendrickson, D.G., Sauvageau, M. and Kelley, D.R. (2014) 'Topological organization of multichromosomal regions by the long intergenic noncoding RNA Firre', *Nature structural & molecular biology,* 21(2), pp. 198-206.

Hahn, M., Dambacher, S., Dulev, S., Kuznetsova, A.Y., Eck, S., Worz, S., Sadic, D., Schulte, M., Mallm, J.P., Maiser, A., Debs, P., von Melchner, H., Leonhardt, H., Schermelleh, L., Rohr, K., Rippe, K., Storchova, Z. and Schotta, G. (2013) 'Suv4-20h2 mediates chromatin compaction and is important for cohesin recruitment to heterochromatin', *Genes & development,* 27(8), pp. 859-872.

Halaschek-Wiener, J. and Brooks-Wilson, A. (2007) 'Progeria of stem cells: stem cell exhaustion in Hutchinson-Gilford progeria syndrome', *The journals of gerontology.Series A, Biological sciences and medical sciences,* 62(1), pp. 3-8.

Haque, F., Lloyd, D.J., Smallwood, D.T., Dent, C.L., Shanahan, C.M., Fry, A.M., Trembath, R.C. and Shackleton, S. (2006) 'SUN1 interacts with nuclear lamin A and cytoplasmic nesprins to provide a physical connection between the nuclear lamina and the cytoskeleton', *Molecular and cellular biology,* 26(10), pp. 3738-3751.

Haraguchi, T., Koujin, T., Segura-Totten, M., Lee, K.K., Matsuoka, Y., Yoneda, Y., Wilson, K.L. and Hiraoka, Y. (2001) 'BAF is required for emerin assembly into the reforming nuclear envelope', *Journal of cell science,* 114(Pt 24), pp. 4575-4585.

Harborth, J., Elbashir, S.M., Bechert, K., Tuschl, T. and Weber, K. (2001) 'Identification of essential genes in cultured mammalian cells using small interfering RNAs', *Journal of cell science,* 114(Pt 24), pp. 4557-4565.

Harley, C.B., Futcher, A.B. and Greider, C.W. (1990) 'Telomeres shorten during ageing of human fibroblasts'.

Harr, J.C., Luperchio, T.R., Wong, X., Cohen, E., Wheelan, S.J. and Reddy, K.L. (2015) 'Directed targeting of chromatin to the nuclear lamina is mediated by

chromatin state and A-type lamins', *The Journal of cell biology,* 208(1), pp. 33-52.

Harris, C.A., Andryuk, P.J., Cline, S., Chan, H.K., Natarajan, A., Siekierka, J.J. and Goldstein, G. (1994) 'Three distinct human thymopoietins are derived from alternatively spliced mRNAs', *Proc Natl Acad Sci U S A,* 91(14), pp. 6283-6287.

Hasan, S., Güttinger, S., Mühlhäusser, P., Anderegg, F., Bürgler, S. and Kutay, U. (2006) 'Nuclear envelope localization of human UNC84A does not require nuclear lamins', *FEBS letters,* 580(5), pp. 1263-1268.

Hassan Ahmed, M. (2013) 'Discovery and restoration of aberrant nuclear structure and genome behaviour in breast cancer cells', *Discovery and restoration of aberrant nuclear structure and genome behaviour in breast cancer cells,* PhD Thesis.

Hastie, N.D., Dempster, M., Dunlop, M.G., Thompson, A.M., Green, D.K. and Allshire, R.C. (1990) 'Telomere reduction in human colorectal carcinoma and with ageing', *Nature,* 346(6287), pp. 866-868.

Hastings, G. (1904) 'Ateleiosis and progeria: continous youth and pre-mature old age', *Br Med J.,* 2, pp. 914-918.

He, D.C., Nickerson, J.A. and Penman, S. (1990) 'Core filaments of the nuclear matrix', *The Journal of cell biology,* 110(3), pp. 569-580.

Hegele, R.A., Cao, H., Liu, D.M., Costain, G.A., Charlton-Menys, V., Rodger, N.W. and Durrington, P.N. (2006) 'Sequencing of the reannotated LMNB2 gene reveals novel mutations in patients with acquired partial lipodystrophy', *The American Journal of Human Genetics,* 79(2), pp. 383-389.

Heitz, E. (1928) 'Translation: Heterochromatin of moss', *Jehrb Wiss Botanik,* 69, pp. 762-818.

Heng, H.H., Goetze, S., Ye, C.J., Liu, G., Stevens, J.B., Bremer, S.W., Wykes, S.M., Bode, J. and Krawetz, S.A. (2004) 'Chromatin loops are selectively anchored using scaffold/matrix-attachment regions', *Journal of cell science,* 117(Pt 7), pp. 999-1008.

Hennekam, R.C. (2006) 'Hutchinson-Gilford progeria syndrome: review of the phenotype', *American journal of medical genetics.Part A ,* 140, pp. 2603-2624.

Herbig, U., Jobling, W.A., Chen, B.P., Chen, D.J., Sedivy, J.M. (2004) 'Telomere shortening triggers senescence of human cells through a pathway involving ATM, p53, and p21(CIP1), but not p16(INK4a).' *Mol Cell* 14(4), pp. 501–513

Hernandez-Verdun, D. and Gautier, T. (1994) 'The chromosome periphery during mitosis', *Bioessays,* 16(3), pp. 179-185.

Herrmann, H. and Aebi, U. (2004) 'Intermediate filaments: molecular structure, assemly mechanism, and integration into functionally distinct intracellular scaffolds.', *Annual Review Biochemistry,* 73, pp. 749-789.

Hibino, Y., Ohzeki, H., Sugano, N. and Hiraga, K. (2000) 'Transcription modulation by a rat nuclear scaffold protein, P130, and a rat highly repetitive DNA component or various types of animal and plant matrix or scaffold attachment regions', *Biochemical and biophysical research communications,* 279(1), pp. 282-287.

Hirano, T. (2012) 'Chromosome territories meet a condensin', *PLoS genetics,* 8(8), pp. 1-2.

Hoffmann, K., Dreger, C.K., Olins, A.L., Olins, D.E., Shultz, L.D., Lucke, B., Karl, H., Kaps, R., Müller, D., Vayá, A., Aznar, J., Ware, R.E., Sotelo Cruz, N., Lindner, T.H., Herrmann, H., Reis, A. and Sperling, K. (2002) 'Mutations in the gene encoding the lamin B receptor produce an altered nuclear morphology in granulocytes (Pelger-Huët anomaly)', *Nat Genet.,* 31(4), pp. 410-414.

Hoffmann, K., Sperling, K., Olins, A.L. and Olins, D.E. (2007) 'The granulocyte nucleus and lamin B receptor: avoiding the ovoid', *Chromosoma,* 116(3), pp. 227-235.

Hohensinner, P.J., Goronzy, J.J. and Weyand, C.M. (2011) 'Telomere dysfunction, autoimmunity and aging', *Aging and disease,* 2(6), pp. 524-537.

Holaska, J.M., Lee, K.K., Kowalski, A.K. and Wilson, K.L. (2003) 'Transcriptional repressor germ cell-less (GCL) and barrier to autointegration factor (BAF) compete for binding to emerin in vitro', *J Biol Chem,* 278(9), pp. 6969-6975.

Holaska, J.M., Kowalski, A.K. and Wilson, K.L. (2004) 'Emerin caps the pointed end of actin filaments: evidence for an actin cortical network at the nuclear inner membrane', *PLoS biology,* 2(9), pp. e231.

Holmer, L. and Worman, H. (2001) 'Inner nuclear membrane proteins: functions and targeting', *Cellular and Molecular Life Sciences CMLS,* 58(12-13), pp. 1741-1747.

Horn, H.F., Brownstein, Z., Lenz, D.R., Shivatzki, S., Dror, A.A., Dagan-Rosenfeld, O., Friedman, L.M., Roux, K.J., Kozlov, S., Jeang, K.T., Frydman, M., Burke, B., Stewart, C.L. and Avraham, K.B. (2013) 'The LINC complex is essential for hearing', *The Journal of clinical investigation,* 123(2), pp. 740-750.

Hozák, P., Hassan, A.B., Jackson, D.A. and Cook, P.R. (1993) 'Visualization of replication factories attached to a nucleoskeleton', *Cell,* 73(2), pp. 361-373.

Hozak, P., Sasseville, A.M., Raymond, Y. and Cook, P.R. (1995) 'Lamin proteins form an internal nucleoskeleton as well as a peripheral lamina in human cells', *Journal of cell science,* 108 (Pt 2)(Pt 2), pp. 635-644.

Hsu, T.C. (1962) 'Differential rate in RNA synthesis between euchromatin and heterochromatin', *Experimental cell research,* 27(2), pp. 332-334.

Huang, S., Risques, R.A., Martin, G.M., Rabinovitch, P.S. and Oshima, J. (2008) 'Accelerated telomere shortening and replicative senescence in human fibroblasts overexpressing mutant and wild-type lamin A', *Experimental cell research,* 314(1), pp. 82-91.

Huang, Y., Cai, M., Clore, G.M. and Craigie, R. (2011) 'No interaction of barrier-to-autointegration factor (BAF) with HIV-1 MA, cone-rod homeobox (Crx) or MAN1-C in absence of DNA', *PloS one,* 6(9), pp. e25123.

Huber, M.D., Guan, T. and Gerace, L. (2009) 'Overlapping functions of nuclear envelope proteins NET25 (Lem2) and emerin in regulation of extracellular signal-regulated kinase signaling in myoblast differentiation', *Mol Cell Biol.,* 29(21), pp. 5718-5728.

Huisinga, K.L., Brower-Toland, B. and Elgin, S.C. (2006) 'The contradictory definitions of heterochromatin: transcription and silencing', *Chromosoma,* 115(2), pp. 110-122.

Hutchinson, J. (1886) 'Congenital Absence of Hair and Mammary Glands with Atrophic Condition of the Skin and its Appendages, in a Boy whose Mother had been almost wholly Bald from Alopecia Areata from the age of Six', *Medico-chirurgical transactions ,* 69, pp. 473-477.

Hutchison, C.J. and Worman, H.J. (2004) 'A-type lamins: guardians of the soma?', *Nature cell biology,* 6(11), pp. 1062-1067.

Hutchison, C. and Kill, I. (1989) 'Changes in the nuclear distribution of DNA polymerase alpha and PCNA/cyclin during the progress of the cell cycle, in a cell-free extract of Xenopus eggs', *Journal of cell science,* 93, pp. 605-613.

Ibrahim, M.X., Sayin, V.I., Akula, M.K., Liu, M., Fong, L.G., Young, S.G. and Bergo, M.O. (2013) 'Targeting isoprenylcysteine methylation ameliorates disease in a mouse model of progeria', *Science (New York, N.Y.),* 340(6138), pp. 1330-1333.

Imai, S., Nishibayashi, S., Takao, K., Tomifuji, M., Fujino, T., Hasegawa, M. and Takano, T. (1997) 'Dissociation of Oct-1 from the nuclear peripheral structure induces the cellular aging-associated collagenase gene expression.', *Mol Biol Cell.,* 8(12), pp. 2407-2419.

Ingram, D.A., Mead, L.E., Tanaka, H., Meade, V., Fenoglio, A., Mortell, K., Pollok, K., Ferkowicz, M.J., Gilley, D. and Yoder, M.C. (2004) 'Identification of a novel hierarchy of endothelial progenitor cells using human peripheral and umbilical cord blood', *Blood,* 104(9), pp. 2752-2760.

Jackson, D.A. (2003) 'The principles of nuclear structure', *Chromosome research : an international journal on the molecular, supramolecular and evolutionary aspects of chromosome biology ,* 11, pp. 387-401.

Jackson, D.A. and Cook, P.R. (1985) 'Transcription occurs at a nucleoskeleton', *The EMBO journal,* 4(4), pp. 919-925.

Jackson, D.A., Iborra, F.J., Manders, E.M. and Cook, P.R. (1998) 'Numbers and organization of RNA polymerases, nascent transcripts, and transcription units in HeLa nuclei', *Molecular biology of the cell,* 9(6), pp. 1523-1536.

James, T.C., Eissenberg, J.C., Craig, C., Dietrich, V., Hobson, A. and Elgin, S.C. (1989) 'Distribution patterns of HP1, a heterochromatin-associated nonhistone

chromosomal protein of Drosophila', *European journal of cell biology,* 50(1), pp. 170-180.

Jedrusik-Bode, M. (2013) 'Histone H1 and heterochromatin protein 1 (HP1) regulate specific gene expression and not global transcription', *Worm,* 2(2), pp. 1-5.

Jegou, T., Chung, I., Heuvelman, G., Wachsmuth, M., Gorisch, S.M., Greulich-Bode, K.M., Boukamp, P., Lichter, P. and Rippe, K. (2009) 'Dynamics of telomeres and promyelocytic leukemia nuclear bodies in a telomerase-negative human cell line', *Molecular biology of the cell,* 20(7), pp. 2070-2082.

Jenuwein, T. and Allis, C.D. (2001) 'Translating the histone code', *Science (New York, N.Y.),* 293(5532), pp. 1074-1080.

Jeyapalan, J.C., Sedivy, J.M. (2008) ' Cellular senescence and organismal aging.' *Mech Ageing Dev*. 129(7-8) pp. 467–474.

Jiang, M., Axe, T., Holgate, R., Rubbi, C.P., Okorokov, A.L., Mee, T. and Milner, J. (2001) 'P53 Binds the Nuclear Matrix in Normal Cells: Binding Involves the Proline-Rich Domain of P53 and Increases Following Genotoxic Stress', *Oncogene,* 20(39), pp. 5449-5458.

Jiang, X.R., Jimenez, G., Chang, E., Frolkis, M., Kusler, B., Sage, M., Beeche, M., Bodnar, A.G., Wahl, G.M., Tlsty, T.D. and Chiu, C.P. (1999) 'Telomerase expression in human somatic cells does not induce changes associated with a transformed phenotype', *Nature genetics,* 21(1), pp. 111-114.

Johnson, B.R., Nitta, R.T., Frock, R.L., Mounkes, L., Barbie, D.A., Stewart, C.L., Harlow, E. and Kennedy, B.K. (2004) 'A-type lamins regulate retinoblastoma protein function by promoting subnuclear localization and preventing proteasomal degradation', *Proceedings of the National Academy of Sciences of the United States of America,* 101(26), pp. 9677-9682.

Junera, H.R., Masson, C., Geraud, G. and Hernandez-Verdun, D. (1995) 'The three-dimensional organization of ribosomal genes and the architecture of the nucleoli vary with G1, S and G2 phases', *Journal of cell science JID - 0052457,* 108(11), pp. 3427-3441.

Jung, H.J., Coffinier, C., Choe, Y., Beigneux, A.P., Davies, B.S., Yang, S.H., Barnes, R.H.,2nd, Hong, J., Sun, T., Pleasure, S.J., Young, S.G. and Fong, L.G. (2012) 'Regulation of prelamin A but not lamin C by miR-9, a brain-specific microRNA', *Proceedings of the National Academy of Sciences of the United States of America,* 109(7), pp. E423-31.

Jung, H.J., Nobumori, C., Goulbourne, C.N., Tu, Y., Lee, J.M., Tatar, A., Wu, D., Yoshinaga, Y., de Jong, P.J., Coffinier, C., Fong, L.G. and Young, S.G. (2013) 'Farnesylation of lamin B1 is important for retention of nuclear chromatin during neuronal migration', *Proceedings of the National Academy of Sciences of the United States of America,* 110(21), pp. E1923-32.

Kandert, S., Luke, Y., Kleinhenz, T., Neumann, S., Lu, W., Jaeger, V.M., Munck, M., Wehnert, M., Muller, C.R., Zhou, Z., Noegel, A.A., Dabauvalle, M.C. and

Karakesisoglou, I. (2007) 'Nesprin-2 giant safeguards nuclear envelope architecture in LMNA S143F progeria cells', *Human molecular genetics JID - 9208958,* 16(23), pp. 2944-2959.

Kanoh, J. and Ishikawa, F. (2001) 'spRap1 and spRif1, recruited to telomeres by Taz1, are essential for telomere function in fission yeast', *Current Biology,* 11(20), pp. 1624-1630.

Karve, T.M. and Cheema, A.K. (2011) 'Small changes huge impact: the role of protein posttranslational modifications in cellular homeostasis and disease', *Journal of amino acids,* 2011, pp. 207691.

Katta, S.S., Smoyer, C.J. and Jaspersen, S.L. (2014) 'Destination: inner nuclear membrane', *Trends in cell biology,* 24(4), pp. 221-229.

Keller, C., Hyrien, O., Knippers, R. and Krude, T. (2002) 'Sitespecific and temporally controlled initiation of DNA replication in a human cell-free system', *Nucleic Acids Res.,* 30, pp. 2114-2123.

Kennedy, B.K., Barbie, D.A., Classon, M., Dyson, N. and Harlow, E. (2000) 'Nuclear organization of DNA replication in primary mammalian cells', *Genes & development,* 14(22), pp. 2855-2868.

Kiel, T., Busch, A., Meyer-Rachner, A. and Hübner, S. (2014) 'Laminopathy-inducing mutations reduce nuclear import of expressed prelamin A', *The international journal of biochemistry & cell biology,* 53, pp. 271-280.

Kieran, M.W., Gordon, L.,B. and Kleinmann, M. (2014) 'The role of farnesyltransferase inhibitor lonafarnib in the treatment of Progeria', *Drug Evaluations,* 2(1), pp. 95-105.

Kieran, M.W., Gordon, L. and Kleinman, M. (2007) 'New approaches to progeria', *Pediatrics,* 120(4), pp. 834-841.

Kilian, A., Bowtell, D.D., Abud, H.E., Hime, G.R., Venter, D.J., Keese, P.K., Duncan, E.L., Reddel, R.R. and Jefferson, R.A. (1997) 'Isolation of a candidate human telomerase catalytic subunit gene, which reveals complex splicing patterns in different cell types', *Human molecular genetics,* 6(12), pp. 2011-2019.

Kill, I.R. (1996) 'Localisation of the Ki-67 antigen within the nucleolus. Evidence for a fibrillarin-deficient region of the dense fibrillar component', *Journal of cell science,* 109(9), pp. 1253-1263.

Kill, I.R., Bridger, J.M., Campbell, K.H., Maldonado-Codina, G. and Hutchison, C.J. (1991) 'The timing of the formation and usage of replicase clusters in S-phase nuclei of human diploid fibroblasts', *Journal of cell science ,* 100, pp. 869-876.

Kill, I.R., Faragher, R.G. A., Lawrence, K. and Shall, S. (1994) 'The expression of proliferation-dependent antigens during the lifespan of normal and progeroid human fibroblasts in culture', *Journal of cell science,* 107 (Pt 2)(Pt 2), pp. 571-579.

Kill, I.R. and Shall, S. (1990) 'Senescent human diploid fibroblasts are able to support DNA synthesis and to express markers associated with proliferation', *Journal of cell science,* 97, pp. 473-478.

Kim, K.S., Seu, Y.B., Baek, S.H., Kim, M.J., Kim ,K.J., Kim, J.H., Kim, J.R. (2007) 'Induction of cellular senescence by insulin-like growth factor binding protein-5 through a p53-dependent mechanism.' *Mol. Biol. Cell* 18, pp. 4543–4552.

Kind, J. and Van Steensel, B. (2014) 'Stochastic genome-nuclear lamina interactions', *Nucleus,* 5(2), pp. 124-130.

King, C.R., Lemmer, J., Campbell, J.R. and Atkins, A.R. (1978) 'Osteosarcoma in a patient with Hutchinson-Gilford progeria', *Journal of medical genetics ,* 15(6), pp. 481-484.

King, M.C., Marks, J.H., Mandell, J.B. and New York Breast Cancer Study Group (2003) 'Breast and ovarian cancer risks due to inherited mutations in BRCA1 and BRCA2', *Science (New York, N.Y.),* 302(5645), pp. 643-646.

Kirkwood, T. (2015) 'Why can't we live forever?', *Scientific American,* 24, pp. 12-19.

Kirkwood, T.B. and Austad, S.N. (2000) 'Why do we age?', *Nature,* 408(6809), pp. 233-238.

Kirschner, J., Brune, T., Wehnert, M., Denecke, J., Wasner, C., Feuer, A., Marquardt, T., Ketelsen, U., Wieacker, P. and Bönnemann, C.G. (2005) 'p. S143F mutation in lamin A/C: a new phenotype combining myopathy and progeria', *Annals of Neurology,* 57(1), pp. 148-151.

Koch, A.J. and Holaska, J.M. (2014) 'Emerin in health and disease', *Seminars in cell & developmental biology.* Elsevier, 95-106.

Kochin, V., Shimi, T., Torvaldson, E., Adam, S.A., Goldman, A., Pack, C.G., Melo-Cardenas, J., Imanishi, S.Y., Goldman, R.D. and Eriksson, J.E. (2014) 'Interphase phosphorylation of lamin A', *J Cell Sci.,* 127(12), pp. 2683-2696.

Korenberg, J.R. and Rykowski, M.C. (1988) 'Human genome organization: Alu, lines, and the molecular structure of metaphase chromosome bands', *Cell,* 53(3), pp. 391-400.

Köster, S., Weitz, D.A., Goldman, R.D., Aebi, U. and Herrmann, H. (2015) 'Intermediate filament mechanics in vitro and in the cell: from coiled coils to filaments, fibers and networks', *Current opinion in cell biology,* 32(0), pp. 82-91.

Kotake, Y., Cao, R., Viatour, P., Sage, J., Zhang, Y. and Xiong, Y. (2007) 'pRB family proteins are required for H3K27 trimethylation and Polycomb repression complexes binding to and silencing p16INK4alpha tumor suppressor gene', *Genes & development,* 21(1), pp. 49-54.

Kracklauer, M.P., Link, J. and Alsheimer, M. (2013) 'Chapter Five - LINCing the Nuclear Envelope to Gametogenesis', *Current topics in developmental biology,* 102(0), pp. 127-157.

Kuilman, T., Michaloglou, C., Vredeveld, L.C., Douma, S., van Doorn, R., Desmet, C.J., Aarden, L.A., Mooi, W.J., Peeper, D.S. (2008) Oncogene-induced senescence relayed by an interleukin-dependent inflammatory network. *Cell* 133, pp. 1019– 1031.

Kumar, P. (2011) 'An Overview: Progeria', *Pharmacologyonline,* 3, pp. 176-184.

Kumaran, R.I., Muralikrishna, B. and Parnaik, V.K. (2002) 'Lamin A/C speckles mediate spatial organization of splicing factor compartments and RNA polymerase II transcription.', *J Cell Biol.,* 159(5), pp. 783-793.

Kumaran, R.I. and Spector, D.L. (2008) 'A genetic locus targeted to the nuclear periphery in living cells maintains its transcriptional competence', *The Journal of cell biology,* 180(1), pp. 51-65.

Lachner, M. and Jenuwein, T. (2002) 'The many faces of histone lysine methylation', *Current opinion in cell biology,* 14(3), pp. 286-298.

Lachner, M., O'Carroll, D., Rea, S., Mechtler, K. and Jenuwein, T. (2001) 'Methylation of histone H3 lysine 9 creates a binding site for HP1 proteins', *Nature,* 410(6824), pp. 116-120.

Laguri, C., Gilquin, B., Wolff, N., Romi-Lebrun, R., Courchay, K., Callebaut, I., Worman, H.J. and Zinn-Justin, S. (2001) 'Structural characterization of the LEM motif common to three human inner nuclear membrane proteins', *Structure,* 9(6), pp. 503-511.

Lam, Y.W. and Trinkle-Mulcahy, L. (2015) 'New insights into nucleolar structure and function', *F1000prime reports,* 7.

Lander, E.S., Linton, L.M., Birren, B., Nusbaum, C., Zody, M.C., Baldwin, J., Devon, K., Dewar, K., Doyle, M. and FitzHugh, W. (2001) 'Initial sequencing and analysis of the human genome', *Nature,* 409(6822), pp. 860-921.

Lansdorp, P.M. (2005) 'Major cutbacks at chromosome ends', *Trends in biochemical sciences,* 30(7), pp. 388-395.

Lattanzi, G., Columbaro, M., Mattioli, E., Cenni, V., Camozzi, D., Wehnert, M., Santi, S., Riccio, M., Del Coco, R., Maraldi, N.M., Squarzoni, S., Foisner, R. and Capanni, C. (2007) 'Pre-Lamin A processing is linked to heterochromatin organization', *Journal of cellular biochemistry,* 102(5), pp. 1149-1159.

Lebkowski, J.S. and Laemmli, U.K. (1982) 'Evidence for two levels of DNA folding in histone-depleted HeLa interphase nuclei', *Journal of Molecular Biology,* 156(2), pp. 309-324.

Lee, K.K. and Wilson, K.L. (2004) 'All in the family: evidence for four new LEM-domain proteins Lem2 (NET-25), Lem3, Lem4 and Lem5 in the human genome', *Symp Soc Exp Biol,* 56, pp. 329-339.

Lee, H.H., Kim, H.S., Kang, J.Y., Lee, B.I., Ha, J.Y., Yoon, H.J., Lim, S.O., Jung, G. and Suh, S.W. (2007) 'Crystal structure of human nucleophosmin-core reveals plasticity of the pentamer-pentamer interface', *Proteins ,* 69(3), pp. 672-678.

Lee, K.K., Starr, D., Cohen, M., Liu, J., Han, M., Wilson, K.L. and Gruenbaum, Y. (2002) 'Lamin-dependent localization of UNC-84, a protein required for nuclear migration in Caenorhabditis elegans', *Molecular biology of the cell,* 13(3), pp. 892-901.

Lee, M.S. and Craigie, R. (1998) 'A previously unidentified host protein protects retroviral DNA from autointegration', *Proceedings of the National Academy of Sciences of the United States of America,* 95(4), pp. 1528-1533.

LeRoy, G., Chepelev, I., DiMaggio, P.A., Blanco, M.A., Zee, B.M., Zhao, K. and Garcia, B.A. (2012) 'Proteogenomic characterization and mapping of nucleosomes decoded by Brd and HP1 proteins', *Genome Biol,* 13(8), pp. R68.

Levis, R., Hazelrigg, T. and Rubin, G.M. (1985) 'Effects of genomic position on the expression of transduced copies of the white gene of Drosophila', *Science (New York, N.Y.),* 229(4713), pp. 558-561.

Li, Y., Danzer, J.R., Alvarez, P., Belmont, A.S. and Wallrath, L.L. (2003) 'Effects of tethering HP1 to euchromatic regions of the Drosophila genome', *Development (Cambridge, England),* 130(9), pp. 1817-1824.

Liang, L., Zhang, H. and Gu, X. (2009) 'Homozygous LMNA mutation R527C in atypical Hutchinson–Gilford progeria syndrome: evidence for autosomal recessive inheritance', *Acta Paediatrica,* 98(8), pp. 1365-1368.

Lichter, P., Cremer, T., Borden, J., Manuelidis, L. and Ward, D.C. (1988) 'Delineation of individual human chromosomes in metaphase and interphase cells by in situ suppression hybridization using recombinant DNA libraries', *Human genetics JID - 7613873,* 80, pp. 224-234.

Lim, R.Y. and Fahrenkrog, B. (2006) 'The nuclear pore complex up close', *Current opinion in cell biology,* 18(3), pp. 342-347.

Lin, F., Blake, D.L., Callebaut, I., Skerjanc, I.S., Holmer, L., McBurney, M.W., Paulin-Levasseur, M. and Worman, H.J. (2000) 'MAN1, an inner nuclear membrane protein that shares the LEM domain with lamina-associated polypeptide 2 and emerin', *J Biol Chem,* 275(7), pp. 4840-4847.

Lin, F. and Worman, H.J. (1993) 'Structural organization of the human gene encoding nuclear lamin A and nuclear lamin C.', 268(22), pp. 16321-16326.

Lin, C.W. and Engelman, A. (2003) 'The barrier-to-autointegration factor is a component of functional human immunodeficiency virus type 1 preintegration complexes', *Journal of virology,* 77(8), pp. 5030-5036.

Lin, F. and Worman, H.J. (1997) 'Expression of Nuclear Lamins in Human Tissues and Cancer Cell Lines and Transcription from the Promoters of the Lamin A/C and B1 Genes', *Experimental cell research,* 236(2), pp. 378-384.

Liokatis, S., Edlich, C., Soupsana, K., Giannios, I., Panagiotidou, P., Tripsianes, K., Sattler, M., Georgatos, S.D. and Politou, A.S. (2012) 'Solution structure and molecular interactions of lamin B receptor Tudor domain', *J Biol Chem.,* 287(2), pp. 1032-1042.

Liu, Y., Drozdov, I., Shroff, R., Beltran, L. E., Shanahan, C.M. (2013) ' Prelamin A Accelerates Vascular Calcification Via Activation of the DNA Damage Response and Senescence-Associated Secretory Phenotype in Vascular Smooth Muscle Cells' *Circ Res*. 112, pp. 99-109.

Liu, B., Wang, J., Chan, K.M., Tjia, W.M., Deng, W., Guan, X., Huang, J.D., Li, K.M., Chau, P.Y. and Chen, D.J. (2005) 'Genomic instability in laminopathy-based premature aging', *Nat. Med,* 11, pp. 780-785.

Liu, Q., Kim, D.I., Syme, J., LuValle, P., Burke, B. and Roux, K.J. (2010) 'Dynamics of lamin-A processing following precursor accumulation', *PloS one,* 5(5), pp. e10874.

Liu, D., O'Connor, M.S., Qin, J. and Songyang, Z. (2004) 'Telosome, a mammalian telomere-associated complex formed by multiple telomeric proteins', *The Journal of biological chemistry,* 279(49), pp. 51338-51342.

Liu, J., Rolef-Ben Shahar, T., Riemer, D., Spann, P., Treinin, M., Weber, K., Fire, A. and Gruenbaum, Y. (2000) 'Essential roles for Caenorhabditis elegans lamin gene in nuclear organization, cell cycle progression, and spatial organization of nuclear pore complexes', *Mol Biol Cell,* 11, pp. 3937-3947.

Liu, Q., Pante, N., Misteli, T., Elsagga, M., Crisp, M., Hodzic, D., Burke, B. and Roux, K.J. (2007) 'Functional association of Sun1 with nuclear pore complexes', *The Journal of cell biology,* 178(5), pp. 785-798.

Liu, Y., Sanoff, H.K., Cho, H., et al., 2009. Expression of p16(INK4a) in peripheral blood T-cells is a biomarker of human aging. *Aging Cell,* 8 (4), pp. 439–448.

Lou, Z., Wei, J., Riethman, H., Baur, J.A., Voglauer, R., Shay, J.W. and Wright, W.E. (2009) 'Telomere length regulates ISG15 expression in human cells', *Aging,* 1(7), pp. 608-621.

Lude´rus, M.E., de Graaf, A., Mattia, E., den Blaauwen, J.L., Grande, M.A., de Jong, L. and Van Driel, R. (1992) 'Binding of matrix attachment regions to lamin B1', *Cell,* 70, pp. 949-959.

Luderus, M.E., den Blaauwen, J.L., de Smit, O.J., Compton, D.A. and van Driel, R. (1994) 'Binding of matrix attachment regions to lamin polymers involves single-stranded regions and the minor groove', *Molecular and cellular biology,* 14(9), pp. 6297-6305.

Luderus, M.E., van Steensel, B., Chong, L., Sibon, O.C., Cremers, F.F. and de Lange, T. (1996) 'Structure, subnuclear distribution, and nuclear matrix association of the mammalian telomeric complex', *The Journal of cell biology,* 135(4), pp. 867-881.

Luger, K., Mäder, A.W., Richmond, R.K., Sargent, D.F. and Richmond, T.J. (1997) 'Crystal structure of the nucleosome core particle at 2.8 Å resolution', *Nature,* 389(6648), pp. 251-260.

Luke, Y., Zaim, H., Karakesisoglou, I., Jaeger, V.M., Sellin, L., Lu, W., Schneider, M., Neumann, S., Beijer, A., Munck, M., Padmakumar, V.C., Gloy, J., Walz, G. and Noegel, A.A. (2008) 'Nesprin-2 Giant (NUANCE) maintains nuclear envelope architecture and composition in skin', *Journal of cell science,* 121(Pt 11), pp. 1887-1898.

Lund, E., Oldenburg, A.R., Delbarre, E., Freberg, C.T., Duband-Goulet, I., Eskeland, R., Buendia, B. and Collas, P. (2013) 'Lamin A/C-promoter interactions specify chromatin state-dependent transcription outcomes', *Genome research,* 23(10), pp. 1580-1589.

Luo, Y.B., Mastaglia, F.L. and Wilton, S.D. (2014) 'Normal and aberrant splicing of LMNA', *Journal of medical genetics,* 51(4), pp. 215-223.

Luporsi, E., André, F., Spyratos, F., Martin, P., Jacquemier, J., Penault-Llorca, F., Tubiana-Mathieu, N., Sigal-Zafrani, B., Arnould, L. and Gompel, A. (2012) 'Ki-67: level of evidence and methodological considerations for its role in the clinical management of breast cancer: analytical and critical review', *Breast cancer research and treatment,* 132(3), pp. 895-915.

Lutz, R.J., Trujillo, M.A., Denham, K.S., Wenger, L. and Sinensky, M. (1992) 'Nucleoplasmic localization of prelamin A: Implications for prenylation-dependent lamin A assembly into the nuclear lamina', *Proc Natl Acad Sci,* 89, pp. 3000-3004.

Ma, H., Siegel, A.J. and Berezney, R. (1999) 'Association of chromosome territories with the nuclear matrix. Disruption of human chromosome territories correlates with the release of a subset of nuclear matrix proteins', *The Journal of cell biology,* 146(3), pp. 531-542.

Maga, G. and Hubscher, U. (2003) 'Proliferating cell nuclear antigen (PCNA): a dancer with many partners', *Journal of cell science,* 116, pp. 3051-3060.

Mais, C., Wright, J.E., Prieto, J.L., Raggett, S.L. and McStay, B. (2005) 'UBF-binding site arrays form pseudo-NORs and sequester the RNA polymerase I transcription machinery', *Genes & development,* 19(1), pp. 50-64.

Maison, C. and Almouzni, G. (2004) 'HP1 and the dynamics of heterochromatin maintenance', *Nature reviews Molecular cell biology,* 5(4), pp. 296-305.

Malhas, A., Lee, C.F., Sanders, R., Saunders, N.J. and Vaux, D.J. (2007) 'Defects in lamin B1 expression or processing affect interphase chromosome position and gene expression', *J Cell Biol.,* 176(5), pp. 593-603.

Malhas, A.N., Lee, C.F. and Vaux, D.J. (2009) 'Lamin B1 controls oxidative stress responses via Oct-1', *J Cell Biol.,* 184(1), pp. 45-55.

Malone, C.J., Fixsen, W.D., Horvitz, H.R. and Han, M. (1999) 'UNC-84 localizes to the nuclear envelope and is required for nuclear migration and anchoring during C. elegans development', *Development (Cambridge, England),* 126(14), pp. 3171-3181.

Malyavantham, K.S., Bhattacharya, S., Barbeitos, M., Mukherjee, L., Xu, J., Fackelmayer, F.O. and Berezney, R. (2008) 'Identifying functional neighborhoods within the cell nucleus: Proximity analysis of early S-phase replicating chromatin domains to sites of transcription, RNA polymerase II, HP1γ, matrin 3 and SAF-A', *Journal of cellular biochemistry,* 105(2), pp. 391-403.

Malyavanthama, K.S., Bhattacharyaa, S. and Berezney, R. (2010) 'The architecture of functional neighborhoods within the mammalian cell nucleus', *Adv Enzyme Regul,* 50(1), pp. 126-134.

Mancini, M.A., Shan, B., Nickerson, J.A., Penman, S. and Lee, W.H. (1994) 'The retinoblastoma gene product is a cell cycle-dependent, nuclear matrix-associated protein', *Proceedings of the National Academy of Sciences of the United States of America,* 91(1), pp. 418-422.

Manilal, S., Sewry, C.A., Pereboev, A., Man, N., Gobbi, P., Hawkes, S., Love, D.R. and Morris, G.E. (1999) 'Distribution of emerin and lamins in the heart and implications for Emery-Dreifuss muscular dystrophy', *Hum Mol Genet,* 8(2), pp. 353-359.

Manilal, S., Nguyen, T.M., Sewry, C.A. and Morris, G.E. (1996) 'The Emery-Dreifuss muscular dystrophy protein, emerin, is a nuclear membrane protein', *Hum Mol Genet.,* 5(6), pp. 801-808.

Mansharamani, M. and and Wilson, K.L. (2005) 'Direct Binding of Nuclear Membrane Protein MAN1 to Emerin *in Vitro* and Two Modes of Binding to Barrier-to-Autointegration Factor', *The Journal of Biological Chemistry,* 280(14), pp. 13863-13870.

Mansharamani, M. and Wilson, K.L. (2005) 'Direct binding of nuclear membrane protein MAN1 to emerin in vitro and two modes of binding to barrier-to-autointegration factor', *J Biol Chem,* 280(14), pp. 13863-13870.

Maraldi, N.M. and Lattanzi, G. (2005) 'Linkage of lamins to fidelity of gene transcription', *Critical reviews in eukaryotic gene expression,* 15(4), pp. 277-294.

Margalit, A., Segura-Totten, M., Gruenbaum, Y. and Wilson, K.L. (2005a) 'Barrier-to-autointegration factor is required to segregate and enclose chromosomes within the nuclear envelope and assemble the nuclear lamina', *Proceedings of the National Academy of Sciences of the United States of America,* 102(9), pp. 3290-3295.

Margalit, A., Vlcek, S., Gruenbaum, Y. and Foisner, R. (2005b) 'Breaking and making of the nuclear envelope', *Journal of cellular biochemistry JID - 8205768,* 95(3), pp. 454-465.

Margalit, A., Brachner, A., Gotzmann, J., Foisner, R. and Gruenbaum, Y. (2007) 'Barrier-to-autointegration factor – a BAFfling little protein', *Trends in cell biology,* 17(4), pp. 202-208.

Margueron, R. and Reinberg, D. (2011) 'The Polycomb complex PRC2 and its mark in life', *Nature,* 469(7330), pp. 343-349.

Marino, G., Ugalde, A.P., Fernandez, A.F., Osorio, F.G., Fueyo, A., Freije, J.M. and Lopez-Otin, C. (2010) 'Insulin-like growth factor 1 treatment extends longevity in a mouse model of human premature aging by restoring somatotroph axis function', *Proceedings of the National Academy of Sciences of the United States of America,* 107(37), pp. 16268-16273.

Markiewicz, E., Dechat, T., Foisner, R., Quinlan, R.A. and Hutchison, C.J. (2002) 'Lamin A/C binding protein LAP2α is required for nuclear anchorage of retinoblastoma protein.', *Mol Biol Cell,* 13, pp. 4401-4413.

Martin, C. and Zhang, Y. (2005) 'The diverse functions of histone lysine methylation', *Nat. Rev. Mol. Cell Biol,* 6, pp. 838-849.

Martins, S., Eikvar, S., Furukawa, K. and Collas, P. (2003) 'HA95 and LAP2B mediate a novel chromatin-nuclear envelope interaction impicated in initiation of DNA replication', *J Cell Biol,* 160, pp. 177-188.

Mattern, K.A., van der Kraan, I., Schul, W., de Jong, L. and van Driel, R. (1999) 'Spatial organization of four hnRNP proteins in relation to sites of transcription, to nuclear speckles, and to each other in interphase nuclei and nuclear matrices of HeLa cells', *Experimental cell research,* 246(2), pp. 461-470.

Mattioli, E., Columbaro, M., Capanni, C., Maraldi, N.M., Cenni, V., Scotlandi, K., Marino, M.T., Merlini, L., Squarzoni, S. and Lattanzi, G. (2011) 'Prelamin A-mediated recruitment of SUN1 to the nuclear envelope directs nuclear positioning in human muscle', *Cell death and differentiation,* 18, pp. 1305-1315.

Mattock, H., Jares, P., Zheleva, D.I., Lane, D.P., Warbrick, E. and Blow, J.J. (2001) 'Use of peptides from p21 (Waf1/Cip1) to investigate PCNA function in Xenopus egg extracts', *Experimental cell research,* 265(2), pp. 242-251.

Mazereeuw-Hautier, J., Wilson, L.C., Mohammed, S., Smallwood, D.F., Shackleton, S., Atherton, D.J. and Harper, J.I. (2007) 'Hutchinson-Gilford progeria syndrome: clinical findings in three patients carrying the G608G mutation in LMNA and review of the literature', *The British journal of dermatology ,* 156(6), pp. 1308-1314.

McClintock, D., Ratner, D., Lokuge, M., Owens, D.M., Gordon, L.B., Collins, F.S. and Djabali, K. (2007) 'The mutant form of lamin A that causes Hutchinson-Gilford progeria is a biomarker of cellular aging in human skin', *PloS one ,* 2(12), pp. 1-20.

McCord, R.P., Nazario-Toole, A., Zhang, H., Chines, P.S., Zhan, Y., Erdos, M.R., Collins, F.S., Dekker, J. and Cao, K. (2013) 'Correlated alterations in genome

organization, histone methylation, and DNA-lamin A/C interactions in Hutchinson-Gilford progeria syndrome', *Genome research,* 23(2), pp. 260-269.

McDonald, D., Carrero, G., Andrin, C., de Vries, G. and Hendzel, M.J. (2006) 'Nucleoplasmic beta-actin exists in a dynamic equilibrium between low-mobility polymeric species and rapidly diffusing populations', *The Journal of cell biology,* 172(4), pp. 541-552.

McIlrath, J., S. D. Bouffler, E. Samper, A. Cuthbert, A. Wojcik, I. Szumiel, P. E. Bryant, A. C. Riches, A. Thompson, M. A. Blasco, R. F. Newbold and P. Slijepcevic (2001). "Telomere length abnormalities in mammalian radiosensitive cells." *Cancer Res,* 61(3): 912-915.

McKeon, F.D., Kirschner, M.W. and Caput, D. (1986) 'Homologies in both primary and secondary structure between nuclear envelope and intermediate filament proteins.', *Nature,* 319(6053), pp. 463-468.

Meaburn, K.J., Cabuy, E., Bonne, G., Levy, N., Morris, G.E., Novelli, G., Kill, I.R. and Bridger, J.M. (2007) 'Primary laminopathy fibroblasts display altered genome organization and apoptosis', *Aging cell,* 6, pp. 139-153.

Meaburn, K.J., Levy, N., Toniolo, D. and Bridger, J.M. (2005) 'Chromosome positioning is largely unaffected in lymphoblastoid cell lines containing emerin or A-type lamin mutations', *Biochemical Society transactions ,* 33(6), pp. 1438-1440.

Mehta, I.S., Amira, M., Harvey, A.J. and Bridger, J.M. (2010) 'Rapid chromosome territory relocation by nuclear motor activity in response to serum removal in primary human fibroblasts', *Genome biology,* 11(1), pp. 1-23.

Mehta, I.S., Bridger, J.M. and Kill, I.R. (2009) 'Progeria, the nucleolus and farnesyltransferase inhibitors', *Biochemical Society transactions,* 38(Pt 1), pp. 287-291.

Mehta, I.S., Eskiw, C.H., Arican, H.D., Kill, I.R. and Bridger, J.M. (2011) 'Farnesyltransferase inhibitor treatment restores chromosome territory positions and active chromosome dynamics in Hutchinson-Gilford progeria syndrome cells', *Genome biology ,* 12(8), pp. 1-23.

Mehta, I.S., Figgitt, M., Clements, C.S., Kill, I.R. and Bridger, J.M. (2007) 'Alterations to nuclear architecture and genome behavior in senescent cells', *Annals of the New York Academy of Sciences ,* 1100, pp. 250-263.

Meinke, P. (2015) 'Nucleoskeleton dynamics and functions in health and disease', *Cell Health and Cytoskeleton,* 7, pp. 55-69.

Meister, P. and Taddei, A. (2013) 'Building silent compartments at the nuclear periphery: a recurrent theme', *Current opinion in genetics & development,* 23(2), pp. 96-103.

Mejat, A. and Misteli, T. (2010) 'LINC complexes in health and disease', *Nucleus (Austin, Tex.) ,* 1(1), pp. 40-52.

Mellad, J.A., Warren, D.T. and Shanahan, C.M. (2011) 'Nesprins LINC the nucleus and cytoskeleton', *Current opinion in cell biology,* 23(1), pp. 47-54.

Mendelsohn, A.R. and Larrick, J.W. (2012) 'Dissecting mammalian target of rapamycin to promote longevity', *Rejuvenation research,* 15(3), pp. 334-337.

Mewborn, S.K., Puckelwartz, M.J., Abuisneineh, F., Fahrenbach, J.P., Zhang, Y., MacLeod, H., Dellefave, L., Pytel, P., Selig, S., Labno, C.M., Reddy, K., Singh, H. and McNally, E. (2010) 'Altered chromosomal positioning, compaction, and gene expression with a lamin A/C gene mutation', *PloS one,* 5(12), pp. 1-13.

Meyerzon, M., Fridolfsson, H.N., Ly, N., McNally, F.J. and Starr, D.A. (2009) 'UNC-83 is a nuclear-specific cargo adaptor for kinesin-1-mediated nuclear migration', *Development,* 136(16), pp. 2725-2733.

Michaloglou, C., Vredeveld, L.C.W., Mooi, W.J., Peeper, D.S.(2008) ' BRAF(E600) in benign and malignant human tumours.' *Oncogene,* 27, pp. 877–895

Mika, S. and Rost, B. (2005) 'NMPdb: Database of Nuclear Matrix Proteins', *Nucleic acids research,* 33(Database issue), pp. 160-163.

Miki, Y., Swensen, J., Shattuck-Eidens, D., Futreal, P.A., Harshman, K., Tavtigian, S., Liu, Q., Cochran, C., Bennett, L.M. and Ding, W. (1994) 'A strong candidate for the breast and ovarian cancer susceptibility gene BRCA1', *Science (New York, N.Y.),* 266(5182), pp. 66-71.

Min, J., Choi, E.S., Hwang, K., Kim, J., Sampath, S., Venkitaraman, A.R. and Lee, H. (2012) 'The breast cancer susceptibility gene BRCA2 is required for the maintenance of telomere homeostasis', *The Journal of biological chemistry,* 287(7), pp. 5091-5101.

Mirkovitch J, Mirault ME, Laemmli UK (1984) ' Organization of the higher-order chromatin loop: specific DNA attachment sites on nuclear scaffold.' *Cell* , 39: 223-232.

Mislow, J.M.K., Holaska, J.M., Kim, M.S., Lee, K.K., Segura-Totten, M., Wilson, K.L. and and McNally, E.M. (2002) 'Nesprin-1a self-associates and binds directly to emerin and lamin A in vitro.', *FEBS Lett.,* 525, pp. 135-140.

Moir, R.D., Montag-Lowy, M. and Goldman, R.D. (1994) 'Dynamic properties of nuclear lamins: lamin B is associated with sites of DNA replication.', *J Cell Biol,* 125(6), pp. 1201-1212.

Moir, R.D., Yoon, M., Khuon, S. and Goldman, R.D. (2000) 'Nuclear lamins A and B1: different pathways of assembly during nuclear envelope formation in living cells', *The Journal of cell biology,* 151(6), pp. 1155-1168.

Monga, D., Mehan, S. and Khanna, D. (2015) 'HUTCHINSON GILFORD PROGERIA SYNDROME: A FUTURE PARADIGM FOR DRUG DISCOVERY', *INTERNATIONAL JOURNAL OF RECENT ADVANCES IN PHARMACEUTICAL RESEARCH,* 5(1), pp. 9-21.

Morales, J.C., Xia, Z., Lu, T., Aldrich, M.B., Wang, B., Rosales, C., Kellems, R.E., Hittelman, W.N., Elledge, S.J. and Carpenter, P.B. (2003) 'Role for the BRCA1 C-terminal repeats (BRCT) protein 53BP1 in maintaining genomic stability', *The Journal of biological chemistry,* 278(17), pp. 14971-14977.

Morton, N.E. (1991) 'Parameters of the human genome', *Proceedings of the National Academy of Sciences of the United States of America,* 88(17), pp. 7474-7476.

Moulson, C.L., Fong, L.G., Gardner, J.M., Farber, E.A., Go, G., Passariello, A., Grange, D.K., Young, S.G. and Miner, J.H. (2007) 'Increased progerin expression associated with unusual LMNA mutations causes severe progeroid syndromes', *Human mutation,* 28(9), pp. 882-889.

Moyzis, R.K., Buckingham, J.M., Cram, L.S., Dani, M., Deaven, L.L., Jones, M.D., Meyne, J., Ratliff, R.L. and Wu, J.R. (1988) 'A highly conserved repetitive DNA sequence, (TTAGGG)n, present at the telomeres of human chromosomes', *Proceedings of the National Academy of Sciences of the United States of America,* 85(18), pp. 6622-6626.

Muck, C., Micutkova, L., Zwerschke, W., Jansen-Durr, P. (2008) 'Role of insulin-like growth factor binding protein-3 in human umbilical vein endothelial cell senescence.' *Rejuvenation Res.* 11, pp. 449–453.

Mukherjee, A.B. and Costello, C. (1998) 'Aneuploidy analysis in fibroblasts of human premature aging syndromes by FISH during in vitro cellular aging', *Mechanisms of ageing and development,* 103(2), pp. 209-222.

Murata, S., Nakazawa, T., Ohno, N., Terada, N., Iwashina, M., Mochizuki, K., Kondo, T., Nakamura, N., Yamane, T. and Iwasa, S. (2007) 'Conservation and alteration of chromosome territory arrangements in thyroid carcinoma cell nuclei', *Thyroid,* 17(6), pp. 489-496.

Nakamura, K.D., Turturro, A. and Hart, R.W. (1988) 'Elevated c-myc expression in progeria fibroblasts', *Biochemical and biophysical research communications,* 155(2), pp. 996-1000.

Navarro, C.L., Cadinanos, J., De Sandre-Giovannoli, A., Bernard, R., Courrier, S., Boccaccio, I., Boyer, A., Kleijer, W.J., Wagner, A., Giuliano, F., Beemer, F.A., Freije, J.M., Cau, P., Hennekam, R.C., Lopez-Otin, C., Badens, C. and Levy, N. (2005) 'Loss of ZMPSTE24 (FACE-1) causes autosomal recessive restrictive dermopathy and accumulation of Lamin A precursors', *Human molecular genetics,* 14(11), pp. 1503-1513.

Nelson, G., Wordsworth, J., Wang C., Jurk D., Lawless, C., Martin-Ruiz, C., and Von Zglinicki T. (2012) ' A senescent cell bystander effect: senescence-induced senescence ' , Aging cells, 11(2), pp. 345–349.

Németh, A., Conesa, A., Santoyo-Lopez, J., Medina, I., Montaner, D., Péterfia, B., Solovei, I., Cremer, T., Dopazo, J. and Längst, G. (2010) 'Initial genomics of the human nucleolus', *PLoS genetics,* 6(3), pp. e1000889.

Newport, J.W., Wilson, K.L. and and Dunphy, W.G. (1990) 'A lamin-independent pathway for nuclear envelope assembly', *Cell Biology,* 111, pp. 2247-2259.

Nickerson, J. (2001) 'Experimental observations of a nuclear matrix', *Journal of cell science,* 114(Pt 3), pp. 463-474.

Nickerson, J.A., Krockmalnic, G., Wan, K.M. and Penman, S. (1997) 'The nuclear matrix revealed by eluting chromatin from a cross-linked nucleus', *Proceedings of the National Academy of Sciences of the United States of America,* 94(9), pp. 4446-4450.

Nigg, E.A., Kitten, G.T. and Vorburger, K. (1992) '
Targeting lamin proteins to the nuclear envelope: the role of CaaX box modifications.', *Biochem Soc Trans,* 20(2), pp. 500-504.

Nikolakaki, E., Simos, G., Georgatos, S.D. and Giannakouros, T. (1996) 'A nuclear envelope-associated kinase phosphorylates arginine-serine motifs and modulates interactions between the lamin B receptor and other nuclear proteins', *J Biol Chem,* 271(4), pp. 8365-8372.

Nili, E., Cojocaru, G.S., Kalma, Y., Ginsberg, D., Copeland, N.G., Gilbert, D.J., Jenkins, N.A., Berger, R., Shaklai, S., Amariglio, N., Brok-Simoni, F., Simon, A.J. and Rechavi, G. (2001) 'Nuclear membrane protein LAP2beta mediates transcriptional repression alone and together with its binding partner GCL (germ-cell-less)', *J Cell Sci.,* 114(18), pp. 3297-3307.

Noma, K., Allis, C.D. and Grewal, S.I. (2001) 'Transitions in distinct histone H3 methylation patterns at the heterochromatin domain boundaries', *Science (New York, N.Y.),* 293(5532), pp. 1150-1155.

Noordermeer, D., Leleu, M., Splinter, E., Rougemont, J., De Laat, W. and Duboule, D. (2011) 'The dynamic architecture of Hox gene clusters', *Science (New York, N.Y.),* 334(6053), pp. 222-225.

Nussinov, R., Tsai, C., Xin, F. and Radivojac, P. (2012) 'Allosteric post-translational modification codes', *Trends in biochemical sciences,* 37(10), pp. 447-455.

Oakes, C.C., Smiraglia, D.J., Plass, C., Trasler, J.M. and Robaire, B. (2003) 'Aging results in hypermethylation of ribosomal DNA in sperm and liver of male rats', *Proceedings of the National Academy of Sciences of the United States of America,* 100(4), pp. 1775-1780.

Obrdlik, A., Kukalev, A., Louvet, E., Farrants, A.K., Caputo, L. and Percipalle, P. (2008) 'The histone acetyltransferase PCAF associates with actin and hnRNP U for RNA polymerase II transcription', *Molecular and cellular biology,* 28(20), pp. 6342-6357.

Ojani, M. (2012) 'Relationship between DNA damage response and telomere maintenance', *PhD thesis,* .

Olins, A.L., Rhodes, G., Welch, D.B., Zwerger, M. and Olins, D.E. (2010) 'Lamin B receptor: multi-tasking at the nuclear envelope', *Nucleus (Austin, Tex.) JID - 101518322,* 1(1), pp. 53-70.

Olive, M., Harten, I., Mitchell, R., Beers, J.K., Djabali, K., Cao, K., Erdos, M.R., Blair, C., Funke, B., Smoot, L., Gerhard-Herman, M., Machan, J.T., Kutys, R., Virmani, R., Collins, F.S., Wight, T.N., Nabel, E.G. and Gordon, L.B. (2010) 'Cardiovascular pathology in Hutchinson-Gilford progeria: correlation with the vascular pathology of aging', *Arteriosclerosis, Thrombosis, and Vascular Biology,* 30(11), pp. 2301-2309.

Olovnikov, A.M. (1971) 'Principle of marginotomy in template synthesis of polynucleotides', *Doklady Akademii nauk SSSR,* 201(6), pp. 1496-1499.

Osborne, C.S., Chakalova, L., Mitchell, J.A., Horton, A., Wood, A.L., Bolland, D.J., Corcoran, A.E. and Fraser, P. (2007) 'Myc dynamically and preferentially relocates to a transcription factory occupied by Igh', *PLoS biology,* 5(8), pp. e192.

Ostlund, C., Ellenberg, J., Hallberg, E., Lippincott-Schwartz, J. and Worman, H.J. (1999) 'Intracellular trafficking of emerin, the Emery-Dreifuss muscular dystrophy protein', *Cell sci,* 112(11), pp. 1709-1719.

Ostlund, C., Sullivan, T., Stewart, C.L. and Worman, H.J. (2006) 'Dependence of diffusional mobility of integral inner nuclear membrane proteins on A-type lamins.', *Biochemistry,* 45, pp. 1374-1382.

O'Sullivan, J.N., Bronner, M.P., Brentnall, T.A., Finley, J.C., Shen, W., Emerson, S., Emond, M.J., Gollahon, K.A., Moskovitz, A.H. and Crispin, D.A. (2002) 'Chromosomal instability in ulcerative colitis is related to telomere shortening', *Nature genetics,* 32(2), pp. 280-284.

O'Sullivan, R.J. and Karlseder, J. (2010) 'Telomeres: protecting chromosomes against genome instability', *Nature reviews Molecular cell biology,* 11(3), pp. 171-181.

Ottaviani, D., Lever, E., Takousis, P. and Sheer, D. (2008) 'Anchoring the genome', *Genome biology,* 9(1), pp. 201-2008-9-1-201.

Ouellette, M.M., McDaniel, L.D., Wright, W.E., Shay, J.W. and Schultz, R.A. (2000) 'The establishment of telomerase-immortalised cell lines representing human chromosome instability syndromes', *Human molecular genetics ,* 9(3), pp. 403-411.

Ozaki, T., Saijo, M., Murakami, K., Enomoto, H., Taya, Y. and and Sakiyama, S. (1994) 'Complex formation between lamin A and the retinoblastoma gene product: identification of the domain on lamin A required for its interaction', *Oncogene,* 140, pp. 3-9.

Ozawa, R., Hayashi, Y.K., Ogawa, M., Kurokawa, R., Matsumoto, H., Noguchi, S., Nonaka, I. and Nishino, I. (2006) 'Emerin-lacking mice show minimal motor and

cardiac dysfunctions with nuclear-associated vacuoles', *The American journal of pathology,* 168(3), pp. 907-917.

Padmakumar, V.C., Libotte, T., Lu, W., Zaim, H., Abraham, S., Noegel, A.A., Gotzmann, J., Foisner, R. and Karakesisoglou, I. (2005) 'The inner nuclear membrane protein Sun1 mediates the anchorage of Nesprin-2 to the nuclear envelope', *Journal of cell science,* 118, pp. 3419-3430.

Palm, W. and de Lange, T. (2008) 'How shelterin protects mammalian telomeres', *Annual Review of Genetics,* 42, pp. 301-334.

Parada, L.A. and Misteli, T. (2002) 'Chromosome positioning in the interphase nucleus', *Trends in cell biology,* 12(9), pp. 425-432.

Park, Y., Hayashi, Y.K., Bonne, G., Arimura, T., Noguchi, S., Nonaka, I. and Nishino, I. (2009) 'Autophagic degradation of nuclear components in mammalian cells', *Autophagy,* 5(6), pp. 795-804.

Parsch, D., Brassat U FAU - Brummendorf,,T.H., FAU, B.T. and Fellenberg, J. (2008) 'Consequences of telomerase inhibition by BIBR1532 on proliferation and chemosensitivity of chondrosarcoma cell lines', *Cancer investigation JID - 8307154,* 26, pp. 590-596.

Passos, J.F., Nelson, G., Wang, C., Richter, T., Simillion, C., Proctor, C.J., Miwa, S., Olijslagers, S., Hallinan, J., Wipat, A., Saretzki, G., Rudolph, K.L., Kirkwood, T.B., von Zglinicki, T. (2010) Feedback between p21 and reactive oxygen production is necessary for cell senescence. *Mol. Syst. Biol*. 6, 347.

Paulin-Levasseur, M., Blake, D.L., Julien, M. and Rouleau, L. (1996) 'The MAN antigens are non-lamin constituents of the nuclear lamina in vertebrate cells', *Chromosoma,* 104(5), pp. 367-379.

Paull, T.T., Rogakou, E.P., Yamazaki, V., Kirchgessner, C.U., Gellert, M. and Bonner, W.M. (2000) 'A critical role for histone H2AX in recruitment of repair factors to nuclear foci after DNA damage', *Current Biology,* 10(15), pp. 886-895.

Pekovic, V., Harborth, J., Broers, J.L., Ramaekers, F.C., van Engelen, B., Lammens, M., von Zglinicki, T., Foisner, R. and Hutchison, C.a.M. (2007) 'Nucleoplasmic LAP2alpha-lamin A complexes are required to maintain a proliferative state in human fibroblasts', *Journal of Cell Biology,* 176(2), pp. 163-172.

Penkner, A., Tang, L., Novatchkova, M., Ladurner, M., Fridkin, A., Gruenbaum, Y., Schweizer, D., Loidl, J. and Jantsch, V. (2007) 'The nuclear envelope protein Matefin/SUN-1 is required for homologous pairing in C. elegans meiosis', *Developmental cell,* 12(6), pp. 873-885.

Pereira, S., Bourgeois, P., Navarro, C., Esteves-Vieira, V., Cau, P., De Sandre-Giovannoli, A. and Lévy, N. (2008) 'HGPS and related premature aging disorders: From genomic identification to the first therapeutic approaches', *Mechanisms of ageing and development,* 129(7–8), pp. 449-459.

Peric-Hupkes, D., Meuleman, W., Pagie, L., Bruggeman, S.W., Solovei, I., Brugman, W., Gräf, S., Flicek, P., Kerkhoven, R.M. and van Lohuizen, M. (2010) 'Molecular maps of the reorganization of genome-nuclear lamina interactions during differentiation', *Molecular cell,* 38(4), pp. 603-613.

Peters, A.H., O'Carroll, D., Scherthan, H., Mechtler, K., Sauer, S., Schöfer, C., Weipoltshammer, K., Pagani, M., Lachner, M. and Kohlmaier, A. (2001) 'Loss of the Suv39h histone methyltransferases impairs mammalian heterochromatin and genome stability', *Cell,* 107(3), pp. 323-337.

Picoraro, J.A. and Chung, W.K. (2015) 'Delineation of New Disorders and Phenotypic Expansion of Known Disorders through Whole Exome Sequencing', *Current Genetic Medicine Reports,* 3(4), pp. 209-218.

Plasilova, M., Chattopadhyay, C., Pal, P., Schaub, N.A., Buechner, S.A., Mueller, H., Miny, P., Ghosh, A. and Heinimann, K. (2004) 'Homozygous missense mutation in the lamin A/C gene causes autosomal recessive Hutchinson-Gilford progeria syndrome', *Journal of medical genetics,* 41(8), pp. 609-614.

Pliss, A., Fritz, A.J., Stojkovic, B., Ding, H., Mukherjee, L., Bhattacharya, S., Xu, J. and Berezney, R. (2015) 'Non-Random Patterns in the Distribution of NOR-Bearing Chromosome Territories in Human Fibroblasts: A Network Model of Interactions', *Journal of cellular physiology,* 230(2), pp. 427-439.

Prieto, J.L. and McStay, B. (2007) 'Recruitment of factors linking transcription and processing of pre-rRNA to NOR chromatin is UBF-dependent and occurs independent of transcription in human cells', *Genes & development,* 21(16), pp. 2041-2054.

Puckelwartz, M.J., Depreux, F.F. and McNally, E.M. (2011) 'Gene expression, chromosome position and lamin A/C mutations', *Nucleus (Austin, Tex.) ,* 2(3), pp. 162-167.

Puckelwartz, M.J., Kessler, E., Zhang, Y., Hodzic, D., Randles, K.N., Morris, G., Earley, J.U., Hadhazy, M., Holaska, J.M., Mewborn, S.K., Pytel, P. and McNally, E.M. (2009) 'Disruption of nesprin-1 produces an Emery Dreifuss muscular dystrophy-like phenotype in mice', *Human molecular genetics,* 18(4), pp. 607-620.

Puente, X.S., Quesada, V., Osorio, F.G., Cabanillas, R., Cadinanos, J., Fraile, J.M., Ordonez, G.R., Puente, D.A., Gutierrez-Fernandez, A., Fanjul-Fernandez, M., Levy, N., Freije, J.M. and Lopez-Otin, C. (2011) 'Exome sequencing and functional analysis identifies BANF1 mutation as the cause of a hereditary progeroid syndrome', *American journal of human genetics ,* 88, pp. 1-7.

Ragnauth, C.D., Warren, D.T., Liu, Y., McNair, R., Tajsic, T., Figg, N., Shroff, R., Skepper, J., Shanahan, C.M. (2010) 'Prelamin A acts to accelerate smooth muscle cell senescence and is a novel biomarker of human vascular aging.' *Circulation*.,121, pp. 200–2210.

Randles, K.N., Lam, L.T., Sewry, C.A., Puckelwartz, M., Furling, D., Wehnert, M., McNally, E.M. and Morris, G.E. (2010) 'Nesprins, but not sun proteins, switch

isoforms at the nuclear envelope during muscle development', *Developmental Dynamics,* 239(3), pp. 998-1009.

Raz, V., Vermolen, B.J., Garini, Y., Onderwater, J.J., Mommaas-Kienhuis, M.A., Koster, A.J., Young, I.T., Tanke, H. and Dirks, R.W. (2008) 'The nuclear lamina promotes telomere aggregation and centromere peripheral localization during senescence of human mesenchymal stem cells', *Journal of cell science,* 121(Pt 24), pp. 4018-4028.

Razin, S.V. and Gromova, I.I. (1995) 'The channels model of nuclear matrix structure', *Bioessays,* 17(5), pp. 443-450.

Razin, S.V., Gromova, I.I. and Iarovaia, O.V. (1996) 'Specificity and functional significance of DNA interaction with the nuclear matrix: new approaches to clarify the old questions', *International review of cytology,* 162, pp. 405-448.

Razin, S., Borunova, V., Iarovaia, O. and Vassetzky, Y. (2014) 'Nuclear matrix and structural and functional compartmentalization of the eucaryotic cell nucleus', *Biochemistry (Moscow),* 79(7), pp. 608-618.

Rea, S., Eisenhaber, F., O'Carroll, D., Strahl, B.D., Sun, Z., Schmid, M., Opravil, S., Mechtler, K., Ponting, C.P. and Allis, C.D. (2000) 'Regulation of chromatin structure by site-specific histone H3 methyltransferases', *Nature,* 406(6796), pp. 593-599.

Reddy, S. and Comai, L. (2012) 'Lamin A, farnesylation and aging', *Experimental cell research,* 318(1), pp. 1-7.

Rehman, N.A., Rehman, A.A., Ashraf, I.N. and Ahmed, S. (2015) 'Can Hutchinson-Gilford progeria syndrome be cured in the future?', *Intractable & Rare Diseases Research,* (0).

Reil, M. and Dabauvalle, M. (2013) 'Essential roles of LEM-domain protein MAN1 during organogenesis in Xenopus laevis and overlapping functions of emerin', *European journal of cell biology,* 92(8–9), pp. 280-294.

Richards, E.J. and Elgin, S.C. (2002) 'Epigenetic codes for heterochromatin formation and silencing: rounding up the usual suspects', *Cell,* 108(4), pp. 489-500.

Richards, S.A., Muter, J., Ritchie, P., Lattanzi, G. and Hutchison, C.J. (2011) 'The accumulation of un-repairable DNA damage in laminopathy progeria fibroblasts is caused by ROS generation and is prevented by treatment with N-acetyl cysteine', *Human molecular genetics,* 20(20), pp. 3997-4004.

Robin, J.D., Ludlow, A.T., Batten, K., Magdinier, F., Stadler, G., Wagner, K.R., Shay, J.W. and Wright, W.E. (2014) 'Telomere position effect: regulation of gene expression with progressive telomere shortening over long distances', *Genes & development,* 28(22), pp. 2464-2476.

Rodier, F. ,Coppé, J.P., Pati, l. C.K., Hoeijmakers, W.A., Muñoz, D.P., Raza, S.R., Freund, A., Campeau, E., Davalos, A.R., Campisi, J. (2009) ' Persistent DNA

damage signalling triggers senescence-associated inflammatory cytokine secretion.' *Nat Cell Biol*. 11(8), pp. 973–979

Rodriguez, S., Coppede, F., Sagelius, H. and Eriksson, M. (2009) 'Increased expression of the Hutchinson-Gilford progeria syndrome truncated lamin A transcript during cell aging', *European journal of human genetics ,* 17(7), pp. 928-937.

Rodriguez, S. and Eriksson, M. (2010) 'Evidence for the involvement of lamins in aging', *Current aging science ,* 3(2), pp. 1-9.

Rogers, L.D. and Overall, C.M. (2013) 'Proteolytic post-translational modification of proteins: proteomic tools and methodology', *Molecular & cellular proteomics : MCP,* 12(12), pp. 3532-3542.

Rosete, M., Padros, M.R. and Vindrola, O. (2007) 'The nucleolus as a regulator of cellular senescence', *Medicina,* 67(2), pp. 183-194.

Roux, K.J., Crisp, M.L., Liu, Q., Kim, D., Kozlov, S., Stewart, C.L. and Burke, B. (2009) 'Nesprin 4 is an outer nuclear membrane protein that can induce kinesin-mediated cell polarization', *Proceedings of the National Academy of Sciences of the United States of America,* 106(7), pp. 2194-2199.

Ruden, M. and Puri, N. (2013) 'Novel anticancer therapeutics targeting telomerase', *Cancer treatment reviews,* 39(5), pp. 444-456.

Rusiñol, A.E. and Sinensky, M.S. (2006) 'Farnesylated lamins, progeroid syndromes and farnesyl transferase inhibitors', *J Cell Sci.,* 119(6), pp. 3265-3272.

Saksouk, N., Simboeck, E. and Déjardin, J. (2015) 'Constitutive heterochromatin formation and transcription in mammals', *Epigenetics & Chromatin,* 8(1), pp. 3.

Salhab, M., Jiang, W.G., Newbold, R.F. and Mokbel, K. (2008) 'The expression of gene transcripts of telomere-associated genes in human breast cancer: correlation with clinico-pathological parameters and clinical outcome', *Breast cancer research and treatment,* 109(1), pp. 35-46.

Scaffidi, P. and Misteli, T. (2006) 'Lamin A-dependent nuclear defects in human aging.', *Science,* 312, pp. 1059-1063.

Scaffidi, P. and Misteli, T. (2005) 'Reversal of the cellular phenotype in the premature aging disease Hutchinson-Gilford progeria syndrome', *Nature medicine,* 11(4), pp. 440-445.

Schirmer, E.C., Florens, L., Guan, T., - Yates,,John R.,3rd, 3rd, Y.J. and Gerace, L. (2003) 'Nuclear membrane proteins with potential disease links found by subtractive proteomics', *Science (New York, N.Y.) ,* 301(5638), pp. 1380-1382.

Schirmer, E.C. and Gerace, L. (2005) 'The nuclear membrane proteome: extending the envelope', *Trends in biochemical sciences,* 30(10), pp. 551-558.

Schmitt, J., Benavente, R., Hodzic, D., Hoog, C., Stewart, C.L. and Alsheimer, M. (2007) 'Transmembrane protein Sun2 is involved in tethering mammalian meiotic telomeres to the nuclear envelope', *Proceedings of the National Academy of Sciences of the United States of America,* 104(18), pp. 7426-7431.

Schoeftner, S. and Blasco, M.A. (2009) 'A 'higher order'of telomere regulation: telomere heterochromatin and telomeric RNAs', *The EMBO journal,* 28(16), pp. 2323-2336.

Schotta, G., Sengupta, R., Kubicek, S., Malin, S., Kauer, M., Callen, E., Celeste, A., Pagani, M., Opravil, S., De La Rosa-Velazquez, I.A., Espejo, A., Bedford, M.T., Nussenzweig, A., Busslinger, M. and Jenuwein, T. (2008) 'A chromatin-wide transition to H4K20 monomethylation impairs genome integrity and programmed DNA rearrangements in the mouse', *Genes & development,* 22(15), pp. 2048-2061.

Schreiber, K. and Kennedy, B. (2013) 'When Lamins Go Bad: Nuclear Structure and Disease', *Cell,* 152(6), pp. 1365-1375.

Schultz, L.B., Chehab, N.H., Malikzay, A. and Halazonetis, T.D. (2000) 'p53 binding protein 1 (53BP1) is an early participant in the cellular response to DNA double-strand breaks', *The Journal of cell biology,* 151(7), pp. 1381-1390.

Scully, R., Chen, J., Plug, A., Xiao, Y., Weaver, D., Feunteun, J., Ashley, T. and Livingston, D.M. (1997) 'Association of BRCA1 with Rad51 in mitotic and meiotic cells', *Cell,* 88(2), pp. 265-275.

Scully, R. and Livingston, D.M. (2000) 'In search of the tumour-suppressor functions of BRCA1 and BRCA2', *Nature,* 408(6811), pp. 429-432.

Segura-Totten, M. and Wilson, K.L. (2004) 'BAF: roles in chromatin, nuclear structure and retrovirus integration', *Trends in cell biology,* 14(5), pp. 261-266.

Segura-Totten, M., Kowalski, A.K., Craigie, R. and Wilson, K.L. (2002) 'Barrier-to-autointegration factor: major roles in chromatin decondensation and nuclear assembly', *The Journal of cell biology,* 158(3), pp. 475-485.

Shaffer, L.G., McGowan-Jordan, J. and Schmid, M. (2013) *ISCN 2013: An International System for Human Cytogenetic Nomenclature (2013).* Karger Medical and Scientific Publishers.

Shah, P.P., Donahue, G., Otte, G.L., Capell, B.C., Nelson, D.M., Cao, K., Aggarwala, V., Cruickshanks, H.A., Rai, T.S., McBryan, T., Gregory, B.D., Adams, P.D. and Berger, S.L. (2013) 'Lamin B1 depletion in senescent cells triggers large-scale changes in gene expression and the chromatin landscape', *Genes & development,* 27(16), pp. 1787-1799.

Shaklai, S., Amariglio, N., Rechavi, G. and Simon, A.J. (2007) 'Gene silencing at the nuclear periphery', *FEBS J,* 274(6), pp. 1383-1392.

Shang, Y., Zhang, J., Zhang, H. and Zheng, Q. (2014) 'Molecular simulation investigation on the interaction between barrier-to-autointegration factor or its Gly25Glu mutant and DNA', *Journal of molecular modeling,* 20(5), pp. 1-9.

Shao, X., Tarnasky, H.A., Lee, J.P., Oko, R. and van der Hoorn, Frans A (1999) 'Spag4, a novel sperm protein, binds outer dense-fiber protein Odf1 and localizes to microtubules of manchette and axoneme', *Developmental biology,* 211(1), pp. 109-123.

Shimi, T., Pfleghaar, K., Kojima, S., Pack, C.G., Solovei, I., Goldman, A.E. and Goldman, R.D. (2008) 'The A- and B-type nuclear lamin networks: microdomains involved in chromatin organization and transcription.', *Genes Dev,* 22(24), pp. 3409-3421.

Shimi, T., Butin-Israeli, V. and Goldman, R.D. (2012) 'The functions of the nuclear envelope in mediating the molecular crosstalk between the nucleus and the cytoplasm', *Current opinion in cell biology,* 24(1), pp. 71-78.

Shumaker, D.K., Lopez-Soler, R.I., Adam, S.A., Herrmann, H., Moir, R.D., Spann, T.P. and Goldman, R.D. (2005) 'Functions and dysfunctions of the nuclear lamin Ig-fold domain in nuclear assembly, growth, and Emery-Dreifuss muscular dystrophy', *Proc Natl Acad Sci U S A.,* 102, pp. 15494-15499.

Shumaker, D.K., Lee, K.K., Tanhehco, Y.C., Craigie, R. and Wilson, K.L. (2001) 'LAP2 binds to BAF· DNA complexes: requirement for the LEM domain and modulation by variable regions', *The EMBO journal,* 20(7), pp. 1754-1764.

Shumaker, D.K., Dechat, T., Kohlmaier, A., Adam, S.A., Bozovsky, M.R., Erdos, M.R., Eriksson, M., Goldman, A.E., Khuon, S., Collins, F.S., Jenuwein, T. and Goldman, R.D. (2006) 'Mutant nuclear lamin A leads to progressive alterations of epigenetic control in premature aging', *Proceedings of the National Academy of Sciences of the United States of America ,* 103(23), pp. 8703-8708.

Shumaker, D.K., Solimando, L., Sengupta, K., Shimi, T., Adam, S.A., Grunwald, A., Strelkov, S.V., Aebi, U., Cardoso, M.C. and Goldman, R.D. (2008) 'The highly conserved nuclear lamin Ig-fold binds to PCNA: its role in DNA replication', *The Journal of cell biology ,* 181(2), pp. 269-280.

Sieprath, T., Corne, T.D., Nooteboom, M., Grootaert, C., Rajkovic, A., Buysschaert, B., Robijns, J., Broers, J.L., Ramaekers, F.C. and Koopman, W.J. (2015) 'Sustained accumulation of prelamin a and depletion of lamin a/c both cause oxidative stress and mitochondrial dysfunction but induce different cell fates', *Nucleus*, pp. 236-246.

Silve, S., Dupuy, P., Ferrara, P. and Loison, G. (1998) 'Human lamin B receptor exhibits sterol C14-reductase activity in Saccharomyces cerevisiae', *Biochimica et Biophysica Acta (BBA) - Lipids and Lipid Metabolism,* 1392(2–3), pp. 233-244.

Simon, D.N., Zastrow, M.S. and Wilson, K.L. (2010) 'Direct actin binding to A-and B-type lamin tails and actin filament bundling by the lamin A tail', *Nucleus,* 1(3), pp. 264-272.

Sims, R.J., Nishioka, K. and Reinberg, D. (2003) 'Histone lysine methylation: a signature for chromatin function', *TRENDS in Genetics,* 19(11), pp. 629-639.

Sinensky, M., Fantle, K. and Dalton, M. (1994) 'An antibody which specifically recognizes prelamin A but not mature lamin A: application to detection of blocks in farnesylation-dependent protein processing', *Cancer research,* 54(12), pp. 3229-3232.

Sinensky, M., Fantle, K., Trujillo, M., McLain, T., Kupfer, A. and Dalton, M. (1994) 'The processing pathway of prelamin A', *Journal of cell science,* 107, (Pt 1), pp. 61-67.

Sinha, J.K., Ghosh, S. and Raghunath, M. (2014) 'Progeria: a rare genetic premature ageing disorder', *The Indian journal of medical research,* 139(5), pp. 667-674.

Skoko, D., Li, M., Huang, Y., Mizuuchi, M., Cai, M., Bradley, C.M., Pease, P.J., Xiao, B., Marko, J.F., Craigie, R. and Mizuuchi, K. (2009) 'Barrier-to-autointegration factor (BAF) condenses DNA by looping', *Proceedings of the National Academy of Sciences of the United States of America,* 106(39), pp. 16610-16615.

Slijepcevic, P., Xiao, Y., Dominguez, I. and Natarajan, A. (1996) 'Spontaneous and radiation-induced chromosomal breakage at interstitial telomeric sites', *Chromosoma,* 104(8), pp. 596-604.

Slotkin, R.K. and Martienssen, R. (2007) 'Transposable elements and the epigenetic regulation of the genome', *Nature Reviews Genetics,* 8(4), pp. 272-285.

Smetana, K., Steele, W. and Busch, H. (1963) 'A nuclear ribonucleoprotein network', *Experimental cell research,* 31(1), pp. 198-201.

Snider, N.T. and Omary, M.B. (2014) 'Post-translational modifications of intermediate filament proteins: mechanisms and functions', *Nature Reviews Molecular Cell Biology,* 15(3), pp. 163-177.

Solovei, I., Schermelleh, L., Düring, K., Engelhardt, A., Stein, S., Cremer, C. and Cremer, T. (2004) 'Differences in centromere positioning of cycling and postmitotic human cell types', *Chromosoma,* 112(8), pp. 410-423.

Solovei, I., Wang, A.S., Thanisch, K., Schmidt, C.S., Krebs, S., Zwerger, M., Cohen, T.V., Devys, D., Foisner, R., Peichl, L., Herrmann, H., Blum, H., Engelkamp, D., Stewart, C.L., Leonhardt, H. and Joffe, B. (2013) 'LBR and lamin A/C sequentially tether peripheral heterochromatin and inversely regulate differentiation', *Cell,* 512, pp. 584-598.

Somech, R., Shaklai, S., Amariglio, N., Rechavi, G. and Simon, A.J. (2005) 'Nuclear envelopathies—raising the nuclear veil', *Pediatric research,* 57, pp. 8R-15R.

Spann, T.P., Moir, R.D., Goldman, A.E., Stick, R. and Goldman, R.D. (1997) 'Disruption of nuclear lamin organization alters the distribution of replication factors and inhibits DNA synthesis', *J. Cell Biol,* 136, pp. 1201-1212.

Spann, T.P., Goldman, A.E., Wang, C., Huang, S. and Goldman, R.D. (2002) 'Alteration of nuclear lamin organization inhibits RNA polymerase II-dependent transcription', *J Cell Biol.,* 156(4), pp. 603-608.

Spector, D.L., Fu, X.D. and Maniatis, T. (1991) 'Associations between distinct pre-mRNA splicing components and the cell nucleus', *The EMBO journal,* 10(11), pp. 3467-3481.

Squarzoni, S., Sabatelli, P., Ognibene, A., Toniolo, D., Cartegni, L., Cobianchi, F., Petrini, S., Merlini, L. and Maraldi, N. (1998) 'Immunocytochemical detection of emerin within the nuclear matrix', *Neuromuscular Disorders,* 8(5), pp. 338-344.

Starr, D.A. (2011) 'KASH and SUN proteins', *Current Biology,* 21(11), pp. 414-415.

Starr, D.A. and Fischer, J.A. (2005) 'KASH'n Karry: The KASH domain family of cargo-specific cytoskeletal adaptor proteins', *Bioessays,* 27(11), pp. 1136-1146.

Starr, D.A. (2009) 'A nuclear-envelope bridge positions nuclei and moves chromosomes', *Journal of cell science ,* 122, pp. 577-586.

Stehbens, W.E., Delahunt, B., Shozawa, T., Gilbert-Barness, E. (2001) 'Smooth muscle cell depletion and collagen types in progeric arteries.' *Cardiovasc Pathol* 10, pp. 133–136

Stewart-Hutchinson, P., Hale, C.M., Wirtz, D. and Hodzic, D. (2008) 'Structural requirements for the assembly of LINC complexes and their function in cellular mechanical stiffness', *Experimental cell research,* 314(8), pp. 1892-1905.

Stewart SA and Weinberg RA (2006) Telomeres: cancer to human aging. Annual Review of Cell and Developmental Biology, 22, pp. 531-557.

Strelkov, S.V., Schumacher, J., Burkhard, P., Aebi, U. and Herrmann, H. (2004) 'Crystal Structure of the Human Lamin A Coil 2B Dimer: Implications for the Head-to-tail Association of Nuclear Lamins', *Journal of Molecular Biology,* 343(4), pp. 1067-1080.

Stuurman, N., Heins, S. and Aebi, U. (1998) 'Nuclear Lamins: Their Structure, Assembly, and Interactions', *Journal of structural biology,* 122(1–2), pp. 42-66.

Sullivan, G.J., Bridger, J.M., Cuthbert, A.P., Newbold, R.F., Bickmore, W.A. and McStay, B. (2001) 'Human acrocentric chromosomes with transcriptionally silent nucleolar organizer regions associate with nucleoli', *The EMBO journal,* 20(11), pp. 2867-2877.

Sullivan, T., Escalante-Alcalde, D., Bhatt, H., Anver, M., Bhat, N., Nagashima, K., Stewart, C.L. and Burke, B. (1999) 'Loss of A-type lamin expression compromises nuclear envelope integrity leading to muscular dystrophy', *J Cell Biol,* 147(5), pp. 913-920.

Sun, H.B., Shen, J. and Yokota, H. (2000) 'Size-dependent positioning of human chromosomes in interphase nuclei', *Biophysical journal,* 79, pp. 184-190.

Suntharalingam, M. and Wente, S.R. (2003) 'Peering through the Pore: Nuclear Pore Complex Structure, Assembly, and Function', *Developmental Cell,* 4(6), pp. 775-789.

Suzuki, M.M. and Bird, A. (2008) 'DNA methylation landscapes: provocative insights from epigenomics', *Nature Reviews Genetics,* 9(6), pp. 465-476.

Swamy, M.V., Cooma, I., Reddy, B.S. and Rao, C.V. (2002) 'Lamin B, caspase-3 activity, and apoptosis induction by a combination of HMG-CoA reductase inhibitor and COX-2 inhibitors: a novel approach in developing effective chemopreventive regimens', *International journal of oncology,* 20(4), pp. 753-759.

Swift, J., Ivanovska, I.L., Buxboim, A., Harada, T., Dingal, P.C., Pinter, J. and Discher, D.E. (2013) 'Nuclear lamin-A scales with tissue stiffness and enhances matrix-directed differentiation', *Science,* 341(6149), pp. 1240104.

Szczerbal, I. and Bridger, J.M. (2010) 'Association of adipogenic genes with SC-35 domains during porcine adipogenesis', *Chromosome research,* 18(8), pp. 887-895.

Szczerbal, I., Foster, H.A. and Bridger, J.M. (2009) 'The spatial repositioning of adipogenesis genes is correlated with their expression status in a porcine mesenchymal stem cell adipogenesis model system', *Chromosoma,* 118(5), pp. 647-663.

Tachibana, M., Sugimoto, K., Nozaki, M., Ueda, J., Ohta, T., Ohki, M., Fukuda, M., Takeda, N., Niida, H., Kato, H. and Shinkai, Y. (2002) 'G9a histone methyltransferase plays a dominant role in euchromatic histone H3 lysine 9 methylation and is essential for early embryogenesis', *Genes & development,* 16(14), pp. 1779-1791.

Taimen, P., Pfleghaar, K., Shimi, T., Moller, D., Ben-Harush, K., Erdos, M.R., Adam, S.A., Herrmann, H., Medalia, O., Collins, F.S., Goldman, A.E. and Goldman, R.D. (2009) 'A progeria mutation reveals functions for lamin A in nuclear assembly, architecture, and chromosome organization', *Proceedings of the National Academy of Sciences of the United States of America,* 106(49), pp. 20788-20793.

Takai, H., Smogorzewska, A., de Lange, T., (2003) ' DNA Damage Foci at Dysfunctional Telomeres ' Current Biology, Vol. 13, pp. 1549–1556

Tamaru, H. (2010) 'Confining euchromatin/heterochromatin territory: jumonji crosses the line', *Genes & development,* 24(14), pp. 1465-1478.

Tanabe, H., Habermann, F.A., Solovei, I., Cremer, M. and Cremer, T. (2002) 'Non-random radial arrangements of interphase chromosome territories: evolutionary considerations and functional implications', *Mutation Research/Fundamental and Molecular Mechanisms of Mutagenesis,* 504(1), pp. 37-45.

Tanabe, H., Kupper, K., Ishida, T., Neusser, M. and Mizusawa, H. (2005) 'Inter-and intra-specific gene-density-correlated radial chromosome territory arrangements

are conserved in Old World monkeys', *Cytogenetic and genome research,* 108(1-3), pp. 255-261.

Tanemura, K., Ogura, A., Cheong, C., Gotoh, H., Matsumoto, K., Sato, E., Hayashi, Y., Lee, H. and Kondo, T. (2005) 'Dynamic rearrangement of telomeres during spermatogenesis in mice', *Developmental biology,* 281(2), pp. 196-207.

Tang, C.W., Maya-Mendoza, A., Martin, C., Zeng, K., Chen, S., Feret, D., Wilson, S.A. and Jackson, D.A. (2008) 'The integrity of a lamin-B1-dependent nucleoskeleton is a fundamental determinant of RNA synthesis in human cells', *Journal of cell science,* 121, pp. 1014-1024.

Taniura, H., Glass, C. and Gerace, L. (1995) 'A chromatin binding site in the tail domain of nuclear lamins that interacts with core histones.', *Cell Biol.,* 131, pp. 33-44.

Taylor, M.R., Slavov, D., Gajewski, A., Vlcek, S., Ku, L., Fain, P.R., Carniel, E., Di Lenarda, A., Sinagra, G. and Boucek, M.M. (2005) 'Thymopoietin (lamina-associated polypeptide 2) gene mutation associated with dilated cardiomyopathy', *Human mutation,* 26(6), pp. 566-574.

Ten Dijke, P. and Hill, C.S. (2004) 'New insights into TGF-beta-Smad signalling', *Trends Biochem Sci.,* 29(5), pp. 265-273.

Tian, X., Chen, B. and Liu, X. (2010) 'Telomere and telomerase as targets for cancer therapy', *Applied Biochemistry and Biotechnology,* 160(5), pp. 1460-1472.

Timme, S., Schmitt, E., Stein, S., Schwarz-Finsterle, J., Wagner, J., Walch, A., Werner, M., Hausmann, M. and Wiech, T. (2011) 'Nuclear position and shape deformation of chromosome 8 territories in pancreatic ductal adenocarcinoma', *Analytical cellular pathology,* 34(1-2), pp. 21-33.

Tchkonia, T., Morbeck, D.E., von Zglinicki, T., van Deursen, J., Lustgarten, J., Heidi Scrable, H., Khosla, S., Jensen, M.D., and Kirkland, J.L., (2010) ' Fat tissue, aging, and cellular senescence.' *Aging Cell*. 9(5), pp.667–684.

Tolhuis, B., Palstra, R., Splinter, E., Grosveld, F. and de Laat, W. (2002) 'Looping and interaction between hypersensitive sites in the active β-globin locus', *Molecular cell,* 10(6), pp. 1453-1465.

Tollefsbol, T.O. and Cohen, H.J. (1984) 'Werner's syndrome: an underdiagnosed disorder resembling premature aging', *Age,* 7(3), pp. 75-88.

Tomás-Loba, A., Flores, I., Fernández-Marcos, P.J., Cayuela, M.L., Maraver, A., Tejera, A., Borrás, C., Matheu, A., Klatt, P. and Flores, J.M. (2008) 'Telomerase reverse transcriptase delays aging in cancer-resistant mice', *Cell,* 135(4), pp. 609-622.

Tran, E.J. and Wente, S.R. (2006) 'Dynamic Nuclear Pore Complexes: Life on the Edge', *Cell,* 125(6), pp. 1041-1053.

Trinkle-Mulcahy, L. and Lamond, A.I. (2006) 'Mitotic phosphatases: no longer silent partners', *Current opinion in cell biology,* 18(6), pp. 623-631.

Tschiersch, B., Hofmann, A., Krauss, V., Dorn, R., Korge, G. and Reuter, G. (1994) 'The protein encoded by the Drosophila position-effect variegation suppressor gene Su(var)3-9 combines domains of antagonistic regulators of homeotic gene complexes', *The EMBO journal,* 13(16), pp. 3822-3831.

Tsiligiri, M., Fekos, C., Theodoridou, E. and Lavdaniti, M. (2015) 'An overview of Hutchinson Gilford Progeria Syndrome (HGPS).', *British Journal of Medicine and Medical Research,* 5(12), pp. 1527-1533.

Tsuchiya, Y., Hase, A., Ogawa, M., Yorifuji, H. and Arahata, K. (1999) 'Distinct regions specify thenuclearmembrane targeting of emerin, the responsible proteinfor EmeryDreifuss muscular dystrophy', *Eur J Biochem,* 259, pp. 859-865.

Tsurumi, A. and Li, W. (2012) 'Global heterochromatin loss: a unifying theory of aging?', *Epigenetics,* 7(7), pp. 680-688.

Tzur, Y.B., Wilson, K.L. and Gruenbaum, Y. (2006) 'SUN-domain proteins:'Velcro'that links the nucleoskeleton to the cytoskeleton', *Nature reviews Molecular cell biology,* 7(10), pp. 782-788.

van Koningsbruggen, S., Gierlinski, M., Schofield, P., Martin, D., Barton, G.J., Ariyurek, Y., den Dunnen, J.T. and Lamond, A.I. (2010) 'High-resolution whole-genome sequencing reveals that specific chromatin domains from most human chromosomes associate with nucleoli', *Molecular biology of the cell,* 21, pp. 3735-3748.

van Noort, V., Seebacher, J., Bader, S., Mohammed, S., Vonkova, I., Betts, M.J., Kuhner, S., Kumar, R., Maier, T., O'Flaherty, M., Rybin, V., Schmeisky, A., Yus, E., Stulke, J., Serrano, L., Russell, R.B., Heck, A.J., Bork, P. and Gavin, A.C. (2012) 'Cross-talk between phosphorylation and lysine acetylation in a genome-reduced bacterium', *Molecular systems biology,* 8, pp. 571.

Van Steensel, B. and Dekker, J. (2010) 'Genomics tools for unraveling chromosome architecture', *Nature biotechnology,* 28(10), pp. 1089-1095.

Varela, I., Pereira, S., Ugalde, A.P., Navarro, C.L., Suárez, M.F., Cau, P., Cadiñanos, J., Osorio, F.G., Foray, N. and Cobo, J. (2008) 'Combined treatment with statins and aminobisphosphonates extends longevity in a mouse model of human premature aging', *Nature medicine,* 14(7), pp. 767-772.

Vassetzky, Y., Hair, A. and Mechali, M. (2000) 'Rearrangement of chromatin domains during development in Xenopus', *Genes & development,* 14(12), pp. 1541-1552.

Vaziri, H., Benchimol, S. (1996) ' From telomere loss to p53 induction and activation of a DNA-damage pathway at senescence: the telomere loss/DNA damage model of cell aging. ' *Exp Gerontol,* 31(1–2), pp. 295–301

Verstraeten, V.L., Ji, J.Y., Cummings, K.S., Lee, R.T. and Lammerding, J. (2008) 'Increased mechanosensitivity and nuclear stiffness in Hutchinson-Gilford progeria cells: effects of farnesyltransferase inhibitors', 7, pp. 383-393.

Verstraeten, V.L., Peckham, L.A., Olive, M., Capell, B.C., Collins, F.S., Nabel, E.G., Young, S.G., Fong, L.G. and Lammerding, J. (2011) 'Protein farnesylation inhibitors cause donut-shaped cell nuclei attributable to a centrosome separation defect', *Proceedings of the National Academy of Sciences of the United States of America,* 108(12), pp. 4997-5002.

Vijg, J. and Campisi, J. (2008) 'Puzzles, promises and a cure for ageing', *Nature,* 454(7208), pp. 1065-1071.

Villeponteau, B. (1997) 'The heterochromatin loss model of aging', *Experimental gerontology,* 32(4), pp. 383-394.

Visser, A.E. and Aten, J.A. (1999) 'Chromosomes as well as chromosomal subdomains constitute distinct units in interphase nuclei', *Journal of cell science,* 112 (Pt 19)(Pt 19), pp. 3353-3360.

Vlcek, S., Korbei, B. and Foisner, R. (2002) 'Distinct functions of the unique C terminus of LAP2alpha in cell proliferation and nuclear assembly', *The Journal of biological chemistry,* 277(21), pp. 18898-18907.

Vlcek, S. and Foisner, R. (2007) 'Lamins and lamin-associated proteins in aging and disease', *Current opinion in cell biology,* 19(3), pp. 298-304.

Voeltz, G.K., Rolls, M.M. and Rapoport, T.A. (2002) 'Structural organization of the endoplasmic reticulum', *EMBO reports,* 3(10), pp. 944-950.

Volpi, E.V. and Bridger, J.M. (2008) 'FISH glossary: an overview of the fluorescence in situ hybridization technique', *BioTechniques,* 45(4), pp. 385-386.

Waaijer ME, *et al.* (2012) The number of p16INK4a positive cells in human skin reflects biological age. *Aging Cell.* 11(4), pp. 722–725.

Wagner, N., Weber, D., Seitz, S. and Krohne, G. (2004) 'The lamin B receptor of Drosophila melanogaster', *J Cell Sci,* 117(10), pp. 2015-2028.

Wallis, C.V., Sheerin, A.N., Green, M.H.L., Jones, C.J., Kipling, D. and Faragher, R.G.A. (2004) 'Fibroblast clones from patients with Hutchinson–Gilford progeria can senesce despite the presence of telomerase', *Experimental gerontology,* 39(4), pp. 461-467.

Wan KM, Nickerson JA, Krockmalnic G and Penman S (1999) ' The nuclear matrix prepared by amine modification.' Proceedings of the National Academy of Sciences of the United States of America, 96 (3), pp. 933-938

Wang, Y., Östlund, C., Choi, J.C., Swayne, T.C., Gundersen, G.G. and Worman, H.J. (2012) 'Blocking farnesylation of the prelamin A variant in Hutchinson-Gilford progeria syndrome alters the distribution of A-type lamins', *Nucleus,* 3(5), pp. 452-462.

Wang, Z., Liu, X., Yang, B. and Gelernter, J. (2013) 'The role and challenges of exome sequencing in studies of human diseases', *Frontiers in genetics,* 4.

Wang, X., Xu, S., Rivolta, C., Li, L.Y., Peng, G.H., Swain, P.K., Sung, C.H., Swaroop, A., Berson, E.L., Dryja, T.P. and Chen, S. (2002) 'Barrier to autointegration factor interacts with the cone-rod homeobox and represses its transactivation function', *The Journal of biological chemistry,* 277(45), pp. 43288-43300.

Warren, D.T., Zhang, Q., Weissberg, P.L. and Shanahan, C.M. (2005) 'Nesprins: intracellular scaffolds that maintain cell architecture and coordinate cell function?', *Expert reviews in molecular medicine,* 7(11), pp. 1-15.

Weinrich, S.L., Pruzan, R., Ma, L., Ouellette, M., Tesmer, V.M., Holt, S.E., Bodnar, A.G., Lichtsteiner, S., Kim, N.W., Trager, J.B., Taylor, R.D., Carlos, R., Andrews, W.H., Wright, W.E., Shay, J.W., Harley, C.B. and Morin, G.B. (1997) 'Reconstitution of human telomerase with the template RNA component hTR and the catalytic protein subunit hTRT', *Nature genetics,* 17(4), pp. 498-502.

Weis, K. (2007) 'The Nuclear Pore Complex: Oily Spaghetti or Gummy Bear?' *Cell,* 130(3), pp. 405-407.

Weyemi U, et al. (2012) 'ROS-generating NADPH oxidase NOX4 is a critical mediator in oncogenic H-Ras-induced DNA damage and subsequent senescence.' *Oncogene*, 31(9), pp. 1117–1129

Wiech, T., Stein, S., Lachenmaier, V., Schmitt, E., Schwarz-Finsterle, J., Wiech, E., Hildenbrand, G., Werner, M. and Hausmann, M. (2009) 'Spatial allelic imbalance of BCL2 genes and chromosome 18 territories in nonneoplastic and neoplastic cervical squamous epithelium', *European Biophysics Journal,* 38(6), pp. 793-806.

Wilson, R.H. and Coverley, D. (2013) 'Relationship between DNA replication and the nuclear matrix', *Genes to Cells,* 18(1), pp. 17-31.

Wilson, K.L. and Foisner, R. (2010) 'Lamin-binding Proteins', *Cold Spring Harbor perspectives in biology,* 2, pp. 1-17.

Winter-Vann, A.M. and Casey, P.J. (2005) 'Post-prenylation-processing enzymes as new targets in oncogenesis', *Nat Rev CanceR,* 5(5), pp. 405-412.

Woglar, A., Daryabeigi, A., Adamo, A., Habacher, C., Machacek, T., La Volpe, A. and Jantsch, V. (2013) 'Matefin/SUN-1 phosphorylation is part of a surveillance mechanism to coordinate chromosome synapsis and recombination with meiotic progression and chromosome movement', *PLoS genetics,* 9(3), pp. e1003335.

Wong, H.P. and Slijepcevic, P. (2004) 'Telomere length measurement in mouse chromosomes by a modified Q-FISH method', *Cytogenetic and genome research,* 105(2-4), pp. 464-470.

Wood, A.M., Rendtlew Danielsen, J.M., Lucas, C.A., Rice, E.L., Scalzo, D., Shimi, T., Goldman, R.D., Smith, E.D., Le Beau, M.M. and Kosak, S.T. (2014) 'TRF2 and lamin A/C interact to facilitate the functional organization of chromosome ends', *Nature communications ,* 5(5467), pp. 1-9.

Woodcock, C.L. (2006) 'Chromatin architecture', *Current opinion in structural biology,* 16(2), pp. 213-220.

Worman, H.J. and Courvalin, J.C. (2000) 'The inner nuclear membrane', 177, pp. 1-11.

Worman, H.J., Evans, C.D. and Blobel, G. (1990) 'The lamin B receptor of the nuclear envelope inner membrane: a polytopic protein with eight potential transmembrane domains', *J Cell Biol.,* 111(4), pp. 1535-1542.

Worman, H.J., Yuan, J., Blobel, G. and Georgatos, S.D. (1988) 'A lamin B receptor in the nuclear envelope', *Proc Natl Acad Sci U S A.,* 85(22), pp. 8531-8534.

Worman, H.J. and Dauer, W.T. (2014) 'The Nuclear Envelope: An Intriguing Focal Point for Neurogenetic Disease', *Neurotherapeutics,* 11(4), pp. 764-772.

Worman, H.J. and Schirmer, E.C. (2015) 'Nuclear membrane diversity: underlying tissue-specific pathologies in disease?', *Current opinion in cell biology,* 34, pp. 101-112.

Worman, H.J. (2012) 'Nuclear lamins and laminopathies', *The Journal of pathology* 226, pp. 316-325.

Worman, H.J., Fong, L.G., Muchir, A. and Young, S.G. (2009) 'Laminopathies and the long strange trip from basic cell biology to therapy', *The Journal of clinical investigation,* 119(7), pp. 1825-1836.

Worman, H.J., Ostlund, C. and Wang, Y. (2010) 'Diseases of the nuclear envelope', *Cold Spring Harbor perspectives in biology,* 2(2), pp. a000760.

Wozniak, R.W. and Lusk, C.P. (2003) 'Nuclear pore complexes', *Current Biology,* 13(5), pp. pR169.

Wu, W., Lin, F. and Worman, H.J. (2002) 'Intracellular trafficking of MAN1, an integral protein of the nuclear envelope inner membrane', *J Cell Sci.,* 115(7), pp. 1361-1371.

Wuyts, W., Biervliet, M., Reyniers, E., D'Apice, M.R., Novelli, G. and Storm, K. (2005) 'Somatic and gonadal mosaicism in Hutchinson-Gilford progeria', *American journal of medical genetics,* 135(1), pp. 66-68.

Xu, Y. (2011) 'Chemistry in human telomere biology: structure, function and targeting of telomere DNA/RNA', *Chemical Society Reviews,* 40(5), pp. 2719-2740.

Xue, W., Zender L., Miething, C., Dickins, R.A., Hernando,E., Krizhanovsky, V., Cordon-Cardo, C., & Lowe, S.W., (2007) 'Senescence and tumour clearance is triggered by p53 restoration in murine liver carcinomas', *Nature* 445, pp. 656-660.

Yang, L., Guan, T. and Gerace, L. (1997) 'Lamin-binding fragment of LAP2 inhibits increase in nuclear volume during the cell cycle and progression into S phase', *The Journal of cell biology,* 139(5), pp. 1077-1087.

Yang, L., Munck, M., Swaminathan, K., Kapinos, L.E., Noegel, A.A. and Neumann, S. (2013) 'Mutations in LMNA modulate the lamin A--Nesprin-2 interaction and cause LINC complex alterations', 8, pp. 1-12.

Yang, S.H., Bergo, M.O., Toth, J.I., Qiao, X., Hu, Y., Sandoval, S., Meta, M., Bendale, P., Gelb, M.H., Young, S.G. and Fong, L.G. (2005) 'Blocking protein farnesyltransferase improves nuclear blebbing in mouse fibroblasts with a targeted Hutchinson-Gilford progeria syndrome mutation', *Proceedings of the National Academy of Sciences of the United States of America,* 102(29), pp. 10291-10296.

Yugami, M., Kabe, Y., Yamaguchi, Y., Wada, T. and Handa, H. (2007) 'hnRNP-U enhances the expression of specific genes by stabilizing mRNA', *FEBS letters,* 581(1), pp. 1-7.

Zakian, V.A. (1995) 'Telomeres: beginning to understand the end', *Science (New York, N.Y.),* 270(5242), pp. 1601-1607.

Zastrow, M.S., Vlcek, S. and Wilson, K.L. (2004) 'Proteins that bind A-type lamins: integrating isolated clues', *J Cell Sci.,* 117(7), pp. 979-987.

Zeng, C., He, D. and Brinkley, B. (1994) 'Localization of NuMA protein isoforms in the nuclear matrix of mammalian cells', *Cell motility and the cytoskeleton,* 29(2), pp. 167-176.

Zeng, W., De Greef, J.C., Chen, Y., Chien, R., Kong, X., Gregson, H.C., Winokur, S.T., Pyle, A., Robertson, K.D. and Schmiesing, J.A. (2009) 'Specific loss of histone H3 lysine 9 trimethylation and HP1gamma/cohesin binding at D4Z4 repeats is associated with facioscapulohumeral dystrophy (FSHD)', *PLoS Genet,* 5(7), pp. e1000559.

Zentner, G.E., Saiakhova, A., Manaenkov, P., Adams, M.D. and Scacheri, P.C. (2011) 'Integrative genomic analysis of human ribosomal DNA', *Nucleic acids research,* 39(12), pp. 4949-4960.

Zhang, F.L. and Casey, P.J. (1996) 'Protein prenylation: molecular mechanisms and functional consequences', *Annu Rev Biochem,* 65, pp. 241-269.

Zhang, Y., McCord, R.P., Ho, Y., Lajoie, B.R., Hildebrand, D.G., Simon, A.C., Becker, M.S., Alt, F.W. and Dekker, J. (2012) 'Spatial organization of the mouse genome and its role in recurrent chromosomal translocations', *Cell,* 148(5), pp. 908-921.

Zhang, Q., Ragnauth, C.D., Skepper, J.N., Worth, N.F., Warren, D.T., Roberts, R.G., Weissberg, P.L., Ellis, J.A. and Shanahan, C.M. (2005) 'Nesprin-2 is a multi-isomeric protein that binds lamin and emerin at the nuclear envelope and forms a subcellular network in skeletal muscle', *Journal of cell science JID - 0052457,* 118(4), pp. 673-687.

Zhang, Y. and Reinberg, D. (2001) 'Transcription regulation by histone methylation: interplay between different covalent modifications of the core histone tails', *Genes & development,* 15(18), pp. 2343-2360.

Zhen, Y.Y., Libotte, T., Munck, M., Noegel, A.A. and Korenbaum, E. (2002) 'NUANCE, a giant protein connecting the nucleus and actin cytoskeleton', *Journal of cell science,* 115(Pt 15), pp. 3207-3222.

Zheng, R., Ghirlando, R., Lee, M.S., Mizuuchi, K., Krause, M. and Craigie, R. (2000) 'Barrier-to-autointegration factor (BAF) bridges DNA in a discrete, higher-order nucleoprotein complex', *Proceedings of the National Academy of Sciences of the United States of America,* 97(16), pp. 8997-9002.

Zhou, L. and Panté, N. (2010) 'The nucleoporin Nup153 maintains nuclear envelope architecture and is required for cell migration in tumor cells', *FEBS letters,* 584(14), pp. 3013-3020.

Zhu, Q., Pao, G.M., Huynh, A.M., Suh, H., Tonnu, N., Nederlof, P.M., Gage, F.H. and Verma, I.M. (2011) 'BRCA1 tumour suppression occurs via heterochromatin-mediated silencing', *Nature,* 477(7363), pp. 179-184.

Zhuang, X., Semenova, E., Maric, D. and Craigie, R. (2014) 'Dephosphorylation of barrier-to-autointegration factor by protein phosphatase 4 and its role in cell mitosis', *The Journal of biological chemistry,* 289(2), pp. 1119-1127.

Zijlmans, J.M., Martens, U.M., Poon, S.S., Raap, A.K., Tanke, H.J., Ward, R.K,, Lansdorp, P.M. (1997) ' Telomeres in the mouse have large inter-chromosomal variations in the number of T2AG3 repeats'. Proc Natl Acad Sci U S A. 1997 Jul 8; 94(14), pp. 7423-8.

Zink, D., Cremer, T., Saffrich, R., Fischer, R., Trendelenburg, M.F., Ansorge, W. and Stelzer, E.H. (1998) 'Structure and dynamics of human interphase chromosome territories in vivo', *Human genetics,* 102(2), pp. 241-251.

Zuber, M., Tan, E.M. and Ryoji, M. (1989) 'Involvement of proliferating cell nuclear antigen (cyclin) in DNA replication in living cells', *Molecular and cellular biology,* 9(1), pp. 57-66.

Zuleger, N., Robson, M.I. and Schirmer, E.C. (2011) 'The nuclear envelope as a chromatin organizer', *Nucleus,* 5, pp. 339-349.

Appendices

❖ Indirect Immunofluorescence

Methanol : Acetone, 1:1 (v/v):

25 ml Methanol in 25 ml acetone

4% Paraformaldehyde:

4 g paraformaldehyde in 100 ml 1X PBS

10X PBS

160 g NaCl, 4g KCl, 22.9g Na_2HPO_4, and 4g KH_2PO_4 adjust this to 2 litres ddH_20 then autoclave it.

1XPBS (v: v):

100 ml 10XPBS in 900 ml ddH_20

1% Triton-X100

1 ml Triton-X100 in 99 ml 1XPBS

1% Fetal Calf serum (FCS)

1 ml Fetal Calf Serum (FCS) in 90 ml 1XPBS (Phosphate Buffer Saline)

❖ Preparation for Running DOP-PCR

❖ Master mix for running DOP-PCR (v/v):

	(µl)
5X KAPA HifI Fidelity Buffer (with 1 mM Mg^{2+} at 1X)	10
dACGTP (2µM)	5
dTTP (2µM)	2
DOP-PCR Primer (20 µM)	5
Sterilised Water	12
DNA Template	5
Biotin-16-dUTP	10
Taq-KAPA-HIFI	1
Total	50

❖ DOP-PCR programme:

Phase	**Step(Cycle)**	**Temperature(^{0}C)**	**Time (Minutes)**
Initial Denaturation	1	94	3
Denaturation	30	94	1
Annealing		62	1
Extension		68	1.5
Final Extension	1	68	8
For Collection		4	∞

❖ Preparation DOP-PCR gel:

1 % Agarose in 1X TBE and 2µl ethidium bromide (10 mg/ml)

❖ Summary of Antibodies Used in Indirect Immunofluorescence Method:

Primary antibodies (v/v)			Secondary antibodies (v/v)	
Protein	**Species**	**Dilution (µl)**	**Species**	**Dilution (µl)**
Lamin A/C	Mouse	1:100	1- Goat (FITC) 2- Goat (TRITC)	1- 1:64 2- 1:30
Progerin	Mouse	1:50		
PCNA	Mouse	1:10		
Lamin B1	Mouse	1:50		
Emerin	Mouse	1:30		
LAP2	Mouse	1:100		
NUP153	Mouse	1:1000		
HP1α	Mouse	1:500		
H2ax	Mouse	1:500		
RNAPOL1	Mouse	1:100		
Nucleophosmin	Mouse	1:2000		
H3me3K9	Mouse	1:100		
Lamin A	Goat	1:50	Rabbit (FITC)	1:50
Pre-lamin A	Goat	1:50		
Fibrillarin	Goat	1:100		
Ki-67	Rabbit	1:30	Swine (TRITC)	1:25
Lamin B2	Rabbit	1:250		
LBR	Rabbit	1:500		
SUN1	Rabbit	1:100		
SUN2	Rabbit	1:50		
H3ME3K27	Rabbit	1:100		
H4ME3K20	Rabbit	1:100		
CREST	Human	1:1000	Goat (FITC)	1:100

❖ Summary of Antibodies Used in Westernblotting Method

Primary antibodies (v/v)			**Secondary antibodies (v/v)**	
Protein	**Species**	**Dilution (µl)**	**Species**	**Dilution**
Lamin A/C	1- Mouse	1: 200	1- Rabbit anti-mouse peroxidase 2- Goat	1- 1:160,000 2- 1:15,000
Lamin B1	Mouse	1: 500		
α-Tubulin	Mouse	1: 4000		
SUN1	Rabbit	1: 1000	Donkey(FITC)	1:15,000
SUN2	Rabbit	1: 1000		
LBR	Rabbit	1: 500		

❖ 2 Dimensional – Fluorescence *In Situ* Hybridisation (2D- FISH)

3M Sodium Acetate (NaAc) pH 5.0:

0.5 g Na acetate in 2 ml ddH_20 adjust pH to 5.0

Methanole: Acetic Acid, 3:1 (v/v):

75 ml methanol in 25 ml acetic acid

0.075M KCl:

0.7 g Kcl IN 125 ML ddH_20

70 % Ethanol:

30 ml ddH_20 in 70 ml ethanol

90% Ethanol:

10 ml ddH_20 in 90 ml ethanol

100 % Ethanol:

100 ML absolute ethanol

20XSSC (w/v):

180.3 g NaCl and 88.2 gr Na Citrate in 1 L ddH_20, then adjust pH to 7.0 and autoclave it.

4XSSC:

20 ml 20XSSC in 80 ml ddH_20

70 % Formamide in 30 ml 2XSSC pH 7.0 (v.v):

70 ml Formamide in 30 ml 2XSSC (20 ml ddH_20 + 10 ml of 2XSSC), then adjust pH to 7.0

Buffer A:

50 % Formamide 2XSSC, pH 7.0:

150 ml Formamide in 30 ml 2XSSC + 120 ml ddH_20, then adjust pH to 7.0

Buffer B:

0.1XSSC pH 7.0 (v/v):

1.5 ml 20XSSC in 298.5 ml ddH_20, then adjust pH to 7.0

4 % Bovine Serum Albumin (BSA):

4g BSA in 10 ml 4XSSC

1% BSA:

0.1 g BSA in 10 ml 4XSSC

Cy3-Streptavidin (1:200 dilution, v/v):

1 µl Cy3 in 199 µl 1% BSA

4XSSC in 0.5% Tween-20 (v/v):

400 ml ddH_20 in 100 ml 20XSSC + 1.5 ml Tween-20

❖ Image of 50bp Hyper™ Ladder II Used for PCR studies

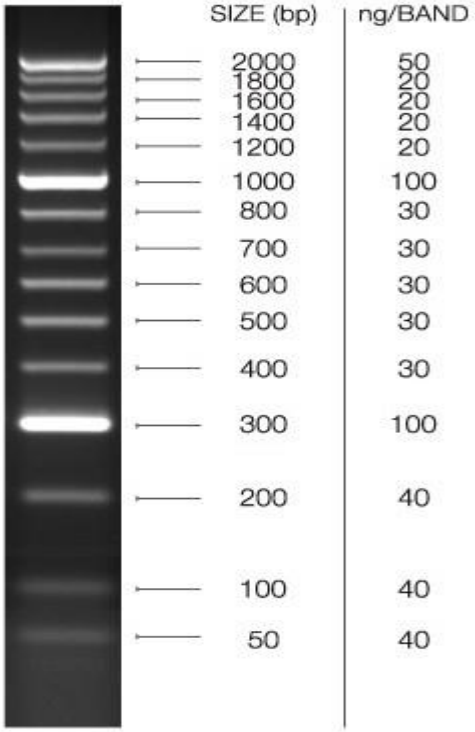

Figure: 50 bp ladder (visualized by ethidium bromide staining on a 1% TAE agarose gel).

❖ Lovastatin Drug Treatment

Lovastatin drug (10µg/ ml) in 100% ethanol:

1M = 404.54g in 1 L

1M = 0.40454g in 1 ml

1M = 1000µM = 404 µg in 1 ml

24 µM = 10 µg in 1 ml

To make it 1000X stock

❖ M-FISH karyotypic results for hTERT progeria cell line T08

Table 1: M-FISH karyotypes of T08 cells

Cell number	Karyotype
0001	61,XXX,del(Xp),der(1)t(1;17),-2,-3,-3,-4,-4,del(4p),-5,del(5p),-6,-6,-7,-8, ,-9,del(9q),-10,-11,-11,-12,-13,-13,del(13q),del(13q),-14,-14,der(15)t(8;15),-15,-15,-16,-16,-17,-18,-18,-19,-20,-21,-22,-22,+2mar
0002	62,XXXY,-1,der(1)t(1;13),der(1)t(1;17),ace(1p),-3,del(3p),-4,-5,-5,-5,del(5p),-6,-7,-8,-8, -9,-9,der(9)t(1;9),-10,-10,-10,-11,-11,-12,-13,-13,-14,der(15)t(8;15),-16,-17,der(17)(1;17),del(18q),-19,-19,-20,-20,der(22)t(18;22),-22
0005	79,XXX,der(X)t(X;18),der(1)t(14;1;17),ins(1;14),del(1q),der(2)t(1;2),del(3p),-4,-5,der(6)t(6;19),der(7)t(7;21),-9,-12,-13,der(14)t(10;14),ace(14;21),-15,-15, der(15)t(8;15),-20,-21,+2mar
0011	76,X,-X,-X,-X,ins(1;14),der(1)t(1;18),del(1q),-2,der(2)t(2;15),del(3p),-4,del(5p),del(5q),der(6)t(6;19),-7,-7,-8,der(12)t(12;20), -13,-14,der(14)t(10;14), der(15)t(8;15),del(15q),-17,-18,-19,-21,-22+3mar
0013	78,XXX,der(X)t(X;18),der(1)t(14;1;17),ins(1;14), der(1)(1;14),del(1q),der(2)t(1;2),del(3p),-4,-5,del(5p),-6,der(6)t(6;10),del(7q),-9,del(9q),-11,-13,-14,der(14)(10;14),der(15)t(8;15),-16,-18,del(18q),-19,-20,-20,-21
0018	66,XXX,der(X)t(X;1),der(1)t(14;1;17),der(1)t(1;18),del(1p),der(1)ins(15;1;X),del(2p),-3,del(3p),der(4)t(4;19),del(5p),del(5q),-6,-6,-6,-6,-7,-7,-9,-10,-11,-11,-12,-13,-13,-14,der(15)t(8;15),del(15q) ,-18,der(18)t(17;18) ,-20,-20,-20,-21,-21,-21,-22,-22
0019	85,XXX,der(X)t(X;18),del(Xq),ins(1;14),der(1)t(14;1;17),der(2)t(1;2),del(3p),-4,del(5p),der(6)t(6;13),der(7)t(7;21),dic(8;17)+ace(8q),-9,-12,-13,-14,der(14)t(10;14),-17,der(18)t(18;20),-19,-21
0020	79,XXX,der(X)t(X;18),ins(1;14),der(2)t(1;2),-3,-4,del(5p),del(5p),-6,der(7)t(7;21),-9,-12,-12,-13,-14,der(14)t(10;14),der(15)t(8;15),-17,del(18p),-19,del(20p)+del(20q),-20,-22,+mar
0021	83,XXX,t(X;1),ins(1;14),der(1)t(14;1;17),del(2p),del(3p),der(4)t(4;19),der(5)t(5;10),del(5p),-6,der(7)t(7;21),-13,-14,der(14)t(10;14),-15,der(15)t(8;15),-16,del(17q)
0025	79,XXX,der(X)t(X;18),ins(1;14),der(1)t(14;1;17), der(2)t(1;2), del(3p),-4,-5,del(5p), der(6)t(6;19), der(7)t(7;21),-8,-9,-11,der(14)t(10;14),del(14q), der(15)t(8;15),-16,-20,-22,-22
0029	86,XXX,t(X;1),ins(1;14),der(1)t(14;1;17),der(1)(1;17),der(1)t(1;18),del(2p),del(3p),der(4)t(4;19), del(5p),-6,der(7)t(7;21),-13,-14,der(14)t(10;14),der(15)t(8;15),ace(15p),-16,der(16)t(14;16),+del(18p)+del(18q),-20,-22,del(22q)+ace(22q)
0030	71,XXX,del(Xp),der(1)t(1;17),ace(1;17),ace(1q),ace(1p),der(1)t(1;13),der(3)t(3;10),-4,-4,del(5p),-6,der(7)t(2;7),-8,del(9p),-10,-14,-15,der(15)t(8;15),-16,-16,-17,-18,-18,-19,-19,-20,-20,-22,-22
0034	73,XXX,der(X)t(X;18),ins(1;14),der(1)t(14;1;17),der(2)t(1;2),del(3p),-4,del(5p),del(5p),-6,-7,-9,-9,-10,-11,-12,-13,-14,der(14)t(10;14),-15,der(15)t(8;15),del(18p),-19,-20,der(20)t(18;20),-21
0041	81,XXX,t(X;1),ins(1;14),der(1)t(14;1;17),del(1p),del(1q),del(2p),del(2q),-3,del(4p),del(5p),-6,der(7)t(7;21),-12,-13,-14,-15,der(15)t(8;15),ace(15p),-17,der(17)t(Y;17),der(18)t(18;21),-19,+mar
0046	81,XXX,der(X)t(X;18),ins(1;14),der(1)t(14;1;17),der(2)t(1;2),der(3)t(3;22),-4,del(5p),-6,der(7)t(7;21),-9,-12,-13,-14,der(14)t(10;14),-15,der(15)t(8;15),-19,der(20)t(18;20),+mar
0049	75,X,-X,-X,t(X;1),ins(1;14),der(1)t(14;1;17),x2ace(1q),-2,del(2p),-3,del(3p),der(4)t(4;19),-5,-6,der(7)t(7;21),-8,-9,-12,-12,-13,-13,-

	14,der(14)t(10;14),-15,-15,-16,der(16)t(16;?),der(17)t(X;17),del(17q),-19,-19,der(20)t18;20),-22,+2mar
0051	70,XXX,der(X)t(X;18),-1,ins(1;14),der(1)t(1;14),der(1)t(1;18),der(2)t(1;2),-4,-5,-5,-5,-6,-6,der(6)t(6;19),-7,-9,-12,-13,-13,-14,der(14)t(10;14),der(15)t(8;15),-16,-16,-17,-17,del(18p),-20,-21,-22,del(22q)+ace(22q),+mar

❖ **Table 2: Occurrence of structural rearrangements in T08 cells**

	Observed in cell number																	**Number of cells**
	1	**2**	**5**	**11**	**13**	**18**	**19**	**20**	**21**	**25**	**29**	**30**	**34**	**41**	**46**	**49**	**51**	
t(Xcen;1)									X		X			X		X		4
der(X)t(Xcen;1)						X												1
der(X)t(Xcen;18?cen)			X		X		X	X		X			X		X		X	8
der(1)t(1cen;13)		X										X						2
der(1)t(1cen;14)					X												X	2
ins(1?cen;14)			X	X	X		X	X		X	X		X	X	X	X	X	12
der(1)ins(15;1;X)						X												1
der(1)t(1;17)	X	X									X	X						4
der(1)t(14;1cen;17)			X		X	X	X		X	X	X		X	X	X	X		11
ace(1;17)												X						1
der(1)t(1cen;18)				X		X					X						X	4
der(2)t(1?cen;2cen)			X		X		X	X		X			X		X		X	8

t(Xcen;1), cell 49: Reciprocaltranslocation

der(X)t(Xcen;1), cell 18 : Non-reciprocal translation

der (1)ins(15;1;X) : Reciprocal translocation with additional exachange resulting in 15; 1; X

	Observed in cell number																	**Number of cells**
	1	**2**	**5**	**11**	**13**	**18**	**19**	**20**	**21**	**25**	**29**	**30**	**34**	**41**	**46**	**49**	**51**	
der(2)t(2pter;15)				X														1
der(3)t(3;10)												X						1
der(3)t(3cen;22)															X			1
der(4)t(4cen;19)	X					X			X		X					X		5
der(5)t(5;10)									X									1
der(6)t(6cen;13)							X											1
der(6)t(6cen;19)			X	X						X							X	4
der(7)t(2;7)												X						1
der(7)t(7?qter;21)			X				X	X	X	X	X			X	X	X		9
dic(8cen;17)							X											1
der(9)t(1;9)		X																1
der(12)t(12cen;20)				X														1
der(14)t(10;14cen)			X	X	X		X	X	X	X	X		X		X	X	X	12
ace(14;21)			X															1

	Observed in cell number																	Number of cells
	1	**2**	**5**	**11**	**13**	**18**	**19**	**20**	**21**	**25**	**29**	**30**	**34**	**41**	**46**	**49**	**51**	
der(15)t(8;15)	X	X	X	X	X	X		X	X	X	X	X	X	X	X		X	15
der(16)t(14;16cen)											X							1
der(16)t(16;?)																X		1
der(17)t(X;17cen)																X		1
der(17)t(Y;17)														X				1
der(17)(?1;17)		X																1
der(18)t(5;18)											X							1
der(18)t(17;18cen)						X												1
der(18)t(18cen;20)							X											1
der(18)t(18cen;21)														X				1
der(20)t(18;20cen)													X		X			2
der(22)t(18;22cen)		X																1

❖ Table 3: Occurrence of structural deletions in T08 cells

	Observed in cell number																	Number of cells
	1	**2**	**5**	**11**	**13**	**18**	**19**	**20**	**21**	**25**	**29**	**30**	**34**	**41**	**46**	**49**	**51**	
del(Xp)	X											X						2
del(Xcenq)							X											1
ace(1p)		X										X						2
ace(1q)												X				X		2
ace(1q)																X		1
del(1q)			X	X	X													3
del(1cenq)						X								X				2
del(2cenp)						X			X		X			X		X		5
del(2cenq)														X				1
del(3p)		X	X	X	X	X	X		X	X	X		X			X		11
del(4cenp)														X				1
del(5cenp)	X	X		X	X	X	X	X	X	X	X	X	X	X	X			14
del(5cenq)				X		X												2
del(7q)					X													1
ace(8q)							X											1
del(9cenp)	X											X						2
del(9q)					X													1
del(13q)	X																	1
del(13q)	X																	1
del(14cenq)										X								1
ace(15p)											X			X				2
del(15q)				X		X												2
del(17q)									X							X		2
del(18cenp)								X			X		X				X	4
del(18cenq)		X			X						X							3
del(20cenq)								X										1
del(22q)											X						X	2
ace(22q)											X						X	2

❖ Table 4: Occurrence of numerical aberrations in untreated T08 cells

	Observed in cell number																	Number of cells
	1	**2**	**5**	**11**	**13**	**18**	**19**	**20**	**21**	**25**	**29**	**30**	**34**	**41**	**46**	**49**	**51**	
-1		X															X	2
-2	X			X												X		3
-3	X	X				X		X						X		X		6
-3	X																	1
-4	X	X	X	X	X		X	X		X		X	X		X		X	12
-4	X											X						2
-5	X	X	X		X					X						X	X	7
-5		X															X	2
-5		X															X	2
-6	X	X			X	X		X	X		X	X	X	X	X	X	X	13
-6	X					X											X	3
-6						X												1
-6						X												1
-7	X	X		X		X							X				X	6
-7				X		X												2
-8	X	X		X						X		X				X		6
-8		X																1
-9	X	X	X		X	X	X	X		X			X		X	X	X	12
-9		X											X					2
-10	X	X				X						X	X					5
-10		X																1
-10		X																1
-11	X	X			X	X				X			X					6
-11	X	X				X												3
-12	X	X	X			X	X	X					X	X	X	X	X	11
-12								X								X		2
-13	X	X	X	X	X	X		X	X		X		X	X	X	X	X	14
-13	X	X				X	X									X	X	6
-14	X	X		X	X	X	X	X	X		X	X	X	X	X	X	X	14
-14	X																	1
-15	X		X						X		X	X	X	X	X	X		9
-15	X		X													X		3
-16	X	X			X				X	X	X	X				X	X	9

	1	**2**	**5**	**11**	**13**	**18**	**19**	**20**	**21**	**25**	**29**	**30**	**34**	**41**	**46**	**49**	**51**	**Number of cells**
-16	X											X					X	3
-17	X	X		X			X	X				X		X			X	8
-17																	X	1
-18	X			X	X	X						X						5
-18	X											X						2
-19	X	X		X	X		X	X				X	X	X	X	X		11
-19		X										X				X		3
-20	X	X	X		X	X		X			X	X	X			X	X	11
-20		X			X	X				X		X						5
-20						X												1
-21	X		X	X	X	X	X						X				X	8
-21						X												1
-21						X												1
-22	X	X		X		X		X		X	X	X				X	X	10
-22	X					X				X		X						4
-X				X												X		2
-X				X												X		2
-X				X														1
+22					X													1

❖ **Table 5: Occurrence of clonal structural rearrangements in T08 cells**

	Observed in cell number																	**Number of cells**
	1	**2**	**5**	**11**	**13**	**18**	**19**	**20**	**21**	**25**	**29**	**30**	**34**	**41**	**46**	**49**	**51**	
t(X;1)									X		X			X		X		4
der(X)t(X;18)			X		X		X	X		X			X		X		X	8
der(1)t(1;13)		X										X						2
der(1)t(1;14)					X												X	2
ins(1;14)			X	X	X		X	X		X	X		X	X	X	X	X	12
der(1)t(1;17)	X	X									X	X						4
der(1)t(14;1;17)			X		X	X	X		X	X	X		X	X	X	X		11
der(1)t(1;18)				X		X					X						X	4
der(2)t(1;2)			X		X		X	X		X			X		X		X	8
der(4)t(4;19)	X					X			X		X					X		5
der(6)t(6;19)			X	X						X							X	4
der(7)t(7;21)			X				X	X	X	X	X			X	X	X		9
der(14)t(10;14)			X	X	X		X	X	X	X	X		X		X	X	X	12
der(15)t(8;15)	X	X	X	X	X	X		X	X	X	X	X	X	X	X		X	15
der(20)t(18;20)													X			X		2

Table 6: Occurrence of clonal structural deletions in T08 cells

	Observed in cell number																	Number of cells
	1	**2**	**5**	**11**	**13**	**18**	**19**	**20**	**21**	**25**	**29**	**30**	**34**	**41**	**46**	**49**	**51**	
del(Xp)	X											X						2
ace(1p)		X										X						2
ace(1q)												X				X		2
del(1q)			X	X	X													3
del(1cenq)						X								X				2
del(2cenp)						X			X		X			X		X		5
del(3p)		X	X	X	X	X	X		X	X	X		X			X		11
del(5cenp)	X	X		X	X	X	X	X	X	X	X	X	X	X	X			14
del(5cenq)				X		X												2
del(9cenp)	X											X						2
ace(15p)											X			X				2
del(15q)				X		X												2
del(17q)									X							X		2
del(18cenp)								X			X		X				X	4
del(18cenq)		X			X						X							3
del(22q)											X						X	2
ace(22q)											X						X	2

Table 7: Occurrence of clonal numerical aberrations in T08 cells

	Observed in cell number																	Number of cells
	1	**2**	**5**	**11**	**13**	**18**	**19**	**20**	**21**	**25**	**29**	**30**	**34**	**41**	**46**	**49**	**51**	
-2	X			X												X		3
-3	X	X				X		X						X		X		6
-4	X	X	X	X	X		X	X		X		X	X		X		X	12
-5	X	X	X		X					X						X	X	7
-6	X	X			X	X		X	X		X	X	X	X	X	X	X	13
-6	X					X											X	3
-7	X	X		X		X							X				X	6
-8	X	X		X						X		X				X		6
-9	X	X	X		X	X	X	X		X			X		X	X	X	12
-10	X	X				X						X	X					5
-11	X	X			X	X				X			X					6
-11	X	X				X												3
-12	X	X	X			X	X	X					X	X	X	X	X	11
-13	X	X	X	X	X	X		X	X		X		X	X	X	X	X	14
-13	X	X				X	X									X	X	6
-14	X	X		X	X	X	X	X	X		X	X	X	X	X	X	X	14
-15	X		X						X		X	X	X	X	X	X		9
-15	X		X													X		3
-16	X	X			X				X	X	X	X				X	X	9
-16	X											X					X	3
-17	X	X		X			X	X				X		X			X	8
-18	X			X	X	X						X						5
-19	X	X		X	X		X	X				X	X	X	X	X		11
-19		X										X				X		3
-20	X	X	X		X	X		X			X	X	X			X	X	11
-20		X			X	X				X		X						5
-21	X		X	X	X	X	X						X				X	8
-22	X	X		X		X		X		X	X	X				X	X	10
-22	X					X				X		X						4

Table 8: Clonal aberrations that occur in 10 or more cells

T08
ins(1;14),der(1)t(14;1;17),del(3p),-4,del(5p),-6,-9,-12,13,-14,der(14)t(10;14),der(15)t(8;15),-19,-20,-22

Table 9: Clonal aberrations that occur in less than 10 cells

T08
t(X;1),der(X)t(X;18),del(Xp),ace(1p),ace(1q),del(1p),del(1q),der(1)t(1;13),der(1)t(1;14),der(1)t(1;17),der(1)t(1;18),der(2)t(1;2),del(2p),-2,-3,del(4p),der(4)t(4;19),del(5q),-5,-6,der(6)t(6;19),-7,der(7)t(7;21),-8,del(9p),-10,-11,-11,-13,-15,-15,ace(15p),del(15q),-16,-16,-17,del(17q),-18,del(18p),del(18q),-19,der(20)t(18;20),-20,-21,del(22q),ace(22q),-22

Table 10: A composite karyotype reflects the heterogeneity of abnormalities in each cell – it describes all of the clonally occurring abnormalities.

T08
61-86,XXX,del(Xp),t(X;1),der(X)t(X;18),ace(1p),ace(1q),del(1p),del(1q),der(1)t(1;13),der(1)t(1;14),ins(1;14),der(1)t(1;17),der(1)t(14;1;17), der(1)t(1;18),der(2)t(1;2),del(2p),-2,-3,del(3p),-4,del(4p),der(4)t(4;19),del(5p),del(5q),-5,-6,der(6)t(6;19),-6,-7,der(7)t(7;21),-8,del(9p),-9,-10,-11,-11,-12,13,-13,-14,der(14)t(10;14),-15,-15,ace(15p),del(15q)der(15)t(8;15),-16,-16,-17,del(17q),-18,del(18p),del(18q),-19,-19,-20,der(20)t(18;20),-20,-21,del(22q),ace(22q),-22,-22 [cp17]

- Regarding clonal abnormalities – no event occurs in all cells analysed. Please see highlighted grey in clonal tables for occurrences in each cell.

List of publications

Papers

1- **Bourne, G., Moir, C., Bikkul, U., Ahmed, M.H., Kill, I.R., Eskiw, C.H., Tosi, S. and Bridger, J.M**. **(2013**) 'Interphase chromosome behavior in normal and diseased cells', in Human Interphase Chromosomes. Springer, pp. 9-33.

2- **Craig, S. C., Bikkul, U., Ahmed, M.H., Foster, H.A., Godwin. L.S., and Bridger**, **J.M. (2015)** 'Visualizing the spatial relationship of the genome with the nuclear envelope using fluorescence in situ hybridization'

3- **Craig, S. C., Bikkul, U., Ofosu, W., Tree, D., Makarov, E., Kill, I.R., and Bridger, J.M. (2015)** ' Drugs that affect farnesylation and anti-oxidant N-acetyl cysteine, bring about positive effects in Hutchinson-Gilford Progeria Syndrome cells with respect to aberrant lamin and progerin distribution'

Conference abstracts

1- **Bikkul, U., Bourne, G., Craig, S. C., Eskiw, C.H., Slijepcevic, P., Faragher, R.G.A. ,Kill, I.R., Bridger, J.M. (2013)** 'Nuclear structure and genome aberrations in immortalised Hutchinson-Gilford Progeria cells.'

Abstract accepted and presented as a poster to EMBO conference series, "nuclear structure and dynamics", L'Isle sur la Sorgue, France, 2013

2- **Bikkul, U., Slijepcevic, P., Anderson, R., Faragher, R.G.A., Kill, I.R., Bridger, J.M. (2014)** 'Structural and genomic aberrations in hTERT immortalised Hutchinson-Gilford Progeria cells.'

Abstract accepted and presented as a poster to “Views into nuclear function”, Patras, Greece, 2014 and to “20th International Chromosome Conference”, University of Kent, England.

3- **Bikkul, U., Slijepcevic, P., Anderson, R., Faragher, R.G.A., Kill, I.R., Bridger, J.M. (2015)** ‘Genome Organisation is affected in immortalised control and Hutchinson-Gilford Progeria Cells.’

Abstract accepted and presented as a poster to “7th UK Conference on the Nuclear Envelope in Disease and Chromatin Organization”, The Wolfson Centre for Inherited Neuromuscular Disease, RJAH Orthopaedic Hospital, Oswestry, UK, 2015.

4- **Bikkul, U., Bourne, G., Slijepcevic, P., Anderson, R., Faragher, R.G.A., Kill, I.R., Bridger, J.M. (2014)** ‘Structural and genomic aberrations in hTERT immortalised Hutchinson-Gilford Progeria cells.’

Abstract accepted and presented as a talk to “the 10th Annual HSSC PhD Conference’, Brunel University, 2014.